DISSERTATION

EPIDITHIODIOXOPIPERAZINES: SYNTHETIC STUDIES OF (+)-CHETOMIN AND (–)-SPORIDESMIN A

Submitted by

Timothy R. Welch

Department of Chemistry

In partial fulfillment of the requirements

For the Degree of Doctor of Philosophy

Colorado State University

Fort Collins, Colorado

Fall 2012

Doctoral Committee:

Advisor: Robert M. Williams

Tomislav Rovis
John L. Wood
Chris Ackerson
Douglas H. Thamm

Copyright by Timothy Ryan Welch 2012

All Rights Reserved

ABSTRACT

EPIDITHIODIOXOPIPERAZINES: SYNTHETIC STUDIES OF

(+)-CHETOMIN AND (–)-SPORIDESMIN A

This dissertation documents efforts toward the asymmetric total syntheses of the natural products (+)-chetomin and (–)-sporidesmin A. Synthetic methods have been developed to efficiently construct the dioxopiperazine core of both molecules. Additionally, a simple epidithiodioxopiperazine has been synthesized to demonstrate a general method for the addition of a sulfur bridge to a dioxopiperazine ring. The work described herein, while not totally successful, provides a basis for future completion of the asymmetric total syntheses of these two epidithiodioxopiperazines and other related fungal metabolites.

ACKNOWLEDGEMENTS

I am truly thankful for all of the supportive individuals who have motivated, inspired, and encouraged me throughout my education. This work and much of my personal and professional development would not have been possible without you. I would first like to thank my advisor, Professor Robert M. Williams, for accepting me into the Williams group and providing a dynamic research environment. It has been an honor to work for you, and I am grateful for all of the advice and insight you have provided me over the years. Thanks to all members of the Williams group, past and present, for all of the ideas, encouragement, and shenanigans. Karen Kahler and Elizabeth McCoy, thank you for making my life at CSU a little easier. Special mention must go to all of my climbing partners; thanks for catching my numerous falls, throwing entertaining wobblers, helping me clear my head, and inspiring me to try harder.

Without question, I would not be here were it not for two professors at KU and several teachers from high school. Professor Brian Blagg, thank you for introducing me to the field of organic synthesis and for your continued support. Professor Givens, it was your skillful course instruction that first inspired me to pursue a career in academia. In high school, I was blessed to have Kristin Seaton (Gunn), John Wachholz, and Linda Nelson as teachers and advisors; thank you all for your encouragement and for always challenging me to do better.

Lastly, I extend my utmost gratitude to my family. My parents taught me the value of hard work and persistence and have always encouraged me to strive for excellence. It was their encouragement and support that nurtured my intellectual curiosity. Mom, Dad, Eric, and Emily, thank you for all of your love and support.

TABLE OF CONTENTS

ABSTRACT ii

ACKNOWLEDGEMENTS iii

TABLE OF CONTENTS iv

LIST OF FIGURES vii

LIST OF SCHEMES xiv

Chapter 1: Epidithiodioxopiperazines

1.1: Introduction 1

1.2: Epidithiodioxopiperazines Derived from Phenylalanine or Tyrosine 3

1.3: Tryptophan-Derived Epidithiodioxopiperazines 13

1.4: Biosynthetic Investigations of Epidithiodioxopiperazines 23

1.5: Concluding Remarks 28

Chapter 2: Total Syntheses of Epidithiodioxopiperazines

2.1: Introduction 29

2.2: Early Epidithiodioxopiperazine Syntheses (1973-1981) 30

2.3: Recent Epidithiodioxopiperazine Syntheses (2009-2012) 35

2.4: Other Relevant Syntheses: Formation of the C3-N1' Bond 45

2.5: Concluding Remarks 49

Chapter 3: Studies Toward the Total Synthesis of Chetomin

3.1: Introduction.....51

3.2: Goals and Early Studies

3.2.1: Goals of the Project.....51

3.2.2: Iminium Ion Approach.....52

3.2.3: Pinacol-type Rearrangement.....53

3.3: Evolution of Coupling Strategy

3.3.1: Witkop's Pyrroloindole.....55

3.3.2: Indole-Aniline Coupling.....57

3.3.3: Coupling to *exo*-3-bromopyrroloindoline.....59

3.3.4: Attempted Coupling to Tetracyclic Bromide.....60

3.4: Epidithiodioxopiperazine Formation.....62

3.5: Attempted Core Construction

3.5.1: Problematic Peptide Couplings.....63

3.6: Synthesis of Heptacyclic Core

3.6.1: Synthesis of Dioxopiperazines.....65

3.6.2: Initial *N*-Methyl Amino Acid Incorporation.....66

3.6.3: Bypassing the Serine Side Chain with Sarcosine.....68

3.6.4: Completion of the Carbon Skeleton of Chetomin.....69

3.6.5: Attempted Epidithiodioxopiperazine Formation.....69

3.7: Proposed Future Studies

3.7.1: Proposed Synthesis of Tetraol.....70

3.7.2: Bypassing the Tetraol.....72

3.7.3: Late-Stage Alkylation of Sarcosine Analogue....72

3.8: Concluding Remarks....73

Chapter 4: Synthetic Approach to Sporidesmin A

4.1: Introduction....75

4.2: Retrosynthetic Analysis....76

4.3: Synthetic Approach to Sporidesmin A

4.3.1: Preparation of Dinitrostyrene Derivative....78

4.3.2: Indole Synthesis and Sharpless Asymmetric Aminohydroxylation 80

4.3.3: Dioxopiperazine Formation....81

4.3.4: Oxidative Cyclization Attempts....83

4.3.5: Toward a Formal Synthesis of Sporidesmin A....86

4.4: Future Direction....88

4.5: Concluding Remarks....89

References....91

Chapter 5: Experimental Procedures....104

Appendix I: Publications....346

Appendix II: Research Proposal....382

List of Abbreviations....395

LIST OF FIGURES

CHAPTER 1

Figure 1.1 Epidithiodioxopiperazines derived from tyrosine and/or phenylalanine.....2

Figure 1.2 Tryptophan-derived epidithiodioxopiperazines.....2

Figure 1.3 Gliotoxins.....3

Figure 1.4 Redox cycling of epidithiodioxopiperazines.....4

Figure 1.5 Mixed disulfide formation.....5

Figure 1.6 Simple biologically active epidithiodioxopiperazines.....6

Figure 1.7 Hyalodendrins and related compounds.....7

Figure 1.8 Silvatins.....7

Figure 1.9 Aranotins.....8

Figure 1.10 Emethallicins.....9

Figure 1.11 Emestrins and related metabolites.....11

Figure 1.12 Epicorazines.....11

Figure 1.13 Scabrosin esters.....12

Figure 1.14 Sirodesmins.....13

Figure 1.15 Sporidesmins.....15

Figure 1.16 Metabolites of the fungus *Chaetomium cochliodes*.....16

Figure 1.17 Chetoseminudins.....16

Figure 1.18 HIF-1 hypoxia response pathway.....17

Figure 1.19 Chaetocins and related metabolites.....19

Figure 1.20 Fungal metabolites related to the chaetocins.....20

Figure 1.21 Verticillin A and related metabolites.....20

Figure 1.22 Verticillin-type epipolythiodioxopiperazines.....21

Figure 1.23 Leptosins.....23

Figure 1.24 Putative epidithiodioxopiperazine gene clusters for sirodesmin PL (**A**) and gliotoxin (**B**).....26

CHAPTER 3

Figure 3.1 Chetomin and related fungal metabolites 52

CHAPTER 4

Figure 4.1 Sporidesmin A and related fungal metabolites 76

CHAPTER 5

Figure 5.1a ^{1}H NMR spectrum of compound **3.5** 106
Figure 5.2a ^{1}H NMR spectrum of compound **3.6** 108
Figure 5.2b ^{13}C NMR spectrum of compound **3.6** 108
Figure 5.3a ^{1}H NMR spectrum of compound **3.15** 110
Figure 5.4a ^{1}H NMR spectrum of compound **3.12** 112
Figure 5.5a ^{1}H NMR spectrum of compound **3.16** 114
Figure 5.6a ^{1}H NMR spectrum of compound **3.17** 116
Figure 5.6b ^{13}C NMR spectrum of compound **3.17** 116
Figure 5.7a ^{1}H NMR spectrum of compound **3.21** 118
Figure 5.8a ^{1}H NMR spectrum of compound **3.31** 120
Figure 5.9a ^{1}H NMR spectrum of compound **3.32** 122
Figure 5.10a ^{1}H NMR spectrum of compound **3.35** 124
Figure 5.11a ^{1}H NMR spectrum of compound **3.40** 126
Figure 5.12a ^{1}H NMR spectrum of compound **3.41** 128
Figure 5.13a ^{1}H NMR spectrum of compound **3.42** 130
Figure 5.14a ^{1}H NMR spectrum of (bromoethynyl)trimethysilane 131
Figure 5.15a ^{1}H NMR spectrum of compound **3.43** 133
Figure 5.16a ^{1}H NMR spectrum of compound **3.44** 135
Figure 5.17a ^{1}H NMR spectrum of compound **3.47** 137

Figure 5.18a ^{1}H NMR spectrum of compound **3.48** 139
Figure 5.19a ^{1}H NMR spectrum of compound **3.56** 141
Figure 5.20a ^{1}H NMR spectrum of compound **3.57a** 143
Figure 5.21a ^{1}H NMR spectrum of compound **3.58a** 145
Figure 5.22a ^{1}H NMR spectrum of compound **3.57c**.....147
Figure 5.22b ^{13}C NMR spectrum of compound **3.57c** 147
Figure 5.23a ^{1}H NMR spectrum of compound **3.57d** 149
Figure 5.23b ^{13}C NMR spectrum of compound **3.57d**.....149
Figure 5.24a ^{1}H NMR spectrum of compound **3.58d** 151
Figure 5.24b ^{13}C NMR spectrum of compound **3.58d**.....151
Figure 5.25a ^{1}H NMR spectrum of compound **3.57e**.....153
Figure 5.25b ^{13}C NMR spectrum of compound **3.57e** 153
Figure 5.26a ^{1}H NMR spectrum of compound **3.58e**.....155
Figure 5.27a ^{1}H NMR spectrum of compound **5.1** 157
Figure 5.28a ^{1}H NMR spectrum of compound **5.2** 159
Figure 5.28b ^{13}C NMR spectrum of compound **5.2** 159
Figure 5.29a ^{1}H NMR spectrum of compound **5.3** 161
Figure 5.29b ^{13}C NMR spectrum of compound **5.3** 161
Figure 5.30a ^{1}H NMR spectrum of compound **3.56** 163
Figure 5.31a ^{1}H NMR spectrum of compound **3.55e**.....165
Figure 5.32a ^{1}H NMR spectrum of compound **3.60** 167
Figure 5.33a ^{1}H NMR spectrum of compound **3.61** 169
Figure 5.34a ^{1}H NMR spectrum of compound **3.63** 172
Figure 5.34b ^{13}C NMR spectrum of compound **3.63** 172
Figure 5.35a ^{1}H NMR spectrum of compound **3.59** 174
Figure 5.36a ^{1}H NMR spectrum of compound **3.34** 176
Figure 5.37a ^{1}H NMR spectrum of compound **3.64** 178
Figure 5.38a ^{1}H NMR spectrum of compound **3.65** 180
Figure 5.38b ^{13}C NMR spectrum of compound **3.65** 180
Figure 5.39a ^{1}H NMR spectrum of compound **3.66** 182
Figure 5.39b ^{13}C NMR spectrum of compound **3.66** 182

Figure 5.40a ^{1}H NMR spectrum of compound **3.67** 184
Figure 5.40b ^{13}C NMR spectrum of compound **3.67** 184
Figure 5.41a ^{1}H NMR spectrum of compound **3.68** 186
Figure 5.42a ^{1}H NMR spectrum of compound **3.69** 188
Figure 5.43a ^{1}H NMR spectrum of compound **5.4** 190
Figure 5.44a ^{1}H NMR spectrum of compound **3.71** 192
Figure 5.45a ^{1}H NMR spectrum of compound **5.5** 194
Figure 5.46a ^{1}H NMR spectrum of compound **3.74** 196
Figure 5.46b ^{13}C NMR spectrum of compound **3.74** 196
Figure 5.47a ^{1}H NMR spectrum of compound **3.75** 198
Figure 5.47b ^{13}C NMR spectrum of compound **3.75** 198
Figure 5.48a ^{1}H NMR spectrum of compound **5.6** 200
Figure 5.48b ^{13}C NMR spectrum of compound **5.6** 200
Figure 5.49a ^{1}H NMR spectrum of compound **3.76** 203
Figure 5.49b ^{13}C NMR spectrum of compound **3.76** 203
Figure 5.50a ^{1}H NMR spectrum of compound **3.77** 205
Figure 5.51a ^{1}H NMR spectrum of compound **5.7** 207
Figure 5.51b ^{13}C NMR spectrum of compound **5.7** 207
Figure 5.52a ^{1}H NMR spectrum of compound **3.80** 209
Figure 5.52b ^{13}C NMR spectrum of compound **3.80** 209
Figure 5.53a ^{1}H NMR spectrum of compound **3.81** 211
Figure 5.54a ^{1}H NMR spectrum of compound **3.82** 214
Figure 5.55a ^{1}H NMR spectrum of compound **5.9** 216
Figure 5.56a ^{1}H NMR spectrum of compound **3.88** 218
Figure 5.56b ^{13}C NMR spectrum of compound **3.88** 218
Figure 5.57a ^{1}H NMR spectrum of compound **5.10** 220
Figure 5.58a ^{1}H NMR spectrum of compound **3.90A** 223
Figure 5.58b ^{13}C NMR spectrum of compound **3.90A** 223
Figure 5.59a ^{1}H NMR spectrum of compound **3.90B**.....224
Figure 5.59b ^{13}C NMR spectrum of compound **3.90B**.....224
Figure 5.60a ^{1}H NMR spectrum of compound **5.11** 226

Figure 5.60b ^{13}C NMR spectrum of compound **5.11** 226
Figure 5.61a ^{1}H NMR spectrum of compound **4.15** 228
Figure 5.61b ^{13}C NMR spectrum of compound **4.15** 228
Figure 5.62a ^{1}H NMR spectrum of compound **4.17** 230
Figure 5.62b ^{13}C NMR spectrum of compound **4.17** 230
Figure 5.63a ^{1}H NMR spectrum of compound **4.18** 232
Figure 5.63b ^{13}C NMR spectrum of compound **4.18** 232
Figure 5.64a ^{1}H NMR spectrum of compound **4.19** 233
Figure 5.65a ^{1}H NMR spectrum of compound **4.7** 235
Figure 5.65b ^{13}C NMR spectrum of compound **4.7** 235
Figure 5.66a ^{1}H NMR spectrum of compound **4.6** 237
Figure 5.66b ^{13}C NMR spectrum of compound **4.6** 237
Figure 5.67a ^{1}H NMR spectrum of compound **5.12** 239
Figure 5.67b ^{13}C NMR spectrum of compound **5.12** 239
Figure 5.68a ^{1}H NMR spectrum of compound **4.20** 241
Figure 5.68b ^{13}C NMR spectrum of compound **4.20** 241
Figure 5.69a ^{1}H NMR spectrum of compound **4.5** 243
Figure 5.69b ^{13}C NMR spectrum of compound **4.5** 243
Figure 5.70a ^{1}H NMR spectrum of compound **4.4** 245
Figure 5.70b ^{13}C NMR spectrum of compound **4.4** 245
Figure 5.71a ^{1}H NMR spectrum of compound **4.23** 247
Figure 5.71b ^{13}C NMR spectrum of compound **4.23** 247
Figure 5.72a ^{1}H NMR spectrum of compound **4.24** 249
Figure 5.73a ^{1}H NMR spectrum of compound **4.25** 251
Figure 5.74a ^{1}H NMR spectrum of compound **4.26** 253
Figure 5.74b ^{13}C NMR spectrum of compound **4.26** 253
Figure 5.75a ^{1}H NMR spectrum of compound **4.27** 255
Figure 5.76a ^{1}H NMR spectrum of compound **4.28** 257
Figure 5.77a ^{1}H NMR spectrum of compound **4.29** 259
Figure 5.77b ^{13}C NMR spectrum of compound **4.29** 259
Figure 5.78a ^{1}H NMR spectrum of compound **4.30** 261

Figure 5.79a ^{1}H NMR spectrum of compound **4.31** 263
Figure 5.80a ^{1}H NMR spectrum of compound **4.32** 265
Figure 5.80b ^{13}C NMR spectrum of compound **4.32** 265
Figure 5.81a ^{1}H NMR spectrum of compound **4.3** 267
Figure 5.81b ^{13}C NMR spectrum of compound **4.3** 267
Figure 5.82a ^{1}H NMR spectrum of compound **4.40** 269
Figure 5.83a ^{1}H NMR spectrum of compound **4.47** 271
Figure 5.84a ^{1}H NMR spectrum of compound **4.50** 274
Figure 5.85a ^{1}H NMR spectrum of compound **4.45** 276
Figure 5.86a ^{1}H NMR spectrum of compound **4.46** 278
Figure 5.87a ^{1}H NMR spectrum of compound **5.14** 281
Figure 5.88a ^{1}H NMR spectrum of compound **5.16** 283
Figure 5.89a ^{1}H NMR spectrum of compound **5.17** 285
Figure 5.90a ^{1}H NMR spectrum of compound **5.18** 287
Figure 5.91a ^{1}H NMR spectrum of compound **5.19** 289
Figure 5.92a ^{1}H NMR spectrum of compound **5.20** 291
Figure 5.93a ^{1}H NMR spectrum of compound **5.22** 294
Figure 5.94a ^{1}H NMR spectrum of compound **5.23** 296
Figure 5.95a ^{1}H NMR spectrum of compound **5.24** 298
Figure 5.96a ^{1}H NMR spectrum of compound **5.25** 300
Figure 5.97a ^{1}H NMR spectrum of compound **5.26** 302
Figure 5.98a ^{1}H NMR spectrum of compound **5.27** 304
Figure 5.99a ^{1}H NMR spectrum of compound **5.28** 306
Figure 5.100a ^{1}H NMR spectrum of compound **5.29** 308
Figure 5.101a ^{1}H NMR spectrum of compound **5.30** 310
Figure 5.102a ^{1}H NMR spectrum of compound **5.31** 312
Figure 5.103a ^{1}H NMR spectrum of compound **5.32** 314
Figure 5.104a ^{1}H NMR spectrum of compound **5.33** 316
Figure 5.105a ^{1}H NMR spectrum of compound **5.34** 318
Figure 5.106a ^{1}H NMR spectrum of compound **5.35** 320
Figure 5.106b ^{13}C NMR spectrum of compound **5.35** 320

Figure 5.107a ^{1}H NMR spectrum of compound **5.36** 322
Figure 5.108a ^{1}H NMR spectrum of compound **5.37** 324
Figure 5.108b ^{13}C NMR spectrum of compound **5.37** 324
Figure 5.109a ^{1}H NMR spectrum of compound **5.38** 326
Figure 5.109b ^{13}C NMR spectrum of compound **5.38** 326
Figure 5.110a ^{1}H NMR spectrum of compound **5.39** 328
Figure 5.110b ^{13}C NMR spectrum of compound **5.39** 328
Figure 5.111a ^{1}H NMR spectrum of compound **5.40** 330
Figure 5.111b ^{13}C NMR spectrum of compound **5.40** 330
Figure 5.112a ^{1}H NMR spectrum of compound **5.41** 332
Figure 5.112b ^{13}C NMR spectrum of compound **5.41** 332
Figure 5.113a ^{1}H NMR spectrum of compound **5.42** 334
Figure 5.113b ^{13}C NMR spectrum of compound **5.42** 334
Figure 5.114a ^{1}H NMR spectrum of compound **5.43** 336
Figure 5.114b ^{13}C NMR spectrum of compound **5.43** 336
Figure 5.115a ^{1}H NMR spectrum of compound **5.44** 338
Figure 5.115b ^{13}C NMR spectrum of compound **5.44** 338
Figure 5.116a ^{1}H NMR spectrum of compound **5.45a** 340
Figure 5.116b ^{13}C NMR spectrum of compound **5.45a** 340
Figure 5.117a ^{1}H NMR spectrum of compound **5.45b** 341
Figure 5.117b ^{13}C NMR spectrum of compound **5.45b** 341
Figure 5.118a ^{1}H NMR spectrum of compound **5.46** 343
Figure 5.118b ^{13}C NMR spectrum of compound **5.46** 343
Figure 5.119a ^{1}H NMR spectrum of compound **1.12** 345
Figure 5.119b ^{13}C NMR spectrum of compound **1.12** 345

LIST OF SCHEMES

CHAPTER 1

Scheme 1.1 Proposed biosynthesis of gliotoxin 24
Scheme 1.2 Proposed oxepine ring formation.....24
Scheme 1.3 Proposed biosynthetic pathway of sirodesmin PL 27

CHAPTER 2

Scheme 2.1 Total synthesis of (±)-sporidesmin A 31
Scheme 2.2 Synthesis of (±)-sporidesmin B 31
Scheme 2.3 Synthesis of (±)-dehydrogliotoxin 32
Scheme 2.4 Synthesis of (+)-gliotoxin 33
Scheme 2.5 Synthesis of (±)-hyalodendrin.....34
Scheme 2.6 Total synthesis of (±)-gliovictin and *epi*-gliovictin 34
Scheme 2.7 Rastetter's total synthesis of (±)-hyalodendrin 35
Scheme 2.8 Biomimetic total synthesis of (+)-11,11'-dideoxyverticillin A 36
Scheme 2.9 Sodeoka's total synthesis of (+)-chaetocin 37
Scheme 2.10 Movassaghi's total synthesis of (+)-chaetocin.....38
Scheme 2.11 Total syntheses of chaetocin C and 12,12'-dideoxychetracin A.....39
Scheme 2.12 Synthesis of (+)-gliocladine C 41
Scheme 2.13 Total synthesis of (+)-gliocladin B 42
Scheme 2.14 Synthesis of (+)-12-deoxybionectin A and (+)-gliocladin B 42
Scheme 2.15 Total synthesis of epicoccin G.....43
Scheme 2.16 Key pyrrolidine synthesis 44
Scheme 2.17 Completion of the total synthesis of (–)-acetylaranotin (**1.35**).....45
Scheme 2.18 Synthesis of (±)-psychotrimine via novel C3-N1' bond formation 46

Scheme 2.19 Total synthesis of kapakahine B 47
Scheme 2.20 Rainier's synthetic C3-N1' bond forming method 47
Scheme 2.21 Total synthesis of kapakahine F.....48
Scheme 2.22 Concise total synthesis of (+)-pestalazine B.....49

CHAPTER 3

Scheme 3.1 Proposed model study for C3-N1' bond formation 52
Scheme 3.2 Attempted iminium ion formation 53
Scheme 3.3 Retrosynthesis of key intermediate **3.8** through a pinacol-type rearrangement 54
Scheme 3.4 Synthesis of 2-alkynyl aniline derivative **3.17**.....54
Scheme 3.5 Synthesis of 2,3-dihydrotryptophan alkyne derivative 55
Scheme 3.6 Witkop's pyrroloindole inspiration.....56
Scheme 3.7 Retrosynthetic plan using pyrroloindoline.....56
Scheme 3.8 Attempted synthesis of 3-bromopyrroloindole 57
Scheme 3.9 Formation of key C-3 quaternary center.....57
Scheme 3.10 Attempted formation of functionalized C3-N bond.....58
Scheme 3.11 Key alkyne synthesis.....58
Scheme 3.12 Larock indole synthesis of tryptophan dimer.....59
Scheme 3.13 Coupling of 3-bromopyrroloindoline.....59
Scheme 3.14 Retrosynthetic analysis of (+)-chetomin.....60
Scheme 3.15 Coupling with more advanced bromopyrroloindoline.....61
Scheme 3.16 Optimized peptide coupling and dioxopiperazine formation.....61
Scheme 3.17 Microwave assisted dioxopiperazine synthesis 62
Scheme 3.18 Attempted coupling with indole.....62
Scheme 3.19 Formation of the disulfide bridge 63
Scheme 3.20 Coupling to 3-bromopyrroloindoline and attempted dioxopiperazine formation.....64
Scheme 3.21 Attempted synthesis of alternate dioxopiperazine precursor.....65
Scheme 3.22 Synthesis of dioxopiperazine **3.77**.....66

Scheme 3.23 Synthesis of (N-Me)$_3$ dioxopiperazine.....67
Scheme 3.24 Attempted protection and deprotection of **3.82** 68
Scheme 3.25 Attempted peptide coupling with N-Me,Boc-Ser(OH).....68
Scheme 3.26 Synthesis of sarcosine-derived dioxopiperazine.....69
Scheme 3.27 Synthesis of (N-Me)$_3$ dioxopiperazine.....69
Scheme 3.28 Attempted epidithiodioxopiperazine formations 70
Scheme 3.29 Key tetraols and iminium intermediates 71
Scheme 3.30 Possible oxidations 72
Scheme 3.31 Alternative sulfenylation.....72
Scheme 3.32 Proposed conversion of **3.91** to chetomin.....73

CHAPTER 4

Scheme 4.1 Retrosynthetic analysis of (–)-sporidesmin A.....77
Scheme 4.2 Nitration of vanillin.....78
Scheme 4.3 Dimethoxyindole synthesis.....79
Scheme 4.4 Synthesis of 5-chloro-dinitrostyrene derivative.....79
Scheme 4.5 Undesired acetal formation.....80
Scheme 4.6 Asymmetric aminohydroxylation 80
Scheme 4.7 Preparation of (DHQD)$_2$AQN.....81
Scheme 4.8 Formation of the dioxopiperazine and an undesired elimination.....81
Scheme 4.9 Preparation of dipeptide.....82
Scheme 4.10 Cyclization to the dioxopiperazine 82
Scheme 4.11 Improved synthesis of dioxopiperazine **4.3** 83
Scheme 4.12 First attempts at oxidative cyclization 84
Scheme 4.13 Model cyclization study.....84
Scheme 4.14 More oxidative cyclization attempts.....85
Scheme 4.15 Progression of cyclization.....86
Scheme 4.16 Attempted cyclization 86
Scheme 4.17 Kishi's final steps in the sporidesmin A synthesis.....87
Scheme 4.18 Preparation of N-Me,Fmoc-Ala-OH 87

Scheme 4.19 Incorporation of *N*-Me-Ala 88
Scheme 4.20 Full panel of oxidation conditions to screen 89
Scheme 4.21 Proposed epidithiodioxopiperazine formation 89

CHAPTER 1

Epidithiodioxopiperazines

1.1: Introduction

Nearly twenty distinct families of epidithiodioxopiperazine fungal metabolites have been characterized since the seminal discovery of gliotoxin in 1936. This unique class of natural products is characterized by a sulfur-bridged dioxopiperazine (**1.1**), a feature generally requisite for the potent biological activity prevalent among the class.[1-5]

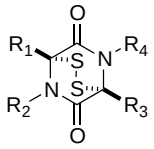

1.1

All natural epidithiodioxopiperazines discovered to date contain at least one aromatic amino acid. Representative molecules from each family to be discussed are shown in **Figure 1.1** (tyrosine- and/or phenylalanine-derived) and **Figure 1.2** (tryptophan-derived). In this chapter, we present an overview of the structures of naturally occurring epidithiodioxopiperazines, relevant physiological properties, and some of the more interesting of the proposed fungal biogeneses.

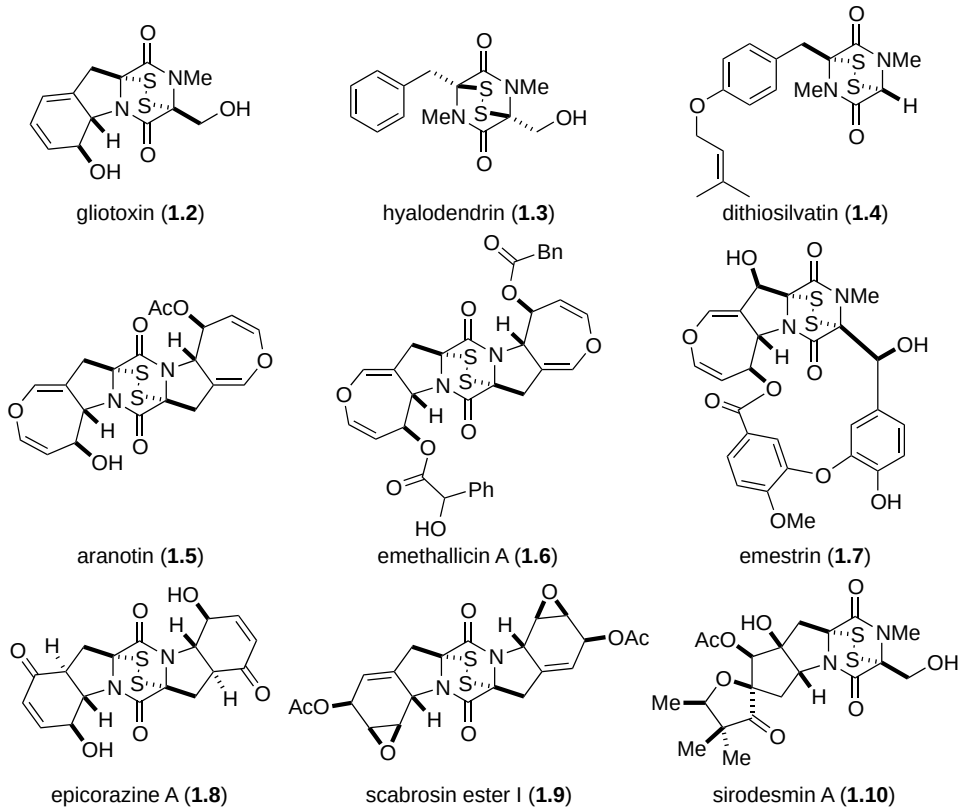

Figure 1.1. Epidithiodioxopiperazines derived from tyrosine and/or phenylalanine.

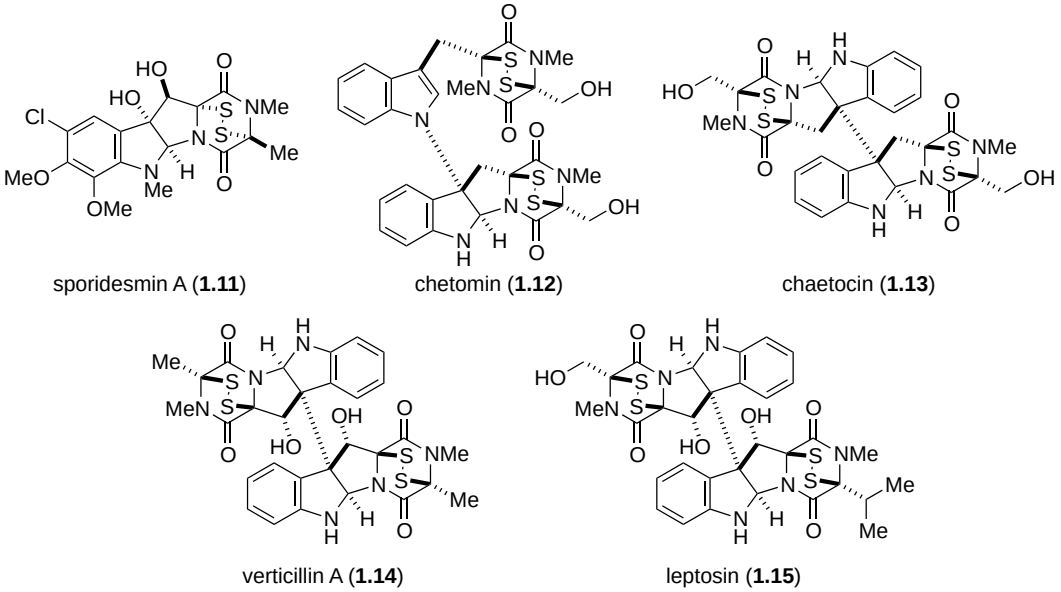

Figure 1.2. Tryptophan-derived epidithiodioxopiperazines.

1.2: Epidithiodioxopiperazines Derived from Phenylalanine or Tyrosine

In 1936, a novel substance with substantial antifungal and antiviral activity was isolated from the wood fungus *Gliocladium fimbriatum* by Weindling and Emerson.[6] A putative structure (**1.16**, **Figure 1.3**) was proposed for the metabolite based on degradation studies. This structure, however, could not account for some experimental observations, leading Johnson and Woodward to propose a revised structure for gliotoxin (**1.2**) in 1958.[7] Absolute stereochemistry was later determined by x-ray analysis.[8] Gliotoxin and related metabolites (**Figure 1.3**) have since been isolated from a variety of fungi—including several *Penicillium* and *Aspergillus* species, *Gliocladium*, *Thermoascus*, and *Candida*—and have been the focus of numerous synthetic and biosynthetic studies that have formed the basis for much of the research discussed herein.[2,3]

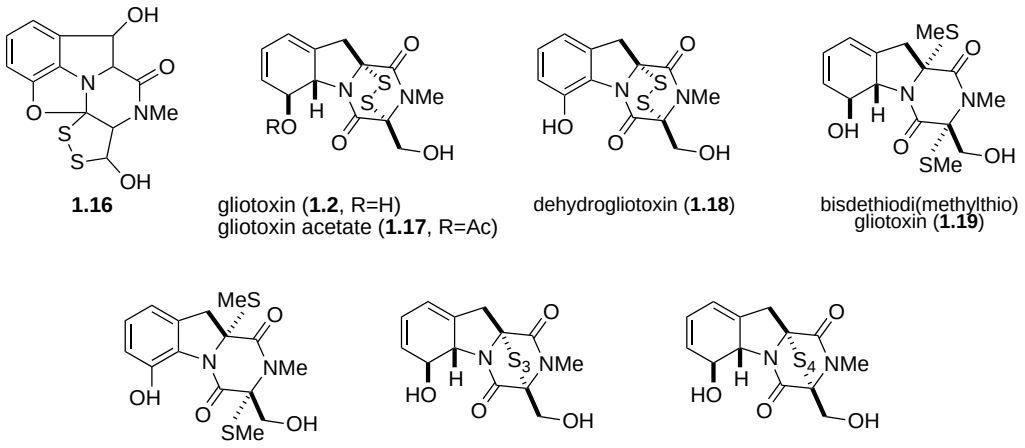

Figure 1.3. Gliotoxins.

The initial interest in the chemotherapeutic potential of gliotoxin as an antifungal or antiviral agent waned as in vivo studies revealed gliotoxin to be generally cytotoxic.[9] Moreover, gliotoxin has been implicated as a virulence factor of *Aspergillus fumigatus*,

the main source of invasive aspergillosis and leading cause of death in immunocompromised patients.[10] However, interest in the molecule was renewed when it was discovered that gliotoxin displayed selective toxicity to cells of the hematopoietic system.[11,12] Specifically, gliotoxin exhibits antiproliferative activity against T and B cells and inhibits phagocytic activity with considerable selectivity toward immune system cells, leading to promising studies that have demonstrated that gliotoxin prevents graft-versus-host disease after bone marrow transplantation.[13]

Generally, the toxicity of gliotoxin and other epidithiodioxopiperazines can be attributed to two mechanisms: generation of reactive oxygen species (**Figure 1.4**) and mixed disulfide formation (**Figure 1.5**). In the presence of a suitable reducing agent such as glutathione or dithiothreitol, epidithiodioxopiperazines are reduced to the corresponding dithiols (**1.23**). Autooxidation back to the disulfide (**1.1**) occurs with the production of superoxide ions and hydrogen peroxide, known to cause oxidative damage to cells.[14,15] Gliotoxin has specifically been shown to induce single- and double-stranded DNA damage in the presence of glutathione, presumably by hydroxyl radicals generated in this redox process.[16]

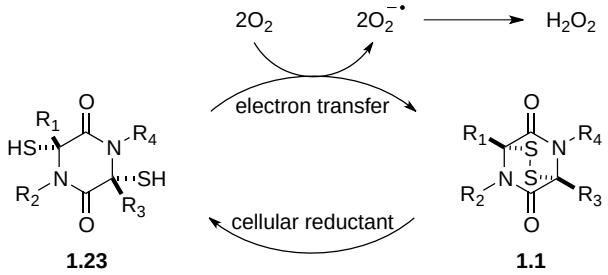

Figure 1.4. Redox cycling of epidithiodioxopiperazines.

Evidence suggests that gliotoxin and other epidithiodioxopiperazines are also capable of forming mixed disulfides with free thiol groups in cells.[17,18] Following

incubation with radiolabelled gliotoxin, cells were shown to contain protein-bound [^{35}S]-gliotoxin (**1.24**).[3] This result could be reversed if cells were treated with both gliotoxin and excess reducing agent (dithiothreitol), suggesting a covalent interaction. Moreover, the antiviral activity of gliotoxin is lost in the presence of excess dithiothreitol. This evidence supports a mechanism of toxicity resulting from mixed disulfide formation between gliotoxin and protein.[19]

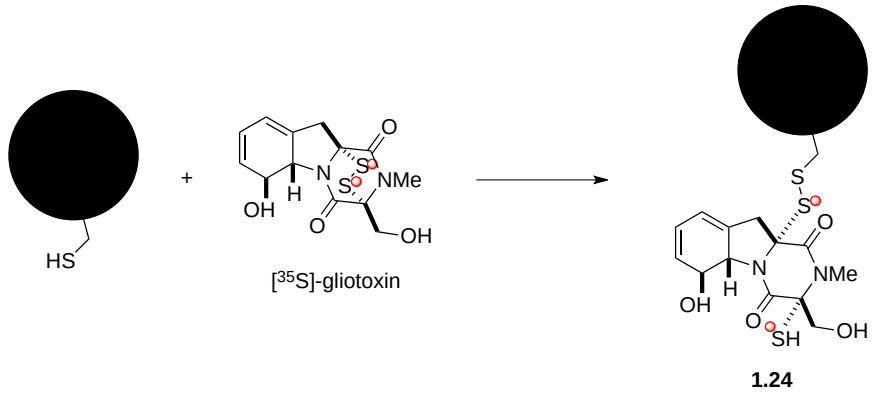

Figure 1.5. Mixed disulfide formation.

Toxicity of epidithiodioxopiperazines would seem to rely on an intact disulfide ring or the reduced dithiol. Indeed, dethiogliotoxin lacks the antibacterial activity of gliotoxin. Reduction and methylation of the disulfide bridge (bisdethiodi(methylthio)gliotoxin, **1.19**) also results in a loss of antiviral activity.[4,20] Not surprisingly, the simple disulfide **1.25** and dithiol **1.26** exhibit potent biological activity, highlighting the importance of the fragment to the observed toxicity of epidithiodioxopiperazines.[21] The great structural diversity in epidithiodioxopiperazines may have evolved only to mask the core disulfide moiety to prevent degradation by target organisms, rather than to impart any sort of selectivity or increased toxicity.[2]

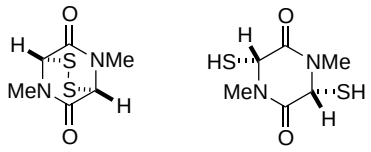

Figure 1.6. Simple biologically active epidithiodioxopiperazines.

Like gliotoxin, the hyalodendrins (**Figure 1.7**) are derived naturally from phenylalanine and serine. Hyalodendrin (**1.3**) was originally isolated by Strunz in 1974 from *Hyalodendron sp.*[22] The same fungus was later shown to produce the bis(methylthio) derivative (**1.29**)[23] and epitetrasulfide **1.28**.[24] Epitrithiohyalodendrin (**1.27**) has only been observed as a product of the unidentified fungus NRRL 3888, along with **1.3** and **1.29**.[25] Not surprisingly, hyalodendrin and the epitri- and epitetrasulfide derivatives exhibit antibacterial activity, while the bisdethiodi(methylthio) analogue is inactive against fungi and bacteria and relatively non-toxic to mice.[22-25] Interestingly, it was observed that hyalodendrin could be converted to epitetrasulfide **1.28** in the presence of HCl with heating in methanol and the culture medium. *Racemic* tetrasulfide was isolated when HCl was omitted from the same conditions.

Enantiomers of the hyalodendrins (except for epitrisulfide **1.27**) have been isolated from both terrestrial and marine sources. Gliovictin (**1.32**) was first isolated from *Helminthosporium victoriae* in 1974,[26] the same year that researchers at Eli Lilly reported the isolation of the same structure (named A26771E) along with the disulfide (A26771A, **1.30**) and epitetrasulfide (A26771C, **1.31**) from *Penicillium turbatum*.[27] Fenical has also isolated gliovictin from the marine deuteromycete *Asteromyces cruciatus*.[28] Predictably, **1.30** and **1.31** both showed antiviral and antibacterial activity, while gliovictin–lacking sulfur atoms capable of redox cycling or mixed disulfide formation–was inactive.[27]

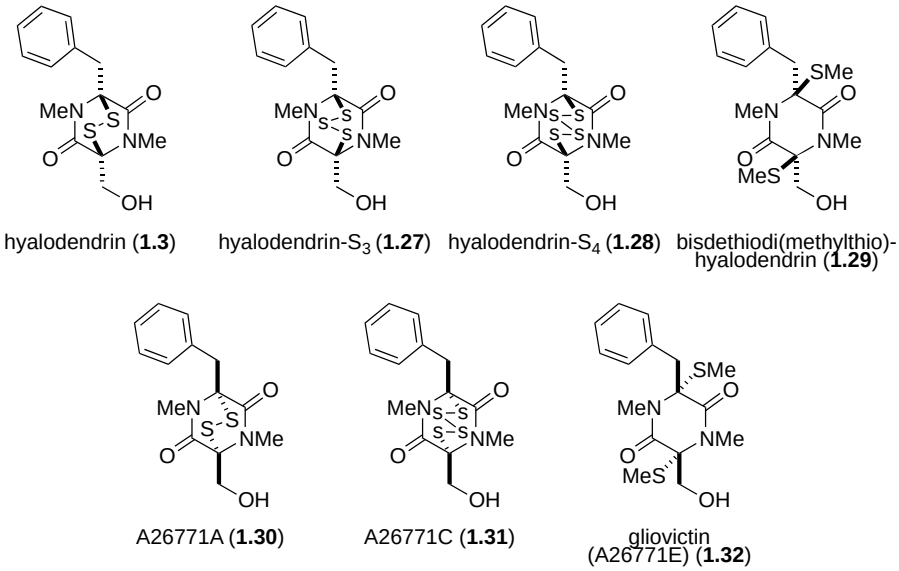

Figure 1.7. Hyalodendrins and related compounds.

Kawahara and coworkers reported the isolation of dithiosilvatin (**1.4**) and silvathione (**1.33**) in 1987 from *Apergillus silvaticus* (**Figure 1.8**).[29] Dioxopiperazinethiones such as **1.33** are rare and are possible intermediates in the formation of trioxopiperazines from epidithiodioxopiperazines. The authors reported the conversion of **1.4** to the bisdethiodi(methylthio) derivative (**1.34**) by reductive methylation ($NaBH_4$, MeI), a compound previously isolated by Hanson and O'Leary from *Gliocladium deliquescens*.[30]

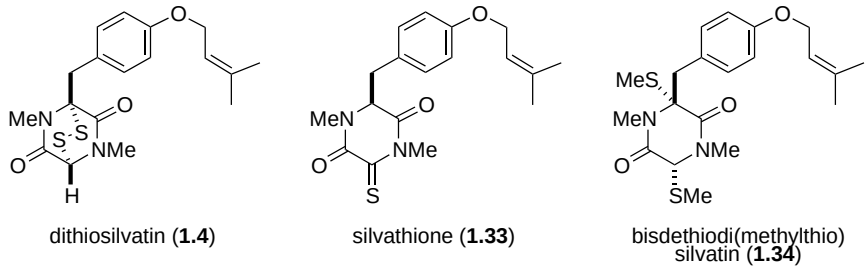

Figure 1.8. Silvatins.

The next subgroup of epidithiodioxopiperazines to be discussed is characterized by the presence of at least one seven-membered dihydrooxepine ring, and includes the

aranotins (**Figure 1.9**), emethallicins (**Figure 1.10**), and emestrins (**Figure 1.11**). Aranotin (**1.5**) and acetylaranotin (**1.35**) have been isolated from *Arachniotus aureus* and *Aspergillus terreus* and exhibit antiviral activity that is apparently selective for RNA viruses such as the polio, Coxsackie (A21), rhino-, and parainfluenza viruses through inhibition of viral RNA synthesis.[31-37] Structurally, the aranotins are related to gliotoxin, with the similarities most evident in apoaranotin (**1.37**). Apoaranotin can be considered a chimera of gliotoxin and aranotin, containing the cyclohexadienol of gliotoxin and the dihydrooxepine ring of aranotin. Asteroxepin (**1.39**) was the first monooxepine derivative to be isolated and is further unique in that it contains one unsubstituted amide. This dioxopiperazine may provide evidence for the sequence of steps in the biosynthesis of the more complex aranotins.

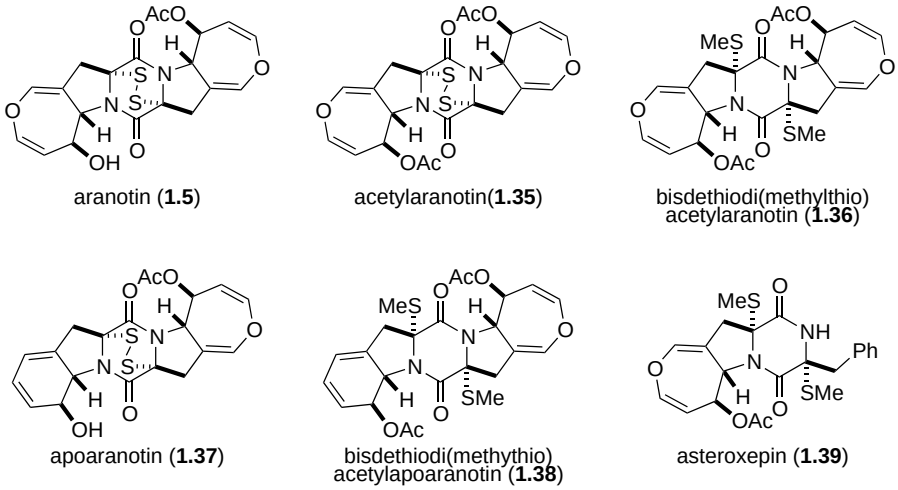

Figure 1.9. Aranotins.

Closely related to the aranotins are the emethallicins (**Figure 1.10**). Both families share the same absolute stereochemistry, and emethallicin A (**1.6**) differs apoaranotin (**1.37**) only in the ester moieties. This observation was experimentally confirmed by hydrolysis of **1.6** followed by acetylation to afford compound **1.37**, identical to naturally

occurring apoaranotin.[38] Emethallicins B, D, and F (**1.40**, **1.42**, and **1.44**) share this same monooxepine core and differ apoaranotin only in ester substitution and sulfur content of the epipolythiodioxopiperazine ring. Emethallicin C (**1.41**) is symmetrical and the only emethallicin to contain two dihydrooxepine rings, more closely resembling aranotin and acetylaranotin.

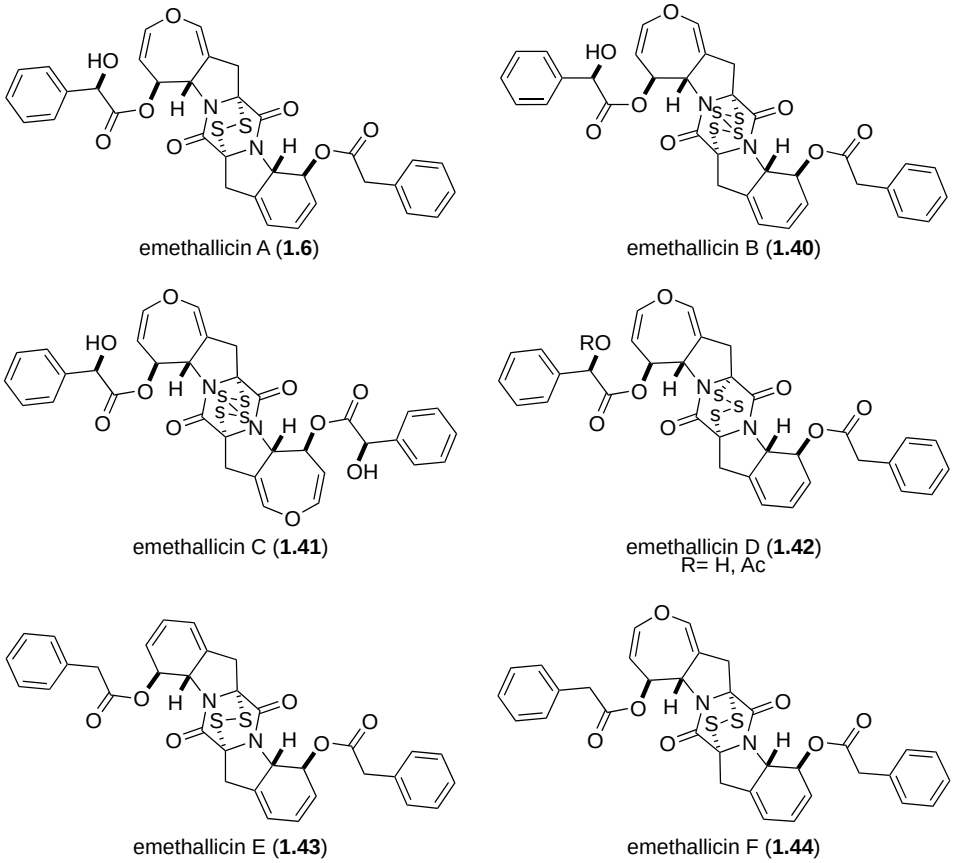

Figure 1.10. Emethallicins.

Emethallicin A (**1.6**) was first isolated from *Emericella heterothallica* in 1989 by Kawai and coworkers, who later reported the isolation of emethallicins B-F (**1.40**-**1.44**) from the same fungus.[38-41] Interestingly, Kawai was unable to convert synthetic emethallicin D monoacetate (**1.42**, R=Ac) to the naturally occurring metabolite (**1.42**, R=H). Basic hydrolytic conditions only succeeded at forming the disulfide and

tetrasulfide monoacetates of **1.6** and **1.40**, respectively.[39] This disproportionation of the trisulfide is similar to a result obtained by Waring and coworkers, who similarly converted trisulfide gliotoxin E (**1.21**) to the disulfide, gliotoxin (**1.2**), and the tetrasulfide, gliotoxin G (**1.22**).[42]

All of the emethallicins exhibit fairly strong inhibitory activities upon histamine release from mast cells, with IC_{50} values ranging from 1.0×10^{-6} to 2.0×10^{-8} M. Generally, activity is stronger for the original emethallicins than for the acetate derivatives. Micromolar inhibition of 5-lipoxygenase has also been reported.[43]

The final class of known epipolythiodioxopiperazine metabolites known to contain at least one dihydrooxepine ring is the macrocyclic emestrins (**Figure 1.11**). Emestrin (**1.7**) was isolated in 1985 from the fungus *Emericella striata*, and later from *E. quadrilineata*, *E. foveolata*, *E. acristata*, and *E. parvathecia*.[44-46] Trisulfide emestrin B (**1.45**), piperazinethione aurantioemestrin (**1.47**), and trioxopiperazine dethiosecoemestrin (**1.48**) were later isolated from *E. striata*.[46-49] It has been postulated that the latter two compounds are derived biosynthetically from emestrin. Emestrin displays potent antifungal and antibacterial activity, but is also very toxic to mammals.

Recently, Kanda and coworkers reported the isolation of MPC1001 (**1.46**) and its analogues (not shown) from *Cladorrhinum* sp. KY4922, contributing eight new members to the emestrin family of natural products.[50] MPC1001 contains a methoxy group rather than the free phenol found in emestrin, but is otherwise structurally and stereochemically identical. MPC1001 and its epipolysulfide analogues all showed antiproliferative activity in the DU145 human prostate cancer cell line.[50]

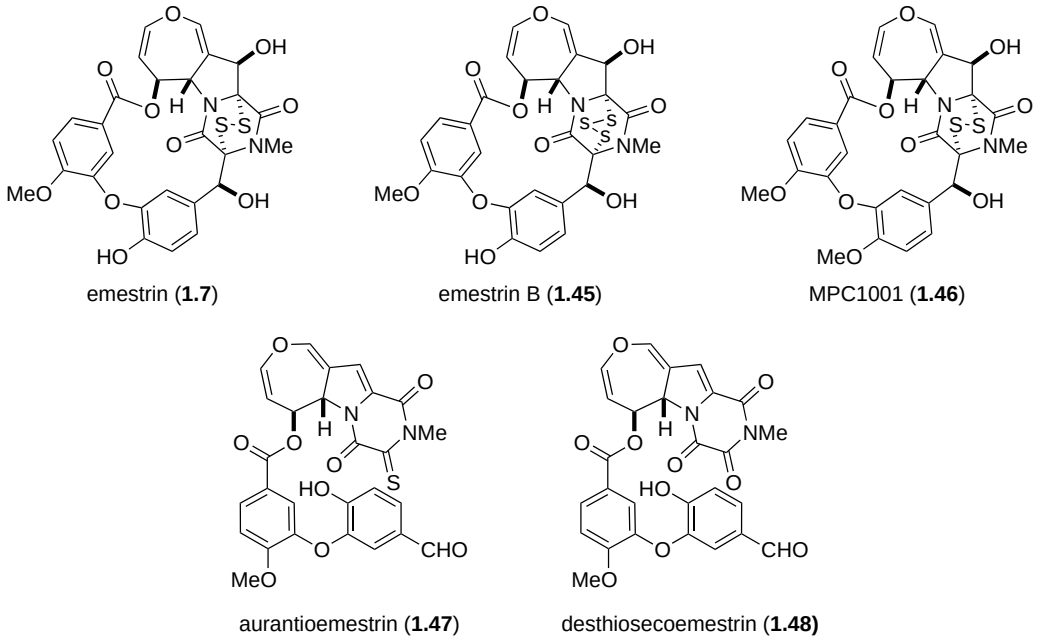

Figure 1.11. Emestrins and related metabolites.

Epicorazines (**Figure 1.12**) have been isolated from several organisms, including *Epicoccum nigrum* (epicorazine A and B, **1.8** and **1.49**),[51-53] *E. purpurascens* (epicorazine B),[54] and *Stereum hirsutum* (epicorazine C, **1.50**).[55] The only difference between **1.8** and **1.49** is the absolute stereochemistry at C6. This cis configuration is shared between **1.49** and **1.50**.

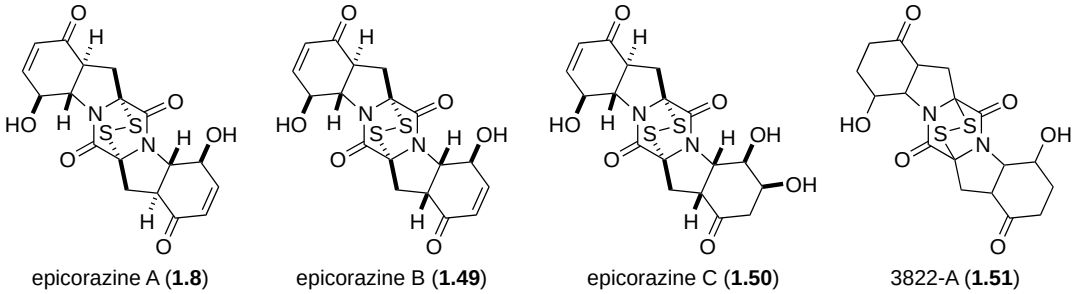

Figure 1.12. Epicorazines.

Epicorazine A, B, and C display only marginal activity against Gram-positive bacteria, including methicillin-resistant *Staphylococcus aureus* (MRSA) and vancomycin-resistant *Enterococcus faecalis* (VRE), and are inactive against Gram-

negative organisms. All three exhibit antiproliferative effects against L929 mouse fibroblast cells and K562 human leukemia cells, as well as cytotoxicity toward the HeLa human cervical carcinoma cell line.[55]

The scabrosin esters were originally isolated from the lichen *Xanthoparmelia scabrosa* in 1978, but it was not until 1999 that the correct structures were determined (**Figure 1.13**).[56,57] The isolation of these compounds was of particular interest, as this report marked the first epidithiodioxopiperazine to be isolated from lichenized fungi. Submicromolar activity, similar to that of gliotoxin (**1.2**), was observed for the scabrosins against the murine P815 mastocytomia cell line, as well as low nanomolar activity in MCF7 human breast carcinoma cell line. Scabrosin esters have also been shown to induce apoptosis concomitantly with a large increase in mitochondrial membrane potential and significant decrease in total cellular ATP. Mitochondrial ATP synthase is the proposed cellular target of the scabrosins.[58]

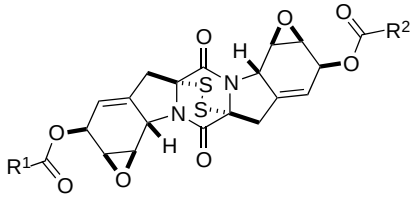

scabrosin ester 1 (R^1=CH_3, R^2=CH_3, **1.9**)
scabrosin ester 2 (R^1=CH_3, R^2=C_3H_7, **1.52**)
scabrosin ester 3 (R^1=C_3H_7, R^2=C_3H_7, **1.53**)
scabrosin ester 4 (R^1=CH_3, R^2=C_5H_{11}, **1.54**)
scabrosin ester 5 (R^1=C_3H_7, R^2=C_5H_{11}, **1.55**)

Figure 1.13. Scabrosin esters.

The sirodesmins (**Figure 1.14**) were first discovered in 1977 as metabolites of *Sirodesmium diversum*[59] and later from the unrelated fungus *Phoma lingam*.[60] Sirodesmins A-H (**1.10**, **1.56**-**1.60**) are characterized by a spirofused tetrahydrofuran cyclopentylpyrrolidine skeleton. Sirodesmins A-C are epimers of G and H at the spirocenter. Notably, sirodesmin H was the first example of a naturally occurring monosulfide.

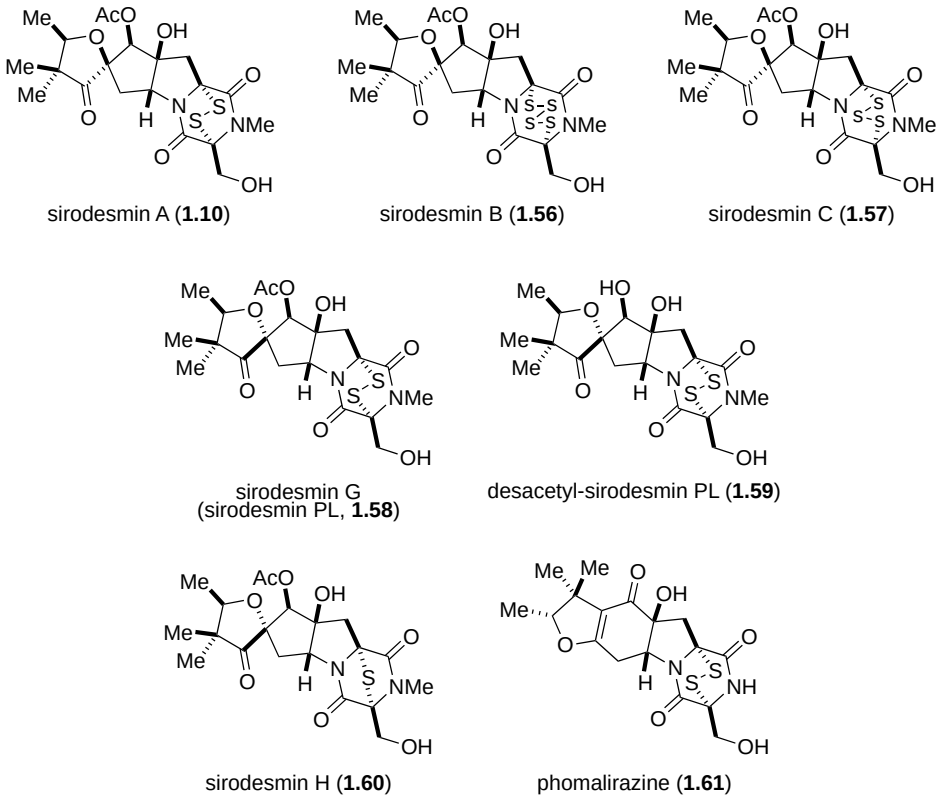

Figure 1.14. Sirodesmins.

Sirodesmins are potent antiviral agents, particularly against the rhinovirus.[59] Sirodesmin G (originally named sirodesmin PL, **1.58**) has specifically been shown to exhibit activity against Gram-positive bacteria,[61] although it has also been implicated as the causative agent of blackleg disease in canola crops (along with phomalirazine, **1.61**). Metabolites **1.58** and **1.61** have both been isolated from the ascomycetous fungus *Leptosphaeria maculans*, the organism known to be responsible for blackleg disease.[62]

1.3: Tryptophan–Derived Epidithiodioxopiperazines

The remaining epidithiodioxopiperazine alkaloids to be discussed are all derived from tryptophan (**Figure 1.2**). Of this subset, the sporidesmins (**Figure 1.15**) are the most densely functionalized and the only members to contain a substituted aromatic ring.

Sporidesmin was discovered by researchers investigating the source of the disease facial eczema that plagued sheep in New Zealand and Australia. The disease caused extensive liver damage in infected sheep and ultimately resulted in death. Thornton and Percival eventually established that ingestion of pasture grasses on which the fungus *Pithomyces chartarum* (previously known as *Sporidesmium bakeri*) was growing was the cause of the serious disease.[63,64] Sporidesmin (**1.11**) was isolated and implicated as the main toxic agent produced by *P. chartarum*.[65] The structure and absolute configuration were subsequently determined by crystallographic means.[8,66,67]

As an interesting aside, veterinarians discovered that zinc sulfate doses gave sheep protection from the effects of sporidesmin.[68] Transition metals such as zinc are now known to inhibit generation of the superoxide anion radical, with epidithiodioxopiperazines shown to form a 2:1 complex with zinc ion.[69,70]

Extensive amounts of research have focused on the sporidesmins, producing the complete characterization of all nine derivatives (**1.11**, **1.62**-**1.69**). All contain a densely functionalized, tryptophan–derived pyrroloindoline core coupled to an alanine residue. Sporidesmin C (**1.63**)[71] is the most unusual, containing a novel trisulfide [4.3.3] ring system.

A great deal of chemistry applicable to most of the epipolythiodioxopiperazines was discovered through investigations of the sporidesmins. For example, the trisulfide sporidesmin E (**1.65**) is readily converted to the disulfide (**1.11**) upon treatment with triphenyl phosphine. Alternatively, di- and trisulfides can be converted to tetrasulfides, achieved using hydrogen polysulfide or dihydrogen disulfide. This was demonstrated by the conversion of sporidesmins A (**1.11**) and E (**1.65**) into sporidesmin G (**1.67**).

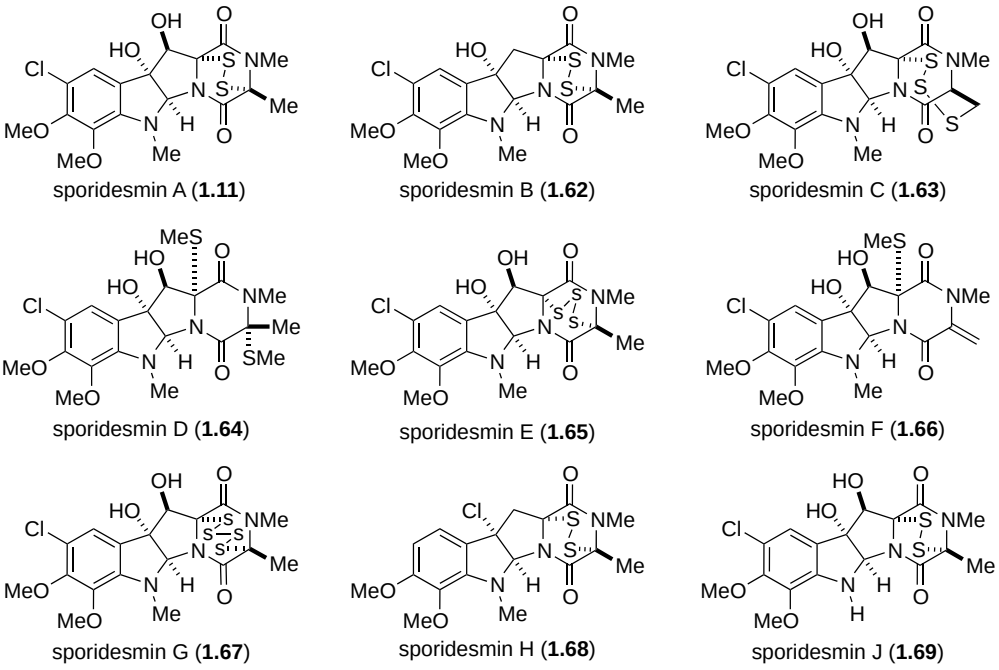

Figure 1.15. Sporidesmins.

In 1944, Waksman and Bugie reported the isolation of a new antibiotic metabolite of the fungus *Chaetomium cochliodes* that they named chetomin.[72] It was not until 30 years later that Walter and coworkers determined the structure of chetomin (**1.12**), revealing a nearly dimeric core likely formed from two molecules each of tryptophan and serine.[73] The two fragments are joined by a bond between the β-pyrrolidinoindoline carbon and the indole nitrogen, a common feature of all five chaetocins (**Figure 1.16**).[74] Chetomin is the only molecule in the family to contain a disulfide bridge within both dioxopiperazine rings. Dethio-tetra(methylthio)chetomin (**1.70**) and chaetocochin C (**1.73**) differ only in the oxidation state of the sulfurs, while chaetocochins A (**1.71**) and B (**1.72**) are macrocyclic analogues of **1.70** and **1.73**, each containing a novel 14-membered ring.

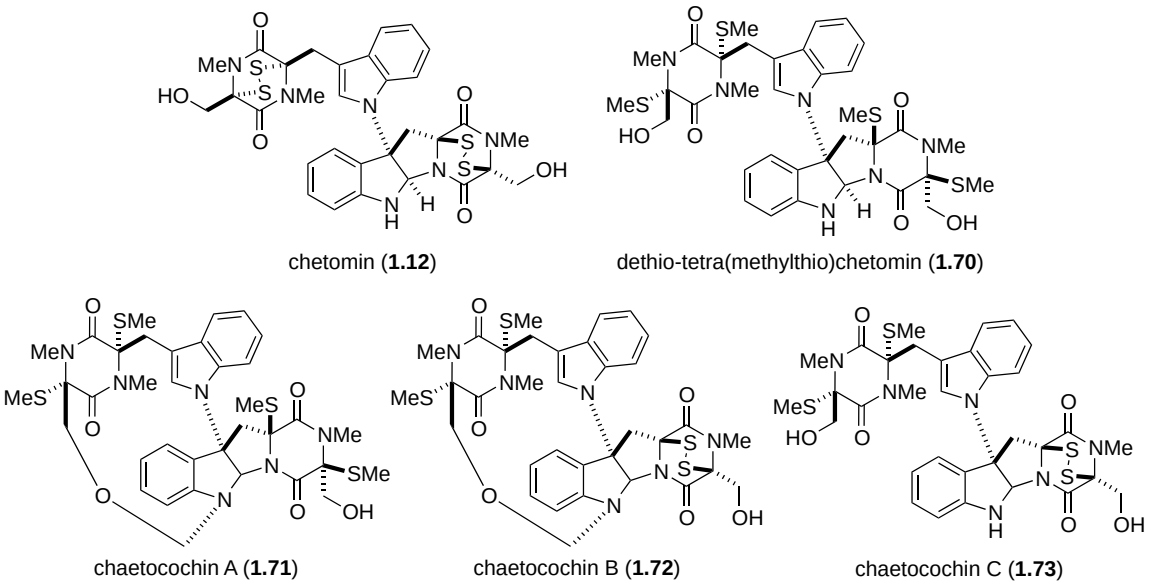

Figure 1.16. Metabolites of the fungus *Chaetomium cochliodes*.

Chetomin was recently isolated from *Chaetomium seminudum* by Fujimoto and coworkers in 2004, along with three new metabolites named the chetoseminudins (**Figure 1.17**).[75] Chetoseminudin A (**1.74**) is merely the pentasulfide homolog of chetomin. From a biosynthetic viewpoint, the more interesting discoveries are chetoseminudins B-D (**1.75**-**1.77**), monomeric bisdethiodi(methylthio) structures that potentially provide insight as to the biosynthetic sequence that produces chetomin, the chaetocochins, and other related epipolythiodioxopiperazines derived from tryptophan and serine.

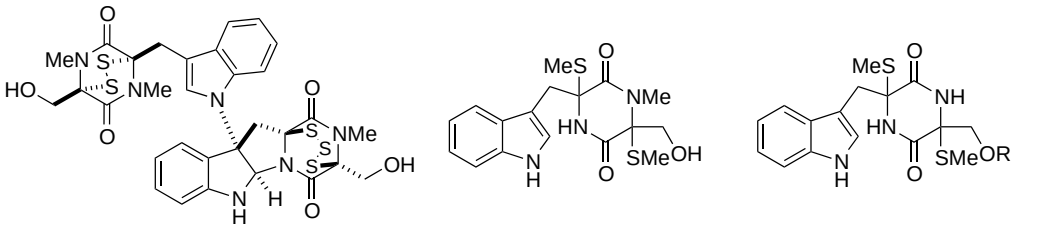

Figure 1.17. Chetoseminudins.

Chetomin (**1.12**) has an unprecedented mechanism of action as a cancer chemotherapeutic agent. Solid tumors must adapt to oxygen deprivation through

induction of the heterodimeric transcription factor hypoxia-inducible factor 1 (HIF-1) in order to survive. Overexpression of HIF-1 is associated with radioresistance in tumors, increased risk of metastasis, and a poor prognosis for patients.[76-78] In normal cells, the α-subunit of HIF-1 (HIF-1α) is hydroxylated and degraded by vHL proteosome (**Figure 1.18**). As oxygen levels decrease and become the rate-limiting reagent in the hydroxylation reaction, HIF-1α accumulates and binds to transcriptional coactivators p300 and CREB binding protein (CBP). Consequent to this binding is the transcription of proteins requisite to the survival of hypoxic cancer cells, facilitating tumor growth and progression.[79]

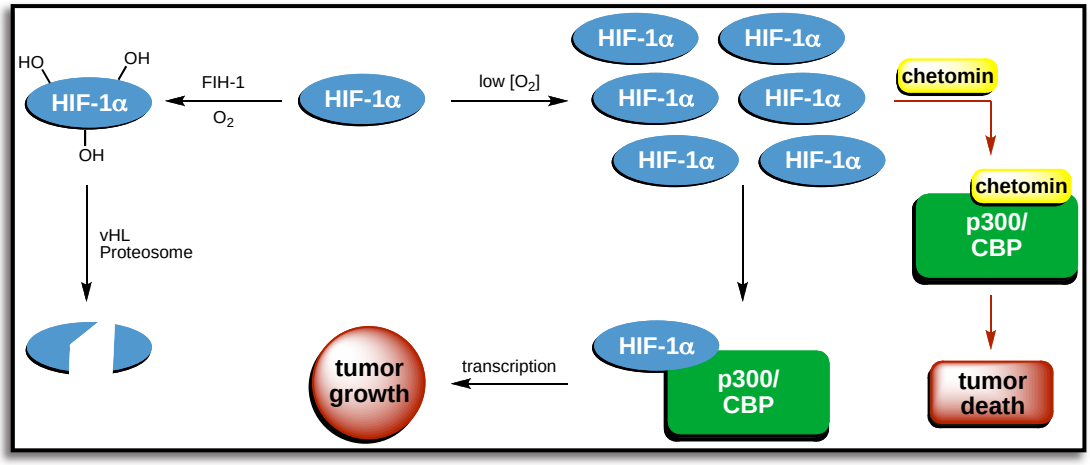

Figure 1.18. HIF-1 hypoxia response pathway.

Chetomin has been shown to inhibit the interaction between HIF-1 and p300 both *in vitro* and in cells, despite extensive surface interactions between the two proteins. Specifically, Kung and coworkers have shown that chetomin disrupts the tertiary structure of p300, inhibiting the transcriptional activity of HIF-1.[76] No other small molecule has been identified to mediate an antitumor response through this mechanism of action. More recently, Hilton and coworkers proposed that chetomin and other

epidithiodioxopiperazines bind zinc at the CH1 domain of p300, ultimately resulting in ejection of a stable zinc–epidithiodioxopiperazine complex. Loss of zinc from the CH1 domain causes the previously observed disruption of the p300 tertiary structure.[1,80]

Chaetocin A (**1.13**, **Figure 1.19**) is a dimeric epidithiodioxopiperazine also derived from two molecules each of tryptophan and serine. It was isolated from *Chaetomium minutum* in 1970.[81,82] Fifteen years passed before the penta- and hexasulfide homologs chaetocin B and C (**1.78** and **1.79**) were isolated from *Chaetomium* spp., along with the novel tetrasulfide chetracin A (**1.80**).[83] In 2012, several related metabolites were isolated from *Oidiodendron truncatum*, including the tetra-, penta- and hexasulfide homologs melinacidin IV, chetracins B and C (**1.82**, **1.83**, and **1.84**), and the dethiotetra(methylthio) derivative chetracin D (**1.81**).[84]

The three chaetocin metabolites (and likely the chetracins) can be interconverted through either desulfurization of **1.78** and **1.79** with triphenyl phosphine to generate chaetocin (**1.13**), or by sulfurization of chaetocin with phosphorus pentasulfide in carbon disulfide to afford a mixture of chaetocins B and C.[83]

Recently, chaetocin A was identified as the first known inhibitor of lysine-specific histone methyltransferases.[85] Histone methylation is an important process in controlling gene expression patterns, especially during cellular differentiation and embryonic development. The activity of histone methyltransferases is disregulated in some tumors, making chaetocin an attractive tool for the study of the molecular mechanism of histone methylation.[85] Additionally, melinacidin IV and chetracin B display nanomolar (3 – 54 nM) activity against five human cancer cell lines (HCT-8, Bel-7402, BGC-823, A549, and A2780).[84]

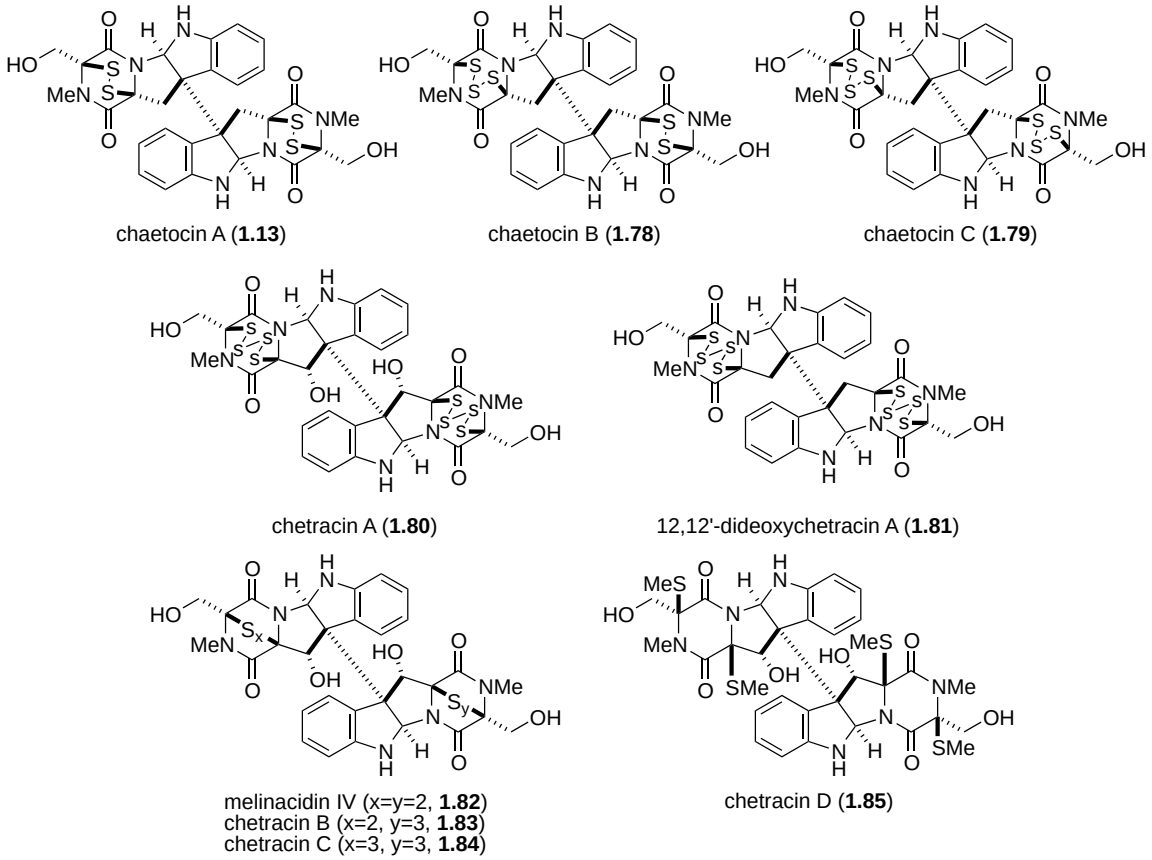

Figure 1.19. Chaetocins and related metabolites.

Several metabolites related to the chaetocins have recently been reported, possessing a C3-C3' linkage to indole rather than the additional monomer found in the chaetocins (**Figure 1.20**). T988 A, B, and C (**1.86**-**1.88**) were originally isolated from *Tilachlidium* sp., although recently it was shown that *Oidiodendron truncatum* also produces the same metabolites, in addition to oidioperazine A (**1.89**) and the chetracins (**1.83**-**1.85**).[75,86] Chetoseminudin C (**1.76**) was also isolated from *O. truncatum*, suggesting that it may be a common intermediate to all of the tryptophan- and serine-derived epipolythiodioxopiperazines discussed thus far. T988 A and B are cytotoxic to P388 leukemia cells.[86]

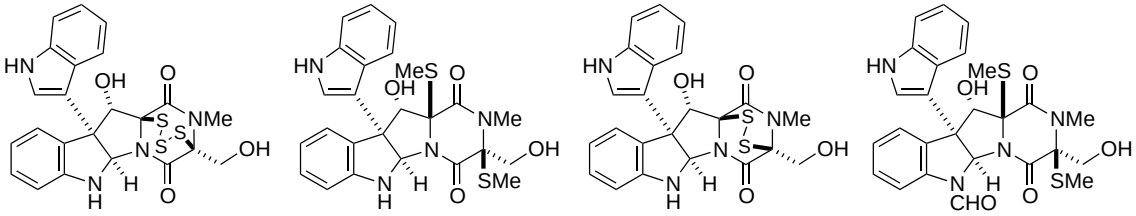

Figure 1.20. Fungal metabolites related to the chaetocins.

Verticillin A (**1.14**, **Figure 1.21**) is quite similar to chaetocin A (**1.13**), derived from two molecules of alanine rather than serine. Only verticillins A, D and E (**1.14**, **1.92** and **1.93**) are symmetrical, while the two tryptophan residues of the remaining verticillins are coupled to different amino acids on the two halves (either alanine, serine, or tyrosine). Verticillin B (**1.90**), for instance, contains alanine and serine residues on the northern and southern halves of the molecule, respectively. Verticillins A-C were isolated from *Verticillium* sp., while the remaining compounds in **Figure 1.21** are produced by *Gliocladium* sp.[87-89]

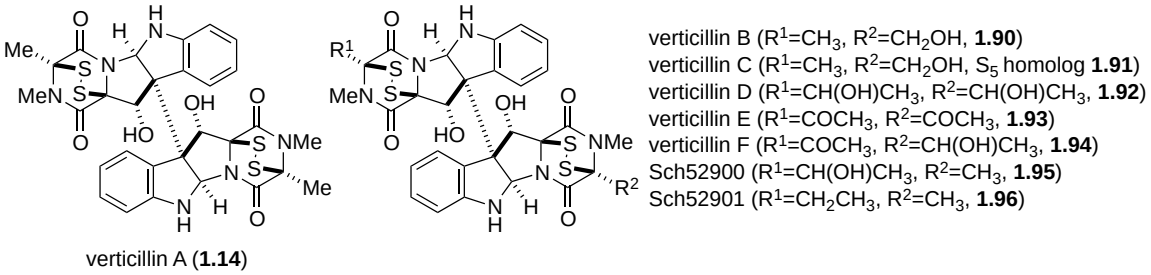

Figure 1.21. Verticillin A and related metabolites.

Gliocladines A-E (**Figure 1.22**, **1.97**-**1.101**) were isolated in 2005 from *Gliocladium roseum*, along with verticillin A, Sch52900, and Sch52901 (**1.14**, **1.95**, and **1.96**).[90] Gliocaldines A and B are simply the penta- and hexasulfide homologs of verticillin A, thus it is not surprising that the same organism produces all three compounds. The structures of gliocladines C and D (**1.99** and **1.100**) should also look

familiar, as they are the alanine derivatives of T988 A and C (**Figure 1.20**). *Bionectra byssicola* F120 has also been shown to produce bionectins A and B (**1.102**, **1.103**), the glycine and tyrosine derivatives of T988C.[91]

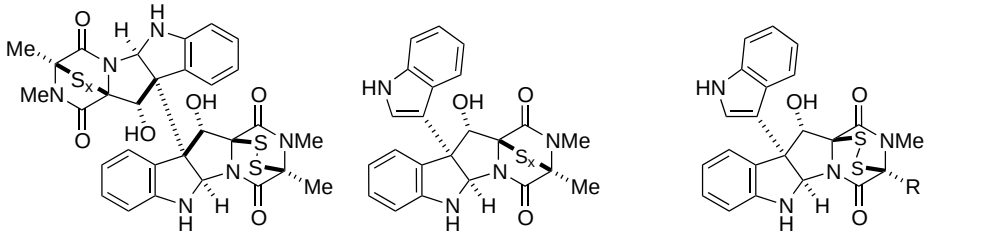

Figure 1.22. Verticillin-type epipolythiodioxopiperazines.

The dimeric subset of epipolythiodioxopiperazines increased greatly in number with the discovery of the leptosins (**Figure 1.23**) from a strain of *Leptosphaeria* sp. attached to the marine alga *Sargassum tortile*.[92-94] Leptosins A-K (**1.104**-**1.118**) all contain at least one valine residue, a feature unique among all epipolythiodioxopiperazines to this family. Leptosins A-C, G, H, and K (**1.104**-**1.113**) share the 12,12'-dihydroxylated, octacyclic core of the verticillins, gliocladines, and chetracins. The C3-C3' linkage to indole is once again produced in leptosins D-F (**1.114**-**1.116**), the valine derivatives of the T988s, gliocladines C-E, and the bionectins. In 1994, two remarkable additions to this family were discovered, the epimers leptosin I and J (**1.117** and **1.118**).[94] These two compounds are characterized by a C12-C11' ether linkage, introducing an additional ring to the structure that prohibits the possibility of topoisomers. Leptosins are generally toxic to P388 leukemia cells.

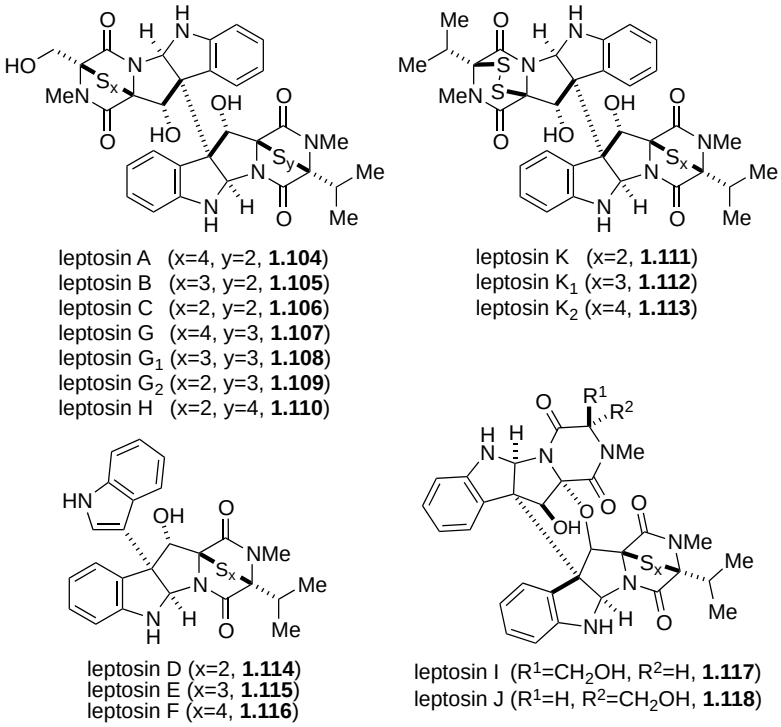

Figure 1.23. Leptosins.

In summary, over 100 epipolythiodioxopiperazine alkaloids have been isolated and characterized to date. While this was intended to be a comprehensive review of all known members of this class of natural products, some were undoubtedly and inadvertently omitted. One cannot help but marvel at the remarkable biological activity of the class as a whole, although it is unlikely that any epipolythiodioxopiperazine will ever achieve therapeutic utility in the clinic due to the general cytotoxicity inherent in the disulfide through mechanisms discussed above. Certainly others have and will continue to argue otherwise, but it is our opinion that the true contribution to medicine will be realized by employing epipolythiodioxopiperazines as tools for the study of novel biological pathways. To date, the natural products chetomin (**1.12**), gliotoxin (**1.2**), and chaetocin A (**1.13**) have already contributed to our understanding of the respective biological targets of the molecules.

Many of the families (particularly those containing a C3-C3' indoline linkage) share a great deal of structural similarity beyond the epipolythiodioxopiperazine moiety that defines the class. It is likely that hundreds of additional variants exist in nature and have yet to be discovered. While numerous biosynthetic studies have been conducted, we still have only a limited understanding of the ease with which nature is able to assemble epipolythiodioxopiperazines, molecules that have for over fifty years taunted synthetic chemists. In the last section of this chapter, we present the notable biosynthetic discoveries reported to date.

1.4: Biosynthetic Investigations of Epidithiodioxopiperazines

Researchers have investigated the biosynthesis of gliotoxin (**1.2**) for nearly forty-five years, but still very little experimental evidence exists to support the numerous proposals. In 1958 and 1960, Suhadolnik reported the only undisputed incorporation study, demonstrating that *Trichoderma viride* incorporates isotopically labeled phenylalanine (**1.119**) and serine (**1.120**) into gliotoxin (**Scheme 1.1**).[95,96] Walsh recently implicated the nonribosomal peptide synthetase GliP in the catalysis of the peptide coupling and dioxopiperazine cyclization reactions.[97] Some debate has occurred as to whether cyclo-Phe-Ser (**1.121**) is a biosynthetic intermediate to gliotoxin. Although doubly labeled **1.121** is incorporated into gliotoxin by *T. viride*, the fungus *Penicillium terlikowskii* poorly incorporates the same compound.[98-100] Walsh observed that release of the dioxopiperazine from the enzyme is slow, allowing for some speculation that further transformations may occur to the enzyme bound compound prior to release.

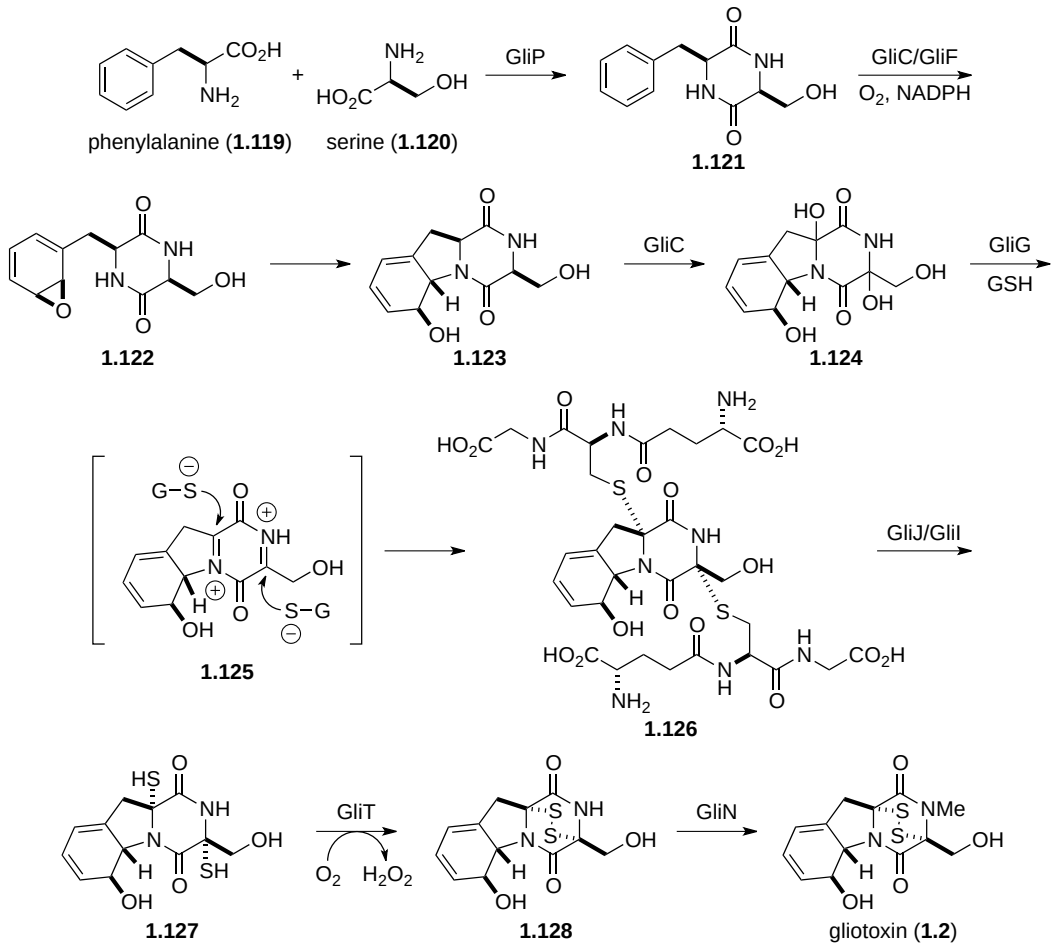

Scheme 1.1. Proposed biosynthesis of gliotoxin.

Arene oxide **1.122** was proposed as a biosynthetic intermediate to both the gliotoxins and aranotins by Neuss in 1968. Cyclization at the ortho position provides the tricyclic core of gliotoxin (**1.123**), whereas a ring enlarging tautomerization of the arene oxide could give the oxepine ring (**1.129**) characteristic of the aranotins (**Scheme 1.2**).[33,34]

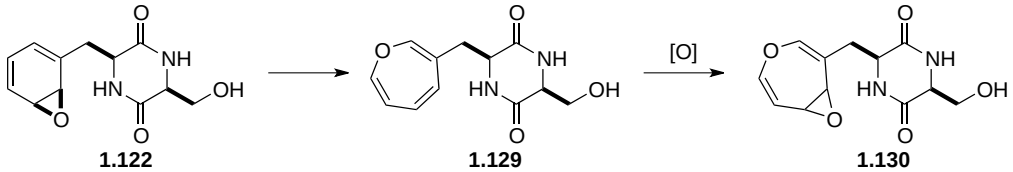

Scheme 1.2. Proposed oxepine ring formation.

The incorporation of sulfur into epidithiodioxopiperazines was until recently poorly understood. Sulfur transfer readily occurs among various potential donors, including methionine, cysteine, and sodium sulfate, complicating [^{35}S] feeding studies.[2,101] In 2011, two groups independently provided evidence supporting a GliC–mediated bishydroxylation of a dioxopiperazine (i.e. **1.123** to **1.124**).[102,103] Elimination of water to generate diiminium **1.125** could be followed by nucleophilic attack of the cysteine thiolate residues of two glutathione (GSH) molecules, catalyzed by the specialized glutathione *S*-transferase GliG.[102-104] Sequential GliJ peptidase and GliI thioesterase activity is proposed to reveal the free dithiol.[102] Scharf and coworkers have unequivocally shown that GliT catalyzes the oxidation to the disulfide (i.e. **1.128**), leaving *N*-methylation to complete the biosynthesis of gliotoxin.[105] The order of tailoring events is up for debate, but recent advances in genomics and proteomics tools to study and manipulate secondary metabolite production will certainly produce much more accurate insight as to the formation of gliotoxin in nature.

Recall that the toxicity of epidithiodioxopiperazines generally arises from redox cycling or mixed disulfide formation (**Figures 1.4** and **1.5**). How is it then that producing fungi, such as *Aspergillus fumigatus*, are immune to toxicity inherent in the structure of gliotoxin? Several studies published in the last two years have provided convincing evidence that GliT is responsible for the self-resistance of *A. fumigatus* to gliotoxin.[105,106] Deletion of the *gliT* gene renders *A. fumigatus* mutants highly sensitive to gliotoxin, toxicity that can be reversed by addition of glutathione. Moreover, concentrations of reduced gliotoxin increase with the concomitant depletion of intracellular glutathione

levels. It is likely that alterations of the cellular redox status and mixed disulfide formation contributes to the growth inhibition observed in the absence of *gliT*.

Perhaps the cytotoxicity of gliotoxin is an indirect consequence of the true role of gliotoxin and other epidithiodioxopiperazines produced by fungi. The same redox cycling that produces deleterious consequences in naïve organisms may, in *Aspergillus fumigatus*, serve as a buffer against cellular oxidative stress.[106] Gliotoxin and other epidithiodioxopiperazines may have evolved as simple antioxidants, with the host protected from unwanted redox cycling and mixed disulfide formation by GliT.

Sirodesmin PL (**1.58**) is the only other epidithiodioxopiperazine to have been extensively studied from a biosynthetic perspective. Putative biosynthetic gene clusters for sirodesmin and gliotoxin identified from *Leptosphaeria maculans* and *Aspergillus fumigatus*, respectively, are given in **Figure 1.24**.[107-109] Based on recent advances to our understanding of gliotoxin biosynthesis and the identification of homologs in the sirodesmin gene cluster, we are able to predict many of the experimentally unverified steps in the biosynthesis of sirodesmin PL (**Scheme 1.3**).

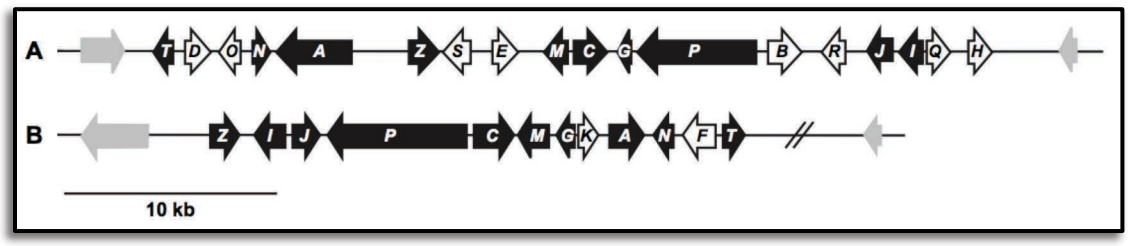

Figure 1.24. Putative epidithiodioxopiperazine gene clusters for sirodemsin PL (**A**) and gliotoxin (**B**).[109]

Feeding studies have shown that *Leptosphaeria maculans* incorporate labeled tyrosine and serine into both sirodesmin PL (**1.58**) and presumed intermediate phomamide (**1.132**).[59,110-112] We propose the incorporation of sulfur to proceed

analogously to the gliotoxin biosynthesis, through dihydroxylation (**1.133**), imine formation, and glutathione addition (**1.134**). Unmasking of the dithiol (**1.135**) and oxidation to the disulfide (**1.136**) could be followed by oxidation and Claisen rearrangement to give **1.137**, which after cyclization and oxidation provides known *L. maculans* metabolite phomalirazine (**1.61**).[59,111] Oxidative spirorearrangement, *N*-methylation, and ketone reduction would lead to another known metabolite, desacetyl-sirodemin PL (**1.59**). Acetylation by SirH would complete the biosynthesis of sirodesmin PL (**1.58**).[2,65,107,109]

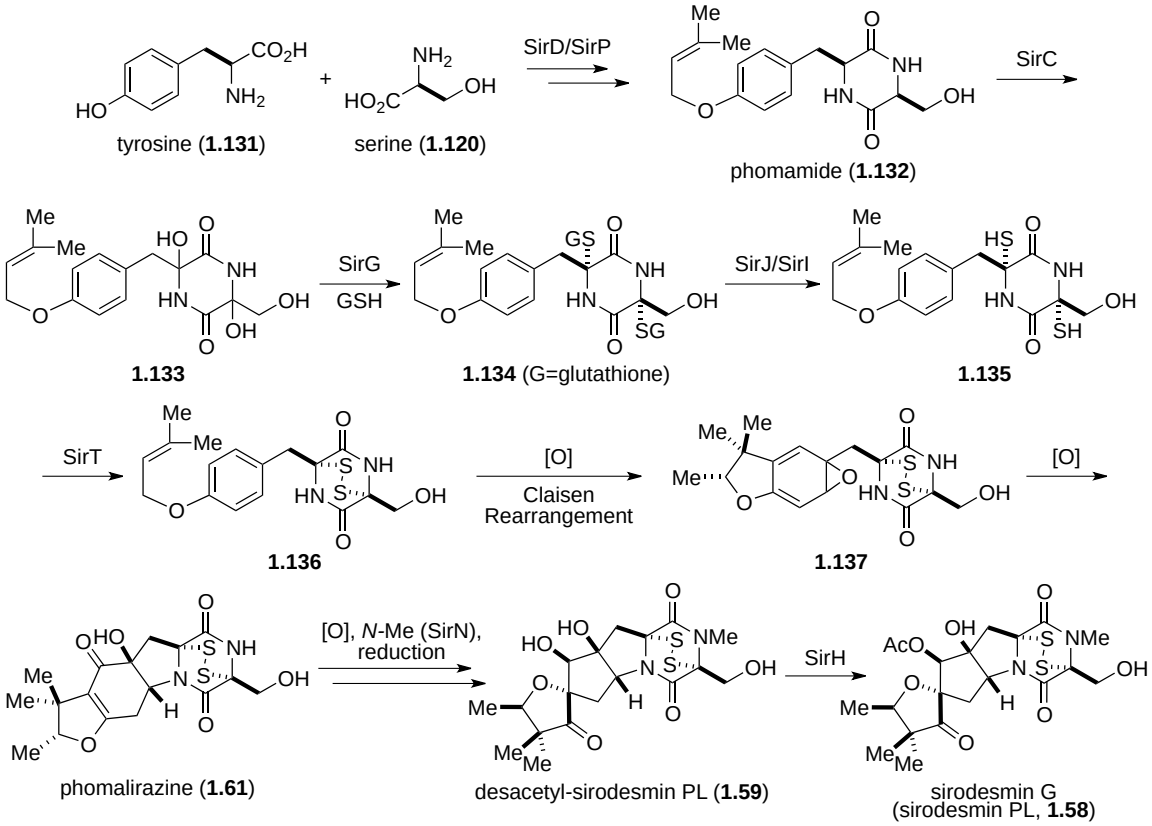

Scheme 1.3. Proposed biosynthetic pathway of sirodesmin PL.

1.5: Concluding Remarks

Epidithiodioxopiperazine alkaloids possess an astonishing array of molecular architecture that has for decades challenged and inspired synthetic chemists. Biosynthetic studies presented in this chapter provide a glimpse at the efficiency and elegance with which Nature is able to assemble these compounds. Synthetic chemists strive to mimic and in turn better understand the mechanisms by which microorganisms are able to produce such complexity, hoping to channel some of Nature's efficiency into novel synthetic pathways. In the next chapter, we present many of the synthetic advances made toward several of the epidithiodioxopiperazines presented above.

CHAPTER 2

Total Syntheses of Epidithiodioxopiperazines

2.1: Introduction

Over 100 naturally occurring epidithiodioxopiperazines have been isolated. However, relatively few have succumbed to total synthesis despite decades of effort, highlighting the challenging synthetic nature of the class of molecules. Initial interest in the biological activity of epidithiodioxopiperazines sparked the synthetic interest of several groups, with six different naturally occurring members of the class yielding to synthetic chemists between 1973 and 1981. Three decades passed before renewed interest in epidithiodioxopiperazines arose, sparked by isolation reports of new metabolites, exciting results from the biological community detailing novel mechanisms of action in cells, and advances in genomics that invigorated interest in elucidating the biosynthesis of these secondary metabolites. Between 2009 and 2012 alone, syntheses of eight additional epidithiodioxopiperazine alkaloids have been reported. A casual glance through Chapter 1 is enough to impress upon the reader the great degree of structural similarity shared among and between families of epidithiodioxopiperazines. We anticipate that in the coming decade total syntheses of entire families of this class of fungal metabolites will be completed concomitantly with great advances in synthetic methods and biosynthetic understanding. In this chapter, we present a comprehensive review of total syntheses of epidithiodioxopiperazines.

2.2: Early Epidithiodioxopiperazine Syntheses (1973-1981)

The total synthesis of sporidesmin A was completed by Kishi and coworkers in 1973. In a series of communications Kishi described a novel strategy for the synthesis of epidithiodioxopiperazines using a dithioacetal moiety as a protecting group for the disulfide bridge.[113-115] Thus protected, the dithioacetal is stable to acidic, basic, and reducing conditions, allowing for the introduction of thiol groups at an early stage in a total synthesis. Synthesis of the sporidesmins began with the treatment of dioxopiperazine **2.1** with the dithiane derivative of *p*-anisaldehyde in the presence of acid to afford dithioacetal-protected dioxopiperazine **2.2** (**Scheme 2.1**).[113] Condensation with acid chloride **2.3** and subsequent methoxymethyl deprotection gave compound **2.4**. Treatment of ketone **2.4** with DIBAL-H at -78 °C resulted in stereoselective reduction to the alcohol, which was then converted into acetate **2.5** in 80% yield. Cyclization to the diacetate (**2.6**) proceeded upon addition of iodosobenzene diacetate, and hydrolysis of the acetates gave the corresponding diol. Treatment of the diol with *m*-chloroperbenzoic acid (*m*CPBA) afforded an intermediate sulfoxide, which decomposed to the disulfide upon exposure to strong Lewis acid, revealing (±)-sporidesmin A (**1.11**).

Intermediate **2.5** was also used by Kishi in a total synthesis of (±)-sporidesmin B (**Scheme 2.2**).[116] Reduction of the acetate gave the methylene (**2.7**), which underwent an oxidative cyclization similar to that reported in the sporidesmin A synthesis to benzoate **2.8**. The disulfide was revealed as described above, completing the synthesis of (±)-sporidesmin B (**1.62**).

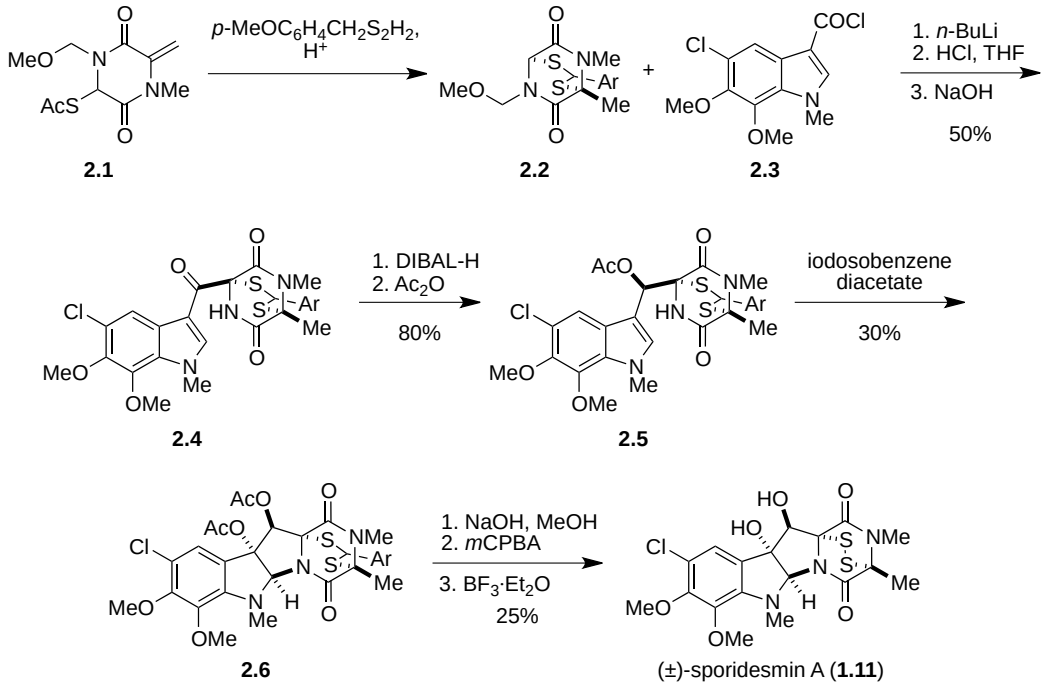

Scheme 2.1. Total synthesis of (±)-sporidesmin A.

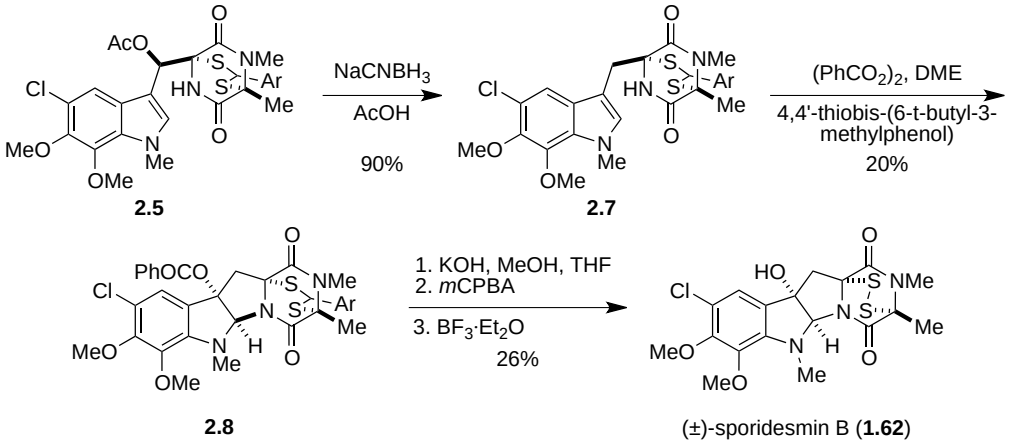

Scheme 2.2. Synthesis of (±)-sporidesmin B.

Fukuyama and Kishi reported the first synthesis of dehydrogliotoxin (**1.18**, **Scheme 2.3**) in 1973.[114] Benzoic acid derivative **2.10** was coupled to dioxopiperazine **2.9** and treated with diazomethane to give methyl ester **2.11**. Radical bromination with NBS and benzoyl peroxide was followed by treatment with potassium thioacetate to give dithioacetate **2.12**. Cleavage of the thioacetates and addition of *p*-methoxybenzaldehyde

and boron trifluoride etherate gave a 1:1 diasteromeric mixture of thioacetals **2.13** in good yield. This masked disulfide is stable to a variety of conditions that the disulfide would not otherwise survive, allowing Kishi to introduce sulfur at an early stage in the synthesis.

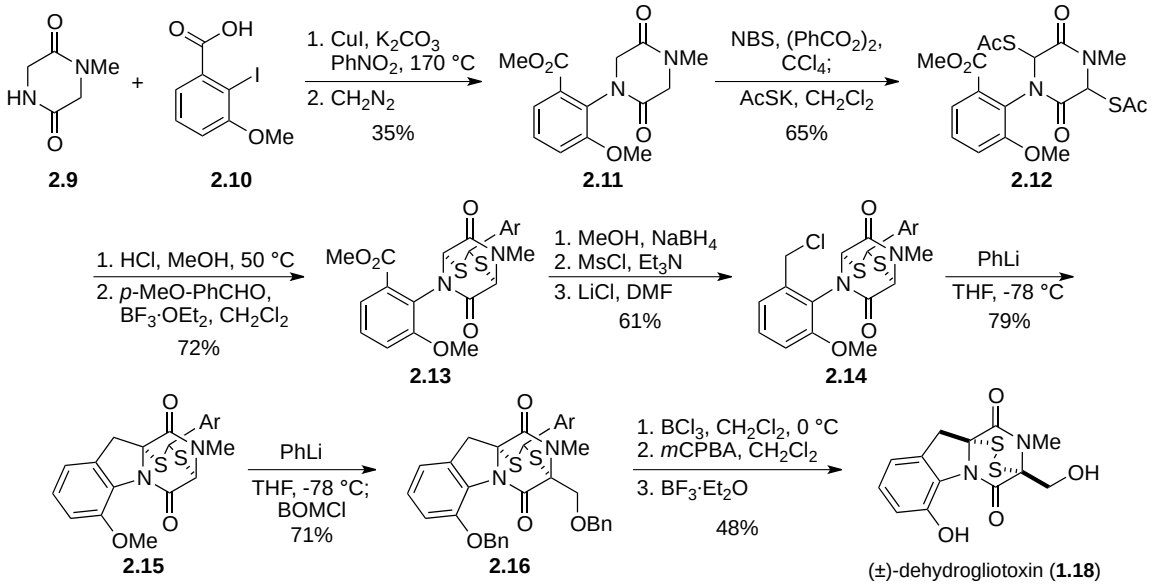

Scheme 2.3. Synthesis of (±)-dehydrogliotoxin.

A three-step conversion to the primary chloride (**2.14**) was followed by addition of phenyllithium to affect cyclization on the desired bridgehead carbon in 79% yield (**2.15**). Addition of phenyllithium with benzyl chloromethyl ether efficiently installed the benzyl protected serine side chain (**2.16**). Cleavage of the benzyl and methyl ethers and conversion to the epidithiodioxopiperazine gave (±)-dehydrogliotoxin (**1.18**).

The biosynthesis of gliotoxin (**1.2**) is believed to proceed through the intramolecular nucleophilic ring-opening of a phenylalanine-derived arene oxide (**1.122**) and has been the subject of considerable speculation and interest. Kishi and coworkers drew inspiration from this biogenetic hypothesis in devising a brilliant total synthesis of gliotoxin. The total synthesis of (±)-gliotoxin was completed in 1976 utilizing the same

disulfide protecting strategy as employed above for the sporidesmins, and was re-engineered in 1981 by the same route starting from optically pure dithioacetal **2.17** obtained from resolution (**Scheme 2.4**).[117,118] Coupling of **2.17** with *t*-butoxy arene oxide **2.18** in the presence of triton B afforded **2.19** and **2.20** in a 2 :1 ratio. Acetylation, deprotection, mixed anhydride formation, and reduction gave alcohol **2.21** in 77% yield from **2.19**. Primary alcohol **2.21** was converted to the chloride following mesylation, and the secondary ester deprotected to reveal alcohol **2.22**. The key stereoselective cyclization-alkylation reaction was achieved upon addition of phenyllithium to **2.22** and benzoxymethyl chloride, affording cycloadduct **2.23** in modest yield (53%). The primary alcohol was revealed upon removal of the benzyl group, and the thioacetal oxidatively removed to afford either (±)- or (+)-gliotoxin (**1.2**).

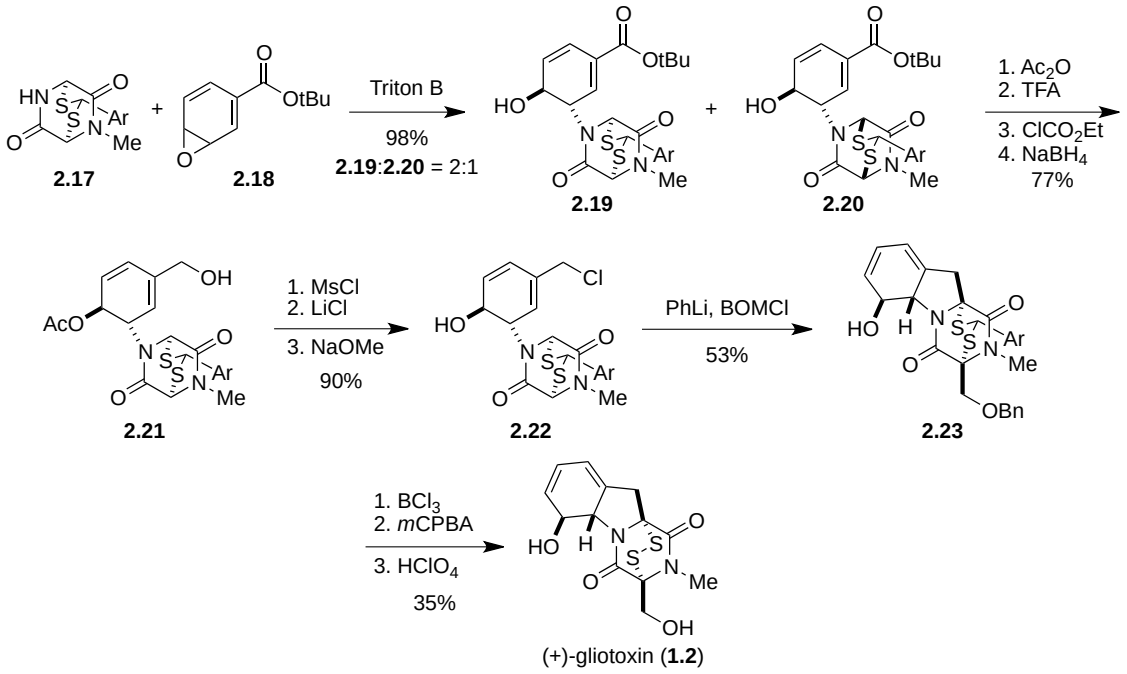

Scheme 2.4. Synthesis of (+)-gliotoxin.

Strunz and Kakushima followed the precedent set by Kishi and completed a total synthesis of hyalodendrin (**1.3**, **Scheme 2.5**).[119] Known thioacetal **2.24** was alkylated

sequentially with chloromethyl methyl ether and benzyl bromide, then deprotected to reveal hyalodendrin (**1.3**).

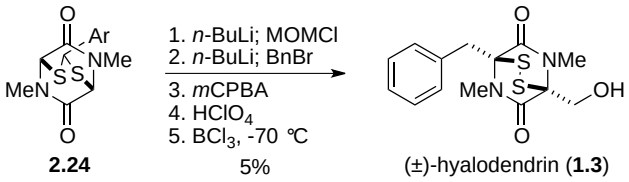

Scheme 2.5. Synthesis of (±)-hyalodendrin.

In 1979 and 1980, Williams and Rastetter reported the total synthesis of gliovictin (**1.32**, **Scheme 2.6**).[120,121] Sarcosine anhydride (**2.25**) was converted in three steps to silyl enol ether **2.27**. Alkylation with benzyl bromide and concomitant sulfenylation and deprotection gave methyl sulfide **2.29**. Additional sulfenylation gave a 3:1 mixture of diastereomers (**2.30**), favoring the undesired anti isomer. Reduction of the mixture of aldehydes completed the total synthesis of gliovictin (**1.32**) and *epi*-gliovictin (**2.31**).

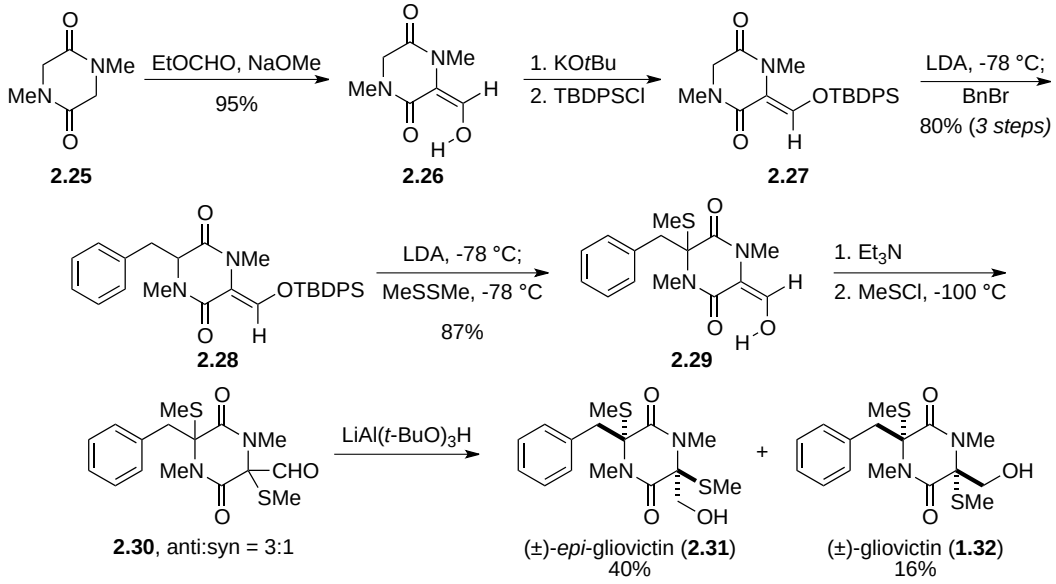

Scheme 2.6. Total synthesis of (±)-gliovictin and *epi*-gliovictin.

A synthesis of hyalodendrin (**1.3**, **Scheme 2.7**) was achieved from silyl enol ether **2.28**, used previously in the gliovictin synthesis.[120] Addition of monoclinic sulfur to the

enolate of **2.28** followed by reductive workup provided thiol **2.32**. Conversion to the enolic methyl disulfide, deprotection of the silyl group, and sulfenylation with triphenylmethyl chlorodisulfide gave a mixture of diastereomers, unfortunately favoring the undesired anti isomer (**2.34**). Reduction and oxidation of **2.34** gave hyalodendrin (**1.3**) in 29% yield.

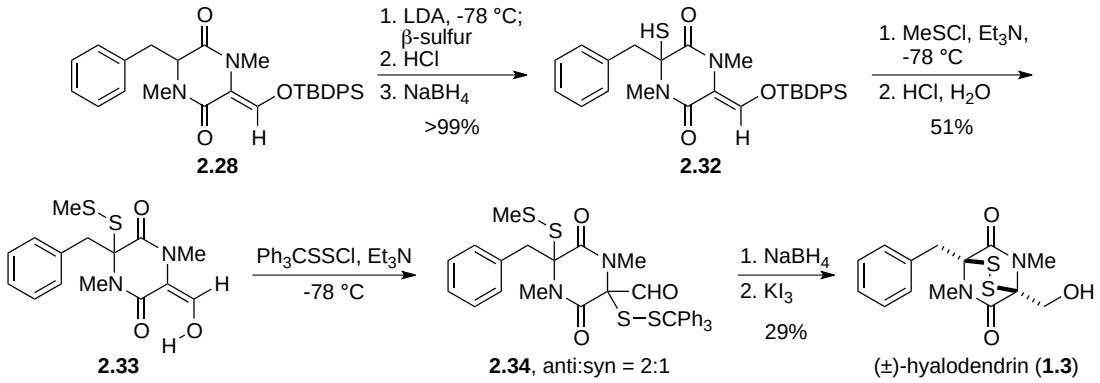

Scheme 2.7. Rastetter's total synthesis of (±)-hyalodendrin.

2.3: Recent Epidithiodioxopiperazine Syntheses (2009-2012)

Several total syntheses of epidithiodioxopiperazines have been reported in the last three years. Movassaghi and coworkers were the first to publish in this modern synthetic revival, reporting the synthesis of (+)-11,11'-dideoxyverticillin A (**2.43**, **Scheme 2.8**).[122] The authors showed that the amine resulting from cleavage of the *N*-Boc carbamate of **2.35** was readily cyclized to dioxopiperazine **2.36** in morpholine. Exposure of **2.36** to bromine produced 3-bromopyrroloindoline **2.37**, and the amides were subsequently methylated upon treatment with iodomethane. Addition of tris(triphenylphosphine)cobalt chloride gave the desired dimeric intermediate **2.38**. After extensive investigation searching for appropriate stereoselective hydroxylation conditions, the dimer was eventually oxidized with bis(pyridine)silver(I) permanganate to a fragile octacyclic

tetraol (**2.39**). Exposure of **2.39** to Fu's (*R*)-(+)-4-pyrrolidinopyridinyl(pentamethyl-cyclopentadienyl)iron (PPY) catalyst with *t*-butyldimethylsilyl chloride (TBSCl) gave selectively the alanine-derived protected hemiaminals (**2.40**). Removal of the benzenesulfonyl groups with sodium amalgam revealed diaminodiol **2.41**. Treatment of **2.41** with K_2CS_3 followed by ethanolamine gave diaminotetrathiol **2.42**, which readily oxidized to (+)-11,11'-dideoxyverticillin A (**2.43**) when partitioned between aqueous hydrochloric acid and dichloromethane and treated with potassium triiodide.

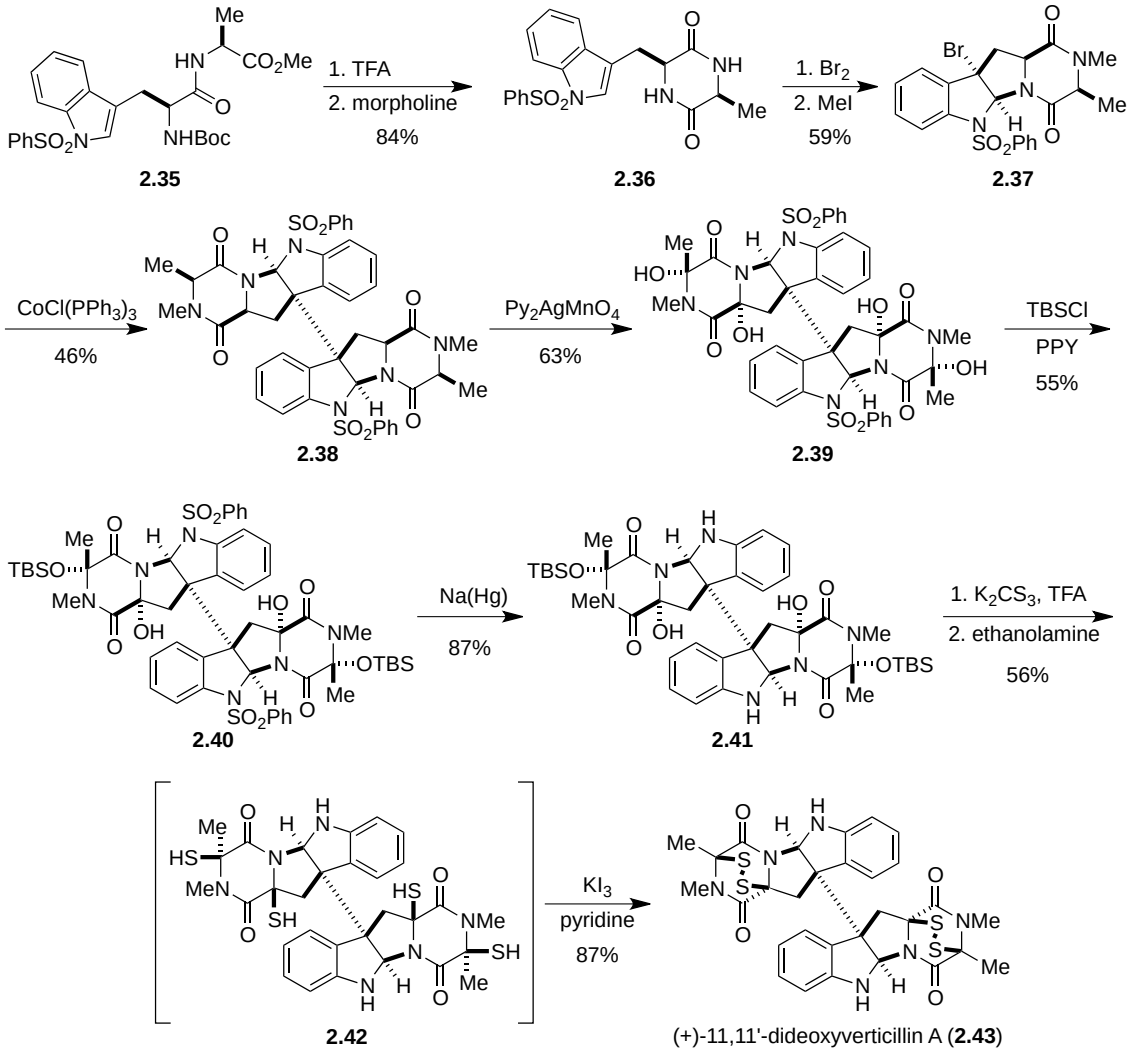

Scheme 2.8. Biomimetic total synthesis of (+)-11,11'-dideoxyverticillin A.

Chaetocin (**1.13**) is quite similar in structure to 11,11'-dideoxyverticillin A, derived from two molecules of serine rather than alanine. Substituted dioxopiperazine **2.46** was prepared in five steps from *N*-Me,Cbz-D-Ser (**2.44**) and D-Trp-OMe (**2.45**).[123,124] Bromocyclization gave tetracycle **2.47**, converted to the tribromide (**2.48**) under radical conditions and hemiaminal **2.49** following addition of water. Movassaghi's reductive dimerization conditions using a Co(I) complex afforded the desired dimer (**2.50**) in modest yield. Addition of **2.50** to condensed hydrogen sulfide and $BF_3{\cdot}OEt_2$ formed the tetrathiol, oxidized to the bis(disulfide) upon addition of iodine to complete the synthesis of (+)-chaetocin (**1.13**).

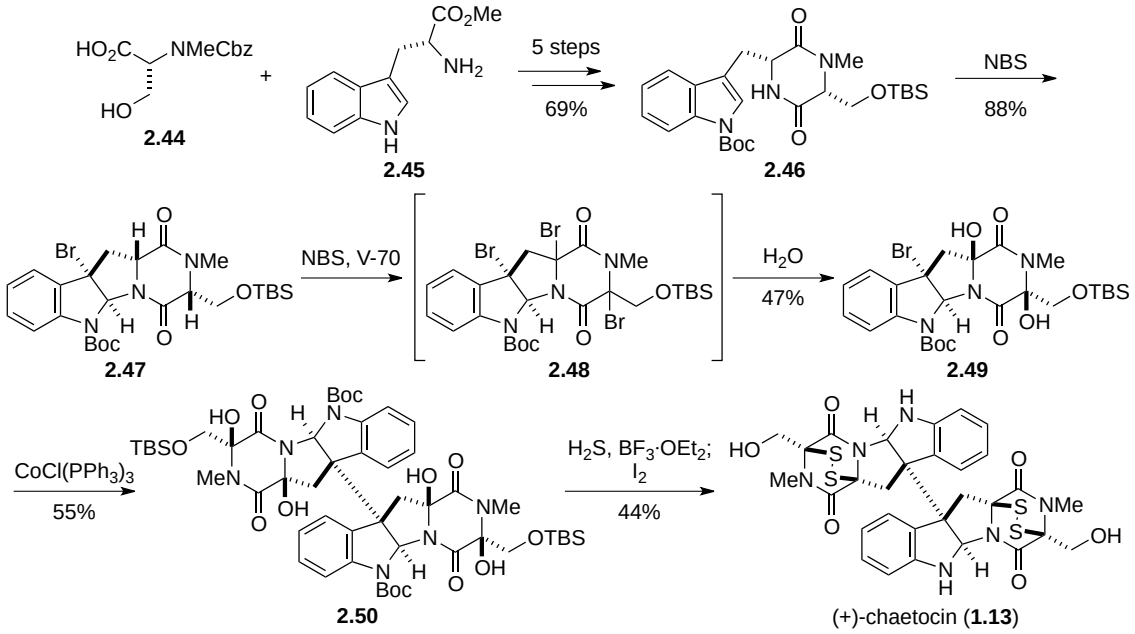

Scheme 2.9. Sodeoka's total synthesis of (+)-chaetocin.

Sodeoka originally planned to form the tetraol from the product resulting from dimerization of **2.47**. It was noted that this dimer was not stable to the radical conditions employed above, so the synthetic plan was altered to that shown in **Scheme 2.9** to

circumvent this problem. Recall that Movassaghi had similar difficulties in forming related tetraol **2.39** and eventually settled on the mild oxidation discussed above.

Mere months after Sodeoka reported the first total synthesis of chaetocin, Movassaghi published the synthesis of (+)-chaetocin (**Scheme 2.10**), the hexasulfide (+)-chaetocin C (**1.79**), and the octasulfide (+)-12,12'-dideoxychetracin A (**1.81**, **Scheme 2.11**), all from the natural amino acids L-serine and L-tryptophan.[125]

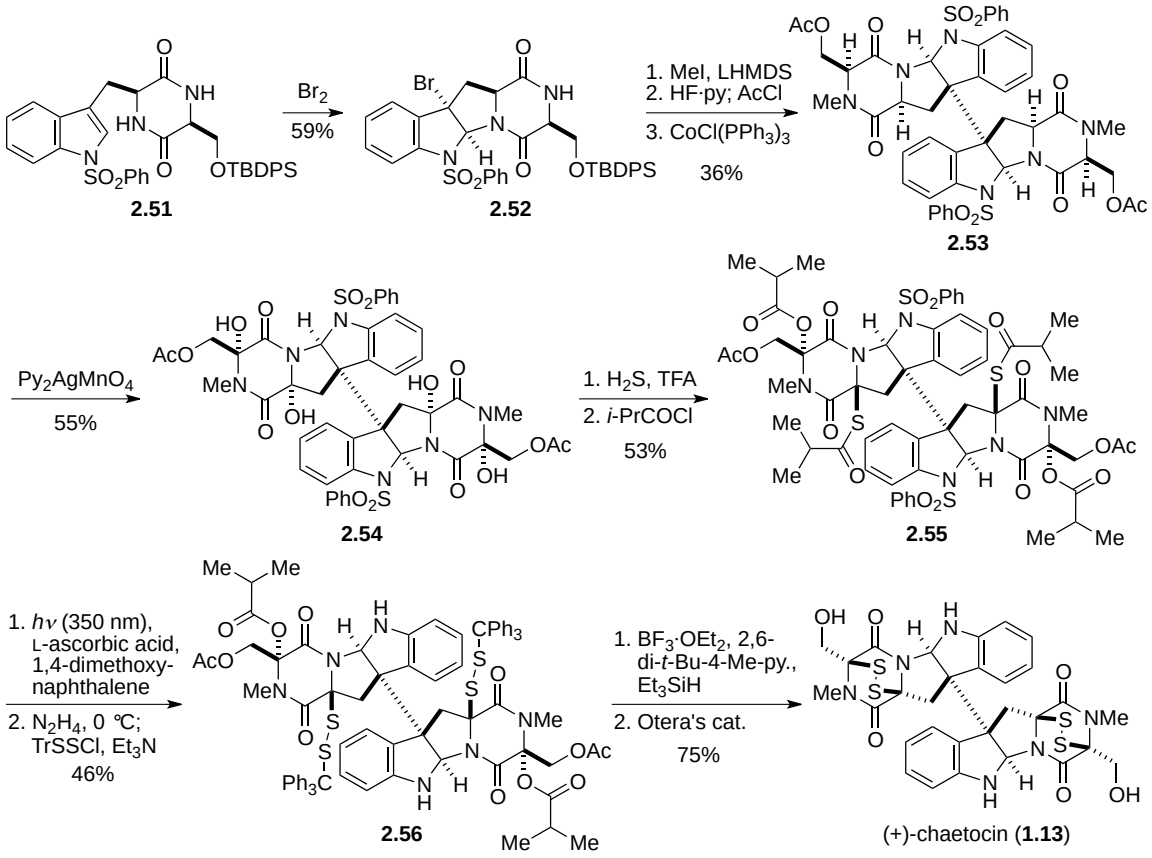

Scheme 2.10. Movassaghi's total synthesis of (+)-chaetocin.

Bromocyclization of dioxopiperazine **2.51** gave *endo*-tetracyclic bromide **2.52**. *N*-methylation, protecting group exchange, and key reductive radical dimerization afforded the dimeric octacycle (**2.53**). Selective tetrahydroxylation was achieved using Py_2AgMnO_4. Tetraol **2.54** is analogous to **2.50** used in Sodeoka's synthesis, but

interestingly the acetate allows for differentiation of the hemiaminals, resulting in regioselective substitution of hydrogen sulfide. Protection of resulting thiohemiaminal as the dithioisobutyrate (**2.55**) served both to prevent opening of the hemiaminal under polar protic conditions and to activate the hemiaminal to mild ionization in future steps. Mild deprotection of the sulfonyl group was followed by chemoselective hydrazinolysis and addition of triphenylmethanesulfenyl chloride to give disulfane **2.56**. Ionization of the isobutyrates and cyclization to the epidithiodioxopiperazines with concomitant loss of a triphenylmethyl cation was followed by removal of the acetates using Otera's catalyst to afford (+)-chaetocin (**1.13**).

Chaetocin C (**1.79**) and 12,12'-dideoxychetracin A (**1.81**), the epitri- and epitetrathiodioxopiperazine analogues of chaetocin, were similarly synthesized from a common intermediate (**Scheme 2.11**).[125]

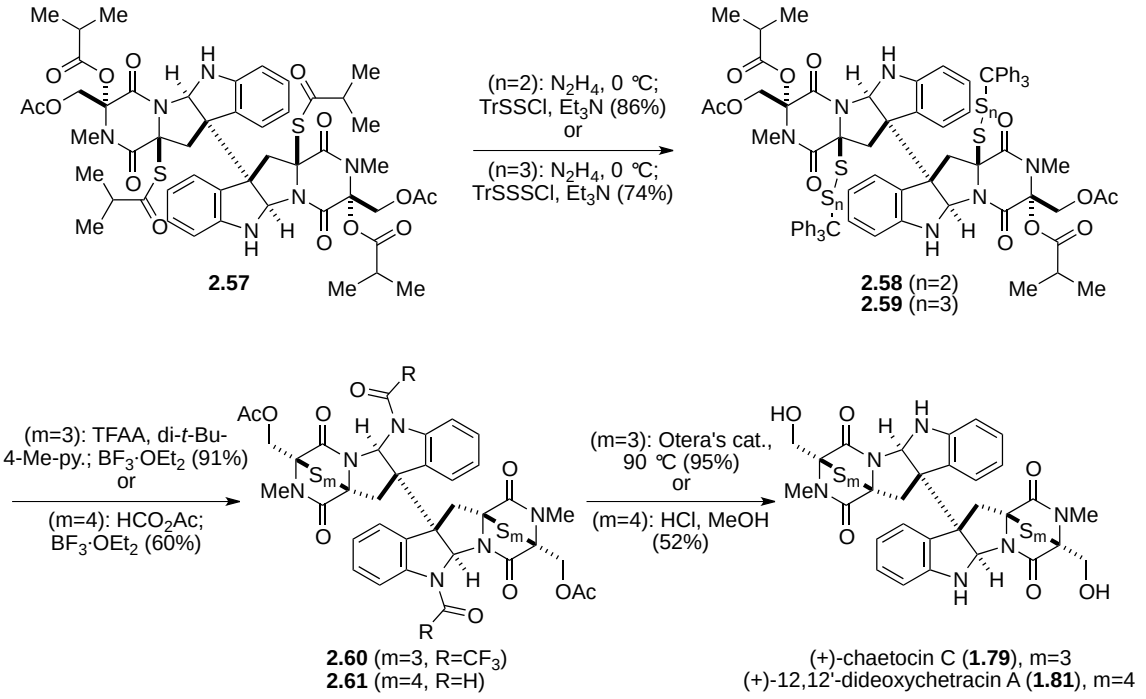

Scheme 2.11. Total syntheses of chaetocin C and 12,12'-dideoxychetracin A.

Hydrazinolysis of diaminodithioisobutyrate **2.57** was followed by treatment with the corresponding sulfur source to give **2.58** or **2.59**. It was necessary to protect the indoline nitrogens as the trifluoroacetates before addition of Lewis acid to form the polysulfide bridges (**2.60** and **2.61**), presumably to prevent decomposition pathways encountered over longer reactions times necessary to the formation of the larger polysulfide bridges. Global deprotection gave either (+)-chaetocin C (**1.79**) or (+)-12,12'-dideoxychetracin A (**1.81**).

In 2011, Overman and coworkers reported the total synthesis of (+)-gliocladine C (**1.99**, **Scheme 2.12**).[126] Known 2-indolinone **2.62** (prepared from isatin and indole) was reduced and Boc-protected to afford compound **2.63**. Conversion to the oxindole ester (**2.64**) proceeded efficiently upon treatment with 2,2,2-trichloro-1,1-dimethylethyl chloroformate, triethyl amine, and 10 mol % of Fu's (*S*)-(–)-4-pyrrolidinopyrindinyl-(pentamethylcyclopentadienyl)iron catalyst. The oxindole was elaborated to indoline **2.65** over four steps in 54% yield. Aldol condensation with the lithium enolate of the piperazinedione provided exclusively the *Z* isomer of **2.66**, which readily cyclized to hexacycle **2.67** upon treatment with $BF_3 \cdot OEt_2$. Grignard addition, silyl protection of the resultant alcohol, asymmetric dihydroxylation, and acetylation gave advanced intermediate **2.68**. Addition of the epimeric mixture of silyl ethers to condensed hydrogen sulfide and $BF_3 \cdot OEt_2$ gave the dithiol, oxidized to the disulfide upon exposure to oxygen. Removal of the acetate revealed (+)-gliocladine C (**1.99**).

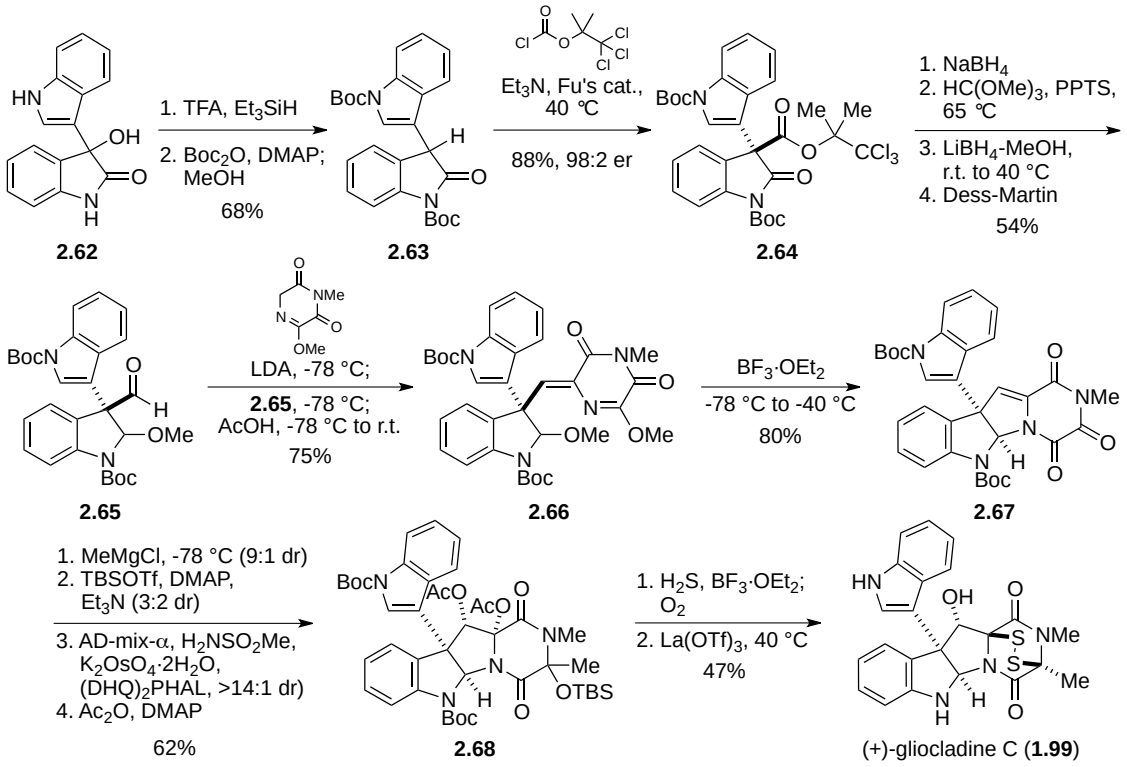

Scheme 2.12. Synthesis of (+)-gliocladine C.

Boyer and Movassaghi recently completed the total synthesis of two compounds related to the gliocladines. The most direct route to the first, (+)-gliocladin B (**2.73**), is detailed in **Scheme 2.13**.[127] Bromocyclization proceeded as above, providing tetracycle **2.70** in good yield with excellent stereoselectivity (97:3 *endo*:*exo*). A Friedel–Crafts type coupling of *N*-TIPS-5-bromoindole with **2.70** formed the desired 3-3' bond. Several indole derivatives were screened, and the 5-bromo derivative was found to give the best yield and selectivity. The bromine and silyl protecting group were removed and the resulting compound oxidized to diol **2.72**. Exposure of this diol to sodium thiomethoxide and trifluoracetic acid gave the bismethylthio derivative. (+)-Gliocladin B (**2.73**) was revealed upon removal of the benzenesulfonyl group.

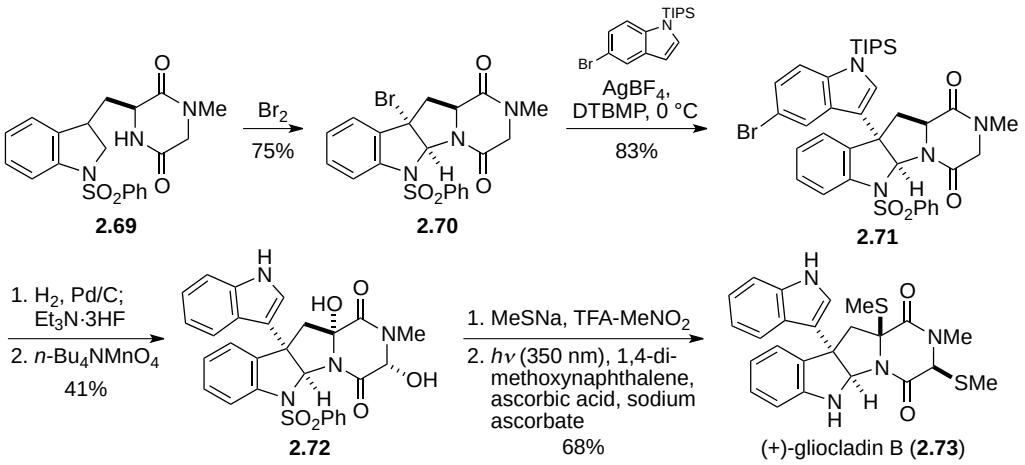

Scheme 2.13. Total synthesis of (+)-gliocladin B.

Although it has not to date been isolated from a natural source, it is worth noting that the authors were able to convert diol **2.72** into the disulfide (+)-12-deoxybionectin A (**2.76**) using conditions analogous to those discussed above in the chaetocin syntheses (**Scheme 2.14**).[127] Disulfide **2.76** is also easily converted to (+)-gliocladin B (**2.73**) by reduction of the disulfide with sodium borohydride in the presence of iodomethane.

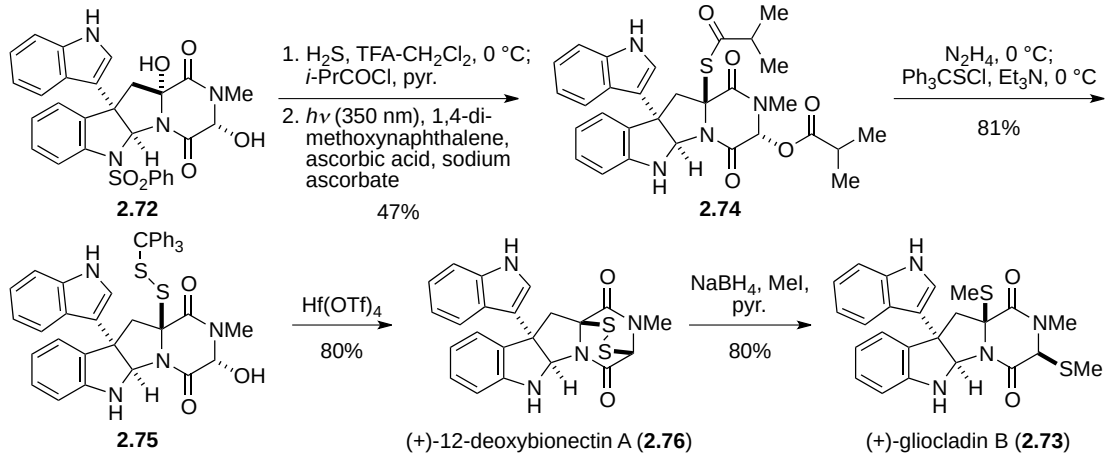

Scheme 2.14. Synthesis of (+)-12-deoxybionectin A and (+)-gliocladin B.

Epiccocin G (**2.84**) lacks a disulfide bridge and was thus not discussed in Chapter 1. Nonetheless, the structure is remarkably similar to that of epicorazine A (**1.8**), and a discussion of Nicolaou's recent total synthesis is certainly relevant in this context.[128]

Hydroxy enone **2.77** (prepared in two steps from *N*-Boc-tyrosine) was converted in four steps to hydroxy methyl ester **2.78** (**Scheme 2.15**). Separate deprotections to either the amine or carboxylic acid gave two derivatives that were coupled to form amide **2.79**. Deprotection and cyclization to the dioxopiperazine was followed by conversion to the bistrifluoroacetate (**2.80**), which eliminated to bisdiene **2.81** upon exposure to $Pd(PPh_3)_4$ catalyst. Treatment with S_8 and NaHMDS gave a mixture of oligosulfenylated compounds (**2.82**) that were readily converted to the bisdimethylthio compound (**2.83**) upon reduction with sodium borohydride and addition of iodomethane. Bisendoperoxide **2.85** was generated on reaction with singlet oxygen, and addition of DBU induced a Kornblum–DeLaMare rearrangement to give a bishydroxy enone. Reduction to the ketone completed the total synthesis of epicoccin G (**2.84**).

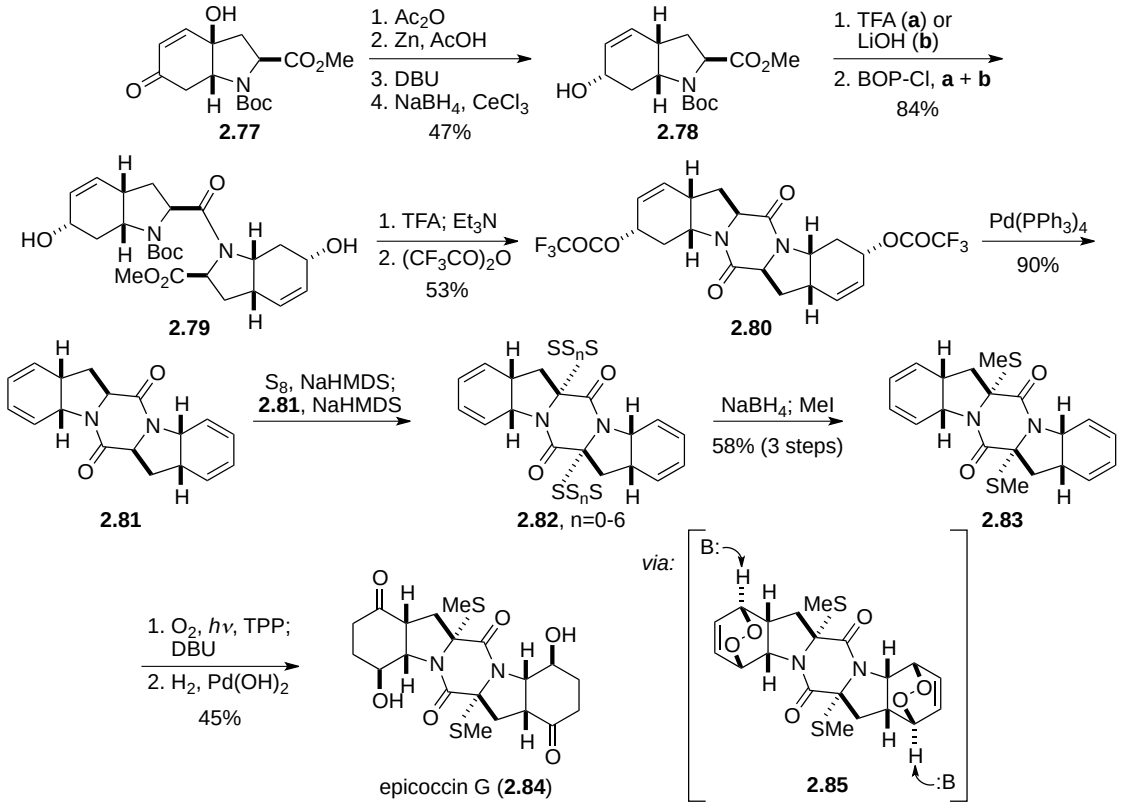

Scheme 2.15. Total synthesis of epicoccin G.

The last epidithiodioxopiperazine total synthesis to be discussed was reported recently by the Reisman group, who completed an elegant synthesis of (–)-acetylaranotin (**1.35**).[129] Pyrrolidine **2.88** was synthesized with >98% ee by (1,3)-dipolar cycloaddition of cinnamaldimine **2.87** to *t*-butyl acrylate (**2.86**) and subsequent cleavage of the *t*-butyl ester (**Scheme 2.16**). Protection of the amine and ozonolytic cleavage of the alkene provided lactone **2.89** in good yield. Ethynylmagnesium bromide was added to the hydroxylactone to form the hydroxy acid, which upon addition of triphenylphosphine and DIAD underwent Mitsunobu lactonization to **2.90**. Reduction to the diol (**2.91**) was followed by bis-TBS protection of the alcohols and selective deprotection of the primary alcohol. The aldehyde obtained following oxidation with Dess–Martin periodinane was efficiently converted to chlorohydrin **2.92**.

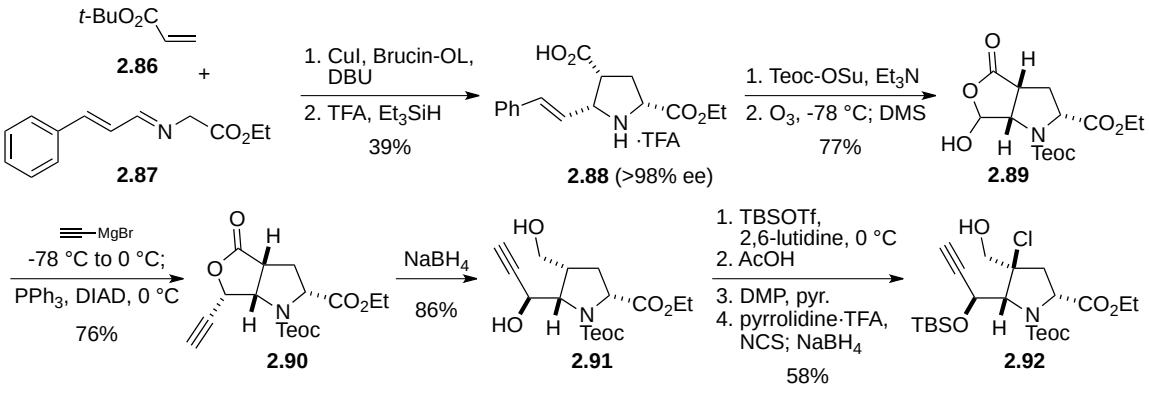

Scheme 2.16. Key pyrrolidine synthesis.

Formation of the dihydrooxepine (**2.93**) was realized upon treatment of alkyne **2.92** with catalytic $[Rh(cod)\text{-}Cl]_2$ and tris(4-fluorophenyl)phosphine (**Scheme 2.17**).[129] Elimination of HCl and hydrolysis of the ester gave acid **2.94**, while deprotection of the Teoc group and HCl elimination of the same compound gave amine **2.95**. BOP-Cl–mediated coupling of **2.94** and **2.95** delivered amide **2.96**, which readily cyclized to dioxopiperazine **2.97** after TBAF·(*t*-BuOH)$_4$–induced desilylation. Synthesis of (–)-

acetylaranotin (**1.35**) was completed following formation of tetrasulfide **2.98**, bisacetylation, mild reduction to the dithiol, and oxidation to the natural disulfide. This publication marked the first total synthesis of a dihydrooxepine-containing epidithiodioxopiperazine natural product.

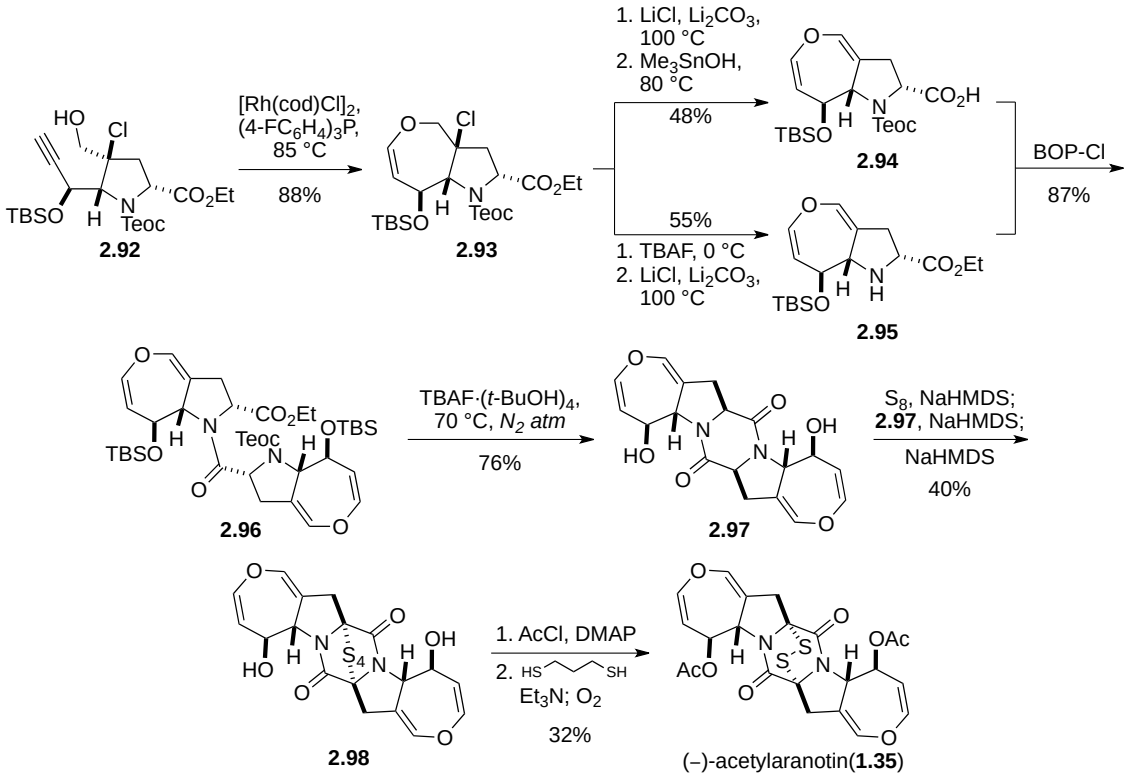

Scheme 2.17. Completion of the total synthesis of (–)-acetylaranotin (**1.35**).

2.4: Other Relevant Syntheses: Formation of the C3-N1' Bond

Recall that chetomin (**1.12**) contains a C3-N1' linkage between two indole–derived fragments. This unique structural feature was synthetically unprecedented when we began our synthetic efforts toward a total synthesis of chetomin. In the last few years, two different methods for the formation of this bond were reported in the literature. We

feel it prudent to discuss in the remainder of this chapter methods for the formation of the challenging C3-N1' bond as it relates to the synthesis of chetomin.

In 2008, Newhouse and Baran reported the total synthesis of (±)-psychotrimine (**Scheme 2.18**).[130,131] The key C3-N1' bond forming reaction was completed by treating tryptamine derivative **2.99** with *N*-iodosuccinimide and 2-iodoaniline to afford compound **2.100**. Larock indole synthesis with alkyne **2.101** completed the carbon framework for the top tryptamine fragment (**2.102**). A total synthesis of psychotrimine (**2.103**) was completed in two steps from **2.102**.

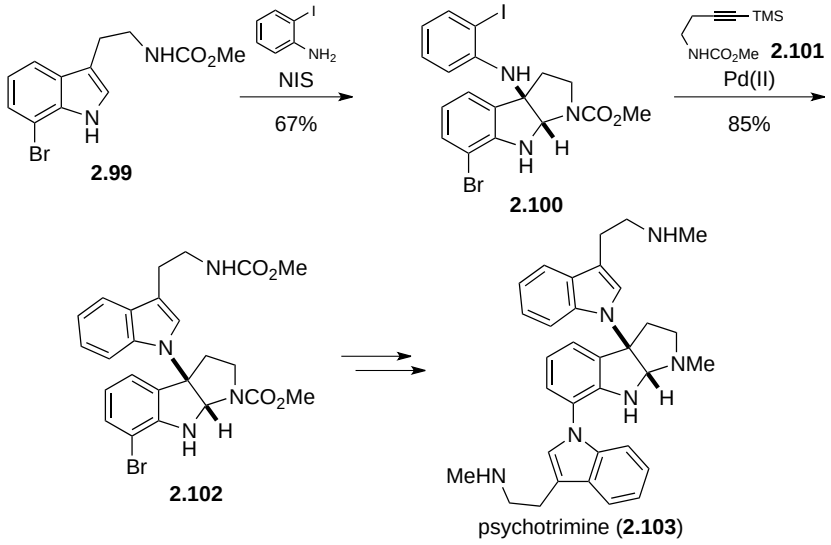

Scheme 2.18. Synthesis of (±)-psychotrimine via novel C3-N1' bond formation.

Baran used the same method in the synthesis of kapakahine B (**2.108**, **Scheme 2.19**).[130,132] In this instance, dipeptide **2.104** was cyclized and coupled to 2-iodoaniline to give **2.105**. Indole formation by a Larock annulation with TES-alkyne **2.106** gave indole **2.107**, converted in several steps to the natural product kapakahine B (**2.108**).

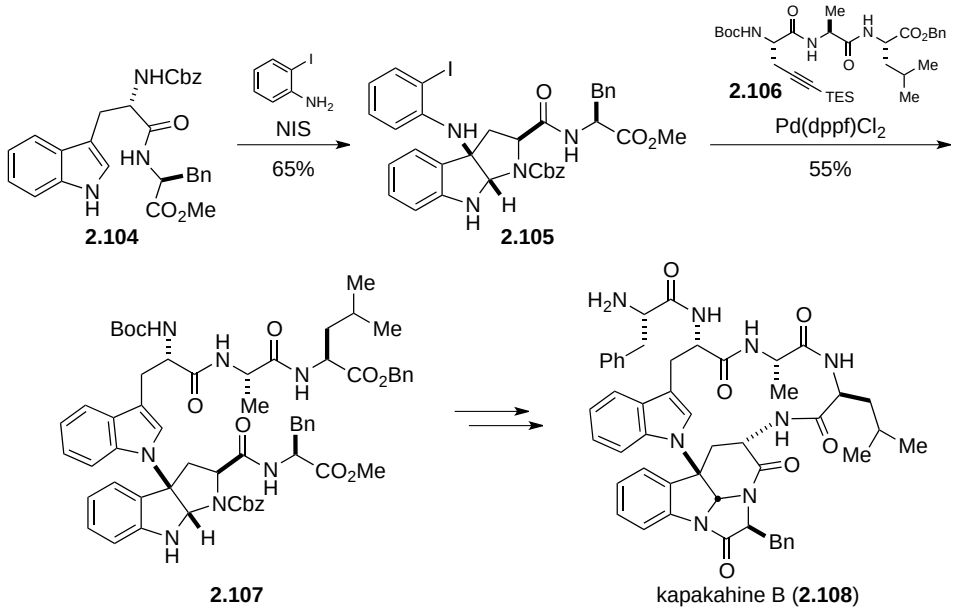

Scheme 2.19. Total synthesis of kapakahine B.

In 2008, Espejo and Rainier reported a new method for the synthesis of C3-N1' heterodimeric indolines from bromopyrroloindoline **2.110** (**Scheme 2.20**, prepared in one step from *N*,*N'*-Boc$_2$-L-Trp-OMe).[133]

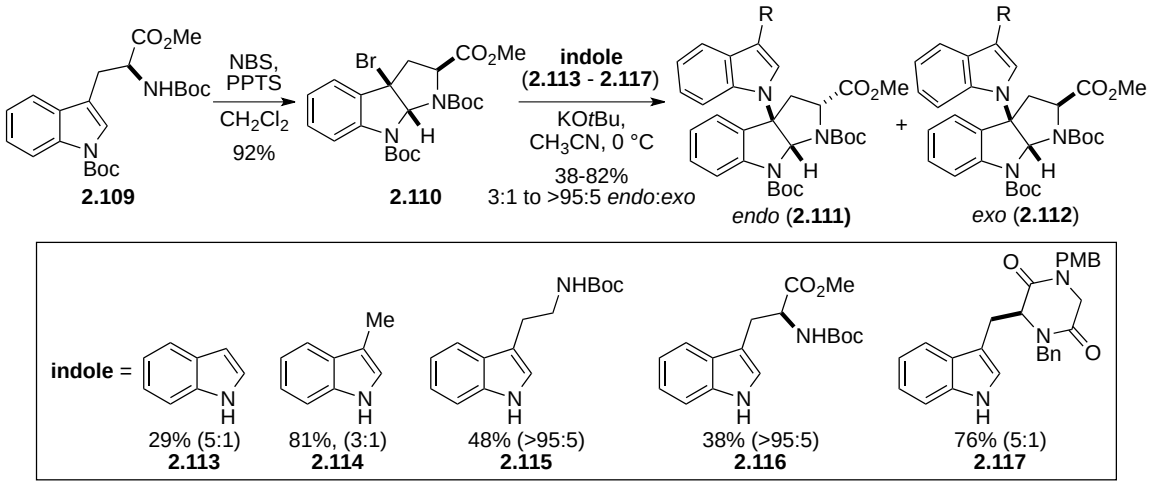

Scheme 2.20. Rainier's synthetic C3-N1' bond forming method.

Addition of potassium *tert*-butoxide to a stirring solution of **2.110** and an indole (i.e. **2.113**-**2.117**) in acetonitrile at 0 °C effects the desired bond formation in 30 minutes.

This method is far more general and cost effective than that reported by Baran, as a variety of indole derivatives can be coupled directly without the added Larock annulation step.

The utility of this method was demonstrated through the total synthesis of kapakahine F (**2.121**, **Scheme 2.21**).[134] Pyrroloindoline dimer **2.118** was synthesized as described above and transformed to phenylalanine derivative **2.119** over several steps. This substrate was originally intended to serve as a model for the subsequent trimethyl aluminum induced rearrangement, but unfortunately the product resulting from the coupling of **2.110** to a tryptophan derivative decomposed under the rearrangement conditions. Thus, indole **2.120** was ultimately used to complete the synthesis of kapakahine F (**2.121**).

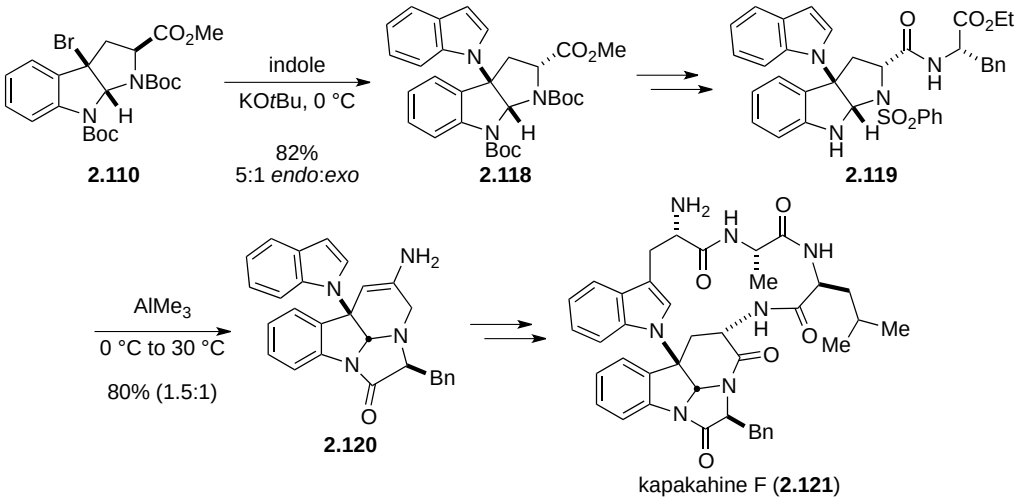

Scheme 2.21. Total synthesis of kapakahine F.

The final total synthesis to be discussed in this chapter featuring a C3-N1' bond forming step is that of (+)-pestalazine B (**2.126**, **Scheme 2.22**), a natural product with similar carbon framework to chetomin (**1.12**).[135] Pestalazine B is unique in this discussion in that, like chetomin, it is enantiomeric at the pyrroloindoline core compared to the

above examples. Accordingly, D-tryptophan was selected as the starting material, converted to bromopyrroloindoline **2.122** using known methods. Rainier's coupling methodology was employed to join **2.122** with dioxopiperazine **2.123** to form key intermediate **2.124**. Removal of the Boc groups and peptide coupling produced tetrapeptide **2.125**. Treatment of **2.125** with diethyl amine resulted in concomitant Fmoc deprotection and cyclization to the naturally occurring dioxopiperazine, completing the total synthesis of pestalazine B (**2.126**).

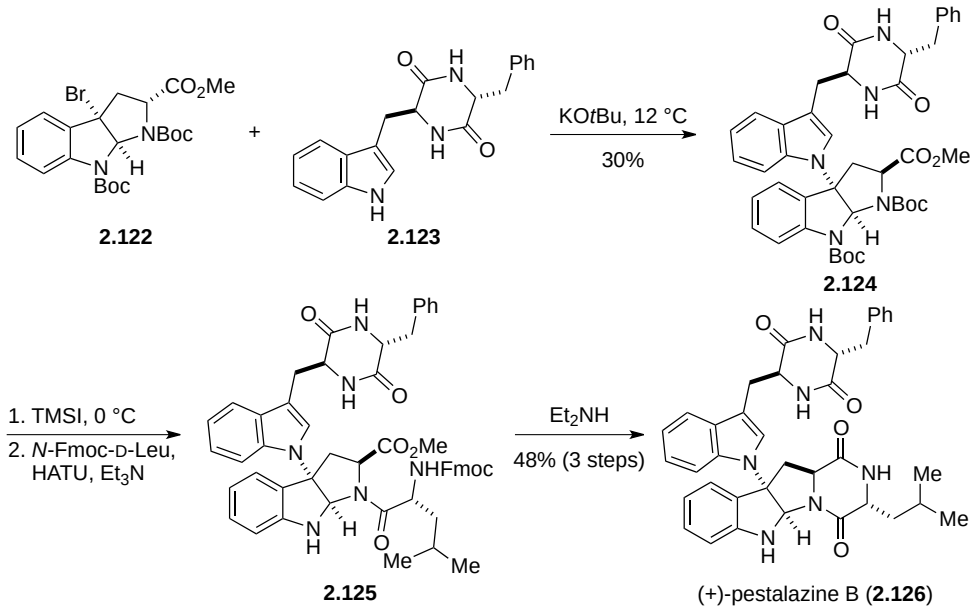

Scheme 2.22. Concise total synthesis of (+)-pestalazine B.

2.5: Concluding Remarks

Epidithiodioxopiperazine alkaloids possess an astonishing array of molecular architecture and, with that, corresponding synthetic challenges to construct such substances. The biosynthesis of many of the natural metabolites touched on in Chapter 1 has certainly inspired many of the chemists cited in this chapter, as several have sought to exploit insights from Nature's strategic bond constructions in a synthetic laboratory

context. Our own synthetic efforts toward chetomin and sporidesmin A as described in the following chapters were undertaken before all of the recent reports were published, although insight and inspiration were drawn from each as new developments in the modern synthetic renaissance of epidithiodioxopiperazines emerged.

CHAPTER 3

Studies Toward the Total Synthesis of Chetomin

3:1: Introduction

Our interest in chetomin stems both from its novel mechanism of action as a potential cancer chemotherapeutic agent and the synthetic challenge posed by the unique architecture of the molecule. Chetomin (**1.12**) and related metabolites isolated from *Chaetomium* sp. (**Figure 3.1**) are the only known epidithiodioxopiperazine alkaloids to contain a nearly dimeric structure joined by a C3-N1' linkage.[73,74] The densely functionalized structure contains five tetrasubstituted carbons and six stereocenters. The synthetic challenge imposed by the epidithiodioxopiperazine rings is also not to be overlooked, as the disulfide bridge is sensitive to oxidative, reductive, basic, and strongly acidic conditions.

3.2: Goals and Early Studies

3.2.1: Goals for the Project

The primary goal of this project was to develop a scalable, divergent synthesis of (+)-chetomin (**1.12**). We hoped to bring in as much functionality as possible when forming the C3-N1' bond to exploit the pseudo-dimeric architecture. Introduction of the disulfide bridges would be reserved for a late stage in the synthesis to circumvent the troubling sensitivity of the functional group. However, no precedent existed in the

infancy of this project for the formation of the key C3-N1' bond. Our initial synthetic efforts were focused on this bond.

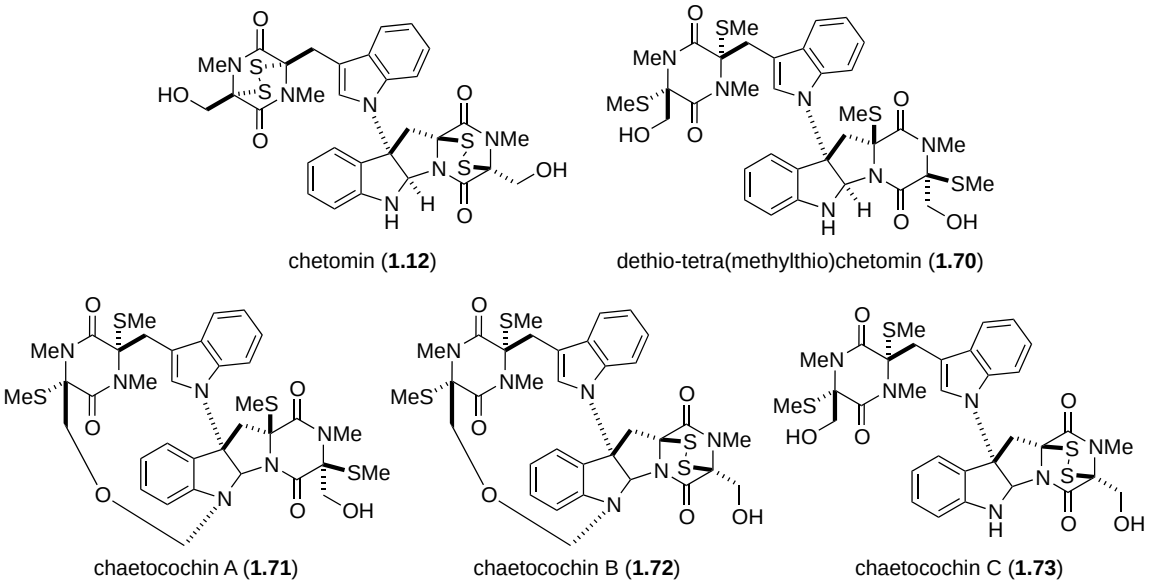

Figure 3.1. Chetomin and related fungal metabolites.

3.2.2: Iminium Ion Approach

A simple model study was designed to gain access to oxindole **3.1** (**Scheme 3.1**). A side chain mimicking the amino acid fragment could be added by nucleophilic addition to iminium **3.2**, formed from condensation of isatin (**3.3**) with indoline (**3.4**).

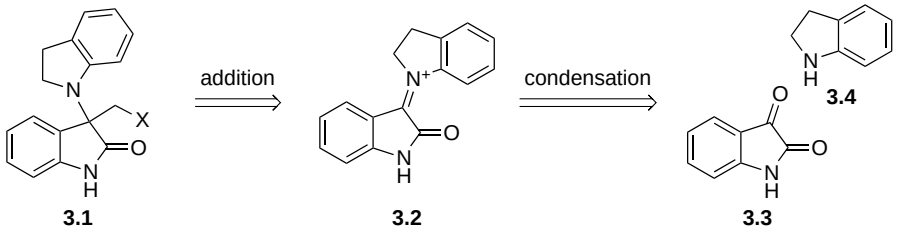

Scheme 3.1. Proposed model study for C3-N1' bond formation.

Condensation of indoline (**3.4**) on *N*-Boc isatin showed promise at forming the desired iminium ion (**3.7**), especially after we observed addition of vinyl Grignard

reagent to the condensation product (**Scheme 3.2**). However, further structural analysis by NMR revealed that water was not eliminated in the condensation, and hemiaminal **3.6** was instead formed through direct addition of indoline to the C3 carbonyl of isatin. Vinyl Grignard reagent was adding to the lactam carbonyl carbon. Numerous conditions were attempted to effect elimination of water, but all failed to produce the desired iminium ion (**3.7**).

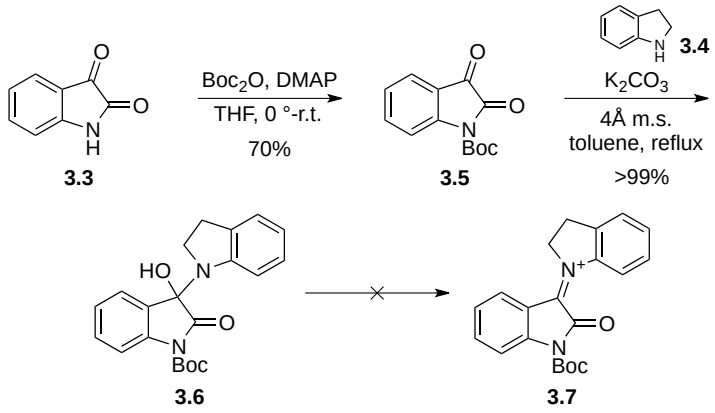

Scheme 3.2. Attempted iminium ion formation.

Looking back, we did achieve our goal of forming a tetrasubstituted carbon on an indole surrogate. However, no reasonable plan existed for the incorporation of the amino acid residue, let alone with any stereocontrol.

3.2.3: Pinacol-type Rearrangement

Inspired by past Williams group chemistry and aryl pinacol-type rearrangements recently reported by Movassaghi, we next envisioned forming the C3 tetrasubstituted center through a pinacol-type rearrangement of tryptophan dimer **3.9** to oxindole **3.8** (**Scheme 3.3**).[136-138] The amino acid fragment of indole **3.9** could be installed through alkylation of **3.10**, which was expected to arise from copper-mediated indole cyclization

of aniline **3.11**. The nitro alkene dimer could be accessed via coupling of bromoalkyne **3.12** with 2,3-dihydrotryptophan (**3.13**).

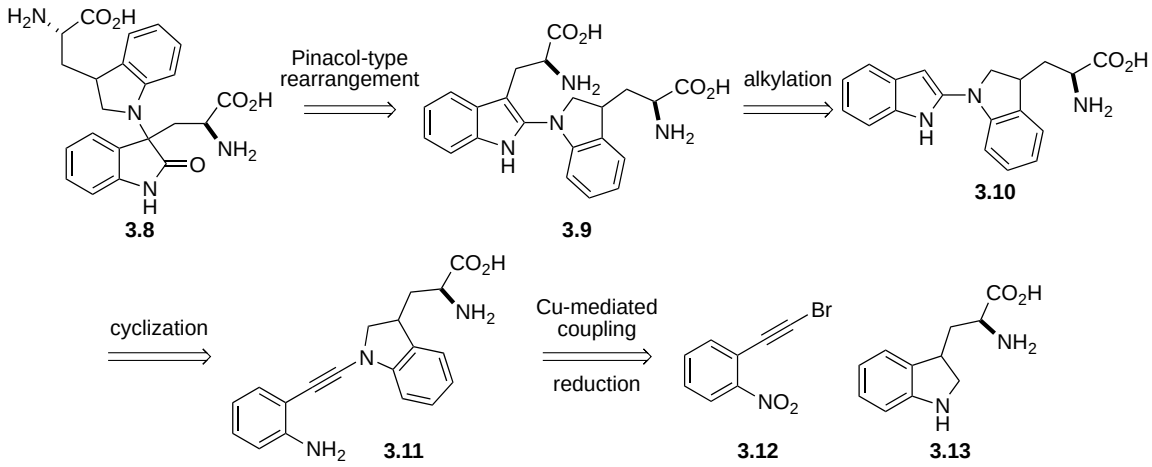

Scheme 3.3. Retrosynthesis of key intermediate **3.8** through a pinacol-type rearrangement.

Bromoalkyne **3.12** was prepared in two steps by treating 2-nitrobenzaldehyde with carbon tetrabromide and triphenylphosphine to afford dibromoalkene **3.15** in 91% yield, which under basic conditions eliminated to form **3.12** in quantitative yield (**Scheme 3.4**).[139]

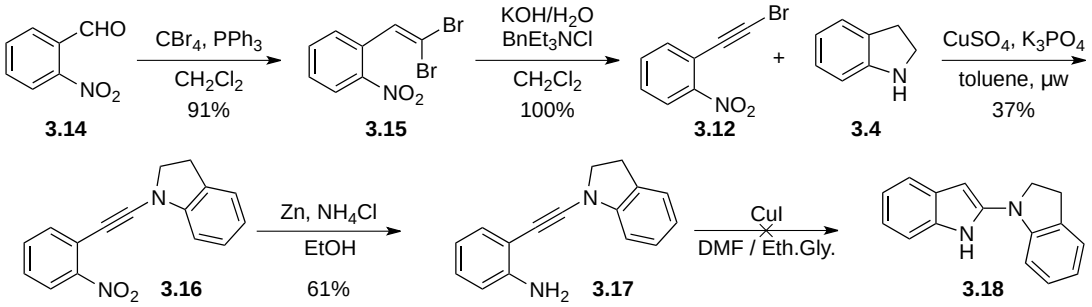

Scheme 3.4. Synthesis of 2-alkynyl aniline derivative **3.17**.

Standard copper-mediated coupling of the bromoalkyne with indoline (**3.4**) failed to proceed in appreciable yields.[140] Microwave-assisted coupling successfully formed alkyne **3.16**, albeit in 37% yield after optimization on small scale (<200 mg). Reduction

of the nitro group using zinc and ammonium chloride gave aniline **3.17** in 61% yield, although copper iodide mediated indole formation failed to produce the desired indole (**3.18**).

Protected 2,3-dihydrotryptophan was synthesized in parallel to this model study to be used in place of indoline (**3.4**) above. *N*-Cbz tryptophan was treated with iodomethane to form the methyl ester (**3.20**) in quantitative yield (**Scheme 3.5**). Reduction of **3.20** using $BH_3 \cdot Me_2S$ in THF and TFA gave 2,3-dihydrotryptophan derivative **3.21** in 79% yield. Coupling using the previously optimized conditions afforded alkyne **3.22** in 45% yield, although reduction to aniline **3.23** gave only trace amounts of the desired product.

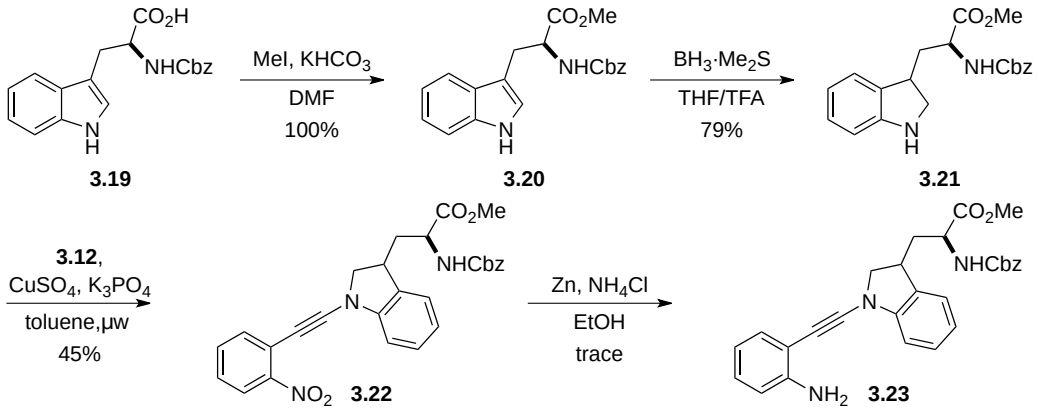

Scheme 3.5. Synthesis of 2,3-dihydrotryptophan alkyne derivative.

3.3: Evolution of Coupling Strategy

3.3.1: Witkop's Pyrroloindole

At this point, we took a step back and looked to nature for inspiration. It is unlikely that fungi synthesize chetomin by such contrived routes. If chetomin is derived naturally from two molecules each of tryptophan and serine, why not start with tryptophan and serine–optically pure, readily available compounds? Moreover, it is likely

that the pyrroloindoline core is formed in nature prior to coupling with the second half of the molecule, if not concomitantly. Witkop's pyrroloindole (**3.24**) was identified as a synthetically useful intermediate in the synthesis of chetomin that could be formed readily from tryptophan.[141] Halogenation of the indole double bond would provide a handle that could be substituted with another indole, ideally tryptophan, all with the potential for some stereocontrol (**Scheme 3.6**).

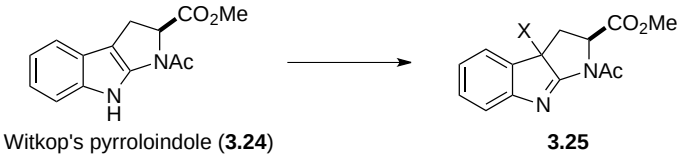

Witkop's pyrroloindole (**3.24**) **3.25**

Scheme 3.6. Witkop's pyrroloindole inspiration.

Retrosynthetically, we could form advanced intermediate **3.26** from the coupling of bromopyrroloindoline **3.28** and a suitably protected tryptophan derivative (**3.27**, **Scheme 3.7**). Both of these coupling partners could be synthesized in a few steps from tryptophan.

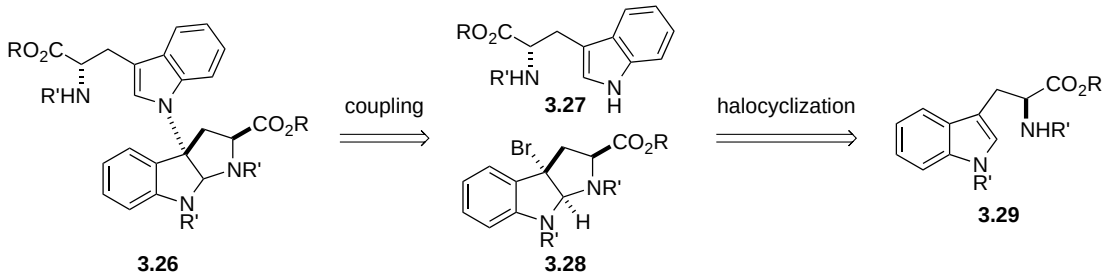

3.26 **3.27** **3.28** **3.29**

Scheme 3.7. Retrosynthetic plan using pyrroloindoline.

Tryptophan methyl ester (**3.30**) was protected as the trifluoroacetate amide (**3.31**), then cyclized to pyrroloindole **3.32** using *t*-BuOCl in 63 % overall yield (**Scheme 3.8**). Treatment of **3.32** with sodium hydride and NBS did not provide the desired bromopyrroloindole.[142]

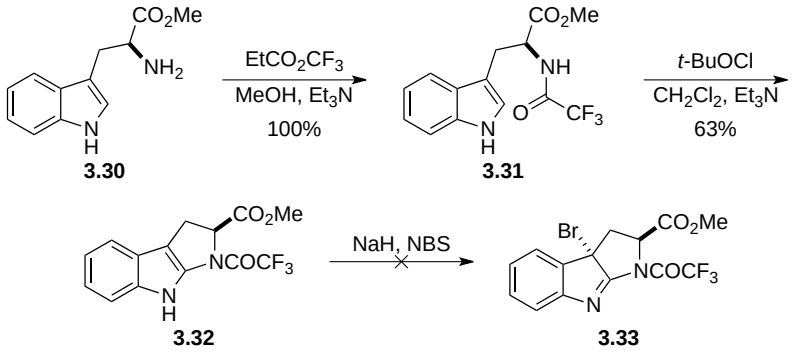

Scheme 3.8. Attempted synthesis of 3-bromopyrroloindole.

3.3.2: Indole–Aniline Coupling

This stepwise procedure to **3.33** was put on hold after a report from the Baran group was published, showing an analogous sequence that showed promise at reducing our synthesis of **3.26** to one step. Baran showed that treatment of *N*-Boc-Trp-OMe (**3.34**) and 2-iodoaniline with *N*-iodosuccinimide in acetonitrile afforded the desired C-N bond and C-3 quaternary center in one pot (**Scheme 3.9**).[130-132]

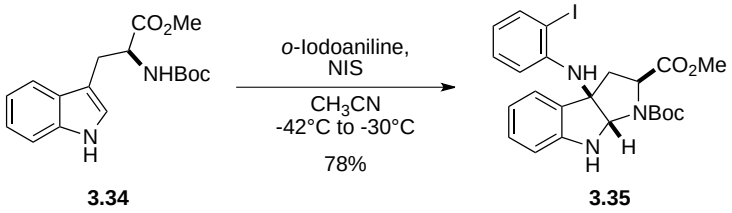

Scheme 3.9. Formation of key C-3 quaternary center.

We repeated this chemistry using indoline in place of 2-iodoaniline, but only starting material was recovered (**Scheme 3.10**). Ideally, this reaction would be done with tryptophan or 2,3-dihydrotryptophan, eliminating the need for a Larock indole synthesis with the iodoaniline. To our disappointment, the reaction only worked as originally reported with 2-iodoaniline, despite numerous attempts at the reaction with indoline (**3.4**), aniline (**3.37**), or 7-iodoindoline[143] (**3.36**).

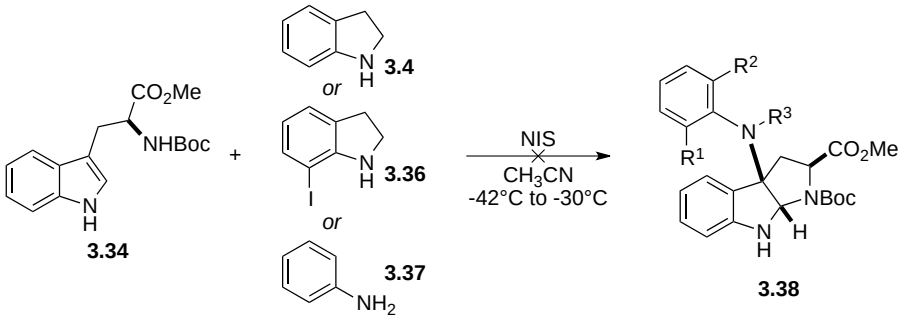

Scheme 3.10. Attempted formation of functionalized C3-N bond.

A suitable TMS-acetylene derivative was synthesized from L-serine methyl ester (**3.39**) and TMS-acetylene (**Scheme 3.11**). Serine methyl ester (**3.39**) was *N*-Boc protected (**3.40**) and the alcohol converted to the iodide (**3.41**) upon treatment with triphenylphosphine, imidazole, and iodine. TMS-acetylene bromide (prepared in one step, 72% yield) was coupled to serine-derived halide **3.41** to afford the desired alkyne (**3.42**) in 40% yield.[132]

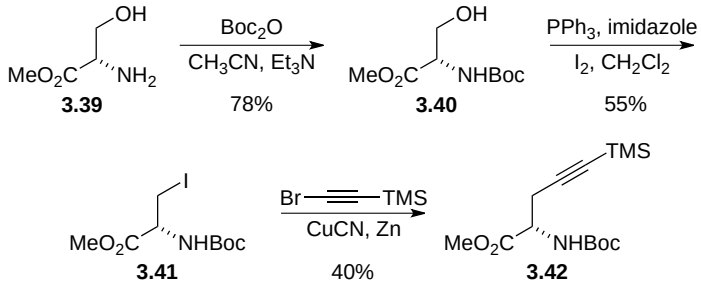

Scheme 3.11. Key alkyne synthesis.

Alkyne **3.42** was subjected to Larock annulation with iodoaniline **3.12** to form indole **3.43**. Saponification to the diacid (**3.44**) proceeded in good yield. While this route afforded access to advanced intermediate **3.44** in decent yields, it suffered from high step count due to the necessary Larock annulation and provided access to a *diastereomer* of chetomin. We again looked back to the convergent, stepwise approach that we had

previously envisioned (**Scheme 3.7**) and attempted the desired sequence in a stepwise manner.

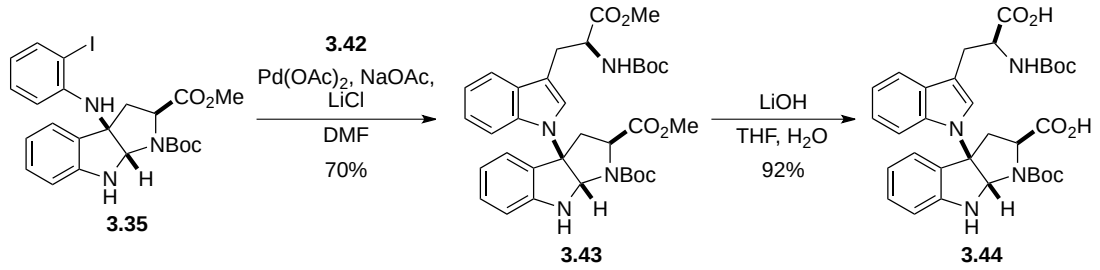

Scheme 3.12. Larock indole synthesis of tryptophan dimer.

3.3.3: Coupling to *exo*-3-bromopyrroloindoline

N-Cbz-Trp-OMe (**3.20**) was synthesized in >99% yield from tryptophan and the indole nitrogen protected as the Boc carbamate (**3.46**). Per a report published by Espejo and Rainier in 2008, addition of NBS and PPTS to **3.46** afforded *exo*-3-bromopyrroloindoline **3.47** in 89% yield (**Scheme 3.13**).[133,144] Deprotonation by KO*t*Bu in the presence of indole formed the C3-N bond in 28% yield and resulted in epimerization of the methyl ester to the thermodynamically more favorable *endo* position (**3.48**).[133]

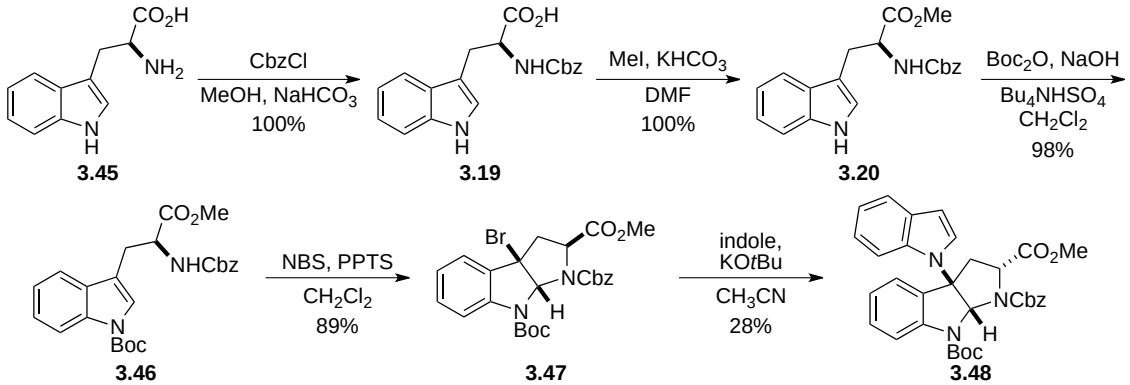

Scheme 3.13. Coupling of 3-bromopyrroloindoline.

This result evolved into our current strategy for the formation of the C3-N1' bond. The stereochemistry of **3.48** matches the enantiomer of what would be needed for a synthesis of chetomin (i.e. **3.51**, **Scheme 3.14**). We could either form the bromopyrroloindoline from L-tryptophan and to it couple D-tryptophan and D-serine to synthesize the enantiomer of chetomin, or we could synthesize the D-tryptophan-derived pyrroloindoline (**3.52**) and use the natural amino acid isomers for the remaining three couplings in a synthesis of (+)-chetomin (**1.12**). Initially, however, only the cheaper L-isomers were used for all four fragments as conditions were worked out for the remaining steps.

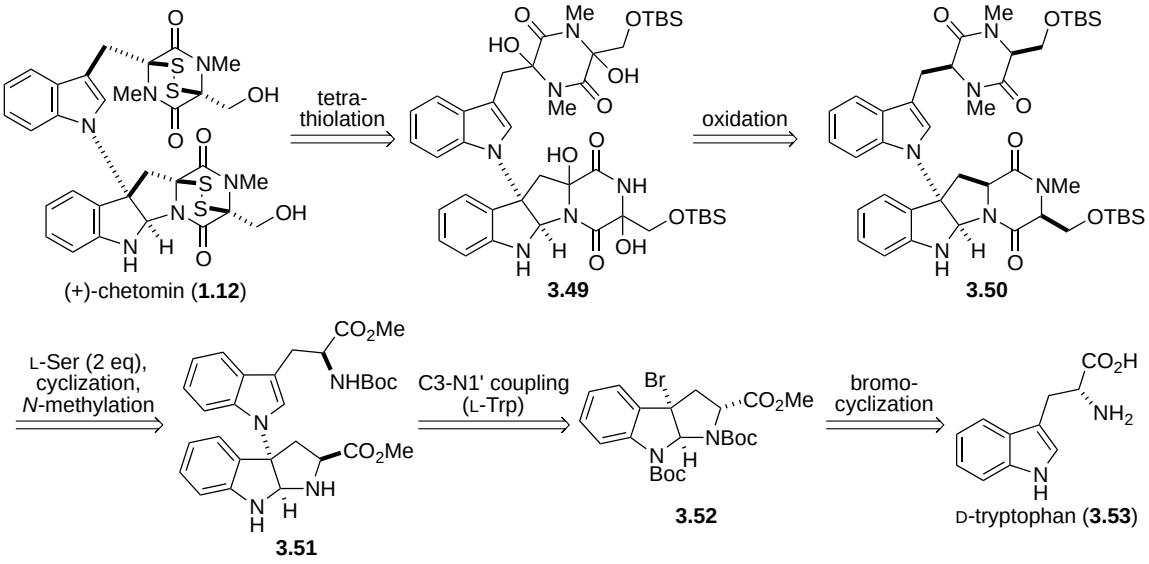

Scheme 3.14. Retrosynthetic analysis of (+)-chetomin.

3.3.4: Attempted Coupling to Tetracyclic Bromide

The next goal was to test a more divergent approach. Ideally, the dioxopiperazine ring could be formed prior to coupling with indole (**Scheme 3.15**).

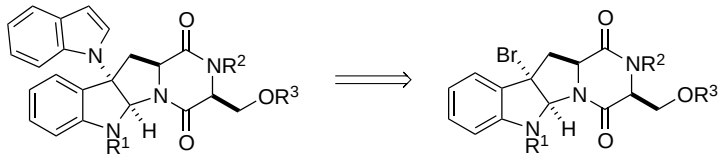

3.54 **3.55**

Scheme 3.15. Coupling with more advanced bromopyrroloindoline.

Unfortunately, synthesis of **3.55** was more challenging than expected. Peptide coupling of tryptophan derivative (**3.56**) with *N*-Me-L-Ser-OMe initially suffered from poor yield. Eventually, the coupling was optimized using EDCI as the coupling reagent to afford dipeptide **3.57a** in good, reproducible yield (**Scheme 3.16**). Cyclization to the dioxopiperazine (**3.58a**) failed under methods traditionally used in the Williams group (i.e. refluxing toluene with catalytic 2-hydroxy pyridine following Boc deprotection). However, microwave heating of neat *N*-Boc dipeptide **3.57a** at 180 °C effected deprotection and cyclization to the dioxopiperazine (**3.58a**) in two minutes. The recovered product did not require any purification before proceeding to the next step.

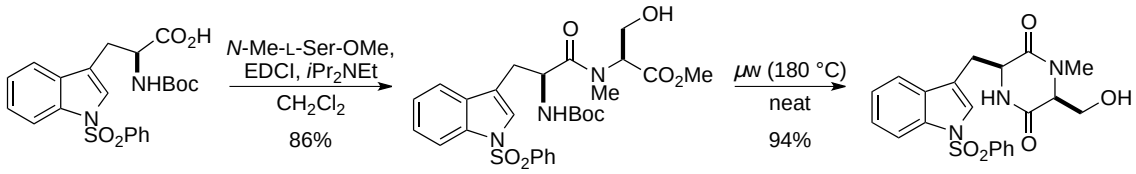

3.56 **3.57a** **3.58a**

Scheme 3.16. Optimized peptide coupling and dioxopiperazine formation.

Gratifyingly, this procedure was generally applicable to a variety of related dipeptides. Dioxopiperazines **3.58a-e** were all synthesized with consistently good yield on scales up to 500 mg (**Scheme 3.17**).

Several of the dioxopiperazines were cyclized to the corresponding bromopyrroloindolines (**3.55**, **Scheme 3.18**). Despite numerous attempts, coupling of indole failed using conditions analogous to those first used in **Scheme 3.13**.

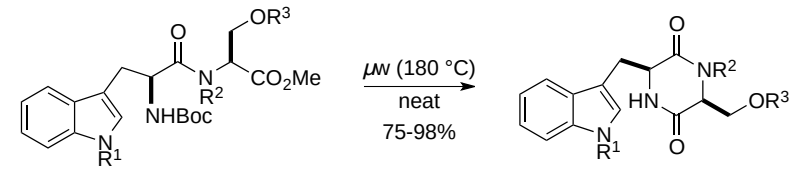

3.57a (R^1=SO_2Ph, R^2=Me, R^3=H)
3.57b (R^1=H, R^2=Me, R^3=H)
3.57c (R^1=H, R^2=H, R^3=H)
3.57d (R^1=SO_2Ph, R^2=H, R^3=H)
3.57e (R^1=SO_2Ph, R^2=H, R^3=TBS)

3.58a-e

Scheme 3.17. Microwave assisted dioxopiperazine synthesis.

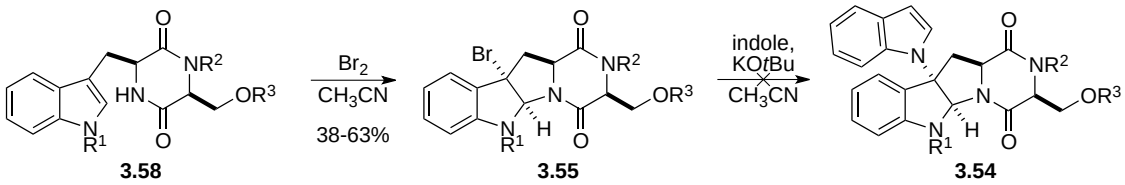

3.58 **3.55** **3.54**

Scheme 3.18. Attempted coupling with indole.

3.4: Epidithiodioxopiperazine Formation

While unsuccessfully attempting to couple indole or tryptophan to **3.55**, we also began to explore methods for the introduction of sulfur to the same dioxopiperazine. Epidithiodioxopiperazine **3.63**, essentially a monomer of chetomin, was synthesized by a general method recently described by the Sodeoka group in Japan (**Scheme 3.19**).[123,124] Benzenesulfonamide protection of L-tryptophan (**3.59**) gave compound **3.56**, to which L-Ser-OMe was coupled to afford dipeptide **3.57d**. The primary alcohol was protected as the silyl ether (**3.57e**) and suffered microwave-induced deprotection and cyclization to dioxopiperazine **3.58e**. Treatment with bromine affected the bromocyclization to *endo*-pyrroloindoline **3.55e**. Addition of iodomethane successfully methylated the secondary amide, but also resulted in the loss of the silyl ether to primary alcohol **3.60**. After reprotecting the alcohol, diol **3.62** was formed following radical bromination and

substitution of **3.61**. Addition of the diol to condensed hydrogen sulfide and $BF_3{\cdot}OEt_2$ and oxidation of the resultant disulfide with iodine gave epidithiodioxopiperazine **3.63**.

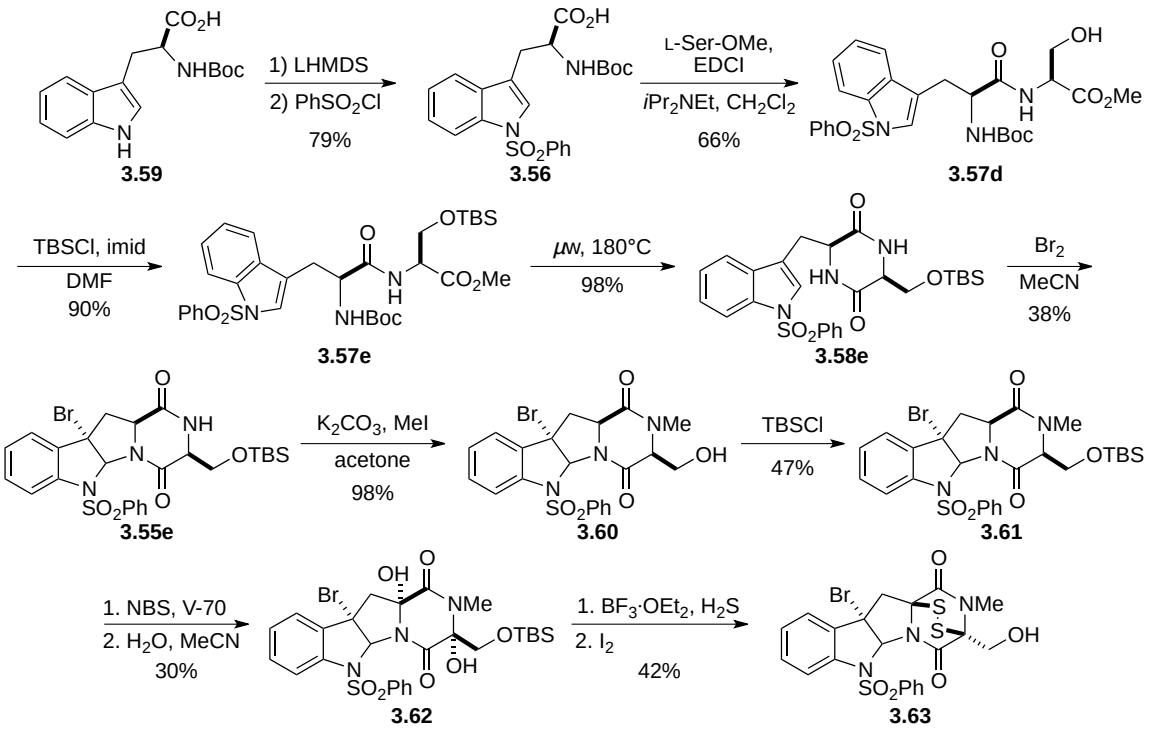

Scheme 3.19. Formation of the disulfide bridge.

3.5: Attempted Core Construction

3.5.1: Problematic Peptide Couplings

With a method for the formation of an epidithiodioxopiperazine in hand, we went back to the method described in **Scheme 3.13** for construction of the key C3-N1' bond. *N*-Boc-tryptophan methyl ester (**3.34**) was prepared and further protected as the benzenesulfonamide (**3.64**, **Scheme 3.20**). Cyclization to the bromopyrroloindoline (**3.65**) proceeded readily upon treatment with NBS and PPTS, and coupling of **3.65** with *N*-Boc-Trp-OMe (**3.34**) gave **3.66** in poor yield (34%). Saponification to diacid **3.67** was followed by peptide coupling with serine methyl ester to give peptide **3.68**. TBS

protection of the primary alcohols proceeded in good yield, although cyclization to the dioxopiperazines (**3.70**) using the previously described microwave conditions failed, as did the reaction with traditional thermal conditions.

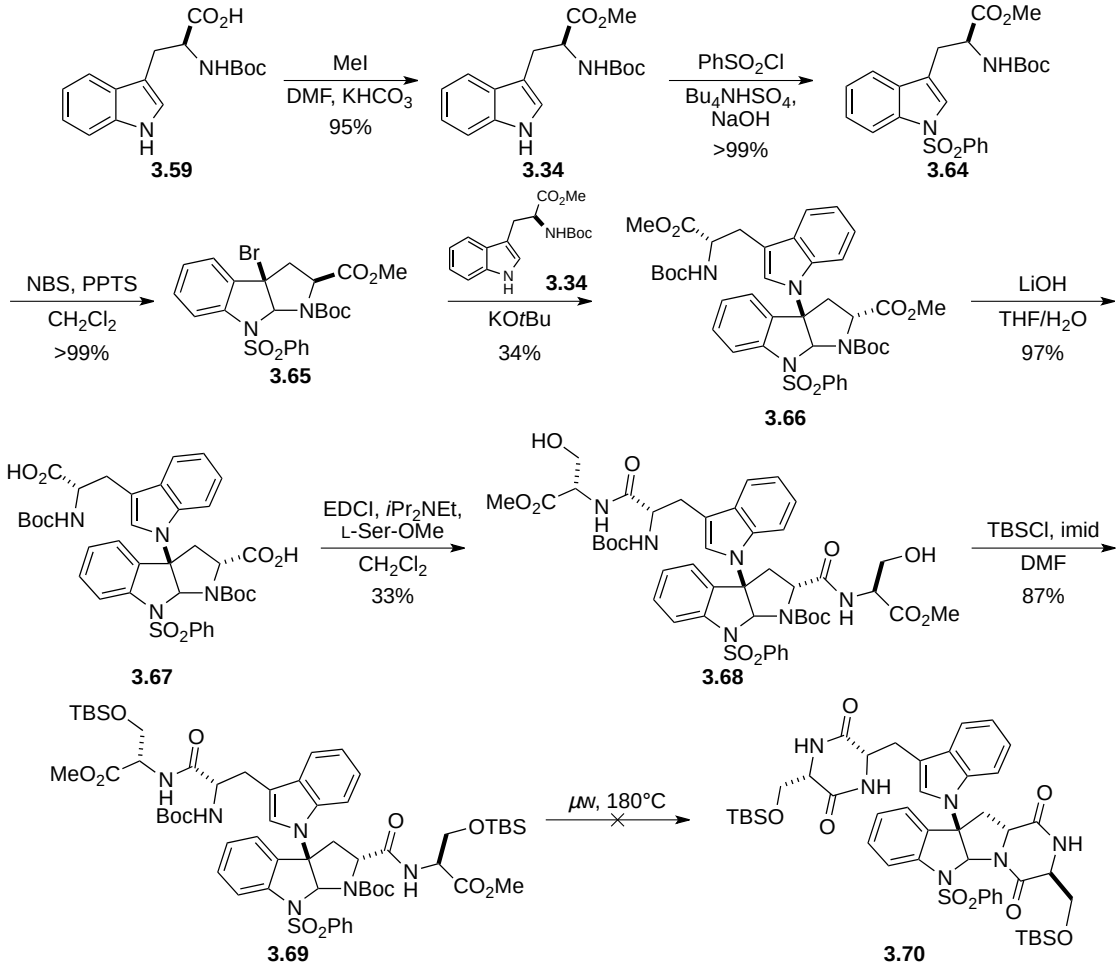

Scheme 3.20. Coupling to 3-bromopyrroloindoline and attempted dioxopiperazine formation.

Deprotection of the Boc groups of intermediate **3.66** and peptide couplings on the resultant amines gave tripeptide **3.71** (**Scheme 3.21**). Intriguingly, formation of the tetrapeptide of **3.66** was never achieved, despite numerous attempts with varying coupling conditions and protecting groups on the amino acid functionalities.

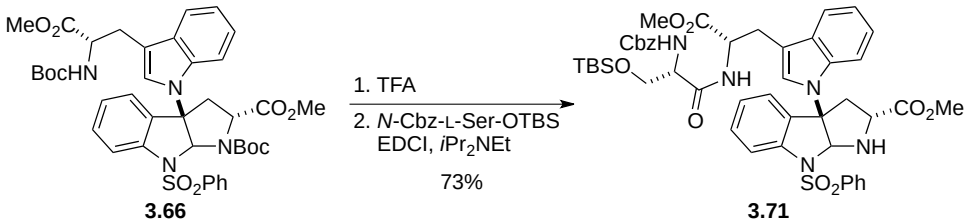

Scheme 3.21. Attempted synthesis of alternate dioxopiperazine precursor.

3.6: Synthesis of Heptacyclic Core

3.6.1: Synthesis of Dioxopiperazines

We reasoned that the failed cyclization attempts in **Scheme 3.20** and peptide coupling problems in **Scheme 3.21** could be due to steric congestion caused by the indoline protecting group. Thus, *N*,*N*'-Boc$_2$-D-Trp-OMe was prepared from D-tryptophan (**3.73**, **Scheme 3.22**). Bromocyclization proceeded stereoselectively to *exo*-bromopyrroloindoline **3.74**. Coupling with *N*-Boc-L-Trp-OMe gave *endo*-intermediate **3.75** in decent yield, while deprotection of the carbamate gave the key intermediate for peptide coupling. In the absence of an aniline protecting group, peptide coupling proceeded in 44% yield to tetrapeptide **3.76**. With the Fmoc amines, deprotection and cyclization to dioxopiperazine **3.77** proceeded in one pot upon treatment with morpholine in THF with gentle heating. At this point, all of the amides needed to be methylated prior to the introduction of sulfur, which first required protection of the aniline nitrogen. Selective Boc protection at this position was never achieved, nor was protection of tetrapeptide **3.76** to **3.78**.

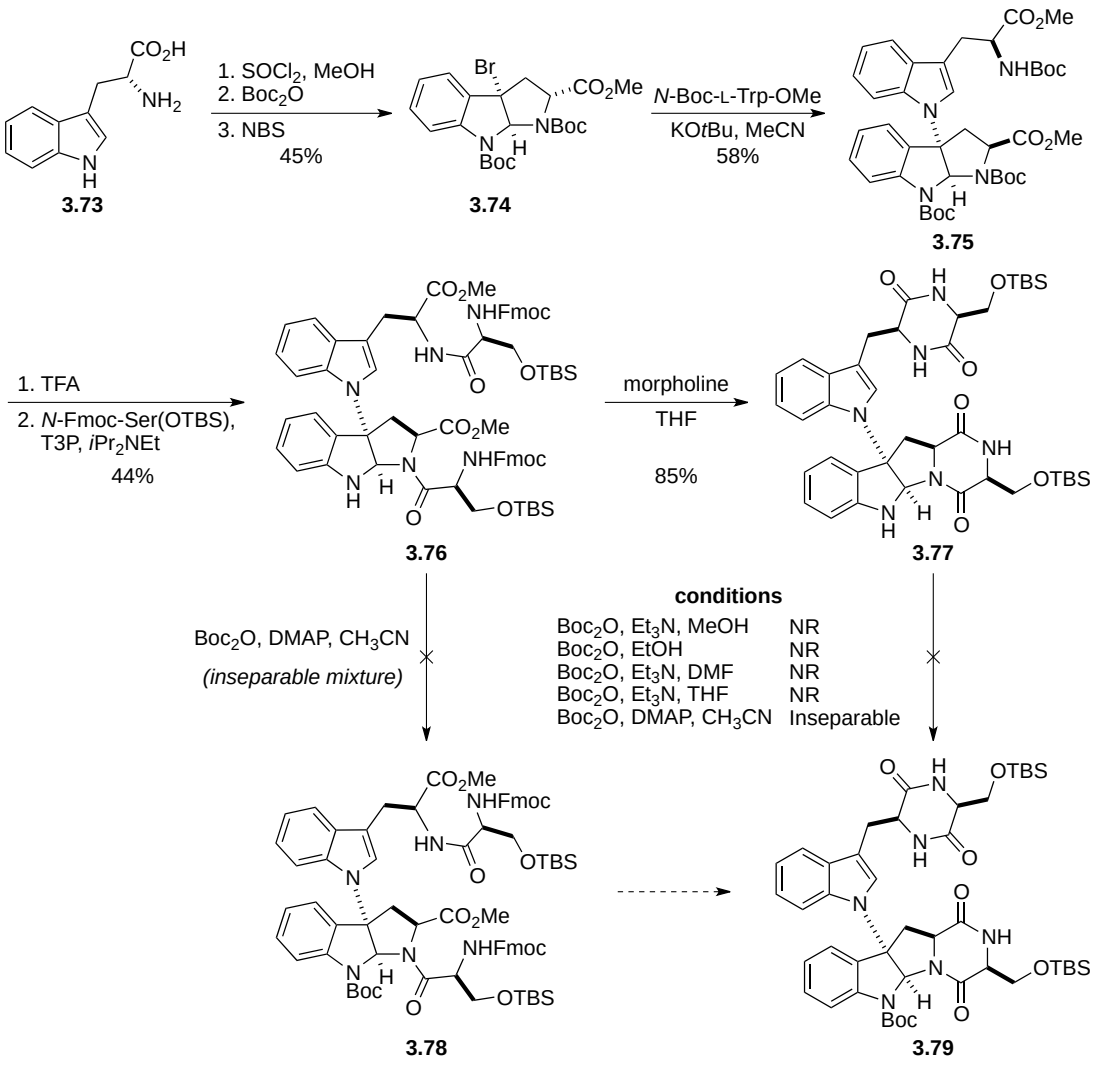

Scheme 3.22. Synthesis of dioxopiperazine **3.77**.

3.6.2: Initial *N*-Methyl Amino Acid Incorporation

It was clear that *N*-methyl tryptophan and serine derivatives needed to be prepared to avoid late stage *N*-methylation. Months of laborious chemistry went in to preparing these seemingly simple derivatives, and ultimately bromopyrroloindoline **3.74** was coupled to *N*-Me,Boc-L-Trp-OMe (**Scheme 3.23**). Deprotection of the two Boc groups gave **3.80**, a key intermediate used extensively in the remainder of this chapter. Peptide coupling with *N*-Me,Boc-Ser(OBn) gave tetrapeptide **3.81**, which was cyclized to

dioxopiperazine **3.82** in excellent yield after Boc deprotection and addition of morpholine.

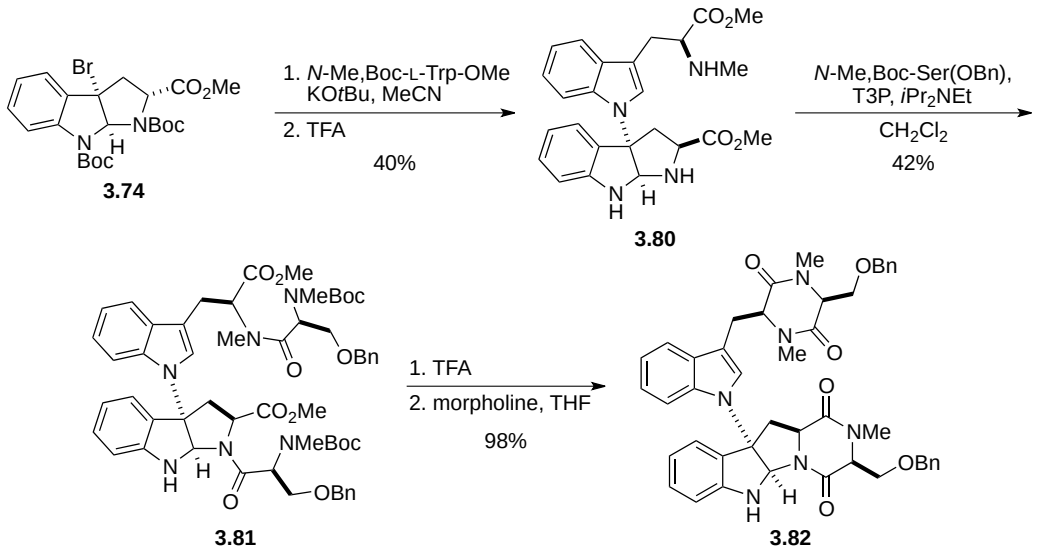

Scheme 3.23. Synthesis of (*N*-Me)$_3$ dioxopiperazine.

Initially we attempted to again protect the aniline nitrogen before subjecting the material to radical bromination conditions. All attempts to Boc or TBS protect **3.82** failed (**Scheme 3.24**). We decided to move forward to try the bromination anyway on diol **3.84**, but the benzyl ether resisted all deprotection attempts.

A serine derivative lacking the benzyl group was added to diamine **3.80**, but this coupling failed to give the desired tetrapeptide (**Scheme 3.25**). The benzyl group seemed to be a poor choice of protecting group for this intermediate, necessitating the synthesis of *N*-Me,Fmoc-Ser(OTBS).

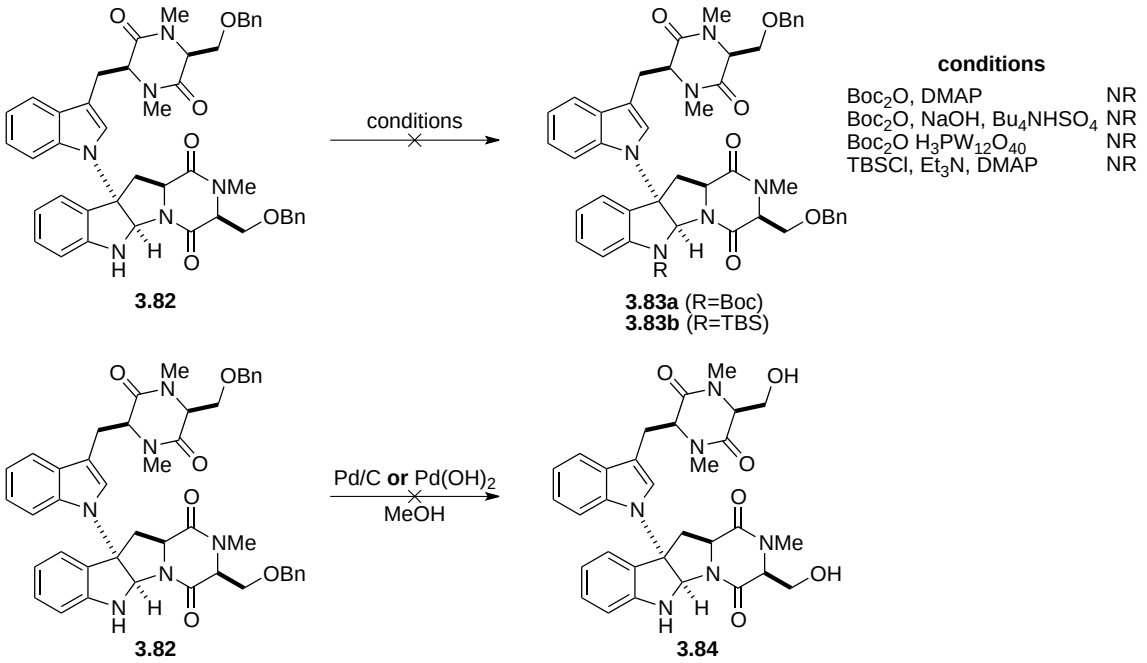

Scheme 3.24. Attempted protection and deprotection of **3.82**.

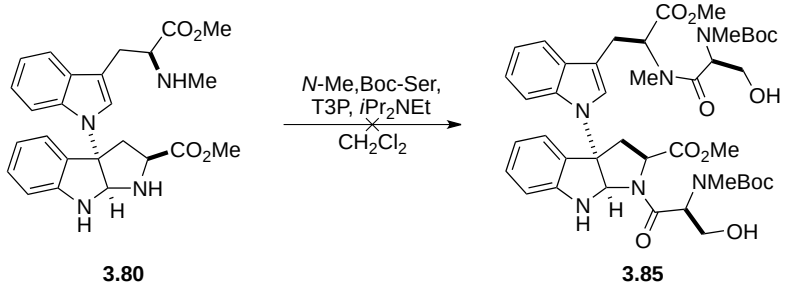

Scheme 3.25. Attempted peptide coupling with *N*-Me,Boc-Ser(OH).

3.6.3: Bypassing the Serine Side Chain with Sarcosine

While working out the synthesis of an appropriate *N*-Me serine derivative, the entire serine side chain was eliminated from the synthesis. *N*-Fmoc sarcosine (**3.87**) was prepared and coupled to diamine **3.80** (**Scheme 3.26**). Cyclization to dioxopiperazine **3.88** proceeded smoothly. However, the radical bromination and hydroxylation did not produce the desired tetraol (**3.89**).

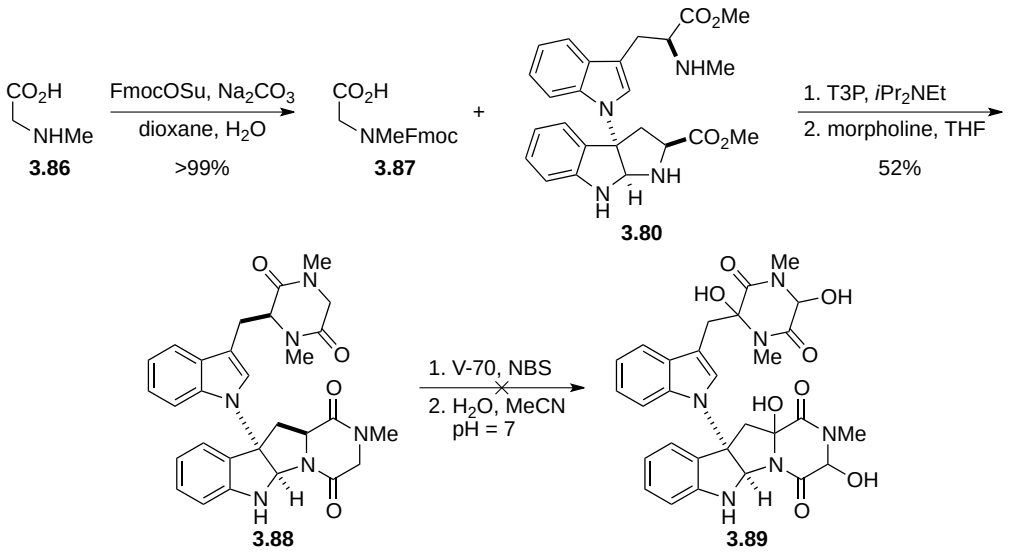

Scheme 3.26. Synthesis of sarcosine-derived dioxopiperazine.

3.6.4: Completion of the Carbon Skeleton of Chetomin

Meanwhile, *N*-Me,Fmoc-Ser(OTBS) was successfully prepared and coupled to **3.80** (**Scheme 3.27**). Dioxopiperazine **3.90** was easily formed as described above.

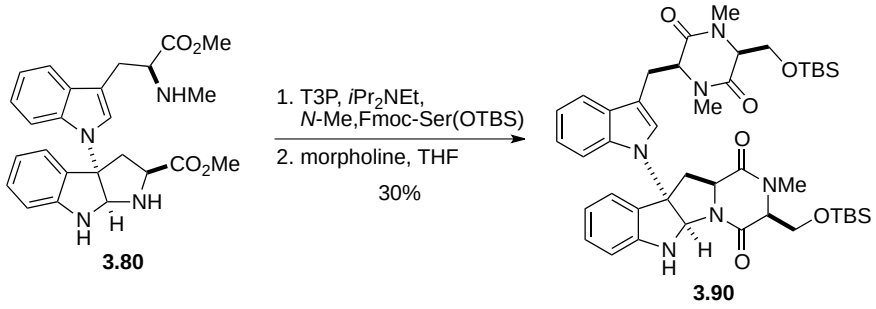

Scheme 3.27. Synthesis of (*N*-Me)$_3$ dioxopiperazine.

3.6.5: Attempted Epidithiodioxopiperazine Formation

Numerous attempts have been made to convert both the serine- and sarcosine-derived dioxopiperazines (**3.90** and **3.88**) to the corresponding epidithiodioxopiperazines

(**1.12** and **3.91**, **Scheme 3.28**). Much to our disappointment, both have refused to yield to our continued efforts.

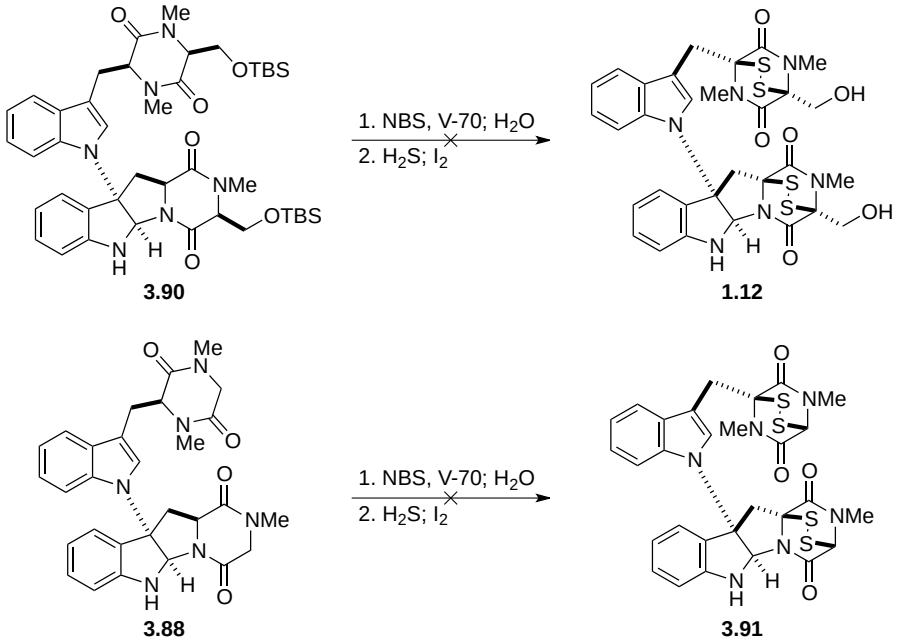

Scheme 3.28. Attempted epidithiodioxopiperazine formations.

3.7: Proposed Future Studies

3.7.1: Proposed Synthesis of Tetraol

We have successfully synthesized the carbon framework of chetomin. The final key to a total synthesis is the oxidation of this core (**3.90** or **3.88**) to tetraols **3.92** or **3.89** (**Scheme 3.29**). Numerous examples (see Chapter 2) suggest that this compound should readily form intermediate iminium ions such as **3.93** and **3.94**. Addition of sulfur should occur at the less hindered faces of the dioxopiperazines.[122-125,127]

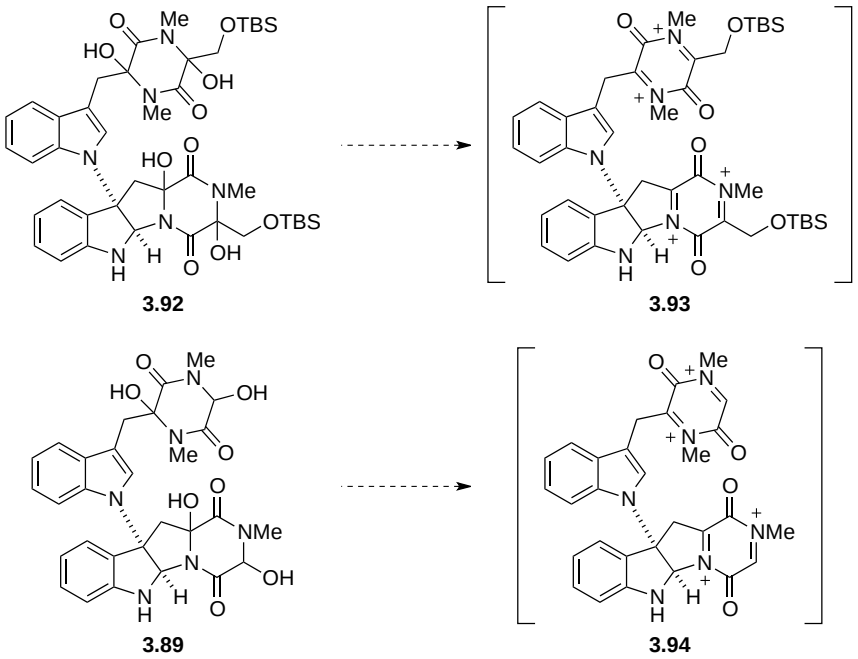

Scheme 3.29. Key tetraols and iminium intermediates.

Synthesis of the tetraols should be possible either by the method previously attempted (radical bromination and substitution) or by mild oxidation with bis(pyridine)silver(I) permanganate (**Scheme 3.30**). In the synthesis of gliocladin B, *n*-Bu_4NMnO_4 was also used as an oxidant for this reaction.[127] Repeated trials will be necessary to produce optimal conditions, requiring sufficient time, material, and persistence. Three potential problems may complicate this route: (1) The free indoline nitrogen may require protection if it proves to be reactive under the proposed radical or oxidation conditions. This has previously been a difficult protection, and while a Boc or silyl group would be ideal, a trifluoroacetate group would also be appropriate (although it would introduce an additional deprotection step). (2) The desired hemiaminal may very well be unstable and require additional functionalization after it is formed before sulfur can be introduced. (3) The serine-derived bis(dioxopiperazine) (**3.90**) is susceptible to elimination of the primary alcohol.

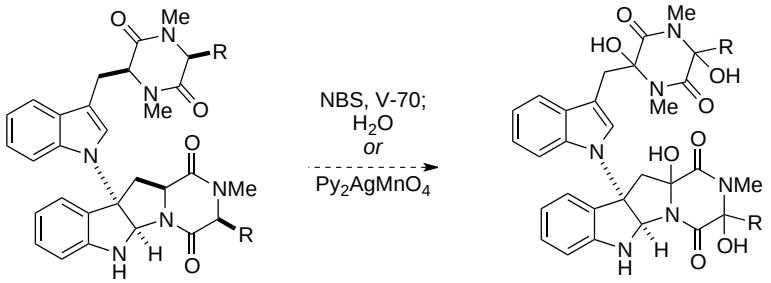

3.90 (R=CH_2OTBS)
3.88 (R=H)

3.92 (R=CH_2OTBS)
3.89 (R=H)

Scheme 3.30. Possible oxidations.

3.7.2: Bypassing the Tetraol

It would also be worth attempting the addition of sulfur directly to dioxopiperazines **3.90** and **3.88**. Both Nicolaou and Reisman took this approach in their respective epidithiodioxopiperazine syntheses, using S_8 and NaHMDS (**Scheme 3.31**).[128,129]

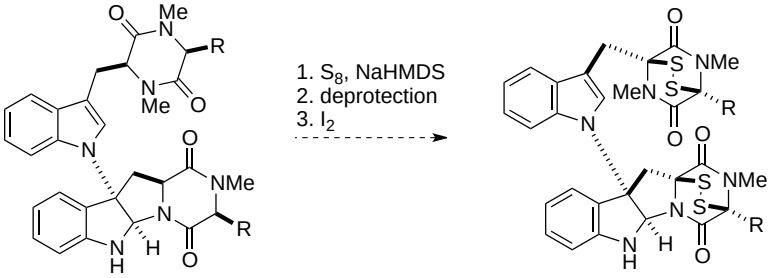

3.90 (R=CH_2OTBS)
3.88 (R=H)

1.12 (R=CH_2OTBS)
3.91 (R=H)

Scheme 3.31. Alternative sulfenylation.

3.7.3: Late-Stage Alkylation of Sarcosine Analogue

Lastly, if access to sarcosine-derived epidithiodioxopiperazine **3.91** proves to be the most efficient route, conversion to chetomin can occur using inspiration from Kishi's early syntheses of sporidesmin and gliotoxin (**Scheme 3.32**).[113-118] Reduction of the

disulfide bridges and protection as the thioacetals would give **3.95**. Alklation with BOMCl would install the protected serine side chain (**3.96**), which could be deprotected and the disulfide revealed to give chetomin (**1.12**).

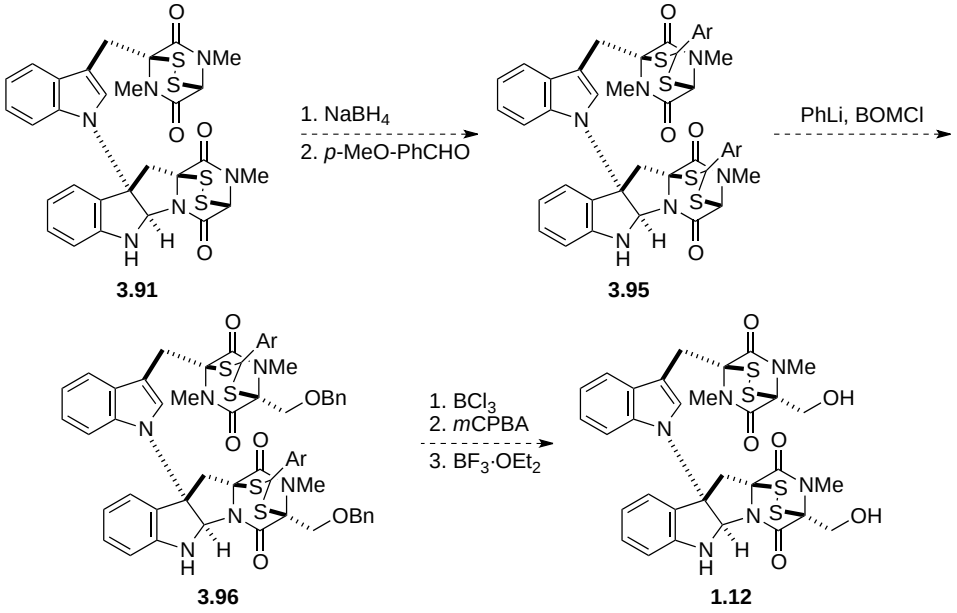

Scheme 3.32. Proposed conversion of **3.91** to chetomin.

3.8: Concluding Remarks

It will be difficult to leave this project behind with the total synthesis of chetomin so near to completion. However, short of a completed synthesis, we did achieve the remaining goals for this project in the synthesis of dioxopiperazines **3.88** and **3.90**. The key C3-N1' bond formation works for a variety of substrates and is a convergent approach to the core structure. A variety of peptide couplings were optimized for this system, producing di- and tetrapeptides in respectable yields. Cyclization of the dioxopiperazine rings is now performed consistently and in high yields. Moreover, the entire sequence is scalable and allows quick access to gram quantities of material. All

that remains is synthesis of the disulfide bridges to complete a total synthesis of (+)-chetomin.

CHAPTER 4

Synthetic Approach to Sporidesmin A

4:1: Introduction

In 2010, we had the opportunity to write a book chapter on biomimetic syntheses of tryptophan-derived dioxopiperazines, in which Kishi's elegant synthesis of (±)-sporidesmin A (**1.11**) was featured (**Figure 4.1**).[145] We were drawn to the densely functionalized structure of sporidesmin A, including the polysubstituted aromatic ring, pyrroloindoline core, hydroxyl groups at C3 and C12, and the epidiothiodioxopiperazine ring. We hoped that chemistry developed for the synthesis of chetomin (see Chapter 3) could be applied to an improved, stereoselective synthesis of sporidesmin A.

As detailed in Chapter 1, sporidesmin A was isolated from *Pithomyces chartarum* in 1959 as part of a forty-year nationwide search for the cause of facial eczema, a disease that was plaguing sheep herds of New Zealand.[63-65] Facial eczema causes extensive liver damage in sheep and has been responsible for massive economic losses in New Zealand since the late 1890s. A dental nurse allegedly discovered that the addition of zinc sulfate to drinking water could prevent the disease, a measure still endorsed by veterinarians.[146] Epidithiodioxopiperazines are known to form a 2:1 complex with zinc ions, inhibiting the generation of the superoxide anion radical and likely providing the observed protective effects of zinc against sporidesmin.[69,70] The toxicity of sporidesmin toward sheep was responsible for many of the early advances made in the study of

epidithiodioxopiperazines, including the isolation and characterization of sporidesmin and related metabolites (**Figure 4.1**).

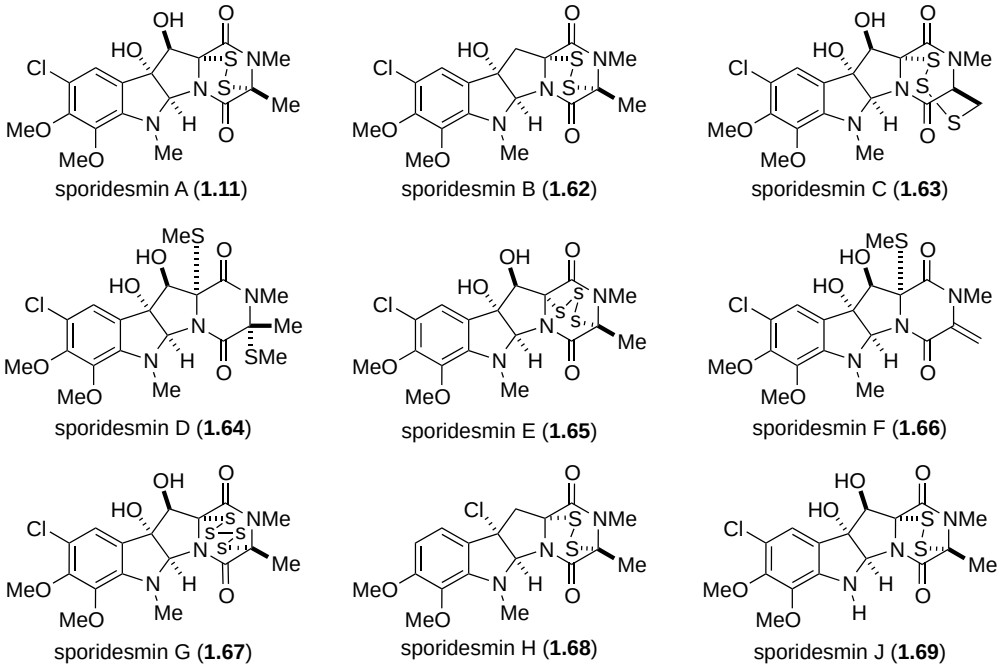

Figure 4.1. Sporidesmin A and related fungal metabolites.

No reasonable argument can be made advocating that a new synthesis of sporidesmin A will have any direct impact on mankind, medicine, or even sheep herds in New Zealand. Our interest is purely academic. Sporidesmin A is a synthetically challenging molecule, and pursuit of a total synthesis will allow us both to explore the scope of similar reactions employed toward the total synthesis of chetomin and to expand our general understanding of the reactivity of epidithiodioxopiperazine alkaloids.

4.2: Retrosynthetic Analysis

The primary goal of this project was to develop a scalable total synthesis of (–)-sporidesmin A (**1.11**). Compared to chetomin (**1.12**), sporidesmin A presents several unique synthetic challenges, the most significant of which is a highly substituted aromatic

ring. We hoped to develop an efficient synthesis of the requisite substituted L-tryptophan derivative and to apply the previously used bromocyclization reaction (**Scheme 3.13**) to form the pyrroloindoline core.

As with chetomin, we planned to introduce the disulfide bridge of (–)-sporidesmin A (**1.11**) at a late stage in the synthesis from hemiaminal **4.1** (**Scheme 4.1**). The hemiaminal could be formed by oxidation of tetracycle **4.2** after forming the pyrroloindoline core through oxidative cyclization and *N*-methylation of dioxopiperazine **4.3**. This intermediate is similar to many of the dioxopiperazines prepared in the previous chapter and was envisioned to arise via coupling of **4.4** with alanine, followed by cyclization.

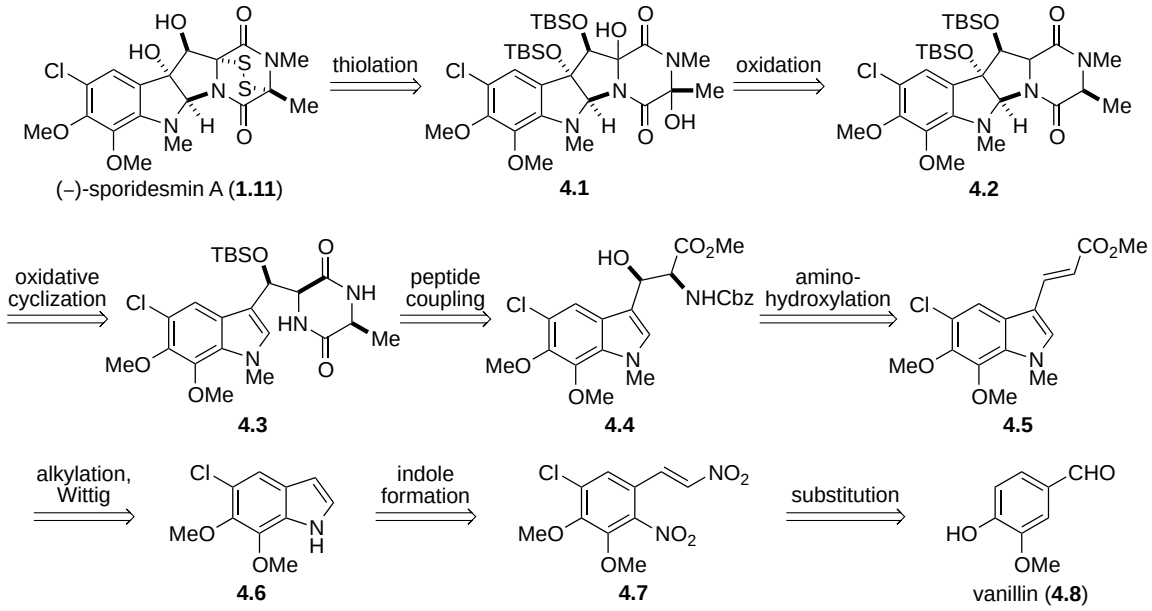

Scheme 4.1. Retrosynthetic analysis of (–)-sporidesmin A.

One key to an asymmetric synthesis is the preparation of β-hydroxytryptophan derivative **4.4**. We hoped to introduce both stereocenters and the amino acid portion of this intermediate through Sharpless asymmetric aminohydroxylation of unsaturated ester **4.5**. This ester could be formed by Wittig olefination of the aldehyde product of a

Vilsmeier–Haack reaction of indole **4.6**. Modified dinitrostyrene Batcho–Leimgruber conditions were planned for the formation of the indole from styrene **4.7**, prepared in several precedented steps from vanillin (**4.8**).

4.3: Synthetic Approach to Sporidesmin A

4.3.1: Preparation of Dinitrostyrene Derivative

Nitration of *O*-acetyl vanillin (**4.9**) afforded **4.10** when fuming nitric acid (>90%) was used as the nitronium source (**Scheme 4.2**). Fuming nitric acid was originally prepared fresh by distillation from a slurry of potassium nitrate and concentrated sulfuric acid, but this procedure seemed quite dangerous on scales producing more than 50 mL of nitric acid, prompting us to obtain the reagent from a commercial source.

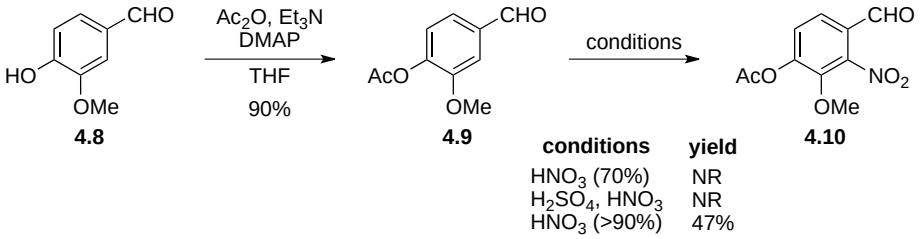

Scheme 4.2. Nitration of vanillin.

Following nitration, **4.10** was heated to reflux in aqueous KOH to afford phenol **4.11**, then *O*-methylation with dimethyl sulfate gave **4.12** in 99% yield (**Scheme 4.3**). The Henry reaction was used to prepare dinitrostyrene derivative **4.13** through addition of nitromethane to the aldehyde and subsequent elimination of water. Indole **4.14** was then prepared in low yield using modified Batcho–Leimgruber conditions.[147]

Originally, we had envisioned preparing chloroindole **4.6** from indole **4.14**. However, it seemed more prudent to chlorinate vanillin, as we would be less concerned with yield and could minimize the amount of chlorine gas used. Accordingly, 5-Cl-

vanillin (**4.15**) was prepared by bubbling chlorine gas through a solution of vanillin in acetic acid (**Scheme 4.4**).[148] Nitration, deacetylation, and methylation proceeded in good yield to provide aldehyde **4.18**. The Henry reaction gave dinitrostyrene **4.7** in low yield.[149]

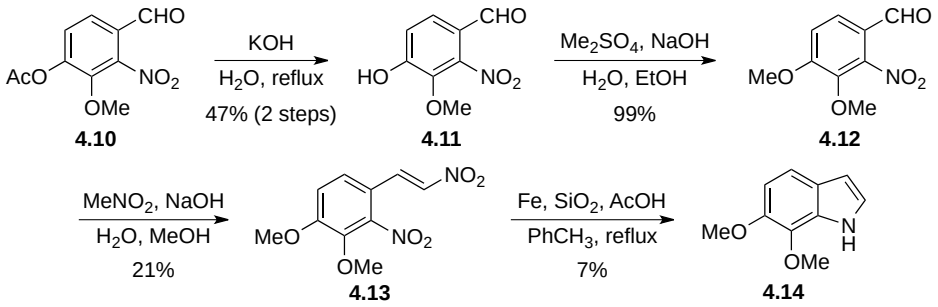

Scheme 4.3. Dimethoxyindole synthesis.

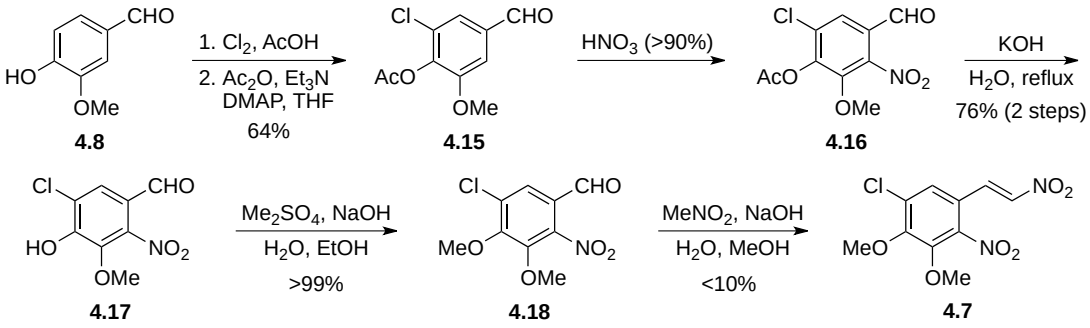

Scheme 4.4. Synthesis of 5-chloro-dinitrostyrene derivative.

We determined that the small amount of ethyl acetal **4.19** formed during the methylation reaction was detrimental to the yield of the Henry reaction (**Scheme 4.5**). To circumvent this problem, the crude mixture of **4.18** and **4.19** was treated with TFA in chloroform to cleave the acetal, affording pure **4.18**. Use of clean material greatly increased the ease of recrystallization and yield of the product of the Henry reaction (**4.7**).

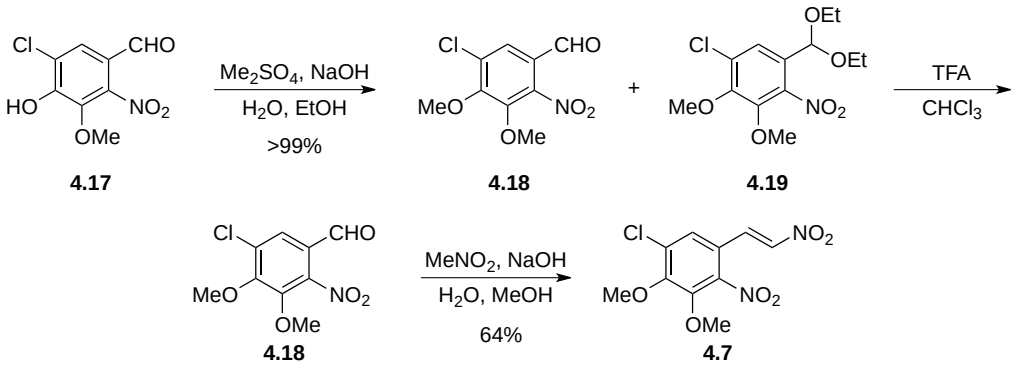

Scheme 4.5. Undesired acetal formation.

4.3.2: Indole Synthesis and Sharpless Asymmetric Aminohydroxylation

Synthesis of indole **4.6** proceeded in good yield using modified Batcho–Leimgruber conditions (**Scheme 4.6**). Following *N*-methylation, an aryl aldehyde was installed at C3 via the Vilsmeier–Haack reaction.[150] This aldehyde (**4.20**) was immediately converted to the unsaturated ester (**4.5**) upon Wittig reaction with the requisite phosphonium ylide. Sharpless asymmetric aminohydroxylation gave β-hydroxytryptophan derivative **4.4**, albeit in modest yield.[151]

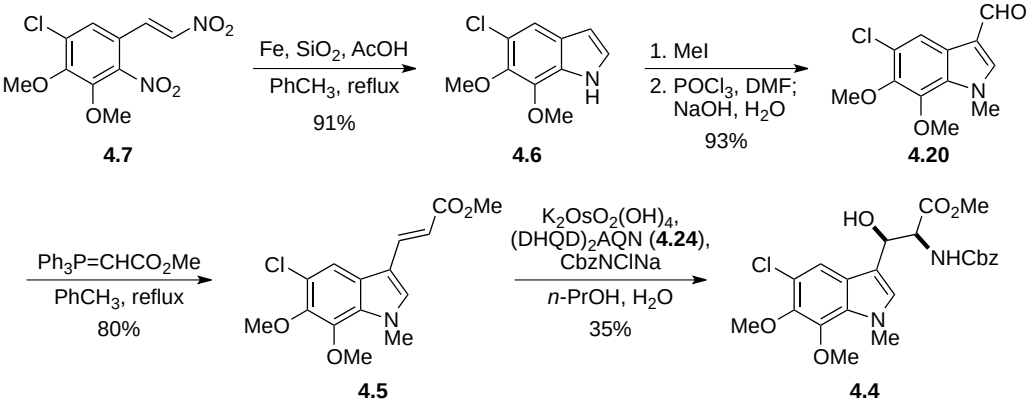

Scheme 4.6. Asymmetric aminohydroxylation.

While it is commercially available, we opted to prepare the ligand for the Sharpless reaction as described in the literature (**Scheme 4.7**).[152] Acylation of

difluorobenzene gave dione **4.23**, which was alkylated to form the dihydroquinidinyl anthraquinone ligand (**4.24**) in good yield.

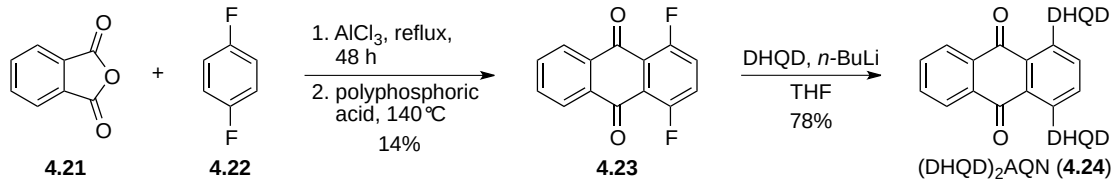

Scheme 4.7. Preparation of $(DHQD)_2AQN$.

4.3.3: Dioxopiperazine Formation

β-hydroxytryptophan derivative **4.4** was protected as the silyl ether (**4.25**) and the Cbz group cleaved to reveal the free amine (**4.26**, **Scheme 4.8**). EDCI-mediated coupling of *N*-Boc-Ala-OH provided dipeptide **4.27** in 59% yield.

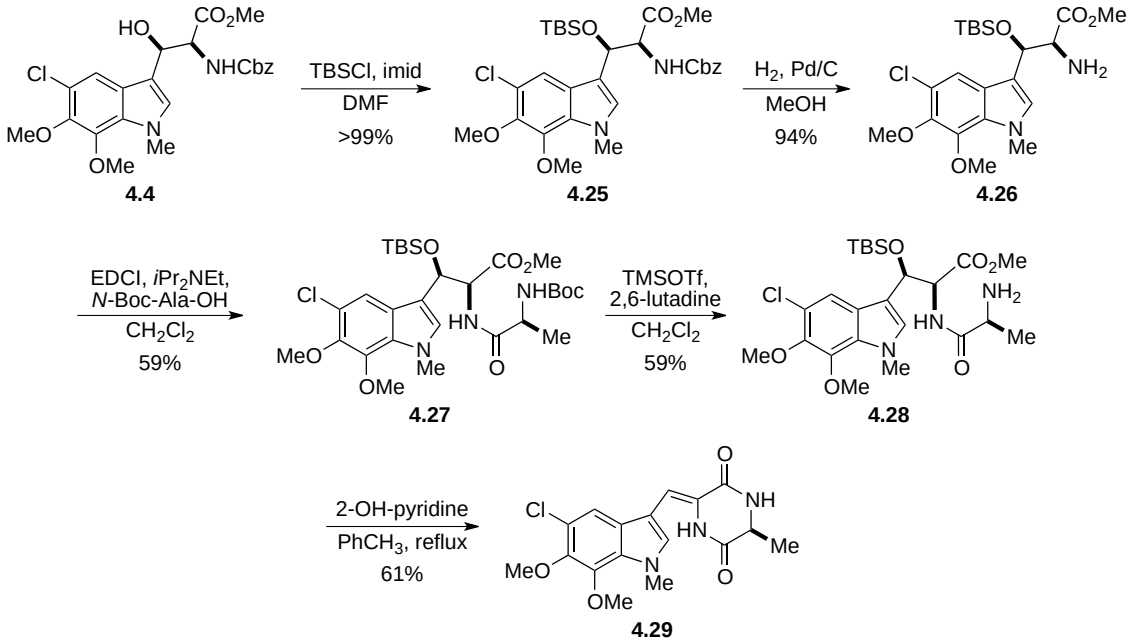

Scheme 4.8. Formation of the dioxopiperazine and an undesired elimination.

Attempts to form the desired dioxopiperazine directly from **4.27** using the microwave conditions described in the previous chapter resulted in decomposition.

Following more traditional methods, we first removed the Boc group, then heated the crude product (**4.28**) in toluene in the presence of 2-hydroxypyridine. The dioxopiperazine was formed, but unfortunately the conditions also caused elimination of the silyl ether to afford **4.29**.

An alternative cyclization precursor was synthesized from **4.25** by saponification of the methyl ester and coupling of L-Ala-OMe (**Scheme 4.9**). The low yielding coupling step forced a quick screen of coupling reagents, through which T3P was identified as the most efficient of those tested, providing dipeptide **4.31** in a mere 34% yield.

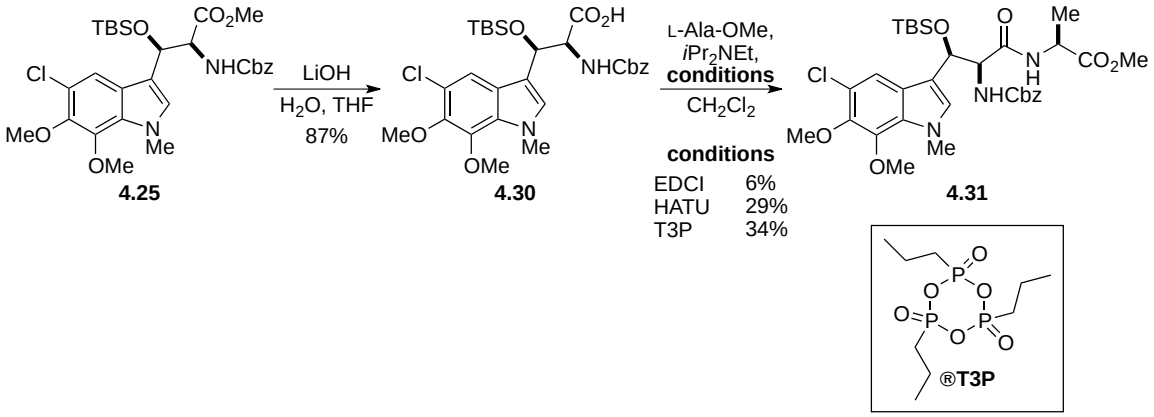

Scheme 4.9. Preparation of dipeptide.

The unoptimized reaction allowed us access to enough material to attempt the cyclization reaction. Dipeptide **4.31** was converted to the free amine and heated gently in toluene with catalytic 2-hydroxypyridine (**Scheme 4.10**). A mixture of the elimination product (**4.29**) and the desired dioxopiperazine (**4.3**) was obtained in poor yield.

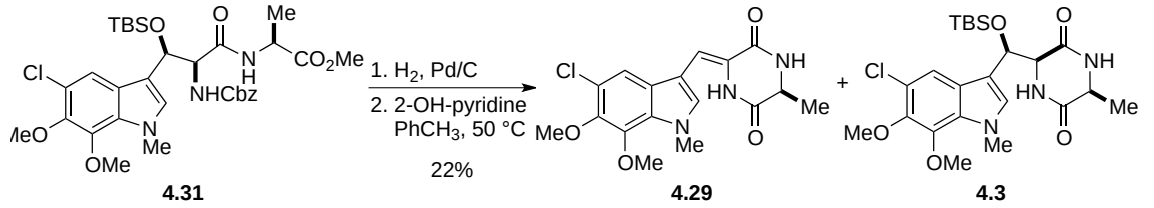

Scheme 4.10. Cyclization to the dioxopiperazine.

We returned to amine **4.26** and to it coupled *N*-Fmoc-L-Ala (**Scheme 4.11**). Again, our standard EDCI-mediated coupling produced dipeptide **4.32** in very poor yield. Use of T3P nearly doubled the yield and greatly simplified purification of **4.32**. Gentle heating of the dipeptide in THF and morpholine resulted in concomitant Fmoc deprotection and cyclization to the desired dioxopiperazine (**4.3**).

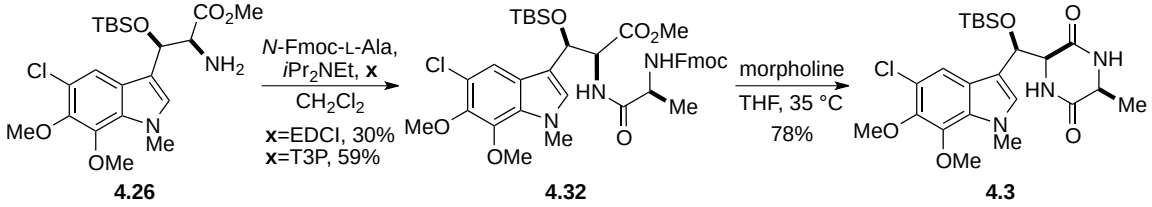

Scheme 4.11. Improved synthesis of dioxopiperazine **4.3**.

4.3.4: Oxidative Cyclization Attempts

Elated to finally have access to dioxopiperazine **4.3**, we pressed forward and attempted the oxidative cyclization to the pyrroloindoline. Treatment of **4.3** with NBS or bromine resulted in products containing two bromine atoms. We turned to the conditions reported in Kishi's synthesis, but only isolated starting material from the reaction mixture (**Scheme 4.12**).[113] Alcohol **4.34** was expected to result from aqueous conditions, but only a small amount of **4.35**, formed by oxidative fission of the indole double bond and elimination of TBSOH, was recovered with starting material.[153]

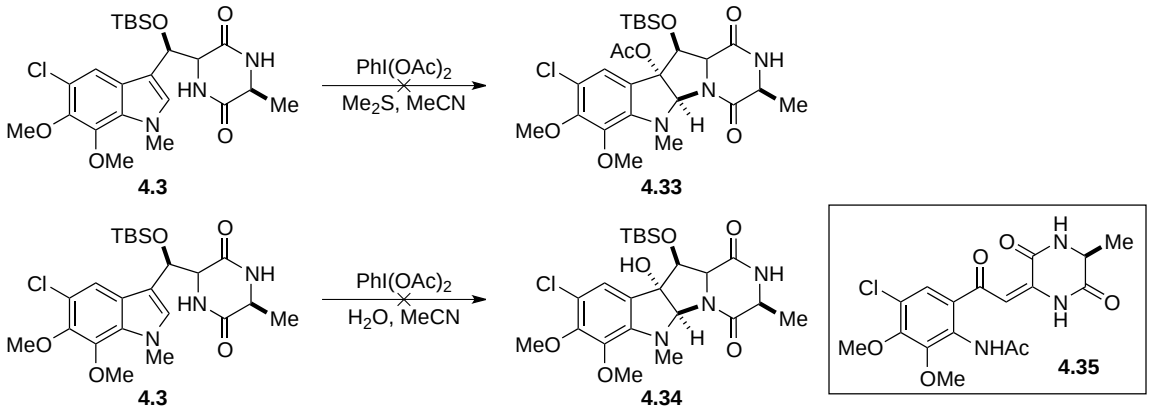

Scheme 4.12. First attempts at oxidative cyclization.

Dioxopiperazine **4.3** was precious material at this point in the synthesis, and we certainly did not have large enough quantities to attempt a variety of conditions. Therefore, simple dioxopiperazine **4.36** was prepared and subjected numerous times to variations of the above conditions (**Scheme 4.13**). Unfortunately, model compound **4.36** also failed to react. Dioxopiperazine **4.36** is nearly insoluble in most solvents, so we were never able to determine if this was the true cause of the failure. The unique electronics of dioxopiperazine **4.3** and the poor solubility of any readily accessible surrogate forced us to study the cyclization using advanced material.

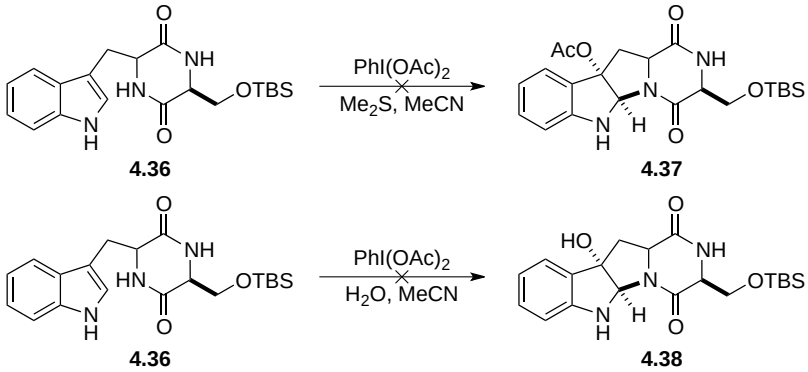

Scheme 4.13. Model cyclization study.

We next attempted the oxidative cyclization using DMDO in acetone and dichloromethane (**Scheme 4.14**).[154,155] No product (**4.34** or **4.39**) was detected from the

reaction of either dioxopiperazine **4.3** or amine **4.26**. However, trace amounts of 3-hydroxypyrroloindoline **4.40** were detected from the reaction with Cbz protected derivative **4.25**.

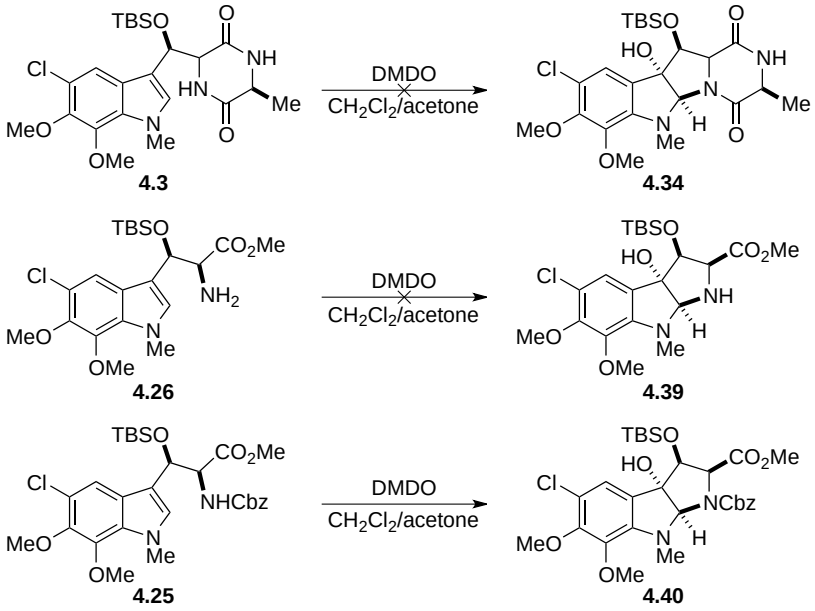

Scheme 4.14. More oxidative cyclization attempts.

Interestingly, only the TBS-protected derivative (**4.25**) would cyclize. The unprotected analogue (**4.4**) also failed to react when treated with DMDO to form the desired tricycle (**4.41**, **Scheme 4.15**). Unfortunately, even the successful cyclization (**4.25** to **4.40**) had limited potential, as the best yield obtained for this sequence was 9%, obtained from the crude reaction mixture by a difficult separation. The recovered alcohol needed to be protected before moving forward, but only trace amounts of the bis-TBS product were obtained. Steric congestion of the two neighboring silyl groups likely contributed to the poor yield of **4.42**.

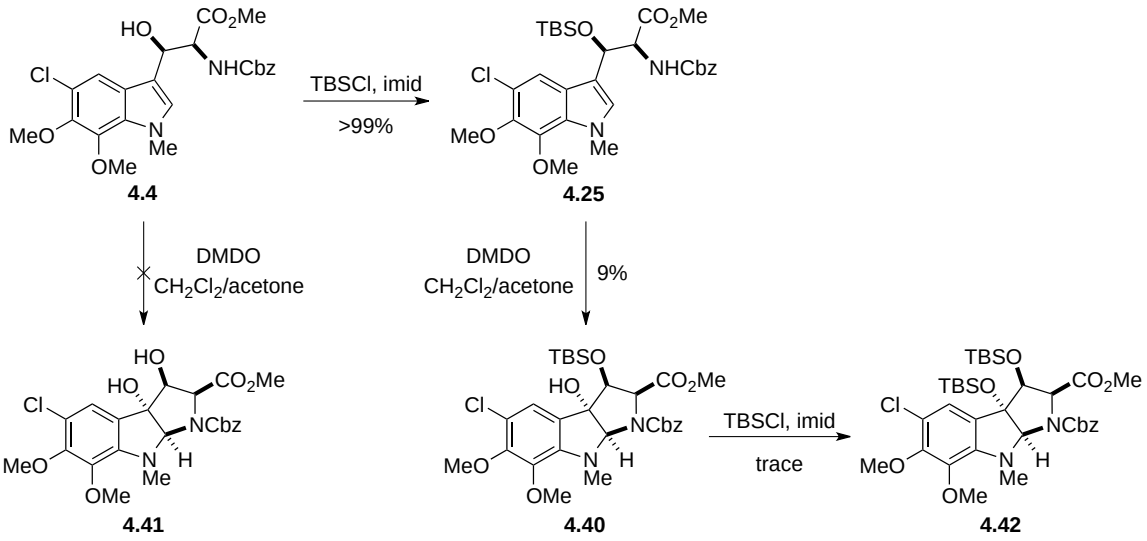

Scheme 4.15. Progression of cyclization.

We also attempted the cyclization using other oxidants, including Davis's oxaziridine and benzoyl peroxide (**Scheme 4.16**).[116,156] Only starting material was recovered, with no trace of the desired products (**4.34** and **4.43**).

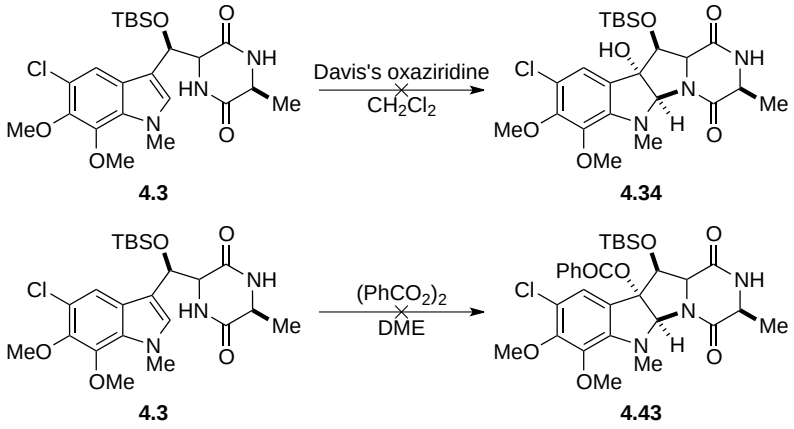

Scheme 4.16. Attempted cyclizations.

4.3.5: Toward a Formal Synthesis of Sporidesmin A

These repeated attempts at forming the requisite 3-hydroxypyrroloindoline were frustrating, especially considering that Kishi had accomplished the same reaction using a

similar substrate. That said, it should be noted that in the original sporidesmin synthesis, the authors only recovered diacetate **2.6** in 30% yield and completed the synthesis using authentic diacetate prepared from the degradation of sporidesmin A (**Scheme 4.17**).[113] One can only conclude that they also were unable to access appreciable quantities of the pyrroloindoline. Moreover, in Kishi's later synthesis of sporidesmin B, benzoyl peroxide was used as the oxidant instead of iodosobenzene diacetate, yielding only 20% of the desired oxidative cyclization product.[116] We recognized that intermediate **2.5** reported in the Kishi sporidesmin A synthesis could be intercepted from alcohol **4.4**.

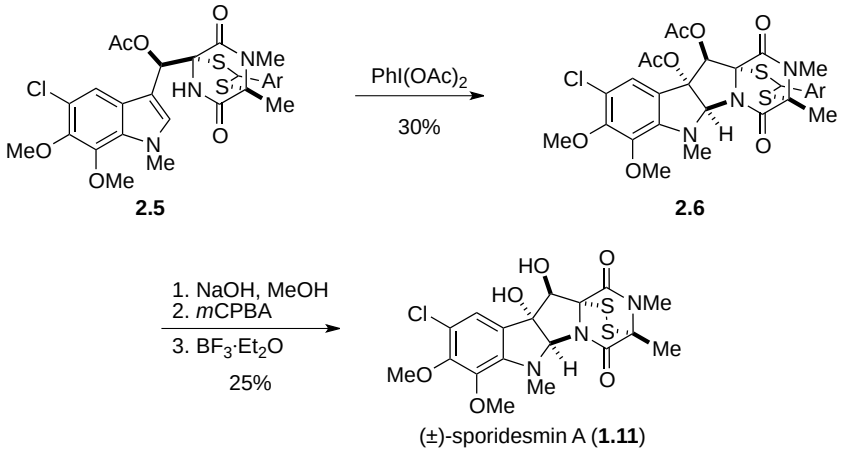

Scheme 4.17. Kishi's final steps in the sporidesmin A synthesis.

A suitable *N*-Me alanine derivative needed to be prepared for the formal synthesis of sporidesmin A. *N*-Fmoc-Ala-OH (**4.44**) was converted to the oxazolidinone (**4.45**), then reduced to afford *N*-Me,Fmoc-Ala-OH (**4.46**, **Scheme 4.18**).[157]

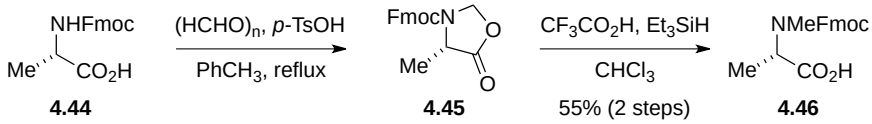

Scheme 4.18. Preparation of *N*-Me,Fmoc-Ala-OH.

Alcohol **4.4** was acetylated by standard procedures to give **4.47**. Amine **4.48** was revealed following deprotection of the Cbz group, then coupled to *N*-Me alanine

derivative **4.46** to afford dipeptide **4.49**. This substrate, however, did not cyclize to the dioxopiperazine when heated in morpholine and THF. Only **4.50**, the product resulting from Fmoc-deprotection and elimination of acetic acid, was recovered.

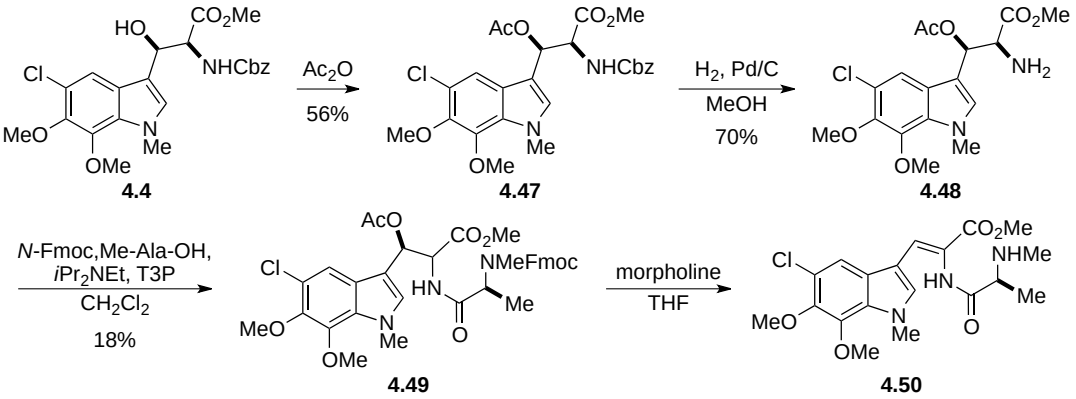

Scheme 4.19. Incorporation of *N*-Me-Ala.

4.4: Future Direction

Given more time, I would like to prepare bis(*N*,*N*'-Cbz) tryptophan derivatives **4.51** and **4.53** from indole **4.6** (**Scheme 4.20**). The bromocyclizations that were carried out for the synthesis of chetomin were all performed on tryptophan derivatives bearing an electron-withdrawing group on the indole nitrogen. Cyclization to the pyrroloindoline should be more favorable with these substrates than for the *N*-Me derivatives. Experience thus far with the oxidative cyclization reaction shows that a complex mixture of products will likely be recovered from each reaction, so sufficient starting material will be required to obtain adequate characterization of the reaction products.

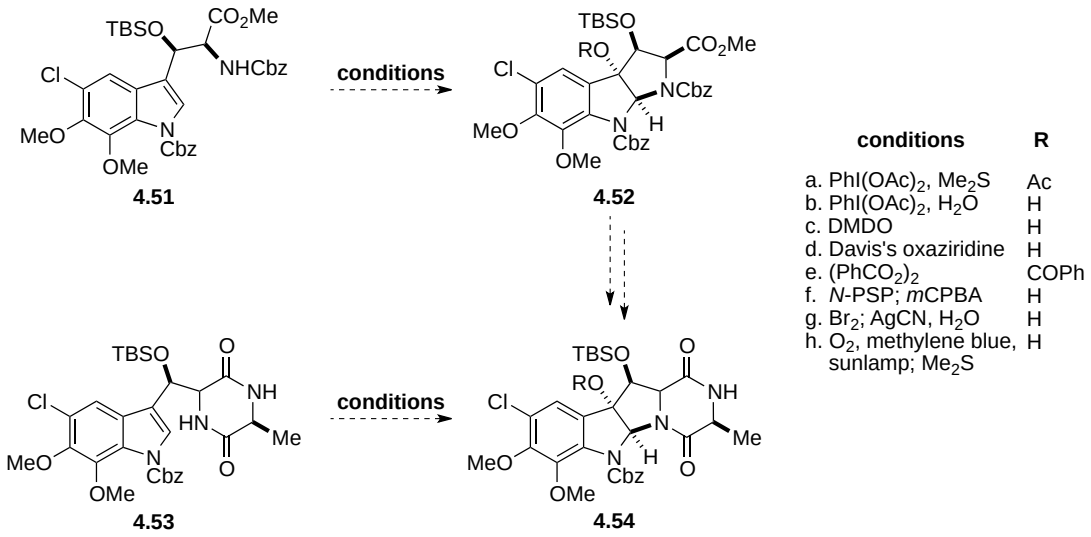

Scheme 4.20. Full panel of oxidation conditions to screen.

The proposed installation of the epidithiodioxopiperazine ring may also be problematic, especially considering the attempts made in the chetomin synthesis. Still, we propose forming (–)-sporidesmin A (**1.11**) through oxidation of the disulfide prepared by reaction of hemiaminal **4.1** with hydrogen sulfide (**Scheme 4.21**). The hemiaminal could be prepared from dioxopiperazine **4.2** or a related derivative.

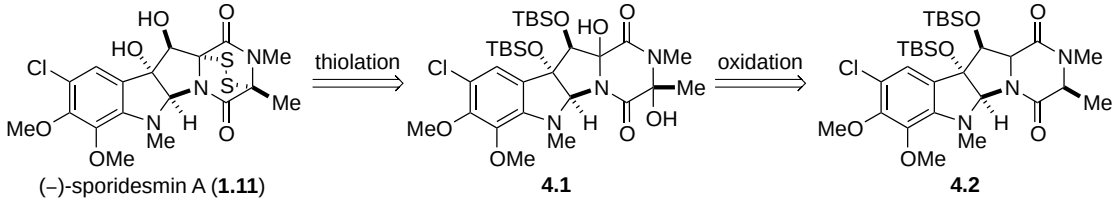

Scheme 4.21. Proposed epidithiodioxopiperazine formation.

4.5: Concluding Remarks

In summary, we have developed an asymmetric approach toward the synthesis of (–)-sporidesmin A. Advanced dioxopiperazine **4.3** can be prepared in decent overall yield and is theoretically three to four steps away from the target natural product. Moreover,

many of the synthetic advances made over the course of this synthesis were applied in our approach to chetomin. Particularly, use of *N*-Fmoc amino acids as precursors to dioxopiperazine rings eliminated a deptrotection step from each synthesis while improving the cyclization yields. While it is difficult to leave this project behind unfinished, I have no doubt that capable hands will pick it up in the future to achieve the total synthesis of (–)-sporidesmin A.

REFERENCES

1. Cook, K. M.; Hilton, S. T.; Mecinovic, J.; Motherwell, W. B.; Figg, W. D.; Schofield, C. J. Epidithiodiketopiperazines Block the Interaction between Hypoxia-Inducible Factor-1alpha (Hif-1alpha) and P300 by a Zinc Ejection Mechanism. *J. Biol. Chem.* **2009**, *284*, 26831-26838.

2. Gardiner, D. M.; Waring, P.; Howlett, B. J. The Epipolythiodioxopiperazine (Etp) Class of Fungal Toxins: Distribution, Mode of Action, Functions and Biosynthesis. *Microbiology* **2005**, *151*, 1021-1032.

3. Waring, P.; Beaver, J. Gliotoxin and Related Epipolythiodioxopiperazines. *Gen. Pharmacol.* **1996**, *27*, 1311-1316.

4. Waring, P.; Eichner, R. D.; Mullbacher, A. The Chemistry and Biology of the Immunomodulating Agent Gliotoxin and Related Epipolythiodioxopiperazines. *Med. Res. Rev.* **1988**, *8*, 499-524.

5. Iwasa, E.; Hamashima, Y.; Sodeoka, M. Epipolythiodiketopiperazine Alkaloids: Total Syntheses and Biological Activities. *Isr. J. Chem.* **2011**, *51*, 420-433.

6. Weindling, R.; Emerson, O. H. The Isolation of a Toxic Substance from the Culture Filtrate of Trichoderma. *Phytopathology* **1936**, *26*, 1068-1070.

7. Bell, M. R.; Johnson, J. R.; Wildi, B. S.; Woodward, R. B. The Structure of Gliotoxin. *J. Am. Chem. Soc.* **1958**, *80*, 1001-1001.

8. Beecham, A. F.; Fridrichsons, J.; Mathieson, A. M. Structure and Absolute Configuration of Gliotoxin and Absolute Configuration of Sporidesmin. *Tetrahedron Lett.* **1966**, 3131.

9. Jordan, T. W.; Cordiner, S. J. Fungal Epipolythiodioxopiperazine Toxins Have Therapeutic Potential and Roles in Disease. *Trends Pharmacol. Sci.* **1987**, *8*, 144-149.

10. Kwon-Chung, K. J.; Sugui, J. A. What Do We Know About the Role of Gliotoxin in the Pathobiology of Aspergillus Fumigatus? *Med. Mycol.* **2009**, *47 Suppl 1*, S97-103.

11. Mullbacher, A.; Eichner, R. D. Immunosuppression Invitro by a Metabolite of a Human Pathogenic Fungus. *Proc. Natl. Acad. Sci., Biol.* **1984**, *81*, 3835-3837.

12. Mullbacher, A.; Waring, P.; Eichner, R. D. Identification of an Agent in Cultures of Aspergillus-Fumigatus Displaying Anti-Phagocytic and Immunomodulating Activity Invitro. *J. Gen. Microbiol.* **1985**, *131*, 1251-1258.

13. Mullbacher, A.; Moreland, A. F.; Waring, P.; Sjaarda, A.; Eichner, R. D. Prevention of Graft-Versus-Host Disease by Treatment of Bone-Marrow with Gliotoxin in Fully Allogeneic Chimeras and Their Cyto-Toxic T-Cell Repertoire. *Transplantation* **1988**, *46*, 120-125.

14. Munday, R. Studies on the Mechanism of Toxicity of the Mycotoxin, Sporidesmin I. Generation of Superoxide Radical by Sporidesmin. *Chem.-Biol. Interact.* **1982**, *41*, 361-374.

15. Chai, C. L.; Waring, P. Redox Sensitive Epidithiodioxopiperazines in Biological Mechanisms of Toxicity. *Redox Rep.* **2000**, *5*, 257-264.

16. Eichner, R. D.; Waring, P.; Geue, A. M.; Braithwaite, A. W.; Mullbacher, A. Gliotoxin Causes Oxidative Damage to Plasmid and Cellular DNA. *J. Biol. Chem.* **1988**, *263*, 3772-3777.

17. Cordiner, S. J.; Jordan, T. W. Inhibition by Sporidesmin of Hepatocyte Bile Acid Transport. *Biochem. J.* **1983**, *212*, 197-204.

18. Mason, J. W.; Kidd, J. G. Effects of Gliotoxin and Other Sulfur-Containing Compounds on Tumor Cells in Vitro; with Observations on the Mechanism of Action of Gliotoxin. *J. Immunol.* **1951**, *66*, 99-106.

19. Hurne, A. M.; Chai, C. L.; Waring, P. Inactivation of Rabbit Muscle Creatine Kinase by Reversible Formation of an Internal Disulfide Bond Induced by the Fungal Toxin Gliotoxin. *J. Biol. Chem.* **2000**, *275*, 25202-25206.

20. Trown, P. W.; Bilello, J. A. Mechanism of Action of Gliotoxin: Elimination of Activity by Sulfhydryl Compounds. *Antimicrob. Agents Chemother.* **1972**, *2*, 261-266.

21. Mullbacher, A.; Waring, P.; Tiwari-Palni, U.; Eichner, R. D. Structural Relationship of Epipolythiodioxopiperazines and Their Immunomodulating Activity. *Mol. Immunol.* **1986**, *23*, 231-235.

22. Stillwell, M. A.; Magasi, L. P.; Strunz, G. M. Production, Isolation, and Antimicrobial Activity of Hyalodendrin, a New Antibiotic Produced by a Species of Hyalodendron. *Can. J. Microbiol.* **1974**, *20*, 759-764.

23. Strunz, G. M.; Heissner, C. J.; Kakushima, M.; Stillwell, M. A. Metabolites of Hyalodendron Sp - Bisdethiodi(Methylthio)Hyalodendrin. *Can. J. Chem.* **1974**, *52*, 325-326.

24. Strunz, G. M.; Kakushima, M.; Stillwell, M. A. Epitetrathiodioxopiperazine with 3s,6s Configuration from Hyalodendron Sp. *Can. J. Chem.* **1975**, *53*, 295-297.

25. DeVault, R. L.; Rosenbrook, W., Jr. A Novel Class of Diketopiperazines. *J. Antibiot.* **1973**, *26*, 532-534.

26. Dorn, F.; Arigoni, D. Gliovictin, New Metabolite of Helminthosporium-Victoriae. *Experientia* **1974**, *30*, 134-135.

27. Michel, K. H.; Chaney, M. O.; Jones, N. D.; Hoehn, M. M.; Nagarajan, R. Epipolythiopiperazinedione Antibiotics from Penicillium Turbatum. *J. Antibiot.* **1974**, *27*, 57-64.

28. Shin, J. H.; Fenical, W. Isolation of Gliovictin from the Marine Deuteromycete Asteromyces-Cruciatus. *Phytochemistry* **1987**, *26*, 3347.

29. Kawahara, N.; Nozawa, K.; Nakajima, S.; Kawai, K. Studies on Fungal Products 13. Isolation and Structures of Dithiosilvatin and Silvathione, Novel Dioxopiperazine Derivatives from Aspergillus-Silvaticus. *J. Chem. Soc., Perkin Trans. 1* **1987**, 2099-2101.

30. Hanson, J. R.; Oleary, M. A. New Piperazinedione Metabolites of Gliocladium-Deliquescens. *J. Chem. Soc., Perkin Trans. 1* **1981**, 218-220.

31. Nagarajan, R.; Huckstep, L. L.; Lively, D. H.; Delong, D. C.; Marsh, M. M.; Neuss, N. Aranotin and Related Metabolites from Arachniotus Aureus I. Determination of Structure. *J. Am. Chem. Soc.* **1968**, *90*, 2980.

32. Nagarajan, R.; Neuss, N.; Marsh, M. M. Aranotin and Related Metabolites 3. Configuration and Conformation of Acetylaranotin. *J. Am. Chem. Soc.* **1968**, *90*, 6518.

33. Neuss, N.; Boeck, L. D.; Brannon, D. R.; Cline, J. C.; DeLong, D. C.; Gorman, M.; Huckstep, L. L.; Lively, D. H.; Mabe, J.; Marsh, M. M.; Molloy, B. B.; Nagarajan, R.; Nelson, J. D.; Stark, W. M. Aranotin and Related Metabolites from Arachniotus Aureus (Eidam) Schroeter Iv. Fermentation, Isolation, Structure Elucidation, Biosynthesis, and Antiviral Properties. *Antimicrob. Agents Chemother.* **1968**, *8*, 213-219.

34. Neuss, N.; Nagarajan, R.; Molloy, B. B.; Huckstep, L. L. Aranotin and Related Metabolites 2. Isolation Characterization and Structures of 2 New Metabolites. *Tetrahedron Lett.* **1968**, 4467.

35. Trown, P. W.; Lindh, H. F.; Milstrey, K. P.; Gallo, V. M.; Mayberry, B. R.; Lindsay, H. L.; Miller, P. A. Ll-S88-Alpha, an Antiviral Substance Produced by Aspergillus Terreus. *Antimicrob. Agents Chemother.* **1968**, *8*, 225-228.

36. Cosulich, D. B.; Nelson, N. R.; Van den Hende, J. H. Crystal and Molecular Structure of L-S88alpha, an Antiviral Epidithiapiperazinedione Derivative from Aspergillus Terreus. *J. Am. Chem. Soc.* **1968**, *90*, 6519.

37. Murdock, K. C. Antiviral Agents. Chemical Modifications of a Disulfide Antibiotic, Acetylaranotin. *J. Med. Chem.* **1974**, *17*, 827-835.

38. Kawahara, N.; Nakajima, S.; Yamazaki, M.; Kawai, K. Structure of a Novel Epidithiodioxopiperazine, Emethallicin a, a Potent Inhibitor of Histamine Release from Emericella Heterothallica. *Chem. Pharm. Bull.* **1989**, *37*, 2592-2595.

39. Kawahara, N.; Nozawa, K.; Yamazaki, M.; Nakajima, S.; Kawai, K. Structures of Novel Epipolythiodioxopiperazines, Emethallicins B, C, and D, Potent Inhibitors of Histamine Release, from Emericella Heterothallica. *Chem. Pharm. Bull.* **1990**, *38*, 73-78.

40. Kawahara, N.; Nozawa, K.; Nakajima, S.; Kawai, K.; Yamazaki, M. Novel Epitetrathiodioxopiperazines, Emethallicin-B and Emethallicin-C, as Potent Inhibitors of Compound 48/80-Induced Histamine-Release, from Emericella-Heterothallica. *J. Chem. Soc., Chem. Commun.* **1989**, 951-952.

41. Kawahara, N.; Nozawa, K.; Yamazaki, M.; Nakajima, S.; Kawai, K. Studies on Fungal Products 32. Novel Epidithiodioxopiperazines, Emethallicin-E and Emethallicin-F, from Emericella-Heterothallica. *Heterocycles* **1990**, *30*, 507-515.

42. Waring, P.; Eichner, R. D.; Tiwaripalni, U.; Mullbacher, A. Gliotoxin-E - a New Biologically-Active Epipolythiodioxopiperazine Isolated from Penicillium-Terlikowskii. *Aust. J. Chem.* **1987**, *40*, 991-997.

43. Ueno, Y.; Umemori, K.; Niimi, E.; Tanuma, S.; Nagata, S.; Sugamata, M.; Ihara, T.; Sekijima, M.; Kawai, K.; Ueno, I.; et al. Induction of Apoptosis by T-2 Toxin and Other Natural Toxins in Hl-60 Human Promyelotic Leukemia Cells. *Nat. Toxins* **1995**, *3*, 129-137.

44. Seya, H.; Nozawa, K.; Nakajima, S.; Kawai, K. I.; Udagawa, S. I. Studies on Fungal Products 8. Isolation and Structure of Emestrin, a Novel Antifungal Macrocyclic Epidithiodioxopiperazine from Emericella-Striata - X-Ray Molecular-Structure of Emestrin. *J. Chem. Soc., Perkin Trans. 1* **1986**, 109-116.

45. Seya, H.; Nakajima, S.; Kawai, K.; Udagawa, S. Structure and Absolute-Configuration of Emestrin, a New Macrocyclic Epidithiodioxopiperazine from Emericella-Striata. *J. Chem. Soc., Chem. Commun.* **1985**, 657-658.

46. Kawai, K.; Nozawa, K.; Seya, H.; Kawahara, N.; Udagawa, S.; Nakajima, S. Studies on Fungal Products 12. Structure of Aurantioemestrin from Emericella-Striata. *Heterocycles* **1987**, *26*, 475-479.

47. Kawahara, N.; Nozawa, K.; Nakajima, S.; Kawai, K. Aurantioemestrin from Emericella-Striata and Silvathione from Aspergillus-Silvaticus, Possible Key Intermediates from Epidithiodioxopiperazines to Trioxopiperazines. *J. Chem. Soc., Chem. Commun.* **1986**, 1495-1496.

48. Seya, H.; Nozawa, K.; Udagawa, S.; Nakajima, S.; Kawai, K. Studies on Fungal Products 9. Dethiosecoemestrin, a New Metabolite Related to Emestrin, from Emericella-Striata. *Chem. Pharm. Bull.* **1986**, *34*, 2411-2416.

49. Nozawa, K.; Udagawa, S. I.; Nakajima, S.; Kawai, K. I. Studies on Fungal Products 14. Emestrin-B, a New Epitrithiodioxopiperazine, from Emericella-Striata. *Chem. Pharm. Bull.* **1987**, *35*, 3460-3463.

50. Onodera, H.; Hasegawa, A.; Tsumagari, N.; Nakai, R.; Ogawa, T.; Kanda, Y. Mpc1001 and Its Analogues: New Antitumor Agents from the Fungus Cladorrhinum Species. *Org. Lett.* **2004**, *6*, 4101-4104.

51. Deffieux, G.; Gadret, M.; Leger, J. M.; Carpy, A. Crystal Structure of Original Fungal Metabolite of 3,6-Epidithio-2,5-Dioxopiperazine Group - Epicorazine-A. *Acta Crystallogr. B.* **1977**, *33*, 1474-1478.

52. Deffieux, G.; Baute, M. A.; Baute, R.; Filleau, M. J. New Antibiotics from Fungus Epicoccum-Nigrum 2. Epicorazine-a - Structure Elucidation and Absolute Configuration. *J. Antibiot.* **1978**, *31*, 1102-1105.

53. Deffieux, G.; Filleau, M. J.; Baute, R. New Antibiotics from Fungus Epicoccum-Nigrum 3. Epicorazine-B - Structure Elucidation and Absolute Configuration. *J. Antibiot.* **1978**, *31*, 1106-1109.

54. Brown, A. E.; Finlay, R.; Ward, J. S. Antifungal Compounds Produced by Epicoccum-Purpurascens against Soil-Borne Plant Pathogenic Fungi. *Soil Biol. Biochem.* **1987**, *19*, 657-664.

55. Kleinwachter, P.; Dahse, H. M.; Luhmann, U.; Schlegel, B.; Dornberger, K. Epicorazine C, an Antimicrobial Metabolite from Stereum Hirsutum Hki 0195. *J. Antibiot.* **2001**, *54*, 521-525.

56. Begg, W. R.; Elix, J. A.; Jones, A. J. Nonacyclic Amides from Lichens of Genus Xanthoparmelia. *Tetrahedron Lett.* **1978**, 1047-1050.

57. Ernst-Russell, M. A.; Chai, C. L. L.; Hurne, A. M.; Waring, P.; Hockless, D. C. R.; Elix, J. A. Structure Revision and Cytotoxic Activity of the Scabrosin Esters, Epidithiopiperazinediones from the Lichen Xanthoparmelia Scabrosa. *Aust. J. Chem.* **1999**, *52*, 279-283.

58. Moerman, K. L.; Chai, C. L. L.; Waring, P. Evidence That the Lichen-Derived Scabrosin Esters Target Mitochondrial Atp Synthase in P388d1 Cells. *Toxicol. Appl. Pharmacol.* **2003**, *190*, 232-240.

59. Curtis, P. J.; Greatbanks, D.; Hesp, B.; Cameron, A. F.; Freer, A. A. Sirodesmins a, B, C, and G, Antiviral Epipolythiopiperazine-2,5-Diones of Fungal Origin - X-Ray Analysis of Sirodesmin-a Diacetate. *J. Chem. Soc., Perkin Trans. 1* **1977**, 180-189.

60. Ferezou, J. P.; Riche, C.; Quesneauthierry, A.; Pascardbilly, C.; Barbier, M.; Bousquet, J. F.; Boudart, G. Structures of 2 Toxins Isolated from Fungus Cultures

Phoma-Lingam Tode - Sirodesmin Pl and Deacetylsirodesmin Pl. *Nouv. J. Chim.* **1977**, *1*, 327-334.

61. Boudart, G. Antibacterial Activity of Sirodesmin Pl Phytotoxin: Application to the Selection of Phytotoxin-Deficient Mutants. *Appl. Environ. Microbiol.* **1989**, *55*, 1555-1559.

62. Elliott, C. E.; Gardiner, D. M.; Thomas, G.; Cozijnsen, A.; Van De Wouw, A.; Howlett, B. J. Production of the Toxin Sirodesmin Pl by Leptosphaeria Maculans During Infection of Brassica Napus. *Mol. Plant Pathol.* **2007**, *8*, 791-802.

63. Thornton, R. H.; Sinclair, D. P. Sporidesmium Bakeri and Facial Eczema of Sheep in the Field. *Nature* **1959**, *184*, 1327-1328.

64. Thornton, R. H.; Percival, J. C. A Hepatotoxin from Sporidesmium Bakeri Capable of Producing Facial Eczema Diseases in Sheep. *Nature* **1959**, *183*, 63.

65. Synge, R. L. M.; White, E. P. Sporidesmin - a Substance from Sporidesmium-Bakeri Causing Lesions Characteristic of Facial Eczema. *Chem. Ind.* **1959**, 1546-1547.

66. Fridrichsons, J.; Mathieson, A. M. Structure of Methylene Dibromide Adduct of Sporidesmin at - 150 Degrees C. *Acta Crystallogr.* **1965**, *18*, 1043.

67. Fridrichsons, J.; Mathieson, A. M. The Structure of Sporidesmin - Causative Agent of Facial Eczema in Sheep. *Tetrahedron Lett.* **1962**, 1265-1268.

68. Smith, B. L.; Embling, P. P.; Towers, N. R.; Wright, D. E.; Payne, E. The Protective Effect of Zinc Sulphate in Experimental Sporidesmin Poisoning of Sheep. *New Zealand veterinary journal* **1977**, *25*, 124-127.

69. Waring, P.; Egan, M.; Braithwaite, A.; Mullbacher, A.; Sjaarda, A. Apoptosis Induced in Macrophages and T Blasts by the Mycotoxin Sporidesmin and Protection by Zn2+ Salts. *Int. J. Immunopharmacol.* **1990**, *12*, 445-457.

70. Munday, R. Studies on the Mechanism of Toxicity of the Mycotoxin Sporidesmin 3. Inhibition by Metals of the Generation of Superoxide Radical by Sporidesmin. *J. Appl. Toxicol.* **1984**, *4*, 182-186.

71. Hodges, R.; Shannon, J. S. Isolation and Structure of Sporidesmin C. *Aust. J. Chem.* **1966**, *19*, 1059.

72. Waksman, S. A.; Bugie, E. Chaetomin, a New Antibiotic Substance Produced by Chaetomium Cochliodes I. Formation and Properties. *J. Bacteriol.* **1944**, *48*, 527-530.

73. Mcinnes, A. G.; Taylor, A.; Walter, J. A. Structure of Chetomin. *J. Am. Chem. Soc.* **1976**, *98*, 6741-6741.

74. Li, G. Y.; Li, B. G.; Yang, T.; Yan, J. F.; Liu, G. Y.; Zhang, G. L. Chaetocochins a-C, Epipolythiodioxopiperazines from Chaetomium Cochliodes. *J. Nat. Prod.* **2006**, *69*, 1374-1376.

75. Fujimoto, H.; Sumino, M.; Okuyama, E.; Ishibashi, M. Immunomodulatory Constituents from an Ascomycete, Chaetomium Seminudum. *J. Nat. Prod.* **2004**, *67*, 98-102.

76. Kung, A. L.; Zabludoff, S. D.; France, D. S.; Freedman, S. J.; Tanner, E. A.; Vieira, A.; Cornell-Kennon, S.; Lee, J.; Wang, B.; Wang, J.; Memmert, K.; Naegeli, H. U.; Petersen, F.; Eck, M. J.; Bair, K. W.; Wood, A. W.; Livingston, D. M. Small Molecule Blockade of Transcriptional Coactivation of the Hypoxia-Inducible Factor Pathway. *Cancer Cell* **2004**, *6*, 33-43.

77. Staab, A.; Loeffler, J.; Said, H. M.; Diehlmann, D.; Katzer, A.; Beyer, M.; Fleischer, M.; Schwab, F.; Baier, K.; Einsele, H.; Flentje, M.; Vordermark, D. Effects of Hif-1 Inhibition by Chetomin on Hypoxia-Related Transcription and Radiosensitivity in Ht 1080 Human Fibrosarcoma Cells. *BMC Cancer* **2007**, *7*, 213.

78. Mohammed, K. A.; Jadulco, R. C.; Bugni, T. S.; Harper, M. K.; Sturdy, M.; Ireland, C. M. Strongylophorines: Natural Product Inhibitors of Hypoxia-Inducible Factor-1 Transcriptional Pathway. *J. Med. Chem.* **2008**, *51*, 1402-1405.

79. Melillo, G. Hypoxia-Inducible Factor 1 Inhibitors. *Methods Enzymol.* **2007**, *435*, 385-402.

80. Block, K. M.; Wang, H.; Szabo, L. Z.; Polaske, N. W.; Henchey, L. K.; Dubey, R.; Kushal, S.; Laszlo, C. F.; Makhoul, J.; Song, Z.; Meuillet, E. J.; Olenyuk, B. Z. Direct Inhibition of Hypoxia-Inducible Transcription Factor Complex with Designed Dimeric Epidithiodiketopiperazine. *J. Am. Chem. Soc.* **2009**, *131*, 18078-18088.

81. Hauser, D.; Weber, H. P.; Sigg, H. P. Isolation and Configuration of Chaetocin. *Helv. Chim. Acta* **1970**, *53*, 1061-1073.

82. Weber, H. P. Molecular Structure and Absolute Configuration of Chaetocin. *Acta Crystallogr. B.* **1972**, *B 28*, 2945.

83. Saito, T.; Suzuki, Y.; Koyama, K.; Natori, S.; Iitaka, Y.; Kinoshita, T. Chetracin-a and Chaetocin-B and Chaetocin-C, 3 New Epipolythiodioxopiperazines from Chaetomium Spp. *Chem. Pharm. Bull.* **1988**, *36*, 1942-1956.

84. Li, L.; Li, D.; Luan, Y.; Gu, Q.; Zhu, T. Cytotoxic Metabolites from the Antarctic Psychrophilic Fungus Oidiodendron Truncatum. *J. Nat. Prod.* **2012**, *75*, 920-927.

85. Greiner, D.; Bonaldi, T.; Eskeland, R.; Roemer, E.; Imhof, A. Identification of a Specific Inhibitor of the Histone Methyltransferase Su(Var)3-9. *Nat. Chem. Biol.* **2005**, *1*, 143-145.

86. Feng, Y.; Blunt, J. W.; Cole, A. L.; Munro, M. H. Novel Cytotoxic Thiodiketopiperazine Derivatives from a Tilachlidium Sp. *J. Nat. Prod.* **2004**, *67*, 2090-2092.

87. Minato, H.; Matsumoto, M.; Katayama, T. Studies on the Metabolites of Verticillium Sp. Structures of Verticillins a, B, and C. *J. Chem. Soc., Perkin Trans. 1* **1973**, *17*, 1819-1825.

88. Joshi, B. K.; Gloer, J. B.; Wicklow, D. T. New Verticillin and Glisoprenin Analogues from Gliocladium Catenulatum, a Mycoparasite of Aspergillus Flavus Sclerotia. *J. Nat. Prod.* **1999**, *62*, 730-733.

89. Chu, M.; Truumees, I.; Rothofsky, M. L.; Patel, M. G.; Gentile, F.; Das, P. R.; Puar, M. S.; Lin, S. L. Inhibition of C-Fos Proto-Oncogene Induction by Sch 52900 and Sch 52901, Novel Diketopiperazine Produced by Gliocladium Sp. *J. Antibiot.* **1995**, *48*, 1440-1445.

90. Dong, J. Y.; He, H. P.; Shen, Y. M.; Zhang, K. Q. Nematicidal Epipolysulfanyldioxopiperazines from Gliocladium Roseum. *J. Nat. Prod.* **2005**, *68*, 1510-1513.

91. Zheng, C. J.; Kim, C. J.; Bae, K. S.; Kim, Y. H.; Kim, W. G. Bionectins a-C, Epidithiodioxopiperazines with Anti-Mrsa Activity, from Bionectra Byssicola F120. *J. Nat. Prod.* **2006**, *69*, 1816-1819.

92. Takahashi, C.; Minoura, K.; Yamada, T.; Numata, A.; Kushida, K.; Shingu, T.; Hagishita, S.; Nakai, H.; Sato, T.; Harada, H. Potent Cytotoxic Metabolites from a Leptosphaeria Species - Structure Determination and Conformational-Analysis. *Tetrahedron* **1995**, *51*, 3483-3498.

93. Takahashi, C.; Numata, A.; Ito, Y.; Matsumura, E.; Araki, H.; Iwaki, H.; Kushida, K. Leptosins, Antitumor Metabolites of a Fungus Isolated from a Marine Alga. *J. Chem. Soc., Perkin Trans. 1* **1994**, 1859-1864.

94. Takahashi, C.; Numata, A.; Matsumura, E.; Minoura, K.; Eto, H.; Shingu, T.; Ito, T.; Hasegawa, T. Leptosins I and J, Cytotoxic Substances Produced by a Leptosphaeria Sp. Physico-Chemical Properties and Structures. *J. Antibiot.* **1994**, *47*, 1242-1249.

95. Winstead, J. A.; Suhadolnik, R. J. Biosynthesis of Gliotoxin 2. Further Studies on the Incorporation of Carbon-14 and Tritium-Labeled Precursors. *J. Am. Chem. Soc.* **1960**, *82*, 1644-1647.

96. Suhadolnik, R. J.; Chenoweth, R. G. Biosynthesis of Gliotoxin 1. Incorporation of Phenylalanine-1-C-14 and Phenylalanine-2-C-14. *J. Am. Chem. Soc.* **1958**, *80*, 4391-4392.

97. Balibar, C. J.; Walsh, C. T. Glip, a Multimodular Nonribosomal Peptide Synthetase in Aspergillus Fumigatus, Makes the Diketopiperazine Scaffold of Gliotoxin. *Biochemistry* **2006**, *45*, 15029-15038.

98. Bulock, J. D.; Leigh, C. Biosynthesis of Gliotoxin. *J. Chem. Soc., Chem. Commun.* **1975**, 628-629.

99. Kirby, G. W.; Patrick, G. L.; Robins, D. J. Cyclo-(L-Phenylalanyl-L-Seryl) as an Intermediate in Biosynthesis of Gliotoxin. *J. Chem. Soc., Perkin Trans. 1* **1978**, 1336-1338.

100. Macdonald, J. C.; Slater, G. P. Biosynthesis of Gliotoxin and Mycelianamide. *Can. J. Biochem.* **1975**, *53*, 475-478.

101. Kirby, G. W.; Rao, G. V.; Robins, D. J. New Co-Metabolites of Gliotoxin in Gliocladium-Virens. *J. Chem. Soc., Perkin Trans. 1* **1988**, 301-304.

102. Davis, C.; Carberry, S.; Schrettl, M.; Singh, I.; Stephens, J. C.; Barry, S. M.; Kavanagh, K.; Challis, G. L.; Brougham, D.; Doyle, S. The Role of Glutathione S-Transferase Glig in Gliotoxin Biosynthesis in Aspergillus Fumigatus. *Chem. Biol.* **2011**, *18*, 542-552.

103. Scharf, D. H.; Remme, N.; Habel, A.; Chankhamjon, P.; Scherlach, K.; Heinekamp, T.; Hortschansky, P.; Brakhage, A. A.; Hertweck, C. A Dedicated Glutathione S-Transferase Mediates Carbon-Sulfur Bond Formation in Gliotoxin Biosynthesis. *J. Am. Chem. Soc.* **2011**, *133*, 12322-12325.

104. Scharf, D. H.; Heinekamp, T.; Remme, N.; Hortschansky, P.; Brakhage, A. A.; Hertweck, C. Biosynthesis and Function of Gliotoxin in Aspergillus Fumigatus. *Appl. Microbiol. Biotechnol.* **2012**, *93*, 467-472.

105. Scharf, D. H.; Remme, N.; Heinekamp, T.; Hortschansky, P.; Brakhage, A. A.; Hertweck, C. Transannular Disulfide Formation in Gliotoxin Biosynthesis and Its Role in Self-Resistance of the Human Pathogen Aspergillus Fumigatus. *J. Am. Chem. Soc.* **2010**, *132*, 10136-10141.

106. Schrettl, M.; Carberry, S.; Kavanagh, K.; Haas, H.; Jones, G. W.; O'Brien, J.; Nolan, A.; Stephens, J.; Fenelon, O.; Doyle, S. Self-Protection against Gliotoxin--a Component of the Gliotoxin Biosynthetic Cluster, Glit, Completely Protects Aspergillus Fumigatus against Exogenous Gliotoxin. *PLoS Pathog.* **2010**, *6*, e1000952.

107. Gardiner, D. M.; Cozijnsen, A. J.; Wilson, L. M.; Pedras, M. S.; Howlett, B. J. The Sirodesmin Biosynthetic Gene Cluster of the Plant Pathogenic Fungus Leptosphaeria Maculans. *Mol. Microbiol.* **2004**, *53*, 1307-1318.

108. Gardiner, D. M.; Howlett, B. J. Bioinformatic and Expression Analysis of the Putative Gliotoxin Biosynthetic Gene Cluster of Aspergillus Fumigatus. *FEMS Microbiol. Lett.* **2005**, *248*, 241-248.

109. Fox, E. M.; Howlett, B. J. Biosynthetic Gene Clusters for Epipolythiodioxopiperazines in Filamentous Fungi. *Mycol. Res.* **2008**, *112*, 162-169.

110. Ferezou, J. P.; Quesneauthierry, A.; Barbier, M.; Kollmann, A.; Bousquet, J. F. Structure and Synthesis of Phomamide, a New Piperazine-2,5-Dione Related to the Sirodesmins, Isolated from the Culture-Medium of Phoma-Lingam Tode. *J. Chem. Soc., Perkin Trans. 1* **1980**, 113-115.

111. Bulock, J. D.; Clough, L. E. Sirodesmin Biosynthesis. *Aust. J. Chem.* **1992**, *45*, 39-45.

112. Kremer, A.; Li, S. M. A Tyrosine O-Prenyltransferase Catalyses the First Pathway-Specific Step in the Biosynthesis of Sirodesmin Pl. *Microbiology* **2010**, *156*, 278-286.

113. Kishi, Y.; Nakatsuka, S.; Fukuyama, T.; Havel, M. Total Synthesis of Sporidesmin-A. *J. Am. Chem. Soc.* **1973**, *95*, 6493-6495.

114. Kishi, Y.; Fukuyama, T.; Nakatsuka, S. Total Synthesis of Dehydrogliotoxin. *J. Am. Chem. Soc.* **1973**, *95*, 6492-6493.

115. Kishi, Y.; Fukuyama, T.; Nakatsuka, S. New Method for Synthesis of Epidithiodiketopiperazines. *J. Am. Chem. Soc.* **1973**, *95*, 6490-6492.

116. Nakatsuka, S.; Fukuyama, T.; Kishi, Y. Total Synthesis of D,L-Sporidesmin B. *Tetrahedron Lett.* **1974**, 1549-1552.

117. Fukuyama, T.; Kishi, Y. Total Synthesis of Gliotoxin. *J. Am. Chem. Soc.* **1976**, *98*, 6723-6724.

118. Fukuyama, T.; Nakatsuka, S.; Kishi, Y. Total Synthesis of Gliotoxin, Dehydrogliotoxin and Hyalodendrin. *Tetrahedron* **1981**, *37*, 2045-2078.

119. Strunz, G. M.; Kakushima, M. Total Synthesis of (+/-) Hyalodendrin. *Experientia* **1974**, *30*, 719-720.

120. Williams, R. M.; Rastetter, W. H. Syntheses of the Fungal Metabolites (+/-)-Gliovictin and (+/-)-Hyalodendrin. *J. Org. Chem.* **1980**, *45*, 2625-2631.

121. Williams, R. M.; Rastetter, W. H. Efficient Synthesis of D,L-Gliovictin - Construction of the Hydroxymethyl Moiety Via a 3-Formyl-2,5-Piperazinedione. *Tetrahedron Lett.* **1979**, 1187-1190.

122. Kim, J.; Ashenhurst, J. A.; Movassaghi, M. Total Synthesis of (+)-11,11'-Dideoxyverticillin A. *Science* **2009**, *324*, 238-241.

123. Iwasa, E.; Hamashima, Y.; Fujishiro, S.; Higuchi, E.; Ito, A.; Yoshida, M.; Sodeoka, M. Total Synthesis of (+)-Chaetocin and Its Analogues: Their Histone Methyltransferase G9a Inhibitory Activity. *J. Am. Chem. Soc.* **2010**, *132*, 4078-4079.

124. Iwasa, E.; Hamashima, Y.; Fujishiro, S.; Hashizume, D.; Sodeoka, M. Total Syntheses of Chaetocin and Ent-Chaetocin. *Tetrahedron* **2011**, *67*, 6587-6599.

125. Kim, J.; Movassaghi, M. General Approach to Epipolythiodiketopiperazine Alkaloids: Total Synthesis of (+)-Chaetocins a and C and (+)-12,12'-Dideoxychetracin A. *J. Am. Chem. Soc.* **2010**, *132*, 14376-14378.

126. DeLorbe, J. E.; Jabri, S. Y.; Mennen, S. M.; Overman, L. E.; Zhang, F. L. Enantioselective Total Synthesis of (+)-Gliocladine C: Convergent Construction of Cyclotryptamine-Fused Polyoxopiperazines and a General Approach for Preparing Epidithiodioxopiperazines from Trioxopiperazine Precursors. *J. Am. Chem. Soc.* **2011**, *133*, 6549-6552.

127. Movassaghi, M.; Boyer, N. Concise Total Synthesis of (+)-Gliocladins B and C. *Chem. Sci.* **2012**, *3*, 1798-1803.

128. Nicolaou, K. C.; Totokotsopoulos, S.; Giguere, D.; Sun, Y. P.; Sarlah, D. Total Synthesis of Epicoccin G. *J. Am. Chem. Soc.* **2011**, *133*, 8150-8153.

129. Codelli, J. A.; Puchlopek, A. L. A.; Reisman, S. E. Enantioselective Total Synthesis of (-)-Acetylaranotin, a Dihydrooxepine Epidithiodiketopiperazine. *J. Am. Chem. Soc.* **2012**, *134*, 1930-1933.

130. Newhouse, T.; Lewis, C. A.; Eastman, K. J.; Baran, P. S. Scalable Total Syntheses of N-Linked Tryptamine Dimers by Direct Indole-Aniline Coupling: Psychotrimine and Kapakahines B and F. *J. Am. Chem. Soc.* **2010**, *132*, 7119-7137.

131. Newhouse, T.; Baran, P. S. Total Synthesis of (+/-)-Psychotrimine. *J. Am. Chem. Soc.* **2008**, *130*, 10886-10887.

132. Newhouse, T.; Lewis, C. A.; Baran, P. S. Enantiospecific Total Syntheses of Kapakahines B and F. *J. Am. Chem. Soc.* **2009**, *131*, 6360-6361.

133. Espejo, V. R.; Rainier, J. D. An Expeditious Synthesis of C(3)-N(1') Heterodimeric Indolines. *J. Am. Chem. Soc.* **2008**, *130*, 12894-12895.

134. Espejo, V. R.; Rainier, J. D. Total Synthesis of Kapakahine E and F. *Org. Lett.* **2010**, *12*, 2154-2157.

135. Perez-Balado, C.; de Lera, A. R. Concise Total Synthesis and Structural Revision of (+)-Pestalazine B. *Org. Biomol. Chem.* **2010**, *8*, 5179-5186.

136. Greshock, T. J.; Williams, R. M. Improved Biomimetic Total Synthesis of D,L-Stephacidin A. *Org. Lett.* **2007**, *9*, 4255-4258.

137. Movassaghi, M.; Schmidt, M. A.; Ashenhurst, J. A. Stereoselective Oxidative Rearrangement of 2-Aryl Tryptamine Derivatives. *Org. Lett.* **2008**, *10*, 4009-4012.

138. Poriel, C.; Lachia, M.; Wilson, C.; Davies, J. R.; Moody, C. J. Oxidative Rearrangement of Indoles: A New Approach to the Efhg-Tetracyclic Core of Diazonamide A. *J. Org. Chem.* **2007**, *72*, 2978-2987.

139. Yao, P. Y.; Zhang, Y.; Hsung, R. P.; Zhao, K. A Sequential Metal-Catalyzed C-N Bond Formation in the Synthesis of 2-Amido-Indoles. *Org. Lett.* **2008**, *10*, 4275-4278.

140. Istrate, F. M.; Buzas, A. K.; Jurberg, I. D.; Odabachian, Y.; Gagosz, F. Synthesis of Functionalized Oxazolones by a Sequence of Cu(Ii)- and Au(I)-Catalyzed Transformations. *Org. Lett.* **2008**, *10*, 925-928.

141. Ohno, M.; Spande, T. F.; Witkop, B. Cyclization of Tryptophan and Tryptamine Derivatives to 2,3-Dihydropyrrolo[2,3-B]Indoles. *J. Am. Chem. Soc.* **1970**, *92*, 343-348.

142. Fuchs, J. R.; Funk, R. L. Total Synthesis of (+/-)-Perophoramidine. *J. Am. Chem. Soc.* **2004**, *126*, 5068-5069.

143. Yamada, Y.; Arima, S.; Okada, C.; Akiba, A.; Kai, T.; Harigaya, Y. Preparation of 7-Halo-Indoles by Thallation of N-Formylindoline and Their Attempted Use for Synthesis of the Right-Hand Segment of Chloropeptin. *Chem. Pharm. Bull.* **2006**, *54*, 788-794.

144. Lopez, C. S.; Perez-Balado, C.; Rodriguez-Grana, P.; de Lera, A. R. Mechanistic Insights into the Stereocontrolled Synthesis of Hexahydropyrrolo[2,3-B]Indoles by Electrophilic Activation of Tryptophan Derivatives. *Org. Lett.* **2008**, *10*, 77-80.

145. Welch, T. R.; Williams, R. M. Biomimetic Synthesis of Alkaloids Derived from Tryptophan: Dioxopiperazine Alkaloids. In *Biomimetic Organic Synthesis*, Poupon, E.; Nay, B., Eds. Wiley-VCH: **2011**, 117-148.

146. Di Menna, M. E.; Smith, B. L.; Miles, C. O. A History of Facial Eczema (Pithomycotoxicosis) Research. *New Zeal. J. Agr. Res.* **2009**, *52*, 345-376.

147. Rege, P. D.; Tian, Y.; Corey, E. J. Studies of New Indole Alkaloid Coupling Methods for the Synthesis of Haplophytine. *Org. Lett.* **2006**, *8*, 3117-3120.

148. Ojo, B.; Findsen, L. A.; Igarashi, N.; Kong, B.; Chowdhury, B. K. Synthesis and Bronchodilatory Activity of Four New Derivatives of Deoxyvasicine. *Drug Des. Discovery* **1996**, *14*, 1-14.

149. Blunt, J. W.; Erasmuson, A. F.; Ferrier, R. J.; Munro, M. H. G. Syntheses of Haptens Related to the Benzenoid and Indole Portions of Sporidesmin-a - C-13 Nmr-Spectra of Indole-Derivatives. *Aust. J. Chem.* **1979**, *32*, 1045-1054.

150. Ishikawa, H.; Elliott, G. I.; Velcicky, J.; Choi, Y.; Boger, D. L. Synthesis of (-)- and Ent-(+)-Vindoline and Related Alkaloids. *J. Am. Chem. Soc.* **2006**, *128*, 10596-10612.

151. Koketsu, K.; Oguri, H.; Watanabe, K.; Oikawa, H. Identification and Stereochemical Assignment of the Beta-Hydroxytryptophan Intermediate in the Echinomycin Biosynthetic Pathway. *Org. Lett.* **2006**, *8*, 4719-4722.

152. Becker, H.; Sharpless, K. B. A New Ligand Class for the Asymmetric Dihydroxylation of Olefins. *Angew. Chem., Int. Ed.* **1996**, *35*, 448-451.

153. Ritchie, R.; Saxton, J. E. Studies on Indolic Mold Metabolites - Total Synthesis of L-Prolyl-2-Methyltryptophan Anhydride and Deoxybrevianamide-E. *Tetrahedron* **1981**, *37*, 4295-4303.

154. Zhao, L.; May, J. P.; Huang, J.; Perrin, D. M. Stereoselective Synthesis of Brevianamide E. *Org. Lett.* **2012**, *14*, 90-93.

155. Schkeryantz, J. M.; Woo, J. C. G.; Siliphaivanh, P.; Depew, K. M.; Danishefsky, S. J. Total Synthesis of Gypsetin, Deoxybrevianamide E, Brevianamide E, and Tryprostatin B: Novel Constructions of 2,3-Disubstituted Indoles. *J. Am. Chem. Soc.* **1999**, *121*, 11964-11975.

156. Greshock, T. J.; Grubbs, A. W.; Williams, R. M. Concise, Biomimetic Total Synthesis of D,L-Marcfortine C. *Tetrahedron* **2007**, *63*, 6124-6130.

157. Luo, Y.; Evindar, G.; Fishlock, D.; Lajoie, G. A. Synthesis of N-Protected N-Methyl Serine and Threonine. *Tetrahedron Lett.* **2001**, *42*, 3807-3809.

CHAPTER 5

Experimental Procedures

Unless otherwise noted, all reagents were obtained from commercial suppliers and were used without further purification**.** All air or moisture sensitive reactions were performed under a positive pressured of argon in flame-dried glassware. Tetrahydrofuran (THF), toluene, diethyl ether (Et_2O), dichloromethane, benzene (PhH), acetonitrile (MeCN), triethylamine (Et_3N), pyridine, diisopropyl amine, methanol (MeOH), dimethylsulfoxide (DMSO), and *N*,*N*-dimethylformamide (DMF) were obtained from a dry solvent system (Ar degassed solvents delivered through activated alumina columns, positive pressure of argon). Column chromatography was performed on Merck silica gel Kieselgel 60 (230-400 mesh). Melting points were determined in open-end capillary tubes and are uncorrected. ^{1}HNMR and ^{13}CNMR spectra were recorded on Varian 300, or 400 MHz spectrometers. Chemical shifts are reported in ppm relative to $CHCl_3$ at δ 7.27 (^{1}HNMR) and δ 77.23 (^{13}CNMR). Mass spectra were obtained on Fisons VG Autospec. IR spectra were obtained from thin films on a NaCl plate using a Bruker Tensor 27 FT-IR spectrometer. Optical rotations were collected at 589 nm on a Rudolph Research automatic polarimeter Autopol III.

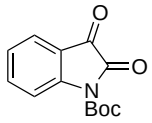

3.5

***Tert*-butyl 2,3-dioxoindoline-1-carboxylate (3.5)**. To a solution of isatin (4.0 g, 27.2 mmol) in THF (100 mL) at 0°C was added Boc_2O (7.1 g, 32.6 mmol) and DMAP (195 mg, 1.6 mmol). The resulting mixture was stirred overnight at r.t. under Ar, then concentrated under reduced pressure. The product was recrystallized in EtOAc/hexanes to afford **3.5** (4.7 g, 70% yield).

^{1}H-NMR (300 MHz; DMSO-d_6): δ 7.92 (d, *J* = 8.2 Hz, 1H), 7.76-7.65 (m, 2H), 7.29 (t, *J* = 7.5 Hz, 1H), 1.56 (s, 9H).

REF: TRW-I-175, **TRW-I-179**.

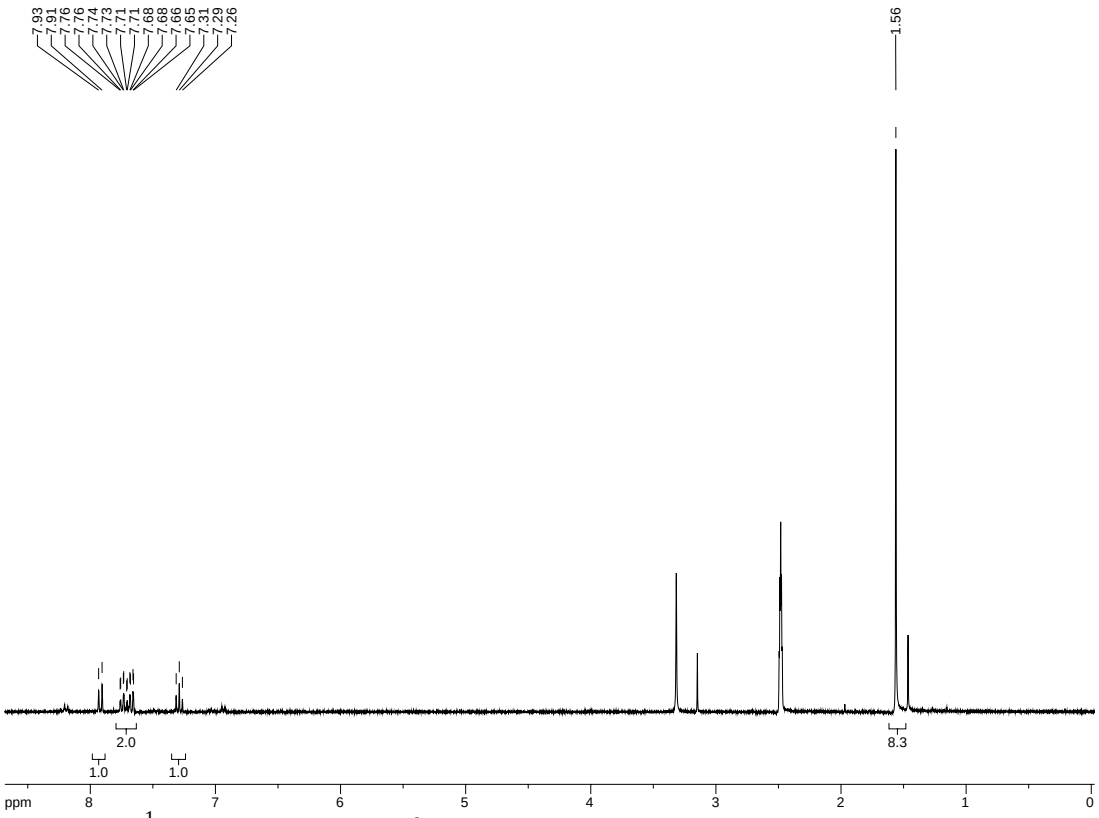

Figure 5.1a. ^{1}H NMR spectrum of compound **3.5**.

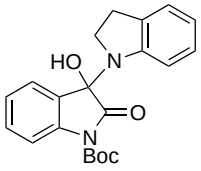

3.6

Boc-Hemiaminal (3.6). To a flame-dried RBF was added **3.5** (500 mg, 2.02 mmol) and toluene (20 mL). Indoline (134 μL, 1.2 mmol), K_2CO_3 (372 mg, 2.7 mmol), and 4 Å M.S. (5 g) were subsequently added, and the resulting suspension heated to reflux for 12 h under Ar. The reaction mixture was filtered through celite and the fitrate concentrated under reduced pressure to afford 419 mg of **3.6** as a tan solid (100% yield) that was taken on without further purification.

^{1}H-NMR (400 MHz; $CDCl_3$): δ 10.59 (s, 1H), 8.55 (d, *J* = 8.7 Hz, 1H), 8.26 (d, *J* = 8.1 Hz, 1H), 7.74 (dd, *J* = 8.1, 1.4 Hz, 1H), 7.57 (dd, *J* = 8.6, 7.2 Hz, 1H), 7.24-7.20 (m, 1H), 7.13-7.11 (m, 1H), 7.03-6.99 (m, 1H), 3.97 (t, *J* = 8.4 Hz, 2H), 3.15 (t, *J* = 8.3 Hz, 2H), 1.54 (s, 9H); ^{13}C-NMR (101 MHz; $CDCl_3$): δ 193.7, 163.4, 152.9, 144.1, 141.7, 137.0, 133.9, 132.0, 129.2, 128.0, 125.5, 121.7, 119.3, 117.7, 81.4, 48.1, 28.49, 28.42.

REF: **TRW-I-180**, TRW-I-185, TRW-I-201.

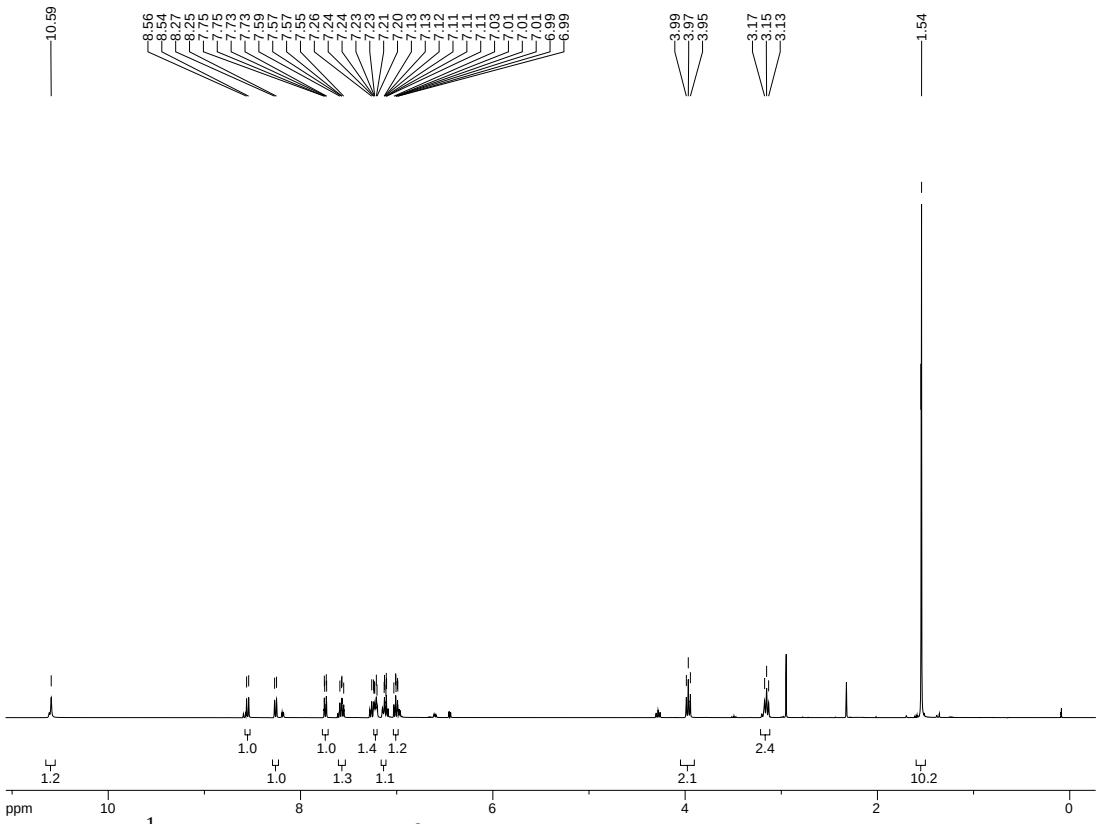

Figure 5.2a. ^{1}H NMR spectrum of compound **3.6**.

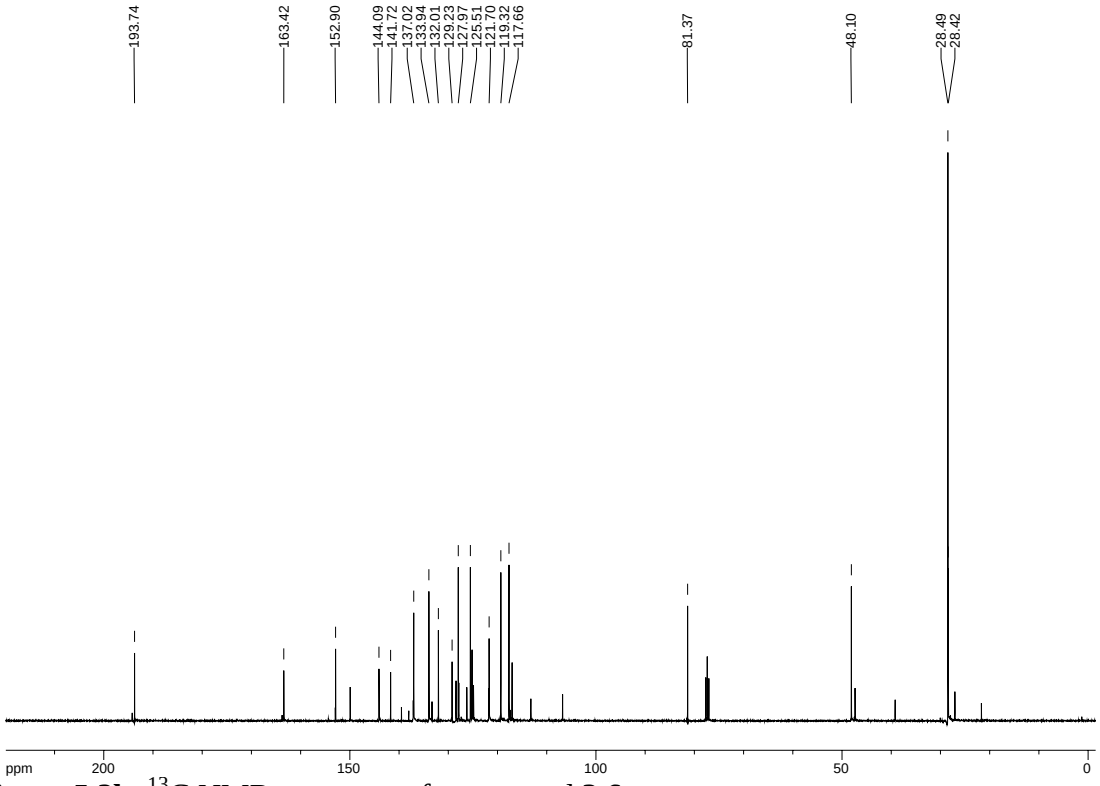

Figure 5.2b. ^{13}C NMR spectrum of compound **3.6**.

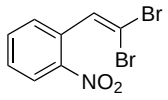

3.15

1-(2,2-dibromovinyl)-2-nitrobenzene (3.15). 2-nitrobenzaldehyde (**3.14**, 2.0 g, 13.2 mmol) and CBr_4 (6.57 g, 19.8 mmol) were dissolved in CH_2Cl_2 (100 mL). The resulting solution was cooled to 0 °C and a solution of PPh_3 (10.38 g, 39.6 mmol) in CH_2Cl_2 (80 mL) slowly added. The reaction was stirred an additional 30 minutes at 0 °C, then concentrated under reduced pressure. The residue was taken up in chloroform (30 mL), filtered, and the solid washed with chloroform (2 x 30 mL). The filtrate was concentrated, then purified by SiO_2 chromatography (8:1 hexanes:EtOAc) to afford **3.15** (3.69 g, 91% yield).

^{1}H-NMR (300 MHz; $CDCl_3$): δ 8.12 (dd, *J* = 8.2, 1.3 Hz, 1H), 7.78 (s, 1H), 7.71-7.65 (m, 1H), 7.60-7.51 (m, 2H).

REF: TRW-I-286, **TRW-I-337**, TRW-I-363.

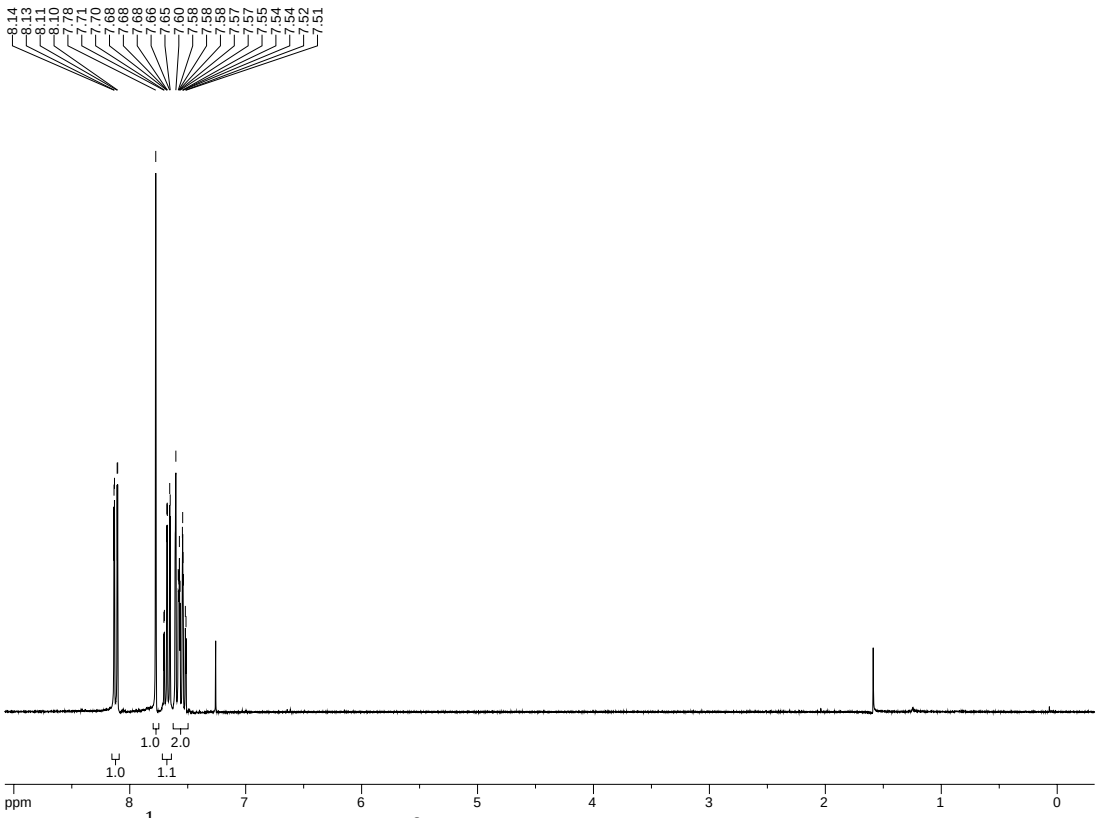

Figure 5.3a. ^{1}H NMR spectrum of compound **3.15**.

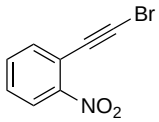

3.12

1-(bromoethynyl)-2-nitrobenzene (3.12). To a solution of dibromoalkene **3.15** (3.60 g, 11.7 mmol) and $BnEt_3NCl$ (1.33 g, 5.85 mmol) in CH_2Cl_2 (46 mL) at 0 °C was added a solution of KOH (30 g) in 23 mL of H_2O. The resulting solution was stirred for 1 h at 0 °C, then extracted with CH_2Cl_2. The organic extracts were dried over Na_2SO_4, filtered, concentrated under reduced pressure, and purified by SiO_2 chromatography (10-20% EtOAc in hexanes) to afford **3.12** in quantitative yield.

^{1}H-NMR (300 MHz; $CDCl_3$): δ 8.06 (dd, *J* = 8.2, 1.4 Hz, 1H), 7.66 (dd, *J* = 7.7, 1.7 Hz, 1H), 7.58 (td, *J* = 7.5, 1.4 Hz, 1H), 7.49 (td, *J* = 7.8, 1.6 Hz, 1H).

REF: TRW-I-291, **TRW-I-338**, TRW-I-364.

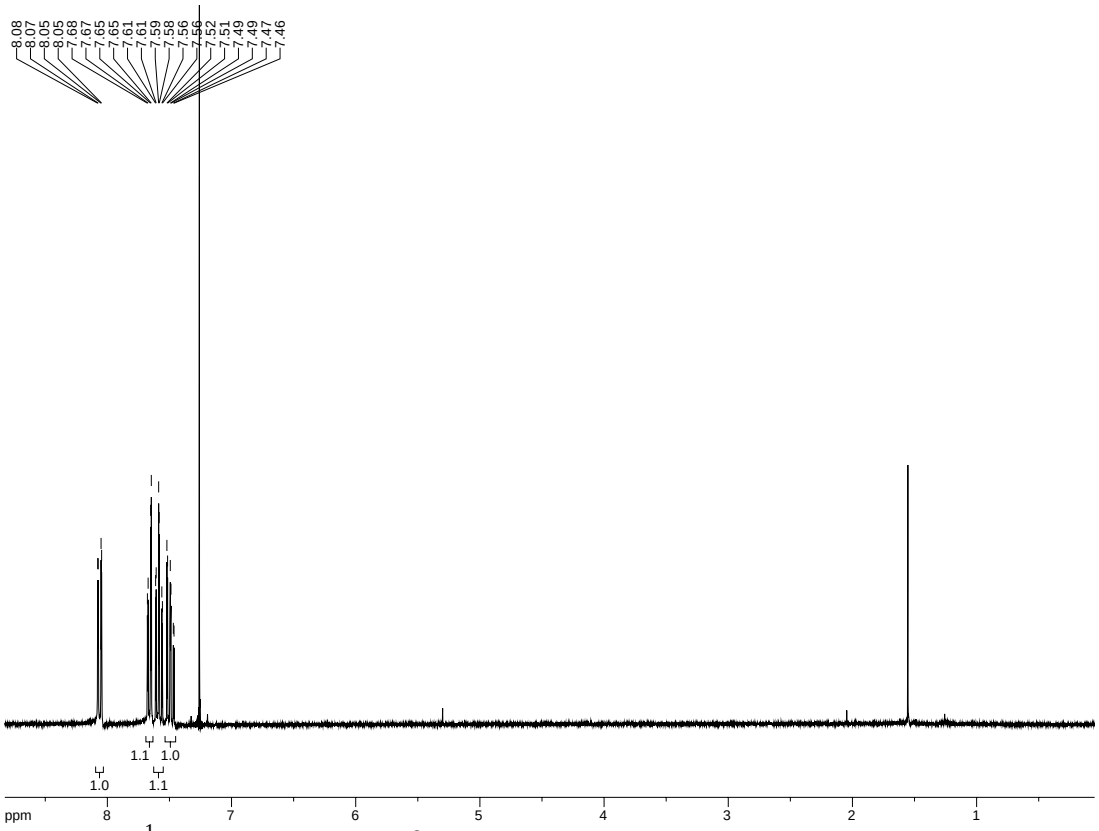

Figure 5.4a. ^{1}H NMR spectrum of compound **3.12**.

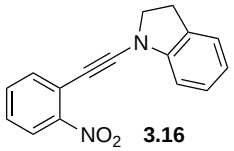

3.16

1-((2-nitrophenyl)ethynyl)indoline (3.16). Bromoalkyne **3.12** (185 mg, 0.82 mmol) was dissolved in toluene (2.75 mL). Indoline (110 μL, 0.98 mmol), K_3PO_4 (418 mg, 1.97 mmol), $CuSO_4 \cdot 5H_2O$ (40 mg, 0.16 mmol), and 1,10-phenanthroline (60 mg, 0.33 mmol) were added successively. The resulting suspension was heated to 120 °C for 4 h in a microwave. Upon completion of the reaction, the solution was cooled and diluted with ether, then filtered through celite. The filtrate was concentrated under reduced pressure and purified by SiO_2 chromatography (10-20% EtOAc in hexanes) to afford **3.16** (80 mg, 37% yield).

^{1}H-NMR (300 MHz; $CDCl_3$): δ 8.38 (d, *J* = 7.9 Hz, 1H), 8.15 (d, *J* = 8.7 Hz, 1H), 7.68 (d, *J* = 9.1 Hz, 1H), 7.40 (t, *J* = 7.7 Hz, 1H), 7.30-7.26 (m, 2H), 7.19 (td, *J* = 10.2, 6.6 Hz, 2H), 4.72 (t, *J* = 8.3 Hz, 2H), 3.32 (t, *J* = 8.3 Hz, 2H).

REF: TRW-I-328, TRW-I-334, TRW-I-342, **TRW-I-343**, TRW-I-353, TRW-I-360, TRW-I-362, TRW-I-385.

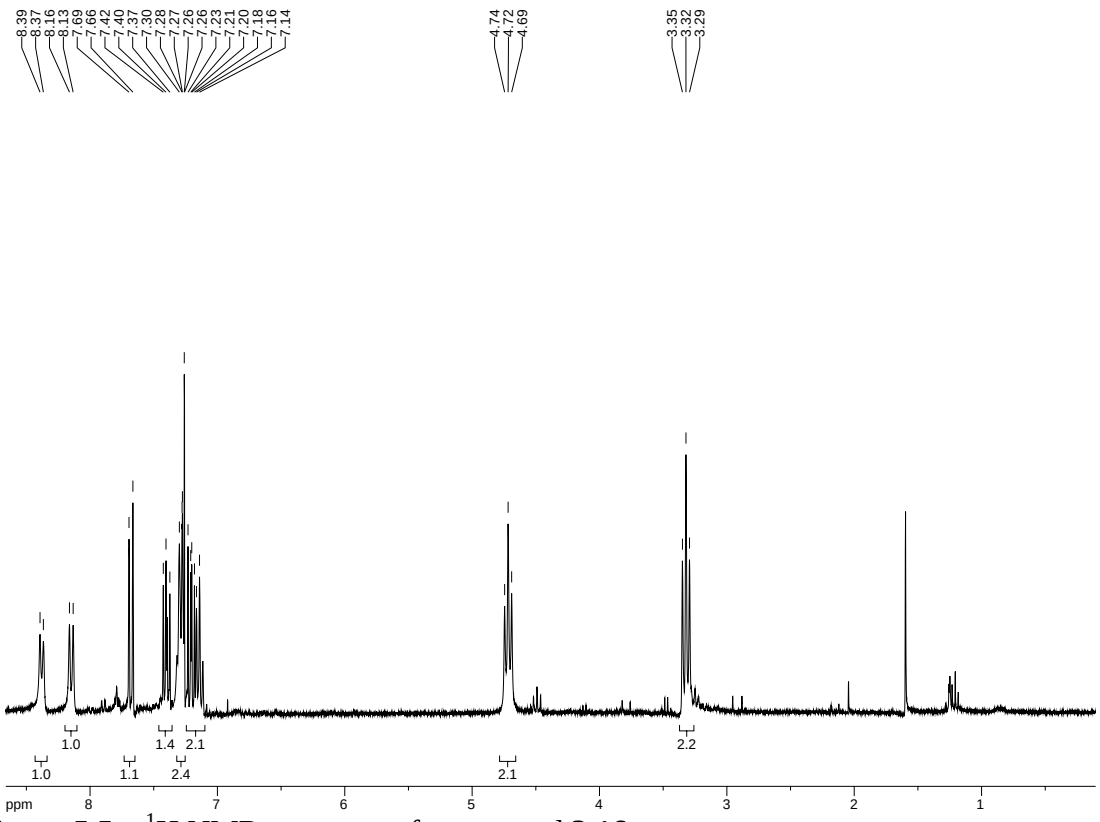

Figure 5.5a. ^{1}H NMR spectrum of compound **3.16**.

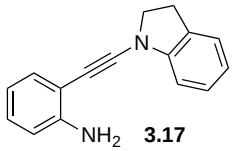

3.17

2-(indolin-1-ylethynyl)aniline (3.17). Nitroalkyne **3.16** was dissolved in a 4 to 1 acetone/water mixture (4.3 mL). Zinc dust (141 mg, 2.15 mmol) and NH_4Cl (228 mg, 4.30 mmol) were added successively, and the resulting suspension stirred briskly for 10 minutes at r.t. The mixture was concentrated under reduced pressure, diluted with EtOAc, washed with water, washed with brine, dried over Na_2SO_4 and concentrated. Purification by SiO_2 chromatography (3:1 hexanes:EtOAc, 1:1 hexanes:EtOAc, then 100% EtOAc) afforded pure aniline derivative **3.17** (61 mg, 61% yield).

^{1}H-NMR (300 MHz; $CDCl_3$): δ 8.33 (d, *J* = 8.1 Hz, 1H), 7.26 (d, *J* = 15.6 Hz, 2H), 7.20-7.04 (m, 4H), 6.72 (dd, *J* = 7.4, 2.3 Hz, 2H), 4.39-4.14 (m, 2H), 3.96 (td, *J* = 10.4, 6.1 Hz, 1H), 3.54 (td, *J* = 10.4, 7.0 Hz, 1H), 3.21-2.99 (m, 2H); ^{13}C-NMR (75 MHz; $CDCl_3$): δ 131.5, 130.1, 129.1, 127.9, 124.98, 124.95, 122.2, 118.8, 117.6, 117.3, 112.5, 71.6, 47.5, 28.4.

REF: TRW-I-331, TRW-I-336, TRW-I-352, TRW-I-357, **TRW-I-361**, TRW-I-366.

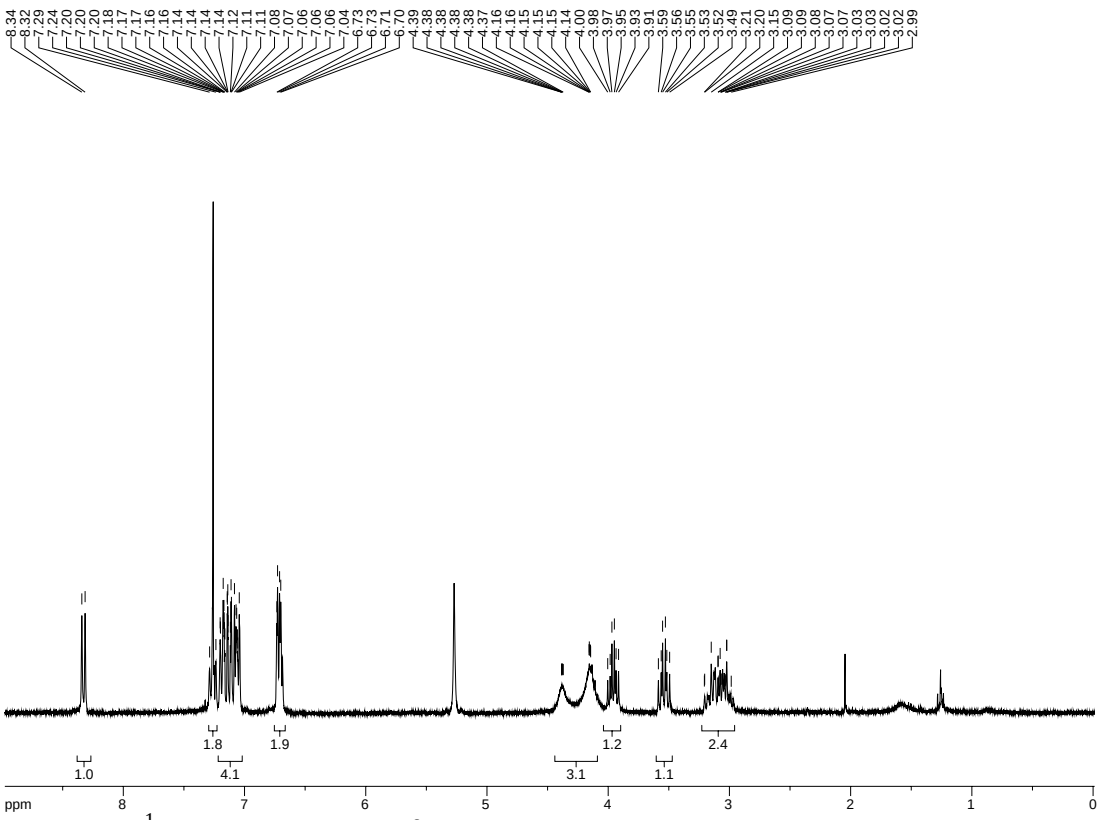

Figure 5.6a. ^{1}H NMR spectrum of compound **3.17**.

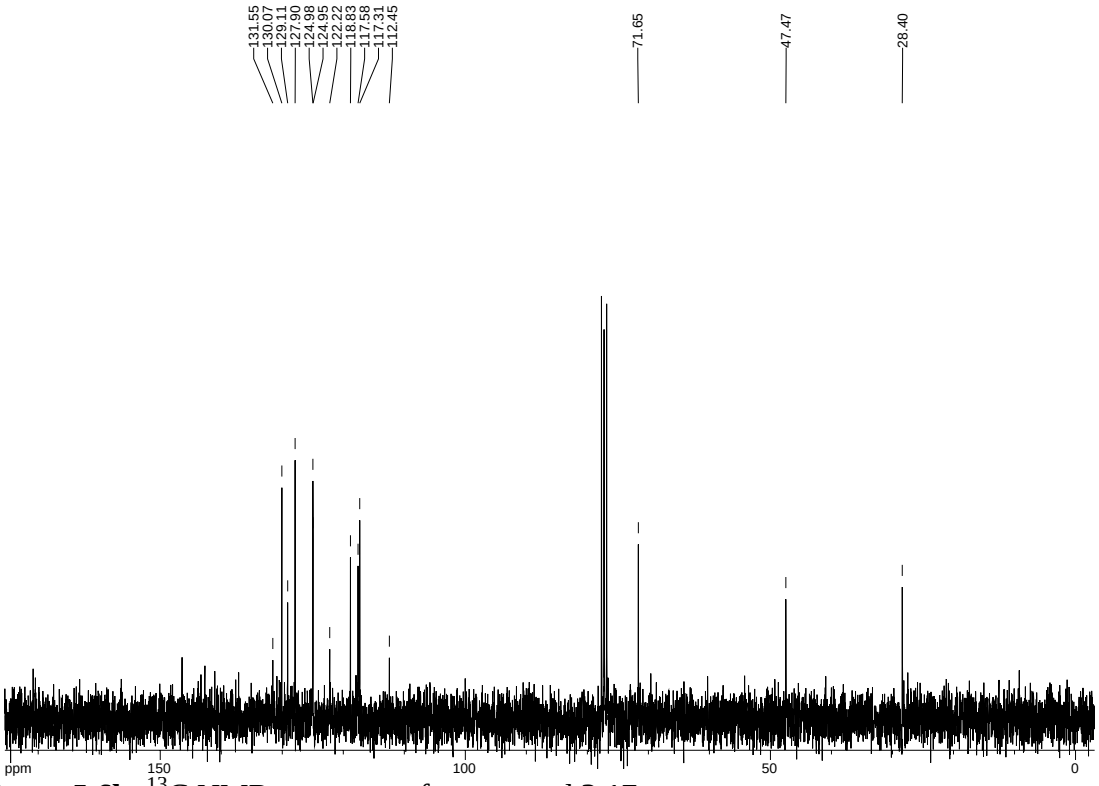

Figure 5.6b. ^{13}C NMR spectrum of compound **3.17**.

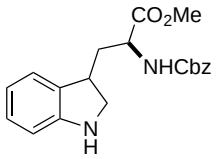

3.21

Methyl 3-(benzyloxycarbonylamino)-4-(indolin-3-yl)butanoate (3.21). *N*-Cbz-L-Trp-OMe (3.52 g, 10.0 mmol) was dissolved in THF/TFA (16.5 mL/16.5 mL) and cooled to 0 °C. $BH_3 \cdot Me_2S$ was added dropwise and the resulting solution stirred 15 min. at 0 °C. Water (33 mL) was added and the mixture stirred 15 min. at r.t. The solvent was removed *in vacuo* and TFA azeotroped off with toluene (3x). The residue was taken up in EtOAc, washed with 1M NaOH (3x), water (1x), and brine (1x) successively. The organic layer was dried over Na_2SO_4, filtered, concentrated under reduced pressure, and purified by SiO_2 chromatography (2:1 – 1:1 hexanes:EtOAc) to afford indoline **3.21** (2.81 g, 79% yield).

^{1}H-NMR (300 MHz; $CDCl_3$): δ 7.36 (s, 5H), 7.03 (t, *J* = 7.1 Hz, 2H), 6.74-6.71 (m, 1H), 6.64 (dd, *J* = 9.5, 1.8 Hz, 1H), 5.37 (dd, *J* = 26.1, 8.8 Hz, 1H), 5.12 (s, 2H), 4.53-4.44 (m, 1H), 3.74-3.68 (m, 4H), 3.36-3.22 (m, 2H), 2.11-2.06 (m, 2H).

REF: **TRW-I-369**.

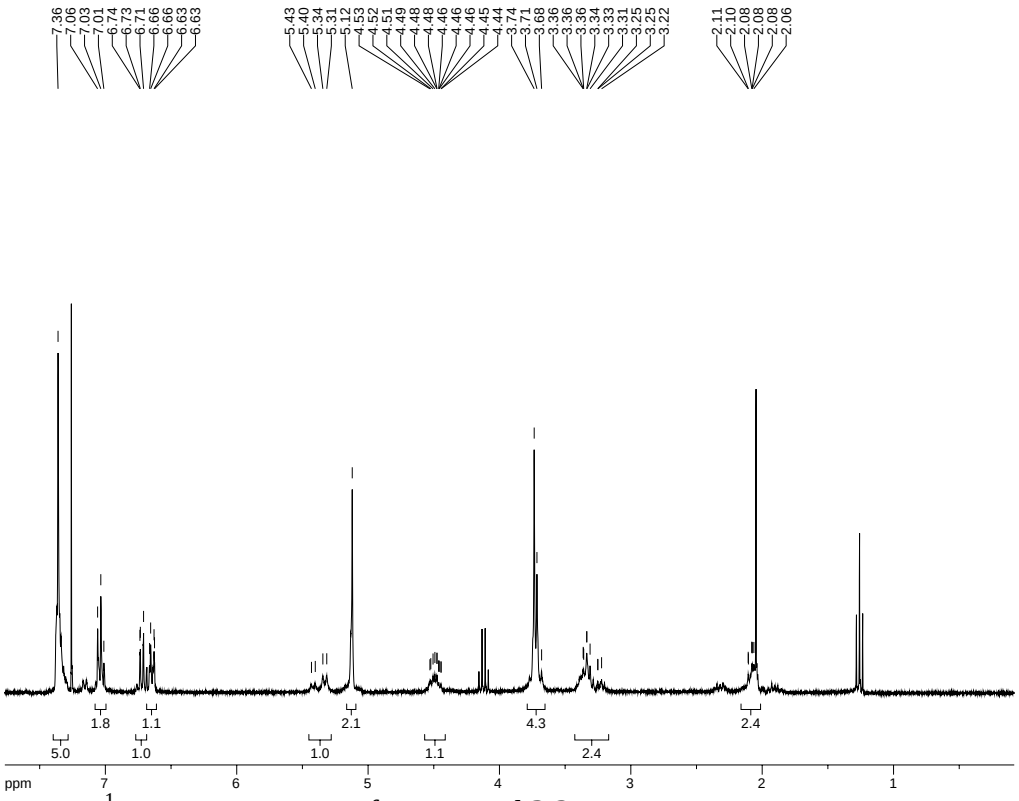

Figure 5.7a. ^{1}H NMR spectrum of compound **3.21**.

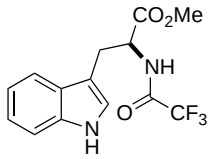

3.31

(*S*)-methyl 3-(1*H*-indol-3-yl)-2-(2,2,2-trifluoroacetamido)propanoate (3.31). To a solution of L-Trp-OMe·HCl (1.0 g, 3.92 mmol) in MeOH was added trifluoromethyl propionate (0.94 mL, 7.84 mmol) and Et_3N (1.1 mL, 7.84 mmol). After stirring 1 h at r.t., the reaction mixture was concentrated and the resulting residue dissolved in CH_2Cl_2. The organic phase was washed with ammonium hydroxide (5%, 1x) and brine (1x), then dried over Na_2SO_4 and concentrated to afford 1.23 g of the title compound, carried forward as crude (>99% yield).

^{1}H-NMR (300 MHz; $CDCl_3$): δ 8.25-8.23 (bs, 1H), 7.49 (d, *J* = 7.8 Hz, 1H), 7.37 (d, *J* = 8.1 Hz, 1H), 7.21 (td, *J* = 7.5, 1.1 Hz, 1H), 7.13 (td, *J* = 7.4, 1.0 Hz, 1H), 6.98 (d, *J* = 2.4 Hz, 1H), 6.87-6.85 (bs, 1H), 4.94 (dt, *J* = 7.8, 5.0 Hz, 1H), 3.73 (s, 3H), 3.42 (d, *J* = 5.1 Hz, 2H).

REF: TRW-I-423, **TRW-I-425**.

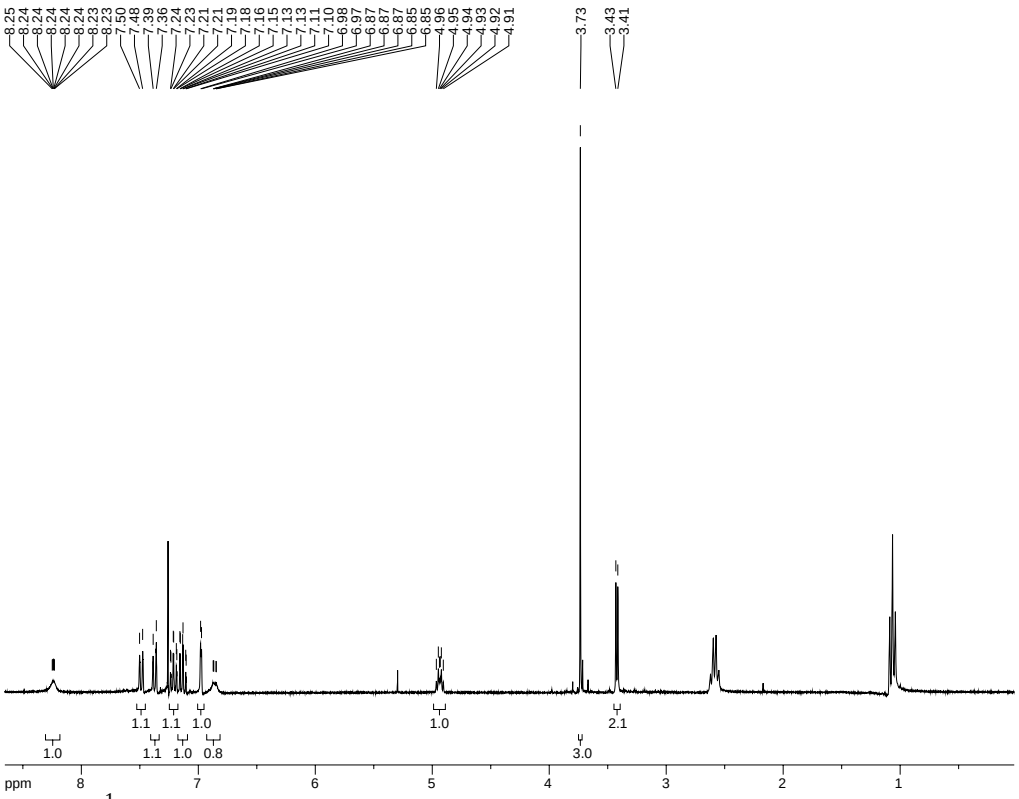

Figure 5.8a. ^{1}H NMR spectrum of compound **3.31**.

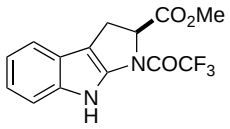

3.32

(*S*)-methyl 1-(2,2,2-trifluoroacetyl)-1,2,3,8-tetrahydropyrrolo[2,3-*b*]indole-2-carboxylate (3.32). To a solution of **3.31** (1.07 g, 3.4 mmol) in CH_2Cl_2 (34 mL) and Et_3N (1.9 mL, 13.6 mmol) at 0 °C was added *t*-BuOCl (0.41 mL, 3.4 mmol) dropwise. The resulting solution was allowed to warm to r.t. O/N with stirring. Water was added and the product extracted in to Et_2O. The combined organic layers were washed with brine, dried over Na_2SO_4, and concentrated. Recrystallization from EtOAc/hexanes provided the pure title compound (670 mg, 63% yield).

^{1}H-NMR (300 MHz; $CDCl_3$): δ 9.17-9.16 (bs, 1H), 7.39 (td, *J* = 6.7, 2.6 Hz, 2H), 7.17 (ddd, *J* = 7.0, 4.3, 2.2 Hz, 2H), 5.55 (dt, *J* = 9.7, 1.8 Hz, 1H), 3.82 (s, 3H), 3.74 (dd, *J* = 14.8, 9.7 Hz, 1H), 3.36 (dd, *J* = 14.8, 2.3 Hz, 1H).

REF: **TRW-I-424**, TRW-I-427.

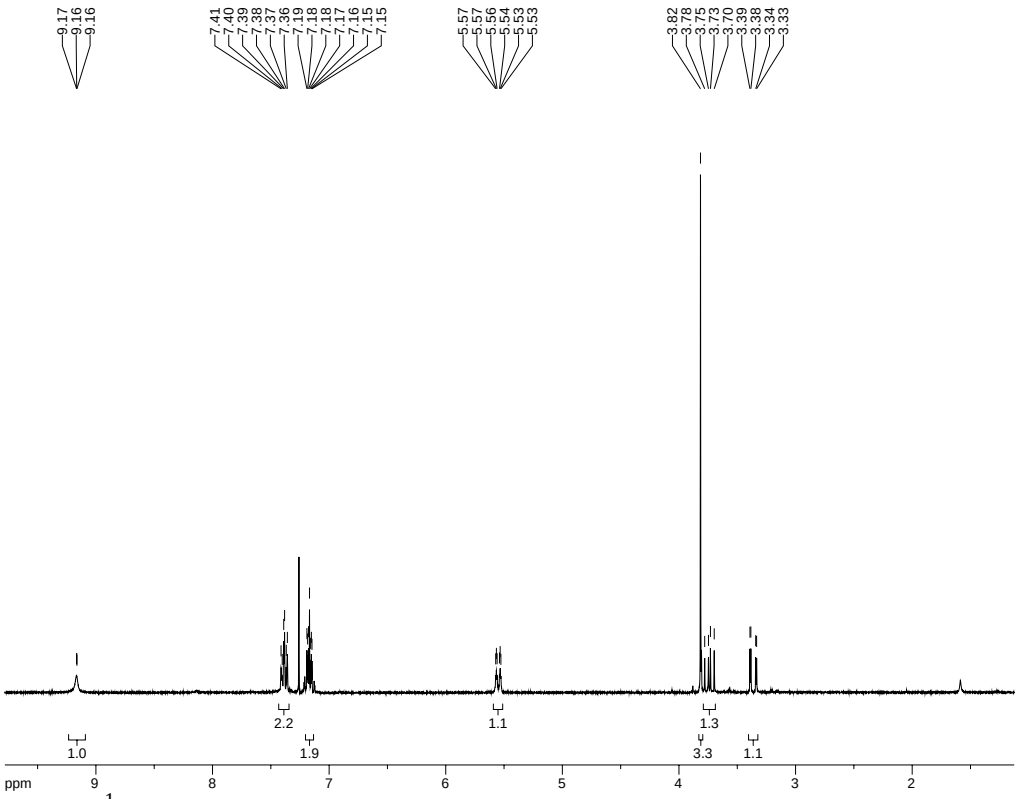

Figure 5.9a. ^{1}H NMR spectrum of compound **3.32**.

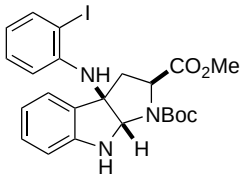

3.35

(2*S*,3a*R*,8a*S*)-1-*tert*-butyl 2-methyl 3a-((2-iodophenyl)amino)-3,3a,8,8a-tetrahydropyrrolo[2,3-*b*]indole-1,2(2*H*)-dicarboxylate (3.35). *N*-Boc-Trp-OMe (100 mg, 0.31 mmol) was dissolved in acetonitrile (6 mL), then 2-iodoaniline (81 mg, 0.37 mmol) added and the resulting solution cooled to -45 °C. Freshly recrystallized NIS (113 mg, 0.50 mmol) was added dropwise over 1 h as a solution in acetonitrile (1.5 mL). The reaction was allowed to warm to -35 °C as it stirred an additional hour. The entire reaction mixture was poured into a separatory funnel containing sat'd $Na_2S_2O_4$ and EtOAc. The product was extracted in EtOAc (3x) and the combined organic layers washed with brine, dried over Na_2SO_4, and concentrated. Crude **3.35** was purified by SiO_2 chromatography (5-10% EtOAc in hexanes) to afford pure **3.35** in 78% yield (130 mg).

^{1}H-NMR (300 MHz; $CDCl_3$): δ 7.64 (t, *J* = 7.8 Hz, 1H), 7.12 (dt, *J* = 13.7, 7.3 Hz, 2H), 6.99 (t, *J* = 7.7 Hz, 1H), 6.75-6.65 (m, 2H), 6.40 (t, *J* = 7.6 Hz, 1H), 6.30 (dd, *J* = 16.2, 8.2 Hz, 1H), 5.89 (d, *J* = 34.7 Hz, 1H), 4.63 (d, *J* = 25.6 Hz, 1H), 4.39 (ddd, *J* = 25.8, 8.3, 4.3 Hz, 1H), 3.82 (s, 3H), 2.72 (qd, *J* = 15.3, 6.6 Hz, 2H), 1.46 (d, *J* = 30.4 Hz, 9H).

REF: **TRW-I-435**, TRW-I-441.

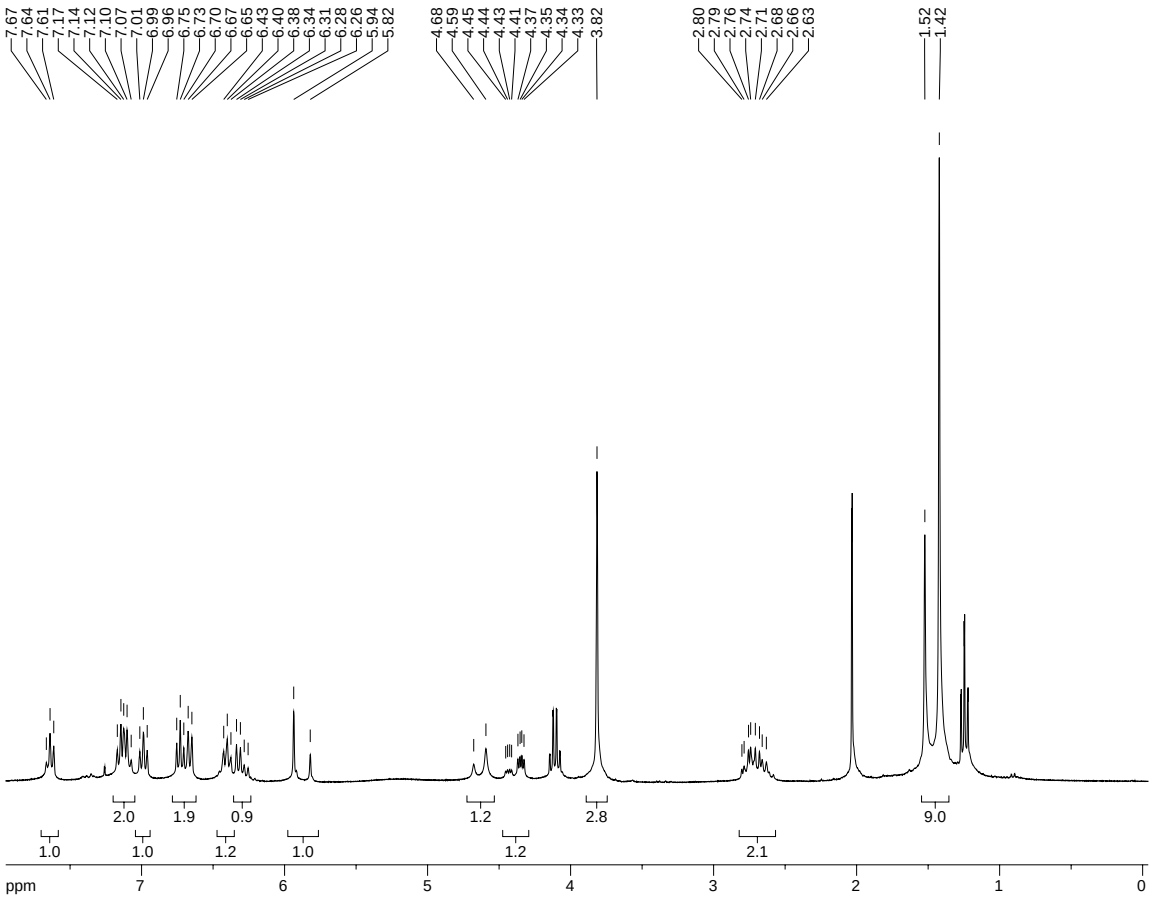

Figure 5.10a. ^{1}H NMR spectrum of compound **3.35**.

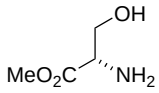

3.39

L-serine-OMe (3.39). To a solution of L-serine (50.0 g, 0.48 mol) in MeOH (450 mL) at 0 °C was added $SOCl_2$ (35 mL, 0.48 mol). The reaction was allowed to warm to r.t. as it stirred O/N. The resulting solution was concentrated, taken up in ether, filtered, and the solid washed with ether. The crude solid material was recrystallized in MeOH/ether to afford pure crystalline methyl ester **3.39** as the HCl salt.

REF: TRW-I-462, **TRW-II-118**.

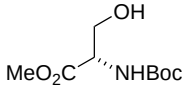

3.40

***N*-Boc-Ser-OMe (3.40)**. Boc anhydride (12.2 g, 56 mmol) was dissolved in acetonitrile (190 mL), then Et_3N (24 mL, 168 mmol) and L-Ser-OMe·HCl (8.74 g, 56 mmol) added. The reaction was allowed to stir for 6 h at r.t., then CH_2Cl_2 (950 mL) and 1M HCl (665 mL) added. The organic layer was separated and washed with sat'd $NaHCO_3$, then dried over Na_2SO_4 and concentrated to afford the title material, used as crude (10.01 g, 82% yield).

^{1}H-NMR (300 MHz; $CDCl_3$): δ 5.43 (m, *J* = 1.6, 0.8 Hz, 1H), 4.40-4.38 (m, 1H), 3.97-3.91 (m, 2H), 3.79 (s, 3H), 2.20-2.19 (m, 1H), 1.46 (s, 9H).

REF: **TRW-I-299**, TRW-I-439.

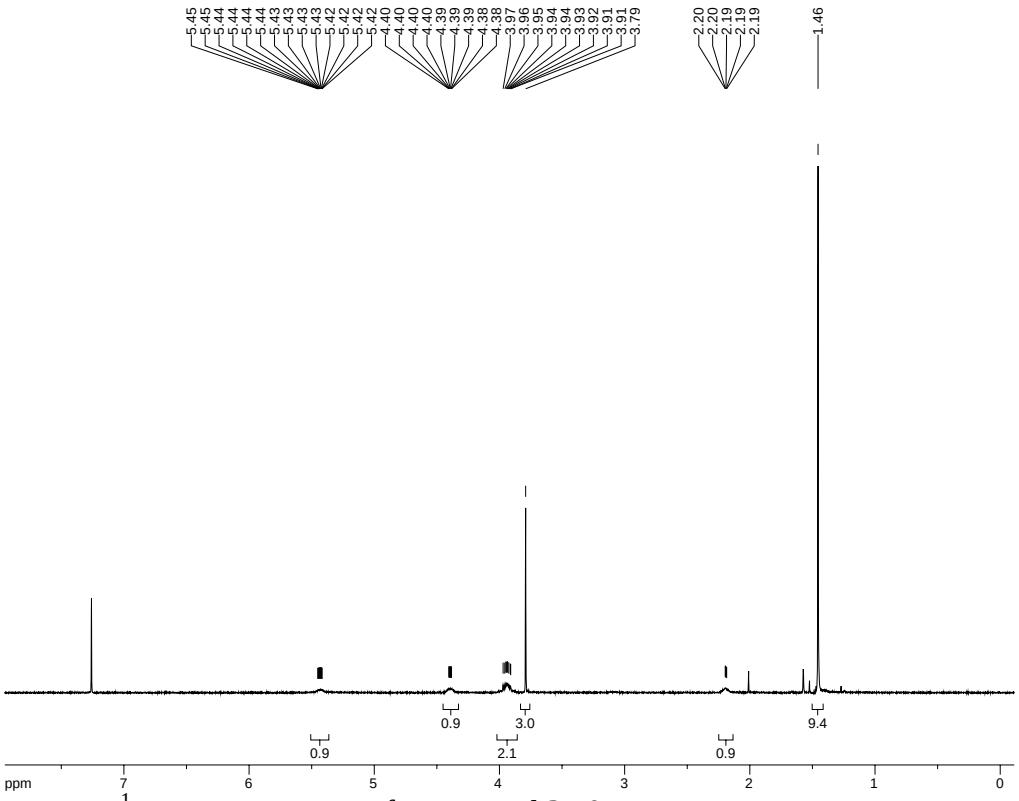

Figure 5.11a. ^{1}H NMR spectrum of compound **3.40**.

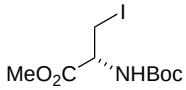

3.41

Methyl 2-(*tert*-butoxycarbonylamino)-3-iodopropanoate (3.41). To a solution of Ph_3P (2.13 g, 8.13 mmol) and imidazole (553 mg, 8.13 mmol) in CH_2Cl_2 (30 mL) at 0 °C was added I_2 (2.07 g, 8.13 mmol) in 3 portions. The reaction mixture was warmed to r.t. for 10 minutes, then cooled to 0 °C before adding dropwise a solution of Boc-Ser-OMe (1.42 g, 6.5 mmol) in 10 mL CH_2Cl_2. The resulting solution was stirred 1 h at 0 °C, then allowed to warm to r.t. as it stirred an additional 1.5 h. The crude reaction mixture was filtered through a plug of silica with 1:1 EtOAC/hexanes. The filtrate was concentrated under reduced pressure and purified by SiO_2 chromatography (5-20% EtOAc in hexanes) to afford iodide **3.41** (1.17 g, 55% yield).

^{1}H-NMR (300 MHz; $CDCl_3$): δ 5.36-5.33 (m, 1H), 4.55-4.50 (m, 1H), 3.80 (s, 3H), 3.56 (dq, *J* = 9.8, 5.0 Hz, 2H), 1.46 (s, 9H).

REF: TRW-I-196, TRW-I-205, **TRW-I-243**, TRW-I-440

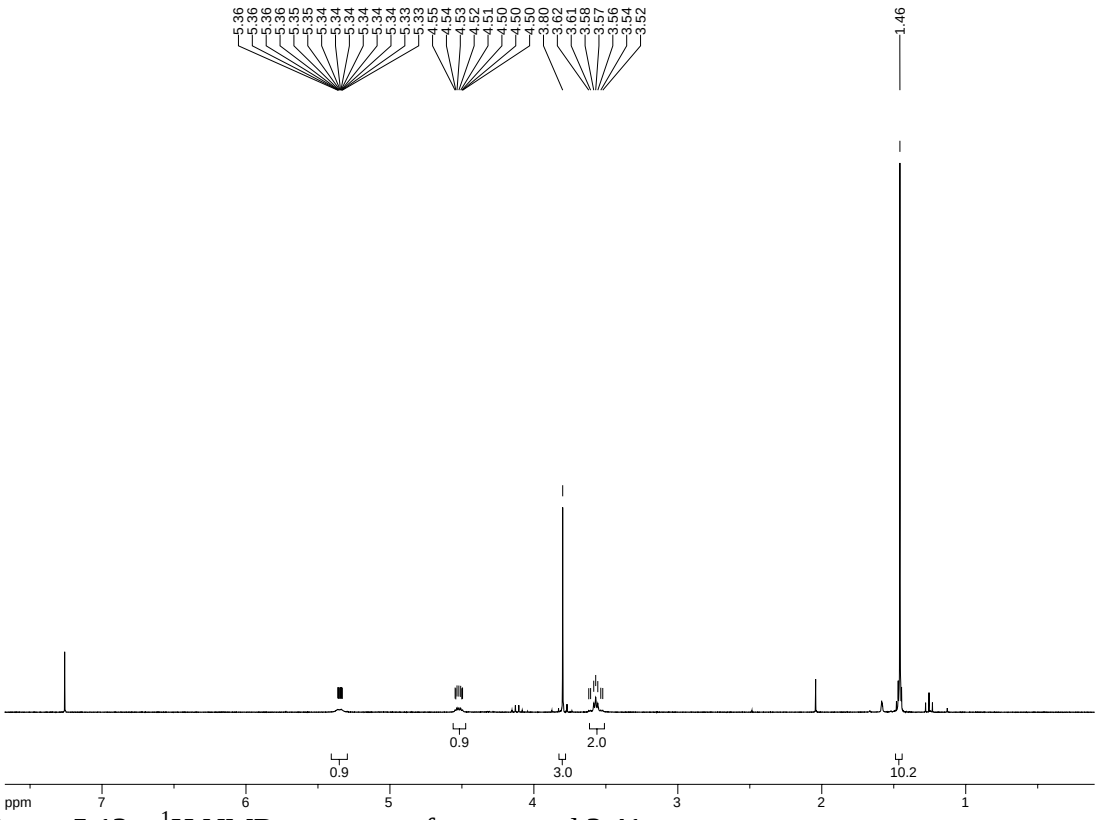

Figure 5.12a. ^{1}H NMR spectrum of compound **3.41**.

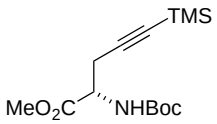

3.42

(*S*)-methyl 2-((*tert*-butoxycarbonyl)amino)-5-(trimethylsilyl)pent-4-ynoate (3.42). A flask (Flask A) containing CuCN (123 mg, 1.37 mmol) and LiCl (115 mg, 2.74 mmol) was heated to 150 °C under vacuum for 2 h, then cooled to r.t. DMF (4 mL) was added and the suspension sonicated until full dissolution was observed. This solution was then cooled to -20 °C. A second flask (Flask B) containing Zn dust (358 mg, 5.47 mmol) was heated under vaccum, cooled to r.t., filled with Ar, then DMF (1.75 mL) and dibromoethane (26 µL, 0.30 mmol) added. The suspension was heated to 80 °C for 30 min, then cooled to r.t. before addition of TMSCl (19 µL, 0.15 mmol). Following an additional 30 min of stirring, *N*-Boc-Ser(I)-OMe (**3.41**, 500 mg, 1.52 mmol) was added slowly as a solution in a minimal amount of DMF. After complete addition, this suspension was transferred to Flask A. The combined reaction mixture was allowed to stir for 15 min at -20 °C, then TMS-acetylene bromide (269 mg, 1.52 mmol) added dropwise. The reaction mixture was allowed to warm to r.t. O/N. Water was added (15 mL) and the product extracted in EtOAc. The combined organic layers were washed with brine, dried over Na_2SO_4, and concentrated. SiO_2 chromatography (3:1 hexanes/EtOAc) afforded the pure title compound (180 mg, 40% yield, stains with vanillin).

^{1}H-NMR (300 MHz; $CDCl_3$): δ 5.28 (d, J = 8.4 Hz, 1H), 4.43-4.37 (m, 1H), 3.70 (s, 3H), 2.75-2.59 (m, 2H), 1.39 (s, 9H), 0.07 (s, 8H).

REF: **TRW-I-444**, TRW-I-452, TRW-I-469.

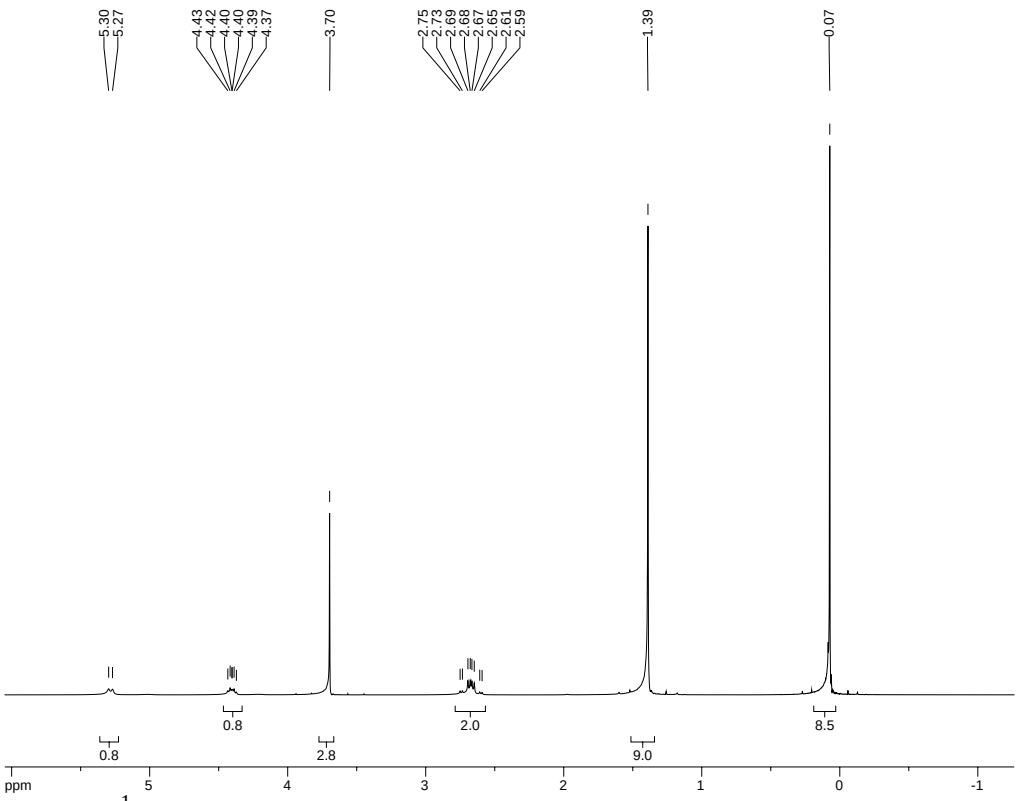

Figure 5.13a. ^{1}H NMR spectrum of compound **3.42**.

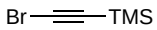

(Bromoethynyl)trimethylsilane. To a solution of TMS-acetylene (5 mL, 35.5 mmol) in acetone (120 mL) was added $AgNO_3$ (604 mg, 3.55 mmol) and NBS (6.94 g, 39 mmol). After stirring 3 h, the reaction was quenched by addition of ice water. The product was extracted in pentane and the combined organic layers washed with brine, dried over Na_2SO_4, and concentrated (bath at 0 °C) to afford pure (bromoethynyl)trimethylsilane (4.51 g, 72% yield).

^{1}H-NMR (300 MHz; $CDCl_3$): δ 0.18 (s, 9H).

REF: TRW-I-442, **TRW-I-457**.

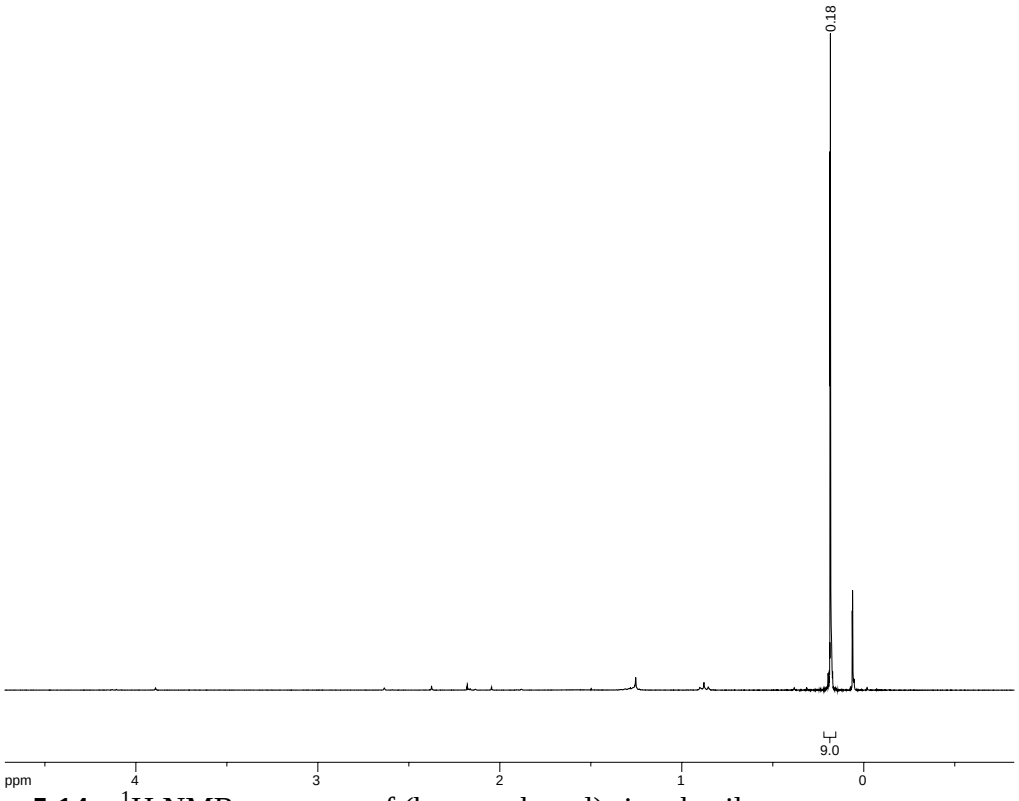

Figure 5.14a. ^{1}H NMR spectrum of (bromoethynyl)trimethysilane.

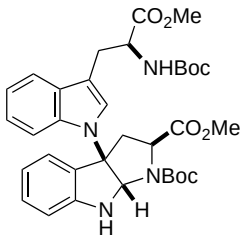

3.43

(2*S*,3a*R*,8a*S*)-1-*tert*-butyl 2-methyl 3a-(3-((*S*)-2-((*tert*-butoxycarbonyl)amino)-3-methoxy-3-oxopropyl)-1*H*-indol-1-yl)-3,3a,8,8a-tetrahydropyrrolo[2,3-*b*]indole-1,2(2*H*)-dicarboxylate (3.43). A flask containing **3.35** (300 mg, 0.56 mmol), **3.42** (370 mg, 1.24 mmol), NaOAc (321 mg, 3.92 mmol), LiCl (24 mg, 0.56 mmol), and $Pd(OAc)_2$ (25 mg, 0.11 mmol) was vacated and backfilled with Ar. DMF (3 mL) was added and the suspension sonicated for 15 minutes while bubbling Ar through reaction. Three freeze-pump-thaw cycles were performed to complete the degassing procedure. The reaction mixture was heated to 100 °C for 24 h, then diluted with toluene and concentrated. The crude residue was taken up in EtOAc, filtered through celite, and washed with 3M HCl. The organic fraction was further washed with brine, dried over Na_2SO_4, and concentrated to afford the title compound (**3.43**, 250 mg, 70% yield).

^{1}H-NMR (300 MHz; $CDCl_3$): δ 7.62 (d, *J* = 8.1 Hz, 1H), 7.52 (d, *J* = 7.6 Hz, 1H), 7.35-7.25 (m, 3H), 7.14 (d, *J* = 7.4 Hz, 1H), 6.92 (d, *J* = 7.5 Hz, 1H), 6.77 (d, *J* = 7.7 Hz, 1H), 6.64 (s, 1H), 6.05-5.91 (m, 1H), 5.02 (d, *J* = 7.9 Hz, 1H), 4.55-4.53 (m, 1H), 4.28-4.20 (m, 1H), 3.80 (d, *J* = 3.1 Hz, 3H), 3.58-3.47 (m, 3H), 3.36 (dd, *J* = 13.1, 9.3 Hz, 1H), 3.15-3.14 (m, 1H), 2.98 (dd, *J* = 13.2, 7.8 Hz, 1H), 1.42 (complex, *J* = 28.4 Hz, 18H).

REF: TRW-I-453, **TRW-I-458**.

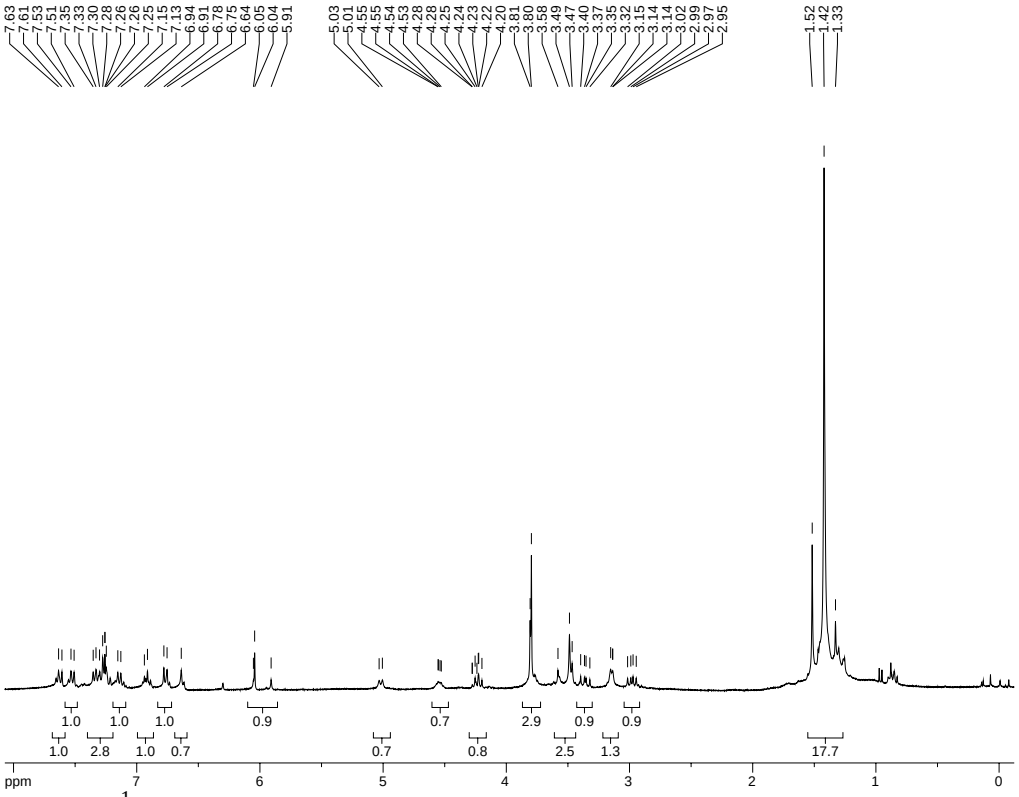

Figure 5.15a. ^{1}H NMR spectrum of compound **3.43**.

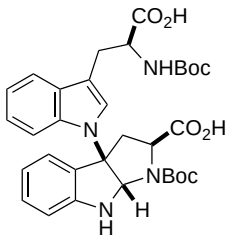

3.44

(2*S*,3a*R*,8a*S*)-1-(*tert*-butoxycarbonyl)-3a-(3-((*S*)-2-((*tert*-butoxycarbonyl)amino)-2-carboxyethyl)-1*H*-indol-1-yl)-1,2,3,3a,8,8a-hexahydropyrrolo[2,3-*b*]indole-2-carboxylic acid (3.44). To a solution of **3.43** (100 mg, 0.136 mmol) in THF and MeOH (2:1, 0.40 mL:0.20 mL) was added LiOH (20 mg, 0.80 mmol). After stirring under Ar O/N, 10% $KHSO_4$ was added until the solution was acidic, then the product extracted in EtOAc. The combined organic extracts were washed with brine, dried over Na_2SO_4, and concentrated. Crude **3.44** recovered as such was carried forward to the next reaction (90.4 mg, 93% yield).

^{1}H-NMR (300 MHz; $CDCl_3$): δ 7.55-7.53 (m, 1H), 7.17 (d, *J* = 8.4 Hz, 2H), 7.06-7.00 (m, 1H), 6.90-6.86 (m, 1H), 6.79-6.62 (m, 3H), 6.48-6.32 (m, 1H), 6.24-6.13 (m, 1H), 4.63-4.34 (m, 2H), 3.56-3.47 (m, 1H), 3.20-3.18 (m, 1H), 3.04-2.82 (m, 2H), 1.50-1.38 (m, 18H).

REF: **TRW-I-456**, TRW-I-460.

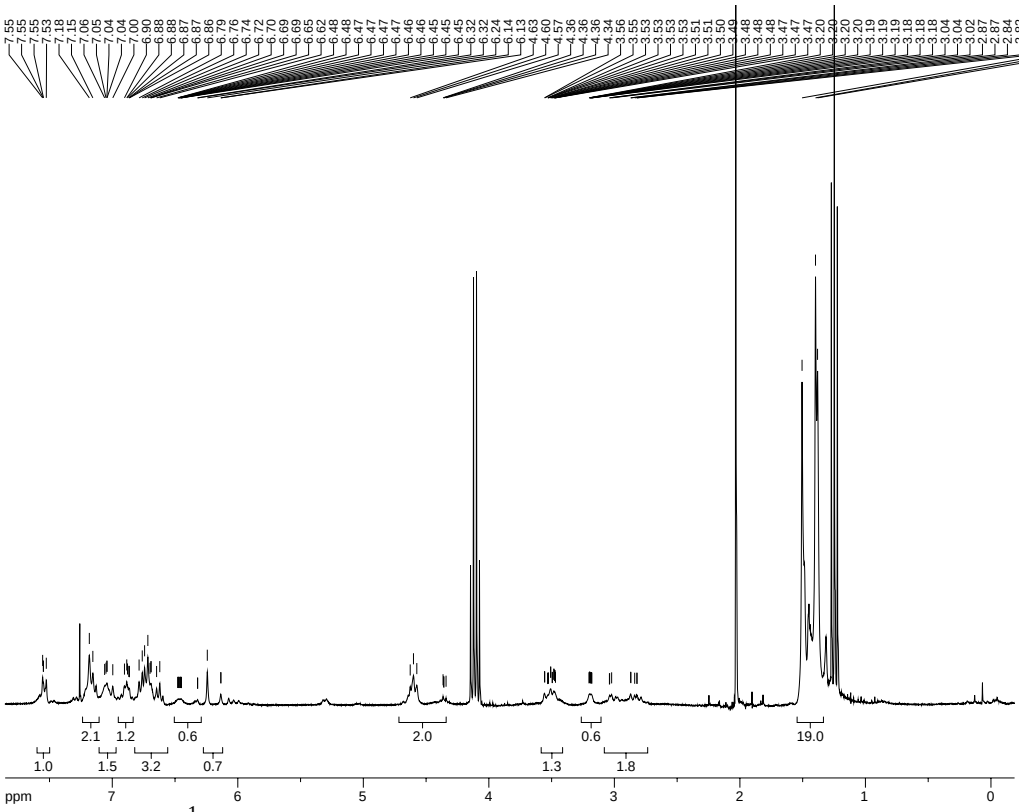

Figure 5.16a. ^{1}H NMR spectrum of compound **3.44**.

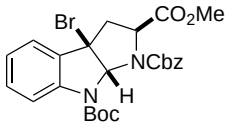

3.47

(2*S*,3a*R*,8a*R*)-1-benzyl 8-*tert*-butyl 2-methyl 3a-bromo-3,3a-dihydropyrrolo[2,3-*b*]indole-1,2,8(2*H*,8a*H*)-tricarboxylate (3.47). To a solution of *N*-Cbz,*N*'-Boc-Trp-OMe (1.0 g, 2.2 mmol) in CH_2Cl_2 (100 mL) was added PPTS (552 mg, 2.2 mmol) and NBS (392 mg, 2.2 mmol). The resulting solution was stirred O/N at r.t, then diluted with CH_2Cl_2, washed with brine, dried over Na_2SO_4, and concentrated. Crude **3.47** was purified by SiO_2 chromatography (25% EtOAc in hexanes) to afford pure material in 88% yield (1.03 g).

^{1}H-NMR (300 MHz; $CDCl_3$): δ 7.37-7.28 (m, 8H), 7.12 (td, *J* = 7.5, 0.7 Hz, 1H), 6.43 (s, 1H), 5.19-5.16 (m, 2H), 3.97 (dd, *J* = 10.3, 6.5 Hz, 1H), 3.69-3.41 (m, 3H), 3.26 (dd, *J* = 12.7, 6.5 Hz, 1H), 2.84 (dd, *J* = 12.7, 10.3 Hz, 1H), 1.52 (s, 9H).

REF: **TRW-I-477**.

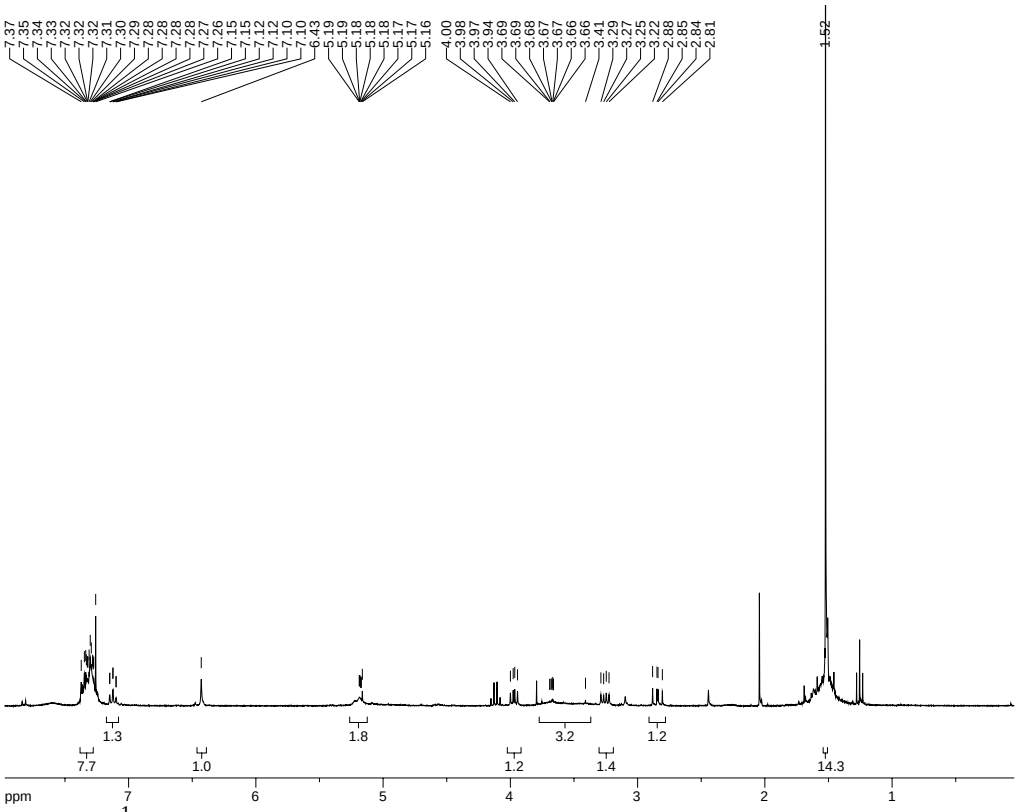

Figure 5.17a. ^{1}H NMR spectrum of compound **3.47**.

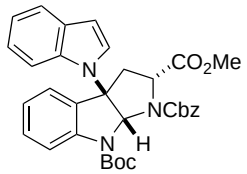

3.48

(2*R*,3a*R*,8a*R*)-1-benzyl 8-*tert*-butyl 2-methyl 3a-(1*H*-indol-1-yl)-3,3a-dihydropyrrolo[2,3-*b*]indole-1,2,8(2*H*,8a*H*)-tricarboxylate (3.48).

Bromopyrroloindoline **3.47** (500 mg, 0.94 mmol) was dissolved in acetonitrile (20 mL), and to it added indole (74 mg, 0.63 mmol). The suspension was cooled to 0 °C, then KO*t*Bu (141 mg, 1.26 mmol) added slowly. Once the reaction was deemed complete by TLC, the mixture was quenched by addition of sat'd $NaHCO_3$ and the product extracted in CH_2Cl_2. The combined organic layers were washed with brine, dried over Na_2SO_4, concentrated, and purified by SiO_2 chromatography (3:1 hexanes:EtOAc) to afford pure **3.48** (100 mg, 28% yield).

^{1}H-NMR (300 MHz; $CDCl_3$): δ 7.79-7.75 (bs, 1H), 7.65-7.62 (m, 1H), 7.44-7.27 (m, 8H), 7.19-7.15 (m, 3H), 6.96 (d, *J* = 3.0 Hz, 1H), 6.44 (d, *J* = 3.4 Hz, 1H), 5.30-5.20 (m, 2H), 4.97 (d, *J* = 8.9 Hz, 1H), 3.57 (dd, *J* = 13.0, 9.3 Hz, 1H), 3.22 (s, 3H), 3.07 (d, *J* = 13.1 Hz, 1H), 1.47 (bs, 9H).

REF: **TRW-I-482**, TRW-I-484.

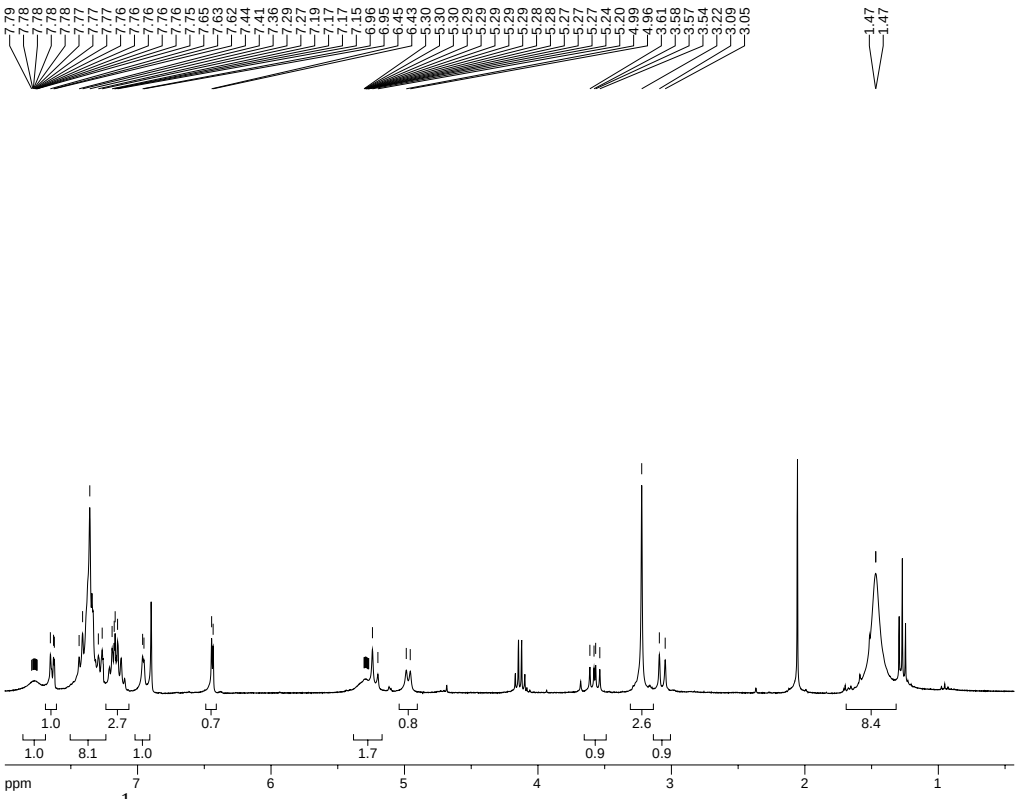

Figure 5.18a. ^{1}H NMR spectrum of compound **3.48**.

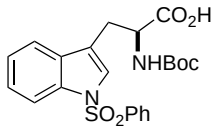

3.56

***N*-Boc-L-tryptophan-*N*-SO_2Ph (3.56)**. *N*-Boc-Trp (14.8 g, 48.7 mmol) was dissolved in THF (100 mL) and the resulting solution cooled to -78 °C. LHMDS (146 mL, 146.1 mmol) was added slowly over 5 minutes. The reaction was stirred at -78 °C for 1 h, then $PhSO_2Cl$ (7.5 mL, 58.4 mmol) added in one portion. After stirring an additional 2 h at -78 °C, the reaction was quenched by addition of 1:1 AcOH:EtOAc then allowed to warm to r.t. The suspension was diluted with 1M HCl and the product extracted in EtOAc. The combined organic layers were dried and concentrated to afford crude **3.56**, purified by SiO_2 chromatography (5% AcOH, 45% hexanes, 50% CH_2Cl_2) to afford pure **3.56** (17.12 g, 79% yield).

^{1}H-NMR (300 MHz; DMSO-d_6): δ 12.64-12.63 (m, 1H), 7.90-7.87 (m, 2H), 7.61 (t, *J* = 7.8 Hz, 2H), 7.56-7.50 (m, 2H), 7.25-7.20 (m, 2H), 7.16-7.13 (m, 2H), 4.20-4.17 (m, 1H), 3.11 (dd, *J* = 14.8, 4.2 Hz, 1H), 2.95 (dd, *J* = 14.8, 10.0 Hz, 1H), 1.31 (s, 9H).

REF: TRW-II-176, **TRW-II-251**.

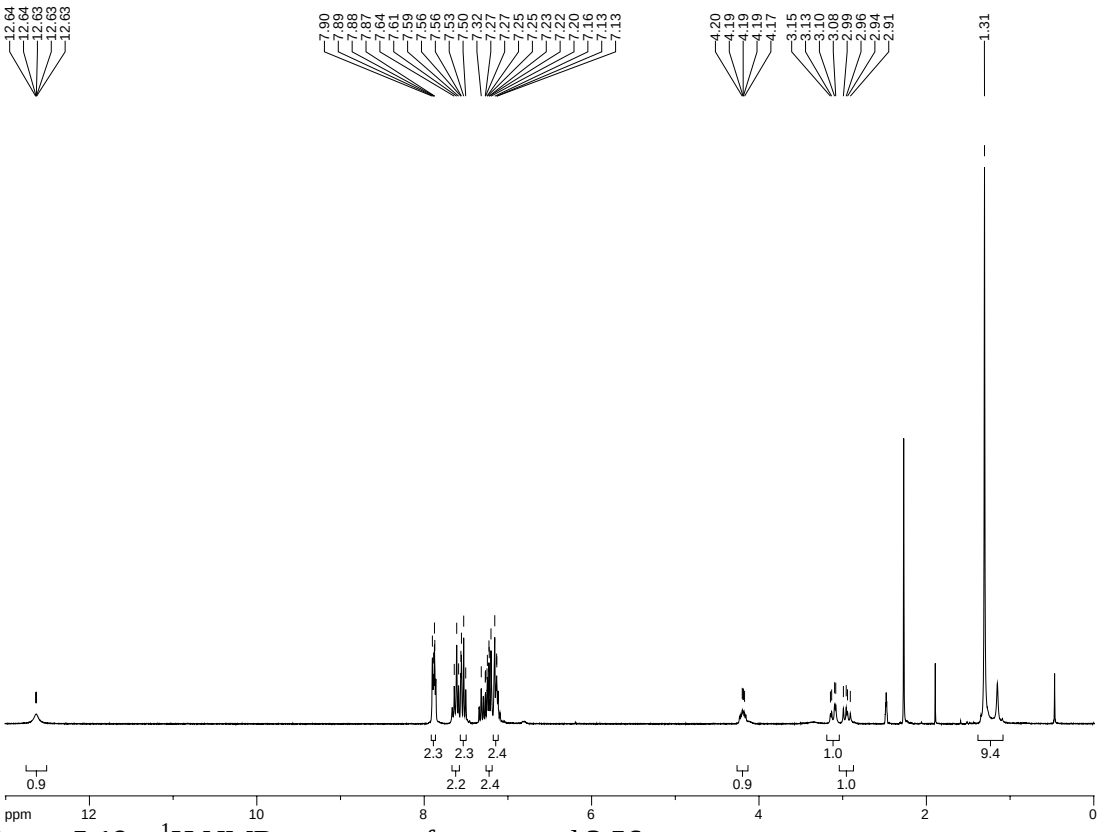

Figure 5.19a. ^{1}H NMR spectrum of compound **3.56**.

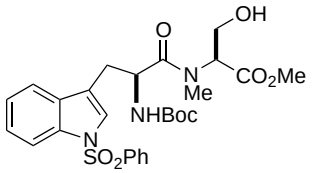

3.57a

Dipeptide (3.57a). To a solution of *N*-Me-L-serine-OMe (2.0 g, 15 mmol) in CH_2Cl_2 (75 mL) was added *i*Pr_2NEt (2.61 mL, 15 mmol). After stirring 15 minutes, the suspension was added to a stirring solution of **3.56** (6.66 g, 15 mmol) and EDCI (2.88 g, 15 mmol) in CH_2Cl_2. The reaction was stirred O/N at r.t., then concentrated and purified through a plug of SiO_2 (100% EtOAc) to afford **3.57a** (86% yield).

^{1}H-NMR (300 MHz; DMSO-d_6): δ 8.40 (d, *J* = 7.4 Hz, 1H), 7.87 (t, *J* = 8.8 Hz, 2H), 7.67 (dt, *J* = 21.1, 6.5 Hz, 2H), 7.54 (t, *J* = 7.7 Hz, 2H), 7.29 (complex, 2H), 6.95 (d, *J* = 8.9 Hz, 1H), 5.14 (dt, *J* = 11.2, 5.6 Hz, 1H), 4.47 (d, *J* = 5.7 Hz, 1H), 4.38-4.34 (m, 1H), 3.77-3.70 (m, 1H), 3.60 (s, 3H), 3.07-3.01 (m, 1H), 2.88-2.80 (m, 1H), 2.48 (s, 3H), 1.25 (s, 9H), 1.06 (s, 1H).

REF: **TRW-II-129**.

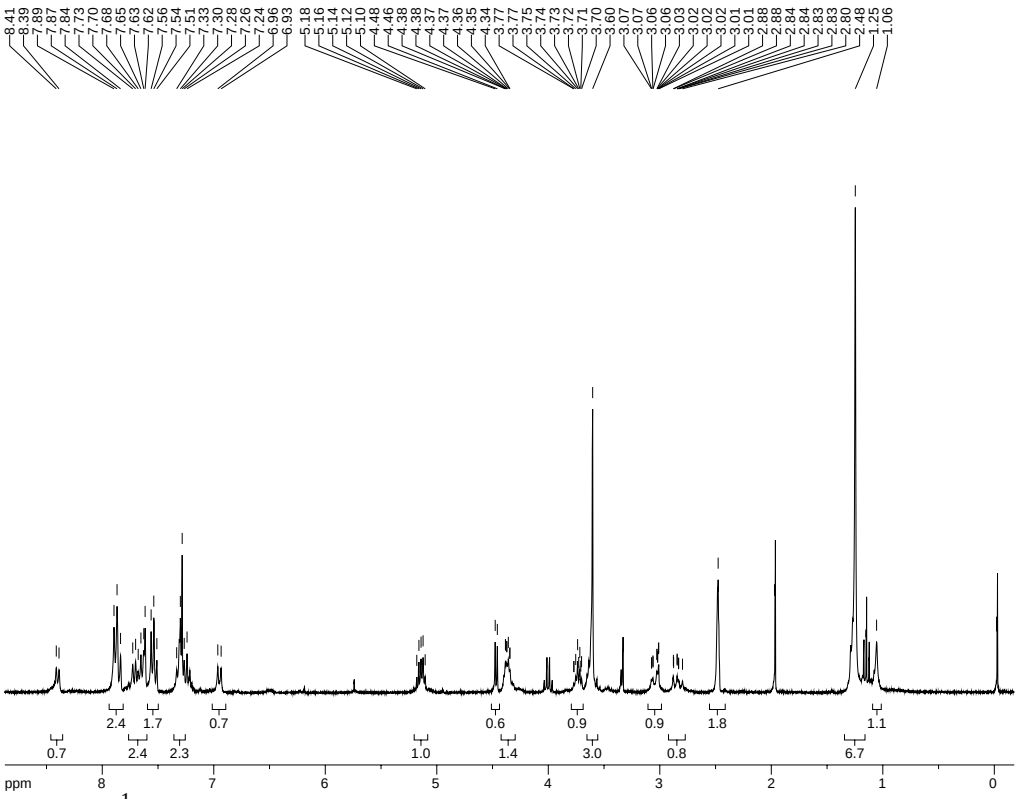

Figure 5.20a. ^{1}H NMR spectrum of compound **3.57a**.

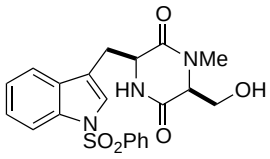

3.58a

Dioxopiperazine (3.58a). Dipeptide **3.57a** (500 mg) was transferred to a microwave tube, then heated neat in the microwave at maximum power to a safe temperature of 180 °C (microwave set to 'open-vessel'). After cooling, the residue was suspended in CH_2Cl_2, transferred to a vial, and concentrated to afford dioxopiperazine **3.58a** (94% yield).

^{1}H-NMR (300 MHz; DMSO-d_6): δ 8.15 (d, *J* = 2.4 Hz, 1H), 8.03 (d, *J* = 2.0 Hz, 1H), 7.89 (dd, *J* = 24.0, 7.8 Hz, 3H), 7.64 (t, *J* = 3.6 Hz, 2H), 7.56 (d, *J* = 4.0 Hz, 1H), 7.33-7.27 (m, 2H), 5.14 (t, *J* = 5.7 Hz, 1H), 4.47 (d, *J* = 5.6 Hz, 1H), 4.05-4.00 (m, 1H), 3.74 (d, *J* = 2.1 Hz, 1H), 3.65-3.60 (m, 1H), 3.42 (t, *J* = 4.2 Hz, 1H), 3.24 (dd, *J* = 59.1, 5.0 Hz, 3H).

REF: **TRW-II-132**.

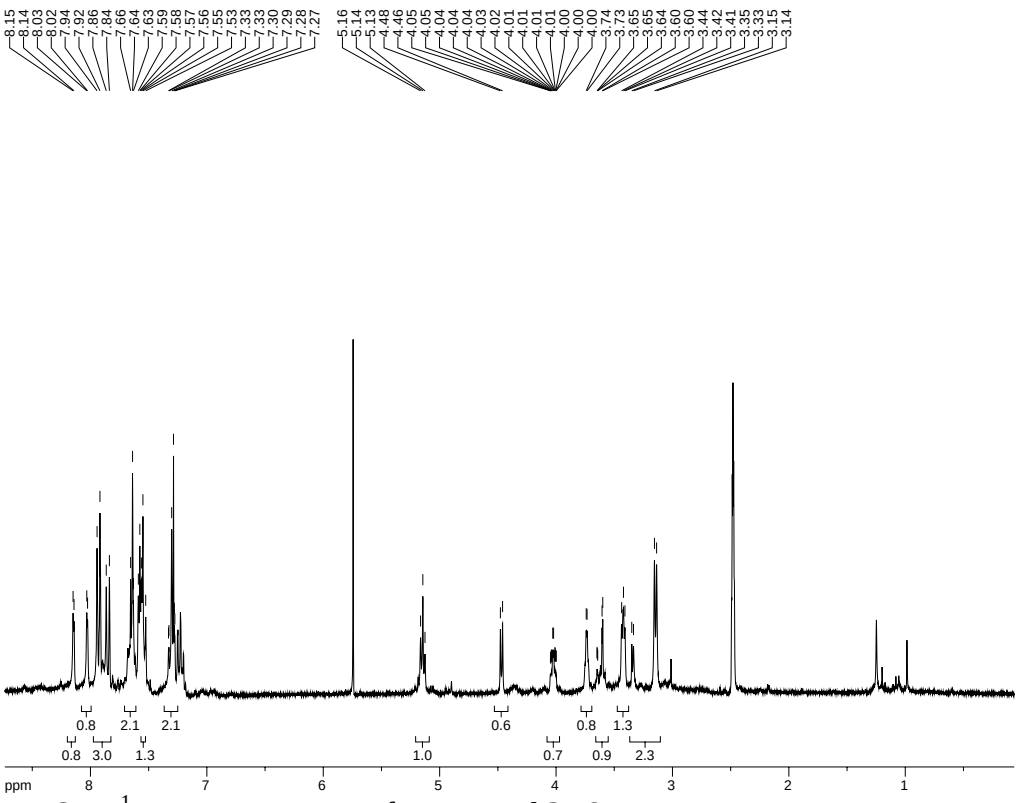

Figure 5.21a. ^{1}H NMR spectrum of compound **3.58a**.

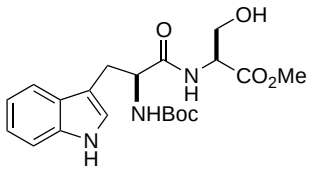

3.57c

(***S*)-methyl 2-((*S*)-2-((*tert*-butoxycarbonyl)amino)-3-(1*H*-indol-3-yl)propan-amido)-3-hydroxypropanoate (3.57c)**. To a solution of L-Ser-OMe·HCl (2.56 g, 16.4 mmol) in CH_2Cl_2 (80 mL) was added *i*Pr_2NEt (2.85 mL, 16.4 mmol). After stirring 15 minutes, *N*-Boc-L-Trp (5.0 g, 16.4 mmol) and EDCI (3.15 g, 16.4 mmol) were added. The reaction was stirred O/N at r.t., then concentrated and purified through a plug of SiO_2 (100% EtOAc) to afford **3.57c** (5.71 g, 86% yield).

^{1}H-NMR (400 MHz; $CDCl_3$): δ 8.69 (bs, 1H), 7.52 (d, *J* = 7.8 Hz, 1H), 7.23 (d, *J* = 8.0 Hz, 1H), 7.06 (t, *J* = 7.4 Hz, 1H), 7.01-6.97 (m, 2H), 5.34 (d, *J* = 7.4 Hz, 1H), 4.42 (bs, 2H), 3.70 (bs, 2H), 3.54 (s, 3H), 3.16 (bs, 2H), 1.30 (s, 9H); ^{13}C-NMR (101 MHz; $CDCl_3$): δ 172.4, 170.6, 155.8, 136.2, 127.5, 123.5, 122.0, 119.4, 118.5, 111.4, 109.8, 80.4, 62.5, 54.8, 52.6, 28.23, 28.14, 28.08.

REF: **TRW-II-043**.

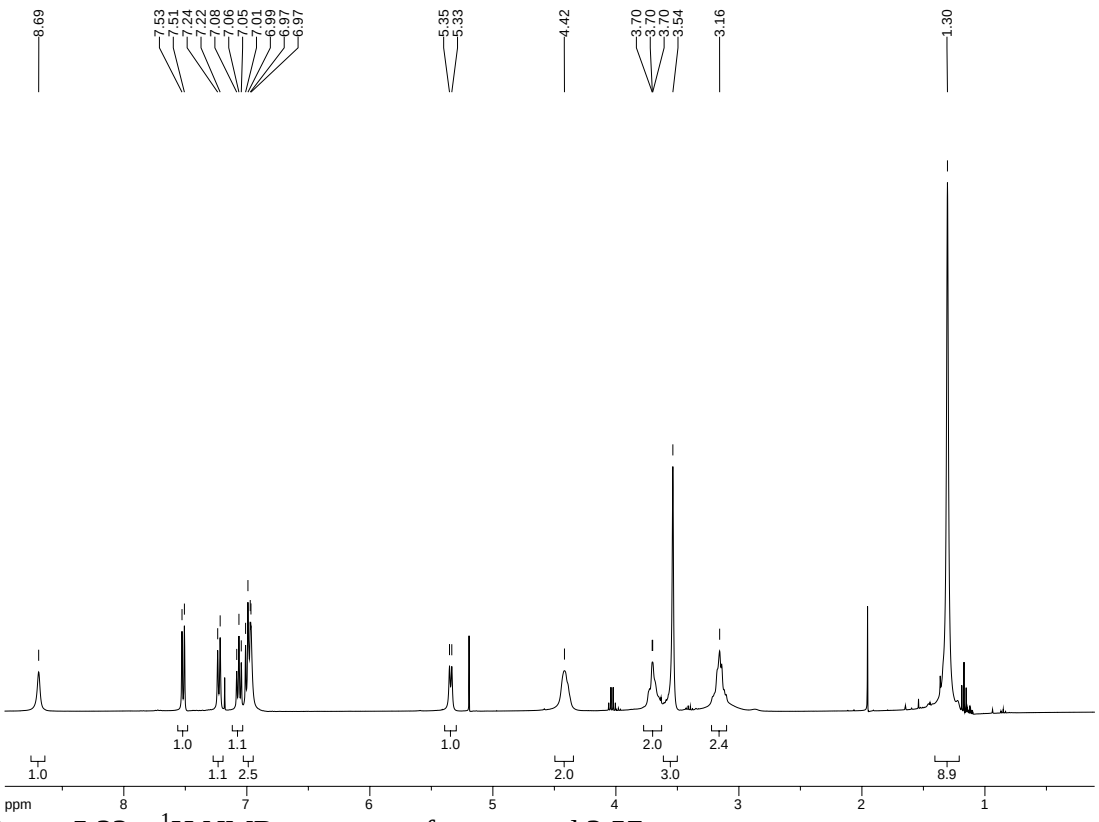

Figure 5.22a. ^{1}H NMR spectrum of compound **3.57c**.

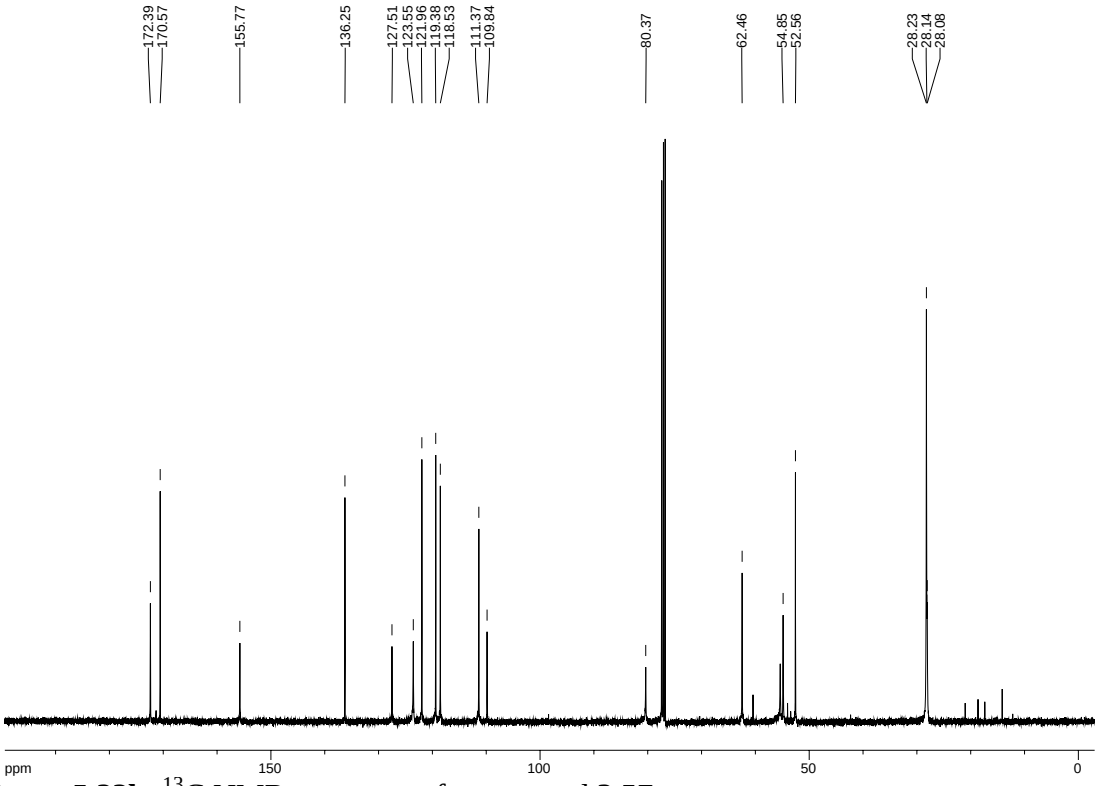

Figure 5.22b. ^{13}C NMR spectrum of compound **3.57c**.

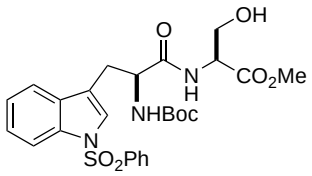

3.57d

Dipeptide (3.57d). To a solution of L-Ser-OMe·HCl (6.0 g, 38.5 mmol) in CH_2Cl_2 (200 mL) was added *i*Pr_2NEt (6.7 mL, 38.5 mmol). After stirring 15 minutes, the suspension was added to a stirring solution of **3.56** (17.12 g, 38.5 mmol) and EDCI (7.39 g, 38.5 mmol) in CH_2Cl_2. The reaction was stirred O/N at r.t., then concentrated and purified through a plug of SiO_2 (100% EtOAc) to afford **3.57d** (13.78 g, 66% yield).

^{1}H-NMR (300 MHz; $CDCl_3$): δ 7.96 (d, *J* = 8.1 Hz, 1H), 7.86 (d, *J* = 7.1 Hz, 2H), 7.52 (t, *J* = 7.0 Hz, 2H), 7.44 (dd, *J* = 13.3, 5.5 Hz, 3H), 7.31 (t, *J* = 7.1 Hz, 1H), 6.96 (d, *J* = 6.7 Hz, 1H), 5.24-5.21 (m, 1H), 4.59-4.56 (m, 1H), 4.44 (q, *J* = 7.2 Hz, 1H), 3.89 (dt, *J* = 1.3, 0.7 Hz, 2H), 3.72 (s, 3H), 3.18 (d, *J* = 6.0 Hz, 2H), 1.40 (s, 9H); ^{13}C-NMR (101 MHz; $CDCl_3$): δ 171.9, 170.7, 155.9, 138.0, 135.0, 133.7, 130.8, 129.2, 126.6, 124.72, 124.70, 123.2, 119.6, 117.9, 113.5, 80.3, 62.4, 54.7, 52.6, 28.16, 28.00.

REF: TRW-II-107, TRW-II-178, **TRW-II-253**.

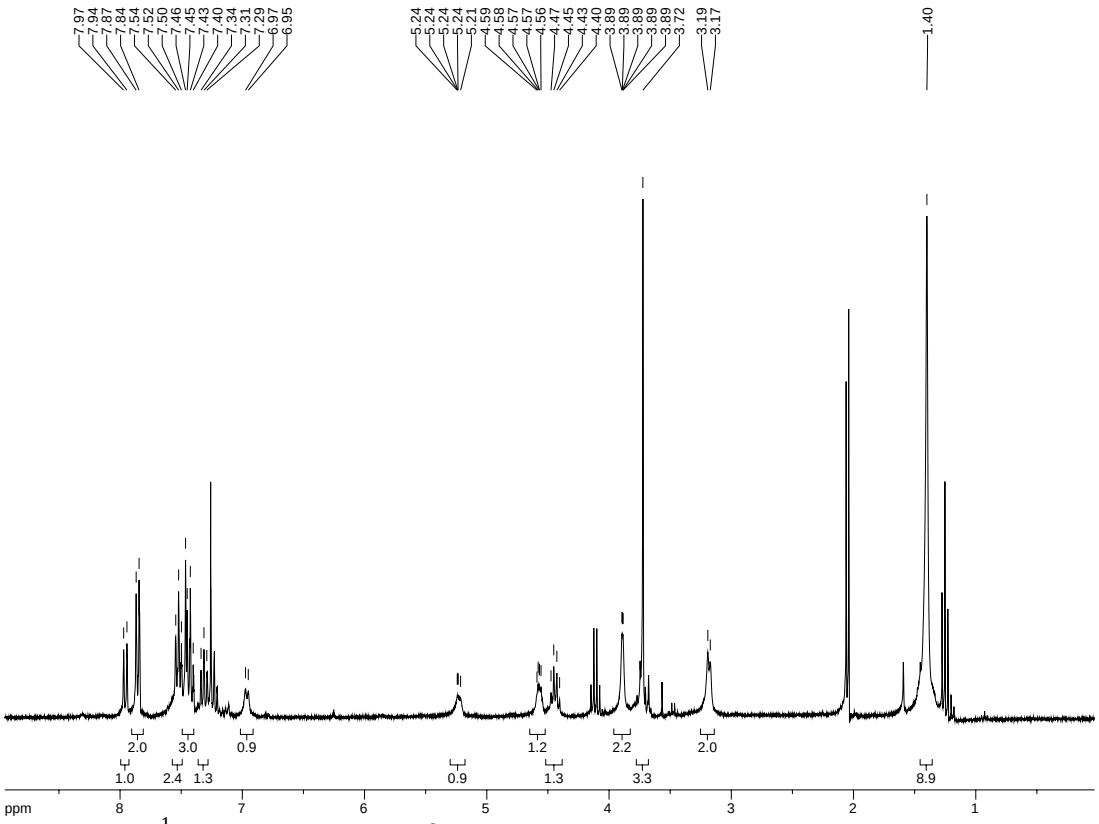

Figure 5.23a. ^{1}H NMR spectrum of compound **3.57d**.

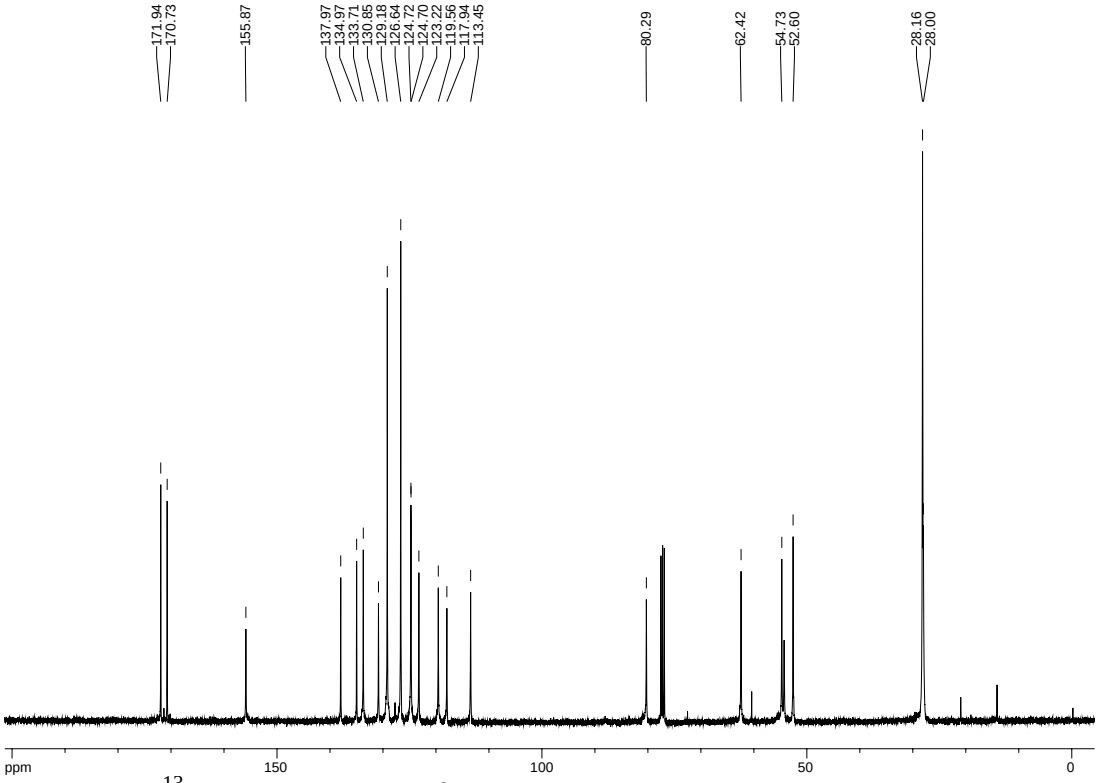

Figure 5.23b. ^{13}C NMR spectrum of compound **3.57d.**

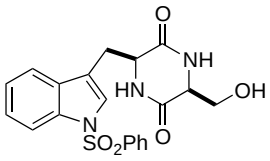

3.58d

(3*S*,6*S*)-3-(hydroxymethyl)-6-((1-(phenylsulfonyl)-1*H*-indol-3-yl)methyl)piperazine-2,5-dione (3.58d). The general cyclization procedure given for compound **3.58a** was repeated.

^{1}H-NMR (300 MHz; DMSO-d_6): δ 8.14-7.86 (m, 4H), 7.64-7.56 (m, 4H), 7.30-7.28 (m, *J* = 5.5, 0.8 Hz, 2H), 5.13-5.13 (m, 1H), 4.38-4.03 (m, 1H), 3.74-3.60 (m, 2H), 3.43-3.33 (m, 2H), 3.15-2.85 (m, 2H); ^{13}C-NMR (101 MHz; DMSO): δ 167.5, 167.3, 137.6, 137.2, 134.8, 131.4, 130.2, 126.9, 125.9, 123.6, 120.4, 118.5, 113.40, 113.31, 63.0, 57.3, 54.7, 50.9.

REF: **TRW-II-063**, TRW-II-186.

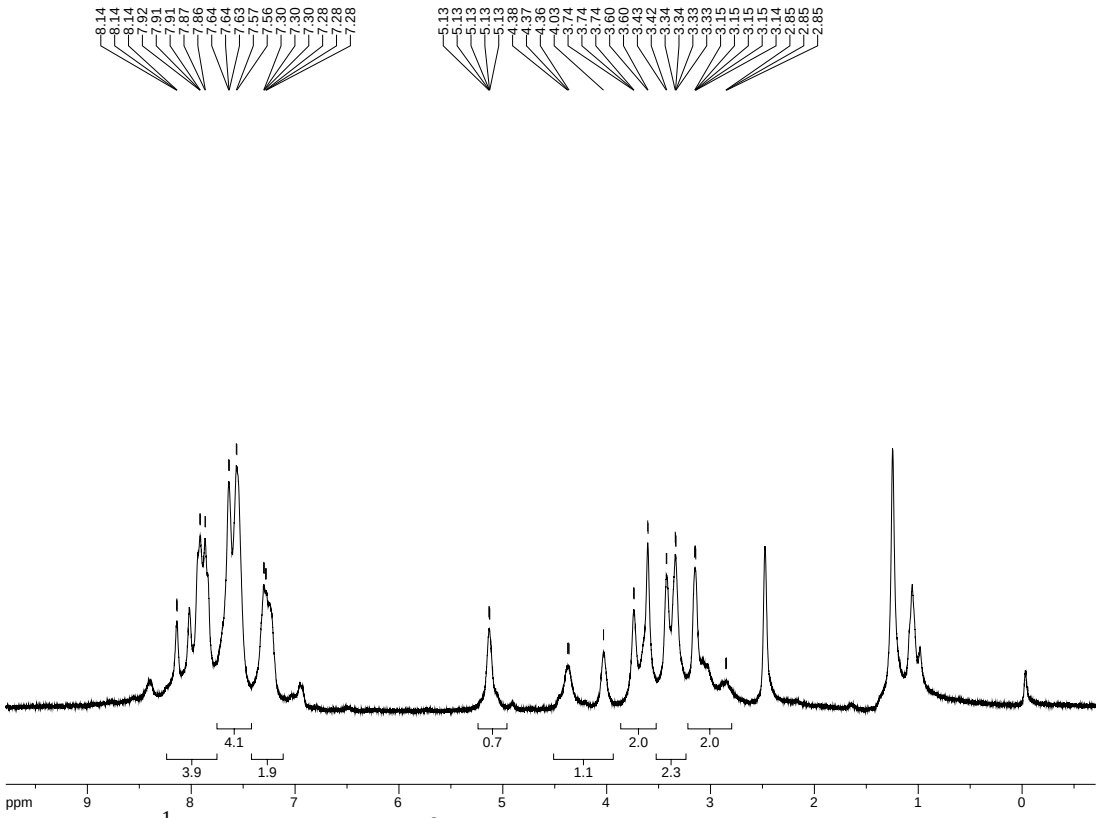

Figure 5.24a. ^{1}H NMR spectrum of compound **3.58d**.

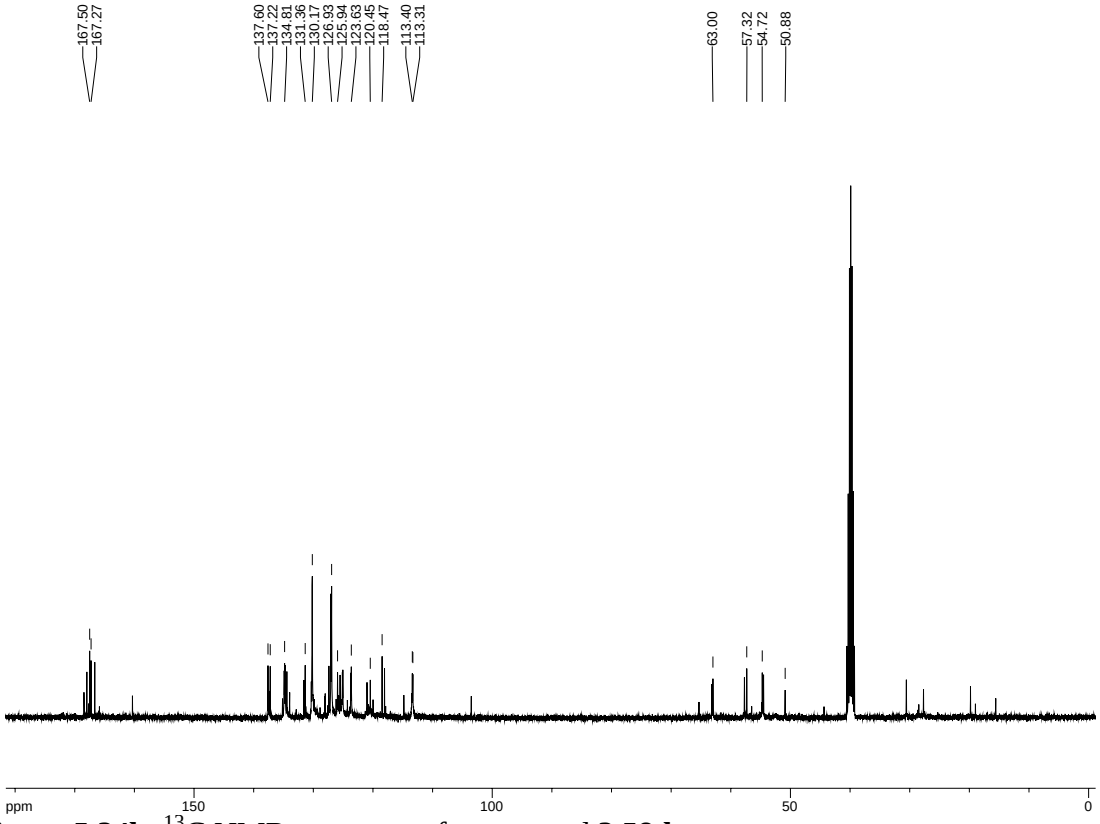

Figure 5.24b. ^{13}C NMR spectrum of compound **3.58d**.

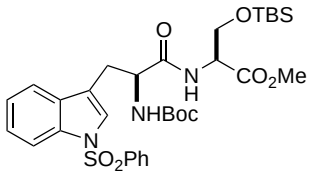

3.57e

Dipeptide (3.57e). Alcohol **3.57d** (2.9 g, 5.3 mmol) was dissolved in DMF (13 mL), and to it added imidazole (864 mg, 12.7 mmol) and TBSCl (2.08 g, 13.8 mmol). The reaction stirred O/N at r.t., then was concentrated, dissolved in EtOAc, washed with H_2O (3x), washed with brine, dried, and concentrated to afford silylether **3.57e** (3.14 g, 90% yield). ^{1}H-NMR (300 MHz; DMSO-d_6): δ 8.14 (d, *J* = 7.8 Hz, 1H), 7.85 (t, *J* = 7.9 Hz, 3H), 7.65 (t, *J* = 7.2 Hz, 2H), 7.58-7.50 (m, 3H), 7.33-7.20 (m, 2H), 7.00 (d, *J* = 8.8 Hz, 1H), 4.46-4.40 (m, 1H), 4.34-4.30 (m, 1H), 3.86 (dd, *J* = 10.3, 4.7 Hz, 1H), 3.74 (dd, *J* = 10.3, 4.9 Hz, 1H), 3.60 (s, 3H), 3.05-2.99 (m, 1H), 2.89-2.80 (m, 1H), 1.25 (s, 9H), 0.82 (s, 9H), 0.00 (d, *J* = 3.2 Hz, 6H); ^{13}C-NMR (101 MHz; $CDCl_3$): δ 170.6, 170.2, 138.2, 135.1, 133.7, 130.8, 129.2, 126.7, 124.9, 124.6, 123.3, 119.6, 117.6, 113.6, 63.3, 54.2, 52.4, 28.20, 28.10, 25.70, 25.61, 18.1, -5.63, -5.77.

REF: TRW-II-196, **TRW-II-222**, TRW-II-254.

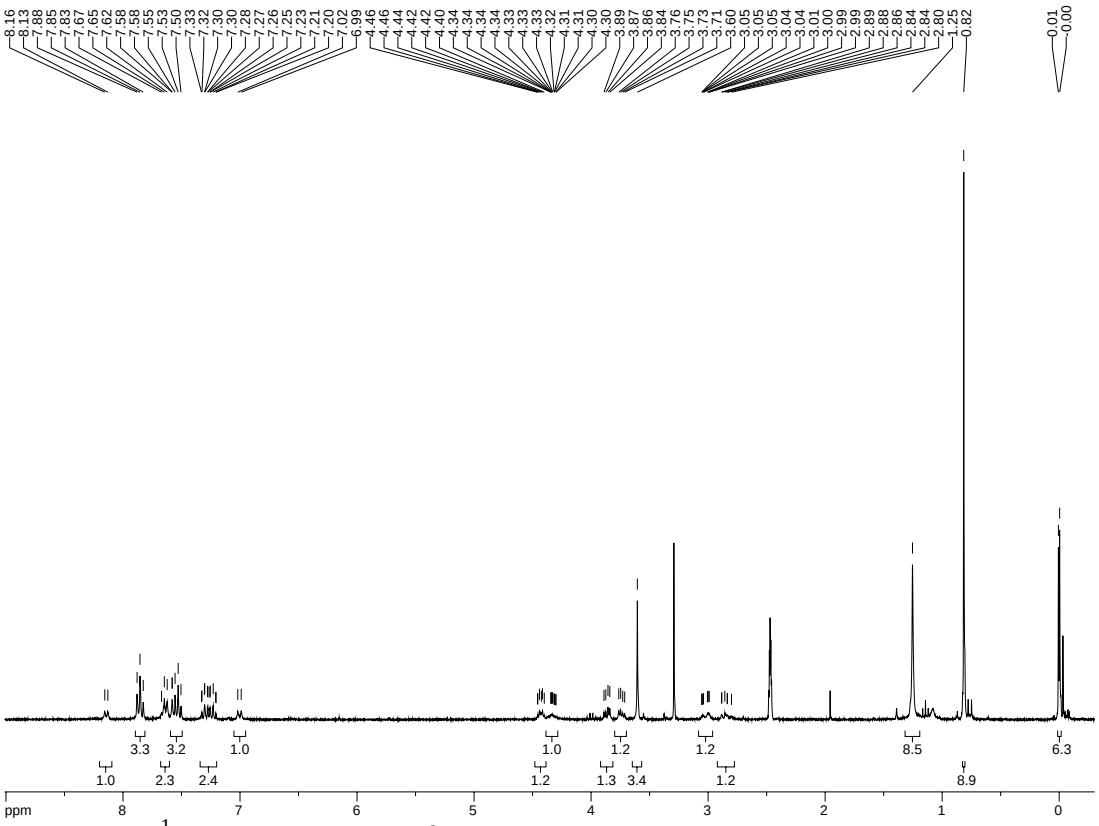

Figure 5.25a. ^{1}H NMR spectrum of compound **3.57e**.

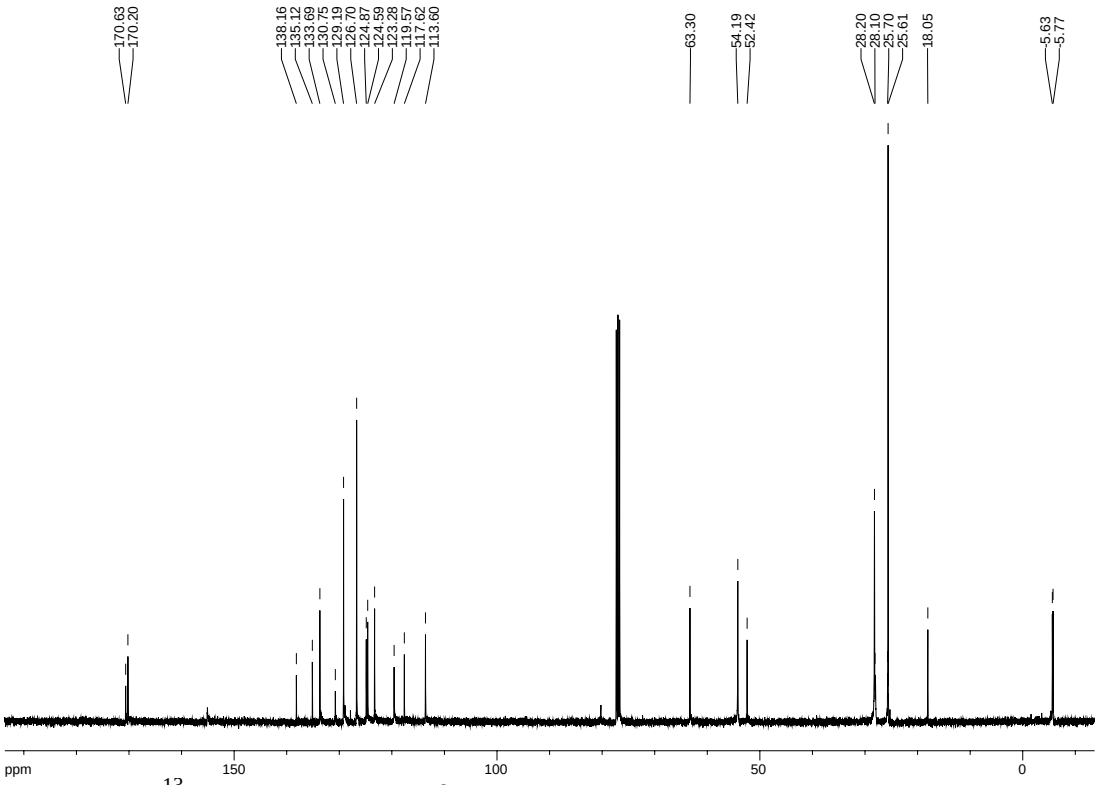

Figure 5.25b. ^{13}C NMR spectrum of compound **3.57e**.

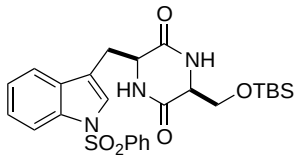

3.58e

Dioxopiperazine (3.58e). Dipeptide **3.57e** (500 mg) was transferred to a microwave tube, then heated neat in the microwave at maximum power to a safe temperature of 180 °C (microwave set to 'open-vessel'). After cooling, the residue was suspended in CH_2Cl_2, transferred to a vial, and concentrated to afford dioxopiperazine **3.57e** (2.47 g over 6 batches, 98%).

^{1}H-NMR (300 MHz; DMSO-d_6): δ 7.92-7.83 (m, 4H), 7.64 (t, *J* = 3.7 Hz, 2H), 7.58-7.52 (m, 4H), 7.33-7.28 (m, 1H), 7.25-7.20 (m, 1H), 4.15-4.05 (m, 1H), 3.84-3.77 (m, 1H), 3.61-3.43 (m, 2H), 3.16-2.94 (m, 2H), 0.79 (s, 9H), -0.02 (s, 3H), -0.06 (s, 3H).

REF: **TRW-II-226**, TRW-II-255.

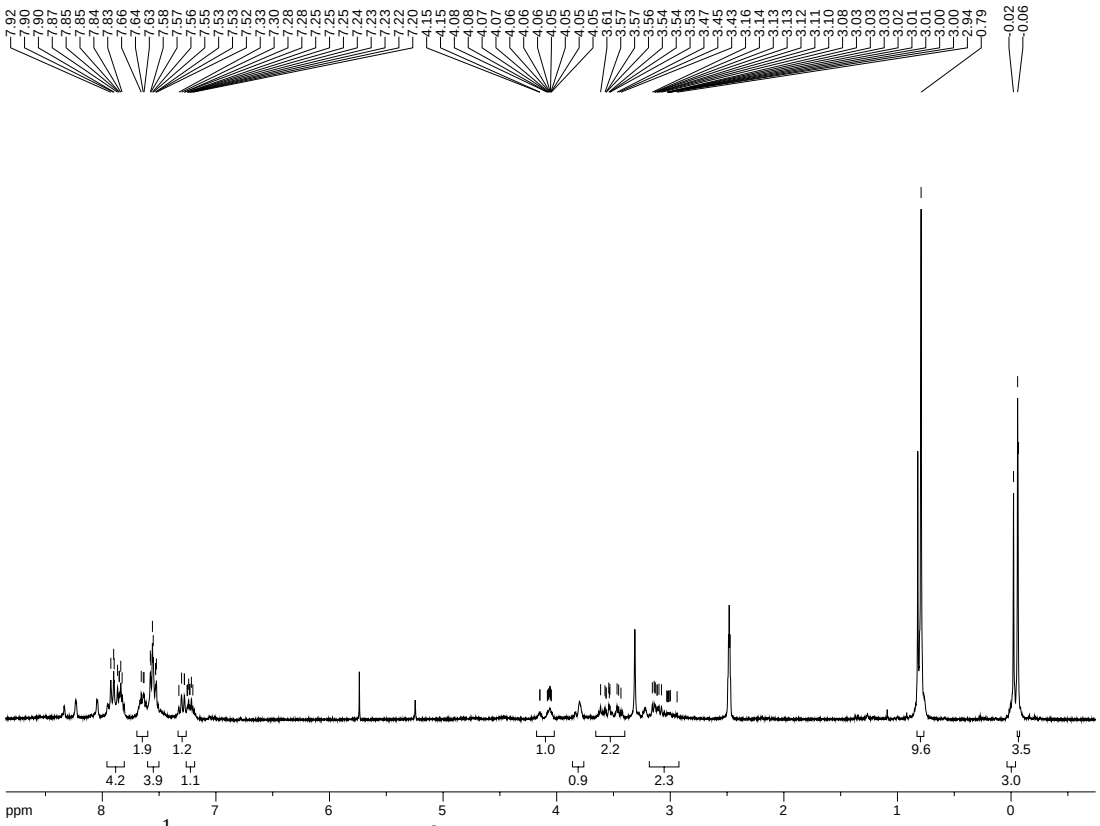

Figure 5.26a. ^{1}H NMR spectrum of compound **3.58e**.

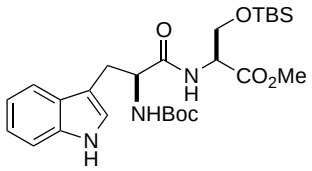

5.1

Dipeptide (5.1). Alcohol **3.57c** (2.0 g, 4.9 mmol) was dissolved in DMF (12 mL), and to it added imidazole (802 mg, 11.8 mmol) and TBSCl (1.92 g, 12.7 mmol). The reaction stirred O/N at r.t., then was concentrated, dissolved in EtOAc, washed with H_2O (3x), washed with brine, dried, and concentrated to afford silylether **5.1** (2.38 g, 93% yield).

^{1}H-NMR (300 MHz; $CDCl_3$): δ 8.18 (bs, *J* = 0.4 Hz, 1H), 7.66 (d, *J* = 7.6 Hz, 1H), 7.34 (d, *J* = 8.0 Hz, 1H), 7.20-7.18 (m, 1H), 7.16-7.11 (m, 2H), 6.55-6.52 (m, 1H), 5.19-5.16 (m, 1H), 4.54 (broad, *J* = 7.0, 4.1 Hz, 2H), 3.95 (dd, *J* = 10.1, 2.7 Hz, 1H), 3.66 (s, 3H), 3.62-3.58 (m, 1H), 3.31-3.30 (m, 1H), 3.21 (dd, *J* = 14.6, 6.9 Hz, 1H), 1.42 (s, 9H), 0.77 (s, 9H), -0.07 (s, 3H), -0.10 (s, 3H).

REF: **TRW-III-196**.

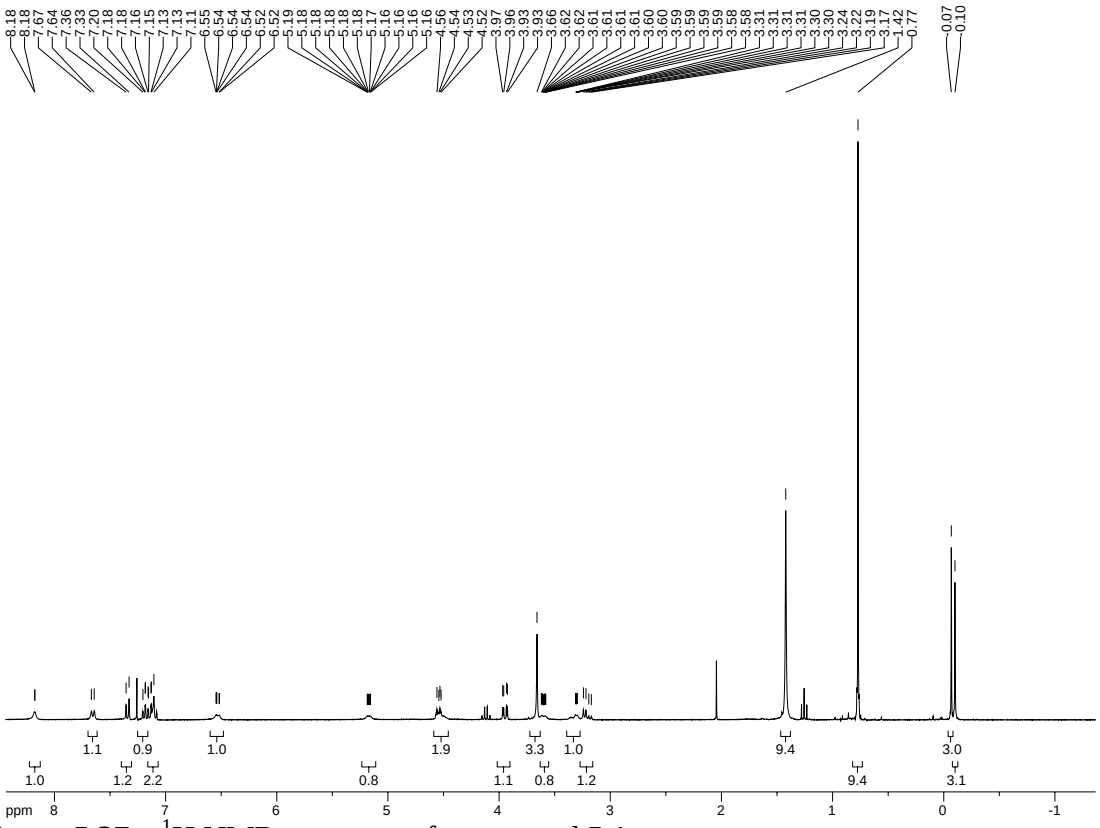

Figure 5.27a. ^{1}H NMR spectrum of compound **5.1**.

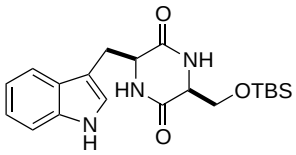

5.2

(3*S*,6*S*)-3-((1*H*-indol-3-yl)methyl)-6-(((*tert*-butyldimethylsilyl)oxy)methyl)piperazine-2,5-dione (5.2). The general cyclization procedure given for compound **3.58a** was repeated.

^{1}H-NMR (300 MHz; DMSO-d_6): δ 10.88 (m, 1H), 7.95 (s, 1H), 7.60-7.48 (m, 1H), 7.29 (t, *J* = 7.8 Hz, 1H), 7.05-6.93 (m, 2H), 4.09-3.97 (m, 1H), 3.82-3.70 (m, 1H), 3.52-3.43 (m, 1H), 3.27-3.14 (m, 2H), 2.79 (d, *J* = 47.6 Hz, 1H), 0.81 (s, 9H), -0.02--0.05 (m, 6H); ^{13}C-NMR (101 MHz; DMSO): δ 167.6, 165.5, 136.5, 127.9, 124.4, 121.3, 118.96, 118.77, 111.7, 109.5, 65.4, 57.5, 55.9, 31.5, 26.33, 26.24, 26.11, 26.05, 25.99, 18.7, -5.0.

REF: **TRW-II-187**.

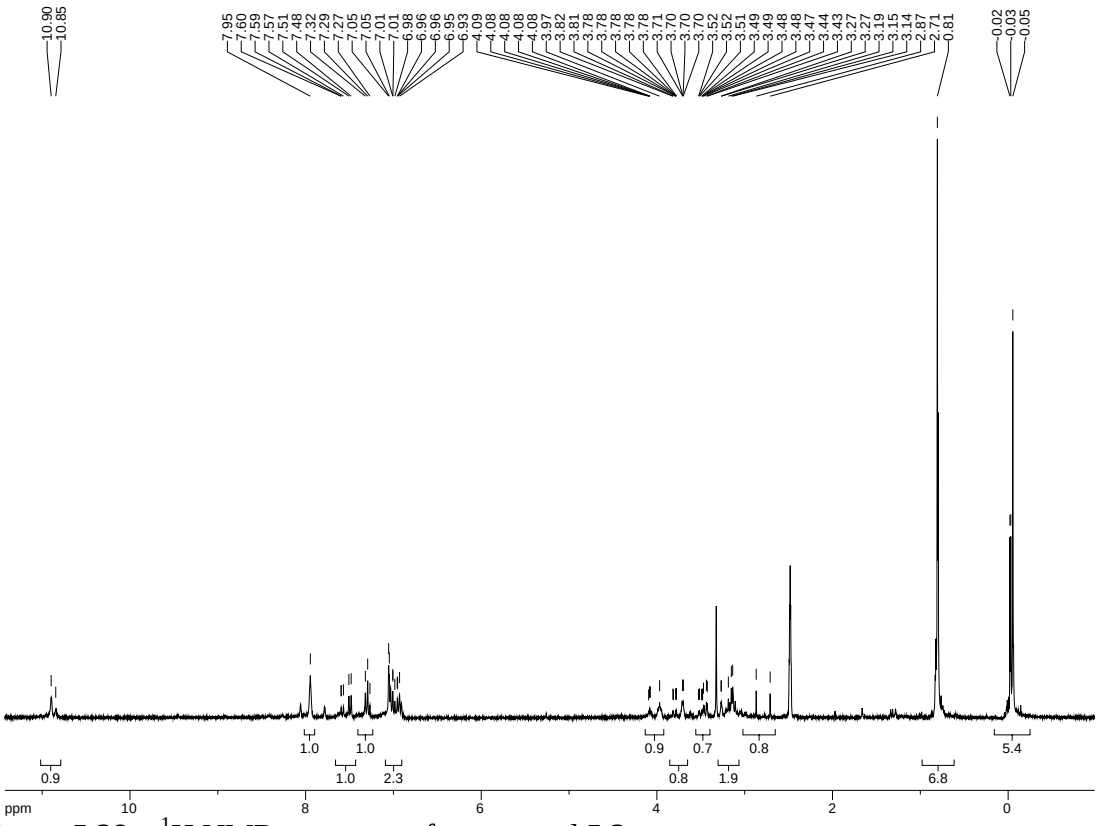

Figure 5.28a. ^{1}H NMR spectrum of compound **5.2**.

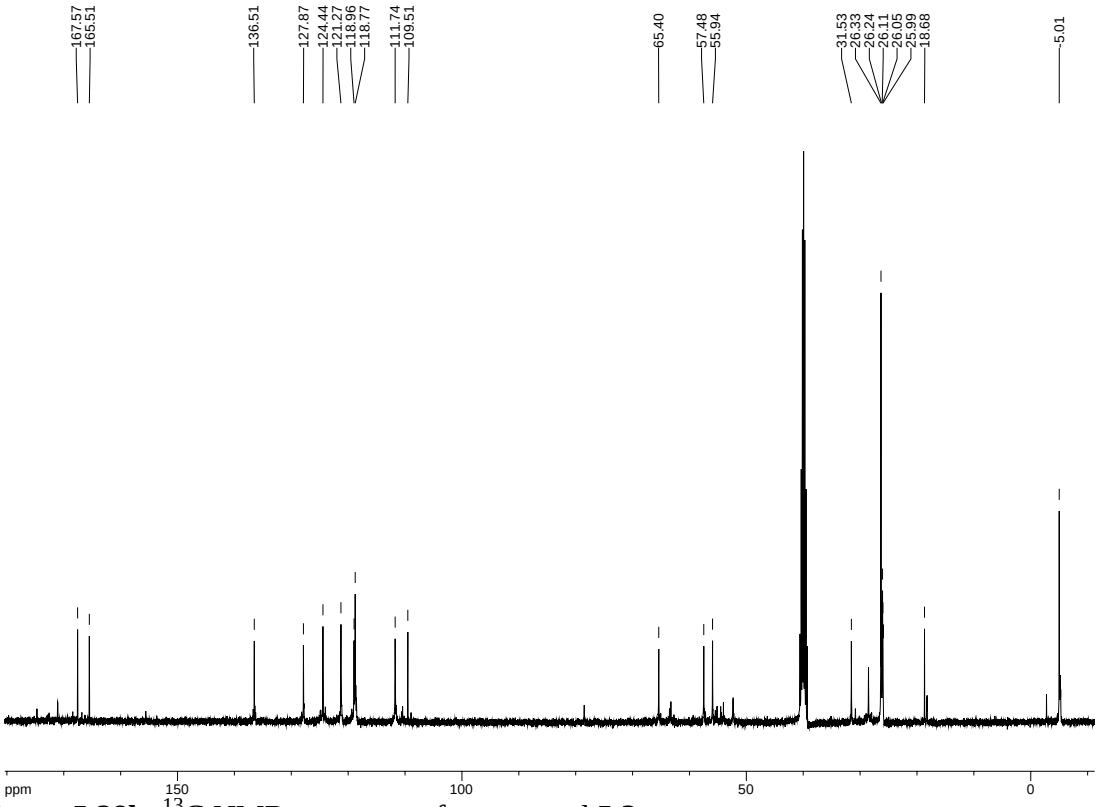

Figure 5.28b. ^{13}C NMR spectrum of compound **5.2**.

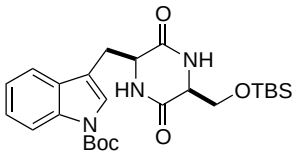

5.3

***tert*-butyl 3-(((2*S*,5*S*)-5-(((*tert*-butyldimethylsilyl)oxy)methyl)-3,6-dioxopiperazin-2-yl)methyl)-1*H*-indole-1-carboxylate**. The general cyclization procedure given for compound **3.58a** was repeated.

^{1}H-NMR (300 MHz; $CDCl_3$): δ 8.01 (d, *J* = 8.2 Hz, 1H), 7.47 (dd, *J* = 7.7, 0.4 Hz, 1H), 7.35 (s, 1H), 7.23-7.10 (m, 2H), 4.16-4.12 (m, 1H), 3.87-3.84 (m, 3H), 3.63 (dd, *J* = 10.1, 3.1 Hz, 1H), 3.31 (dd, *J* = 10.1, 5.8 Hz, 2H), 3.05 (dd, *J* = 14.4, 8.8 Hz, 1H), 1.54 (s, 9H), 0.75 (s, 9H), -0.09 (s, 6H); ^{13}C-NMR (101 MHz; $CDCl_3$): δ 173.3, 171.6, 135.4, 130.61, 130.58, 130.50, 128.6, 124.8, 121.0, 120.2, 89.7, 70.5, 62.7, 60.5, 54.7, 54.5, 36.5, 33.7, 31.4, 24.1, 0.06, -0.00.

REF: **TRW-III-187**.

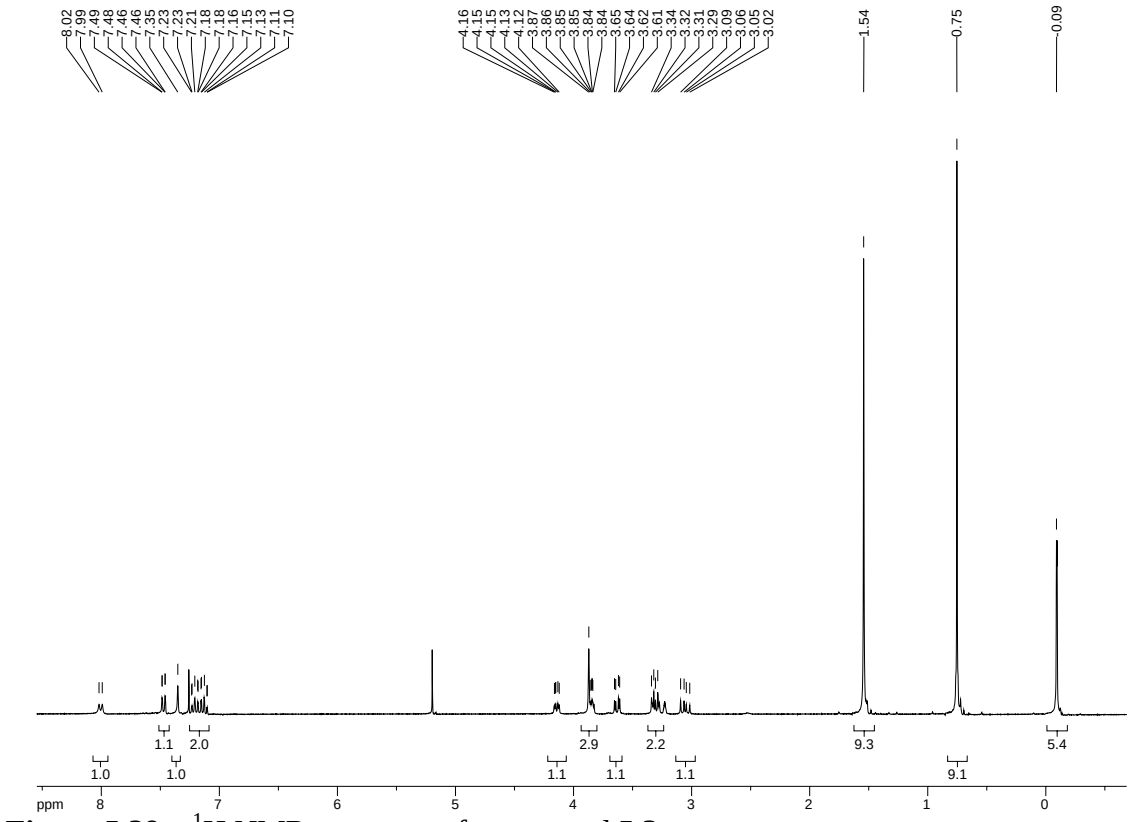

Figure 5.29a. ^{1}H NMR spectrum of compound **5.3**.

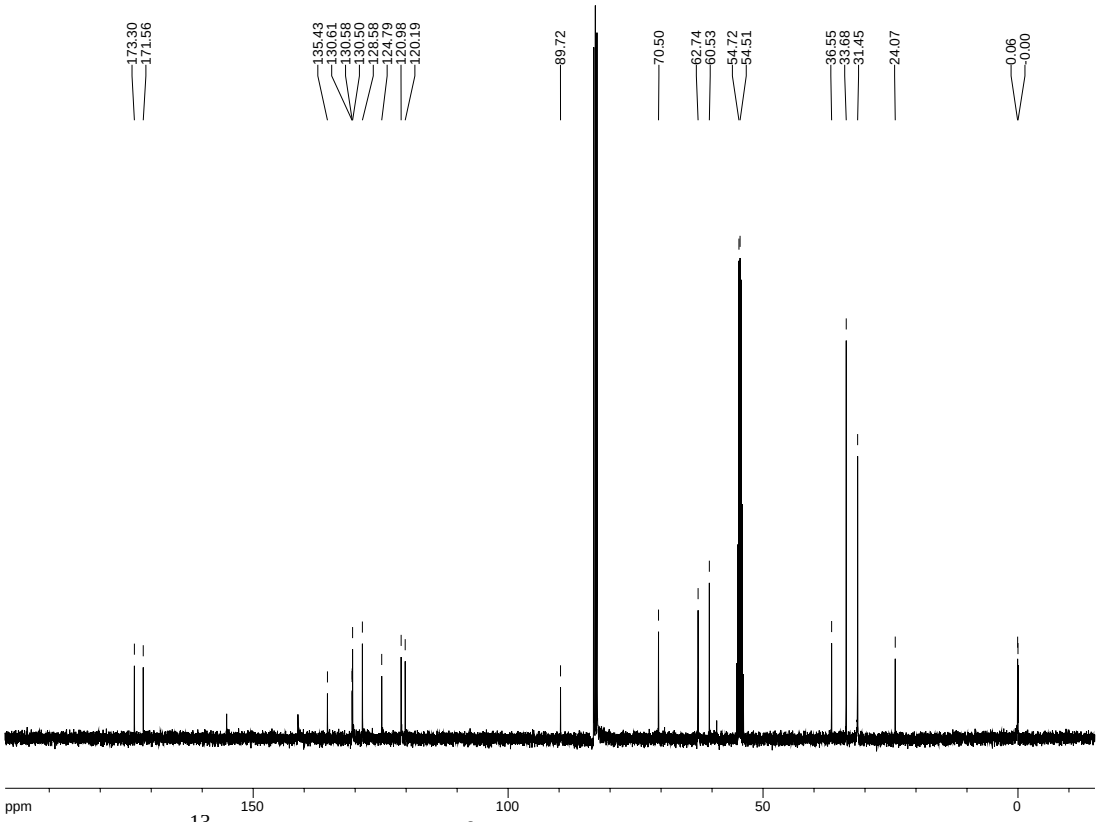

Figure 5.29b. ^{13}C NMR spectrum of compound **5.3**.

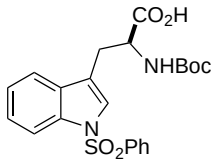

3.56

***N*-Boc-L-tryptophan-*N'*-SO_2Ph (3.56)**. Compound **3.59** (14.8 g, 48.7 mmol) was dissolved in THF (100 mL) and the resulting solution cooled to -78 °C. LHMDS (146 mL, 146.1 mmol) was added slowly over 5 minutes. The reaction was stirred at -78 °C for 1 h, then $PhSO_2Cl$ (7.5 mL, 58.4 mmol) added in one portion. After stirring an additional 2 h at -78 °C, the reaction was quenched by addition of 1:1 AcOH:EtOAc then allowed to warm to r.t. The suspension was diluted with 1M HCl and the product extracted in EtOAc. The combined organic layers were dried and concentrated to afford crude **3.56**, purified by SiO_2 chromatography (5% AcOH, 45% hexanes, 50% CH_2Cl_2) to afford pure **3.56** (17.12 g, 79% yield).

^{1}H-NMR (300 MHz; DMSO-d_6): δ 12.64-12.63 (m, 1H), 7.90-7.87 (m, 2H), 7.61 (t, *J* = 7.8 Hz, 2H), 7.56-7.50 (m, 2H), 7.25-7.20 (m, 2H), 7.16-7.13 (m, 2H), 4.20-4.17 (m, 1H), 3.11 (dd, *J* = 14.8, 4.2 Hz, 1H), 2.95 (dd, *J* = 14.8, 10.0 Hz, 1H), 1.31 (s, 9H).

REF: TRW-II-176, **TRW-II-251**.

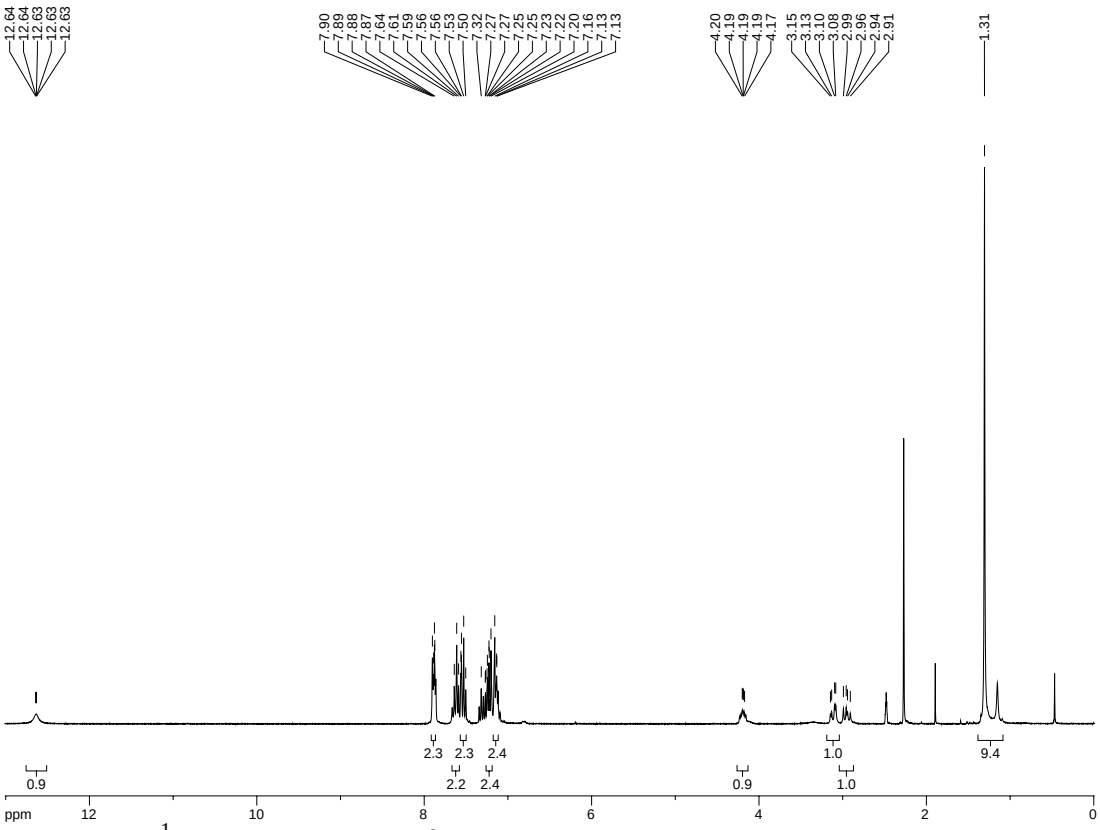

Figure 5.30a. ^{1}H NMR spectrum of compound **3.56**.

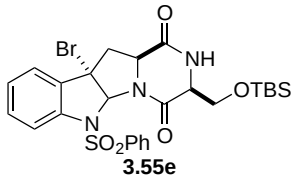

3.55e

Bromopyrroloindoline (3.55e). A solution of dioxopiperazine **3.58e** (2.47 g, 4.68 mmol) in MeCN (50 mL) was cooled to 0 °C and to it added bromine (0.962 mL, 18.7 mmol) dropwise. After stirring 5 minutes, 1:1 $Na_2S_2O_3$:$NaHCO_3$ was added and the product extracted in EtOAc. The combined organic layers were washed with brine, dried over Na_2SO_4 and concentrated. Purification by SiO_2 chromatgraphy (10/40/50 *i*PrOH/hexanes/ CH_2Cl_2) afforded pure pyrroloindoline **3.55e** in 38% yield (1.09 g).

^{1}H-NMR (300 MHz; DMSO-d_6): δ 8.06 (s, 1H), 7.87-7.84 (m, 2H), 7.66-7.53 (m, 4H), 7.42 (d, *J* = 2.3 Hz, 2H), 7.27-7.22 (m, 1H), 6.46 (s, 1H), 4.05 (d, *J* = 1.0 Hz, 1H), 3.77-3.75 (m, 2H), 3.73-3.68 (m, 2H), 3.60-3.56 (m, 2H), 1.01 (d, *J* = 6.1 Hz, 9H), -0.02 (s, 6H).

REF: **TRW-II-228**, TRW-II-256.

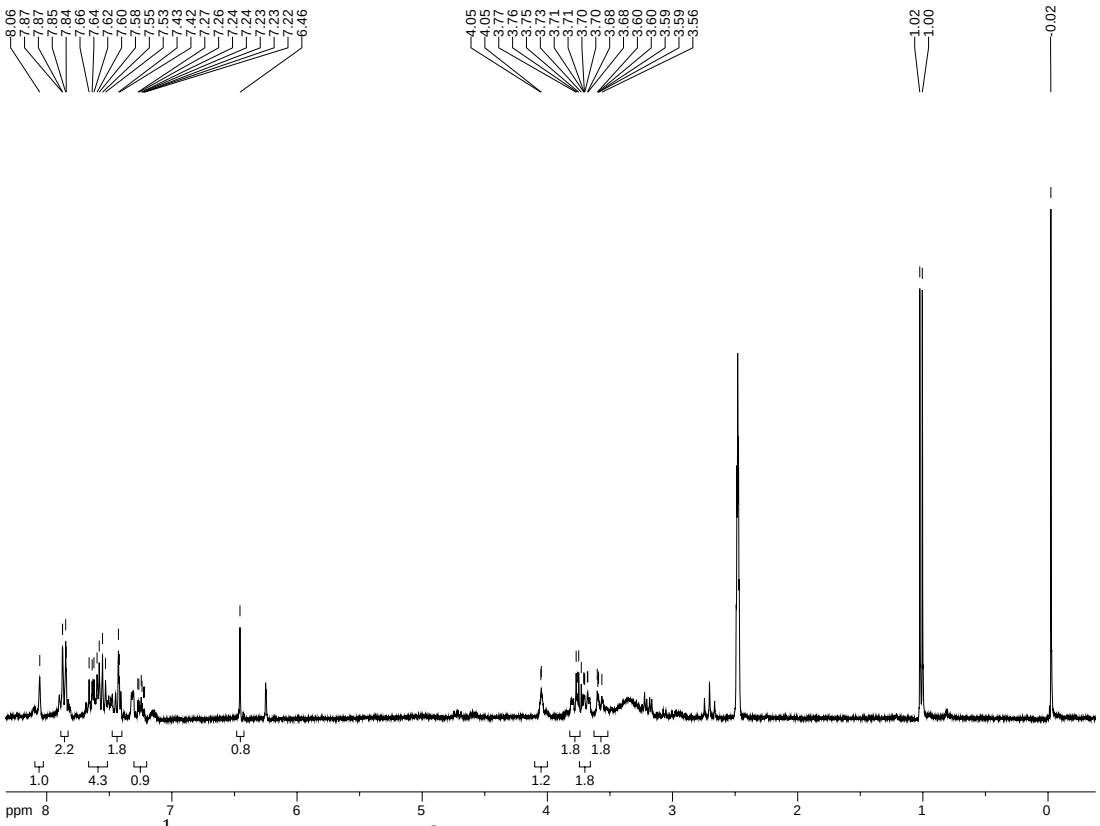

Figure 5.31a. ^{1}H NMR spectrum of compound **3.55e**.

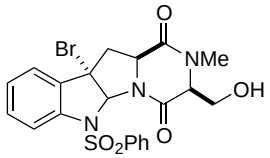

3.60

***N*-Me-bromopyrroloindoline (3.60)**. Dioxopiperazine **3.55e** (2.09 g, 3.4 mmol) was dissolved in acetone (50 mL). Potassium carbonate (11.73 g, 85 mmol) and MeI (27.5 mL, 442 mmol) were added, the flask covered with foil, and the reaction allowed to stir at r.t. under Ar for 5 d. The crude reaction mixture was concentrated, partitioned between EtOAc and H_2O (200 mL each), and the product extracted in EtOAc. The combined organic layers were dried and concentrated. SiO_2 chromatography (10/40/50 *i*PrOH/hexanes/CH_2Cl_2) gave the pure title compound (1.69 g, 98% yield).

^{1}H-NMR (300 MHz; $CDCl_3$): δ 7.89-7.71 (m, *J* = 1.6 Hz, 2H), 7.69 (d, *J* = 8.2 Hz, 1H), 7.58-7.52 (m, 1H), 7.44 (ddd, *J* = 8.4, 6.8, 1.4 Hz, 2H), 7.38-7.32 (m, 2H), 7.21 (d, *J* = 7.0 Hz, 1H), 6.54 (d, *J* = 28.9 Hz, 1H), 4.08-3.78 (m, 4H), 3.17 (ddd, *J* = 28.8, 12.6, 5.2 Hz, 1H), 2.98 (s, 3H), 2.89-2.76 (m, 1H).

REF: TRW-II-235, **TRW-II-258**.

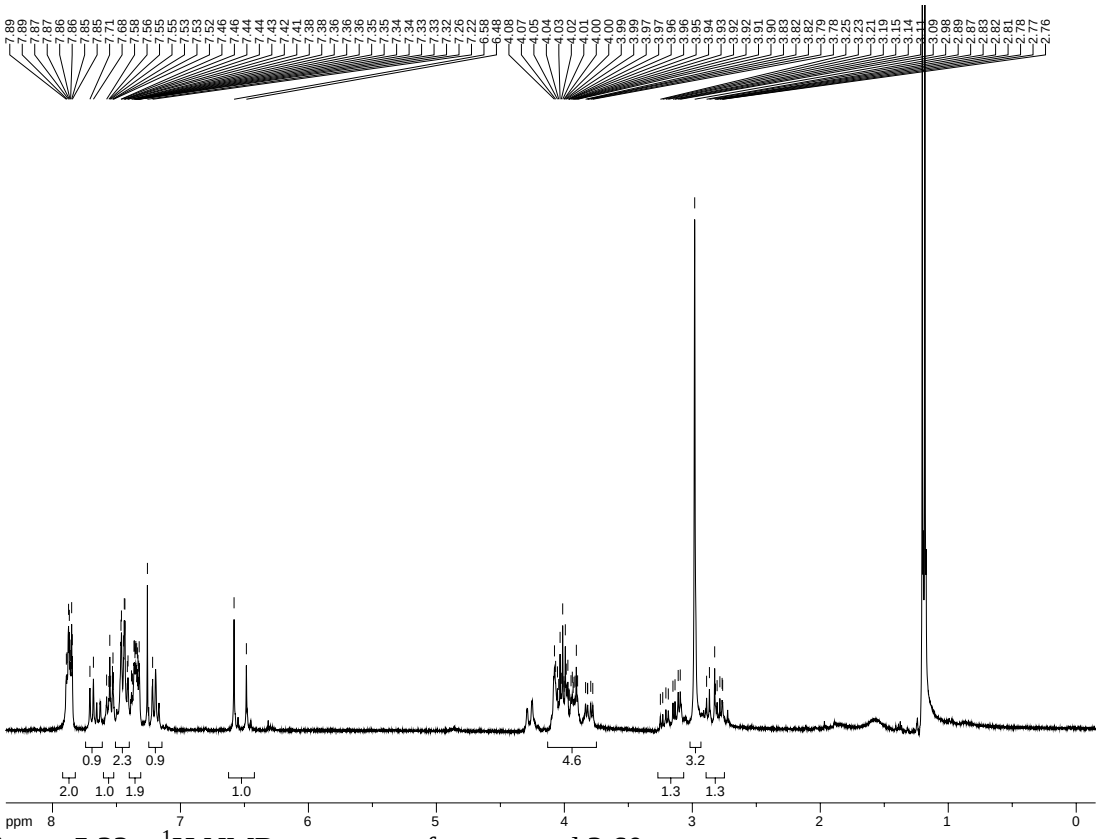

Figure 5.32a. ^{1}H NMR spectrum of compound **3.60**.

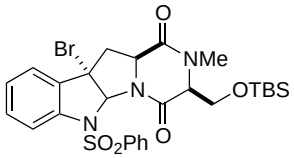

3.61

OTBS-*N*-Me-bromopyrroloindoline (3.61). The same general procedure for TBS protection was followed as for **3.57e**. Instead of carrying the crude product forward as before, it was necessary for the subsequent radical bromination to purify the product by SiO_2 chromatography (20-60% EtOAc in hexanes) to afford **3.61** (47% yield).

^{1}H-NMR (300 MHz; $CDCl_3$): δ 7.89 (dd, *J* = 8.1, 1.0 Hz, 2H), 7.70 (dd, *J* = 7.9, 0.6 Hz, 1H), 7.56-7.53 (m, 1H), 7.48-7.43 (m, 2H), 7.35-7.32 (m, 2H), 7.21-7.16 (m, 1H), 6.63 (s, 1H), 4.28 (dd, *J* = 10.2, 1.3 Hz, 1H), 4.06 (s, 1H), 3.94 (dd, *J* = 10.1, 2.7 Hz, 1H), 3.78 (dd, *J* = 12.4, 4.5 Hz, 1H), 3.09 (dd, *J* = 12.0, 4.5 Hz, 1H), 2.91 (s, 3H), 2.73 (t, *J* = 12.2 Hz, 1H), 0.89 (s, 9H), 0.10 (s, 6H).

REF: TRW-II-236, **TRW-II-242**.

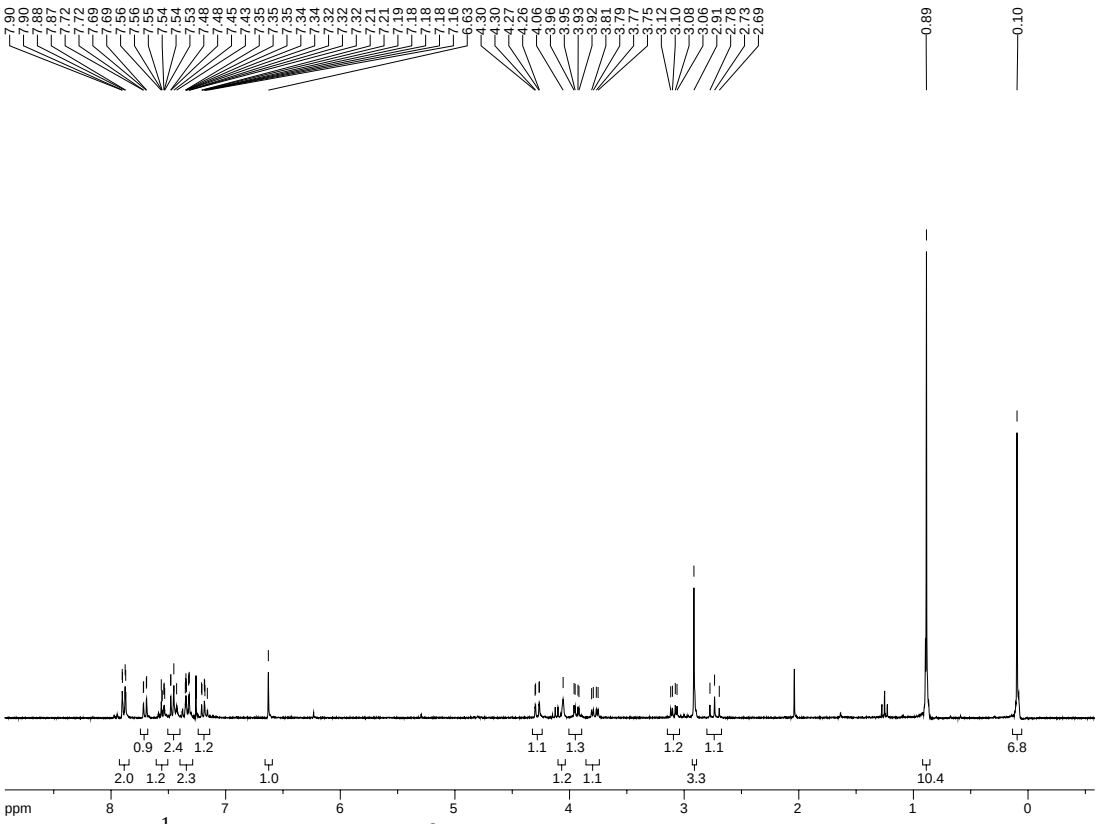

Figure 5.33a. ^{1}H NMR spectrum of compound **3.61**.

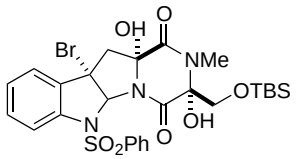

3.62

Diol (3.62). To a solution of Br-dioxopiperazine **3.61** (710 mg, 1.14 mmol) in CCl_4 (40 mL) was added NBS (406 mg, 2.28 mmol) and V-70 (89 mg, 0.29 mmol). The resulting suspension was stirred 8 h. at r.t., then filtered through a cotton plug, the solid washed with CCl_4, and the combined filtrate concentrated. The resulting residue was dissolved in 1:1 MeCN:pH 7 phosphate buffer (58 mL) and stirred 3 h. at r.t. The product was extracted in EtOAc (3x), washed with brine, dried, and concentrated to afford the diol in 97% yield (720 mg), carried forward to the next step as the crude material.

REF: TRW-II-244, 245, **TRW-II-368, 370**.

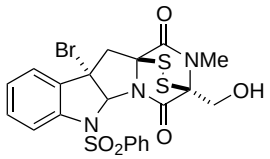

3.63

Epidithiodioxopiperazine (3.63). Hydrogen sulfide (ca. 8 mL) gas was condensed in a sealed tube capped with a rubber septum at -78 °C. Diol **3.62** (125 mg, 0.19 mmol) and $BF_3 \cdot OEt_2$ (0.119 mL, 0.95 mmol) were added as a solution in CH_2Cl_2 (7.6 mL). The rubber septum was removed and the sealed tube capped with a teflon cap and placed behind a blast shield. The reaction mixture stirred at r.t. for 90 min., recooled to -78 °C, uncapped and sealed with a rubber septum, then allowed to warm to r.t. with 3 NaOH and 1 bleach trap in place as the gas vented. The resulting solution was diluted with EtOAc, washed with sat'd NH_4Cl, and the product extracted in EtOAc. Iodine (100 mg, 2 eq) was added to the EtOAc extracts and the mixture allowed to stir 1 min. 10% $Na_2S_2O_3$ was added and the product extracted in EtOAc, dried, and concentrated. Purification by SiO_2 chromatography (1:1 hexanes:EtOAc) afforded pure epidithiodioxopiperazine **3.63** in 42% yield (44.9 mg).

^{1}H-NMR (300 MHz; $CDCl_3$): δ 7.78 (dd, *J* = 8.4, 1.1 Hz, 2H), 7.64 (d, *J* = 8.2 Hz, 1H), 7.52-7.49 (m, 1H), 7.41-7.36 (m, 4H), 7.28-7.26 (m, 1H), 6.49 (s, 1H), 4.33 (d, *J* = 12.8 Hz, 1H), 4.18 (d, *J* = 12.7 Hz, 1H), 3.85 (d, *J* = 15.3 Hz, 1H), 3.21 (d, *J* = 15.3 Hz, 1H), 3.13 (s, 3H); ^{13}C-NMR (101 MHz; $CDCl_3$): δ 176.9, 163.7, 134.83, 134.82, 134.3, 133.8, 132.8, 131.23, 131.22, 131.0, 123.9, 114.6, 72.4, 66.2, 37.6, 31.3, 26.9, 23.7, 20.0; HRMS (ESI-APCI): $[M+H]^+$ 567.9670 calcd for $C_{21}H_{19}BrN_3O_5S_3$, found: 567.9641. REF: **TRW-II-246, 247**, TRW-II-372, 373.

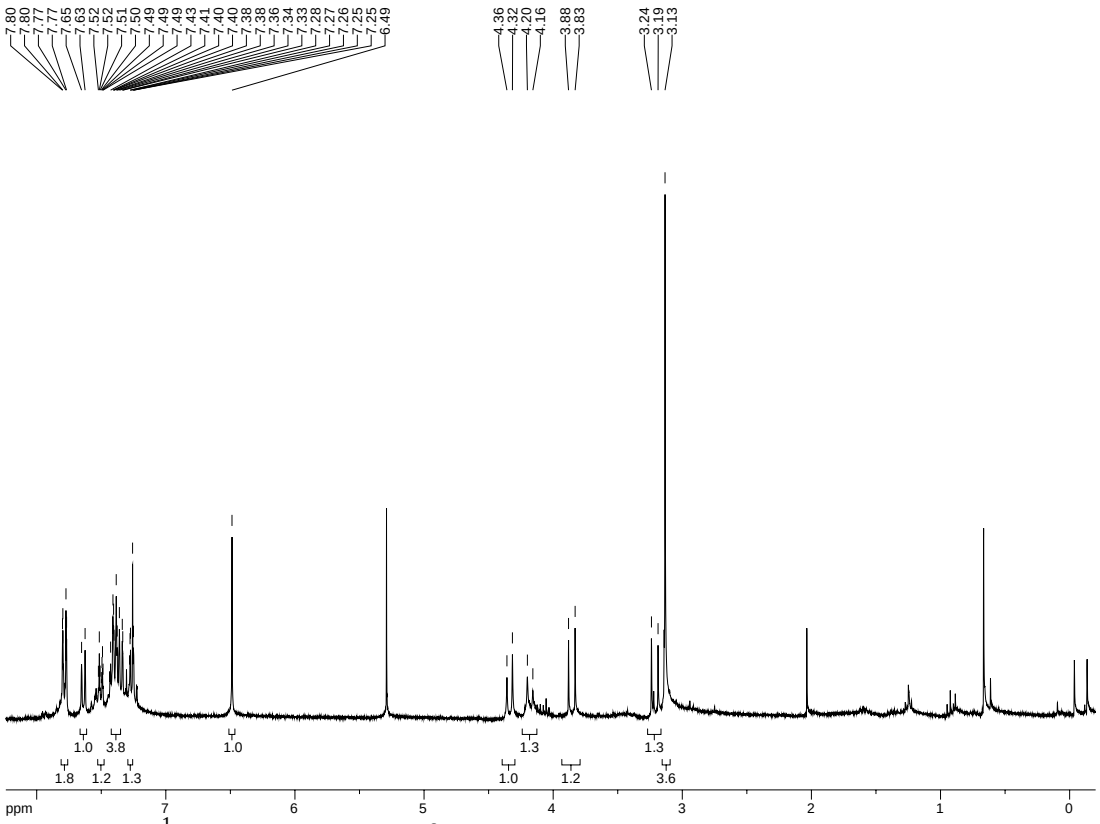

Figure 5.34a. ^{1}H NMR spectrum of compound **3.63**.

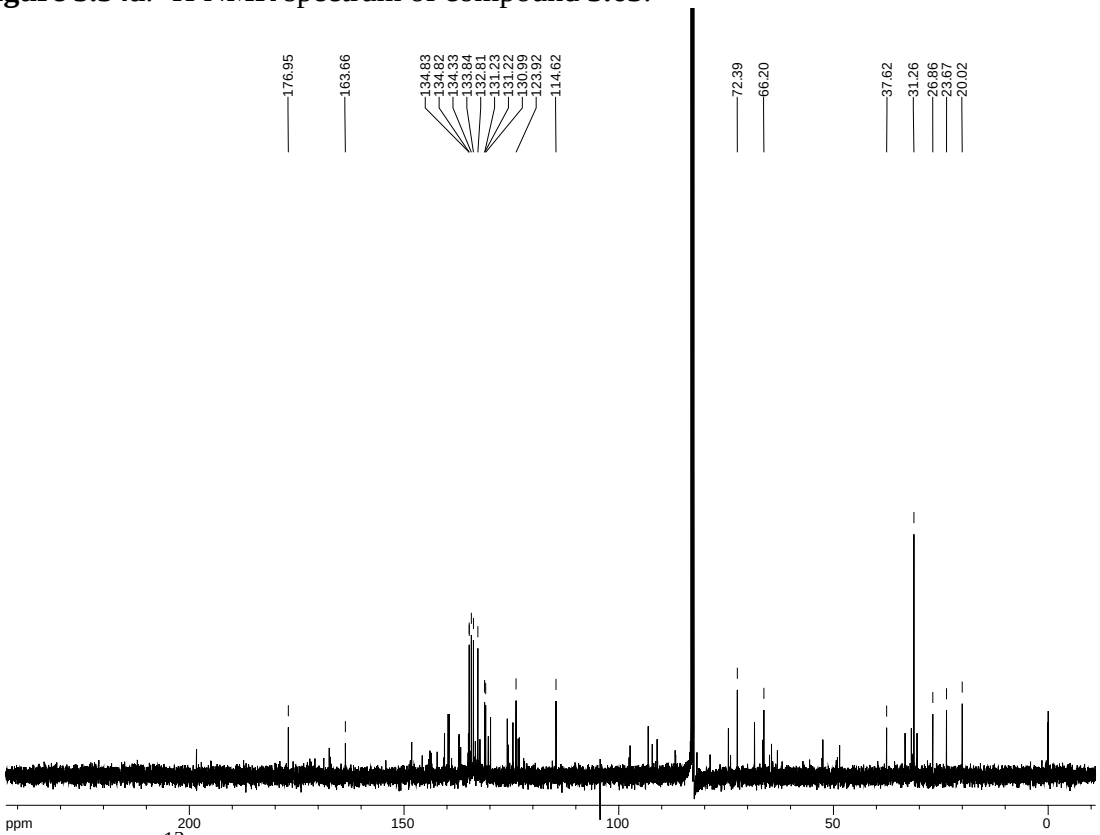

Figure 5.34b. ^{13}C NMR spectrum of compound **3.63**.

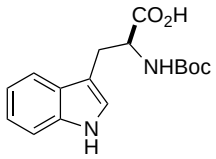

3.59

***N*-Boc-L-tryptophan (3.59)**. To a solution of L-tryptophan (50 g, 245 mmol) in 1:1 THF:H_2O (700 mL) was added NaOH (10.8 g, 270 mmol) and Boc_2O (58.9 g, 270 mmol). The resulting solution was stirred O/N at r.t. The volume was reduced and the product extracted in CH_2Cl_2. The aqueous layer was acidified with 1M HCl to pH 4, and the product extracted in CH_2Cl_2. The combined organic layers were dried over Na_2SO_4 and concentrated to afford **3.59** (70.23 g, 94% yield).

^{1}H-NMR (300 MHz; $CDCl_3$): δ 7.50 (d, *J* = 7.6 Hz, 1H), 7.26 (d, *J* = 7.9 Hz, 1H), 7.09-6.98 (m, 2H), 6.96 (s, 1H), 4.45 (t, *J* = 5.4 Hz, 1H), 3.28-3.17 (m, 2H), 1.31 (s, 9H).

REF: **TRW-II-252**.

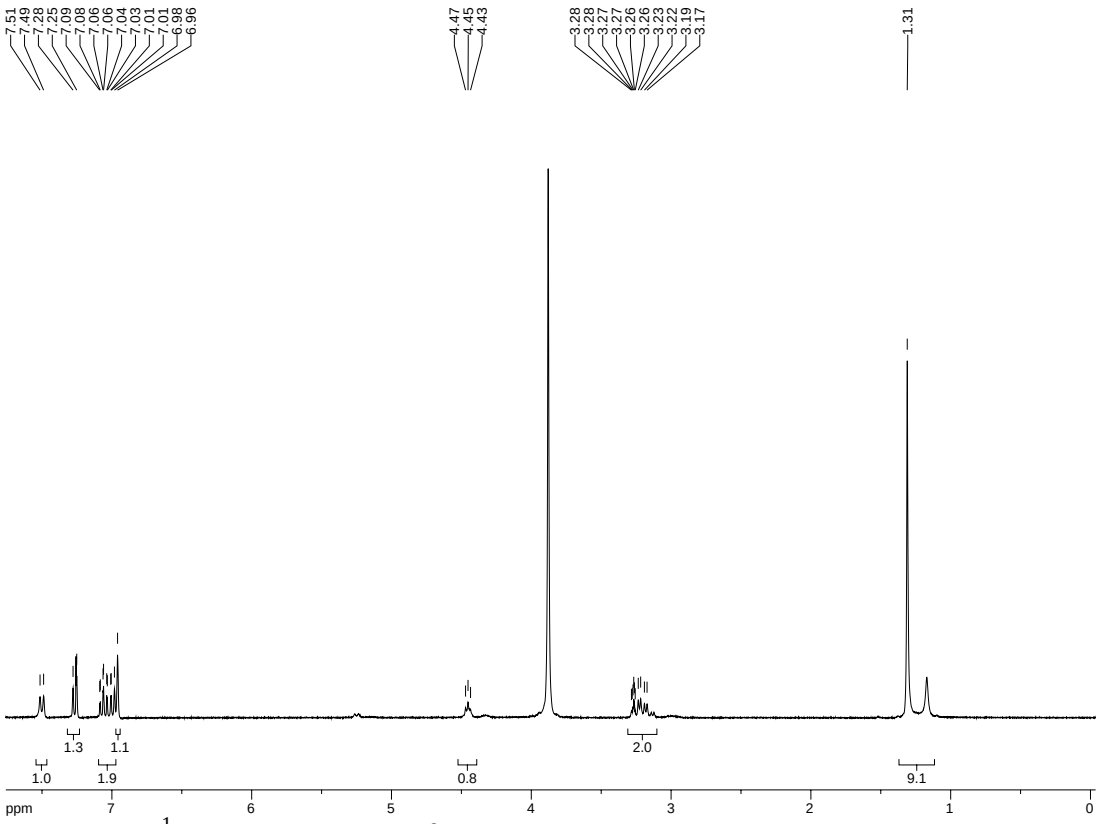

Figure 5.35a. ^{1}H NMR spectrum of compound **3.59**.

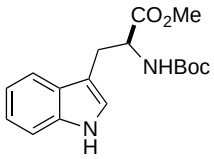

3.34

***N*-Boc-L-tryptophan-OMe (3.34)**. To a solution of *N*-Boc-L-tryptophan (30 g, 98.7 mmol) in DMF (200 mL) at 0 °C was added MeI (9.2 mL, 148 mmol) and $KHCO_3$ (19.7 g, 197 mmol). After stirring O/N at r.t., the mixture was diluted with ether, washed with H_2O (2x), 1M $KHSO_4$ (1x), and brine (1x). The combined organic layers were dried and concentrated to afford the title compound (29.86 g, 95% yield).

^{1}H-NMR (300 MHz; $CDCl_3$): δ 8.10-8.08 (m, 1H), 7.55 (d, *J* = 7.9 Hz, 1H), 7.36 (d, *J* = 8.0 Hz, 1H), 7.22-7.09 (m, 2H), 7.01 (d, *J* = 2.4 Hz, 1H), 5.09-5.06 (m, 1H), 4.68-4.62 (m, 1H), 3.68 (s, 3H), 3.29 (d, *J* = 5.2 Hz, 2H), 1.43 (s, 9H).

REF: TRW-II-273, **TRW-II-285**, TRW-II-349.

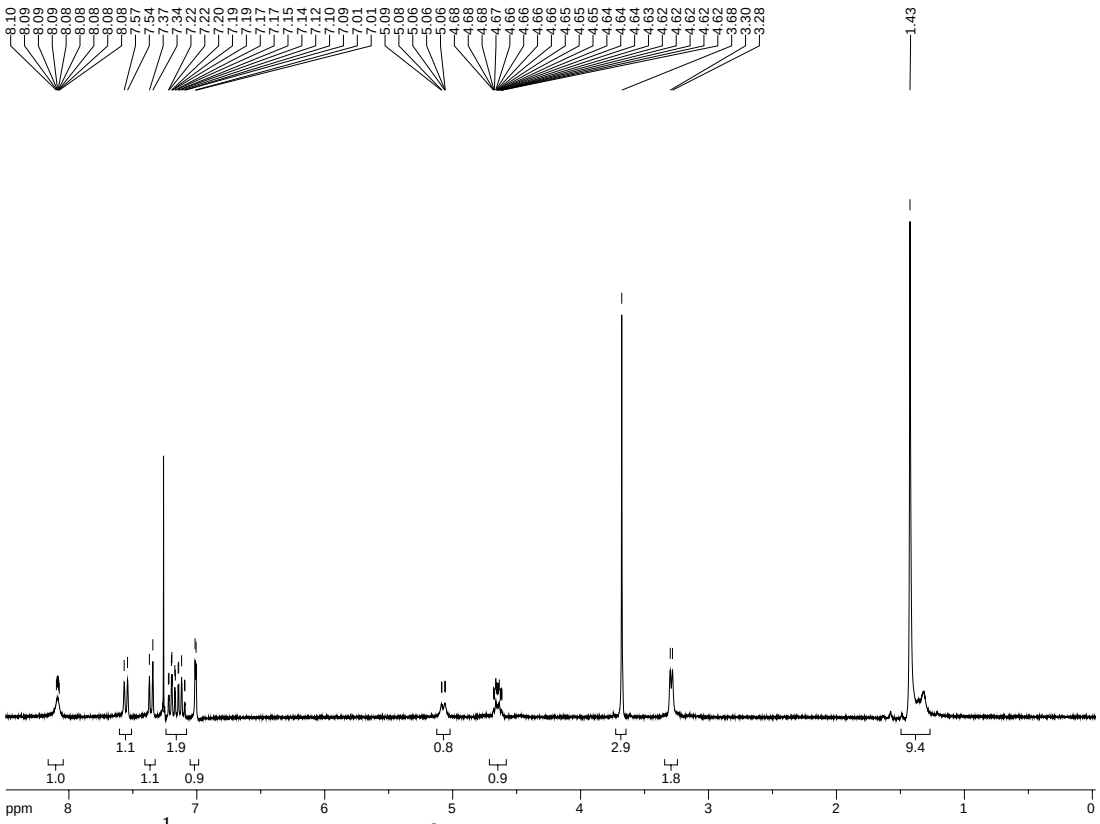

Figure 5.36a. ^{1}H NMR spectrum of compound **3.34**.

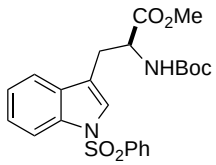

3.64

***N*-Boc-L-tryptophan-OMe-*N'*-SO_2Ph (3.64)**. *N*-Boc-L-tryptophan-OMe (10.0 g, 31.4 mmol), NaOH (3.77 g, 94.2 mmol), and Bu_4NHSO_4 (544 mg, 1.6 mmol) were suspended in CH_2Cl_2 (150 mL), then $PhSO_2Cl$ (4.8 mL, 37.7 mmol) added dropwise. After stirring 6 h. at r.t., aqueous NH_4Cl (300 mL) and EtOAc (300 mL) were added and the product extracted in EtOAc (3x). The combined organic extracts were dried and concentrated to afford the title compound (14.4 g, >99% yield).

^{1}H-NMR (300 MHz; $CDCl_3$): δ 7.97 (d, *J* = 8.2 Hz, 1H), 7.84 (d, *J* = 7.5 Hz, 2H), 7.56-7.50 (m, 1H), 7.47-7.44 (m, 2H), 7.42 (d, *J* = 7.2 Hz, 1H), 7.36 (s, 1H), 7.31-7.20 (m, 2H), 5.05 (dt, *J* = 7.9, 0.6 Hz, 1H), 4.66-4.59 (m, 1H), 3.61 (s, 3H), 3.27-3.11 (m, 2H), 1.44 (s, 9H).

REF: **TRW-II-263**, TRW-II-275, TRW-II-350.

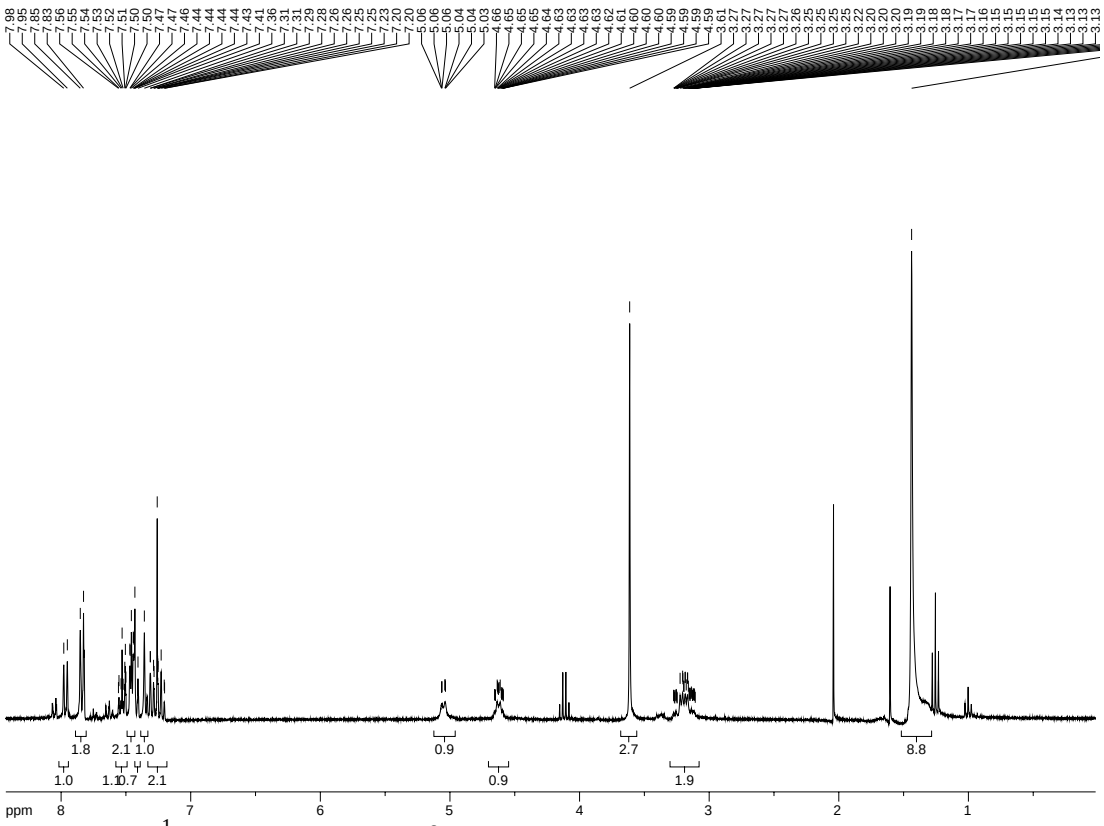

Figure 5.37a. ^{1}H NMR spectrum of compound **3.64**.

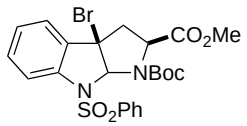

3.65

Bromopyrroloindoline (3.65). To a solution of *N*-Boc-L-tryptophan-OMe-*N*'-SO_2Ph (42 g, 91.5 mmol) in CH_2Cl_2 (1000 mL) was added NBS (16.29 g, 91.5 mmol) and PPTS (22.97 g, 91.5 mmol). The reaction was stirred O/N at r.t., then washed with 10% $NaHCO_3$ and 10% $Na_2S_2O_4$ (1:1), and the organic extract concentrated to afford **3.65** in quantitative yield.

^{1}H-NMR (300 MHz; $CDCl_3$): δ 7.83-7.79 (bs, 2H), 7.57 (d, *J* = 8.0 Hz, 1H), 7.46 (ddd, *J* = 8.4, 6.4, 1.6 Hz, 1H), 7.34 (td, *J* = 7.7, 1.4 Hz, 3H), 7.27-7.25 (m, 1H), 7.17 (td, *J* = 7.5, 1.0 Hz, 1H), 6.33-6.31 (bs, 1H), 3.85-3.80 (m, 1H), 3.73 (s, 3H), 3.06 (dd, *J* = 12.6, 5.9 Hz, 1H), 2.81-2.73 (m, 1H), 1.54-1.53 (bs, 9H); ^{13}C-NMR (101 MHz; $CDCl_3$): δ 171.9, 138.0, 133.8, 133.4, 130.9, 129.2, 128.6, 128.3, 127.3, 126.6, 124.9, 124.3, 123.9, 123.3, 113.6, 86.7, 80.0, 59.4, 52.4, 28.26, 28.17, 27.8, 21.0, 14.2.

REF: TRW-II-264, **TRW-II-277**, TRW-II-351.

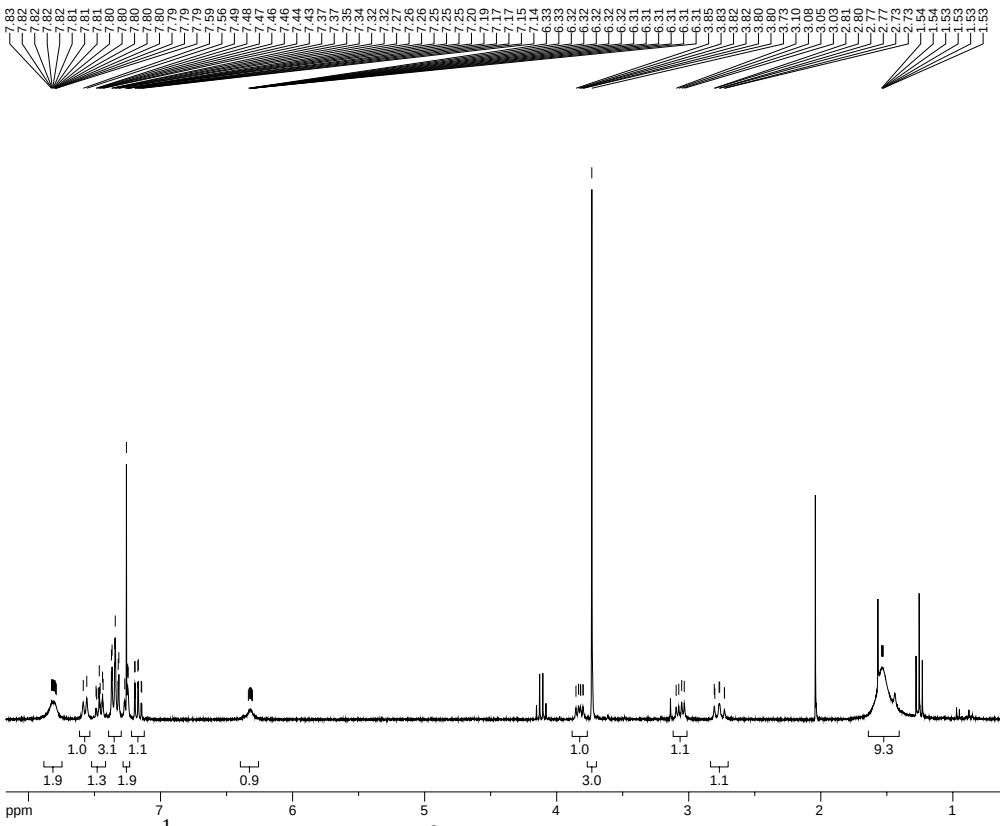

Figure 5.38a. ^{1}H NMR spectrum of compound **3.65**.

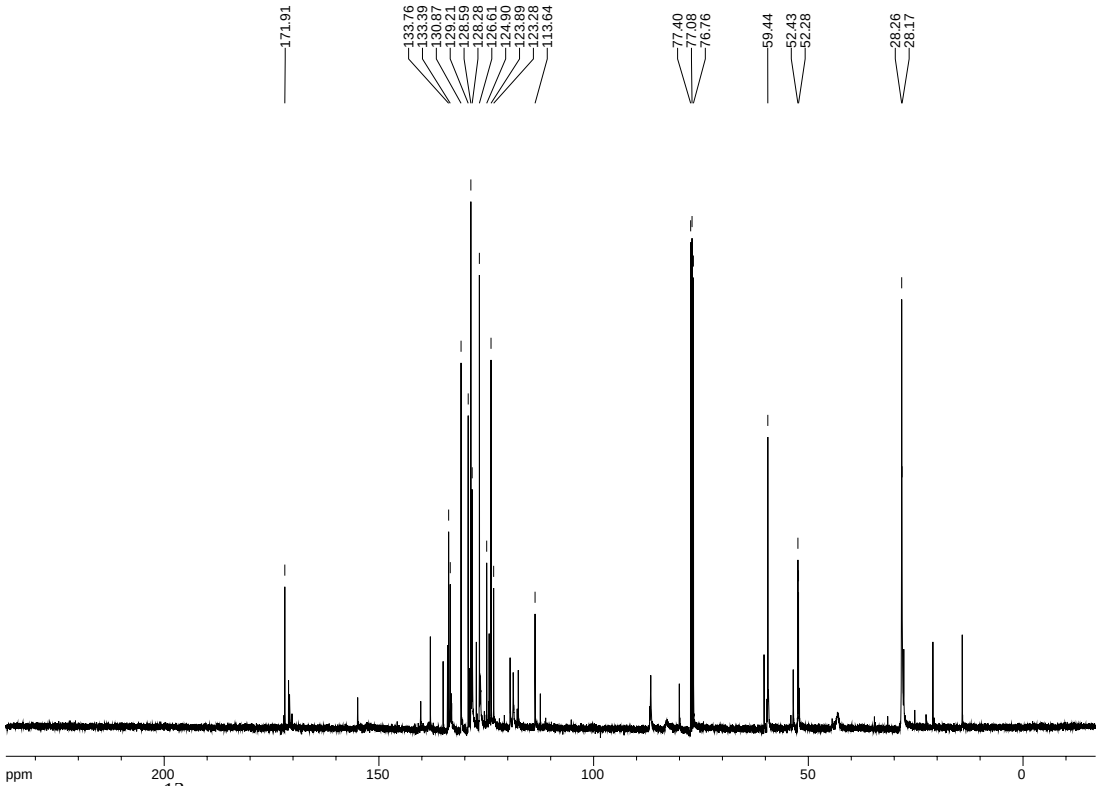

Figure 5.38b. ^{13}C NMR spectrum of compound **3.65**.

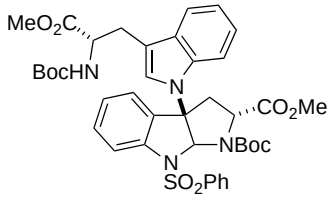

3.66

Indole (3.66). Bromopyrroloindoline **3.65** (16.41 g, 30.6 mmol) was dissolved in CH_3CN, and to the resulting solution added *N*-Boc-L-tryptophan-OMe (6.49 g, 20.4 mmol). The solution was cooled to 0 °C, then KO*t*Bu (4.57 g, 40.8 mmol) added. After stirring 1 h at 0 °C, the reaction was quenched with $NaHCO_3$, extracted in CH_2Cl_2, washed with brine, dried, and concentrated. Purification by SiO_2 chromatography (40% EtOAc in hexanes) afforded **3.66** in 34% yield (5.36 g).

^{1}H-NMR (300 MHz; $CDCl_3$): δ 7.85-7.79 (m, 1H), 7.85-7.79 (m, 1H), 7.60-7.43 (m, 2H), 7.60-7.43 (m, 2H), 7.34 (t, *J* = 7.7 Hz, 3H), 7.34 (t, *J* = 7.7 Hz, 3H), 7.22-7.01 (m, 7H), 7.22-7.01 (m, 7H), 6.85 (s, 1H), 6.85 (s, 1H), 6.31 (bs, 1H), 6.31 (s, 1H), 5.06 (bs, 1H), 5.06 (s, 1H), 4.64-4.61 (m, 1H), 4.64-4.61 (m, 1H), 3.73 (s, 3H), 3.73 (s, 3H), 3.68 (s, 3H), 3.68 (s, 3H), 3.28-3.21 (m, 2H), 3.28-3.21 (m, 2H), 3.07 (dd, *J* = 12.6, 5.9 Hz, 1H), 3.07 (dd, *J* = 12.6, 5.9 Hz, 1H), 2.77 (t, *J* = 11.6 Hz, 1H), 2.77 (t, *J* = 11.6 Hz, 1H), 1.58-1.55 (bs, 9H), 1.58-1.55 (m, 9H), 1.43 (s, 9H), 1.43 (s, 9H); ^{13}C-NMR (101 MHz; $CDCl_3$): δ 172.4, 161.2, 154.9, 143.2, 133.7, 132.9, 132.2, 131.61, 131.58, 131.52, 130.5, 128.9, 128.5, 128.1, 127.0, 126.46, 126.35, 125.2, 124.1, 122.4, 121.82, 121.76, 120.24, 120.17, 119.57, 119.43, 114.8, 82.2, 59.44, 59.36, 54.4, 53.3, 52.1, 51.6, 37.9, 37.7, 28.18, 28.14, 28.08, 28.01, 27.99, 27.97, 27.94, 27.93, 27.91, 27.79; HRMS (ESI-APCI+): $[M+Na]^+$ 797.2832 calcd for $C_{40}H_{46}N_4NaO_{10}S$, found: 797.2829.

REF: **TRW-II-266**, TRW-II-278, TRW-II-352.

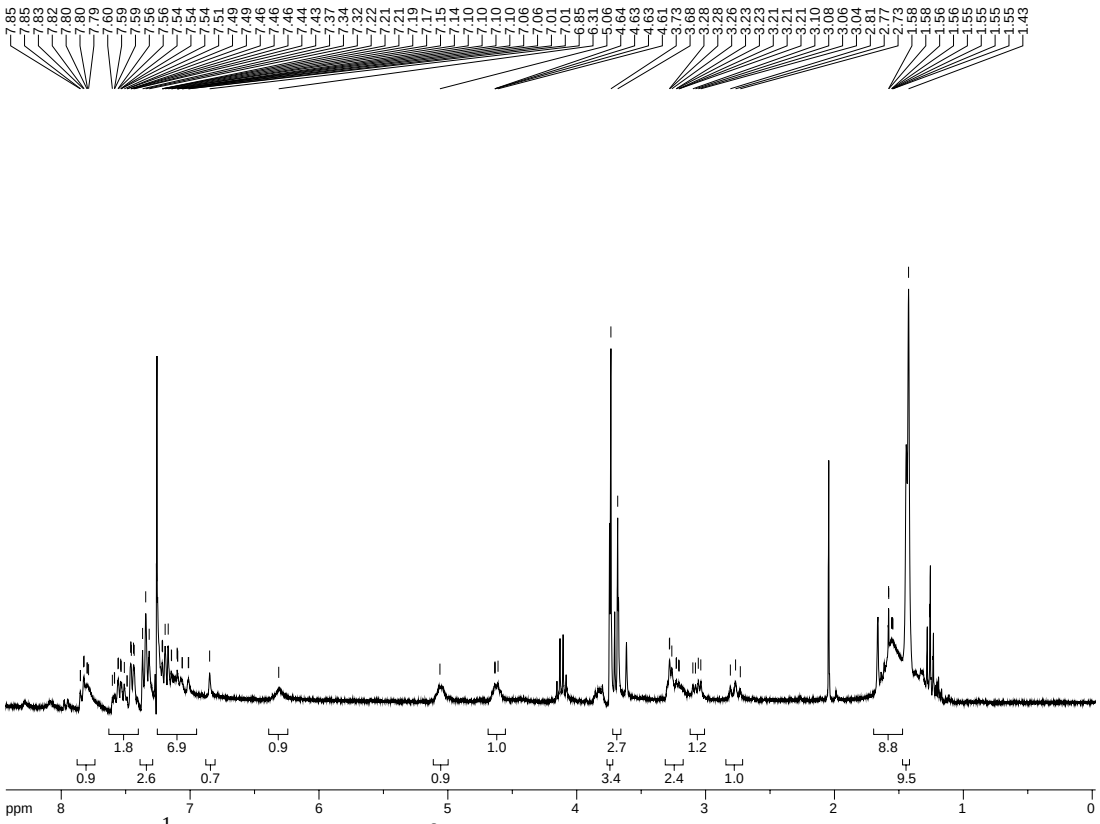

Figure 5.39a. ^{1}H NMR spectrum of compound **3.66**.

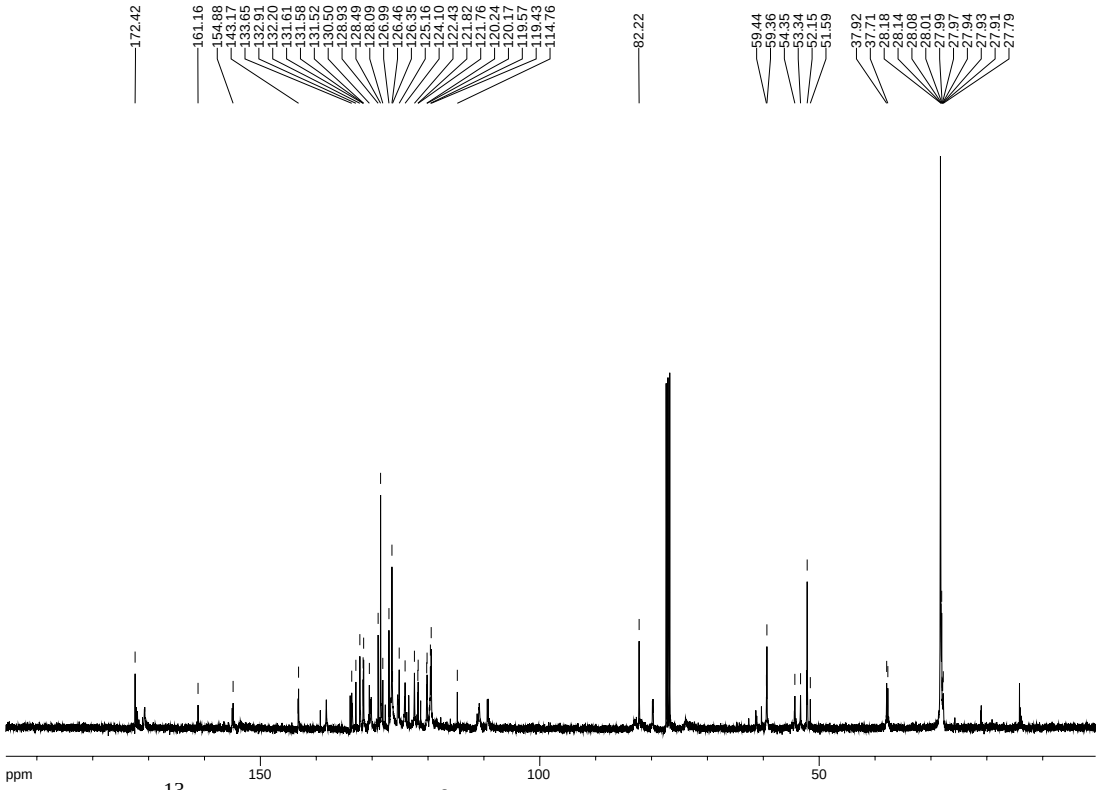

Figure 5.39b. ^{13}C NMR spectrum of compound **3.66**.

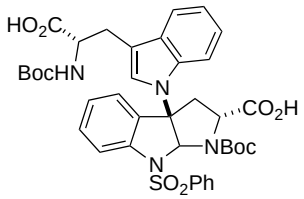

3.67

Diacid (3.67). To a solution of **3.66** (5.35 g, 6.9 mmol) in 2:1 THF:H_2O (24 mL) was added LiOH (828 mg, 34.5 mmol). The reaction stirred O/N before acidifying with 10% $KHSO_4$. The product was extracted in EtOAc, and the combined organic extracts washed with brine, dried, and concentrated. SiO_2 chromatography (1:1 hexanes:EtOAc) gave the pure diacid (5.01 g, 97% yield).

^{1}H-NMR (300 MHz; $CDCl_3$): δ 9.51 (bs, 2H), 7.70-7.67 (m, 1H), 7.55 (dt, *J* = 7.0, 0.8 Hz, 1H), 7.42-7.38 (m, 1H), 7.19-7.13 (m, 8H), 6.95-6.88 (m, 2H), 6.70 (d, *J* = 5.8 Hz, 1H), 6.06-5.93 (m, 1H), 4.99-4.92 (m, 1H), 4.54-4.40 (m, 1H), 3.43-3.34 (m, 1H), 3.19-3.05 (m, 1H), 2.81-2.72 (m, 2H), 1.56 (s, 8H), 1.42 (d, *J* = 11.7 Hz, 9H); ^{13}C-NMR (101 MHz; $CDCl_3$): δ 178.03, 177.95, 159.41, 159.30, 146.7, 141.6, 137.56, 137.44, 136.8, 136.3, 135.3, 134.47, 134.33, 132.8, 132.4, 131.7, 130.8, 130.4, 129.5, 128.35, 128.18, 126.2, 123.97, 123.91, 123.64, 123.63, 123.58, 123.54, 123.52, 123.50, 123.47, 113.45, 113.42, 98.4, 86.33, 86.25, 83.81, 83.68, 64.5, 63.3, 32.0, 31.8.

REF: **TRW-II-268**, TRW-II-446.

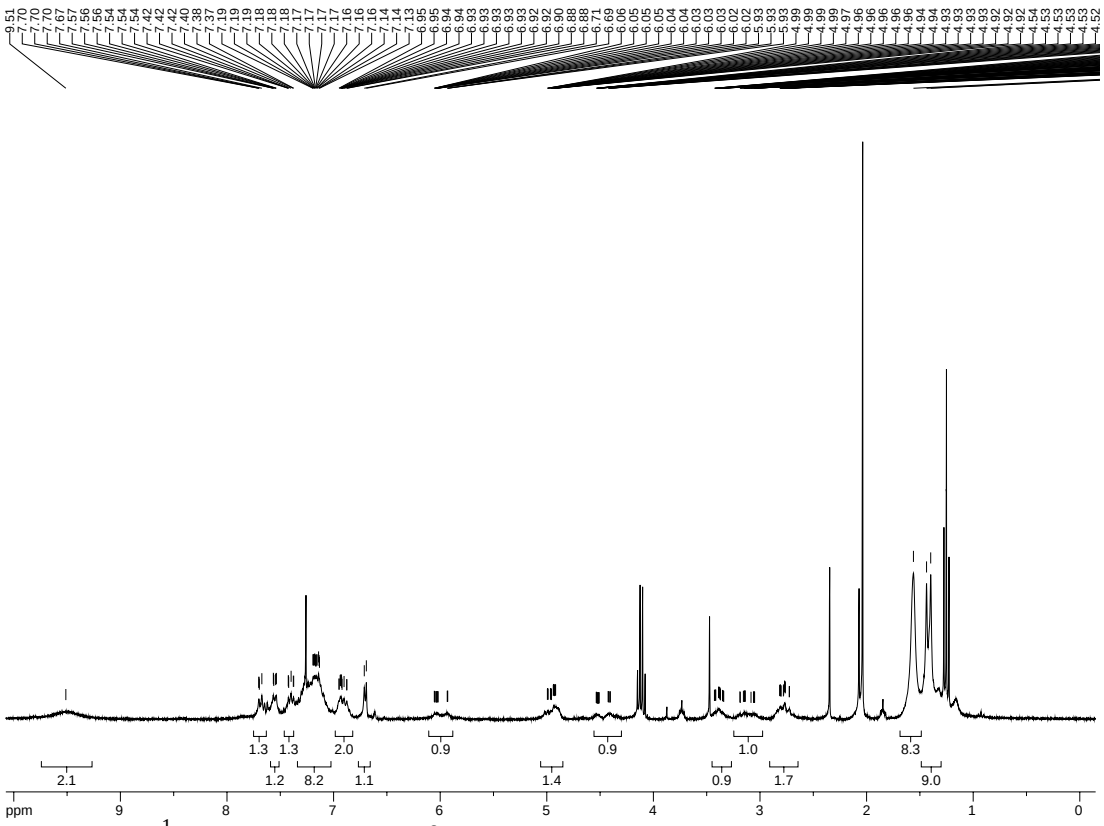

Figure 5.40a. ^{1}H NMR spectrum of compound **3.67**.

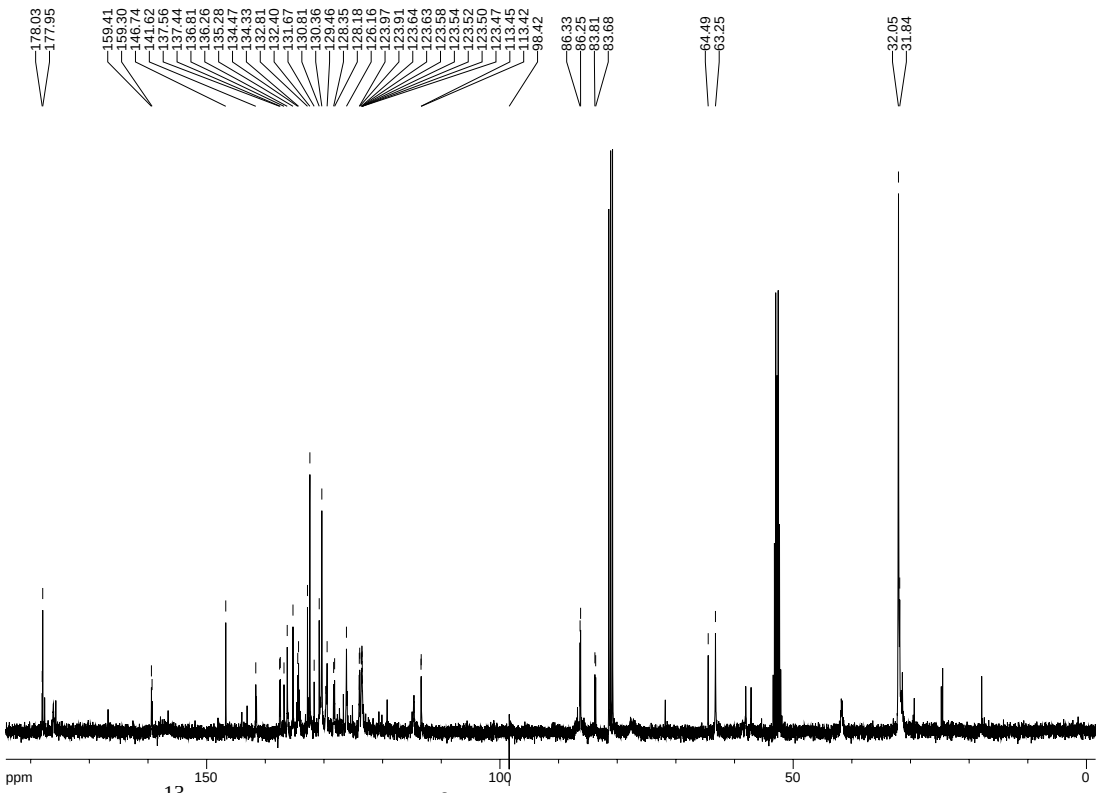

Figure 5.40b. ^{13}C NMR spectrum of compound **3.67**.

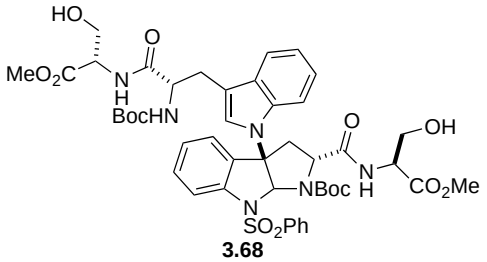

3.68

Tetrapeptide (3.68). To a solution of L-serine-OMe·HCl (2.09 g, 13.4 mmol) in CH_2Cl_2 (70 mL) was added *i*Pr_2NEt (2.3 mL, 13.4 mmol). After stirring 15 minutes, the suspension was added to a stirring solution of **3.67** (5.01 g, 6.69 mmol) and EDCI (2.57 g, 13.4 mmol) in CH_2Cl_2. The reaction was stirred O/N at r.t., then concentrated and purified through a plug of SiO_2 (100% EtOAc) to afford **3.68** (2.11 g, 33% yield).

^{1}H-NMR (300 MHz; DMSO-d_6): δ 8.10-8.08 (broad, 1H), 7.73-7.58 (m, 5H), 7.44-7.31 (m, 3H), 7.10-7.07 (m, 3H), 6.83-6.74 (m, 1H), 6.44-6.42 (m, 1H), 5.04-4.86 (m, 3H), 4.34-4.22 (m, 3H), 3.61-3.43 (m, 9H), 3.02-2.83 (m, 1H), 2.76-2.51 (m, 2H), 1.34-1.27 (m, 18H).

REF: **TRW-II-270**, TRW-II-447.

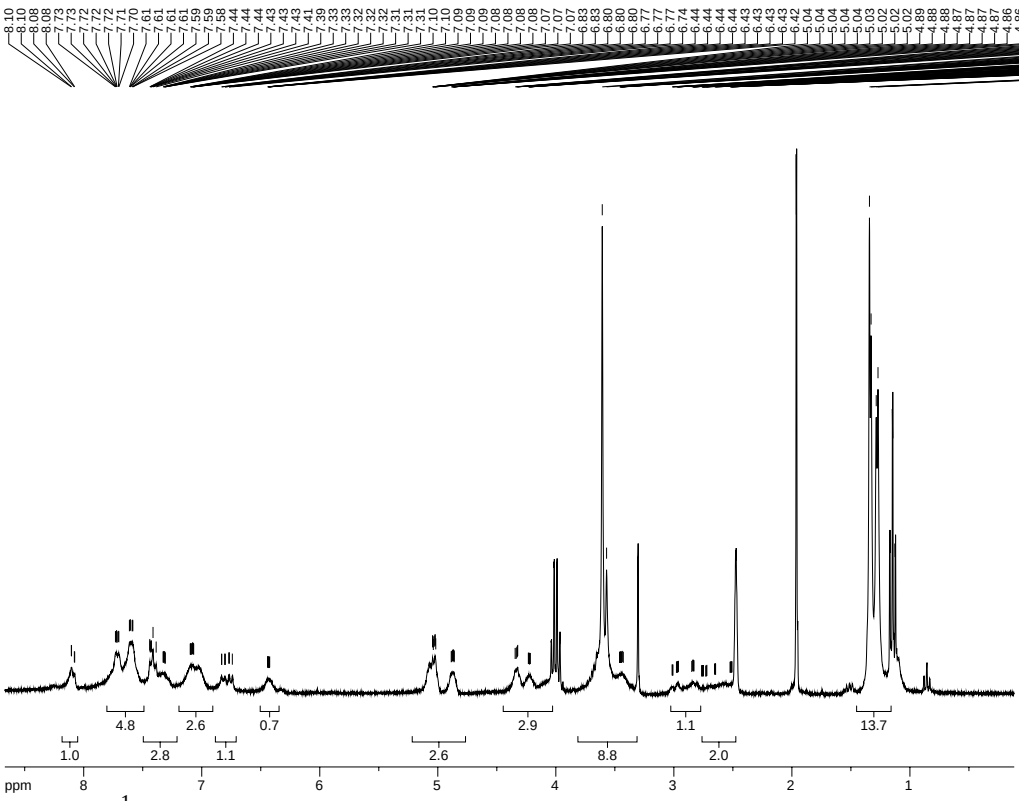

Figure 5.41a. ^{1}H NMR spectrum of compound **3.68**.

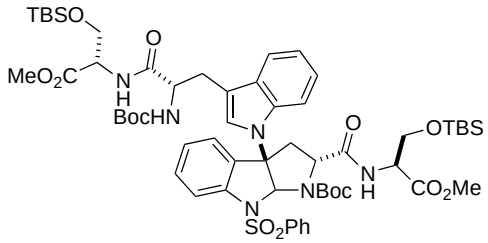

3.69

TBS_2-Tetrapeptide (3.69). To a solution of diol **3.68** (2.11 g, 2.22 mmol) in DMF (12 mL) was added imidazole (728 mg, 10.7 mmol) and TBSCl (1.74 g, 11.5 mmol). The reaction mixture stirred O/N at r.t., then was concentrated. The crude residue was taken up in EtOAc and washed with water (3x), brine (1x), dried over Na_2SO_4, and concentrated to afford the title compound (2.27 g, 87% yield).

^{1}H-NMR (300 MHz; DMSO-d_6): δ 8.02-7.99 (m, 1H), 7.72-7.42 (m, 6H), 7.37-7.21 (m, 2H), 7.13-6.86 (m, 4H), 6.48-6.39 (m, 1H), 4.92-4.89 (m, 1H), 4.43-4.39 (m, 1H), 4.21-4.06 (m, 2H), 3.82-3.69 (m, 3H), 3.63-3.58 (m, 6H), 3.00-2.89 (m, 1H), 2.86-2.80 (m, 1H), 2.66-2.52 (m, 3H), 1.31 (dd, *J* = 22.1, 8.9 Hz, 18H), 0.81 (s, 18H), -0.01--0.03 (m, 12H).

REF: **TRW-II-272**.

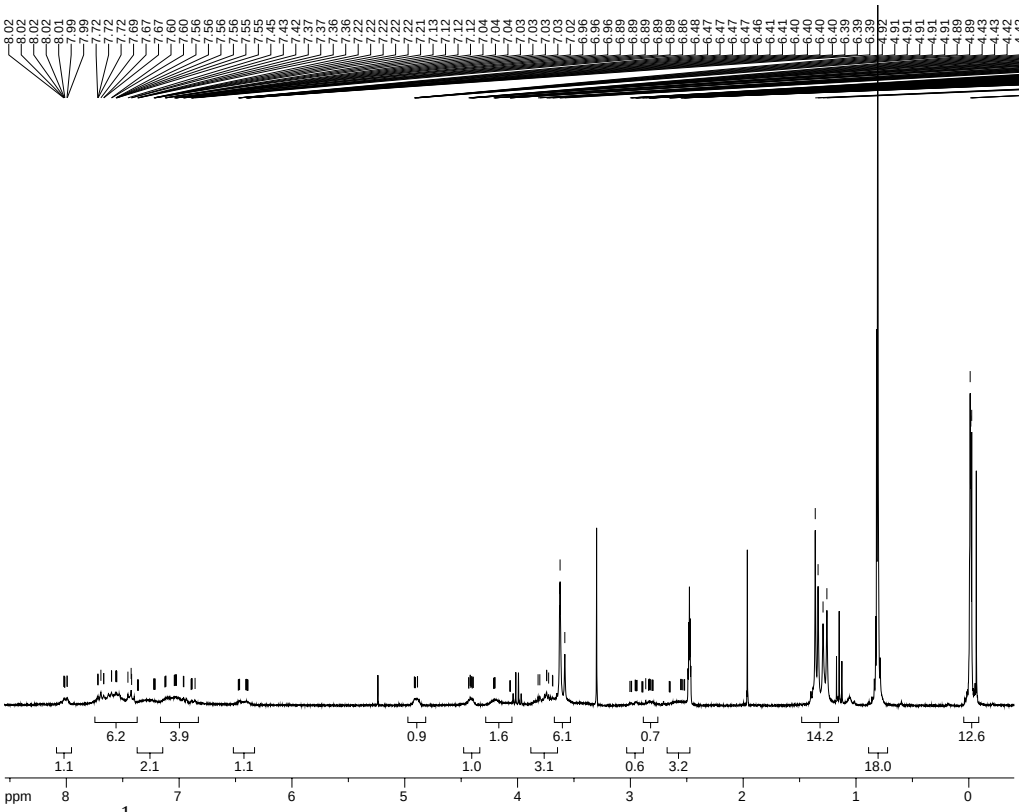

Figure 5.42a. ^{1}H NMR spectrum of compound **3.69**.

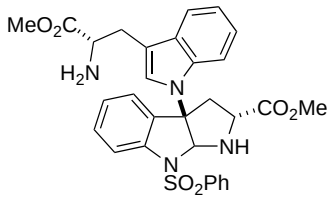

5.4

Diamine (5.4). To a solution of **3.66** (2 g, 2.58 mmol) in CH_2Cl_2 (50 mL) at 0 °C was added TFA (4.8 mL). The resulting solution was warmed to r.t. and stirred for 2 h under Ar. The reaction was quenched with sat'd $NaHCO_3$, and the product extracted in CH_2Cl_2. The combined organic layers were dried and concentrated to afford **5.4** in quantitative yield (1.48 g).

^{1}H-NMR (300 MHz; DMSO-d_6): δ 7.69 (d, *J* = 7.4 Hz, 2H), 7.63-7.58 (m, 2H), 7.50-7.36 (m, 6H), 7.20-7.15 (m, 1H), 7.09-7.04 (m, 1H), 6.99-6.98 (m, 1H), 6.82-6.75 (m, 2H), 5.89 (d, *J* = 4.1 Hz, 1H), 4.51 (t, *J* = 4.2 Hz, 1H), 4.33-4.29 (m, 1H), 3.78 (s, 1H), 3.52 (d, *J* = 6.2 Hz, 3H), 3.39-3.32 (m, 3H), 2.95-2.78 (m, 2H), 2.71-2.65 (m, 2H), HRMS (ESI-APCI-): $[M-H]^-$ 574.1886 calcd for $C_{30}H_{30}N_4O_6S$, found: 574.1867.

REF: **TRW-II-282**, TRW-II-289, TRW-II-292, TRW-II-300, TRW-II-335, TRW-II-353.

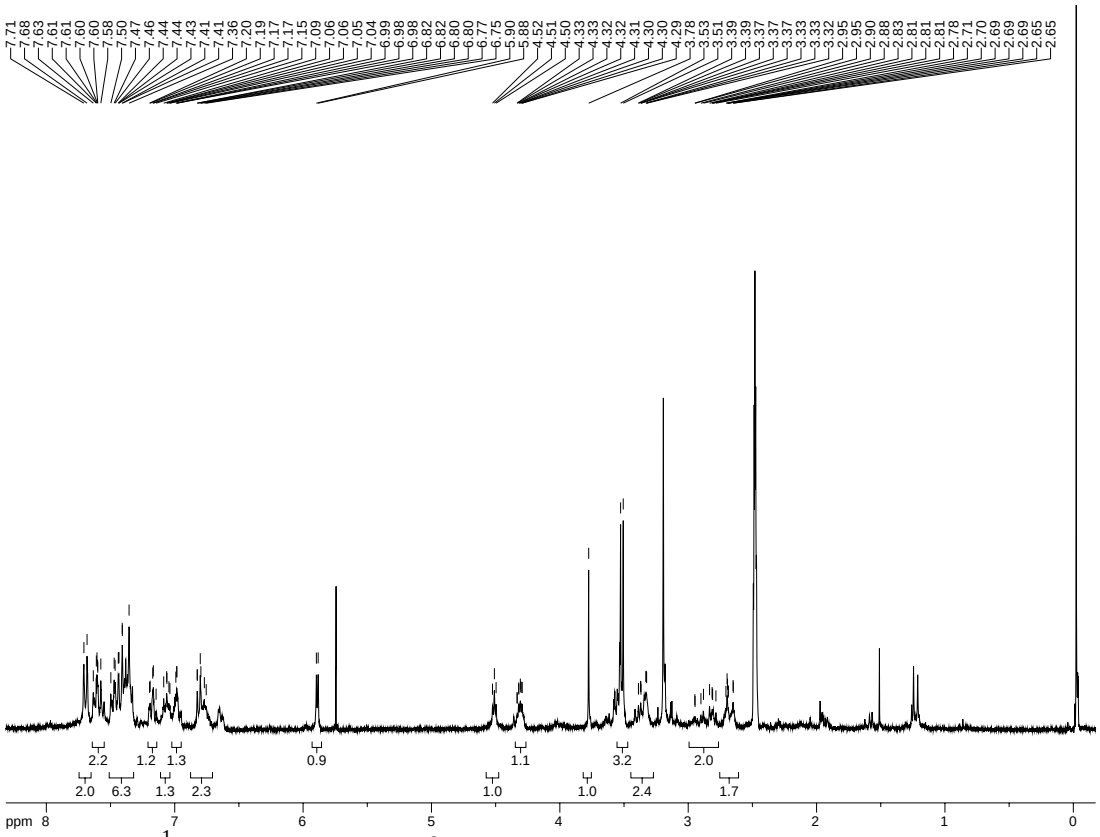

Figure 5.43a. ^{1}H NMR spectrum of compound **5.4**.

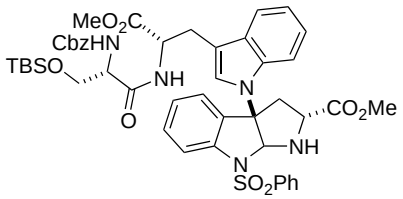

3.71

Tripeptide (3.71). *N*-Cbz-L-serine(OTBS) (2.52 g, 7.14 mmol), *i*Pr_2NEt (1.3 mL, 7.14 mmol), and EDCI (1.37 g, 7.14 mmol) were added to a solution of **5.4** (2.05 g, 3.57 mmol) in CH_2Cl_2 (20 mL). The reaction stirred O/N, then was concentrated and purified through an SiO_2 plug to afford pure **3.71** (2.37 g, 73% yield).

^{1}H-NMR (300 MHz; DMSO-d_6): δ 8.48-8.37 (m, 1H), 7.70-7.58 (m, 5H), 7.48-7.42 (m, 3H), 7.37-7.29 (m, 8H), 7.09-6.99 (m, 3H), 6.79-6.71 (m, 2H), 5.90-5.87 (m, 1H), 5.03-4.96 (m, 2H), 4.49-4.40 (m, 2H), 4.31-4.29 (m, 1H), 4.23-4.19 (m, 1H), 3.78 (s, 1H), 3.64-3.61 (m, 1H), 3.53 (d, *J* = 4.4 Hz, 3H), 3.41-3.34 (m, 1H), 3.19 (d, *J* = 9.1 Hz, 3H), 3.01-2.93 (m, 1H), 2.68-2.64 (m, 1H), 0.78 (d, *J* = 10.3 Hz, 9H), -0.02 (s, 6H); HRMS (ESI-APCI): $[M+H]^+$ 910.3517 calcd for $C_{47}H_{56}N_5O_{10}SSi$, found: 910.3543.

REF: **TRW-II-354**, TRW-II-341, TRW-II-359.

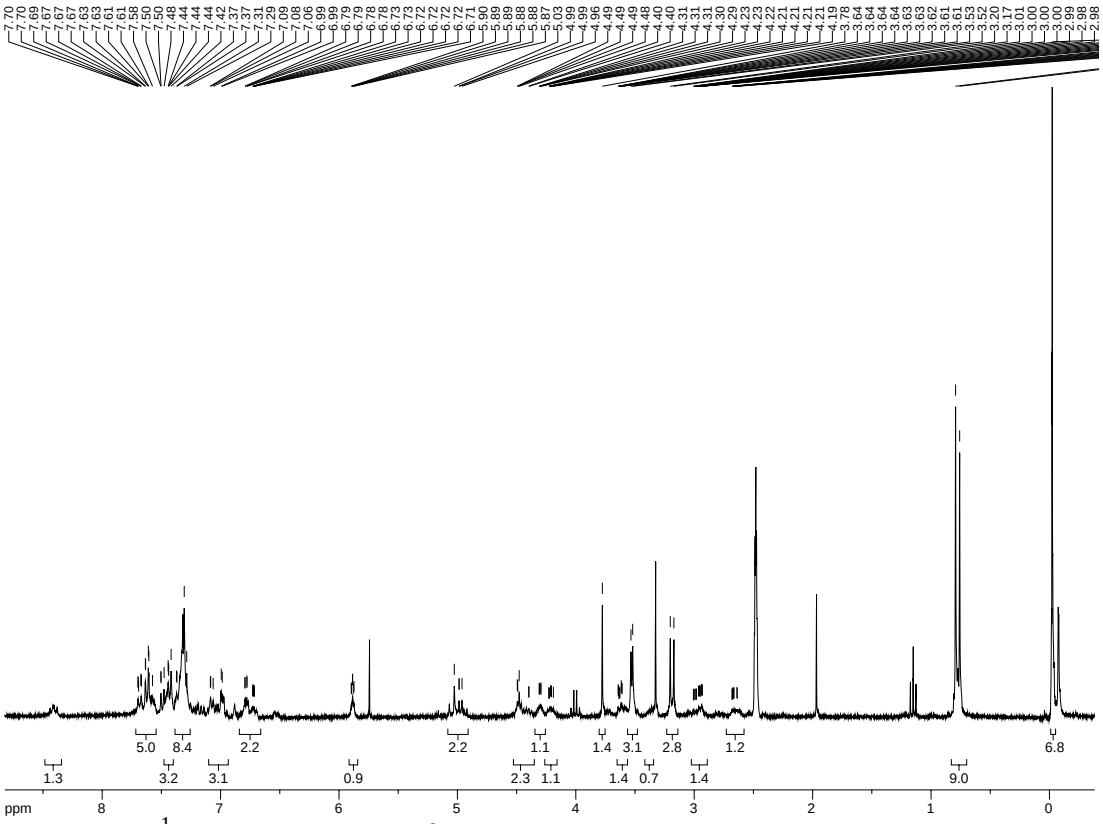

Figure 5.44a. ^{1}H NMR spectrum of compound **3.71**.

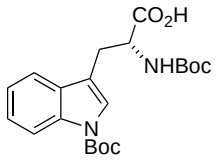

5.5

(*R*)-*tert*-butyl 3-(2-((*tert*-butoxycarbonyl)amino)-3-methoxy-3-oxopropyl)-1*H*-indole-1-carboxylate (5.5). Powdered NaOH (19.0 g, 475 mmol) was added to a stirring suspension of D-Trp-OMe·HCl (24.14 g, 95 mmol) and Bu_4NHSO_4 (3.23 g, 9.5 mmol) in CH_2Cl_2 (950 mL). After stirring 2.5 h, Boc_2O (62.1 g, 285 mmol) was added, and the resulting suspension stirred O/N at r.t. The mixture was filtered through celite, concentrated, and purified by SiO_2 chromatography (9:1 hexanes:EtOAc) to afford *N*,*N*'-Boc_2-D-Trp-OMe (18.53 g, 47% yield).

^{1}H-NMR (300 MHz; $CDCl_3$): δ 8.11 (d, *J* = 7.4 Hz, 1H), 7.49 (d, *J* = 7.6 Hz, 1H), 7.39 (s, 1H), 7.27 (td, *J* = 16.1, 8.4 Hz, 2H), 5.11 (d, *J* = 7.2 Hz, 1H), 4.65 (q, *J* = 6.4 Hz, 1H), 3.69 (s, 3H), 3.22 (qd, *J* = 13.5, 5.5 Hz, 2H), 1.66 (s, 9H), 1.43 (s, 9H).

REF: TRW-III-171, **TRW-III-239**.

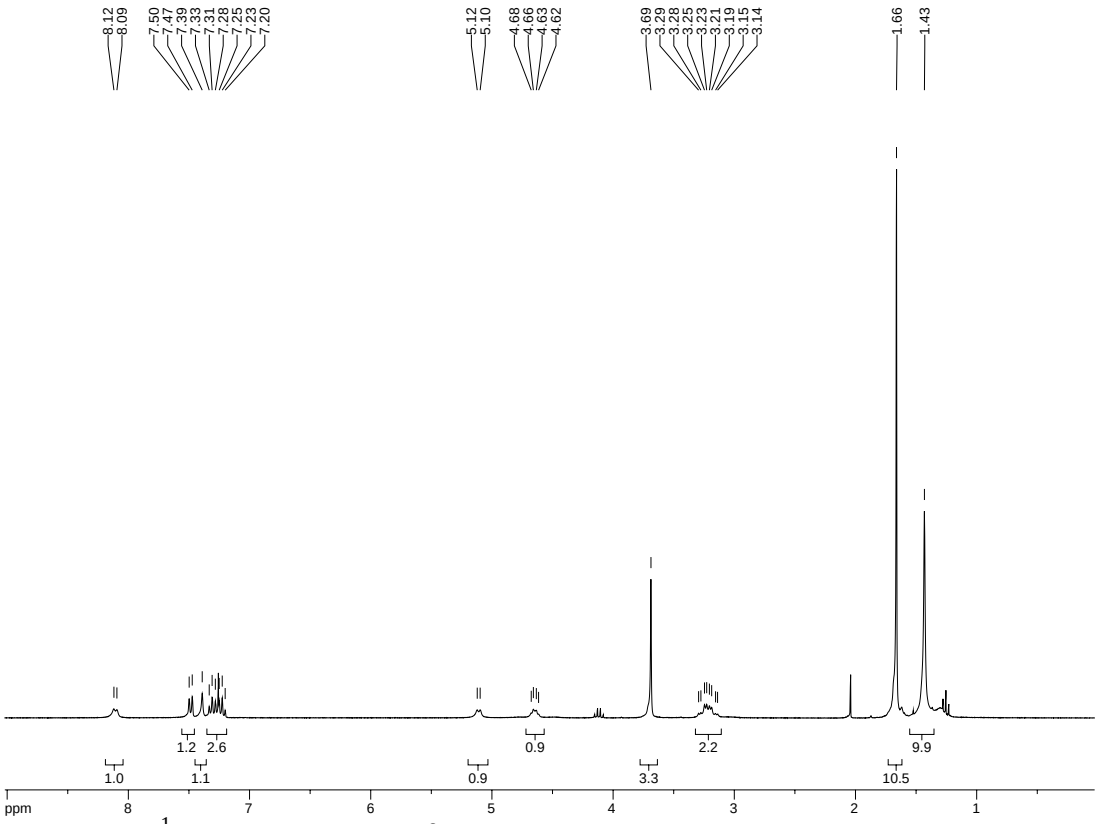

Figure 5.45a. ^{1}H NMR spectrum of compound **5.5**.

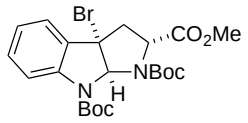

3.74

Bromopyrroloindoline (3.74). To a solution of *N*,*N'*-Boc_2-D-Trp-OMe (18.53 g, 44.3 mmol) in CH_2Cl_2 (1000 mL) was added NBS (7.89 g, 44.3 mmol) and PPTS (11.12 g, 44.3 mmol). The resulting solution was allowed to stir at r.t. O/N. The reaction mixture was washed with brine, the organic layer dried (Na_2SO_4) and concentrated. Purification by SiO_2 chromatography (30% EtOAc in hexanes) gave the desired product in 96% yield (21.20 g).

$[\alpha]_D$ = +150.0 (CH_2Cl_2); ^{1}H-NMR (400 MHz; $CDCl_3$): δ 7.53-7.52 (bs, 1H), 7.34-7.24 (m, 2H), 7.09 (t, *J* = 7.6 Hz, 1H), 6.37 (s, 1H), 3.86 (dd, *J* = 10.3, 6.3 Hz, 1H), 3.71 (s, 3H), 3.18 (dd, *J* = 12.6, 6.3 Hz, 1H), 2.79 (dd, *J* = 12.6, 10.3 Hz, 1H), 1.56 (s, 9H), 1.37 (bs, 9H); ^{13}C-NMR (101 MHz; $CDCl_3$): δ 171.46, 171.41, 171.0, 152.1, 141.5, 130.6, 124.37, 124.35, 123.2, 83.8, 82.2, 59.4, 52.3, 36.4, 28.6, 28.2, 24.1, 21.0, 14.2; IR (NaCl, film) 2980, 1719, 1395, 1334, 1163, 753 cm^{-1}; HRMS (ESI-APCI): $[M+Na]^+$ 519.1107 calcd for $C_{22}H_{29}BrN_2NaO_6$, found: 519.1102.

REF: TRW-III-174, **TRW-III-246**.

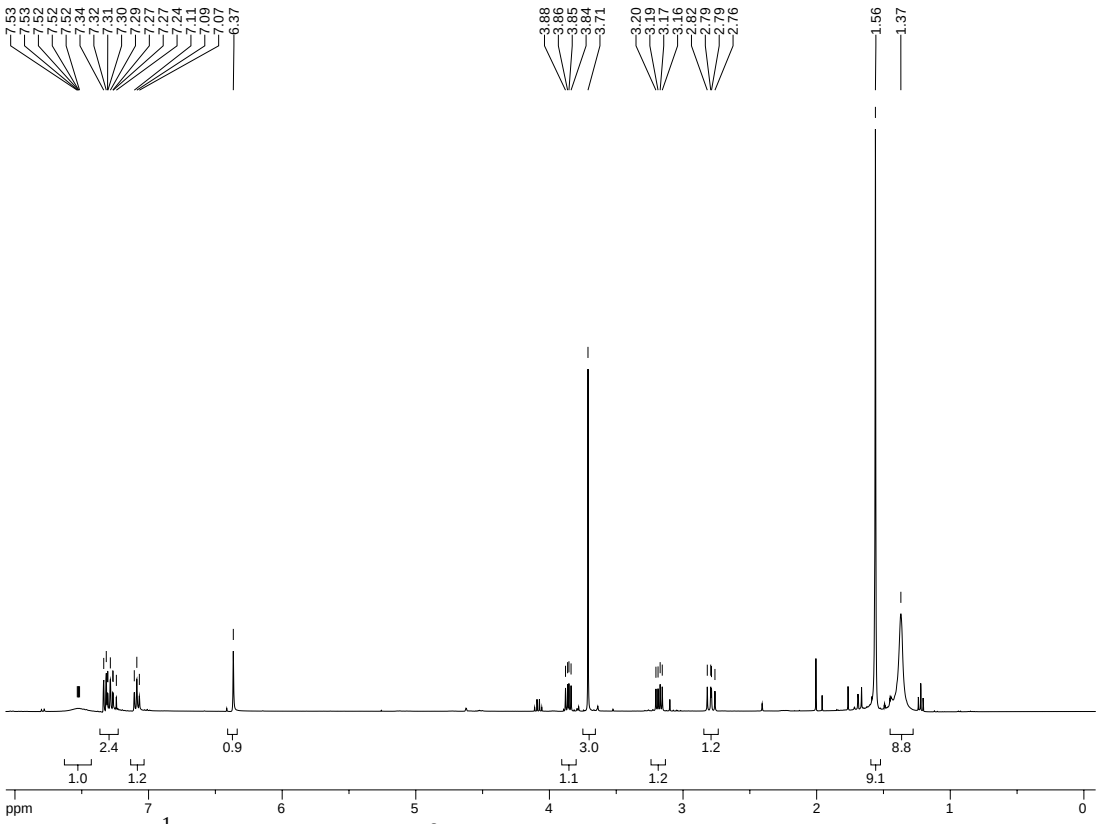

Figure 5.46a. ^{1}H NMR spectrum of compound **3.74**.

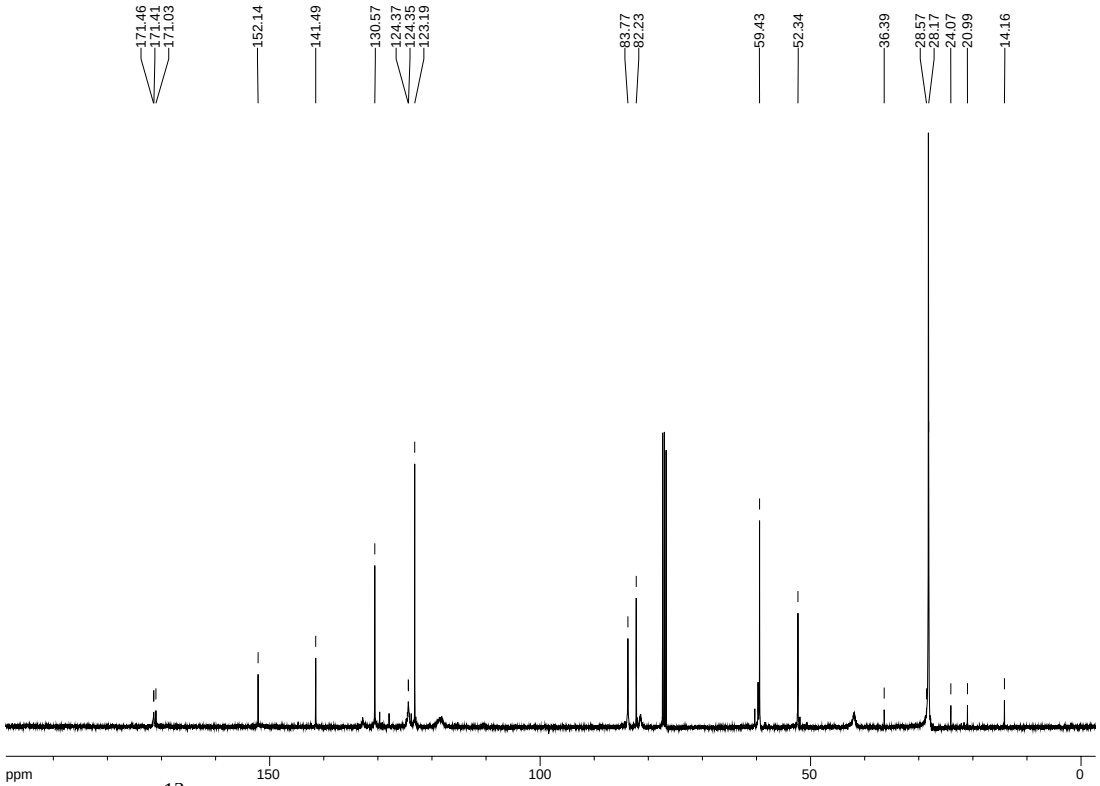

Figure 5.46b. ^{13}C NMR spectrum of compound **3.74**.

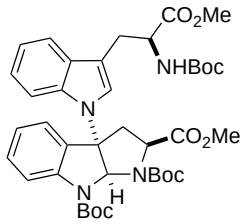

3.75

(2*S*,3a*S*,8a*S*)-1,8-di-*tert*-butyl 2-methyl 3a-(3-((*S*)-2-((*tert*-butoxycarbonyl)amino)-3-methoxy-3-oxopropyl)-1*H*-indol-1-yl)-3,3a-dihydropyrrolo[2,3-*b*]indole-1,2,8(2*H*,8a*H*)-tricarboxylate (3.75). KO*t*Bu (3.02 g, 27 mmol) was added to a solution of bromopyrroloindoline **3.74** (10.0 g, 20.2 mmol) and *N*-Boc-Trp-OMe (4.29 g, 13.5 mmol) in CH_3CN (1000 mL) at 0 °C at stirred 1h under Ar. $NaHCO_3$ was added and the product extracted in CH_2Cl_2, washed with brine, dried (Na_2SO_4), and concentrated. Purification by SiO_2 chromatography (40% EtOAc in hexanes) afforded pure dipeptide (5.47 g, 55% yield).

$[\alpha]_D$ = -7.2 (CH_2Cl_2); ^{1}H-NMR (400 MHz; $CDCl_3$): δ 7.70-7.64 (bs, 1H), 7.51 (t, *J* = 7.5 Hz, 1H), 7.37-7.32 (m, 1H), 7.26 (s, 1H), 7.20-7.05 (m, *J* = 7.8 Hz, 4H), 6.74 (s, 1H), 6.67 (s, 1H), 4.97 (t, *J* = 6.4 Hz, 1H), 4.88 (d, *J* = 7.2 Hz, 1H), 4.53 (s, 1H), 3.58 (s, 2H), 3.53-3.46 (m, 2H), 3.20 (s, 3H), 3.13 (s, 3H), 1.51-1.48 (m, 18H), 1.39 (d, *J* = 7.7 Hz, 9H); ^{13}C-NMR (101 MHz; $CDCl_3$): δ 172.7, 171.0, 155.0, 151.9, 143.6, 134.7, 131.00, 130.89, 124.80, 124.78, 122.9, 122.31, 122.30, 122.0, 120.0, 119.55, 119.37, 111.5, 109.7, 82.1, 79.7, 72.57, 72.54, 60.3, 54.2, 52.1, 28.29, 28.17; IR (NaCl, film) 2979, 1716, 1457, 1207, 739 cm^{-1}; HRMS (ESI-APCI): $[M+Na]^+$ 757.3425 calcd for $C_{39}H_{50}N_4NaO_{10}$, found: 757.3427.

REF: TRW-III-183, **TRW-III-194**.

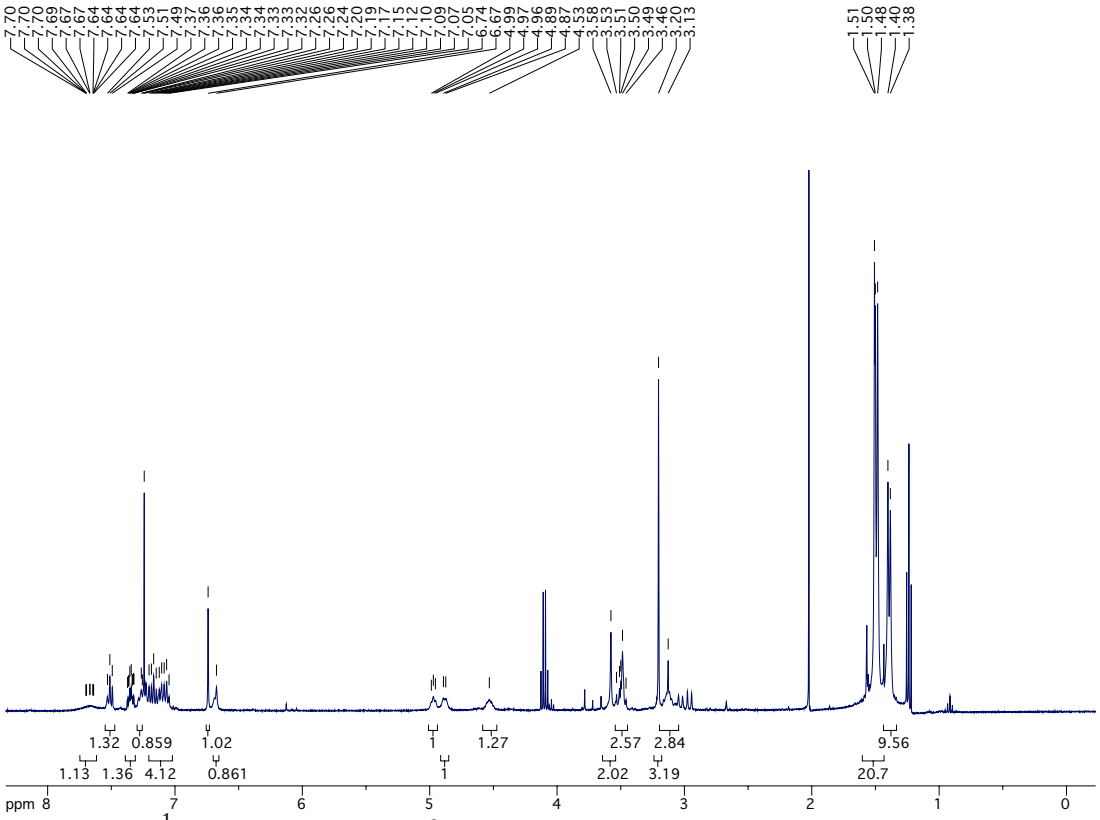

Figure 5.47a. ^{1}H NMR spectrum of compound **3.75**.

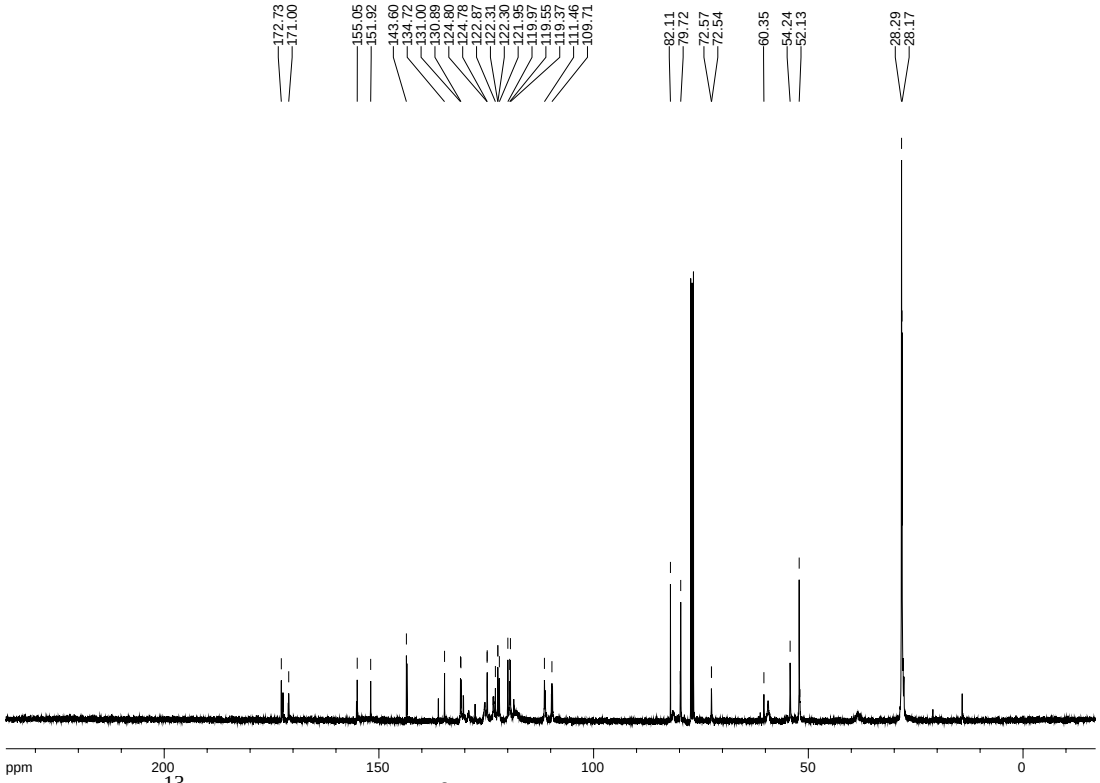

Figure 5.47b. ^{13}C NMR spectrum of compound **3.75**.

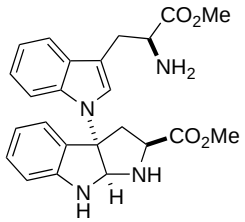

5.6

(2*S*,3a*S*,8a*S*)-methyl 3a-(3-((*S*)-2-amino-3-methoxy-3-oxopropyl)-1*H*-indol-1-yl)-1,2,3,3a,8,8a-hexahydropyrrolo[2,3-*b*]indole-2-carboxylate (5.6). TFA (15 mL) was slowly added to a solution of the Boc-protected compound **3.75** (5.47 g, 7.5 mmol) in CH_2Cl_2 (150 mL) at 0 °C. The reaction mixture was allowed to warm to r.t. as it stirred O/N. $NaHCO_3$ was added and the product extracted into CH_2Cl_2. The combined organic extracts were dried (Na_2SO_4) and concentrated to afford the deprotected product (3.02 g, 93% yield), used without further purification.

$[\alpha]_D$ = +80.0 (CH_2Cl_2); ^{1}H-NMR (400 MHz; $CDCl_3$): δ 7.52 (dt, *J* = 6.6, 3.0 Hz, 1H), 7.40-7.37 (m, 1H), 7.11-6.99 (m, 5H), 6.70 (t, *J* = 7.4 Hz, 1H), 6.62 (dd, *J* = 7.9, 3.4 Hz, 1H), 5.44 (s, 1H), 4.14 (dd, *J* = 7.8, 2.6 Hz, 1H), 3.72 (t, *J* = 6.0 Hz, 1H), 3.60 (d, *J* = 17.0 Hz, 3H), 3.40 (ddd, *J* = 13.0, 7.9, 2.3 Hz, 1H), 3.29 (s, 3H), 3.15 (dt, *J* = 14.4, 4.3 Hz, 1H), 2.95-2.86 (m, 2H), 1.99-1.90 (bs, 3H); ^{13}C-NMR (101 MHz; $CDCl_3$): δ 175.6, 173.8, 149.7, 135.2, 130.5, 129.80, 129.76, 127.5, 125.4, 125.0, 121.8, 119.5, 119.2, 112.1, 110.9, 109.7, 81.8, 75.7, 60.3, 55.0, 52.1, 40.6, 30.5, 28.4; IR (NaCl, film) 3373, 2950, 1735, 1459, 1207, 744 cm^{-1}; HRMS (ESI-APCI): $[M+H]^+$ 435.2032 calcd for $C_{24}H_{27}N_4O_4$, found: 435.2036.

REF: TRW-III-184, **TRW-III-195**.

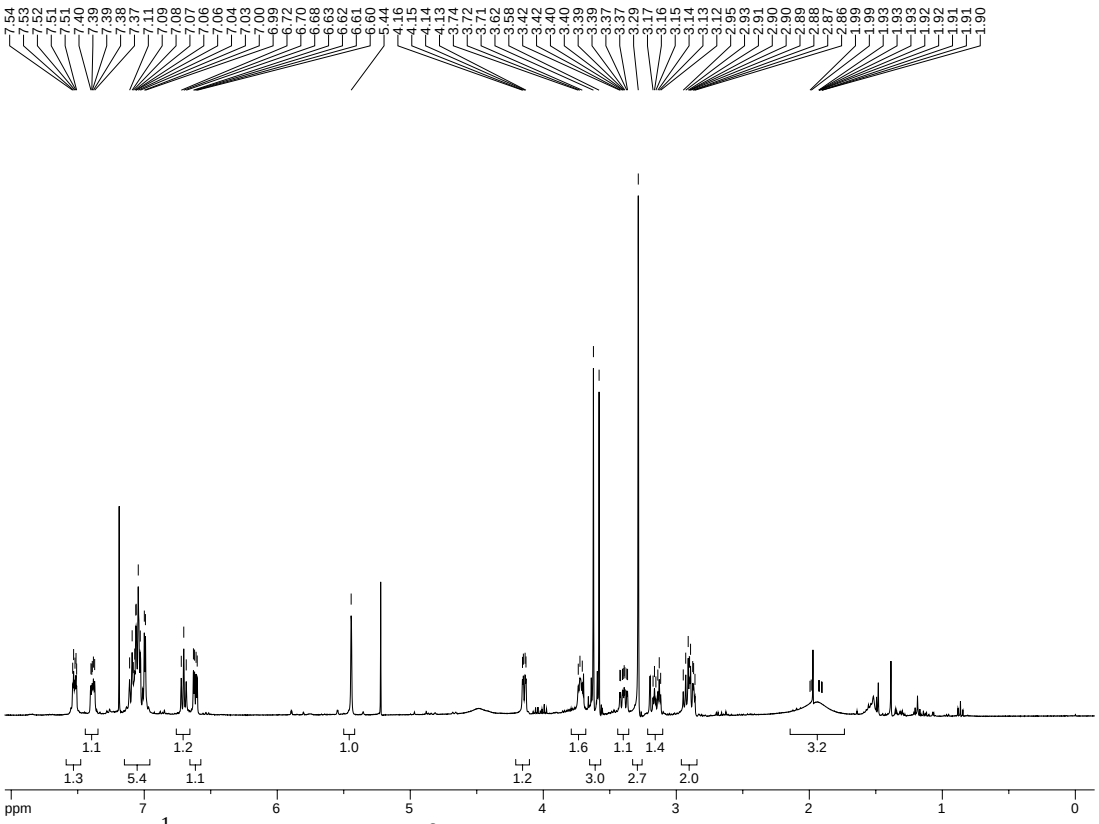

Figure 5.48a. ^{1}H NMR spectrum of compound **5.6**.

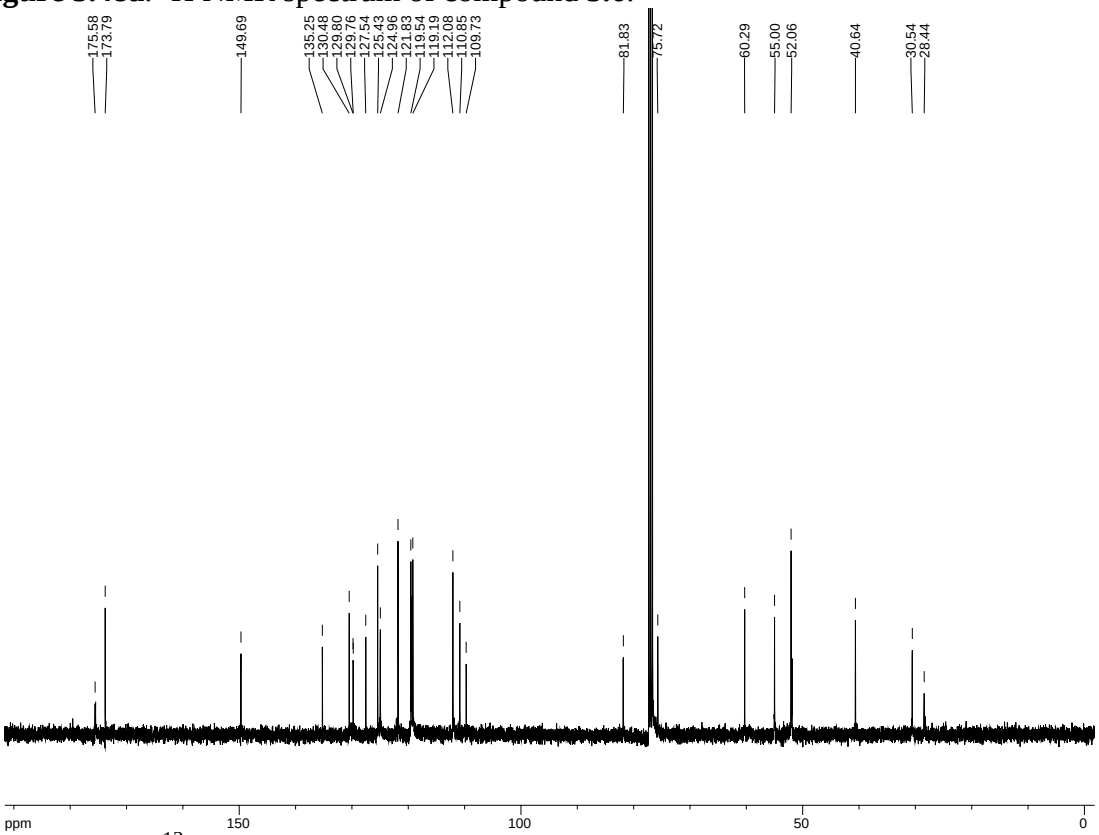

Figure 5.48b. ^{13}C NMR spectrum of compound **5.6**.

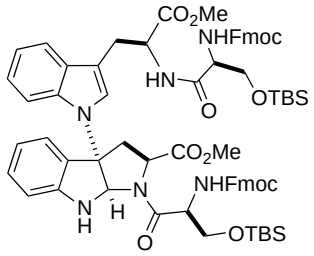

3.76

(2*S*,3a*S*,8a*R*)-methyl 3a-(3-((*S*)-2-((*S*)-2-((((9*H*-fluoren-9-yl)methoxy)-carbonyl)amino)-3-((*tert*-butyldimethylsilyl)oxy)propanamido)-3-methoxy-3-oxopropyl)-1*H*-indol-1-yl)-1-((*S*)-2-((((9*H*-fluoren-9-yl)methoxy)carbonyl)-amino)-3-((*tert*-butyldimethylsilyl)oxy)propanoyl)-1,2,3,3a,8,8a-hexahydro-pyrrolo[2,3-*b*]indole-2-carboxylate (3.76). Diamine **5.6** (1.03 g, 2.4 mmol), *N*-Fmoc-L-Ser(OTBS)-OH (2.12 g, 4.8 mmol), T3P (50% by weight in DMF, 3.51 g, 5.5 mmol), *i*Pr_2NEt (2.1 mL, 12 mmol), and CH_2Cl_2 (24 mL) were combined and stirred under Ar O/N at 35 °C. Water was added, the product extracted in EtOAc, the combined extracts washed with brine, dried (Na_2SO_4), concentrated, and purified by SiO_2 chromatography (10-25% EtOAc in hexanes) to afford the tetrapeptide (2.15 g, 70% yield).

$[\alpha]_D$ = +61.9 (CH_2Cl_2); ^{1}H-NMR (300 MHz; $CDCl_3$): δ 7.77 (d, *J* = 7.4 Hz, 4H), 7.60 (d, *J* = 8.0 Hz, 5H), 7.41 (t, *J* = 7.3 Hz, 5H), 7.35-7.30 (m, 4H), 7.26-7.15 (m, 4H), 6.82-6.67 (m, 2H), 5.68 (d, *J* = 7.7 Hz, 1H), 5.42 (s, 1H), 4.90 (s, 1H), 4.40-4.33 (m, 4H), 4.24-4.10 (m, 3H), 4.05-3.88 (m, 2H), 3.74 (s, 1H), 3.63 (d, *J* = 13.3 Hz, 3H), 3.20 (s, 4H), 2.95 (s, 1H), 0.94-0.82 (m, 18H), 0.08 (dd, *J* = 35.4, 2.8 Hz, 12H); ^{13}C-NMR (101 MHz; $CDCl_3$): δ 177.5, 177.3, 175.7, 175.35, 175.20, 160.8, 156.0, 150.0, 149.48, 149.34, 149.30, 147.1, 146.9, 140.3, 137.11, 137.00, 135.96, 135.82, 133.25, 133.17, 132.6, 131.5, 130.75, 130.70, 130.64, 130.60, 130.57, 130.4, 130.1, 127.8, 125.65, 125.58, 125.48, 125.1, 124.7, 117.28, 117.22, 116.21, 116.13, 114.93, 114.83, 84.8, 78.3, 73.0, 72.78, 72.75,

72.62, 70.8, 68.7, 65.3, 59.06, 58.90, 58.4, 57.7, 56.0, 52.75, 52.72, 52.69, 35.3, 33.9, 33.4, 31.8, 31.52, 31.43, 24.1, 23.75, 23.71, 0.23, 0.11, 0.08, 0.03, -0.01; IR (NaCl, film) 2953, 1724, 1673, 1450, 1253, 1107, 740 cm^{-1}; HRMS (ESI-APCI): $[M+H]^+$ 1281.5764 calcd for $C_{72}H_{85}N_6O_{12}Si_2$, found: 1281.5759.

REF: TRW-III-185, TRW-III-196, **TRW-III-202**.

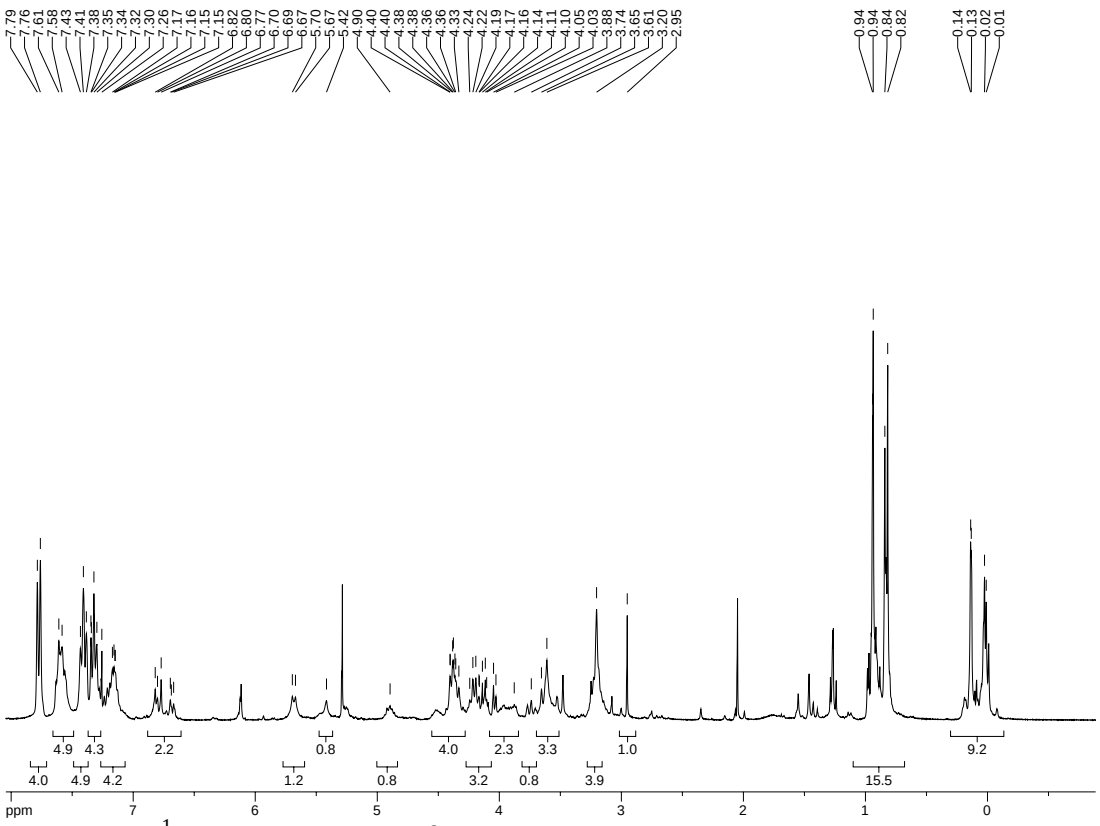

Figure 5.49a. ^{1}H NMR spectrum of compound **3.76**.

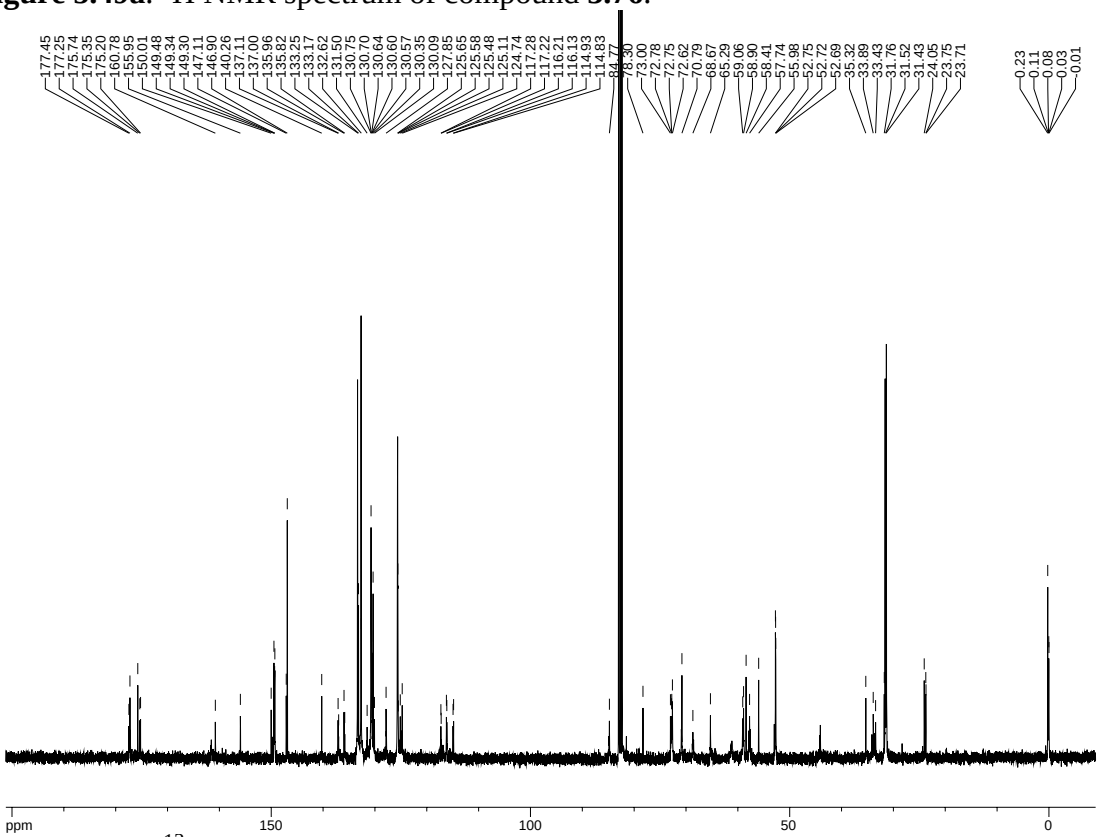

Figure 5.49b. ^{13}C NMR spectrum of compound **3.76**.

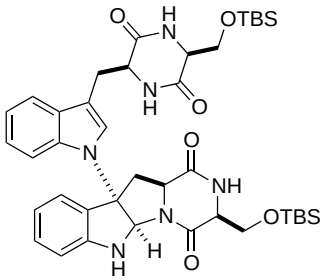

3.77

Dioxopiperazine$_2$ (3.77). Tetrapeptide **3.76** (2.18 g, 1.7 mmol) and morpholine (17 mL) were dissolved in THF (70 mL) and heated to 35 °C. After stirring O/N, the reaction mixture was concentrated and purified by SiO_2 chromatography (5% MeOH in CH_2Cl_2) to afford pure dioxopiperazine **3.77** (1.11 g, 85% yield).

^{1}H-NMR (400 MHz; $CDCl_3$): δ 7.68 (d, *J* = 8.0 Hz, 1H), 7.56 (s, 1H), 7.29 (d, *J* = 7.4 Hz, 1H), 7.16 (t, *J* = 7.4 Hz, 1H), 7.09 (d, *J* = 7.8 Hz, 1H), 7.00 (d, *J* = 7.7 Hz, 1H), 6.81-6.79 (m, 2H), 6.63 (d, *J* = 17.9 Hz, 1H), 6.42 (s, 1H), 6.13 (d, *J* = 3.5 Hz, 1H), 5.53 (d, *J* = 3.5 Hz, 1H), 4.83 (dd, *J* = 11.1, 6.1 Hz, 1H), 4.37-4.35 (m, 1H), 4.25 (q, *J* = 5.4 Hz, 2H), 4.11 (t, *J* = 3.8 Hz, 1H), 4.03 (dd, *J* = 10.0, 3.5 Hz, 1H), 3.85 (dd, *J* = 19.1, 8.2 Hz, 2H), 3.72 (d, *J* = 14.7 Hz, 2H), 3.59 (dd, *J* = 9.9, 8.0 Hz, 1H), 3.54 (s, 1H), 3.34-3.29 (m, 1H), 3.19 (dd, *J* = 14.6, 9.8 Hz, 1H), 2.83 (dd, *J* = 14.7, 11.4 Hz, 1H), 0.96 (s, 18H), 0.16 (s, 12H); HRMS (ESI-APCI): $[M+Na]^+$ 795.3698 calcd for $C_{40}H_{56}N_6NaO_6Si_2$, found: 795.3696.

REF: TRW-III-191, **TRW-III-198**.

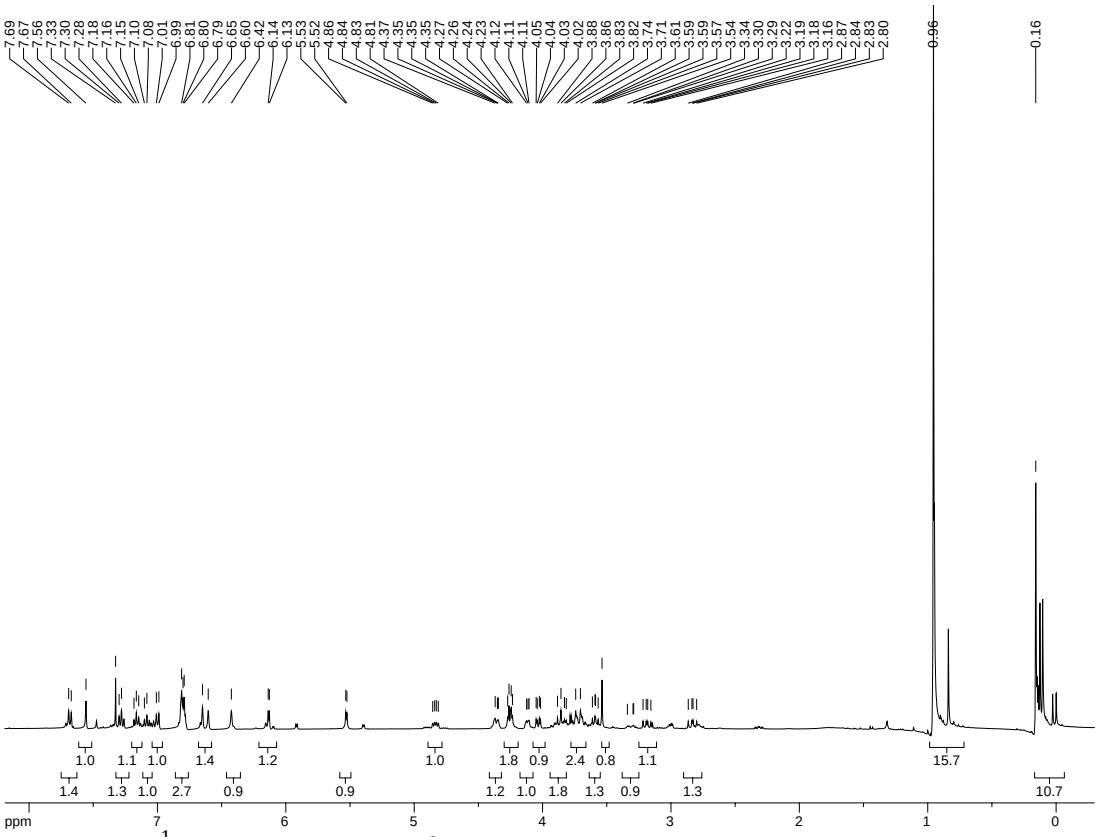

Figure 5.50a. ^{1}H NMR spectrum of compound **3.77**.

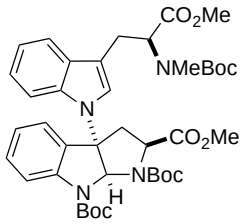

5.7

(2*S*,3a*S*,8a*S*)-1,8-di-*tert*-butyl 2-methyl 3a-(3-((*S*)-2-((*tert*-butoxycarbonyl) (methyl)amino)-3-methoxy-3-oxopropyl)-1*H*-indol-1-yl)-3,3a-dihydro-pyrrolo[2,3-*b*]indole-1,2,8(2*H*,8a*H*)-tricarboxylate (5.7). KO*t*Bu (3.04 g, 27.2 mmol) was added to a solution of bromopyrroloindoline **3.74** (10.08 g, 20.3 mmol) and *N*-Me,Boc-Trp-OMe (4.50 g, 13.6 mmol) in CH_3CN (1000 mL) at 0 °C and stirred 1h under Ar. $NaHCO_3$ was added and the product extracted in CH_2Cl_2, washed with brine, dried (Na_2SO_4), and concentrated. Purification by SiO_2 chromatography (10-20% EtOAc in hexanes) afforded pure dipeptide (5.41 g, 53% yield).

$[\alpha]_D$ = -3.1 (CH_2Cl_2); ^{1}H-NMR (400 MHz; $CDCl_3$): δ 7.68-7.67 (bs, 1H), 7.56 (d, *J* = 7.5 Hz, 1H), 7.35-7.32 (m, 2H), 7.23 (s, 1H), 7.16-7.08 (m, 3H), 6.84 (d, *J* = 15.2 Hz, 1H), 6.74 (d, *J* = 3.3 Hz, 1H), 4.87-4.86 (bs, 1H), 4.73-4.56 (broad, 2H), 3.69 (broad, *J* = 7.1 Hz, 3H), 3.49-3.43 (m, 1H), 3.29 (dd, *J* = 15.0, 4.9 Hz, 1H), 3.20 (s, 3H), 3.02-2.91 (m, 2H), 2.67-2.59 (m, 3H), 1.57-1.11 (m, 27H); ^{13}C-NMR (101 MHz; $CDCl_3$): δ 171.7, 170.9, 151.9, 134.7, 130.97, 130.82, 129.9, 125.0, 123.3, 122.2, 119.88, 119.86, 119.2, 111.6, 110.6, 82.0, 79.9, 72.59, 72.57, 59.9, 59.32, 59.30, 52.12, 52.09, 52.05, 52.00, 51.97, 34.6, 31.5, 28.19, 28.17, 25.2, 22.6, 20.7, 14.1; IR (NaCl, film) 2978, 1703, 1482, 1394, 1157, 738 cm^{-1}; HRMS (ESI-APCI): $[M+Na]^+$ 771.3581 calcd for $C_{40}H_{52}N_4NaO_{10}$, found: 771.3600.

REF: TRW-III-211, **TRW-III-258**.

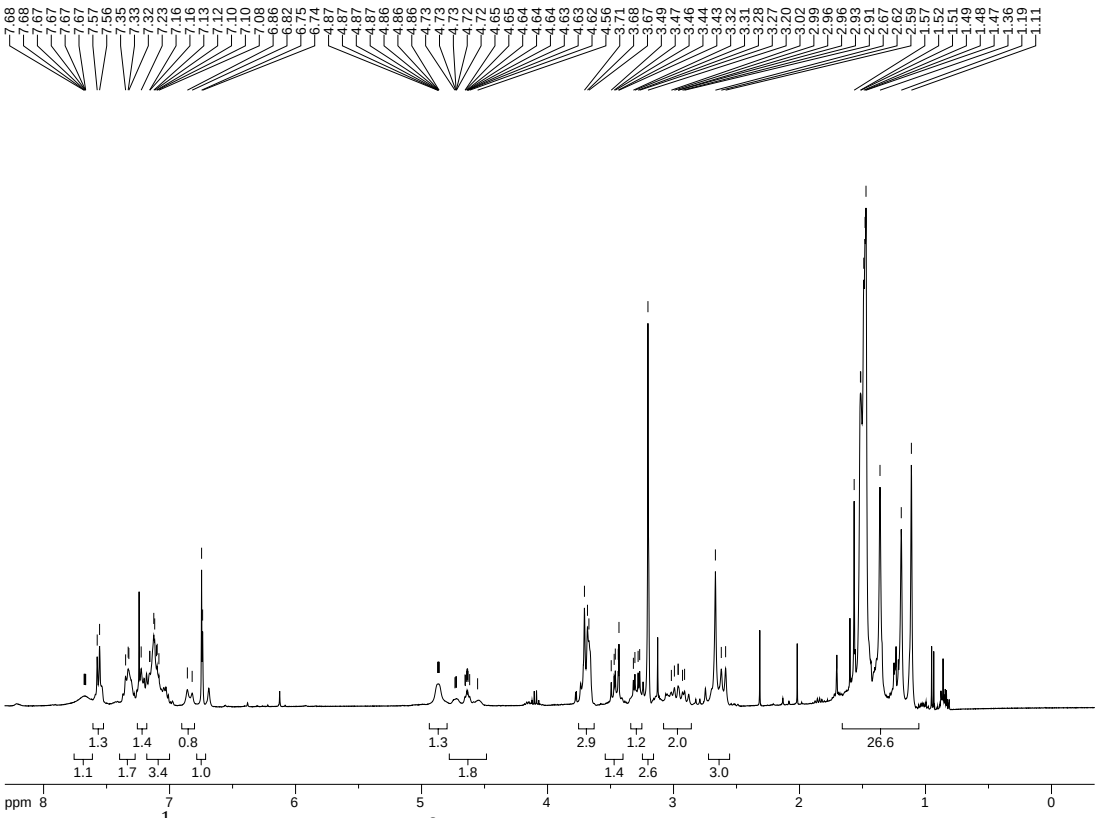

Figure 5.51a. ^{1}H NMR spectrum of compound **5.7**.

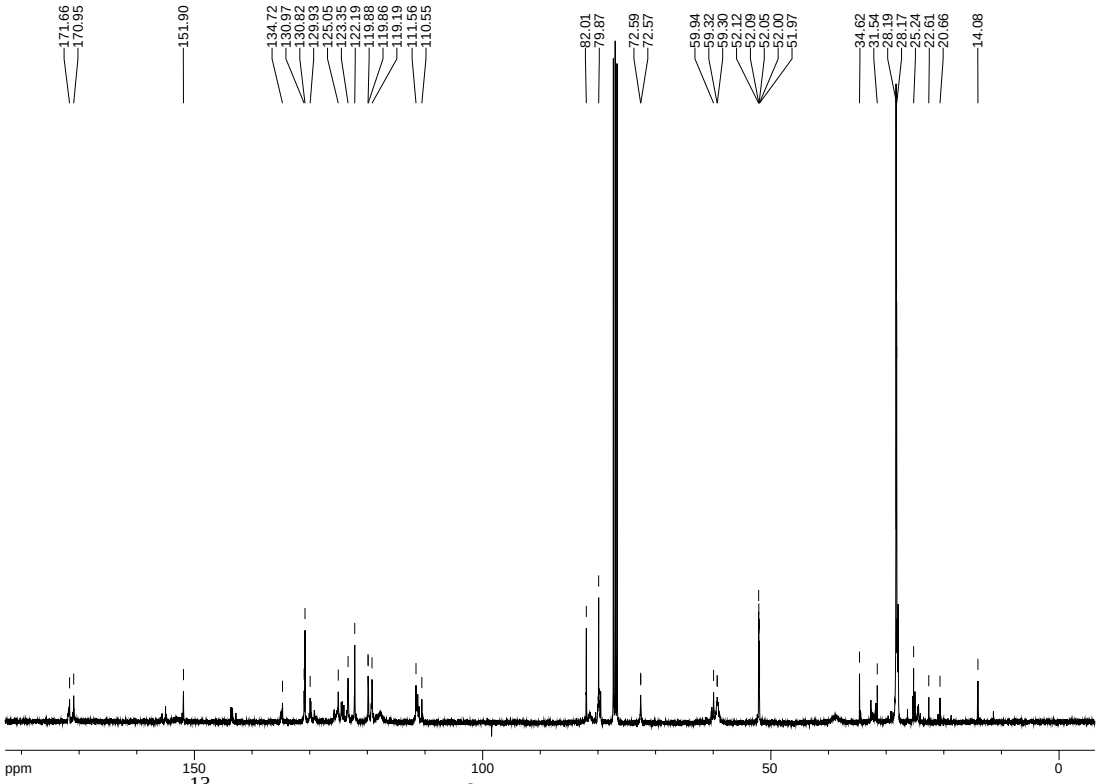

Figure 5.51b. ^{13}C NMR spectrum of compound **5.7**.

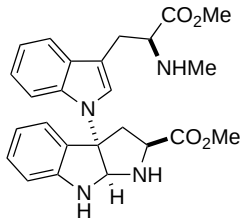

3.80

(2*S*,3a*S*,8a*S*)-methyl 3a-(3-((*S*)-3-methoxy-2-(methylamino)-3-oxopropyl)-1*H*-indol-1-yl)-1,2,3,3a,8,8a-hexahydropyrrolo[2,3-*b*]indole-2-carboxylate (3.80). TFA (11 mL) was slowly added to a solution of Boc-protected material **5.7** (4.11 g, 5.49 mmol) in CH_2Cl_2 (110 mL) at 0 °C. The reaction mixture was allowed to warm to r.t. as it stirred O/N. $NaHCO_3$ was added and the product extracted into CH_2Cl_2. The combined organic extracts were dried (Na_2SO_4) and concentrated to afford the deprotected product (2.35 g, 96% yield), used without further purification.

$[\alpha]_D$ = +73.3 (CH_2Cl_2); ^{1}H-NMR (300 MHz; $CDCl_3$): δ 7.61-7.58 (m, 1H), 7.46-7.43 (m, 1H), 7.18-7.05 (m, 6H), 6.77 (t, *J* = 7.4 Hz, 1H), 6.68 (dd, *J* = 7.9, 0.9 Hz, 1H), 5.51 (s, 1H), 4.55 (bs, 1H), 4.21 (d, *J* = 7.6 Hz, 1H), 3.61 (d, *J* = 9.5 Hz, 3H), 3.53-3.46 (m, 2H), 3.36 (d, *J* = 1.1 Hz, 3H), 3.10-2.93 (m, 4H), 2.35 (s, 3H); ^{13}C-NMR (101 MHz; $CDCl_3$): δ 174.7, 173.8, 149.69, 149.66, 135.26, 135.23, 130.4, 129.7, 127.58, 127.54, 125.3, 125.00, 124.89, 121.8, 119.5, 119.30, 119.13, 112.1, 110.74, 110.71, 109.55, 109.49, 82.0, 75.72, 75.69, 63.71, 63.69, 60.2, 52.1, 51.7, 40.76, 40.70, 34.68, 34.62, 28.91, 28.81; IR (NaCl, film) 2950, 1734, 1459, 1206, 742 cm^{-1}; HRMS (ESI-APCI): $[M+H]^+$ 449.2189 calcd for $C_{25}H_{29}N_4O_4$, found: 449.2179.

REF: **TRW-III-216**, TRW-III-267.

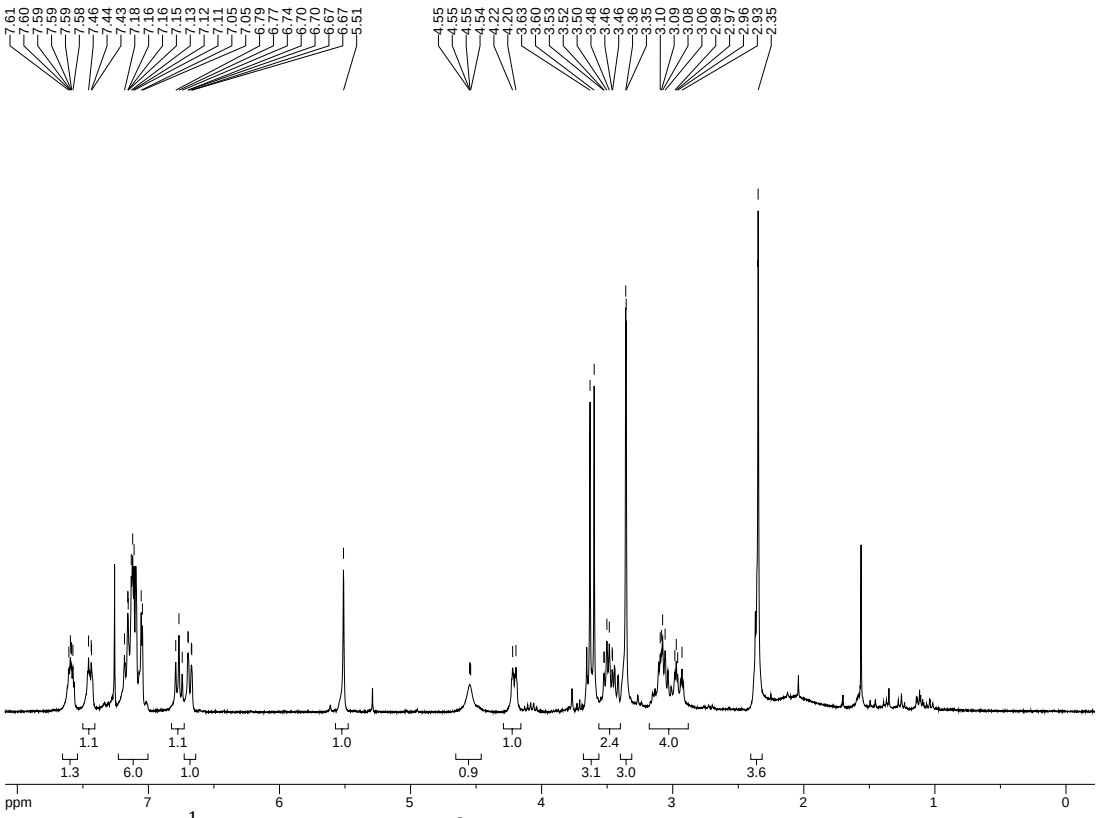

Figure 5.52a. ^{1}H NMR spectrum of compound **3.80**.

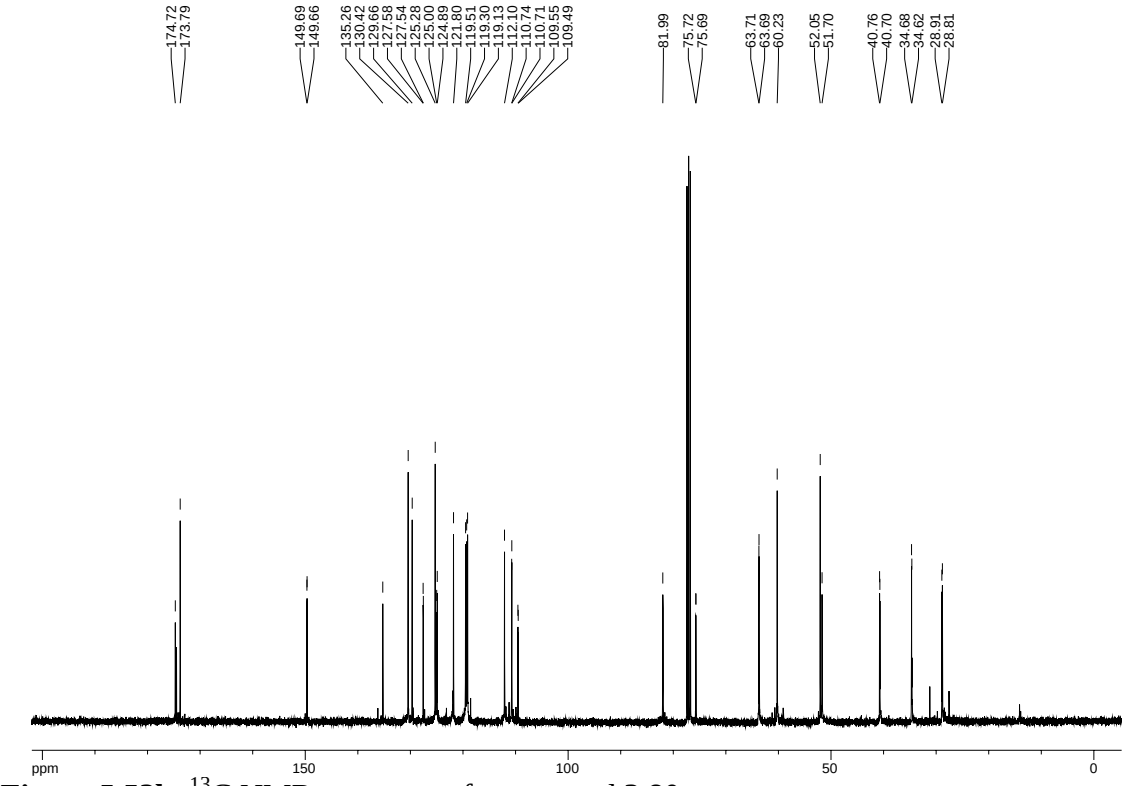

Figure 5.52b. ^{13}C NMR spectrum of compound **3.80**.

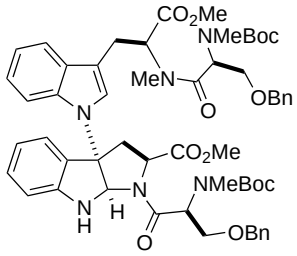

3.81

(2*S*,3a*S*,8a*R*)-methyl 3a-(3-((*S*)-2-((*S*)-3-(benzyloxy)-2-((*tert*-butoxycarbonyl)(methyl)amino)-*N*-methylpropanamido)-3-methoxy-3-oxopropyl)-1*H*-indol-1-yl)-1-((*S*)-3-(benzyloxy)-2-((*tert*-butoxycarbonyl)(methyl)amino)propanoyl)-1,2,3,3a,8,8a-hexahydropyrrolo[2,3-*b*]indole-2-carboxylate (3.81). The diamine (**3.80**, 430 mg, 0.96 mmol), *N*-Me,Boc-L-Ser(OBn)-OH (591 mg, 1.91 mmol), T3P (50% by weight in DMF, 1.41 g, 2.21 mmol), *i*Pr_2NEt (0.835 mL, 4.8 mmol), and CH_2Cl_2 (10 mL) were combined and stirred under Ar O/N at 35 °C. Water was added, the product extracted in EtOAc, the combined extracts washed with brine, dried (Na_2SO_4), concentrated, and purified by SiO_2 chromatography (60% EtOAc in hexanes) to afford the tetrapeptide (420 mg, 42% yield).

^{1}H-NMR (300 MHz; $CDCl_3$): δ 7.58-7.55 (m, 1H), 7.41-7.15 (m, 16H), 6.99 (s, 1H), 6.76-6.69 (m, 1H), 6.26-6.02 (m, 1H), 5.42-5.12 (m, 3H), 4.96-4.86 (m, 1H), 4.61-4.41 (m, 5H), 3.71-3.54 (m, 7H), 3.40-3.35 (m, 2H), 3.18 (d, *J* = 16.2 Hz, 5H), 2.93-2.67 (m, 8H), 1.42 (t, *J* = 8.2 Hz, 18H); HRMS (ESI-APCI): $[M+H]^+$ 1031.5130 calcd for $C_{57}H_{71}N_6O_{12}$, found: 1031.5126.

REF: **TRW-III-231**, TRW-III-237, TRW-III-253.

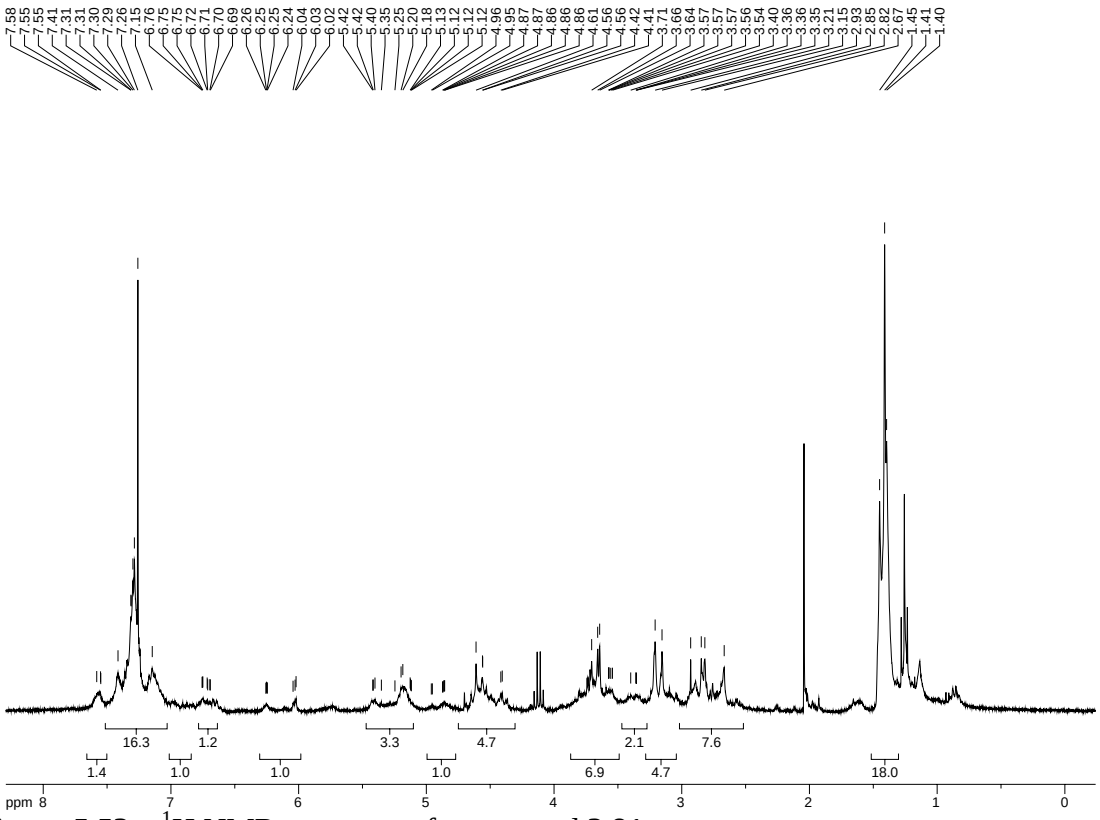

Figure 5.53a. ^{1}H NMR spectrum of compound **3.81**.

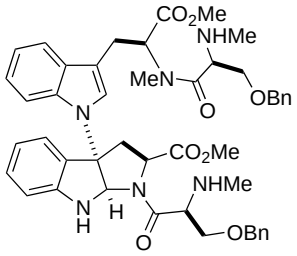

5.8

(2*S*,3a*S*,8a*R*)-methyl 1-((*S*)-3-(benzyloxy)-2-(methylamino)propanoyl)-3a-(3-((*S*)-2-((*S*)-3-(benzyloxy)-*N*-methyl-2-(methylamino)propanamido)-3-methoxy-3-oxopropyl)-1*H*-indol-1-yl)-1,2,3,3a,8,8a-hexahydropyrrolo[2,3-*b*]indole-2-carboxylate (5.8). TFA (0.2 mL) was slowly added to a solution of Boc-protected material **3.81** (103 mg, 0.1 mmol) in CH_2Cl_2 (2 mL) at 0 °C. The reaction mixture was allowed to warm to r.t. as it stirred O/N. $NaHCO_3$ was added and the product extracted into CH_2Cl_2. The combined organic extracts were dried (Na_2SO_4) and concentrated to afford the deprotected product (81 mg, 98% yield), used without further purification.

REF: **TRW-III-233**, TRW-III-243, TRW-III-254.

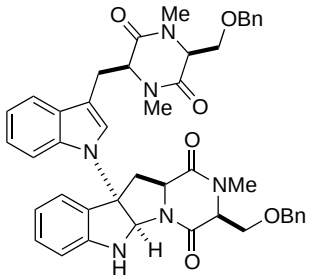

3.82

Dioxopiperazine$_2$ (3.82). Tetrapeptide **5.8** (81 mg, 0.098 mmol) and morpholine (1 mL) were dissolved in THF (4 mL) and heated to 35 °C. After stirring O/N, the reaction mixture was concentrated and purified by SiO_2 chromatography (5% MeOH in CH_2Cl_2) to afford pure dioxopiperazine (75 mg, >99% yield).

^{1}H-NMR (300 MHz; $CDCl_3$): δ 7.53-7.05 (m, 23H), 6.91 (t, *J* = 7.1 Hz, 2H), 6.76-6.71 (m, 2H), 6.46-6.34 (m, 2H), 5.72 (d, *J* = 4.1 Hz, 1H), 4.99-4.92 (m, 1H), 4.63-4.52 (m, 3H), 4.29-4.23 (m, 2H), 3.96 (dd, *J* = 9.7, 4.1 Hz, 2H), 3.69-3.54 (m, 5H), 3.26-3.21 (m, 2H), 3.08 (s, 3H), 2.87 (d, *J* = 3.9 Hz, 2H), 2.71 (dd, *J* = 12.2, 2.8 Hz, 1H), 2.21 (s, 3H); HRMS (ESI-APCI): $[M+Na]^+$ 789.3377 calcd for $C_{45}H_{46}N_6NaO_6$, found: 789.3379.

REF: **TRW-III-235**, TRW-III-245, TRW-III-257.

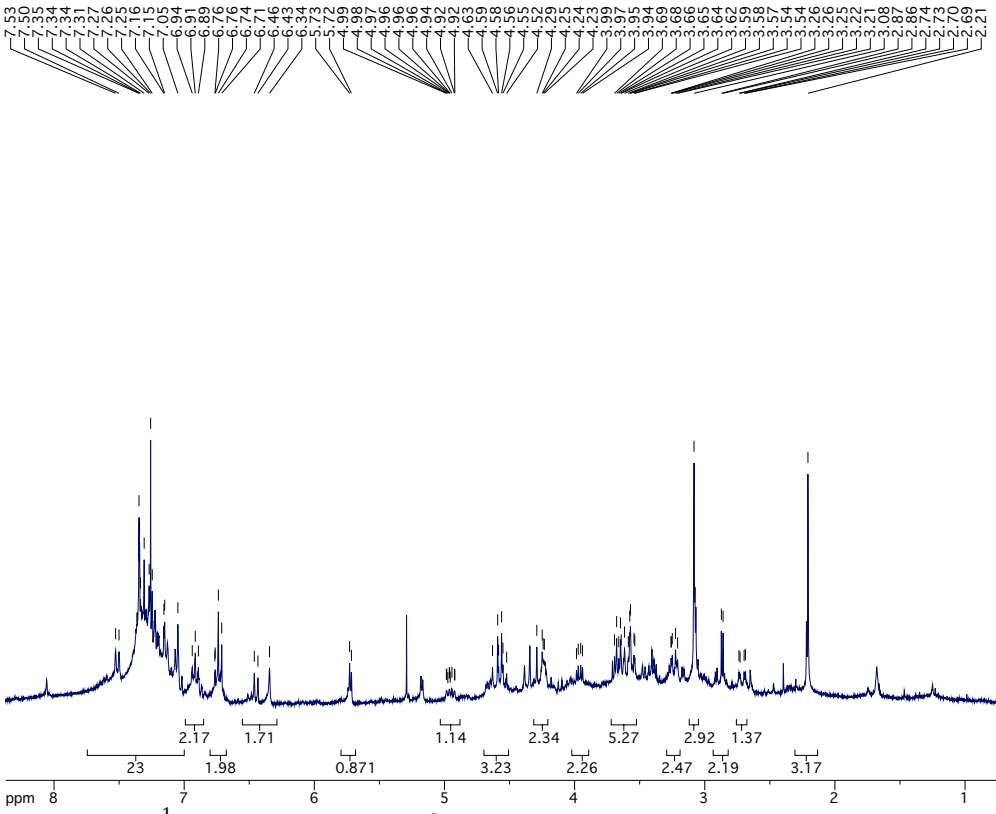

Figure 5.54a. ^{1}H NMR spectrum of compound **3.82**.

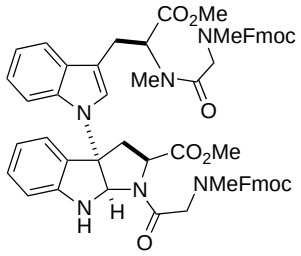

5.9

(2*S*,3a*S*,8a*R*)-methyl 3a-(3-((*S*)-2-(2-((((9*H*-fluoren-9-yl)methoxy)carbonyl)(methyl)amino)-*N*-methylacetamido)-3-methoxy-3-oxopropyl)-1*H*-indol-1-yl)-1-(2-((((9*H*-fluoren-9-yl)methoxy)carbonyl)(methyl)amino)acetyl)-1,2,3,3a,8,8a-hexahydropyrrolo[2,3-*b*]indole-2-carboxylate (5.9). The diamine (**3.80**, 896 mg, 2.0 mmol), *N*-Fmoc-sarcosine-OH (1.24 g, 4.0 mmol), T3P (50% by weight in DMF, 2.93 g, 4.6 mmol), *i*Pr_2NEt (1.7 mL, 10.0 mmol), and CH_2Cl_2 (20 mL) were combined and stirred under Ar O/N at 35 °C. Water was added, the product extracted in EtOAc, the combined extracts washed with brine, dried (Na_2SO_4), concentrated, and purified by SiO_2 chromatography (50-100% EtOAc in hexanes) to afford tetrapeptide **5.9** (1.17 g, 57% yield).

$[\alpha]_D$ = +92.1 (CH_2Cl_2); ^{1}H-NMR (300 MHz; $CDCl_3$): δ 7.78-7.74 (m, 4H), 7.63-7.59 (m, 6H), 7.35 (dd, *J* = 19.2, 7.0 Hz, 8H), 7.16-7.04 (m, 5H), 6.78-6.65 (m, 2H), 6.10-6.00 (m, 1H), 4.54-4.20 (m, 7H), 3.99-3.86 (m, 2H), 3.72-3.61 (m, 5H), 3.37-3.33 (m, 3H), 3.23-3.08 (m, 6H), 2.99-2.90 (m, 4H), 2.80-2.56 (m, 4H); IR (NaCl, film) 2951, 1703, 1451, 1229, 740 cm^{-1}; HRMS (ESI-APCI): $[M+H]^+$ 1035.4293 calcd for $C_{61}H_{59}N_6O_{10}$, found: 1035.4285.

REF: **TRW-III-292**.

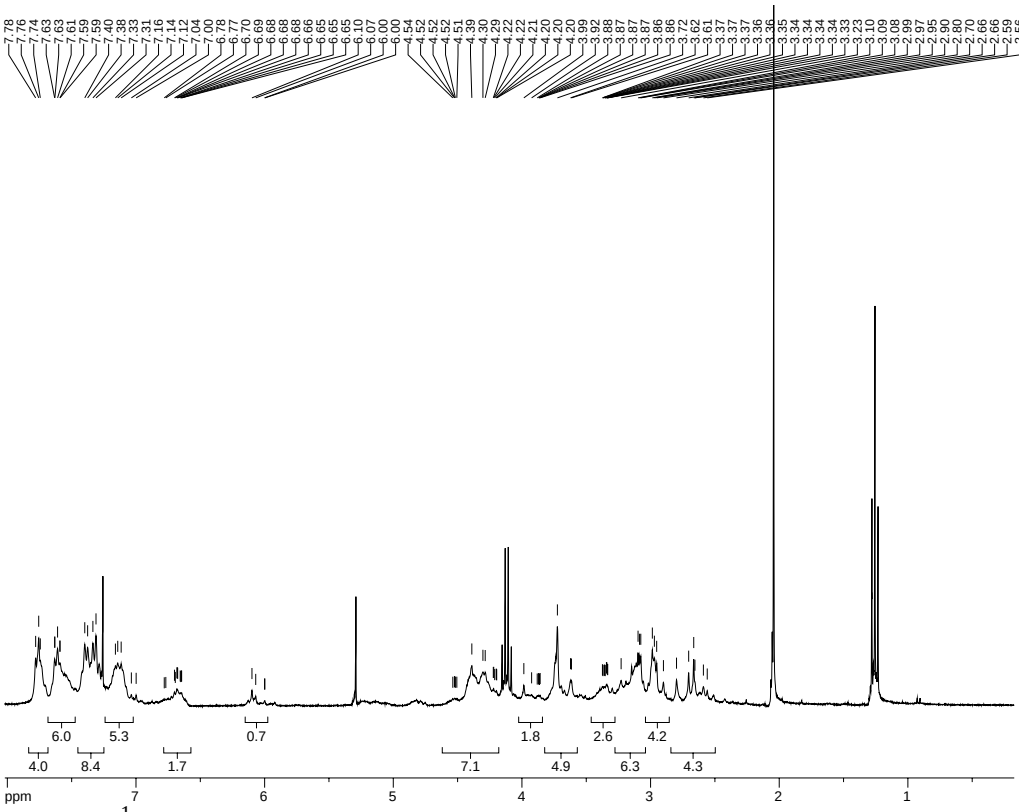

Figure 5.55a. ^{1}H NMR spectrum of compound **5.9**.

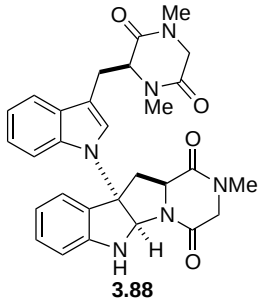

3.88

(5a*R*,10b*S*,11a*S*)-10b-(3-(((*S*)-1,4-dimethyl-3,6-dioxopiperazin-2-yl)methyl)-1*H*-indol-1-yl)-2-methyl-2,3,5a,6,11,11a-hexahydro-1*H*-pyrazino[1',2':1,5]pyrrolo[2,3-*b*]indole-1,4(10b*H*)-dione (3.88). Tetrapeptide **5.9** (1.0 g, 0.97 mmol) and morpholine (10 mL) were dissolved in THF (40 mL) and heated to 35 °C. After stirring O/N, the reaction mixture was concentrated and purified by SiO_2 chromatography (2-6% MeOH in CH_2Cl_2) to afford pure dioxopiperazine **3.88** (470 mg, 92% yield).

$[\alpha]_D$ = +145.5 (CH_2Cl_2); ^{1}H-NMR (300 MHz; $CDCl_3$): δ 7.49 (t, *J* = 7.3 Hz, 1H), 7.26-7.15 (m, 2H), 7.09-6.91 (m, 3H), 6.79-6.73 (m, 2H), 6.01 (dd, *J* = 51.3, 3.1 Hz, 1H), 5.45 (dd, *J* = 53.9, 3.8 Hz, 1H), 4.57-4.49 (m, 1H), 4.18 (t, *J* = 3.2 Hz, 1H), 3.84-3.46 (m, 4H), 3.23-3.12 (m, 2H), 3.06-2.98 (m, 6H), 2.68 (ddd, *J* = 15.3, 11.5, 4.2 Hz, 1H), 2.33 (d, *J* = 32.5 Hz, 3H), 2.06-1.94 (m, 1H); ^{13}C-NMR (101 MHz; $CDCl_3$): δ 166.3, 166.0, 164.6, 164.2, 146.7, 135.4, 130.1, 129.1, 128.1, 127.8, 124.7, 124.4, 122.8, 122.5, 120.2, 119.7, 112.4, 110.2, 108.3, 82.6, 82.0, 74.1, 62.7, 57.2, 53.5, 40.1, 39.7, 33.5, 32.9, 32.0; IR (NaCl, film) 2931, 1664, 1459, 1324, 1259 cm^{-1}; HRMS (ESI-APCI): $[M+H]^+$ 527.2407 calcd for $C_{29}H_{31}N_6O_4$, found: 527.2402.

REF: **TRW-III-293**.

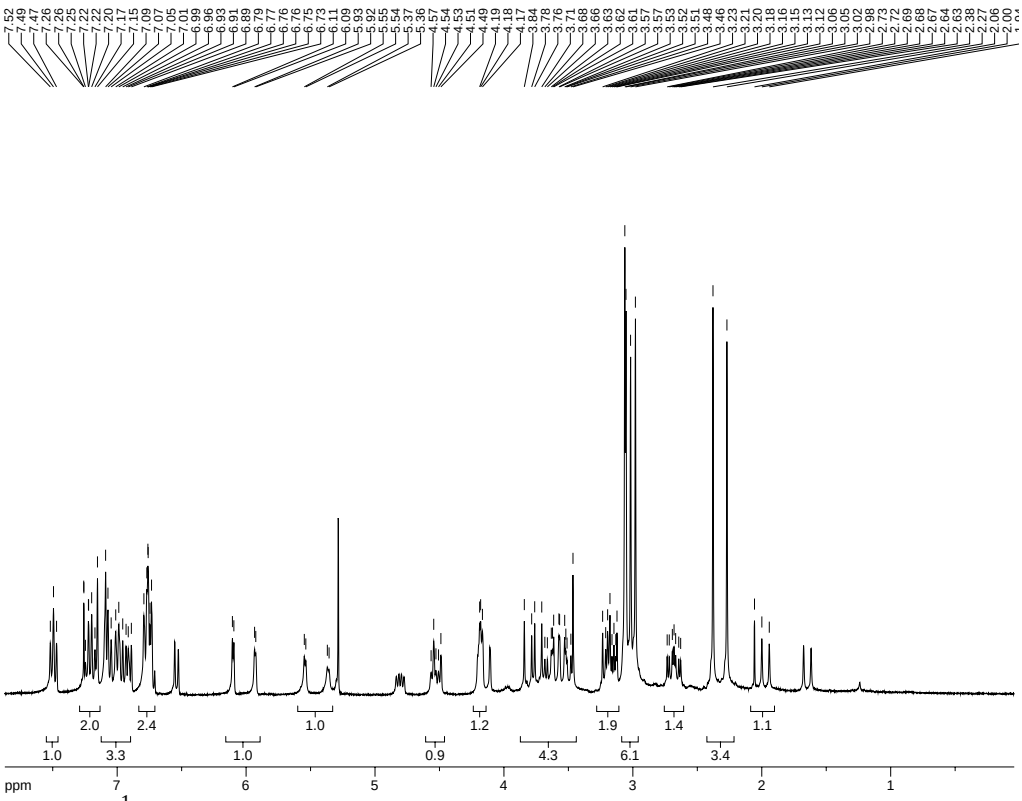

Figure 5.56a. ^{1}H NMR spectrum of compound **3.88**.

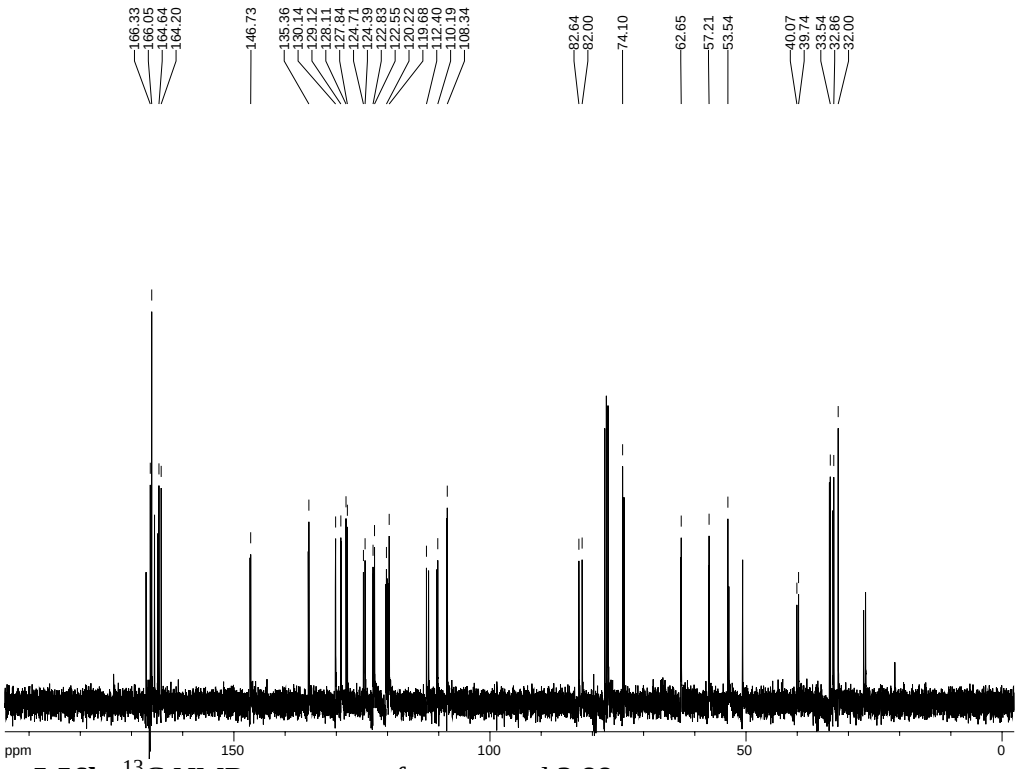

Figure 5.56b. ^{13}C NMR spectrum of compound **3.88**.

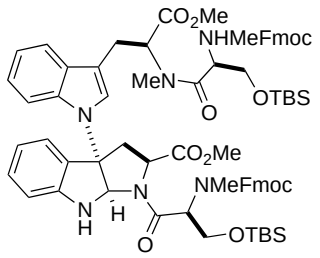

5.10

Tetrapeptide (5.10). The diamine (**3.80**, 327 mg, 0.73 mmol), *N*-Me,Fmoc-L-Ser(OTBS)-OH (663 g, 1.46 mmol), T3P (50% by weight in DMF, 1.07 g, 1.68 mmol), *i*Pr_2NEt (0.635 mL, 5.0 mmol), and CH_2Cl_2 (7.3 mL) were combined and stirred under Ar O/N at 35 °C. Water was added, the product extracted in EtOAc, the combined extracts washed with brine, dried (Na_2SO_4), concentrated, and purified by SiO_2 chromatography (35% EtOAc in hexanes) to afford tetrapeptide **5.10** (351 mg, 36% yield).

$[\alpha]_D$ = -1.5 (CH_2Cl_2); ^{1}H-NMR (300 MHz; $CDCl_3$): δ 7.78-7.71 (m, 4H), 7.61-7.53 (m, 5H), 7.41-7.15 (m, 14H), 6.93-6.66 (m, 3H), 5.13-5.07 (m, 2H), 4.41 (d, *J* = 6.8 Hz, 2H), 4.16-4.01 (m, 5H), 3.93-3.89 (m, 1H), 3.75-3.66 (m, 5H), 3.40-3.35 (m, 2H), 3.25 (d, *J* = 10.7 Hz, 2H), 3.09-2.94 (m, 5H), 2.82-2.81 (m, 4H), 2.72-2.66 (m, 2H), 2.34 (dd, *J* = 6.3, 3.2 Hz, 1H), 2.10-1.95 (m, 2H), 0.87-0.81 (m, 18H), 0.09--0.02 (m, 12H); IR (NaCl, film) 2953, 1696, 1651, 1451, 1317, 1154, 740 cm^{-1}; HRMS (ESI-APCI): $[M+H]^+$ 1323.6234 calcd for $C_{75}H_{91}N_6O_{12}Si_2$, found:1323.6253.

REF: **TRW-III-299**, TRW-III-314.

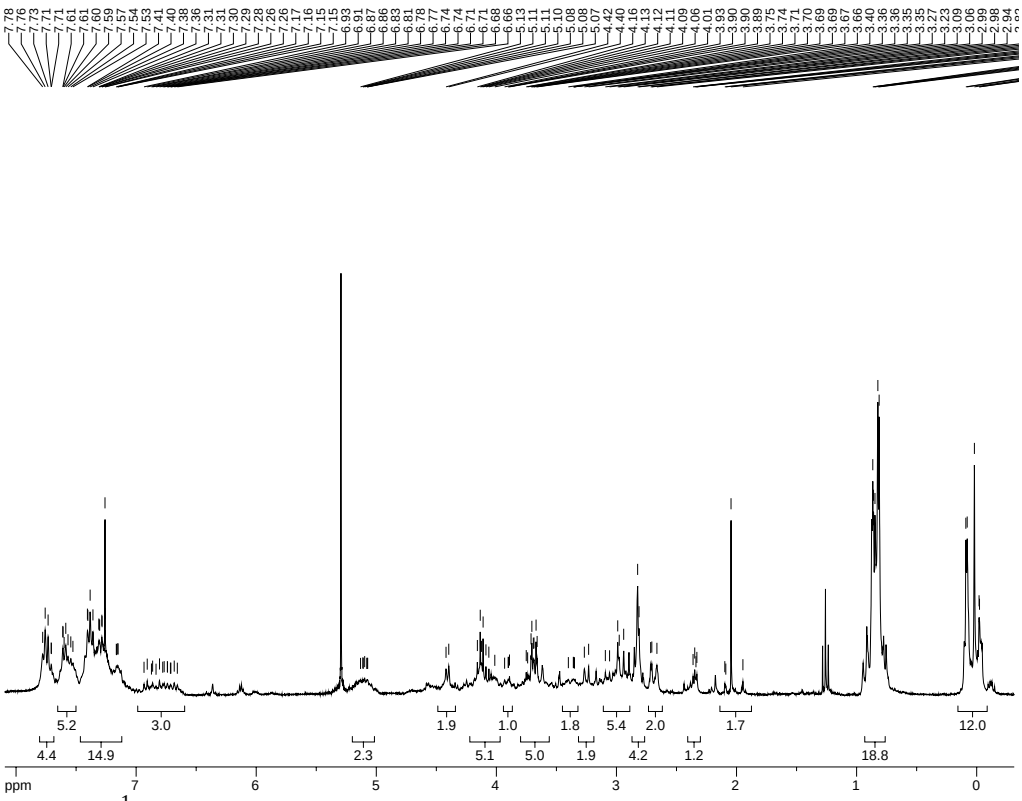

Figure 5.57a. ^{1}H NMR spectrum of compound **5.10**.

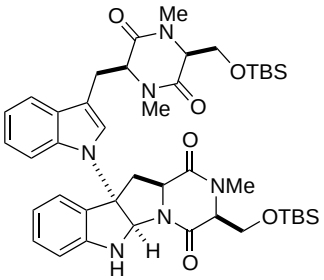

3.90

(3*S*,5a*R*,10b*S*,11a*S*)-3-(((*tert*-butyldimethylsilyl)oxy)methyl)-10b-(3-(((2*S*,5*S*)-5-(((*tert*-butyldimethylsilyl)oxy)methyl)-1,4-dimethyl-3,6-dioxopiperazin-2-yl)methyl)-1*H*-indol-1-yl)-2-methyl-2,3,5a,6,11,11a-hexahydro-1*H*-pyrazino[1',2':1,5]pyrrolo[2,3-*b*]indole-1,4(10b*H*)-dione (3.90). Tetrapeptide **5.10** (300 mg, 0.227 mmol) and morpholine (2.3 mL) were dissolved in THF (9 mL) and heated to 35 °C. After stirring O/N, the reaction mixture was concentrated and purified by SiO_2 chromatography (4% MeOH in CH_2Cl_2) to afford pure dioxopiperazine **3.90** (153 mg, 83% yield).

3.90A: $[\alpha]_D$ = +56.6 (CH_2Cl_2); ^{1}H-NMR (300 MHz; $CDCl_3$): δ 7.51 (d, *J* = 7.9 Hz, 1H), 7.18 (t, *J* = 7.6 Hz, 1H), 7.05 (d, *J* = 11.2 Hz, 2H), 6.90 (t, *J* = 6.1 Hz, 2H), 6.69 (t, *J* = 7.5 Hz, 2H), 6.50 (d, *J* = 8.4 Hz, 1H), 5.70 (s, 1H), 4.80 (dd, *J* = 11.9, 5.9 Hz, 1H), 4.33-4.09 (m, 4H), 3.76 (d, *J* = 10.4 Hz, 1H), 3.66 (dt, *J* = 9.9, 4.9 Hz, 2H), 3.50-3.43 (m, 2H), 3.37 (t, *J* = 4.8 Hz, 1H), 3.19 (dd, *J* = 14.8, 4.6 Hz, 1H), 3.10 (s, 3H), 3.02 (s, 3H), 2.31 (s, 3H), 0.82 (s, 9H), 0.74 (s, 9H), 0.04 (d, *J* = 4.6 Hz, 6H), -0.11 (d, *J* = 4.3 Hz, 6H); ^{13}C-NMR (101 MHz; $CDCl_3$): δ 167.9, 166.5, 165.73, 165.62, 146.6, 135.6, 130.2, 129.5, 124.4, 123.1, 122.5, 120.2, 112.3, 110.0, 108.6, 82.9, 62.6, 62.2, 62.0, 60.5, 59.9, 56.9, 40.7, 32.5, 30.4, 30.0, 27.2, 25.64, 25.52, 18.1, 17.9, -5.60, -5.66, -5.69; IR (NaCl, film) 2930, 2857, 1662, 1461, 1256, 1116 cm^{-1}; HRMS (ESI-APCI): $[M+H]^+$ 815.4348 calcd for $C_{43}H_{63}N_6O_6Si_2$, found:815.4352.

3.90B: $[\alpha]_D$ = +80.0 (CH_2Cl_2); ^{1}H-NMR (300 MHz; $CDCl_3$): δ 7.60 (d, *J* = 7.9 Hz, 1H), 7.30 (s, 1H), 7.15 (td, *J* = 7.7, 1.0 Hz, 1H), 7.07 (t, *J* = 7.4 Hz, 1H), 6.99-6.94 (m, 1H), 6.88 (d, *J* = 7.4 Hz, 1H), 6.76 (d, *J* = 8.3 Hz, 1H), 6.69-6.63 (m, 2H), 5.91 (d, *J* = 2.6 Hz, 1H), 5.59 (d, *J* = 2.6 Hz, 1H), 4.57-4.52 (m, 1H), 4.26-4.19 (m, 2H), 4.03 (dd, *J* = 10.8, 2.7 Hz, 1H), 3.87-3.77 (m, 2H), 3.68-3.61 (m, 2H), 3.40 (dd, *J* = 9.4, 5.6 Hz, 2H), 3.26-3.21 (m, 1H), 2.99 (d, *J* = 9.6 Hz, 6H), 2.71 (s, 3H), 2.60-2.55 (m, 1H), 0.84 (s, 9H), 0.74 (s, 9H), -0.01--0.08 (m, 12H); ^{13}C-NMR (101 MHz; $CDCl_3$): δ 166.0, 164.56, 164.55, 164.35, 146.7, 135.6, 130.1, 129.5, 123.1, 122.6, 120.4, 119.5, 112.1, 111.2, 109.7, 82.7, 65.1, 64.2, 63.7, 63.3, 60.6, 56.8, 41.5, 33.8, 33.1, 31.1, 30.7, 25.9, 25.5, 18.4, 18.0, -5.38, -5.40, -5.71, -5.74; IR (NaCl, film) 2930, 2857, 1654, 1462, 1255, 1112 cm^{-1}; HRMS (ESI-APCI): $[M+H]^+$ 815.4348 calcd for $C_{43}H_{63}N_6O_6Si_2$, found:815.4349.

REF: **TRW-III-301**, TRW-III-315.

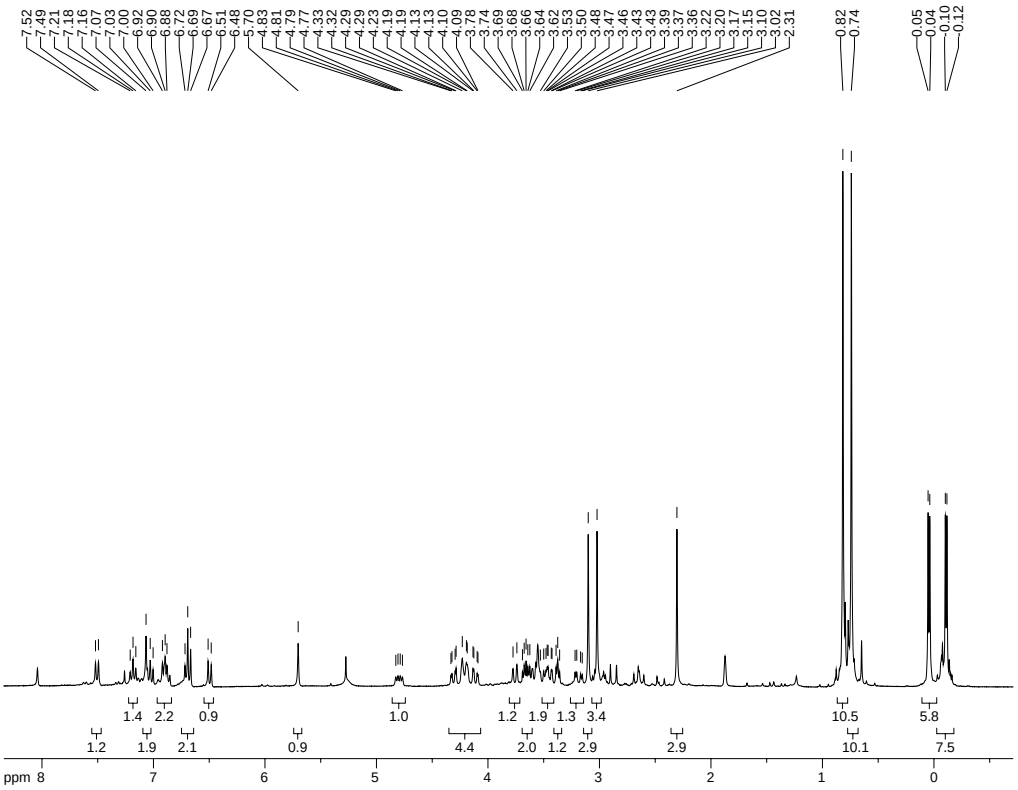

Figure 5.58a. ^{1}H NMR spectrum of compound **3.90A**.

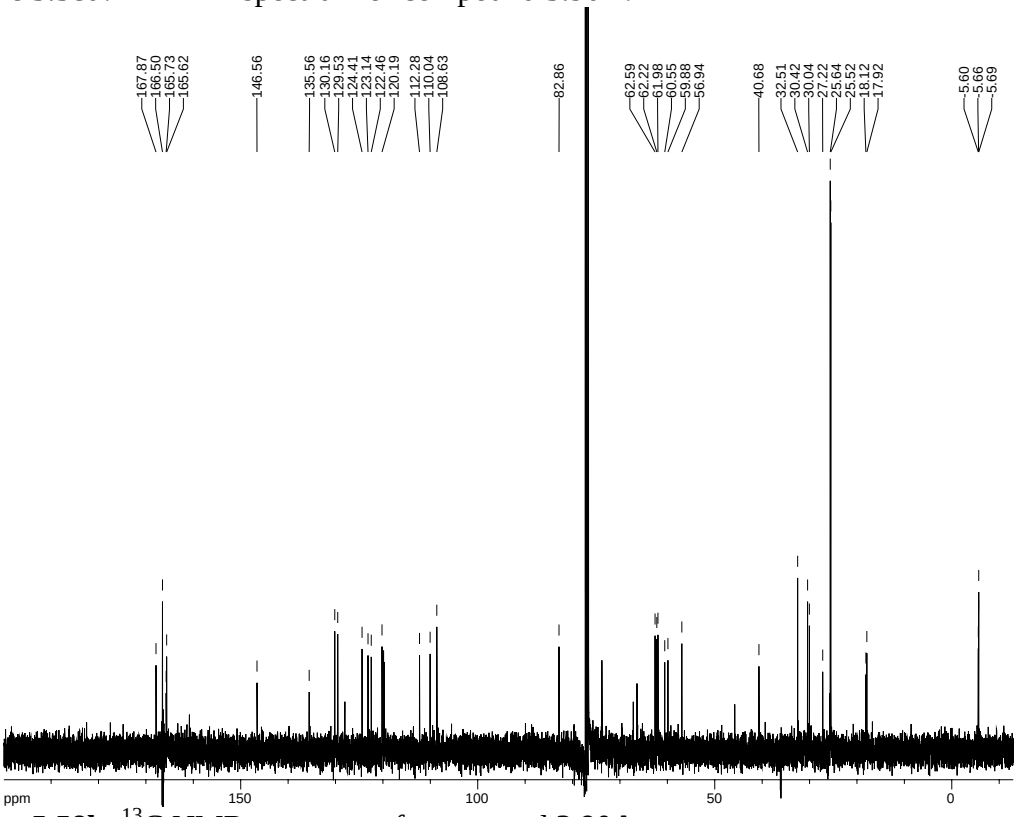

Figure 5.58b. ^{13}C NMR spectrum of compound **3.90A**.

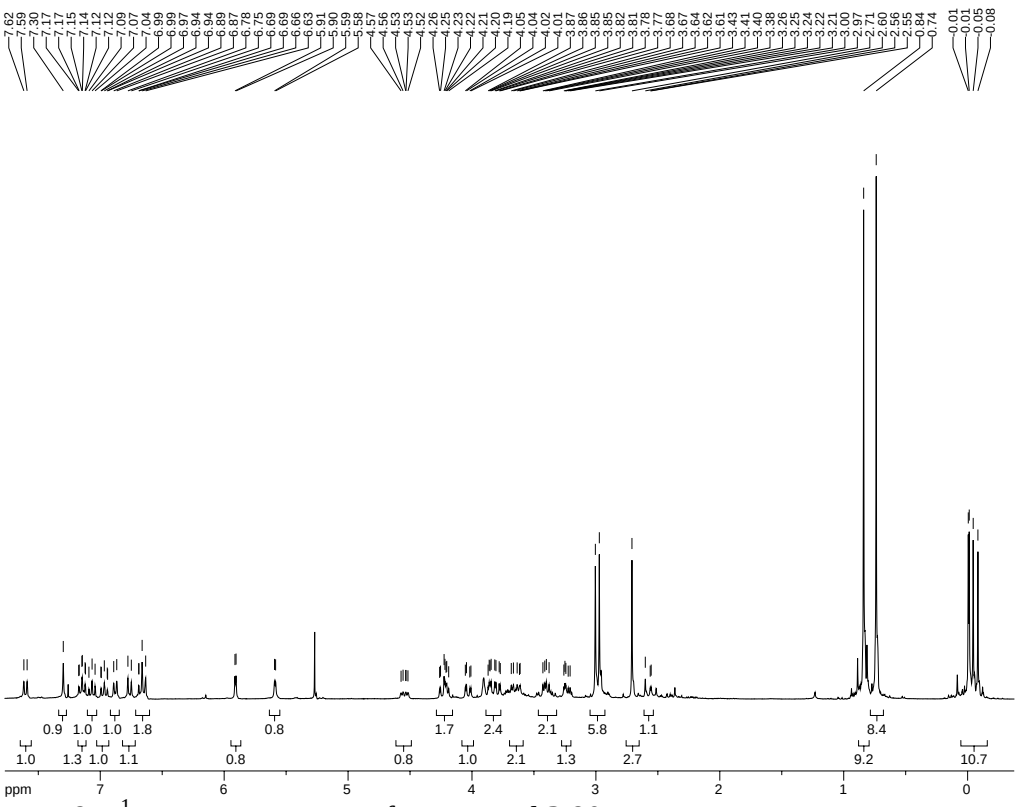

Figure 5.59a. ^{1}H NMR spectrum of compound **3.90B**.

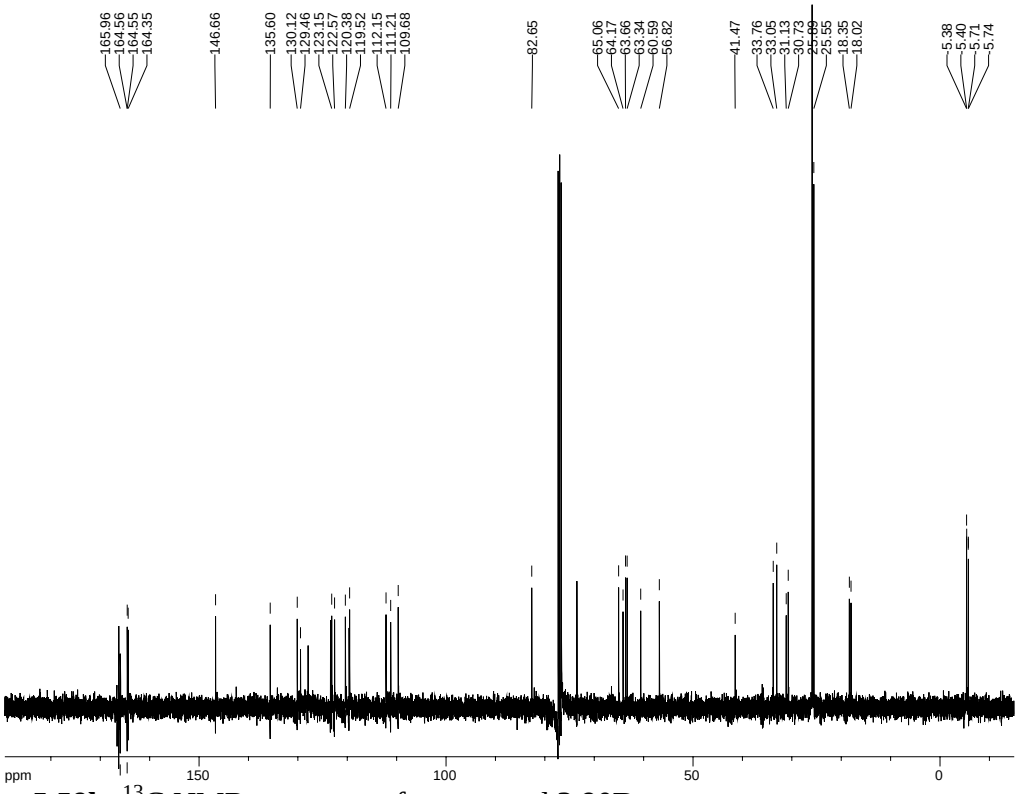

Figure 5.59b. ^{13}C NMR spectrum of compound **3.90B**.

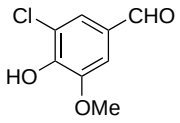

5.11

5-chlorovanillin (5.11). Vanillin (25 g, 164 mmol) was dissolved in AcOH (150 mL), then chlorine gas bubbled through the solution. After a significant amount of white solid had precipitated, the solution was filtered and the solid washed with hexanes. To the AcOH filtrate was added an additional batch of vanillin (25 g), and chlorine gas again bubbled through the solution. The resulting precipitate was filtered, washed with hexanes, combined with the first yield, and dried to afford 5-chlorovanillin (39.30 g, 64% yield). ^{1}H-NMR (400 MHz; acetone-d_6): δ 9.83 (s, 1H), 7.58 (d, *J* = 1.7 Hz, 1H), 7.43 (d, *J* = 1.7 Hz, 1H), 3.98 (s, 3H); ^{13}C-NMR (101 MHz; acetone): δ 189.5, 148.7, 129.2, 125.6, 120.0, 108.7, 56.0.

REF: **TRW-II-413**, TRW-II-463, TRW-II-479, TRW-III-076.

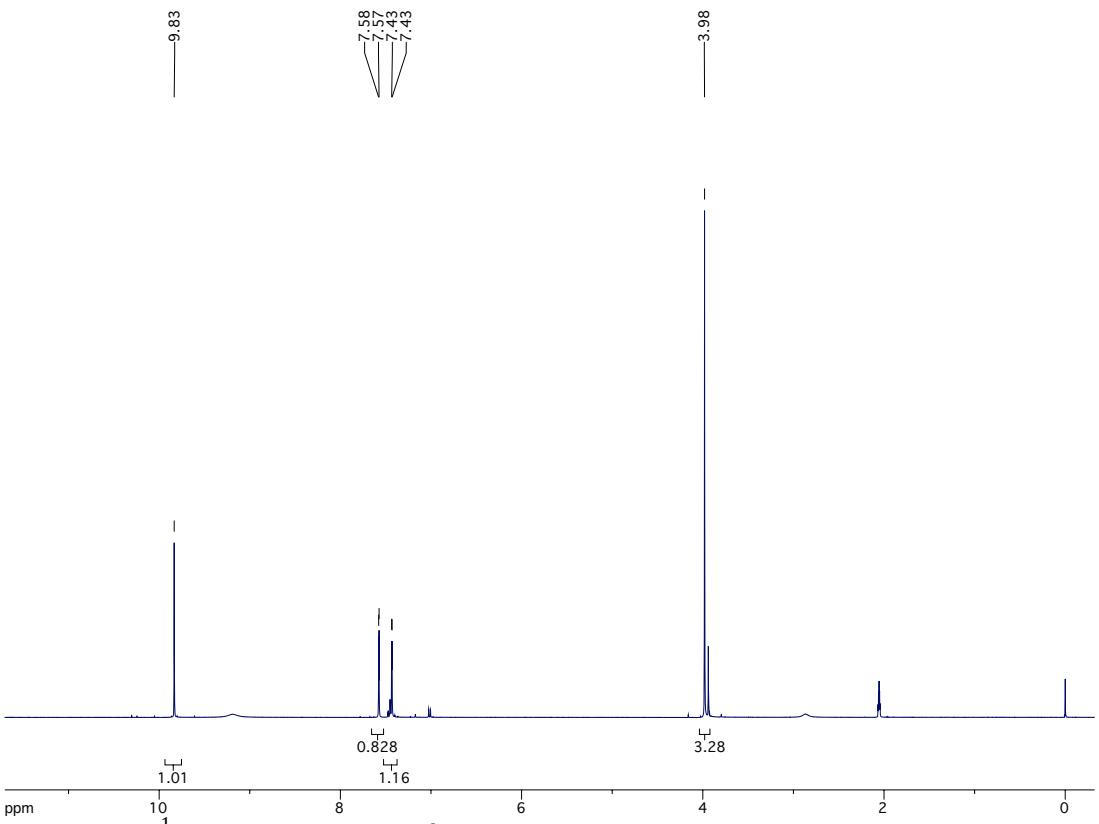

Figure 5.60a. ^{1}H NMR spectrum of compound **5.11**.

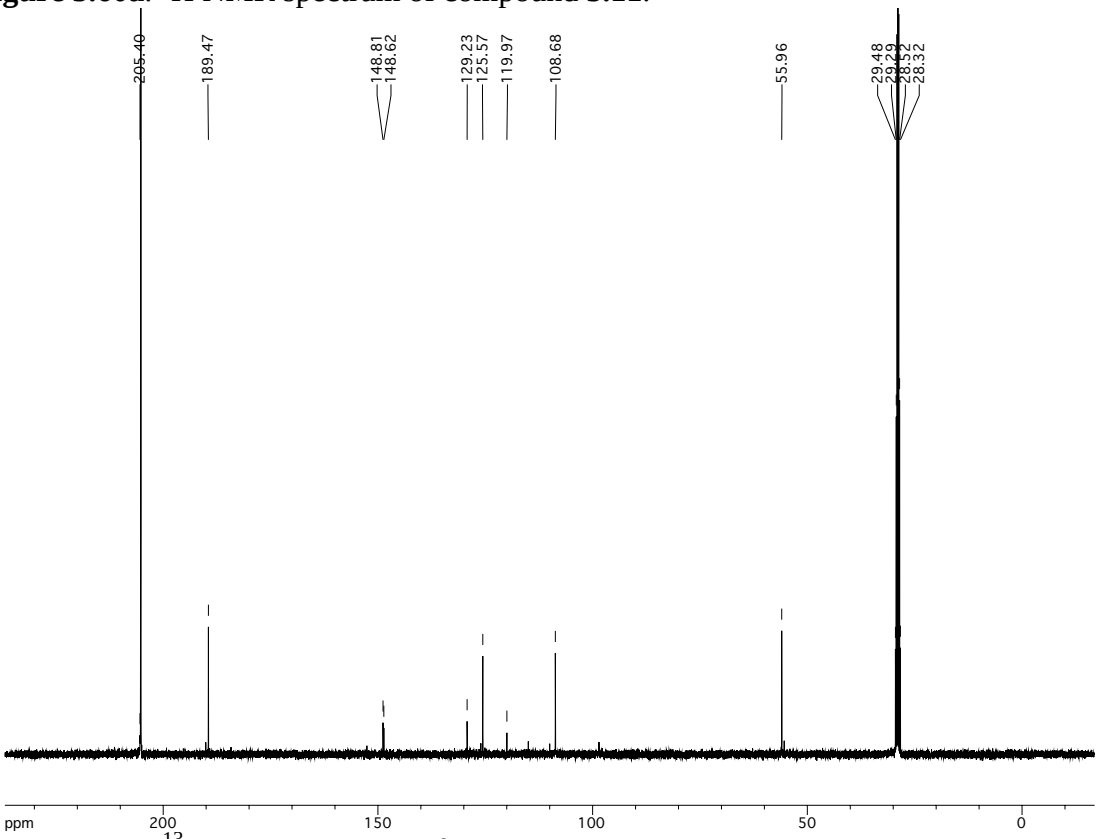

Figure 5.60b. ^{13}C NMR spectrum of compound **5.11**.

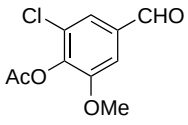

4.15

5-chlorovanillin-OAc (4.15). To a solution of 5-chlorovanillin (58.5 g, 313 mmol) in THF (1000 mL) was added Ac_2O (35.5 mL, 376 mmol), Et_3N (65.5 mL, 470 mmol), and DMAP (200 mg). The resulting solution was stirred O/N, then concentrated. The product was extracted in CH_2Cl_2 from 1M HCl, the combined organic extracts washed with brine, dried over Na_2SO_4, and concentrated to give **4.15** (71.45 g, >99% yield).

^{1}H-NMR (400 MHz; acetone-d_6): δ 9.98 (s, 1H), 7.67 (d, *J* = 1.7 Hz, 1H), 7.59 (d, *J* = 1.7 Hz, 1H), 3.97 (s, 3H), 2.36 (s, 3H); ^{13}C-NMR (101 MHz; acetone): δ 190.0, 166.8, 153.6, 141.3, 135.4, 128.5, 123.2, 110.4, 56.2, 19.2; HRMS (ESI-APCI): $[M-H]^-$ 229.0268 calcd for $C_{10}H_9ClO_4$, found: 229.9854.

REF: TRW-II-415, **TRW-II-464**, TRW-II-481, TRW-III-078.

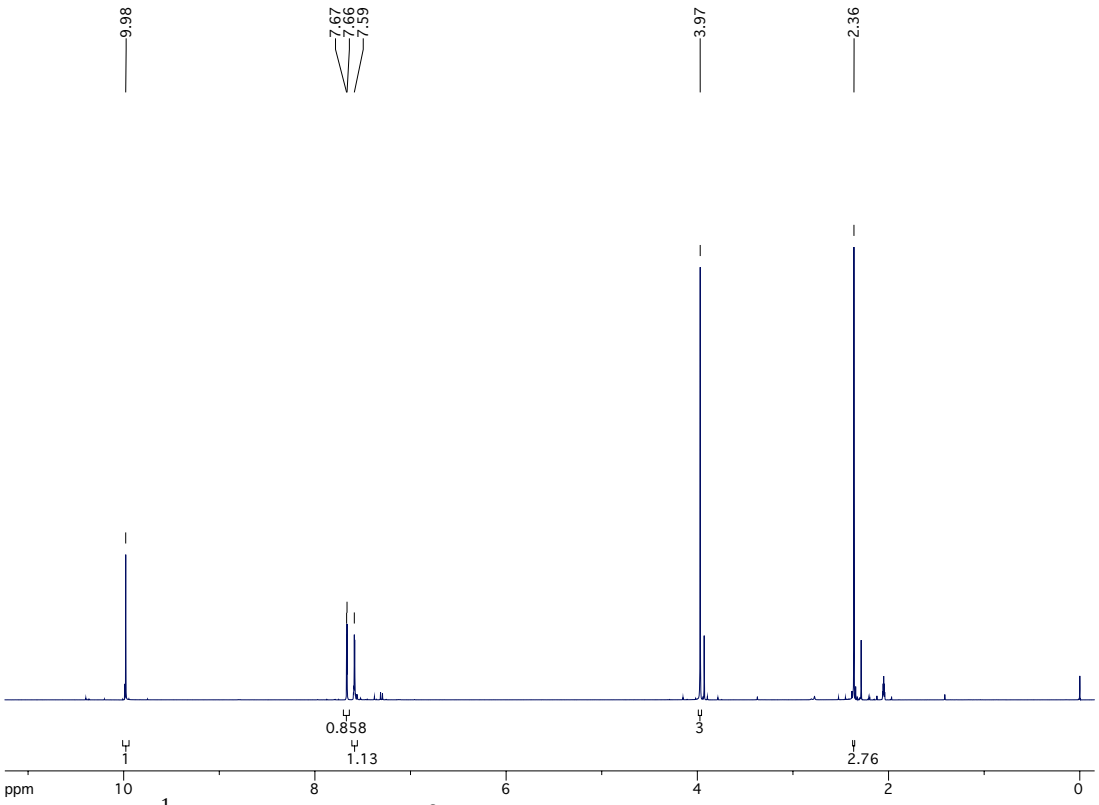

Figure 5.61a. ^{1}H NMR spectrum of compound **4.15**.

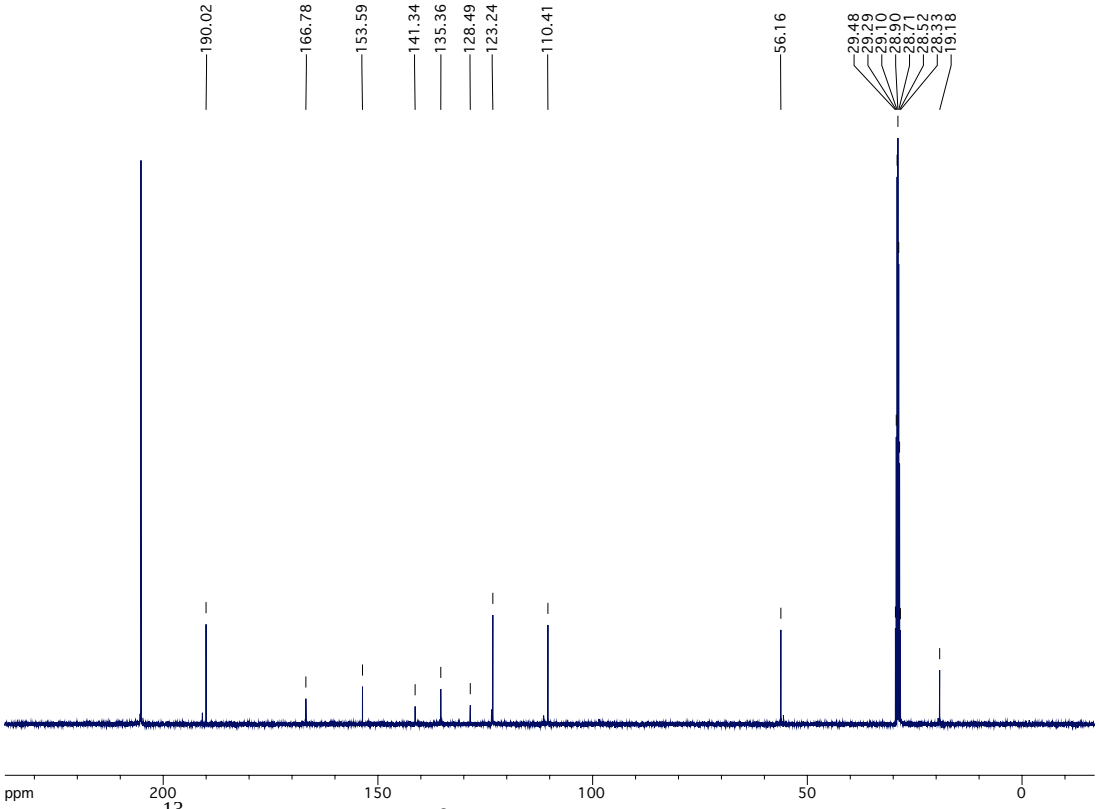

Figure 5.61b. ^{13}C NMR spectrum of compound **4.15**.

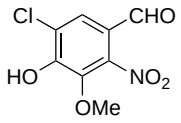

4.17

5-chloro-2-nitrovanillin (4.17). Nitric acid (fuming, 125) was chilled in an ethylene glycol/dry ice bath, then **4.15** (28 g) added in small batches *such that the internal temperature did not rise above 5 °C.* Following the addition, the reaction was stirred for 2 additional hours at -15 °C. The reaction mixture was carefully poured into ice water, and the resulting bright orange precipitate filtered and rinsed with cold water until the washings were pH neutral. This solid (combined from 2x28 g batches) was dissolved in 2M KOH (500 mL) and the solution heated to a boil for 10 min. After cooling to r.t., the solution was poured into ice-cold concentrated HCl, and the resulting precipitate filtered, washed with cold water, and dried to afford **4.17** (43.21 g, 76% yield).

^{1}H-NMR (400 MHz; acetone-d_6): δ 9.82 (s, 1H), 7.94 (s, 1H), 3.95 (s, 3H); ^{13}C-NMR (101 MHz; acetone): δ 186.0, 153.0, 140.9, 129.6, 123.2, 119.6, 98.5, 62.4; HRMS (-APCI): $[M-H]^-$ 229.9856 calcd for $C_8H_6ClNO_5$, found: 229.9860.

REF: TRW-II-417,419; TRW-II-424,425; **TRW-II-484**, TRW-III-080.

Nitric acid (fuming). Potassium nitrate (500 g) was added to concentrated sulfuric acid (500 mL) in a flask equipped with a distillation column, and the resulting suspension heated in an oil bath at 170 °C. Fuming nitric acid (75 mL) was collected over a 4 hour period. *This can be purchased commercially from VWR.*

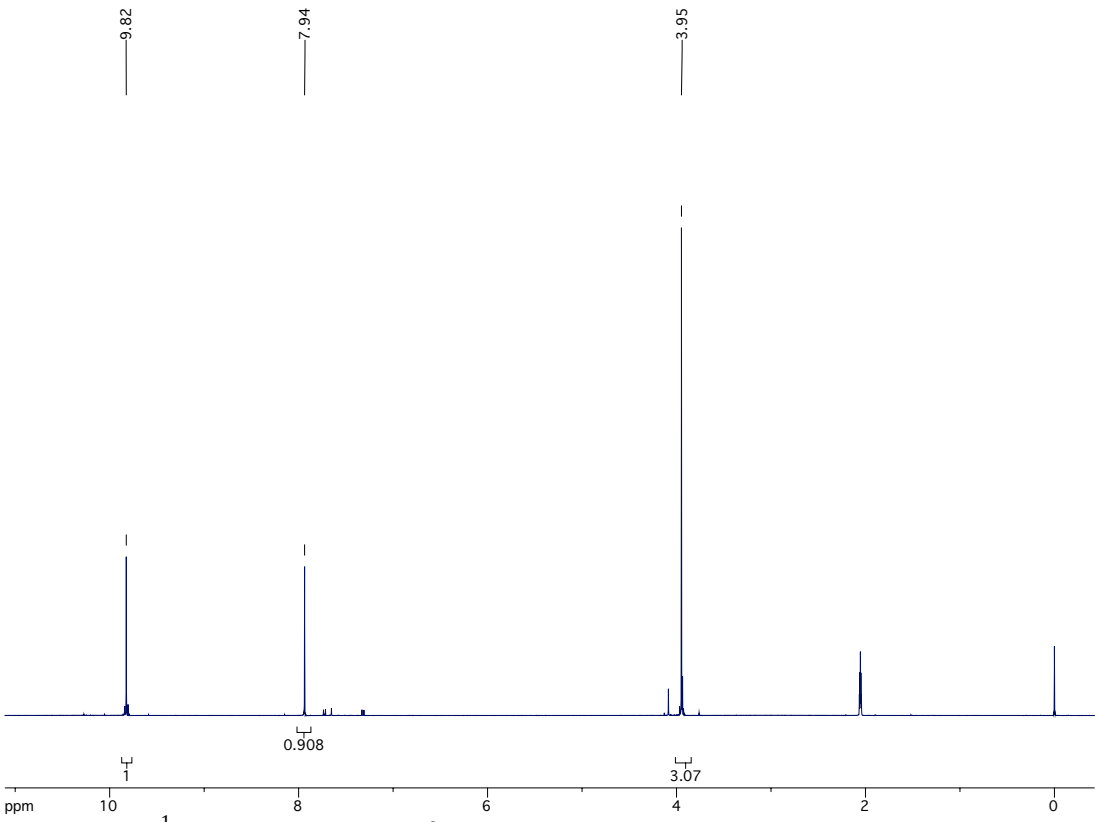

Figure 5.62a. ^{1}H NMR spectrum of compound **4.17**.

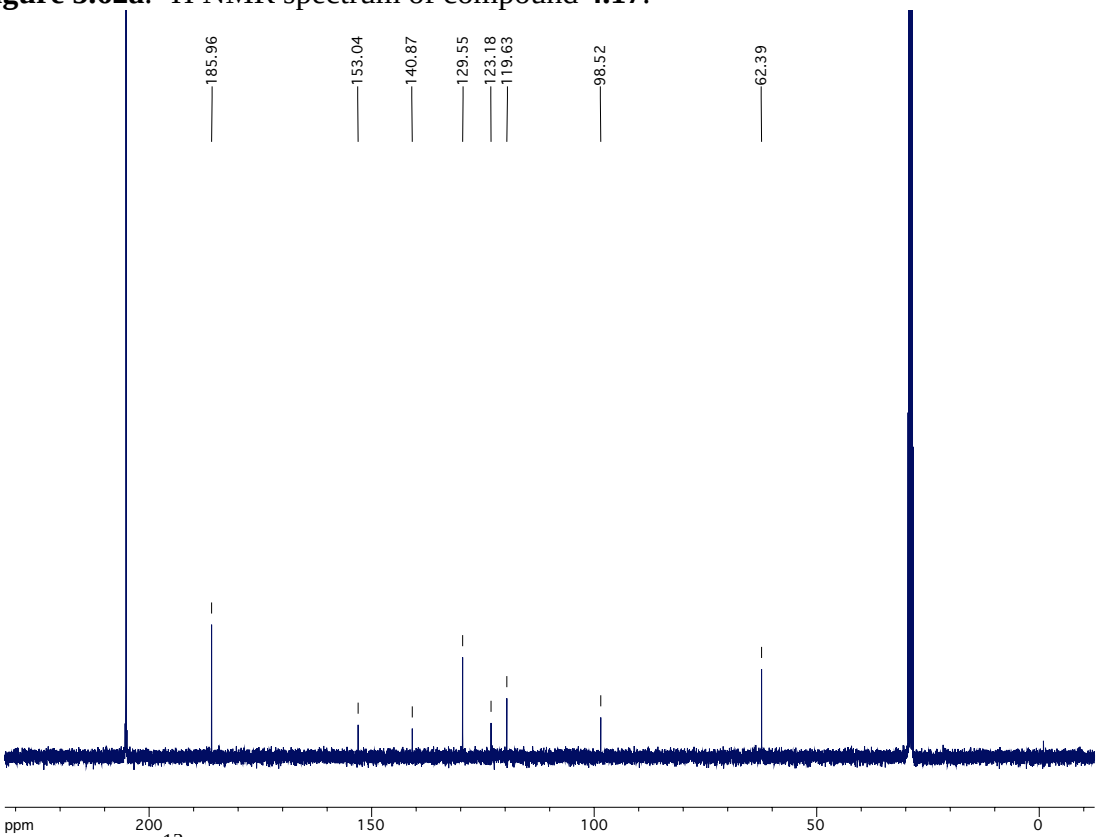

Figure 5.62b. ^{13}C NMR spectrum of compound **4.17**.

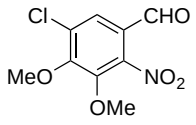

4.18

5-chloro-3,4-dimethoxy-2-nitrobenzaldehyde (4.18). Phenol **4.17** (15.0 g, 64.7 mmol) was dissolved in absolute EtOH (26.3 mL), then Me_2SO_4 (26.3 mL, 278 mmol) added. The resulting solution was immersed in an ice/brine bath before adding a solution of NaOH (11.1 g, 278 mmol) in water (13.2 mL) dropwise. The reaction was heated to 50 °C for 3 hours, then cooled to r.t. and diluted with water. The product was extracted into ether, and the organic extracts dried and concentrated to afford the title compound (15.9 g, >99% yield).

^{1}H-NMR (400 MHz; $CDCl_3$): δ 9.80 (d, *J* = 17.5 Hz, 1H), 7.73 (s, 1H), 4.05 (s, 3H), 4.01 (s, 3H); ^{13}C-NMR (101 MHz; $CDCl_3$): δ 184.7, 155.3, 151.4, 131.6, 126.7, 123.1, 120.3, 62.7, 61.4; HRMS (-APCI): $[M-H]^-$ 245.0091 calcd for $C_{10}H_9ClN_2O_6$, found: 245.0080.

4.19: ^{1}H-NMR (300 MHz; $CDCl_3$): δ 7.45 (s, 1H), 5.58 (s, 1H), 3.97 (s, 3H), 3.93 (s, 3H), 3.65-3.50 (m, 4H), 1.22 (t, *J* = 7.1 Hz, 6H).

REF: TRW-II-421, **TRW-II-429**, TRW-II-485, TRW-III-081.

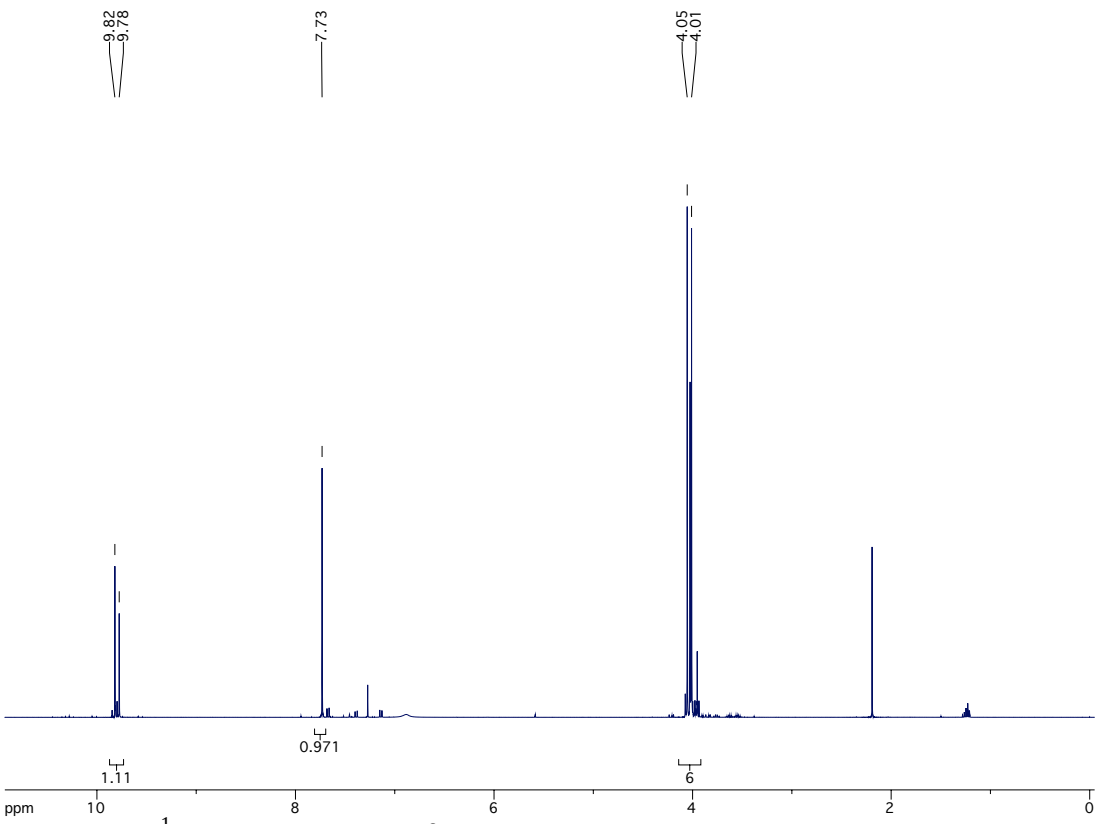

Figure 5.63a. ^{1}H NMR spectrum of compound **4.18**.

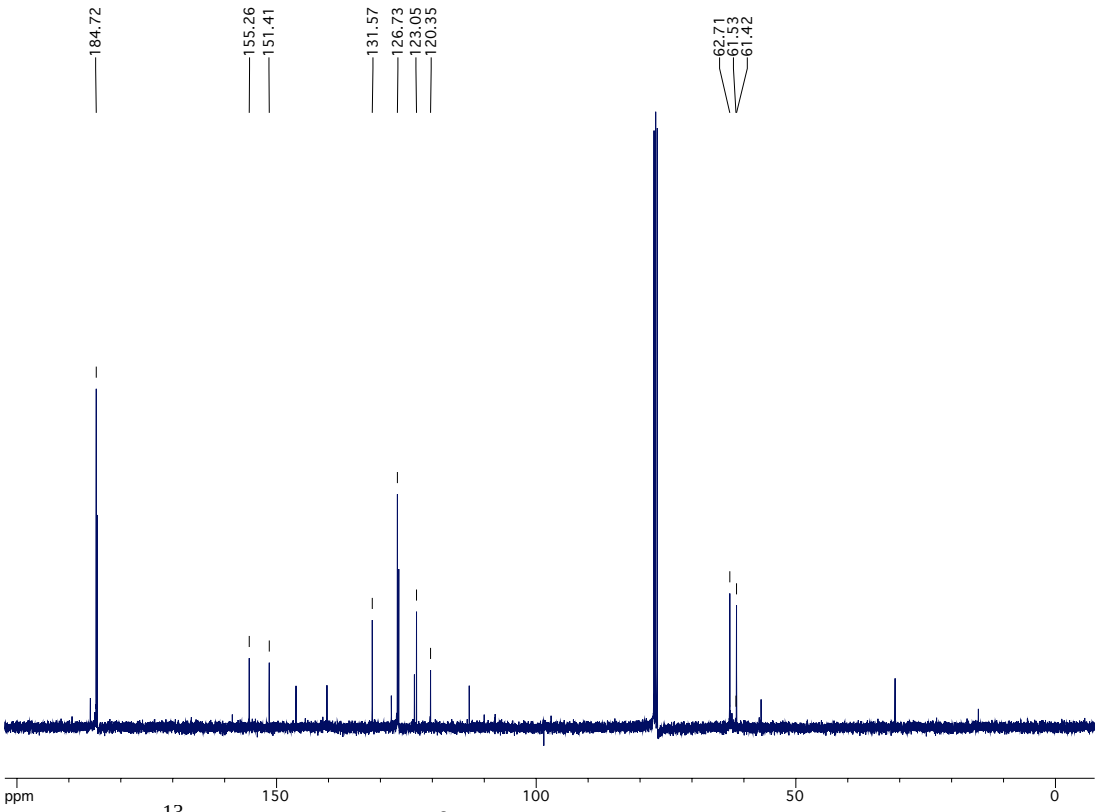

Figure 5.63b. ^{13}C NMR spectrum of compound **4.18**.

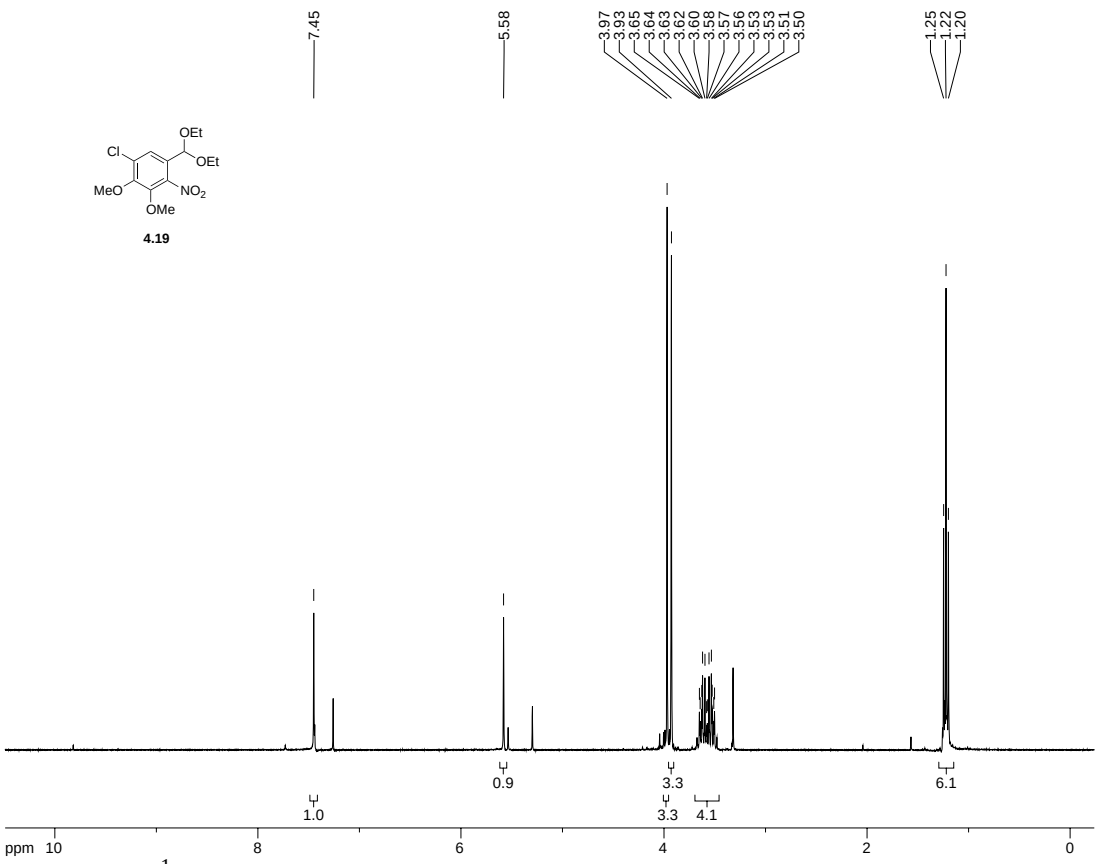

Figure 5.64a. ^{1}H NMR spectrum of compound **4.19**.

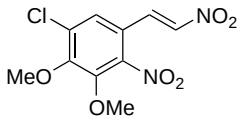

4.7

Dinitrostyrene (4.7). Aldehyde **4.18** (13.64 g, 55.4 mmol) was suspended in EtOH (180 mL), and to it added nitromethane (4.4 mL, 77.6 mmol). The mixture was cooled to -15 °C, then a solution of KOH (13.3 g, 238 mmol) in water (18 mL) and EtOH (180 mL) added dropwise over 2 hours. Upon complete addition of the KOH solution, the reaction was acidified with concentrated HCl (34 mL), diluted with H_2O (200 mL), and the product extracted into chloroform. The organic extracts were dried and concentrated. To the resulting oil was added 55 mL acetic anhydride and sodium acetate (5.5 g). The solution was heated to reflux for 30 min., then poured into water and stirred. Water was decanted from the brown paste then EtOH added and heated to dissolve the crude product. Pure nitrostyrene crystals were recovered (10.3 g, 64% yield).

^{1}H-NMR (400 MHz; DMSO-d_6): δ 8.33 (d, *J* = 13.3 Hz, 1H), 8.15 (s, 1H), 7.63 (d, *J* = 13.4 Hz, 1H), 3.98 (s, 3H), 3.97 (s, 3H); ^{13}C-NMR (101 MHz; DMSO): δ 152.3, 146.3, 145.0, 142.2, 131.5, 129.8, 124.9, 119.3, 63.1, 61.9; IR (NaCl, film) 1639, 1519 cm^{-1}; HRMS (-APCI): $[M-H]^-$ 288.0149 calcd for $C_{10}H_9ClN_2O_6$, found: 288.0141.

REF: TRW-II-426, TRW-II-431, TRW-II-489, TRW-III-003, **TRW-III-011**, TRW-III-084.

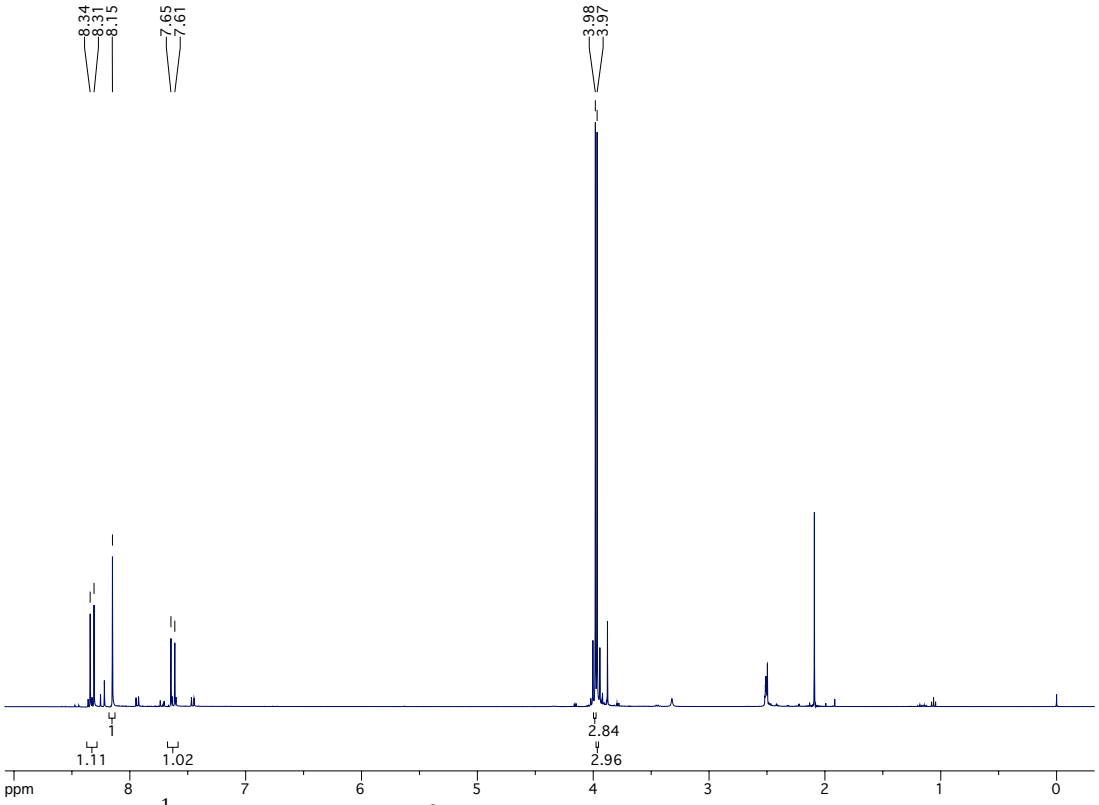

Figure 5.65a. ^{1}H NMR spectrum of compound **4.7**.

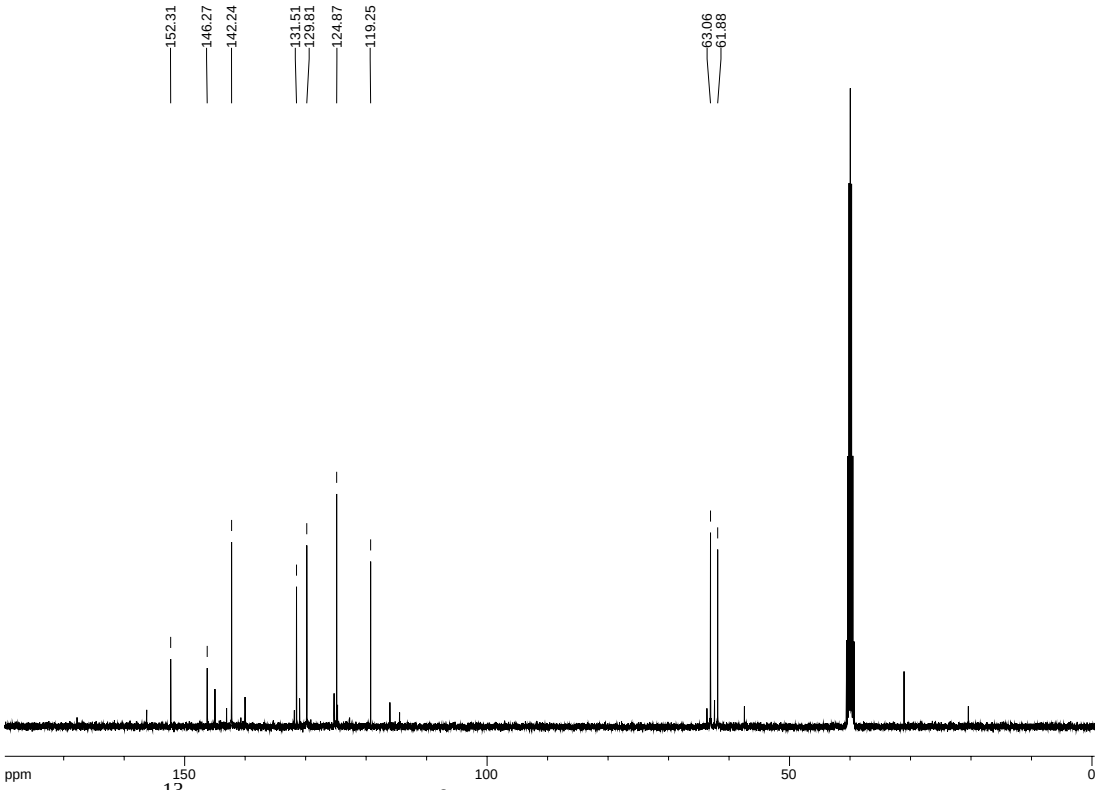

Figure 5.65b. ^{13}C NMR spectrum of compound **4.7**.

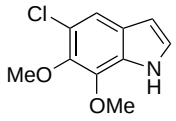

4.6

5-chloro-6,7-dimethoxy-1H-indole (4.6). A suspension of **4.7** (380 mg, 1.3 mmol), SiO_2 (3.8 g, 1000 wt%), Fe powder (1.37 g, 24.4 mmol), AcOH (7.6 mL), and $PhCH_3$ (13 mL) was heated to reflux for 3 h, then cooled to r.t. and diluted with CH_2Cl_2. The mixture was filtered and the solid washed with CH_2Cl_2. The filtrate was washed with $NaHSO_3$ (5% aq), $NaHCO_3$ (sat'd aq), and brine, then dried and concentrated. The resulting oil was dissolved in CH_2Cl_2 (13 mL) and SiO_2 added until the suspension was just fluid. After stirring under Ar for 30 min, the suspension was filtered and the solid washed with MeOH. The filtrate was concentrated and the product deemed sufficiently pure as crude (250 mg, 91% yield).

^{1}H-NMR (400 MHz; $CDCl_3$): δ 8.40 (bs, 1H), 7.27 (s, 1H), 7.03 (t, *J* = 2.8 Hz, 1H), 6.32 (t, *J* = 2.6 Hz, 1H), 3.94 (s, 3H), 3.82 (s, 3H).; ^{13}C-NMR (101 MHz; $CDCl_3$): δ 191.9, 142.7, 139.1, 130.6, 128.8, 121.1, 115.8, 102.5, 61.4, 61.0; IR (NaCl, film) 3357, 2939, 2831, 1655 cm^{-1}; HRMS (ESI-APCI+): $[M+H]^+$ 212.0478 calcd for $C_{10}H_{11}ClNO_2$, found: 212.0472.

REF: **TRW-II-430**, TRW-II-434, TRW-II-490, TRW-III-086.

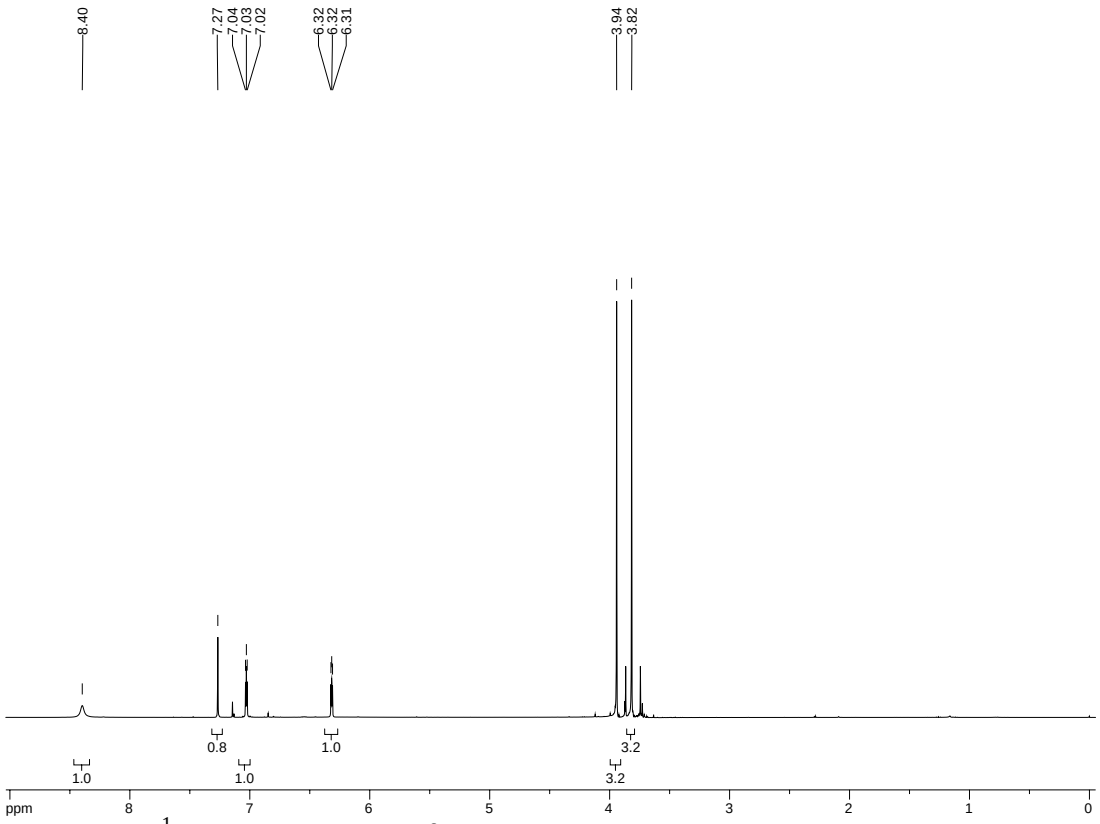

Figure 5.66a. ^{1}H NMR spectrum of compound **4.6**.

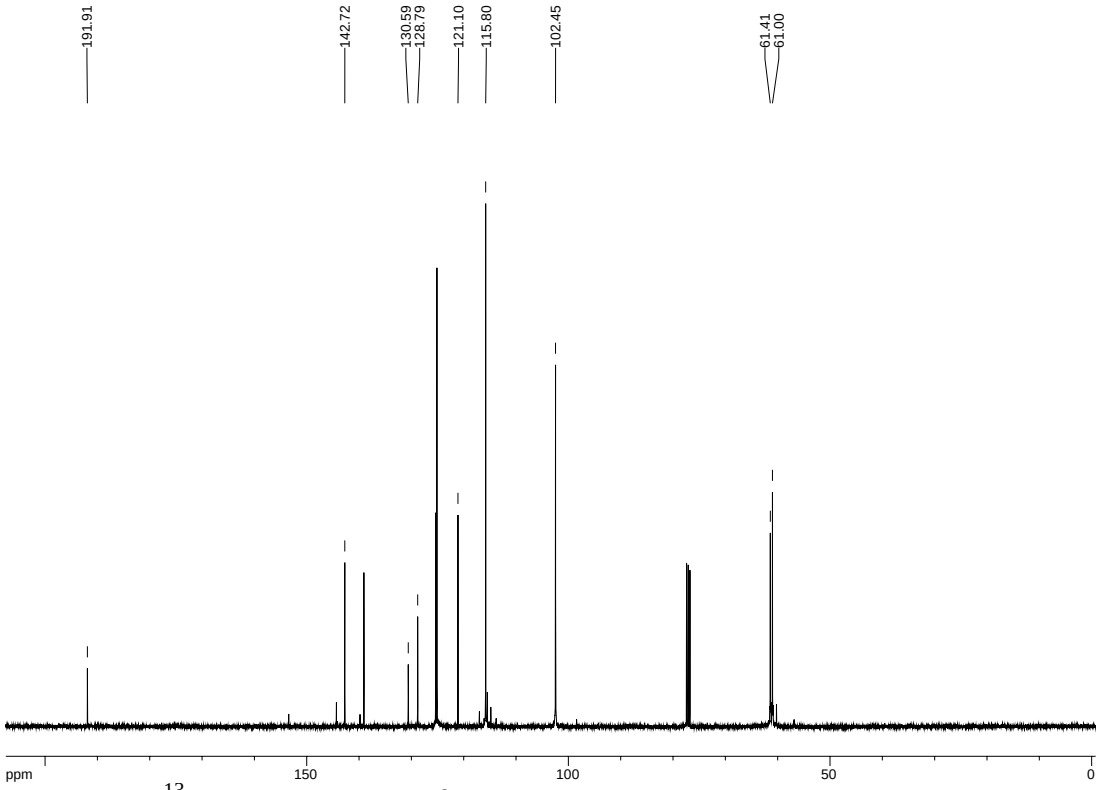

Figure 5.66b. ^{13}C NMR spectrum of compound **4.6**.

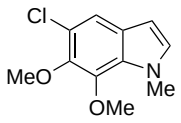

5.12

5-chloro-6,7-dimethoxy-1-methyl-1H-indole (5.12). To a solution of indole **4.6** (126 mg, 0.59 mmol) in DMF (1.5 mL) at 0 °C was slowly added NaH (47 mg). After stirring 30 minutes, iodomethane (0.044 mL, 0.71 mmol) was added dropwise, and the reaction stirred an additional 30 minutes at 0 °C. The reaction was warmed to r.t. and stirred 5 h before adding water. The product was extracted in EtOAc, washed with water (2x) and brine, then dried and concentrated to afford the title compound, deemed sufficiently pure as crude (133 mg, >99% yield).

^{1}H-NMR (300 MHz; $CDCl_3$): δ 7.35 (s, 1H), 6.93 (d, *J* = 3.1 Hz, 1H), 6.34 (d, *J* = 3.1 Hz, 1H), 4.02 (s, 3H), 3.98 (s, 3H), 3.93 (s, 3H); ^{13}C-NMR (101 MHz; $CDCl_3$): δ 143.7, 140.6, 131.0, 126.9, 120.6, 116.0, 115.7, 100.6, 61.8, 61.2, 35.4; IR (NaCl, film) 2928, 1048 cm^{-1}; HRMS (ESI-APCI+): $[M+H]^+$ 226.0635 calcd for $C_{11}H_{13}ClNO_2$, found: 226.0618.

REF: **TRW-II-433**, TRW-II-437, TRW-III-087.

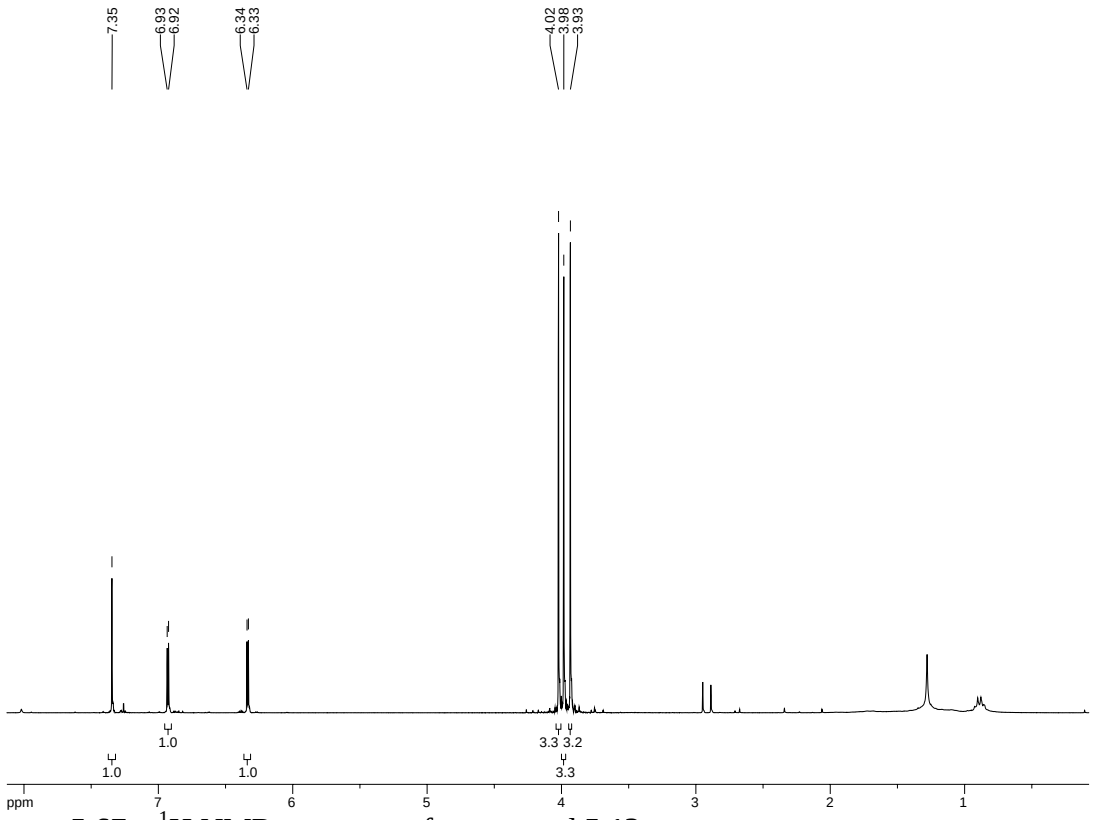

Figure 5.67a. ^{1}H NMR spectrum of compound **5.12**.

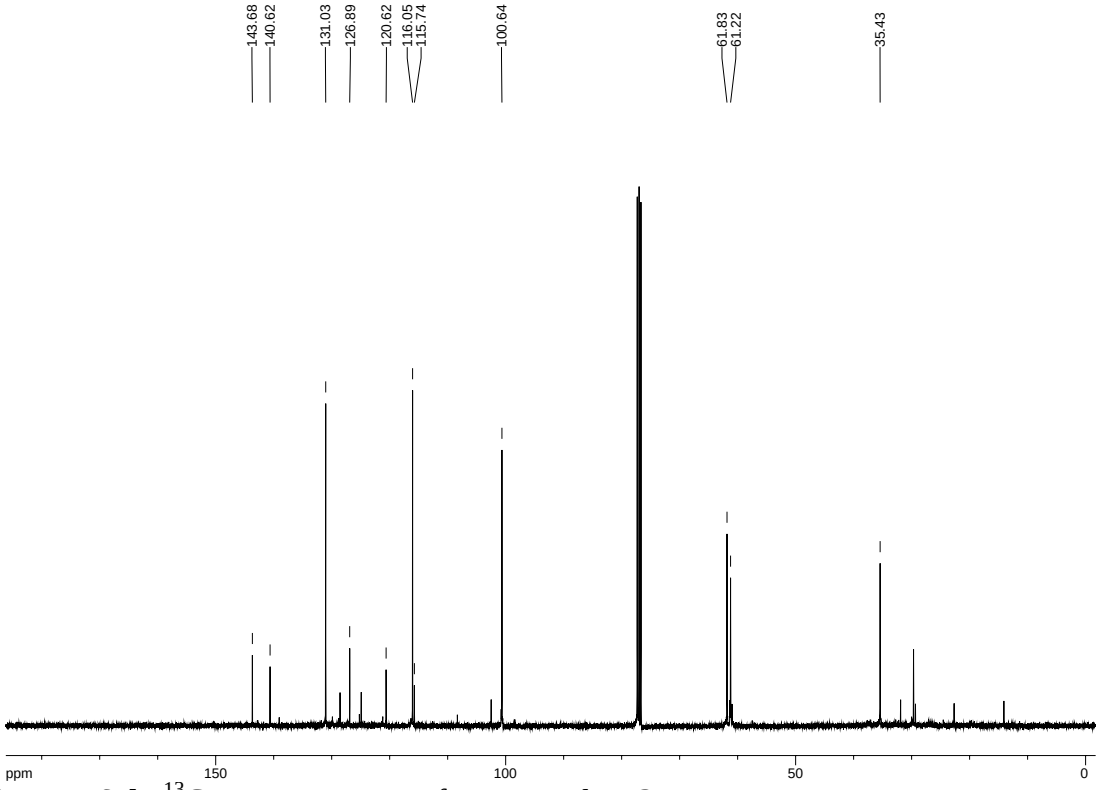

Figure 5.67b. ^{13}C NMR spectrum of compound **5.12**.

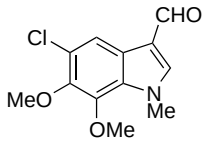

4.20

5-chloro-6,7-dimethoxy-1-methyl-1H-indole-3-carbaldehyde (4.20). DMF (6.5 mL) was cooled to 0 °C, then $POCl_3$ (0.586 mL, 6.42 mmol) added dropwise. Indole **5.12** (1.32 g, 5.84 mmol) was added dropwise as a solution in DMF. After warming the mixture to 35 °C and stirring an additional 1.5 h, ice water was added followed by 2M NaOH (15 mL). The resulting solution was boiled for 10 min, then cooled and diluted with EtOAc. The organic layer was washed with water and brine, then dried and concentrated to give the aldehyde (1.38 g, 93% yield), used as crude in the next reaction.

^{1}H-NMR (400 MHz; $CDCl_3$): δ 9.76 (s, 1H), 7.96 (s, 1H), 7.44 (s, 1H), 3.95 (s, 3H), 3.94 (s, 3H), 3.82 (s, 3H); ^{13}C-NMR (101 MHz; $CDCl_3$): δ 183.9, 145.4, 140.92, 140.89, 129.6, 124.5, 123.1, 117.26, 117.20, 61.9, 61.1, 36.7; IR (NaCl, film) 2930, 2853, 1656, 1044 cm^{-1}; HRMS (ESI-APCI+): $[M+H]^+$ 254.0584 calcd for $C_{12}H_{13}ClNO_3$, found: 254.0581.

REF: TRW-II-436, **TRW-II-439**, TRW-III-090.

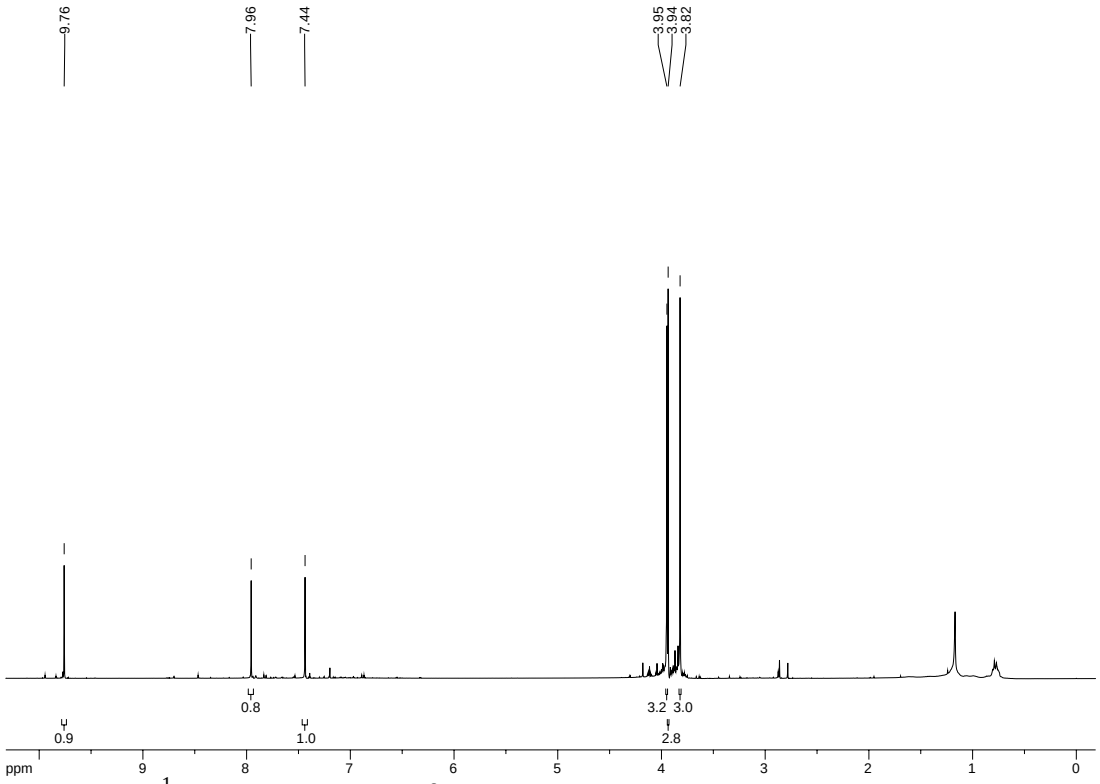

Figure 5.68a. ^{1}H NMR spectrum of compound **4.20**.

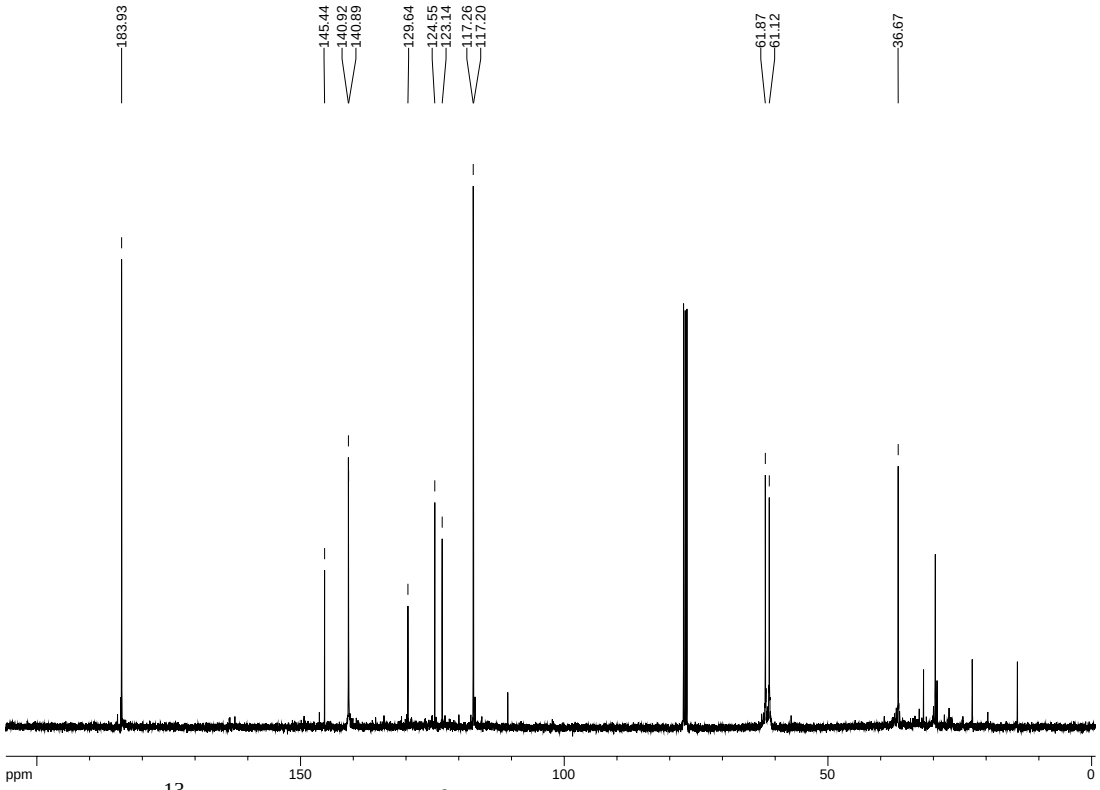

Figure 5.68b. ^{13}C NMR spectrum of compound **4.20**.

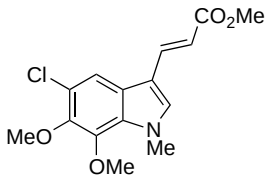

4.5

(E)-methyl 3-(5-chloro-6,7-dimethoxy-1-methyl-1H-indol-3-yl)acrylate (4.5). To a solution of aldehyde **4.20** (133 mg, 0.52 mmol) in toluene (1.8 mL) was added methyl(triphenyl-phosphoranylidene)acetate (347 mg, 1.04 mmol). The resulting solution was heated to reflux O/N, then concentrated and purified by SiO_2 chromatography (9:1 – 4:1 – 2:1 hexanes:EtOAc) to afford olefin **4.5** (128 mg, 80% yield).

^{1}H-NMR (400 MHz; $CDCl_3$): δ 7.67 (d, *J* = 16.0 Hz, 1H), 7.51 (s, 1H), 7.11 (s, 1H), 6.20 (d, *J* = 16.0 Hz, 1H), 3.93 (s, 3H), 3.89 (s, 3H), 3.83 (s, 3H), 3.71 (s, 3H); ^{13}C-NMR (101 MHz; $CDCl_3$): δ 168.4, 144.7, 141.0, 137.2, 134.8, 129.9, 124.3, 122.8, 115.7, 112.5, 111.4, 61.8, 61.2, 51.4, 36.1; IR (NaCl, film) 2940, 1736, 1626, 1043 cm^{-1}; HRMS (ESI-APCI+): $[M+H]^+$ 310.0846 calcd for $C_{15}H_{17}ClNO_4$, found: 310.0840.

REF: **TRW-II-441**, TRW-II-443, TRW-III-091.

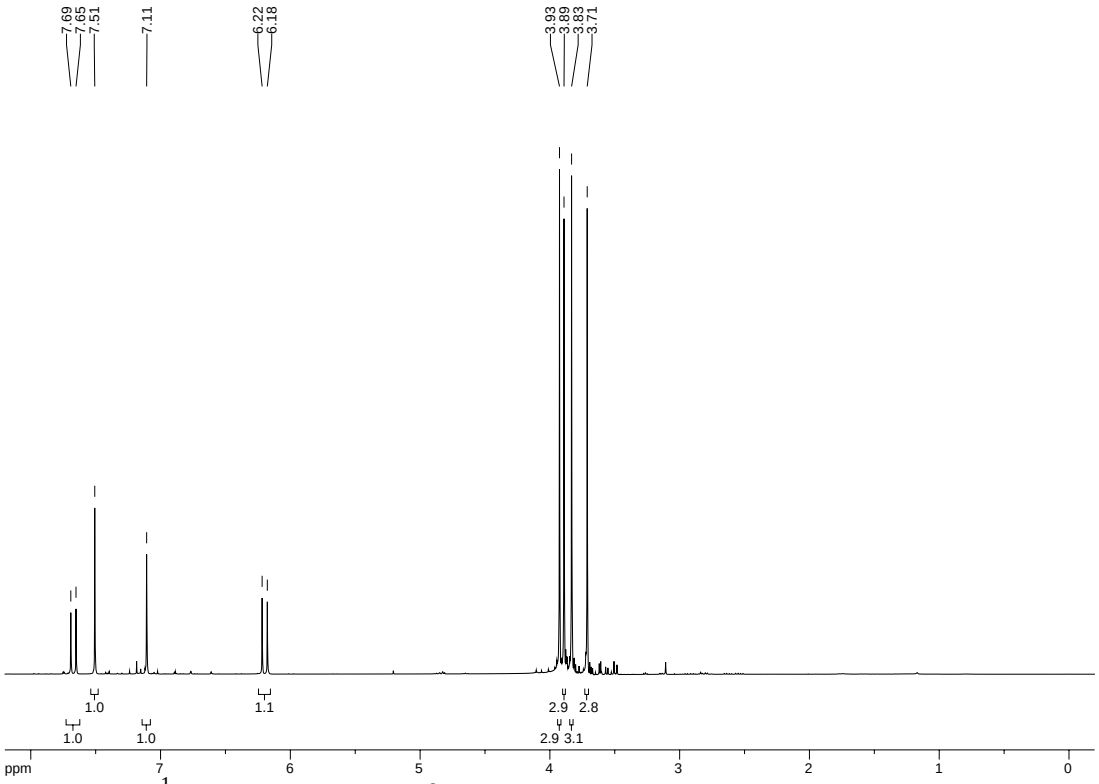

Figure 5.69a. ^{1}H NMR spectrum of compound **4.5**.

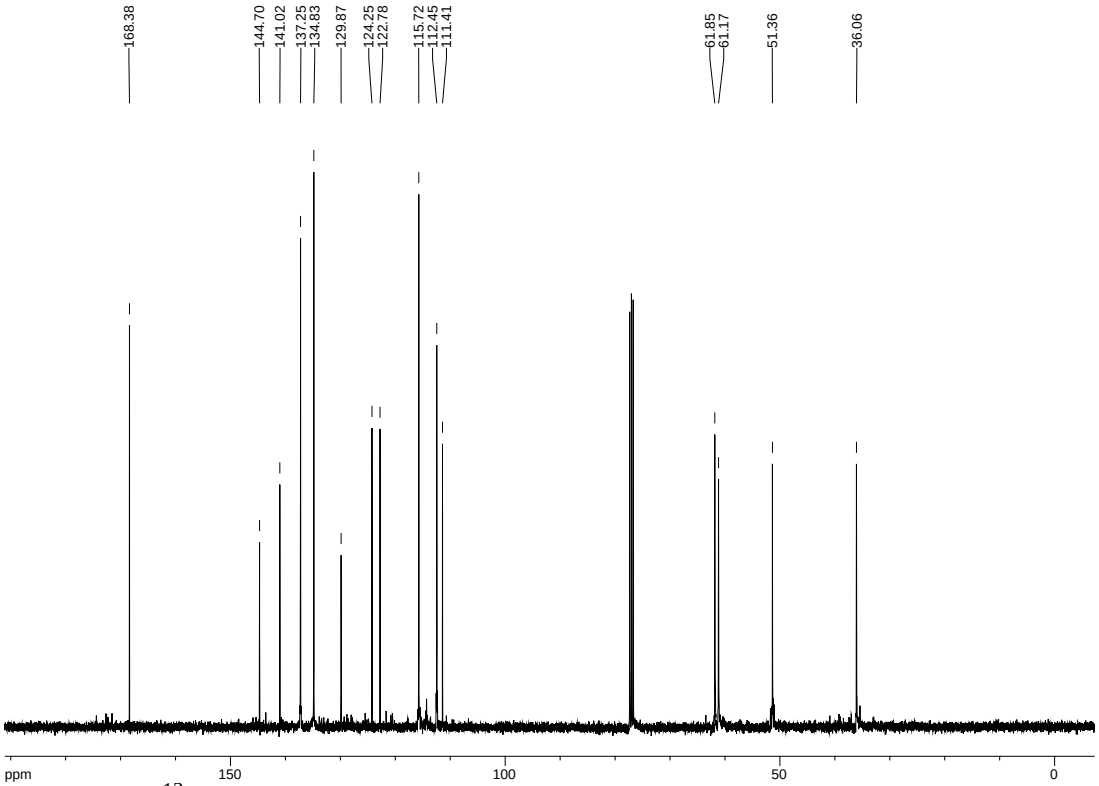

Figure 5.69b. ^{13}C NMR spectrum of compound **4.5**.

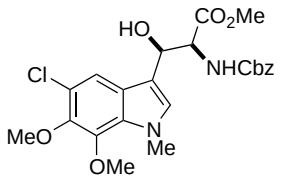

4.4

(2S,3R)-methyl 2-(((benzyloxy)carbonyl)amino)-3-(5-chloro-6,7-dimethoxy-1-methyl-1H-indol-3-yl)-3-hydroxypropanoate (4.4). To a solution of benzyl carbamate (178 mg, 1.18 mmol) in 0.4 M NaOH (2.5 mL) and *n*-propanol (2 mL) in a flask covered with foil was added fresh *t*-butyl hypochlorite (0.135 mL, 1.20 mmol). After stirring 5 min, $(DHQD)_2AQN$ (14 mg, 0.016 mmol) in *n*-propanol (0.5 mL), olefin **4.5** (100 mg, 0.32 mmol) in *n*-propanol (1 mL), and $K_2OsO_2(OH)_4$ (5 mg, 0.013 mmol) in 0.4 M NaOH (0.5 mL) were added successively, and the resulting solution stirred O/N. Sodium bisulfite (0.2 g) was added and the product extracted into EtOAc. The organic layer was washed with water, then brine, dried over Na_2SO_4, and concentrated. SiO_2 chromatography (10:1 – 1:1 hexanes:EtOAc) gave pure tryptophan derivative **4.4** (54 mg, 35% yield).

$[\alpha]_D$ = -20.9 (CH_2Cl_2); 1H-NMR (300 MHz; $CDCl_3$): δ 7.40 (s, 1H), 7.32 (s, 5H), 6.92 (s, 1H), 5.77 (d, *J* = 9.2 Hz, 1H), 5.46-5.45 (bs, 1H), 5.06 (s, 2H), 4.69-4.65 (m, 1H), 3.98 (s, 3H), 3.89 (s, 3H), 3.88 (d, *J* = 9.3 Hz, 3H), 3.78 (s, 3H), 2.69 (bs, 1H); ^{13}C-NMR (101 MHz; $CDCl_3$): δ 166.1, 144.6, 140.9, 133.75, 133.73, 128.66, 128.60, 128.46, 128.43, 128.28, 128.18, 128.07, 126.3, 122.6, 114.2, 108.6, 72.9, 67.3, 66.9, 61.9, 61.2, 52.3, 36.2; IR (NaCl, film) 3346, 2952, 1723, 1465, 1218, 1040 cm^{-1}; HRMS (ESI-APCI+): $[M+Na]^+$ 499.1248 calcd for $C_{23}H_{25}ClN_2NaO_7$, found: 499.1249.

REF: **TRW-II-459**, TRW-II-461, TRW-III-093.

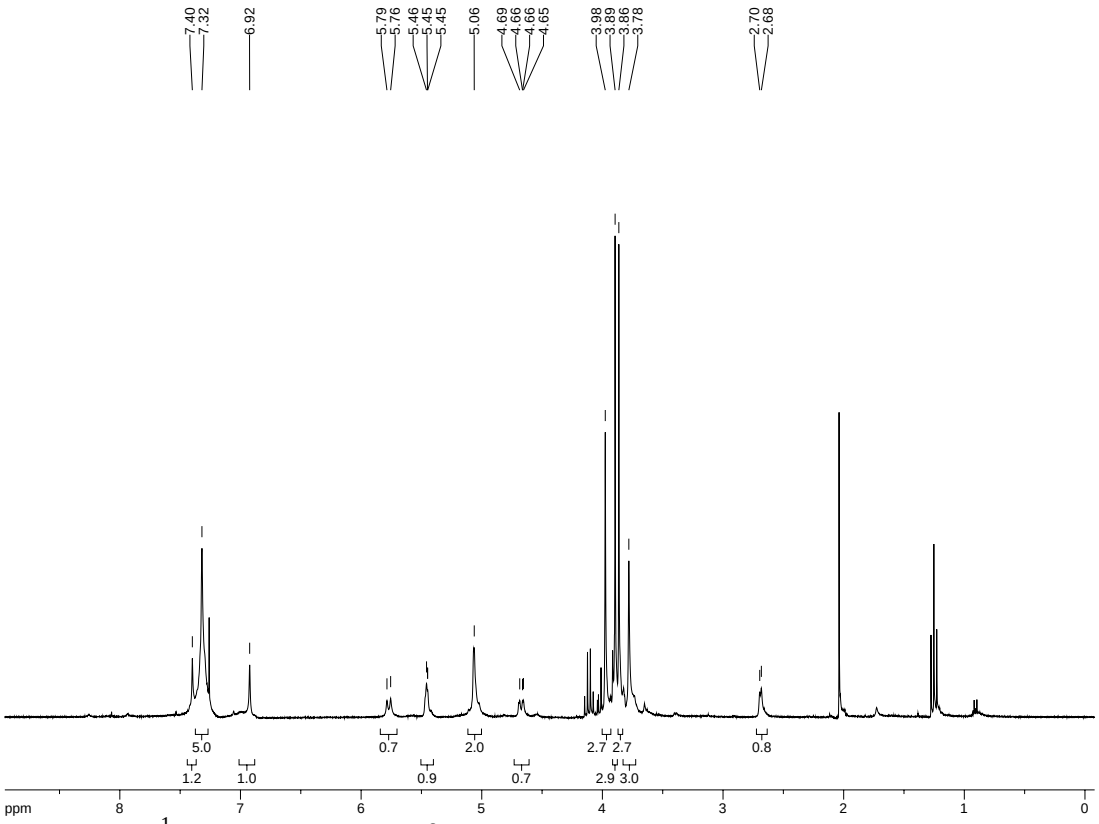

Figure 5.70a. ^{1}H NMR spectrum of compound **4.4**.

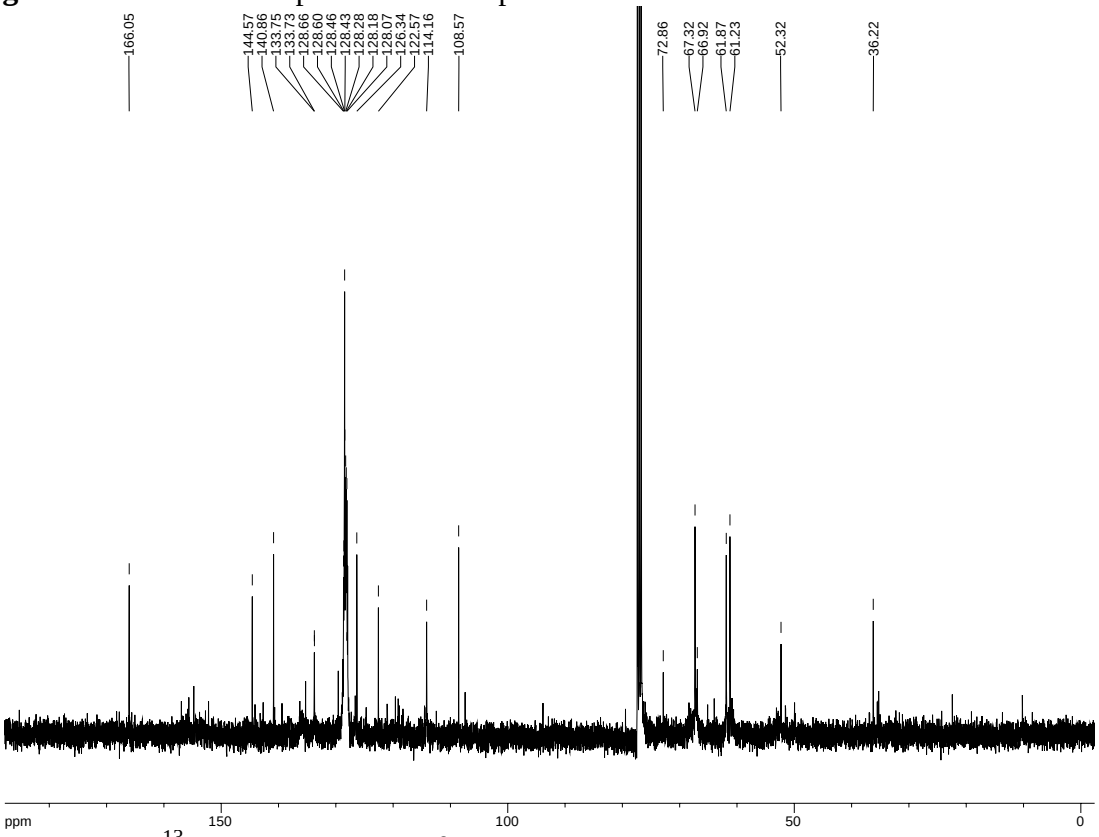

Figure 5.70b. ^{13}C NMR spectrum of compound **4.4**.

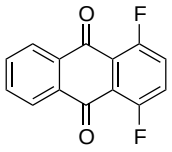

4.23

1,4-difluoroanthracene-9,10-dione (4.23). To a solution of phthalic anhydride (10 g, 67.6 mmol) in 1,4-difluorobenzene (68 mL) was added $AlCl_3$ (36 g, 270 mmol). The resulting solution was stirred at reflux for 48h before removing the solvent by distillation. HCl (1M, 400 mL) was added and the product extracted into CH_2Cl_2 (3x). The combined organic extracts were filtered through a cotton plug and concentrated. The crude residue was taken up in chloroform (40 mL) and to it added hexanes (100 mL). The solution was cooled to -20 °C then filtered to collect the resultant precipitate. After drying the precipitate under vacuum, polyphosphoric acid (50 mL) was added and the mixture heated to 140 °C for 2h. The mixture was poured over approximately 400 g ice and allowed to warm to r.t. while stirring. Solid K_2CO_3 was added to neutralize the solution, then the product was extracted into CH_2Cl_2. The combined organic extracts were dried (Na_2SO_4) and concentrated. The residue was dissolved in CH_2Cl_2, filtered through basic alumina using CH_2Cl_2 as the eluent, and concentrated to afford the title compound (920 mg).

^{1}H-NMR (400 MHz; $CDCl_3$): δ 8.21-8.16 (m, 2H), 7.76-7.72 (m, 2H), 7.43-7.39 (m, 2H); ^{13}C-NMR (101 MHz; $CDCl_3$): δ 134.3, 133.2, 127.0, 124.7, 124.48, 124.34.

REF: **TRW-II-451**, TRW-III-079.

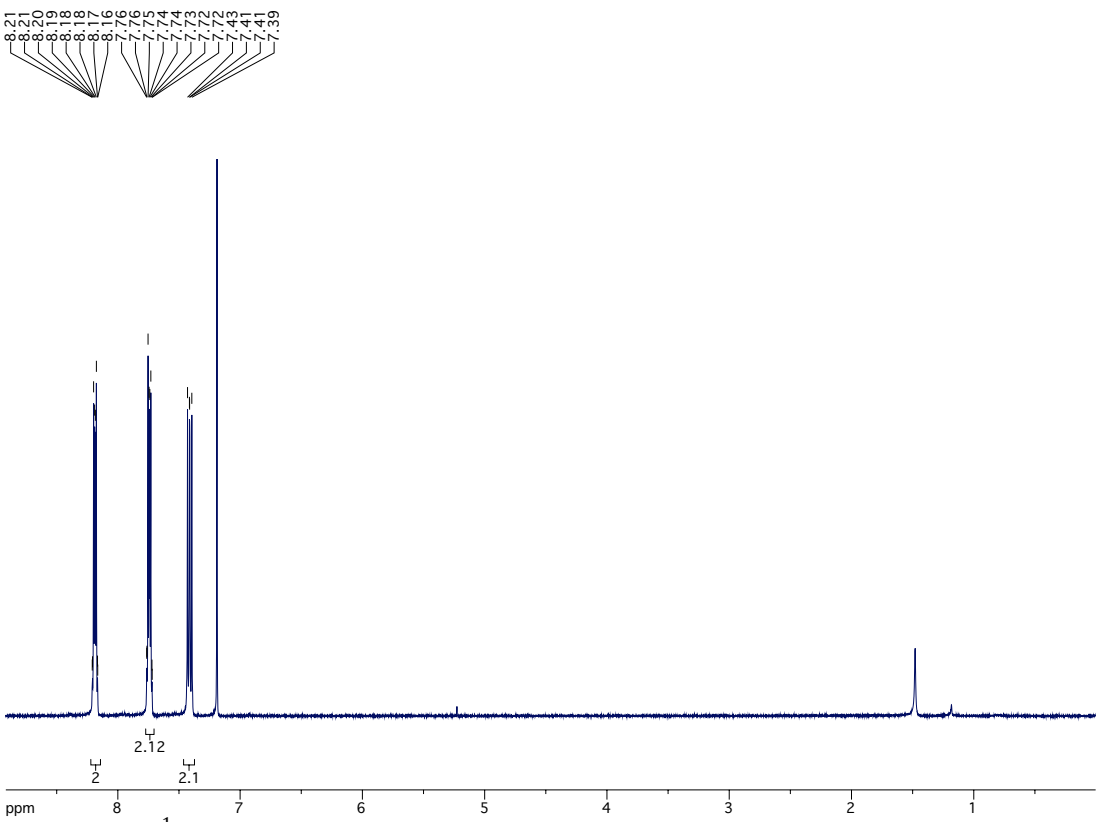

Figure 5.71a. ^{1}H NMR spectrum of compound **4.23**.

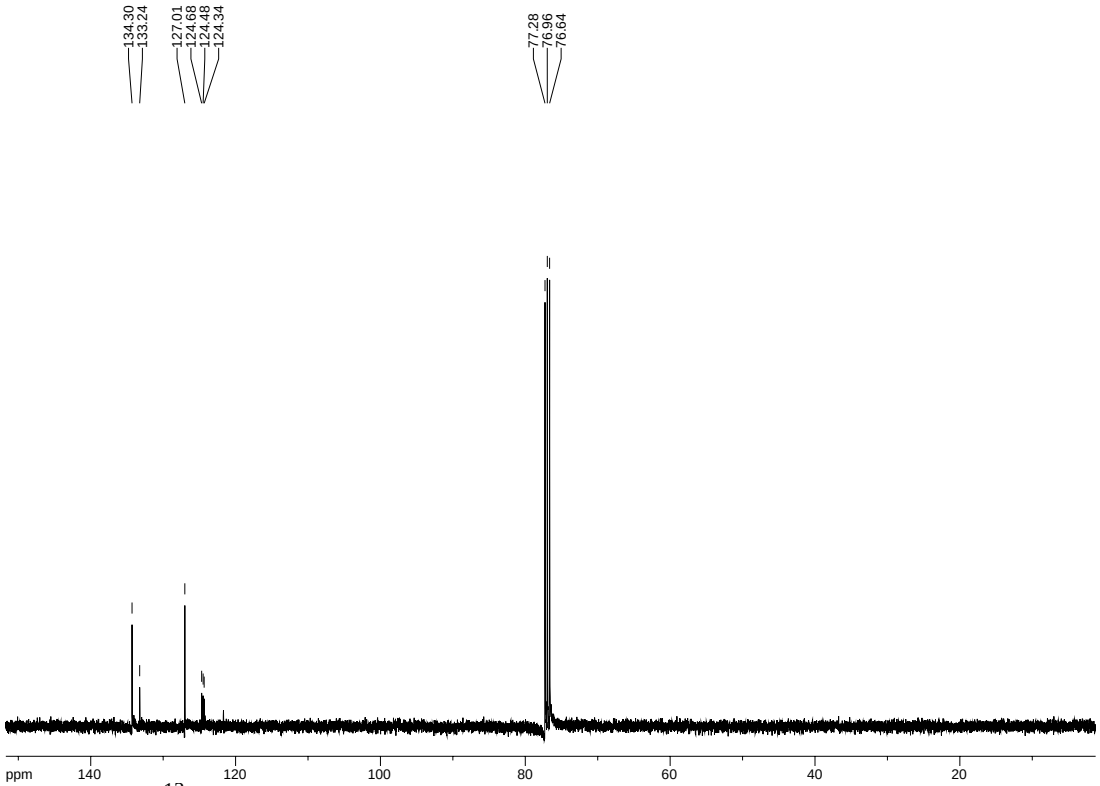

Figure 5.71b. ^{13}C NMR spectrum of compound **4.23**.

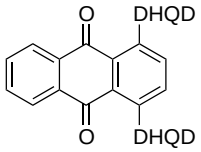

$(DHQD)_2AQN$ (**4.24**)

$(DHQD)_2AQN$ (4.24). To a solution of DHQD (3.1 g, 9.5 mmol) in THF (19 mL) at -50 °C was added *n*BuLi (1.6M in hexanes, 6.0 mL, 9.5 mmol) dropwise over 10 min. After stirring 15 min at -50 °C, the reaction mixture was warmed to 0 °C and the difluoro compound added (920 mg, 3.8 mmol). The reaction was allowed to warm to r.t. as it stirred O/N under Ar, then warmed to 40 °C and stirred an additional 2h. EtOAc was added and the reaction quenched by addition of sat'd $NaHCO_3$. The product was extracted in EtOAc, dried (Na_2SO_4), concentrated, and purified by SiO_2 chromatography (5% MeOH, 0.5% NH_4OH, in $CHCl_3$) to afford $(DHQD)_2AQN$ (2.55 g, 78% yield).

^{1}H-NMR (300 MHz; $CDCl_3$): δ 8.63 (d, *J* = 4.5 Hz, 2H), 8.22 (dd, *J* = 5.8, 3.3 Hz, 2H), 8.01 (d, *J* = 9.2 Hz, 2H), 7.79 (dd, *J* = 5.8, 3.3 Hz, 2H), 7.49 (d, *J* = 4.5 Hz, 3H), 7.37 (dd, *J* = 9.2, 2.5 Hz, 3H), 6.80 (bs, 2H), 5.28 (s, 2H), 3.95 (s, 6H), 3.28-3.26 (bs, 2H), 3.00-2.53 (broad, 10H), 1.83 (bs, 2H), 1.61-1.45 (broad, 12H), 0.84 (t, *J* = 7.3 Hz, 6H).

REF: TRW-II-457, TRW-III-002, **TRW-III-082**.

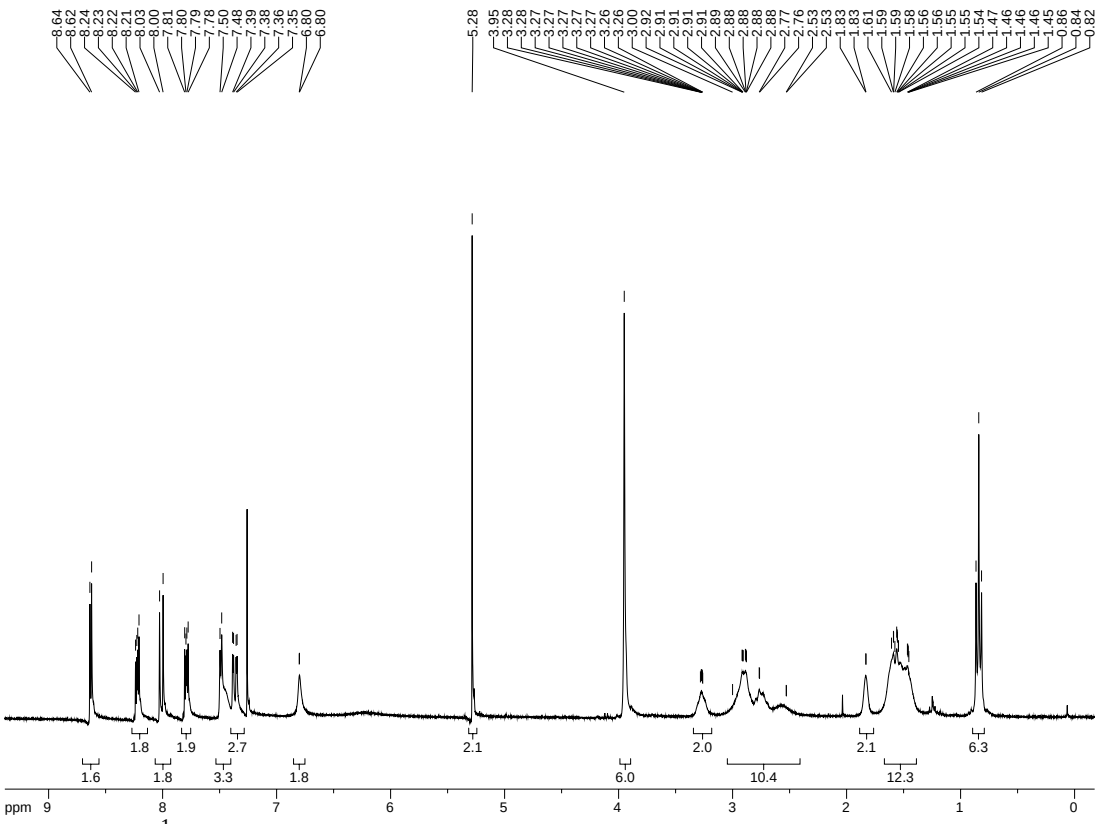

Figure 5.72a. ^{1}H NMR spectrum of compound **4.24**.

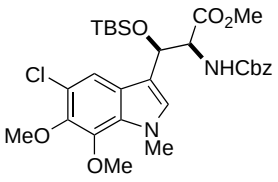

4.25

(2S,3R)-methyl 2-(((benzyloxy)carbonyl)amino)-3-((tert-butyldimethylsilyl) oxy)-3-(5-chloro-6,7-dimethoxy-1-methyl-1H-indol-3-yl)propanoate (4.25). Alcohol **4.4** (296 mg, 0.62 mmol) was dissolved in DMF (1.6 mL), and to it added imidazole (102 mg, 1.5 mmol) and TBSCl (242 mg, 1.6 mmol). After stirring O/N, the solution was diluted with EtOAc, washed with water (3x), brine (1x), dried over Na_2SO_4, and concentrated to give the title compound (366 mg, >99% yield).

^{1}H-NMR (300 MHz; $CDCl_3$): δ 7.36 (s, 1H), 7.32 (s, 5H), 6.83 (s, 1H), 5.49 (dd, *J* = 12.6, 2.3 Hz, 1H), 5.07 (s, 2H), 4.98 (s, 1H), 4.47 (dd, *J* = 9.6, 2.1 Hz, 1H), 4.00 (s, 3H), 3.91 (s, 3H), 3.89 (s, 3H), 3.79 (s, 3H), 0.86 (s, 9H), 0.09 (s, 6H); HRMS (ESI-APCI+): $[M+Na]^+$ 613.2113 calcd for $C_{29}H_{39}ClN_2NaO_7Si$, found: 613.2109.

REF: TRW-II-460, **TRW-II-465**, TRW-III-096.

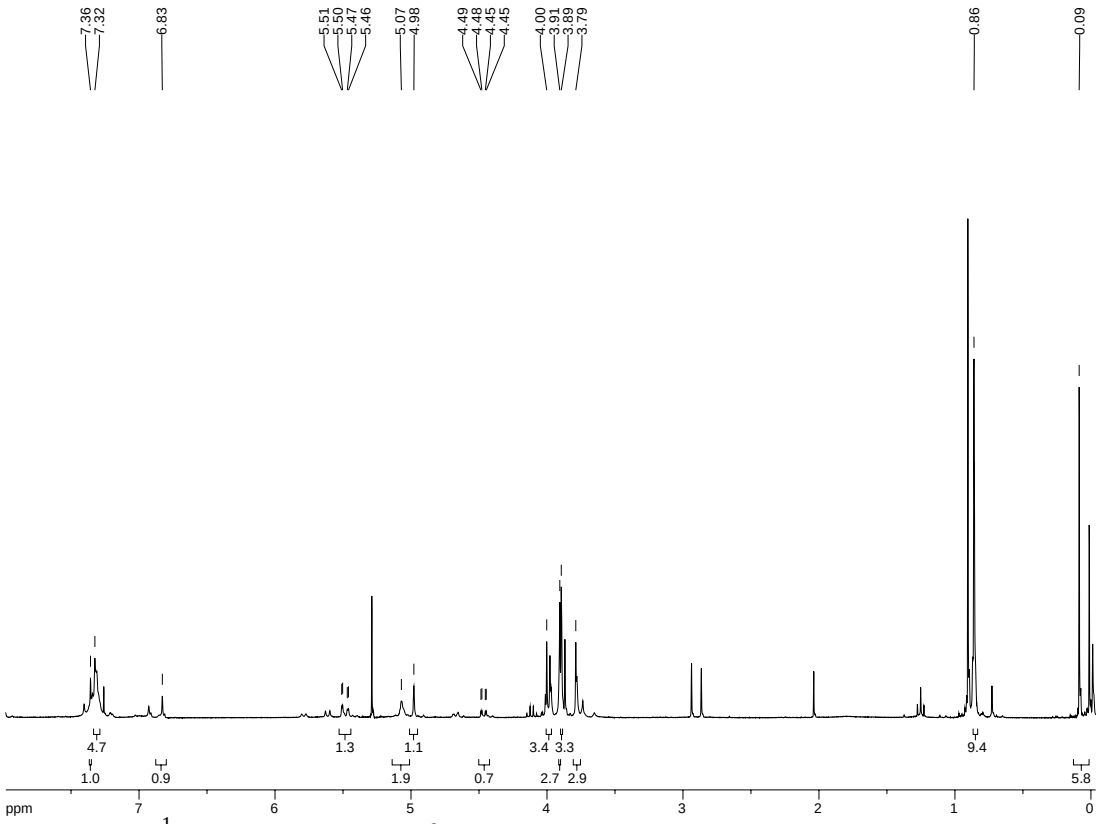

Figure 5.73a. ^{1}H NMR spectrum of compound **4.25**.

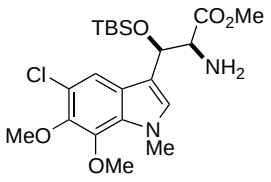

4.26

(2S,3R)-methyl 2-amino-3-((tert-butyldimethylsilyl)oxy)-3-(5-chloro-6,7-dimethoxy-1-methyl-1H-indol-3-yl)propanoate (4.26). To a suspension of **4.25** (366 mg, 0.61 mmol) and Pd/C (37 mg) in MeOH (3 mL) was added hydrogen gas. After stirring O/N, the reaction was flushed with argon and filtered through celite to afford the free amine (262 mg, 94% yield).

$[\alpha]_D$ = +6.4 (CH_2Cl_2); ^{1}H-NMR (300 MHz; $CDCl_3$): δ 7.32 (s, 1H), 6.90 (s, 1H), 5.40 (d, *J* = 1.8 Hz, 1H), 4.85-4.63 (m, 1H), 4.00 (s, 3H), 3.94 (s, 3H), 3.90 (s, 3H), 3.75 (s, 3H), 2.24-2.14 (bs, 2H), 0.88 (s, 9H), -0.01 (s, 3H), -0.15 (s, 3H); ^{13}C-NMR (101 MHz; $CDCl_3$): δ 173.3, 143.8, 140.7, 129.3, 129.0, 123.9, 120.6, 114.8, 114.3, 70.4, 61.8, 61.1, 60.8, 52.0, 35.5, 25.66, 25.61, 25.52, 18.0, -4.6, -5.6; IR (NaCl, film) 3332, 2953, 2858, 1750, 1464, 1038 cm^{-1}; HRMS (ESI-APCI+): $[M+Na]^+$ 479.1745 calcd for $C_{21}H_{33}ClN_2NaO_5Si$, found: 479.1746.

REF: TRW-II-462, **TRW-II-468**, TRW-III-098.

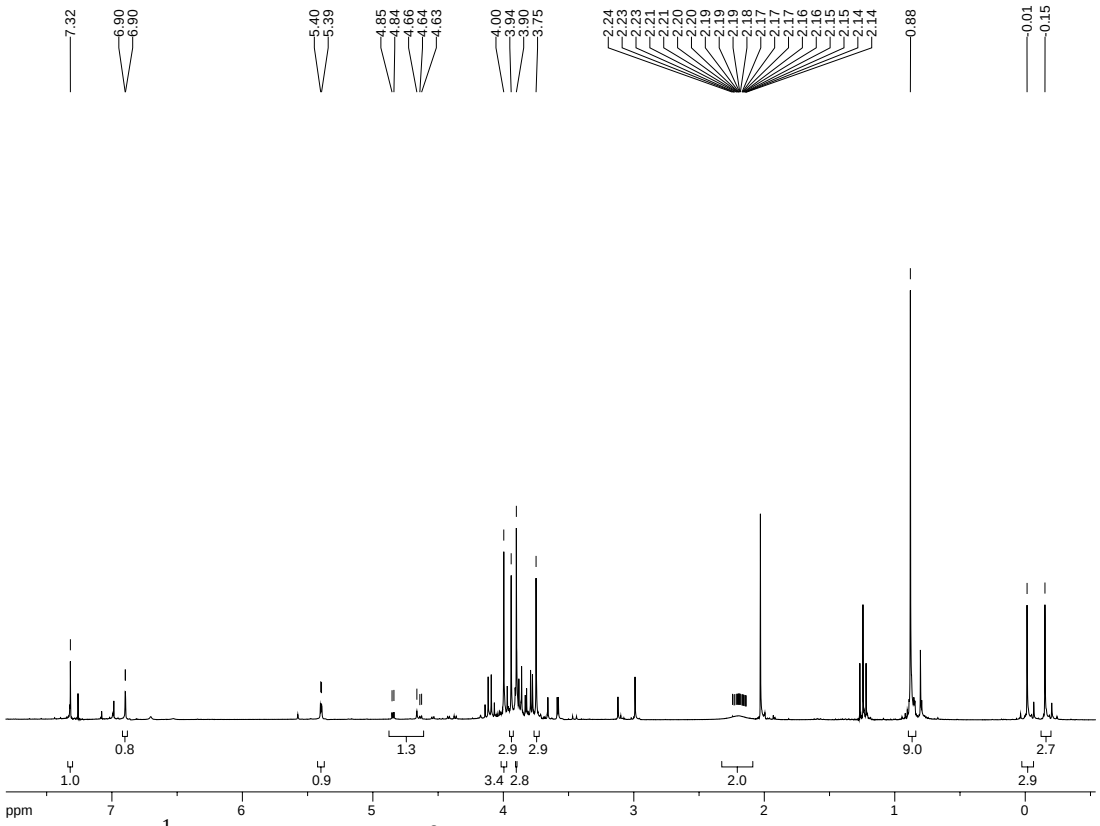

Figure 5.74a. ^{1}H NMR spectrum of compound **4.26**.

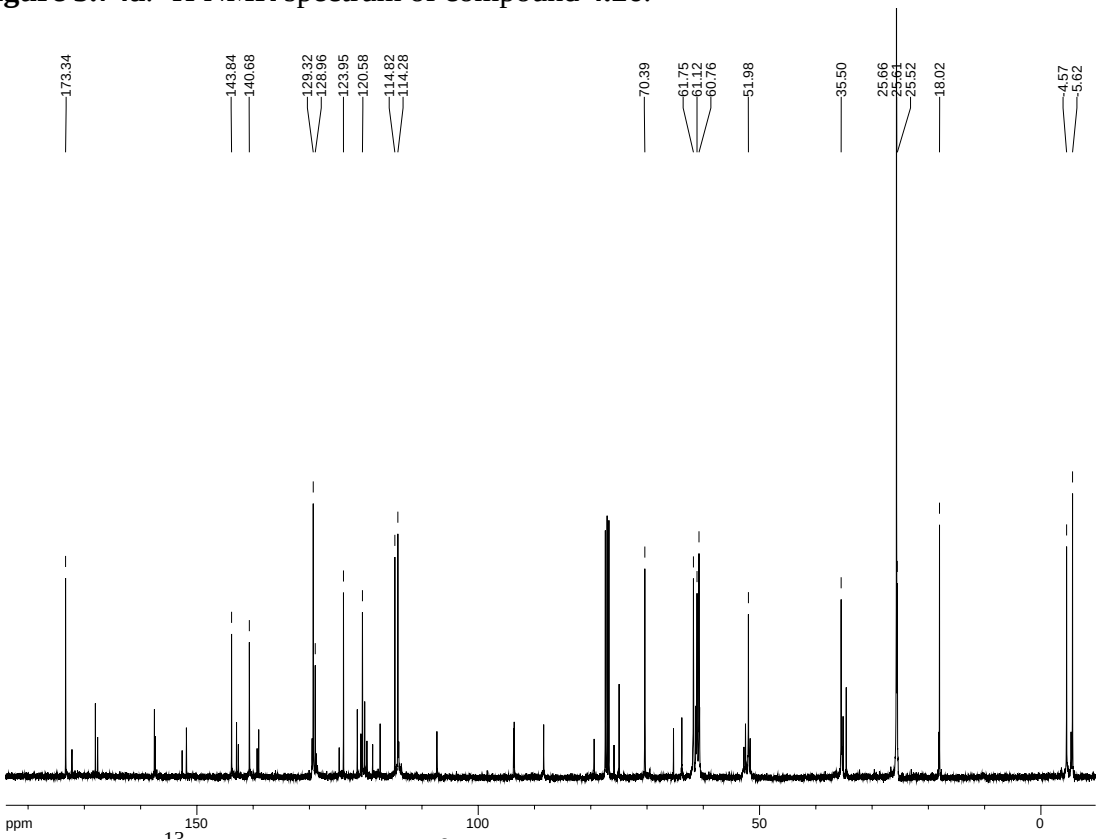

Figure 5.74b. ^{13}C NMR spectrum of compound **4.26**.

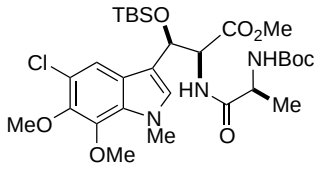

4.27

(2S,3R)-methyl 2-((S)-2-((tert-butoxycarbonyl)amino)propanamido)-3-((tert-butyl-dimethylsilyl)oxy)-3-(5-chloro-6,7-dimethoxy-1-methyl-1H-indol-3-yl)propanoate (4.27). To a solution of amine **4.26** (262 mg, 0.57 mmol) in CH_2Cl_2 (3 mL) was added *N*-Boc-ala-OH (108 mg, 0.57 mmol), *i*Pr_2NEt (0.1 mL, 0.57 mmol), and EDCI (110 mg, 0.57 mmol). The reaction was stirred at r.t. O/N, the concentrated and purified by SiO_2 chromatography (10% - 25% - 50% EtOAc in hexanes) to afford **4.27** (210 mg, 59% yield).

^{1}H-NMR (300 MHz; $CDCl_3$): δ 7.36 (s, 1H), 6.86 (s, 1H), 6.73-6.70 (bs, 1H), 5.53 (d, *J* = 2.0 Hz, 1H), 4.97-4.96 (bs, 1H), 4.67 (dd, *J* = 9.1, 1.7 Hz, 1H), 4.19-4.15 (bs, 1H), 3.99 (s, 3H), 3.92 (s, 3H), 3.90 (s, 3H), 3.78 (s, 3H), 1.45 (s, 9H), 1.24 (dd, *J* = 7.1, 0.8 Hz, 3H), 0.89 (s, 9H), 0.01 (s, 3H), -0.15 (s, 3H).

REF: TRW-II-466, **TRW-II-471**.

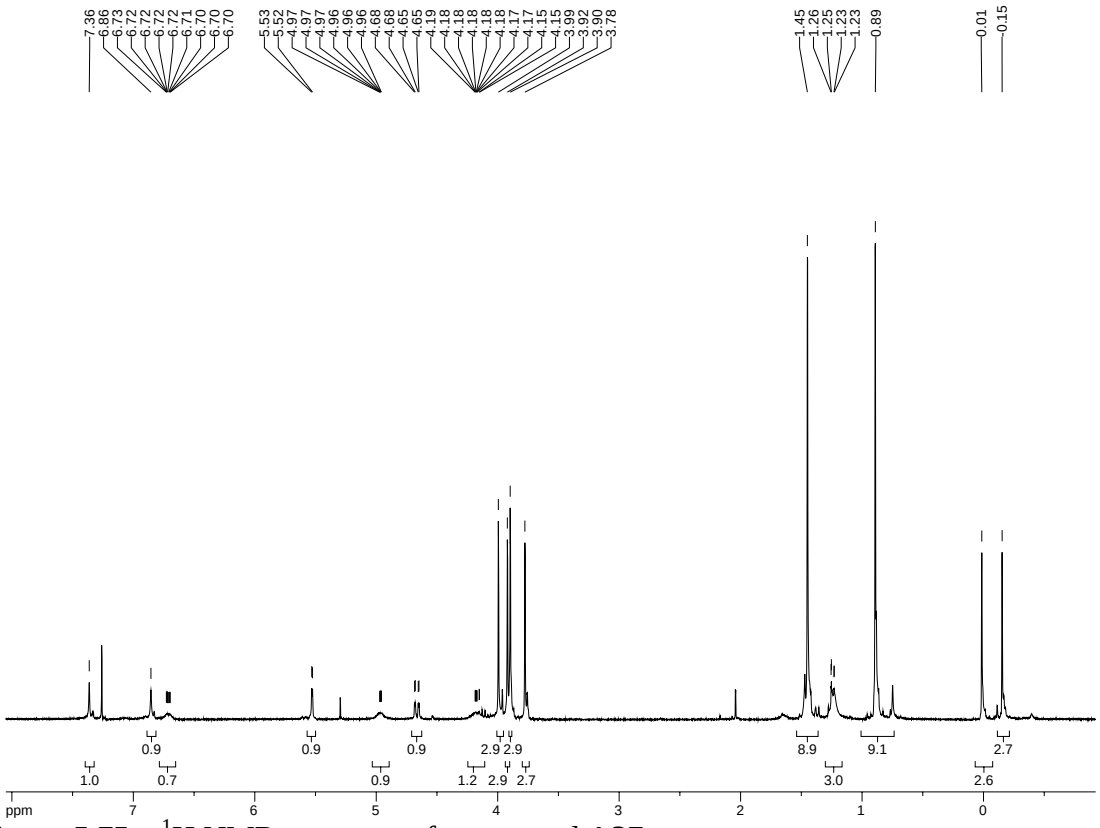

Figure 5.75a. ^{1}H NMR spectrum of compound **4.27**.

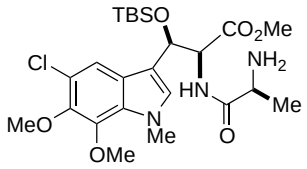

4.28

(2S,3R)-methyl 2-((S)-2-aminopropanamido)-3-((tert-butyldimethylsilyl)oxy)-3-(5-chloro-6,7-dimethoxy-1-methyl-1H-indol-3-yl)propanoate (4.28). Compound **4.27** (105 mg, 0.167 mmol) was dissolved in CH_2Cl_2 (1.7 mL), then 2,6-lutadine (0.039 mL, 0.334 mmol) added. The solution was cooled to 0 °C, then TMSOTf (0.045 mL, 0.251 mmol) added. After warming to r.t., the reaction was monitored by TLC and once complete, quenched with sat'd NH_4Cl. The product was extracted into CH_2Cl_2, the organic extracts dried and concentrated, and the product purified by SiO_2 chromatography to afford the title compound (52 mg, 59% yield).

^{1}H-NMR (300 MHz; $CDCl_3$): δ 7.36 (s, 1H), 6.92 (s, 1H), 5.53 (s, 1H), 4.79-4.77 (bs, 2H), 4.59 (d, *J* = 8.8 Hz, 1H), 3.97 (s, 3H), 3.90 (s, 3H), 3.88 (s, 3H), 3.82 (d, *J* = 7.4 Hz, 1H), 3.74 (s, 3H), 1.29 (d, *J* = 8.4 Hz, 3H), 0.87 (s, 9H), -0.01 (s, 3H), -0.16 (s, 3H).

REF: **TRW-II-476**; for TFA version, see TRW-II-474.

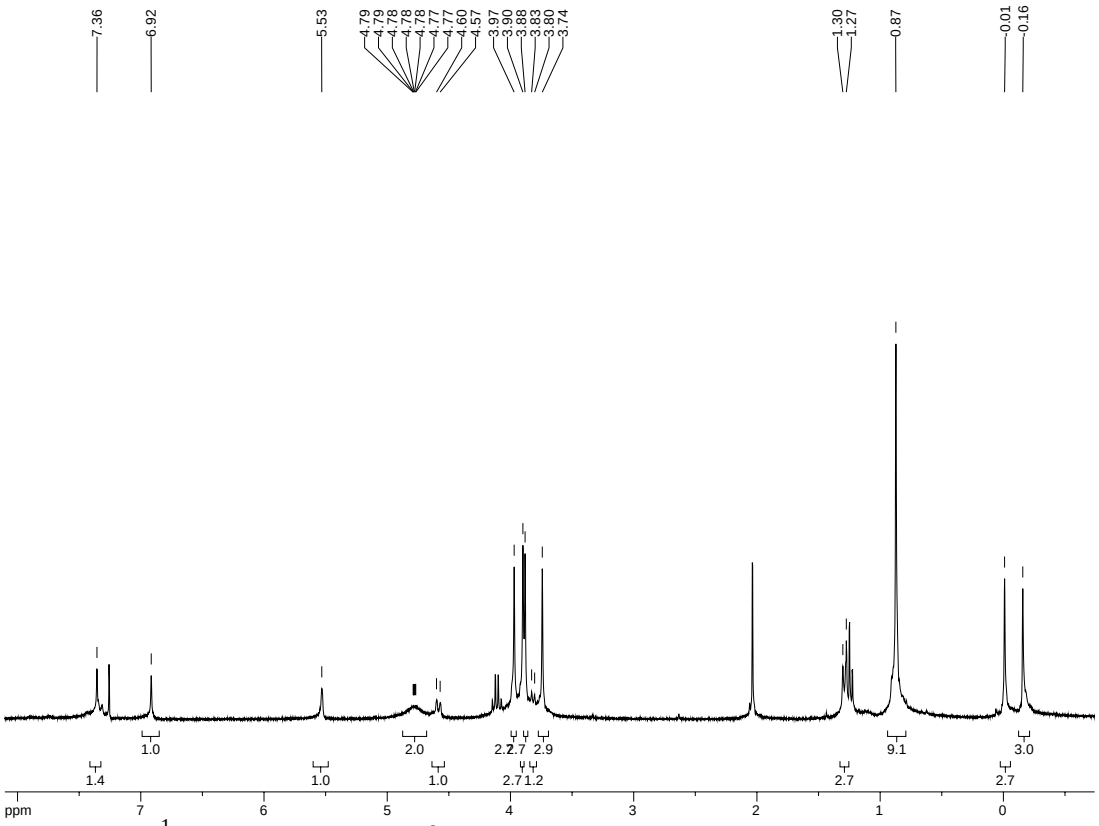

Figure 5.76a. ^{1}H NMR spectrum of compound **4.28**.

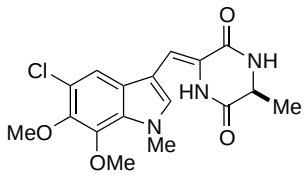

4.29

(S,Z)-3-((5-chloro-6,7-dimethoxy-1-methyl-1H-indol-3-yl)methylene)-6-methylpiperazine-2,5-dione (4.29). To a solution of amine **4.28** (69 mg, 0.167 mmol) in toluene (5 mL) was added a small amount of 2-OH-pyridine. The solution was heated to reflux O/N, then cooled to r.t. The solvent was decanted off and the remaining solid washed with toluene and dried to afford pure **4.29** (37 mg, 61% yield).

^{1}H-NMR (300 MHz; DMSO-d_6): δ 9.43 (s, 1H), 8.32 (s, 1H), 7.87 (s, 1H), 7.43 (s, 1H), 6.81 (s, 1H), 4.11 (q, *J* = 6.9 Hz, 1H), 3.96 (s, 3H), 3.93 (s, 3H), 3.81 (s, 3H), 1.32 (d, *J* = 6.8 Hz, 3H); ^{13}C-NMR (101 MHz; DMSO): δ 167.9, 160.77, 160.73, 144.2, 141.0, 133.1, 128.4, 126.3, 123.8, 120.9, 114.2, 107.2, 106.2, 62.4, 61.4, 50.7, 36.0, 19.9; HRMS (ESI-APCI+): $[M+H]^+$ 364.1064 calcd for $C_{17}H_{19}ClN_3O_4$, found: 364.1075.

REF: **TRW-II-475**, TRW-II-477.

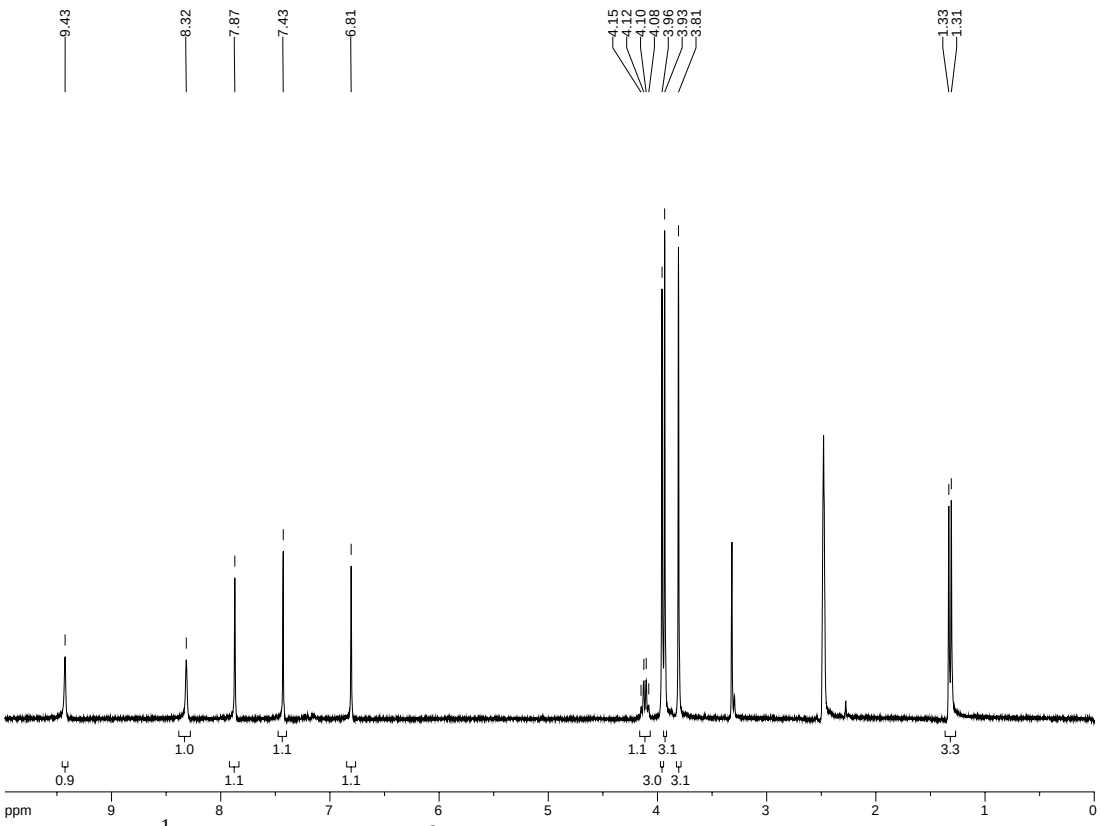

Figure 5.77a. ^{1}H NMR spectrum of compound **4.29**.

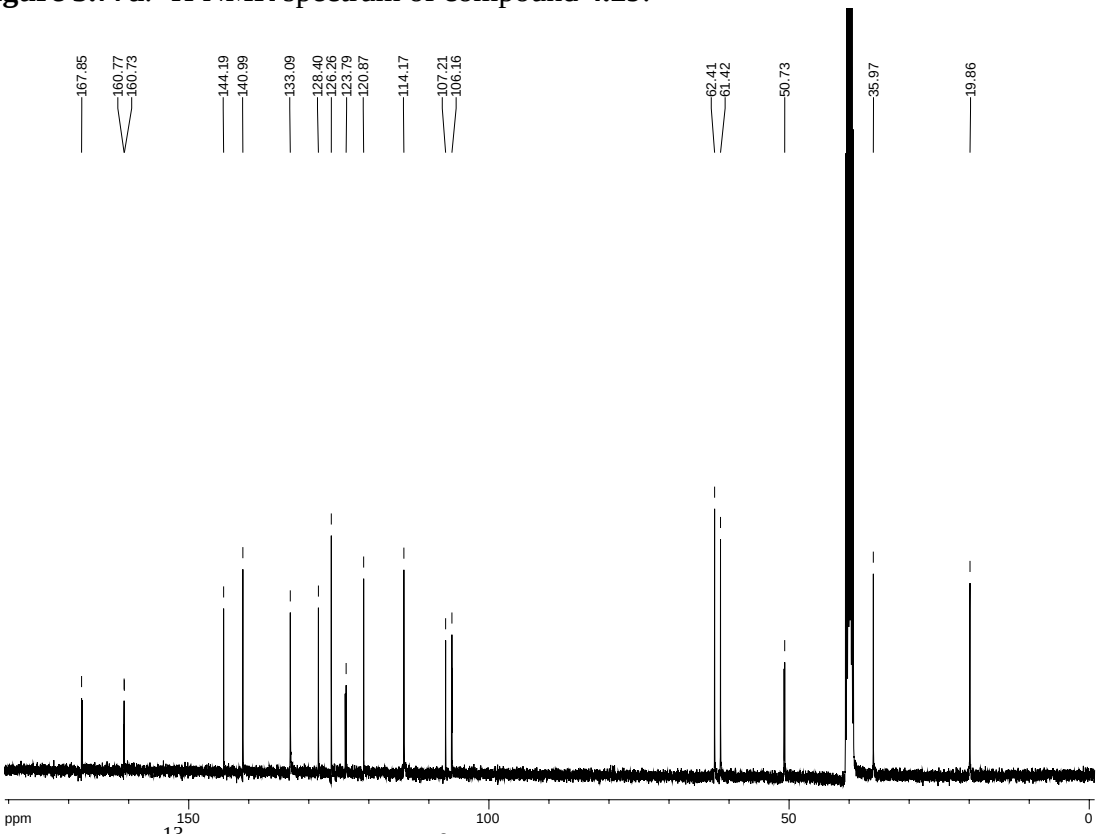

Figure 5.77b. ^{13}C NMR spectrum of compound **4.29**.

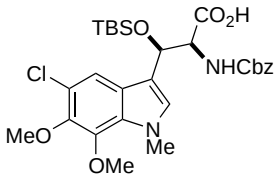

4.30

(2*S*,3*R*)-2-(((benzyloxy)carbonyl)amino)-3-((*tert*-butyldimethylsilyl)oxy)-3-(5-chloro-6,7-dimethoxy-1-methyl-1*H*-indol-3-yl)propanoic acid (4.30). To a solution of methyl ester **4.25** (682 mg, 1.2 mmol) in THF/H_2O (2:1, 2.6:1.3 mL) was added LiOH (144 mg, 6.0 mmol) and the resulting suspension stirred O/N. The reaction mixture was acidified with 10% $KHSO_4$, then the product extracted in EtOAc. The combined organic extracts were washed with brine, dried over Na_2SO_4, and concentrated to afford **4.30** (545 mg, 82% yield).

^{1}H-NMR (300 MHz; $CDCl_3$): δ 7.37-7.28 (m, 6H), 6.87 (bs, 1H), 5.62-5.58 (broad, 1H), 5.10-5.00 (m, 2H), 4.70 (s, 1H), 4.51-4.49 (bs, 1H), 3.99-3.89 (broad, 9H), 0.91-0.86 (m, 9H), 0.10-0.01 (m, 6H).

REF: **TRW-III-023**.

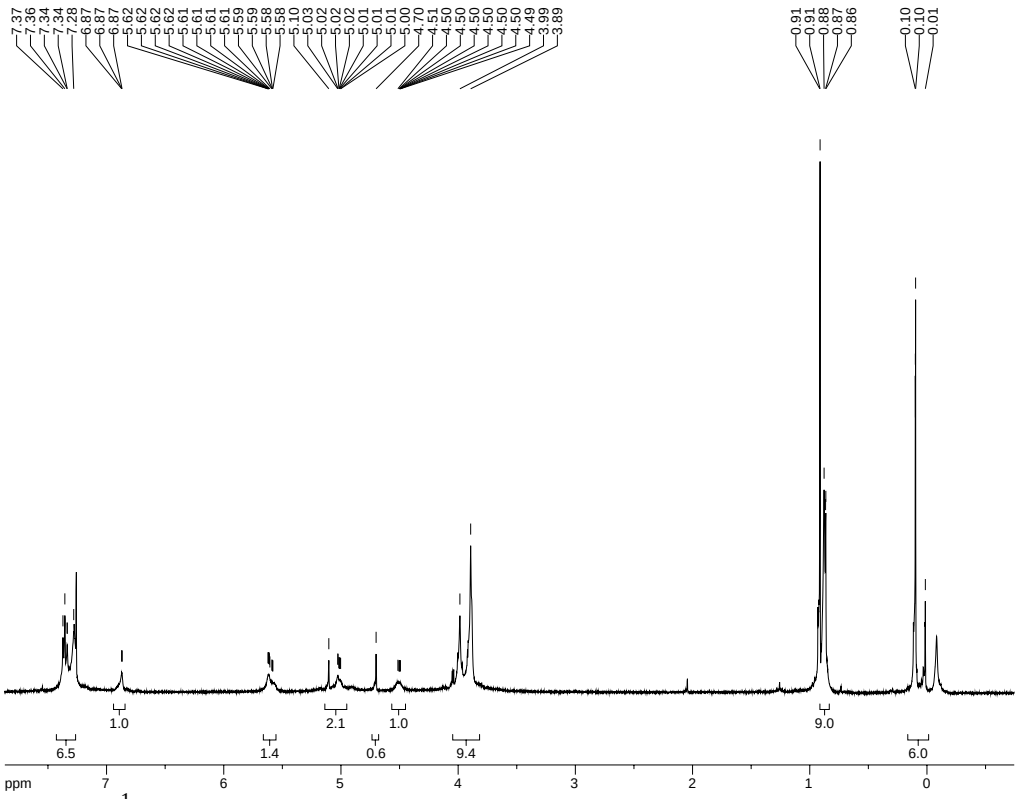

Figure 5.78a. ^{1}H NMR spectrum of compound **4.30**.

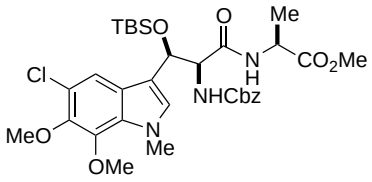

4.31

(*S*)-methyl 2-((2*S*,3*R*)-2-(((benzyloxy)carbonyl)amino)-3-((*tert*-butyldimethylsilyl)oxy)-3-(5-chloro-6,7-dimethoxy-1-methyl-1*H*-indol-3-yl)propanamido)propanoate (4.31). To a solution of acid **4.30** (100 mg, 0.173 mmol), L-Ala-OMe·HCl (24 mg, 0.173 mmol), and *i*Pr_2NEt (0.075 mL, 0.433 mmol) in CH_2Cl_2 (2 mL) was added T3P (50 wt % in DMF, 127 mg of solution). The resulting solution was stirred O/N under Ar at r.t., then quenched by addition of water. The product was extracted in EtOAc and the combined organic layers dried over Na_2SO_4 and concentrated to afford the crude material. Purification by SiO_2 chromatography (10-40% EtOAc in hexanes) gave **4.31** (39 mg, 34% yield).

^{1}H-NMR (300 MHz; $CDCl_3$): δ 7.58 (d, *J* = 7.4 Hz, 1H), 7.35 (d, *J* = 3.1 Hz, 5H), 7.04 (s, 1H), 5.56 (dd, *J* = 29.0, 5.4 Hz, 2H), 5.13-5.10 (broad, 3H), 4.76-4.74 (bs, 1H), 4.57-4.50 (m, 1H), 3.98 (s, 3H), 3.89 (d, *J* = 3.7 Hz, 6H), 3.78 (s, 3H), 1.42 (d, *J* = 7.2 Hz, 3H), 0.94 (s, 9H), 0.06 (d, *J* = 48.3 Hz, 6H).

REF: **TRW-III-026**.

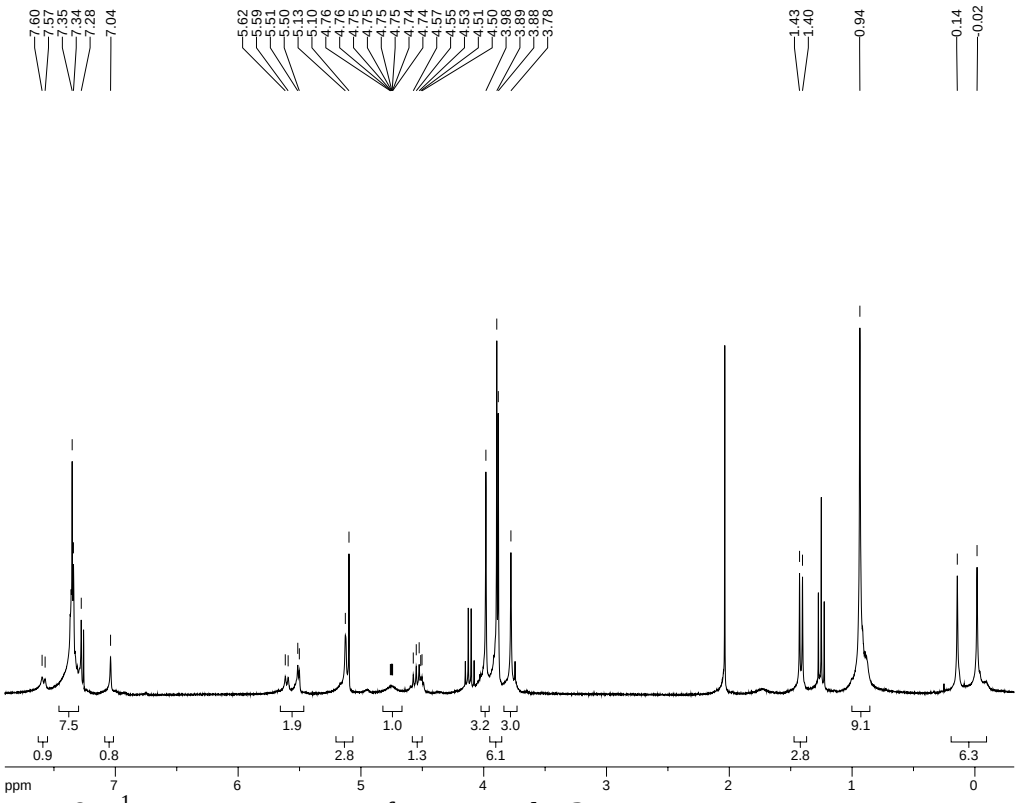

Figure 5.79a. ^{1}H NMR spectrum of compound **4.31**.

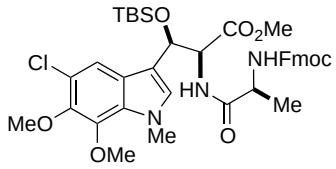

4.32

(2*S*,3*R*)-methyl 2-((*S*)-2-((((9*H*-fluoren-9-yl)methoxy)carbonyl)amino)propanamido)-3-((*tert*-butyldimethylsilyl)oxy)-3-(5-chloro-6,7-dimethoxy-1-methyl-1*H*-indol-3-yl)propanoate (4.32). To a solution of amine **4.26** (100 mg, 0.22 mmol) in CH_2Cl_2 (2.2 mL) was added *N*-Fmoc-Ala (68 mg, 0.22 mmol), *i*Pr_2NEt (0.1 mL, 0.55 mmol), and T3P (160 mg 50 wt% solution in DMF, 0.25 mmol). The resulting solution was allowed to stir O/N at r.t. under Ar, then quenched with water and the product extracted in EtOAc. The combined organic layers were dried over Na_2SO_4, filtered, and concentrated. Purification by SiO_2 chromatography (1:1 hexanes:EtOAc) afforded **4.32** in 59% yield (97 mg).

$[\alpha]_D$ = -3.9 (CH_2Cl_2); ^{1}H-NMR (300 MHz; $CDCl_3$): δ 7.76 (d, *J* = 7.5 Hz, 2H), 7.58 (d, *J* = 7.4 Hz, 2H), 7.40 (d, *J* = 7.5 Hz, 2H), 7.36 (s, 1H), 7.31 (d, *J* = 7.4 Hz, 2H), 6.85 (s, 1H), 6.65 (s, 1H), 5.54 (d, *J* = 1.4 Hz, 1H), 5.41-5.38 (m, 1H), 4.68 (dd, *J* = 9.0, 1.7 Hz, 1H), 4.33-4.27 (m, 2H), 3.97 (s, 3H), 3.89 (s, 3H), 3.86 (s, 3H), 3.79 (s, 3H), 1.36 (d, *J* = 6.8 Hz, 3H), 0.89 (s, 9H), 0.02 (s, 3H), -0.13 (s, 3H); ^{13}C-NMR (101 MHz; $CDCl_3$): δ 171.4, 165.8, 156.4, 144.4, 143.7, 143.3, 141.27, 141.15, 140.9, 135.1, 128.3, 127.78, 127.70, 127.5, 127.10, 127.06, 126.5, 124.87, 124.82, 122.4, 119.98, 119.92, 117.9, 113.9, 108.1, 67.0, 61.8, 61.2, 52.3, 51.5, 47.1, 36.0, 25.61, 25.48, 25.3, 17.94, 17.91, -3.6; IR (NaCl, film) 3302, 2953, 2857, 1714, 1462, 1254, 1040 cm^{-1}; HRMS (ESI-APCI+): $[M+Na]^+$ 772.2797 calcd for $C_{39}H_{48}ClN_3NaO_8Si$, found: 772.2799.

REF: **TRW-III-056**, TRW-III-064, TRW-III-113.

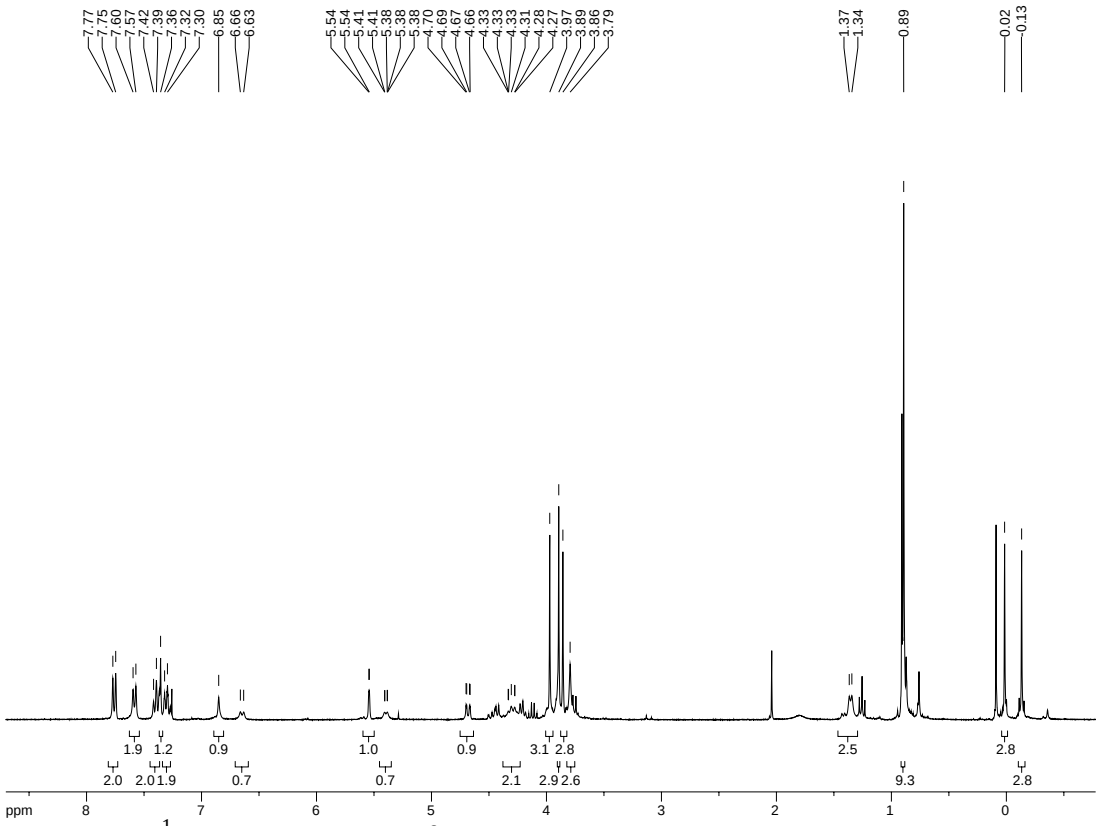

Figure 5.80a. ^{1}H NMR spectrum of compound **4.32**.

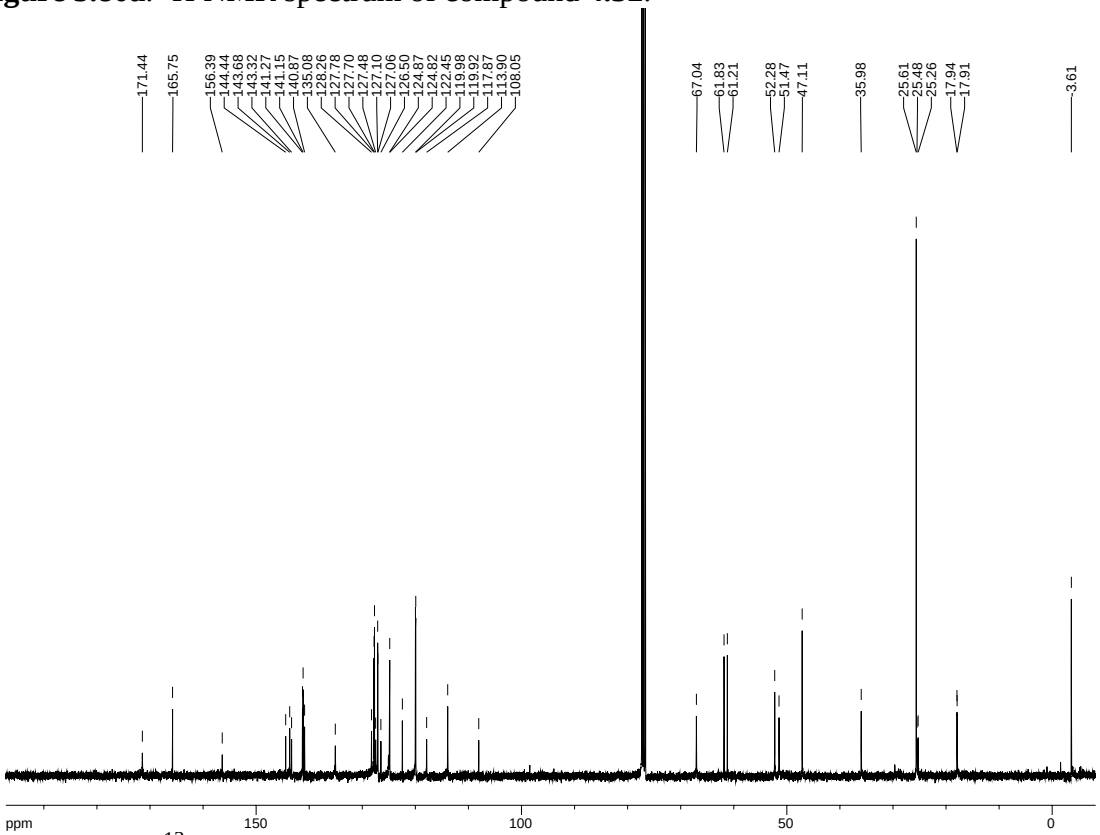

Figure 5.80b. ^{13}C NMR spectrum of compound **4.32**.

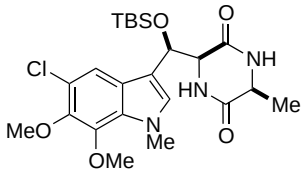

4.3

(6S)-3-((R)-((tert-butyldimethylsilyl)oxy)(5-chloro-6,7-dimethoxy-1-methyl-1H-indol-3-yl)methyl)-6-methylpiperazine-2,5-dione (4.3). Dipeptide **4.32** (350 mg, 0.47 mmol) was dissolved in THF (20 mL), then morpholine (4.7 mL) added. The resulting solution was stirred O/N at r.t., then concentrated. The crude residue was purified by SiO_2 chromatography (10% methanol in CH_2Cl_2) to afford 181 mg of the title dioxopiperazine (78% yield).

$[\alpha]_D$ = -5.8 (CH_2Cl_2); ^{1}H-NMR (300 MHz; $CDCl_3$): δ 7.31 (s, 1H), 6.98 (s, 1H), 5.67 (s, 2H), 4.13 (q, *J* = 6.7 Hz, 1H), 4.05 (d, *J* = 1.5 Hz, 1H), 4.02 (s, 3H), 3.97 (s, 3H), 3.91 (s, 3H), 3.76 (s, 1H), 1.61 (d, *J* = 7.0 Hz, 3H), 0.88 (s, 9H), 0.03 (s, 3H), -0.03 (s, 3H); ^{13}C-NMR (101 MHz; $CDCl_3$): δ 166.5, 160.4, 140.9, 136.1, 129.7, 127.4, 125.7, 122.7, 114.6, 108.6, 61.9, 61.2, 51.6, 51.3, 36.02, 36.00, 25.8, 25.6, 25.3, 20.4, 17.9, -1.6, -3.6; IR (NaCl, film) 3225, 2932, 1681, 1449, 1259, 1042 cm^{-1}; HRMS (ESI-APCI+): $[M+Na]^+$ 518.1854 calcd for $C_{23}H_{34}ClN_3NaO_5Si$, found: 518.1852.

REF: TRW-III-057, **TRW-III-065**.

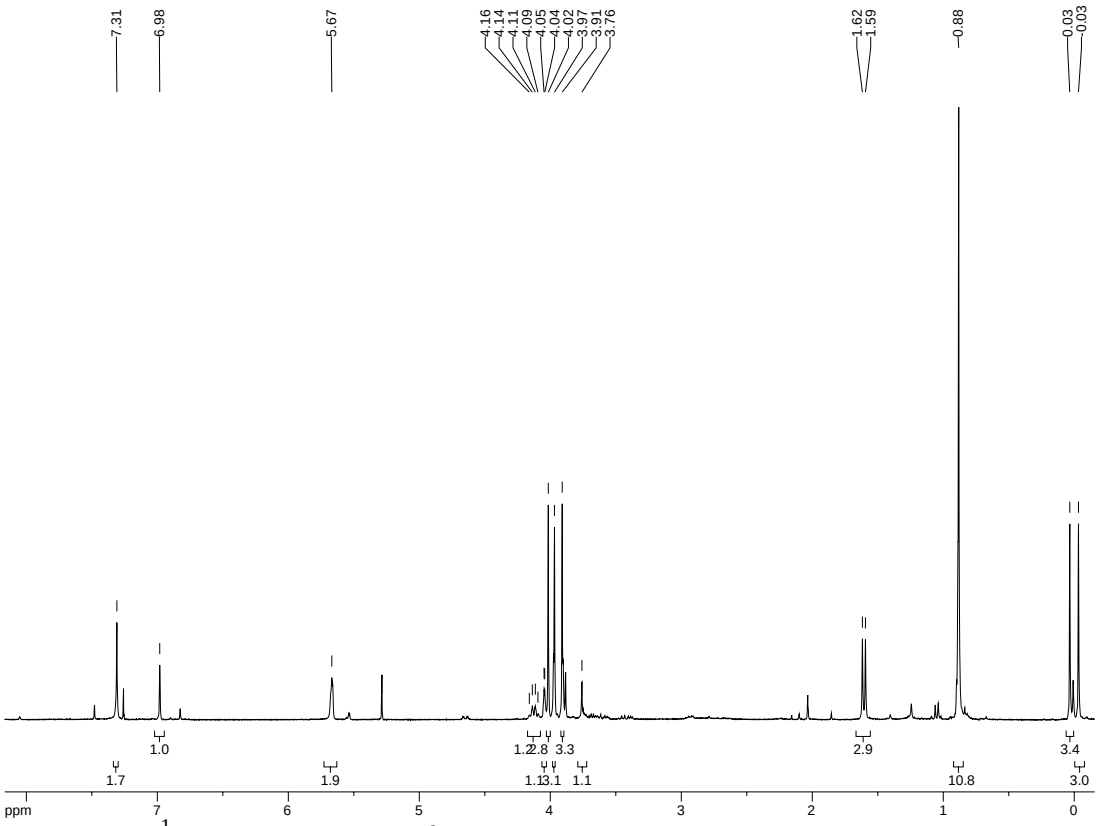

Figure 5.81a. ^{1}H NMR spectrum of compound **4.3**.

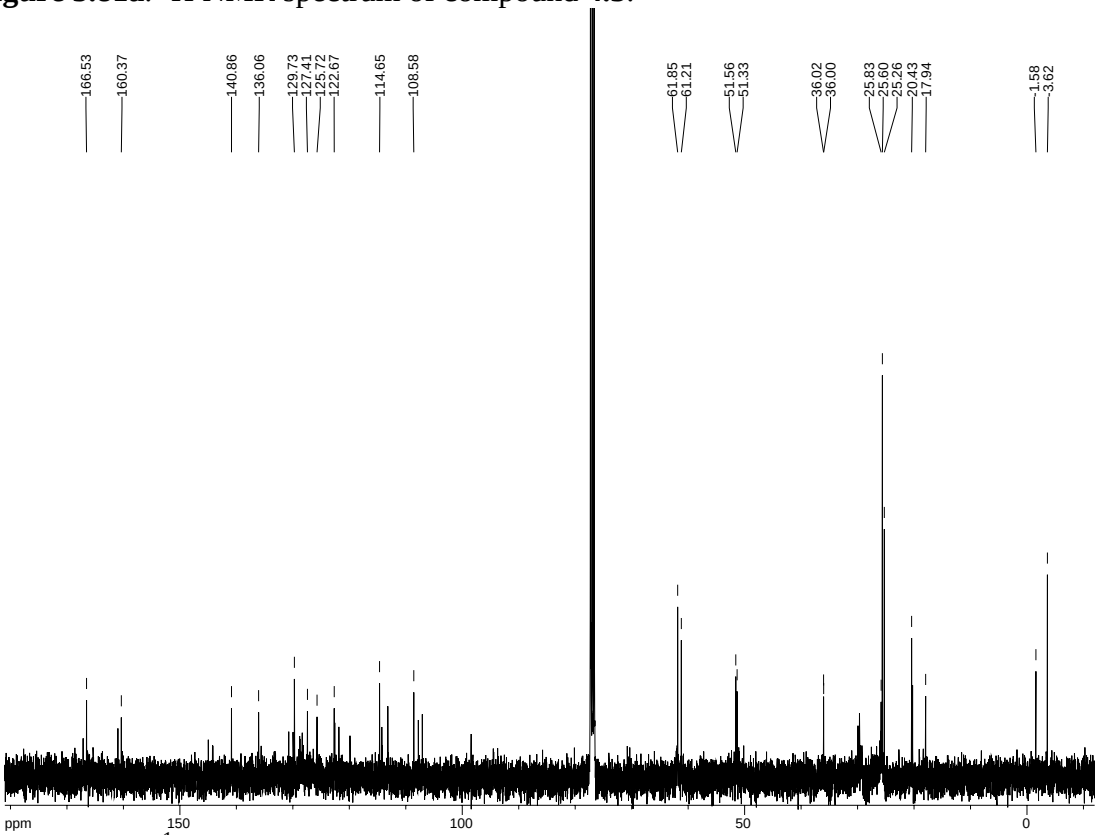

Figure 5.81b. ^{1}H NMR spectrum of compound **4.3**.

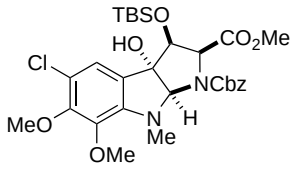

4.40

(2*S*,3*S*,3a*S*,8a*R*)-1-benzyl 2-methyl 3-((*tert*-butyldimethylsilyl)oxy)-5-chloro-3a-hydroxy-6,7-dimethoxy-8-methyl-3,3a,8,8a-tetrahydropyrrolo[2,3-*b*]indole-1,2(2*H*)-dicarboxylate (4.40). Indole **4.25** (70 mg, 0.118 mmol) was dissolved in CH_2Cl_2 (6 mL) and the resulting solution cooled to -78 °C. Freshly prepared DMDO (0.056 M in acetone, 3 mL, 0.165 mmol) was added and the reaction mixture allowed to warm to r.t. O/N. Sodium thiosulfate (sat'd aq) was added and the product extracted in CH_2Cl_2. The combined organic extracts were washed with brine, dried over Na_2SO_4, and concentrated. Purification by pTLC (40% EtOAc in hexanes) afforded pure **4.25** (6.2 mg, 9% yield).

^{1}H-NMR (400 MHz; $CDCl_3$): δ 7.46-7.40 (m, 5H), 7.05 (t, *J* = 9.1 Hz, 1H), 5.59 (s, 1H), 5.42-5.37 (m, 2H), 5.11-5.08 (m, 1H), 4.67-4.61 (m, 1H), 3.97-3.87 (m, 6H), 3.55 (s, 3H), 3.39 (s, 3H), 0.96 (s, 9H), 0.04 (d, *J* = 36.9 Hz, 6H); HRMS (ESI-APCI+): $[M+H]^+$ 607.2242 calcd for $C_{29}H_{40}ClN_2O_8Si$, found: 607.2240.

REF: TRW-III-107, **TRW-III-110**.

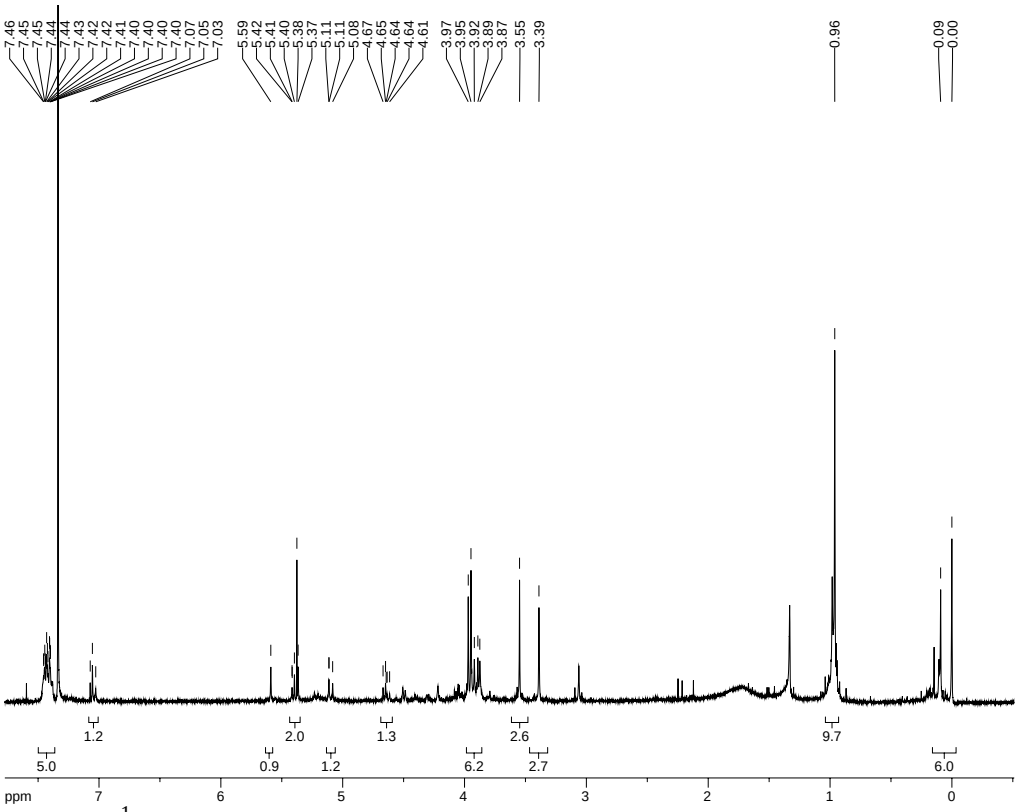

Figure 5.82a. ^{1}H NMR spectrum of compound **4.40**.

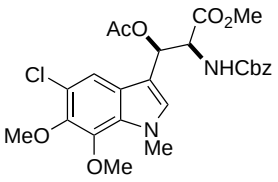

4.47

(2*S*,3*R*)-methyl 3-acetoxy-2-(((benzyloxy)carbonyl)amino)-3-(5-chloro-6,7-dimethoxy-1-methyl-1*H*-indol-3-yl)propanoate (4.47). To a solution of alcohol **4.4** (250 mg, 0.52 mmol) in THF (2.5 mL) was added Ac_2O (0.059 mL, 0.62 mmol), Et_3N (0.109 mL, 0.78 mmol), and DMAP (small amt). The resulting solution was stirred at r.t. O/N, then concentrated and 1M HCl added. The product was extracted in CH_2Cl_2, washed with brine, dried over Na_2SO_4, and concentrated. The crude material was purified by SiO_2 chromatography (1:1 hexanes:EtOAc) to afford **4.47** (150 mg, 56% yield).

^{1}H-NMR (300 MHz; $CDCl_3$): δ 7.38-7.35 (broad, 6H), 6.92 (d, *J* = 38.1 Hz, 1H), 5.61-5.54 (m, 1H), 5.18 (s, 1H), 5.09-5.06 (m, 2H), 4.82 (dd, *J* = 9.7, 3.7 Hz, 1H), 4.00-3.98 (m, 3H), 3.92-3.87 (m, 6H), 3.75 (d, *J* = 7.0 Hz, 3H), 2.17 (s, 3H).

REF: **TRW-III-137**.

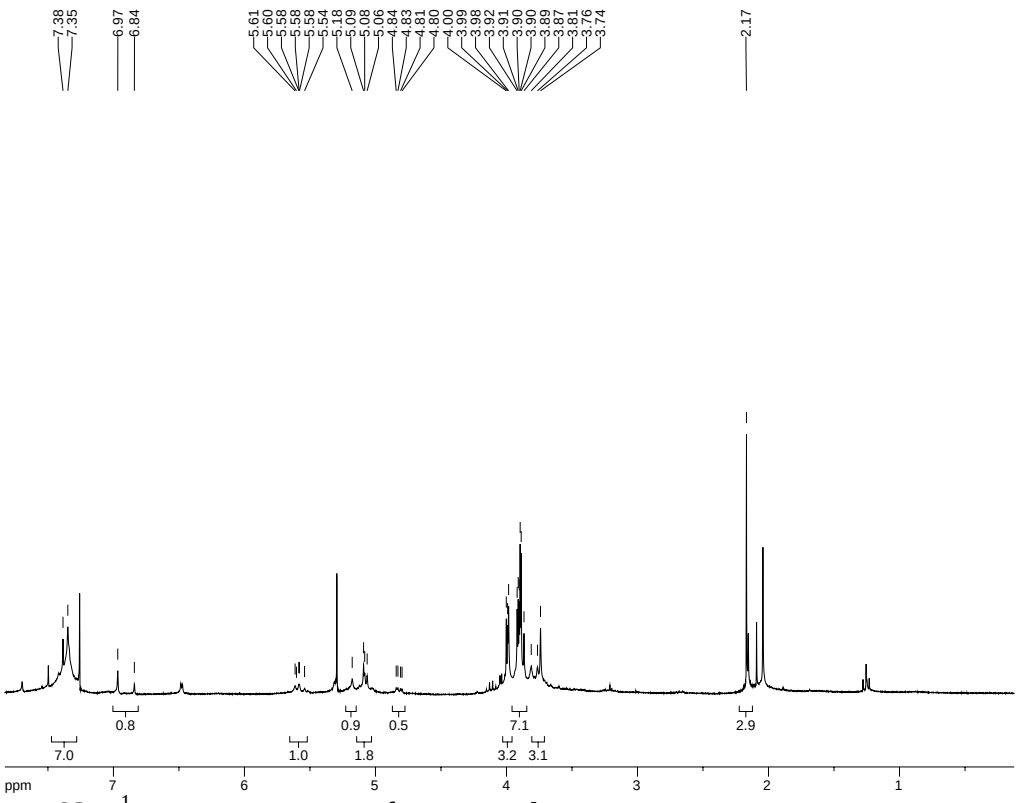

Figure 5.83a. ^{1}H NMR spectrum of compound **4.47**.

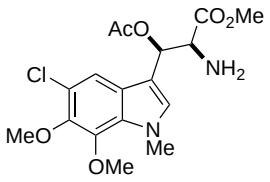

4.48

(2*S*,3*R*)-methyl 3-acetoxy-2-amino-3-(5-chloro-6,7-dimethoxy-1-methyl-1*H*-indol-3-yl)propanoate (4.48). Compound **4.47** (150 mg, 0.29 mmol) was dissolved in MeOH (1.5 mL) and to it added Pd/C (15 mg). The suspension was treated with H_2 (atm) O/N, then filtered through celite and concentrated to afford crude **4.48**, used as crude in the next step.

REF: **TRW-III-141**.

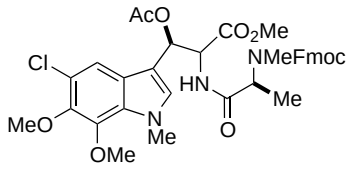

4.49

(3*R*)-methyl 2-((*S*)-2-((((9*H*-fluoren-9-yl)methoxy)carbonyl)(methyl)amino)propanamido)-3-acetoxy-3-(5-chloro-6,7-dimethoxy-1-methyl-1*H*-indol-3-yl)propanoate (4.49). Crude **4.48** (78 mg, 0.203 mmol) was dissolved in CH_2Cl_2 (2 mL) and to it added *N*-Me,Fmoc-Ala (66 mg, 0.203 mmol), *i*Pr_2NEt (0.088 mL, 0.233 mmol), and T3P (150 mg 50 wt% solution in DMF, 0.233 mmol). The resulting solution was allowed to stir O/N at r.t. under Ar, then quenched with water and the product extracted in EtOAc. The combined organic layers were dried over Na_2SO_4, filtered, and concentrated. Purification by SiO_2 chromatography afforded **4.49** in 18% yield (25 mg). A clean NMR could not be obtained for this sample.

REF: **TRW-III-145**.

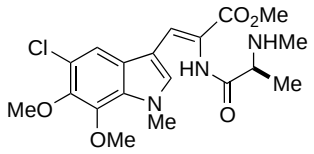

4.50

(*S*,*Z*)-methyl 3-(5-chloro-6,7-dimethoxy-1-methyl-1*H*-indol-3-yl)-2-(2-(methylamino)propanamido)acrylate (4.50). Dipeptide **4.49** (25 mg, 0.037 mmol) was dissolved in THF (1.5 mL), then morpholine (0.37 mL) added. The resulting solution was stirred O/N at r.t., then concentrated. The crude residue was purified by SiO_2 chromatography (10% methanol in CH_2Cl_2) to afford the title product as a 1:1 mixture of diasteromers (trace yield).

^{1}H-NMR (400 MHz; $CDCl_3$): δ 7.44 (d, *J* = 17.9 Hz, 2H), 6.86 (d, *J* = 4.3 Hz, 2H), 5.07 (dt, *J* = 15.5, 4.8 Hz, 2H), 4.84-4.77 (m, 2H), 3.98 (s, 3H), 3.96 (s, 3H), 3.90 (s, 3H), 3.89 (s, 3H), 3.77 (s, 3H), 3.71 (s, 2H), 3.66 (s, 3H), 3.32 (s, 3H), 3.27 (s, 3H), 2.40 (s, 3H), 2.29 (s, 3H), 1.18 (d, *J* = 6.9 Hz, 3H), 0.94 (d, *J* = 7.0 Hz, 3H); HRMS (ESI-APCI+): $[M+H]^+$ 410.1483 calcd for $C_{19}H_{25}ClN_3O_5$, found: 410.1471.

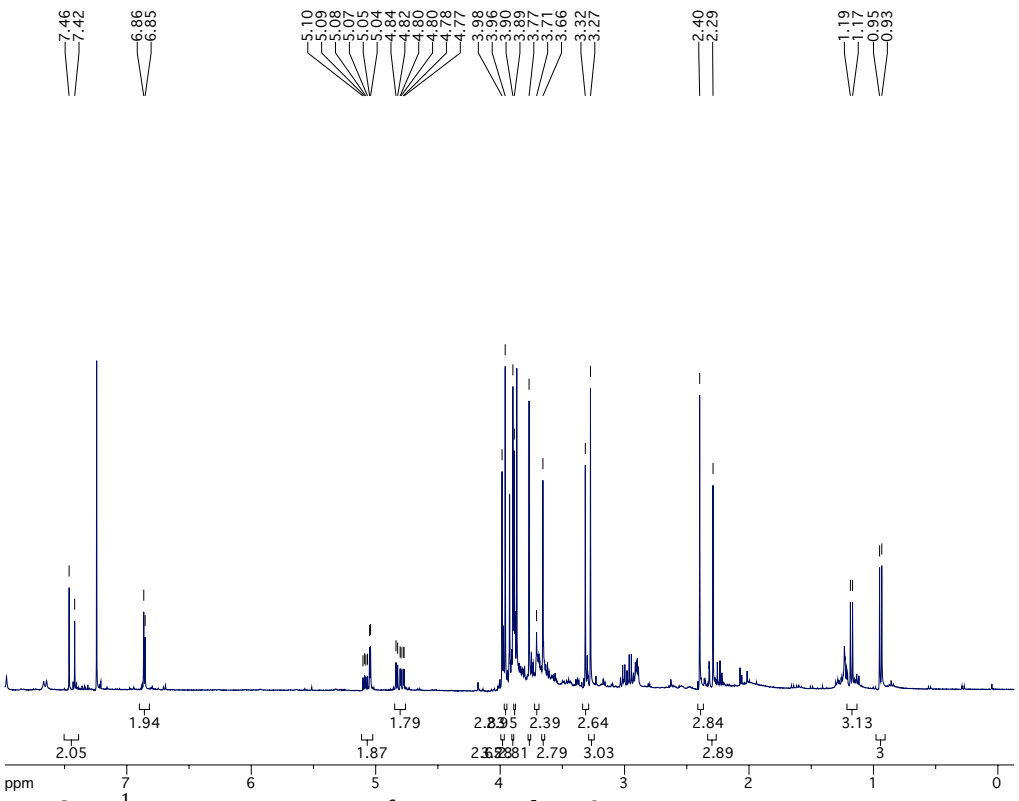

Figure 5.84a. ^{1}H NMR spectrum of compound **4.50**.

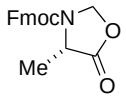

4.45

(*S*)-(9*H*-fluoren-9-yl)methyl 4-methyl-5-oxooxazolidine-3-carboxylate (4.45). To a solution of *N*-Fmoc-Ala (5.0 g, 16.1 mmol) in PhMe (50 mL) was added paraformaldehyde (3.15 g, 105 mmol) and *p*-TsOH (247 mg, 1.3 mmol). The resulting suspension was heated to reflux for 1 h with a Dean-Stark trap in place. Upon cooling, EtOAc was added and the organic phase washed with sat'd $NaHCO_3$, dried over Na_2SO_4, and concentrated to afford **4.45**, carried forward as crude.

^{1}H-NMR (300 MHz; $CDCl_3$): δ 7.78 (d, *J* = 7.3 Hz, 2H), 7.54 (d, *J* = 7.4 Hz, 2H), 7.38 (dt, *J* = 26.6, 7.4 Hz, 4H), 5.38-5.14 (broad, 3H), 4.61-4.60 (broad, 2H), 4.25 (t, *J* = 5.6 Hz, 1H), 1.51-1.14 (broad, 3H).

REF: **TRW-III-125**.

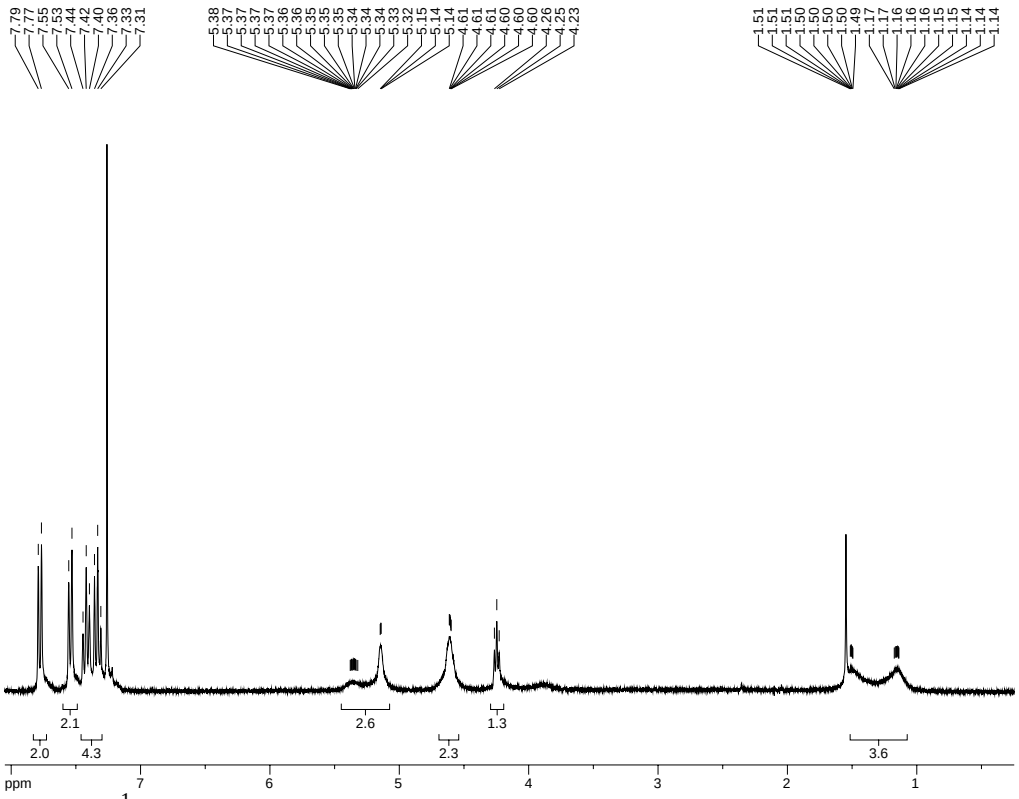

Figure 5.85a. ^{1}H NMR spectrum of compound **4.45**.

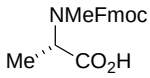

4.46

***N*-Me,Fmoc-L-Ala-OH (4.46)**. Compound **4.45** (crude, directly from previous reaction) was dissolved in $CHCl_3$ (4.1 mL) and to the resulting solution added TFA (4.1 mL) and Et_3SiH (1.0 mL). After stirring 10 h, additional Et_3SiH (3.0 mL) was added. The reaction stirred another 24 h, then was concentrated and TFA removed by repeated azeotropic distillations with toluene. The crude product was recrystallized from ether/EtOAc to afford pure **4.46** (2.87 g, 55% yield over 2 steps).

^{1}H-NMR (300 MHz; $CDCl_3$): δ 7.77 (d, *J* = 7.2 Hz, 2H), 7.61-7.53 (m, 2H), 7.43-7.29 (m, 4H), 4.76 (dq, *J* = 84.6, 7.2 Hz, 1H), 4.44 (qd, *J* = 11.3, 9.0 Hz, 2H), 4.28 (t, *J* = 6.9 Hz, 1H), 2.92 (s, 3H), 1.42 (dd, *J* = 28.0, 7.2 Hz, 3H).

REF: **TRW-III-126**.

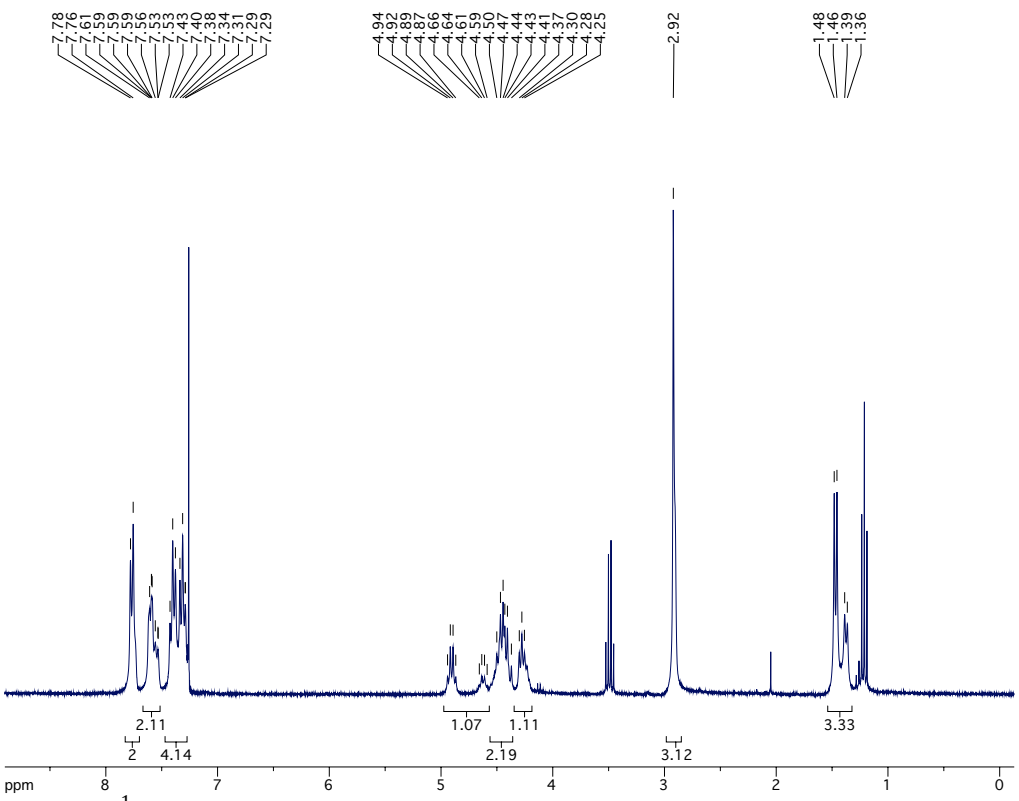

Figure 5.86a. ^{1}H NMR spectrum of compound **4.46**.

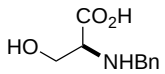

5.13

***N*-Bn-L-Ser-OH (5.13)**. To a solution of serine (14.7 g, 140 mmol) in 2M NaOH (70 mL) was added freshly distilled benzaldehyde (14.0 mL, 138 mmol). After stirring for 1 h at r.t., the reaction mixture was cooled to 0 °C and $NaBH_4$ (1.5 g, 40 mmol) added portionwise such that the internal temperature did not exceed 10 °C. The resulting solution was stirred 30 min at 5 °C, 1 h at r.t., then recooled to 0 °C. Additional $NaBH_4$ (1.5 g, 40 mmol) was added portionwise as before. The reaction was allowed to warm to r.t. as it stirred O/N. The crude reaction mixture was washed with ether (3x), then the aqueous phase acidified to pH 5 with HCl. The resulting precipitate was filtered and washed with water, then dried O/N to afford the crude product (6.55 g, 24% yield).

REF: **TRW-III-288**.

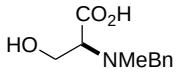

5.14

***N*-Me,Bn-L-Ser-OH (5.14)**. *N*-Bn-Ser (**5.13**, 2.49 g, 12.8 mmol) was dissolved in formic acid (1.6 mL, 38.4 mmol) and formaldehyde (37% in H_2O, 1.1 mL, 15.4 mmol) and heated to 90 °C for 2 h. The reaction mixture was concentrated, then acetone added and a solid triturated out of the solution. The suspension was concentrated, acetone added, and the trituration process repeated 3x. Following the final concentration, acetone was again added and the suspension allowed to stir 1 h at r.t, then 3 h at -20 °C. The solid was filtered, washed with cold acetone, and dried to afford **5.14** (1.47 g, 55% yield).

^{1}H-NMR (300 MHz; CD_3OD): δ 7.58-7.45 (m, 5H), 4.52 (d, *J* = 12.6 Hz, 1H), 4.37 (d, *J* = 12.7 Hz, 1H), 4.12 (qd, *J* = 11.8, 5.6 Hz, 2H), 3.73 (t, *J* = 3.5 Hz, 1H), 2.89 (s, 3H).

REF: **TRW-III-289**.

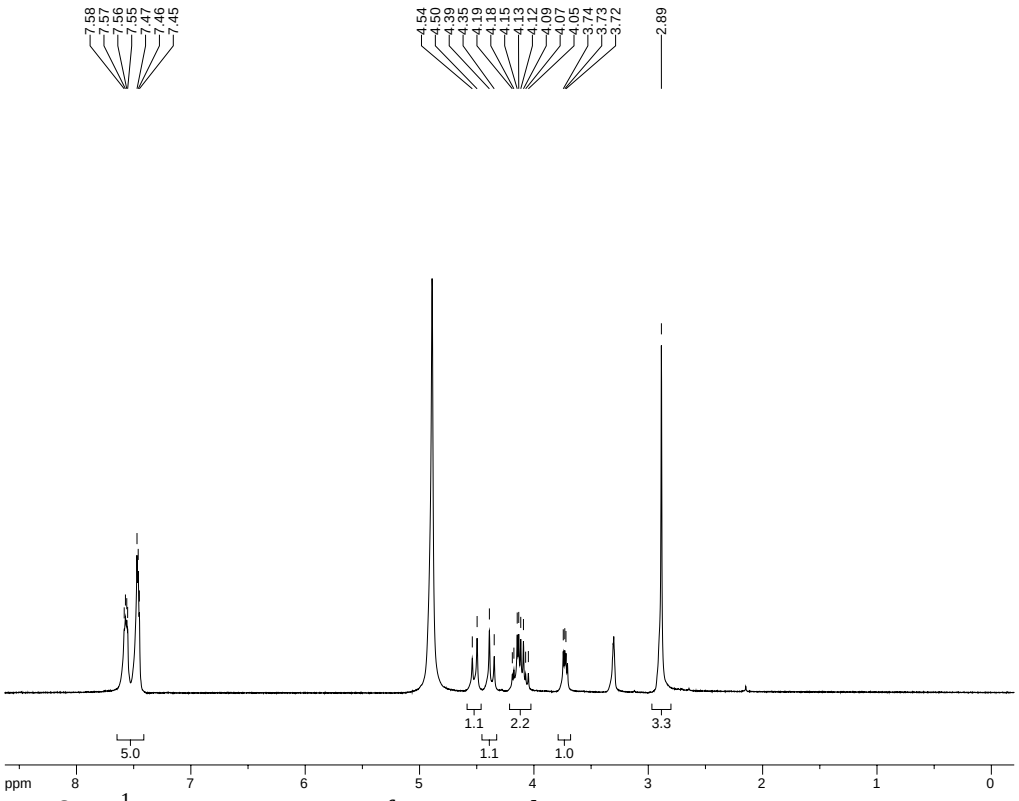

Figure 5.87a. ^{1}H NMR spectrum of compound **5.14**.

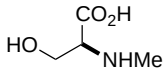

5.15

***N*-Me-L-Ser-OH (5.15)**. **5.14** (1.47 g, 7.0 mmol) was dissolved in MeOH (70 mL) and to it added $Pd(OH)_2$ (700 mg). The resulting suspension was treated with H_2 (55 psi) for 40 h, then filtered through celite and concentrated to afford the title compound (660 mg, 79% yield), carried forward as crude.

REF: **TRW-III-291**.

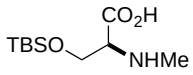

5.16

***N*-Me-L-Ser(OTBS)-OH (5.16)**. To a solution of **5.15** (660 mg, 5.55 mmol) in DMF (12 mL) was added TBSCl (923 mg, 6.11 mmol) and imidazole (755 mg, 11.1 mmol). The resulting solution was allowed to stir at r.t. O/N, then concentrated. To the crude residue was added H_2O and hexanes (1:1) and the resulting suspension stirred 4 h. The solid was filtered, rinsed with hexanes, and dried to give **5.16** (685 mg, 53% yield).

^{1}H-NMR (300 MHz; CD_3OD): δ 4.09 (d, *J* = 4.1 Hz, 2H), 3.50 (t, *J* = 4.1 Hz, 1H), 2.72 (s, 3H), 0.92 (s, 9H), 0.12 (s, 6H).

REF: **TRW-III-296**.

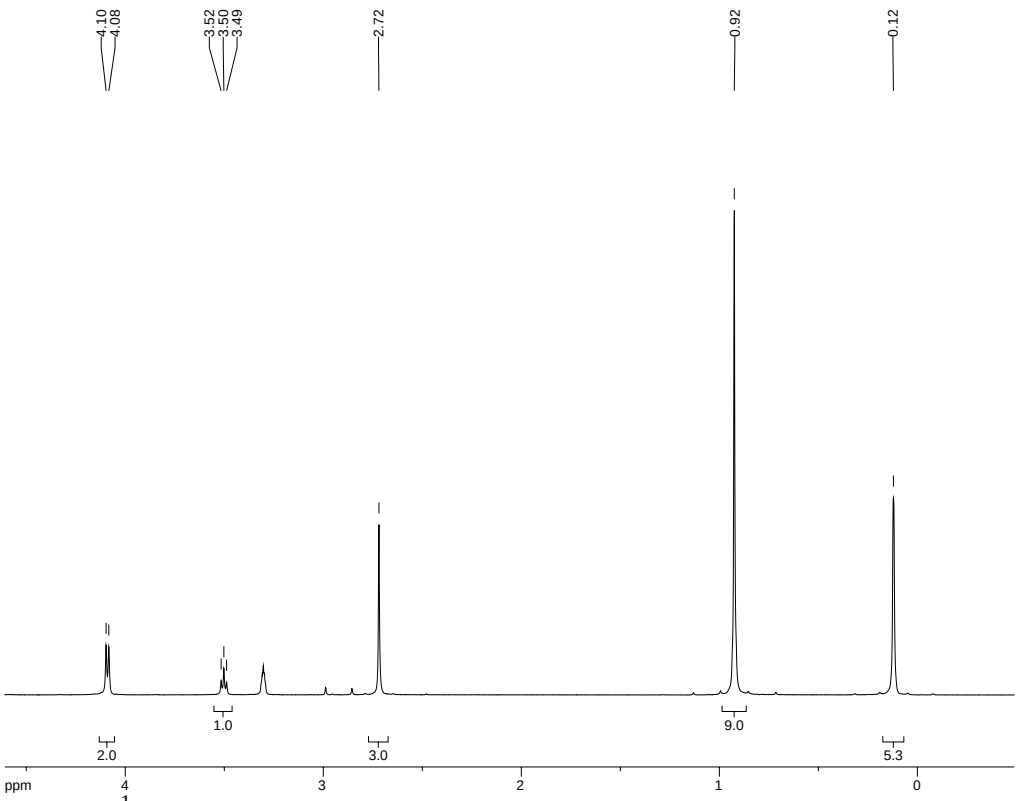

Figure 5.88a. ^{1}H NMR spectrum of compound **5.16**.

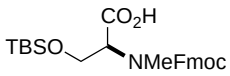

5.17

***N*-Me,Fmoc-L-Ser(OTBS)-OH (5.17)**. To a suspension of **5.16** (375 mg, 1.61 mmol) in Na_2CO_3 (aq, 10%, 3.2 mL) and dioxane (1.3 mL) at 0 °C was added dropwise FmocOSu (570 mg, 1.69 mmol) as a solution in dioxane (2.1 mL). The resulting solution was allowed to warm to r.t. as it stirred O/N. After concentration, the crude mixture was diluted with water, acidified to pH 3-4 with 10% $KHSO_4$, and the product extracted in EtOAc. The combined organic layer was washed with brine, dried over Na_2SO_4, and concentrated to afford **5.17** (663 mg, 90% yield).

^{1}H-NMR (300 MHz; $CDCl_3$): δ 7.77 (d, *J* = 7.6 Hz, 2H), 7.61 (d, *J* = 7.2 Hz, 2H), 7.36 (dt, *J* = 27.2, 7.4 Hz, 4H), 4.82 (t, *J* = 5.9 Hz, 1H), 4.49-4.40 (m, 2H), 4.30-4.22 (m, 1H), 4.14-4.05 (m, 2H), 3.88 (t, *J* = 5.1 Hz, 1H), 3.04 (d, *J* = 24.1 Hz, 3H), 0.86 (s, 9H), 0.08-0.03 (m, 6H); HRMS (ESI-APCI+): $[M+H]^+$ 456.2206 calcd for $C_{25}H_{34}NO_5Si$, found 456.2200.

REF: **TRW-III-298**.

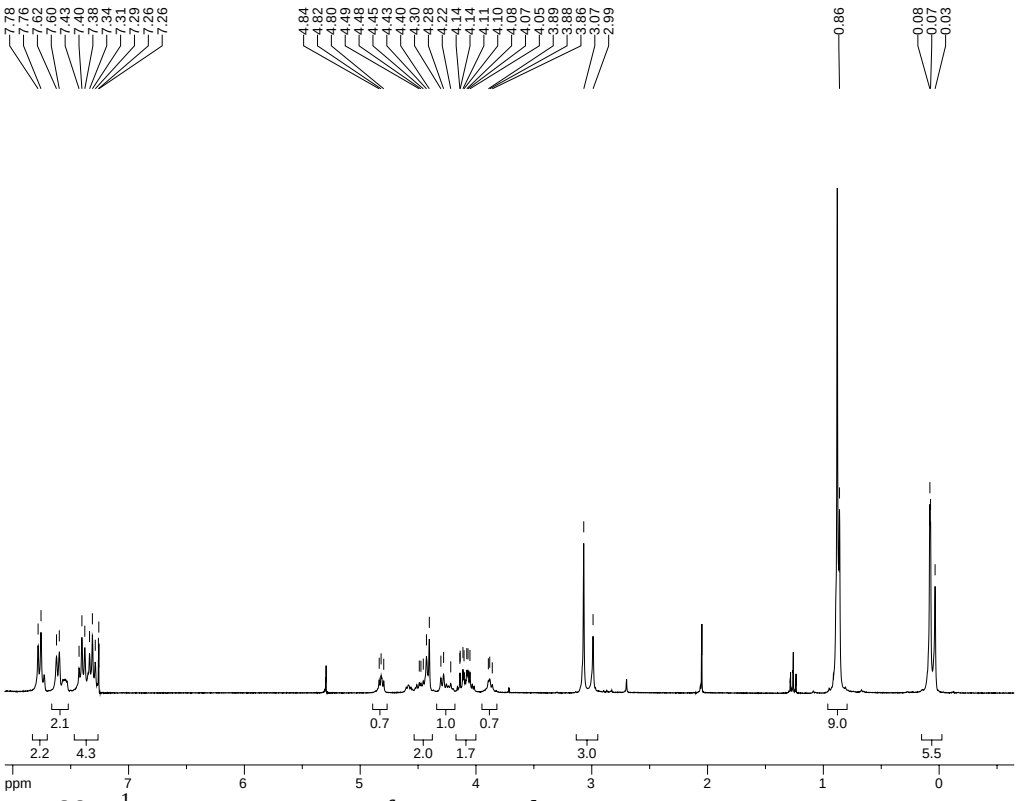

Figure 5.89a. ^{1}H NMR spectrum of compound **5.17**.

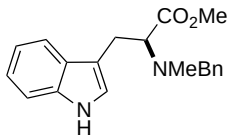

5.18

***N*-Me,Bn-L-Trp-OMe (5.18)**. To a solution of L-Trp-OMe·HCl (500 mg, 2 mmol) in MeOH (20 mL) and Et_3N (1.67 mL) was added PhCHO (212 μL, 2.1 mmol). The resulting mixture was stirred at r.t. for 1 h, then $NaBH_3CN$ (132 mg, 2.1 mmol) added. The reaction mixture was stirred overnight at r.t., at which time paraformaldehyde (180 mg, 2 mmol) was added. After full dissolution (ca. 5 h), PhCHO (132 mg, 2.1 mmol) was added and the reaction stirred overnight. The crude reaction mixture was concentrated and the residue dissolved in EtOAc, filtered through celite, and concentrated. Purification by SiO_2 chromatography (5-30% EtOAc in hexanes) afforded diprotected amine **5.18** (300 mg, 47% yield).

^{1}H-NMR (300 MHz; $CDCl_3$): δ 8.11 (s, 1H), 7.55 (d, *J* = 7.9 Hz, 1H), 7.35 (t, *J* = 4.3 Hz, 6H), 7.23 (t, *J* = 6.9 Hz, 1H), 7.14 (t, *J* = 6.9 Hz, 1H), 7.02 (d, *J* = 2.2 Hz, 1H), 3.92 (d, *J* = 13.5 Hz, 1H), 3.82 (dd, *J* = 9.1, 5.8 Hz, 1H), 3.72-3.68 (m, 4H), 3.42 (dd, *J* = 14.4, 9.1 Hz, 1H), 3.17 (ddd, *J* = 14.3, 5.8, 0.6 Hz, 1H), 2.44 (s, 3H).

REF: **TRW-I-278**, TRW-I-284.

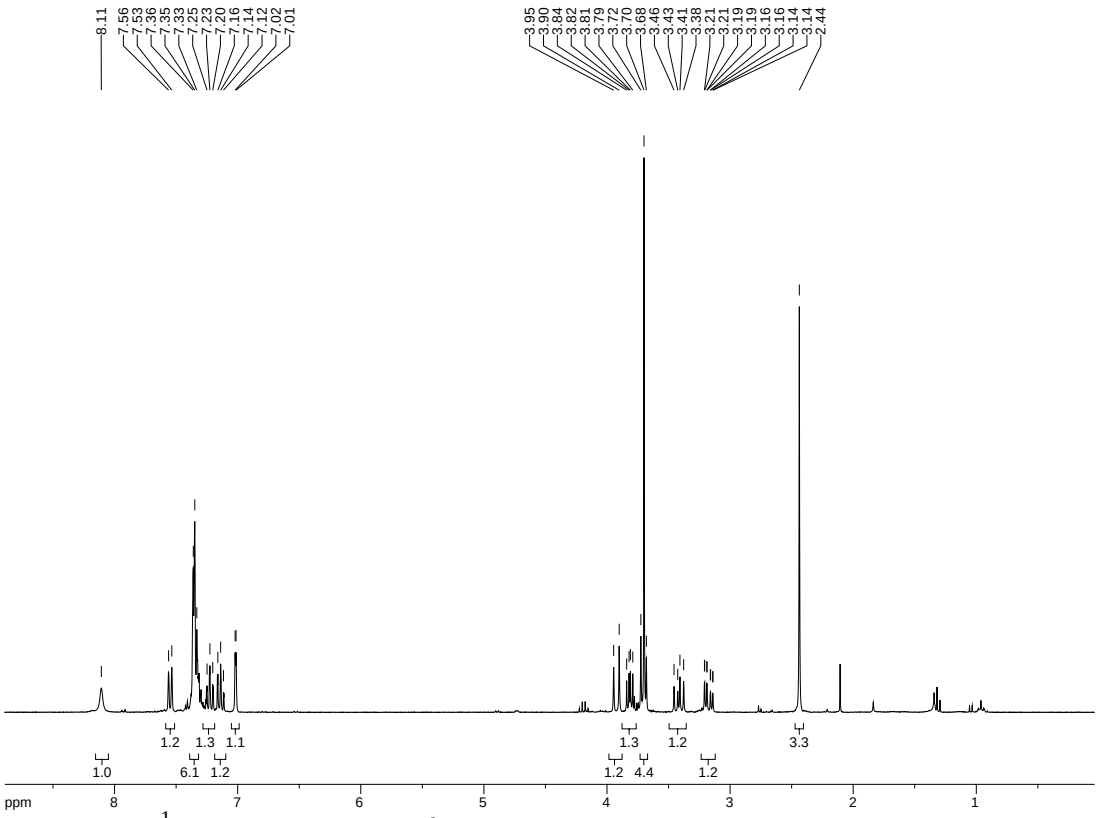

Figure 5.90a. ^{1}H NMR spectrum of compound **5.18**.

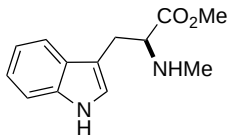

5.19

***N*-Me-L-Trp-OMe (5.19)**. To a degassed solution of **5.18** (300 mg, 0.93 mmol) in MeOH (9 mL) was added $Pd(OH)_2/C$ (150 mg). The resulting suspension was treated with H_2 (55 psi) for 18 h, then filtered through celite and concentrated to afford methylamine **5.19** (215 mg, 99.5% yield), deemed sufficiently pure to carry forward without further purification.

^{1}H-NMR (300 MHz; $CDCl_3$): δ 8.26 (s, 1H), 7.61 (d, *J* = 7.7 Hz, 1H), 7.36-7.33 (m, 1H), 7.15 (tdd, *J* = 14.4, 6.5, 1.2 Hz, 2H), 7.04 (d, *J* = 2.3 Hz, 1H), 3.66 (s, 3H), 3.57 (t, *J* = 6.6 Hz, 1H), 3.16 (qd, *J* = 13.0, 6.6 Hz, 2H), 2.38 (s, 3H), 2.05-1.99 (bs, 1H).

REF: **TRW-I-282**.

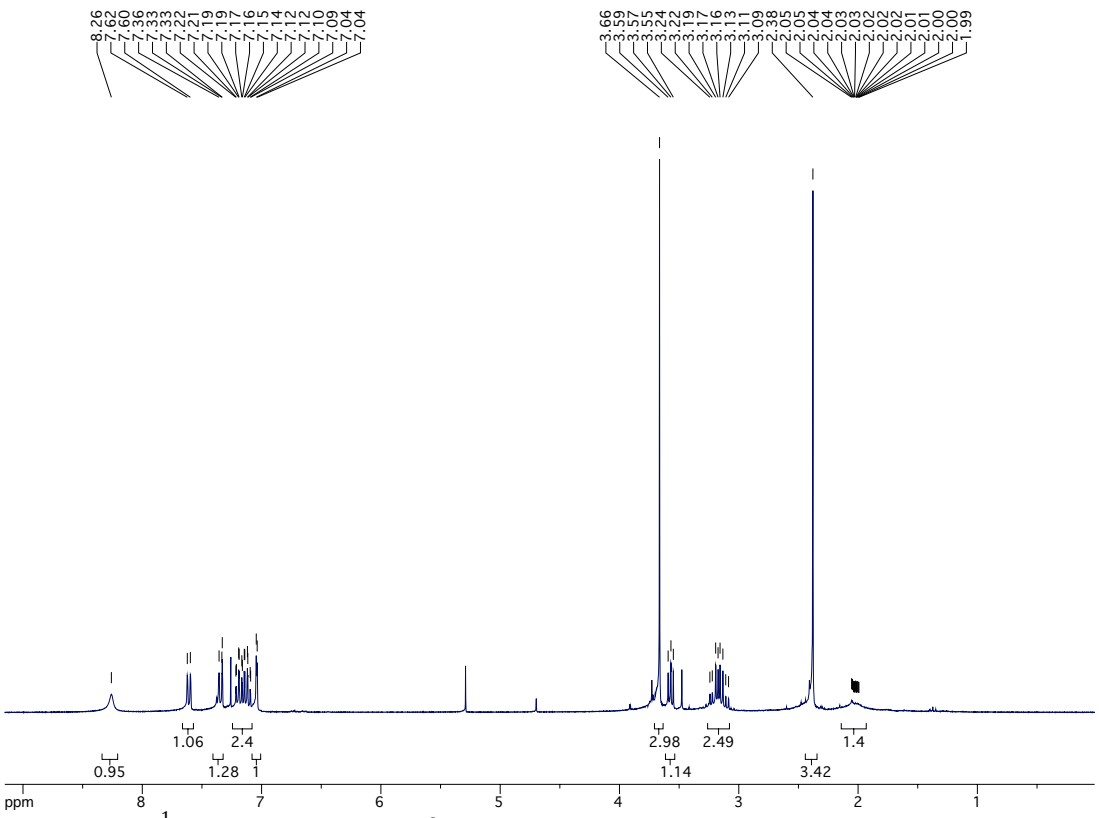

Figure 5.91a. ^{1}H NMR spectrum of compound **5.19**.

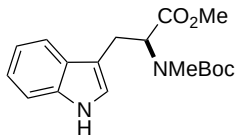

5.20

***N*-Me,Boc-L-Trp-OMe (5.20)**. To a solution of **5.19** (6.40 g, 27.6 mmol) in water/dioxane (1:1, 110 mL) was added NaOH (1.10 g, 27.6 mmol) and Boc anhydride (7.22 g, 33.1 mmol). The resulting solution was allowed to stir O/N at r.t., then acidified with HCl to pH 6-7. The product was extracted in $CHCl_3$ and the organic phase dried over Na_2SO_4 and concentrated. Crude material was purified by SiO_2 chromatography (25% EtOAc in hexanes) to afford **5.20** (4.50 g, 49% yield).

^{1}H-NMR (300 MHz; $CDCl_3$): δ 8.07-8.06 (m, 1H), 7.61 (d, *J* = 7.8 Hz, 1H), 7.36 (d, *J* = 7.5 Hz, 1H), 7.16 (dt, *J* = 21.1, 7.3 Hz, 2H), 7.06-7.00 (broad, 1H), 5.07-4.73 (m, 1H), 3.76 (s, 3H), 3.48-3.40 (m, 1H), 3.27-3.11 (m, 1H), 2.75 (d, *J* = 14.1 Hz, 3H), 1.29 (d, *J* = 61.0 Hz, 9H).

REF: **TRW-III-209**.

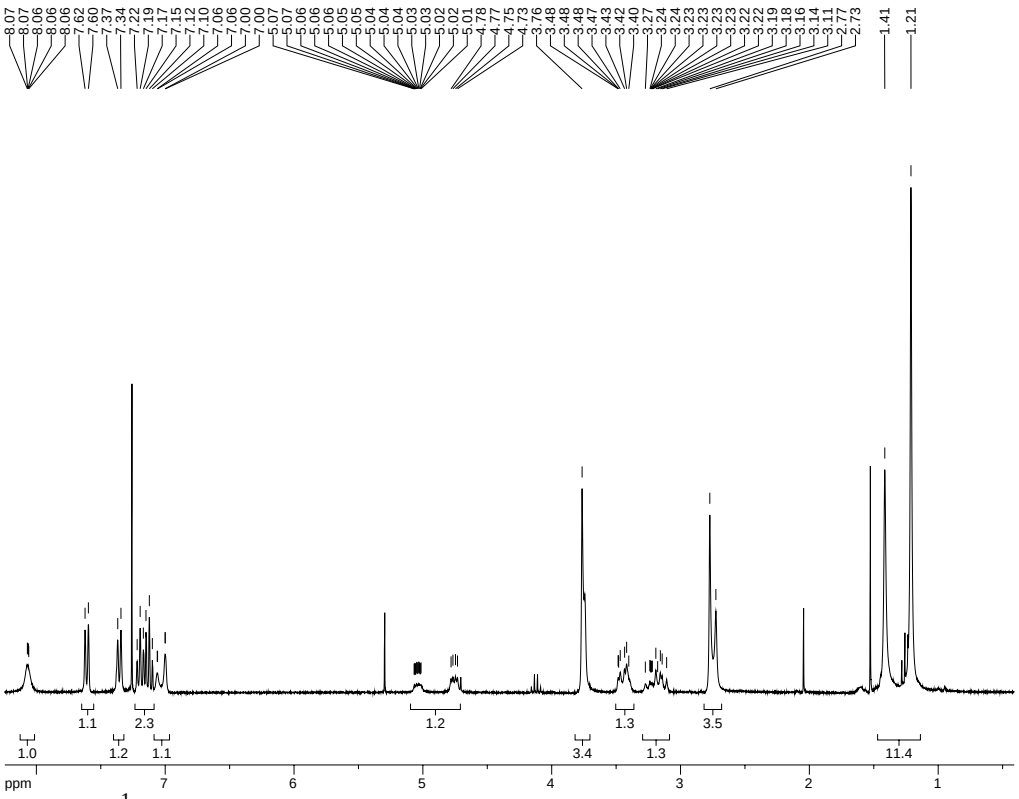

Figure 5.92a. ^{1}H NMR spectrum of compound **5.20**.

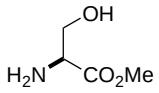

5.21

L-Ser-OMe (5.21). To a solution of L-serine (50.0 g, 0.48 mol) in MeOH (450 mL) at 0 °C was added $SOCl_2$ (35 mL, 0.48 mol). The reaction was allowed to warm to r.t. as it stirred O/N. The resulting solution was concentrated, taken up in ether, filtered, and the solid washed with ether. The crude solid material was recrystallized in MeOH/ether to afford pure crystalline methyl ester **5.21** as the HCl salt.

REF: **TRW-II-118**.

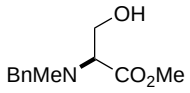

5.22

***N*-Bn,Me-L-Ser-OMe (5.22)**. To a solution of L-Ser-OMe·HCl (10.0 g, 64.1 mmol) in MeOH (500 mL) and Et_3N (50.0 mL, 385 mmol) was added PhCHO (6.8 mL, 67.3 mmol). The resulting mixture was stirred at r.t. for 1 h, then $NaBH_3CN$ (4.24 g, 67.3 mmol) added. The reaction mixture was stirred overnight at r.t., at which time paraformaldehyde (5.78 g, 64.1 mmol) was added. After full dissolution (ca. 5 h), $NaBH_3CN$ (4.24 g, 67.3 mmol) was added and the reaction stirred overnight. The crude reaction mixture was concentrated and the residue dissolved in EtOAc, filtered through celite, and concentrated. Purification by SiO_2 chromatography (2:1 hexanes:EtOAc) afforded diprotected amine **5.22** (7.41 g, 52% yield).

^{1}H-NMR (300 MHz; $CDCl_3$): δ 7.37-7.29 (m, 5H), 4.69 (d, *J* = 5.9 Hz, 1H), 3.79-3.71 (m, 5H), 3.54 (dd, *J* = 8.8, 6.6 Hz, 1H), 2.78 (dd, *J* = 8.6, 3.0 Hz, 1H), 2.33 (s, 3H).

REF: **TRW-II-019**, TRW-II-120, TRW-III-208.

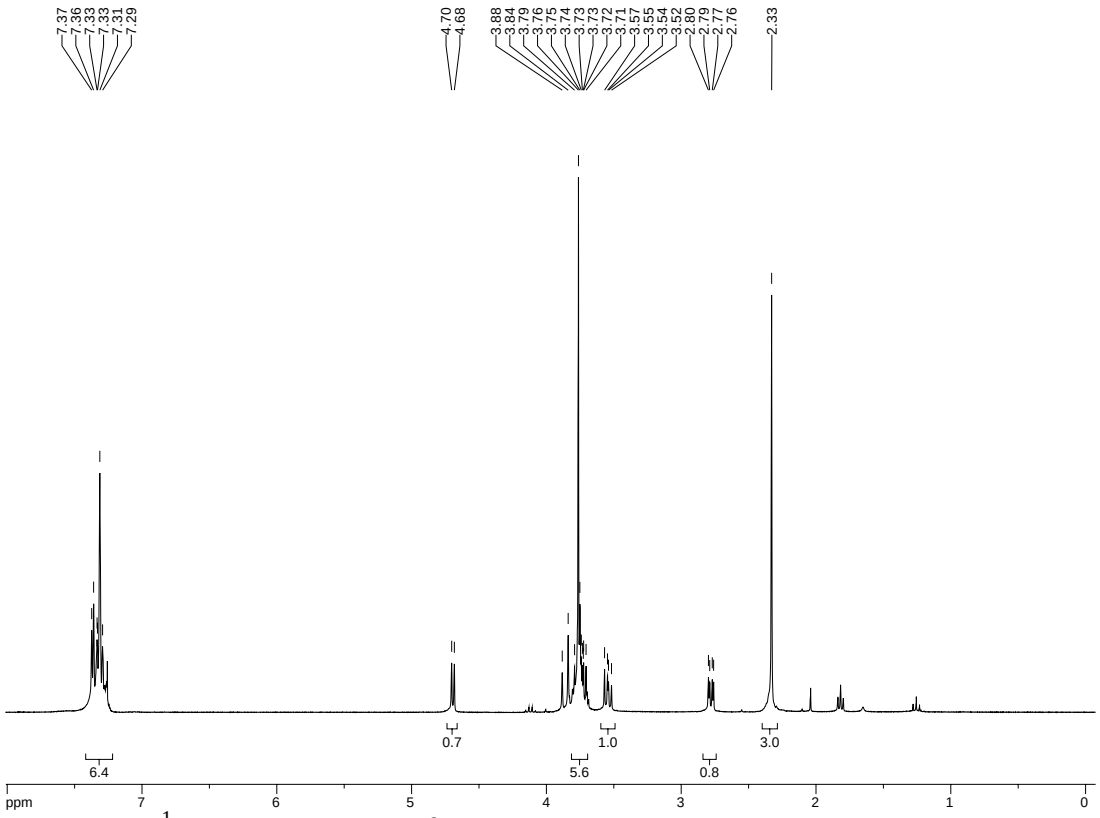

Figure 5.93a. ^{1}H NMR spectrum of compound **5.22**.

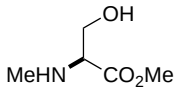

5.23

***N*-Me-L-Ser-OMe (5.23)**. To a degassed solution of **5.22** (3.7 g, 16.6 mmol) in MeOH (140 mL) was added $Pd(OH)_2$ (1.85 g). The resulting suspension was treated with H_2 (55 psi) for 18 h, then filtered through celite and concentrated to afford methylamine **5.23** (99.5% yield), deemed sufficiently pure to carry forward without further purification.

^{1}H-NMR (300 MHz; $CDCl_3$): δ 3.82-3.77 (m, 4H), 3.63 (dd, *J* = 10.9, 6.1 Hz, 1H), 3.28 (t, *J* = 5.2 Hz, 1H), 2.43 (s, 3H).

REF: **TRW-II-020**, TRW-II-123.

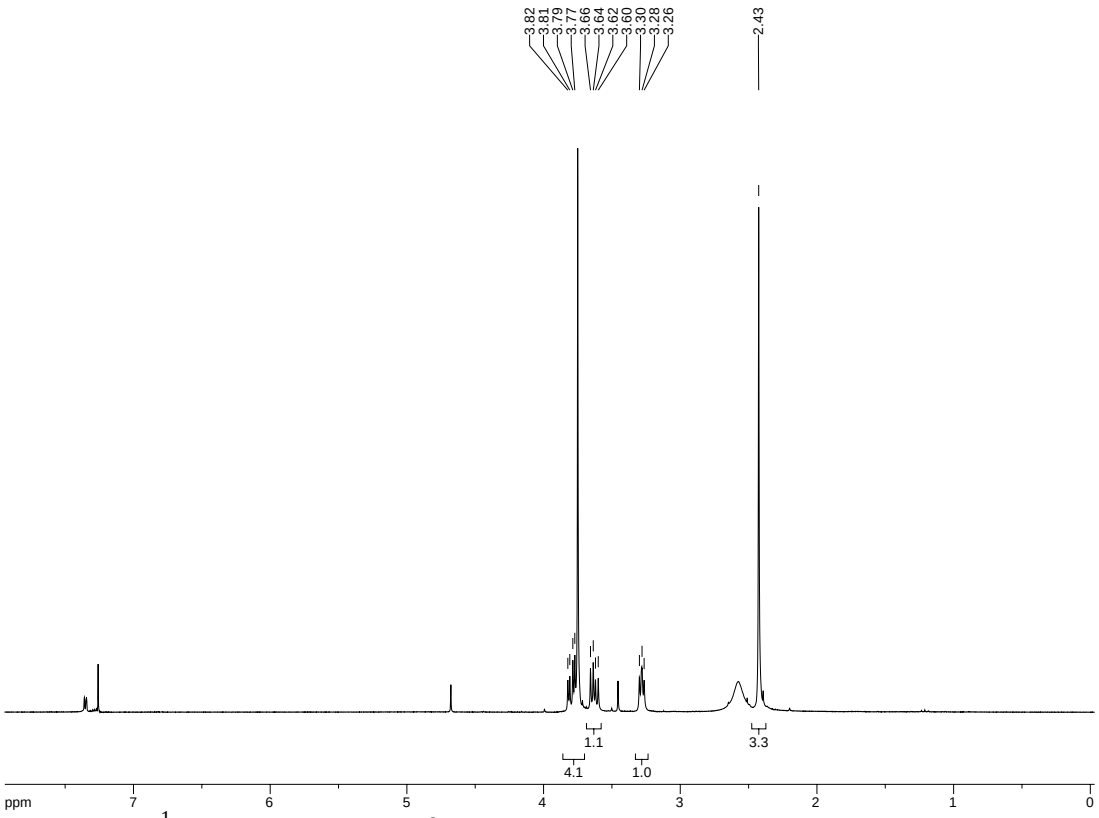

Figure 5.94a. ^{1}H NMR spectrum of compound **5.23**.

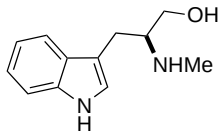

5.24

3-(1*H*-indol-3-yl)-2-(methylamino)propan-1-ol (5.24). To a suspension of LAH (813 mg, 21.4 mmol) in THF (20 mL) at 0°C was added methyl ester **5.19** (1.70 g, 5.35 mmol) dropwise. The resulting mixture was heated to reflux and stirred O/N. After cooling to 0°C, 15% NaOH (8 mL) was added and the reaction stirred an additional 1 h at r.t. The suspension was filtered through celite and the filtrate dried over Na_2SO_4 before concentrating to afford 1.09 g (100% yield) of methylamine alcohol **5.24**.

^{1}H-NMR (300 MHz; $CDCl_3$): δ 8.76 (s, 1H), 7.62 (d, *J* = 7.7 Hz, 1H), 7.34 (d, *J* = 8.0 Hz, 1H), 7.23-7.10 (m, 2H), 6.92 (s, 1H), 3.71 (dd, *J* = 11.5, 2.1 Hz, 1H), 3.47 (dd, *J* = 10.9, 4.3 Hz, 1H), 2.98-2.90 (m, 3H), 2.41 (s, 3H).

REF: TRW-I-294, **TRW-I-310**, TRW-I-323, TRW-I-327.

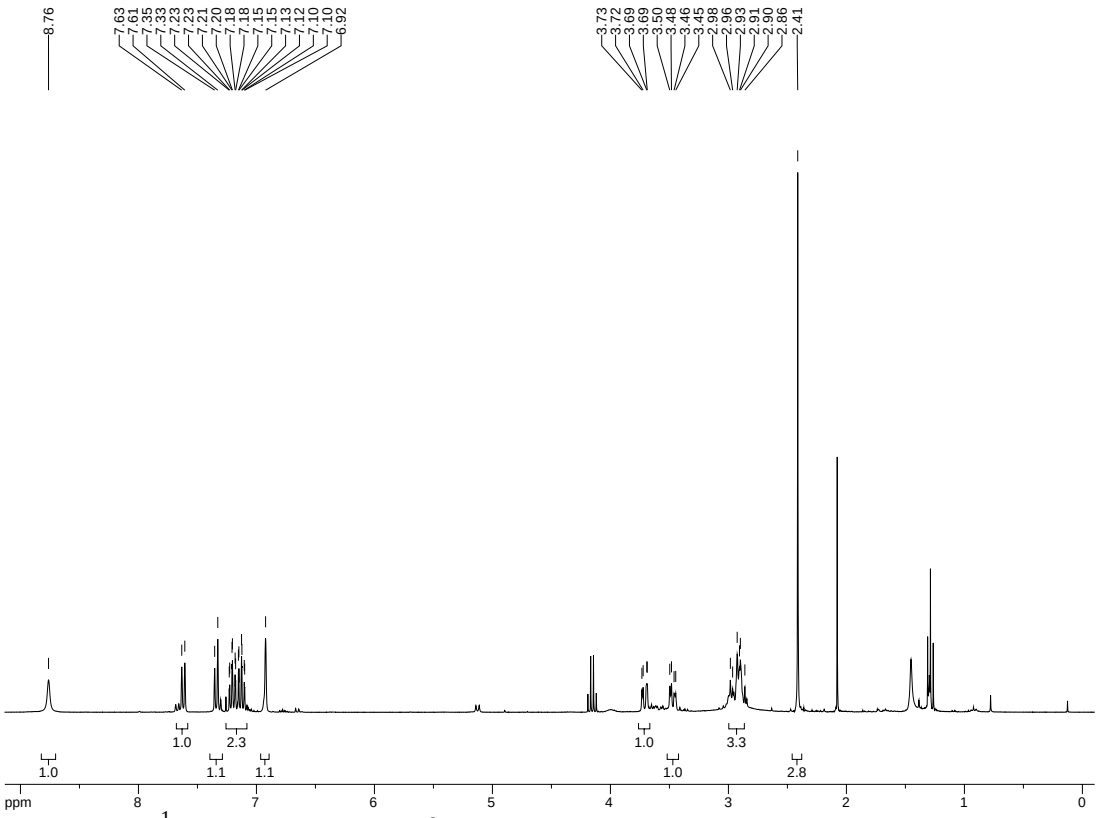

Figure 5.95a. ^{1}H NMR spectrum of compound **5.24**.

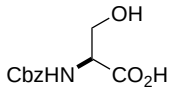

5.25

***N*-Cbz-L-Ser-OH (5.25)**. To a solution of L-Ser (10.0 g, 95 mmol) in saturated aqueous $NaHCO_3$ (380 mL) was added CbzCl (15 mL, 100 mmol). The resulting solution was stirred O/N at r.t., then acidified to ph 4 with 1M HCl. The product was extracted in EtOAc (3x), and the combined organic layers dried and concentrated to afford *N*-Cbz-L-Ser-OH (21.78 g, 96% yield).

^{1}H-NMR (300 MHz; CD_3OD): δ 7.38-7.28 (m, 5H), 5.10 (s, 2H), 4.27 (t, *J* = 4.3 Hz, 1H), 3.91-3.80 (m, 2H).

REF: **TRW-II-337**, TRW-II-398.

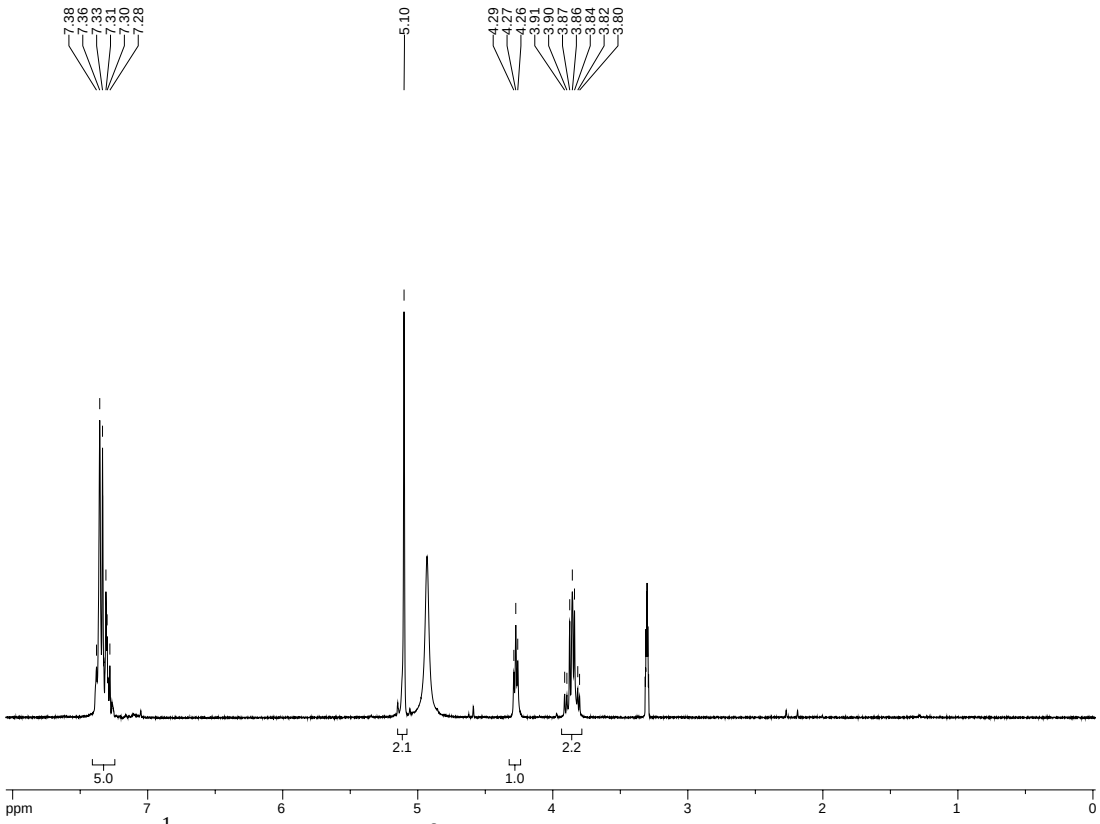

Figure 5.96a. ^{1}H NMR spectrum of compound **5.25**.

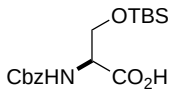

5.26

***N*-Cbz-L-Ser(OTBS)-OH (5.26)**. *N*-Cbz-L-Ser-OH (10.0 g, 41.8 mmol), TBSCl (6.95 g, 46.0 mmol), and imidazole (5.68 g, 83.6 mmol) were dissolved in DMF (100 mL). The resulting solution was stirred at r.t. under Ar for 48 h before concentrating. The residue was suspended in hexanes and the product extracted into 5% aqueous $NaHCO_3$. $KHSO_4$ (1M) was added to acidify the aqueous layer to pH 3, from which the product was extracted into EtOAc. The combined organic extracts were washed with brine, dried over Na_2SO_4, and concentrated to afford *N*-Cbz-L-Ser(OTBS)-OH (10.04 g, 68% yield).

^{1}H-NMR (300 MHz; $CDCl_3$): δ 7.33-7.30 (m, 5H), 5.08 (d, *J* = 3.4 Hz, 2H), 4.33-4.31 (m, 1H), 4.05 (dd, *J* = 10.2, 2.8 Hz, 1H), 3.82 (dd, *J* = 10.2, 2.8 Hz, 1H), 0.82 (d, *J* = 2.8 Hz, 9H), -0.02 (s, 6H).

REF: TRW-II-198, **TRW-II-338**, TRW-II-399.

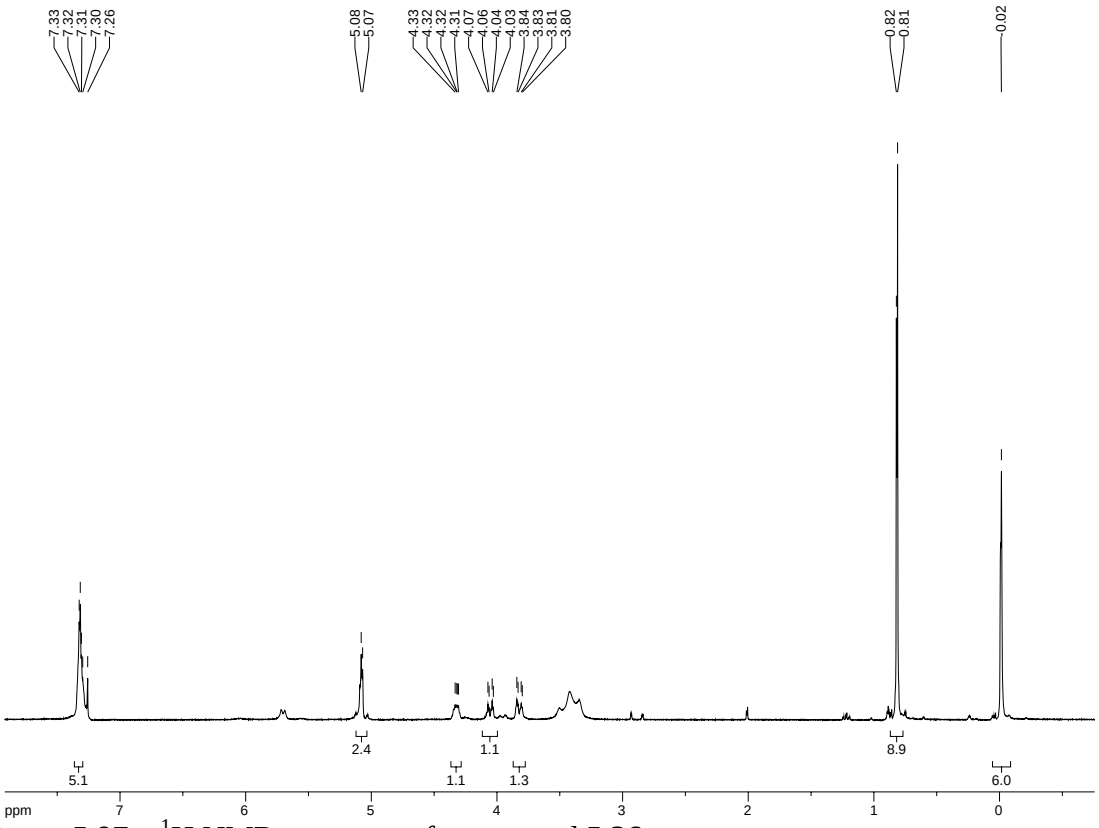

Figure 5.97a. ^{1}H NMR spectrum of compound **5.26**.

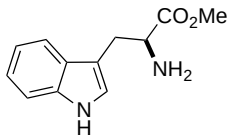

5.27

L-Trp-OMe·HCl (5.27). To a solution of L-tryptophan (25 g, 123 mmol) in MeOH (250 mL) at 0 °C was added $SOCl_2$ (8.9 mL, 123 mmol) dropwise. The reaction was allowed to warm to r.t. as it stirred O/N. Upon completion, the reaction was concentrated, then MeOH (2x) and ether (3x) separately added and the mixture concentrated to thoroughly dry the crude product. Pure L-tryptophan-OMe·HCl crystals were recovered following recrystallization in MeOH/ether (25.08 g, 80% yield).

^{1}H-NMR (300 MHz; CD_3OD): δ 10.62 (bs, 1H), 7.53 (d, *J* = 7.8 Hz, 1H), 7.39 (d, *J* = 8.1 Hz, 1H), 7.20 (d, *J* = 2.3 Hz, 1H), 7.17-7.03 (m, 2H), 4.33 (dd, *J* = 7.4, 5.5 Hz, 1H), 3.79 (s, 3H), 3.42 (dq, *J* = 24.1, 7.9 Hz, 2H).

REF: **TRW-II-391**.

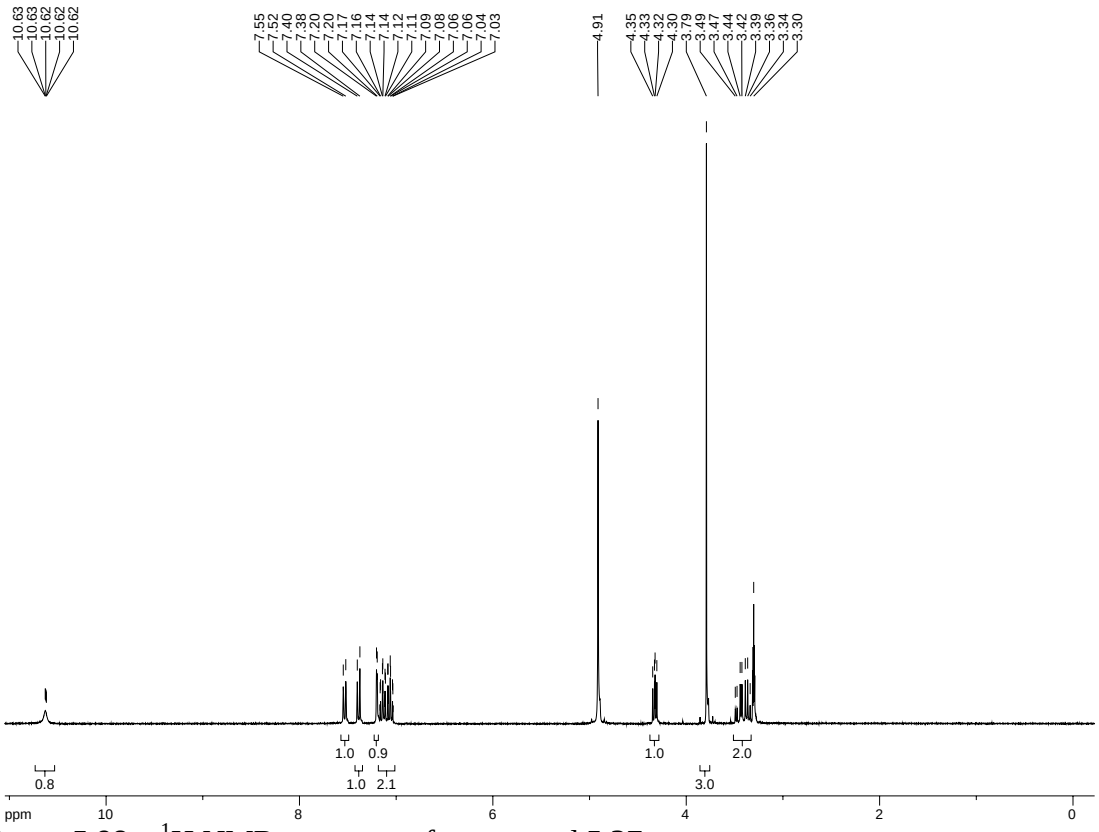

Figure 5.98a. ^{1}H NMR spectrum of compound **5.27**.

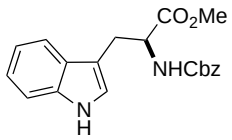

5.28

***N*-Cbz-L-Trp-OMe (5.28)**. To a suspension of L-tryptophan-OMe·HCl (15 g, 58.8 mmol) in dioxane (75 mL) at 0 °C was added 1M NaOH (60 mL). CbzCl (9.7 mL, 64.7 mmol) was added, followed by a second portion of 1M NaOH (60 mL). The reaction mixture was allowed to stir for 20 minutes at 0 °C, then diluted with EtOAc. The organic layer was separated, washed with 1M HCl and brine, then dried and concentrated to afford the title compound.

^{1}H-NMR (300 MHz; $CDCl_3$): δ 8.22 (bs, 1H), 7.53 (d, *J* = 7.9 Hz, 1H), 7.34 (bs, 6H), 7.26-7.17 (m, 2H), 7.13-7.08 (m, 1H), 6.93 (s, 1H), 5.39 (d, *J* = 8.1 Hz, 1H), 5.11 (d, *J* = 4.4 Hz, 2H), 4.77-4.70 (m, 1H), 3.68 (s, 3H), 3.32 (d, *J* = 5.3 Hz, 2H).

REF: **TRW-II-448**.

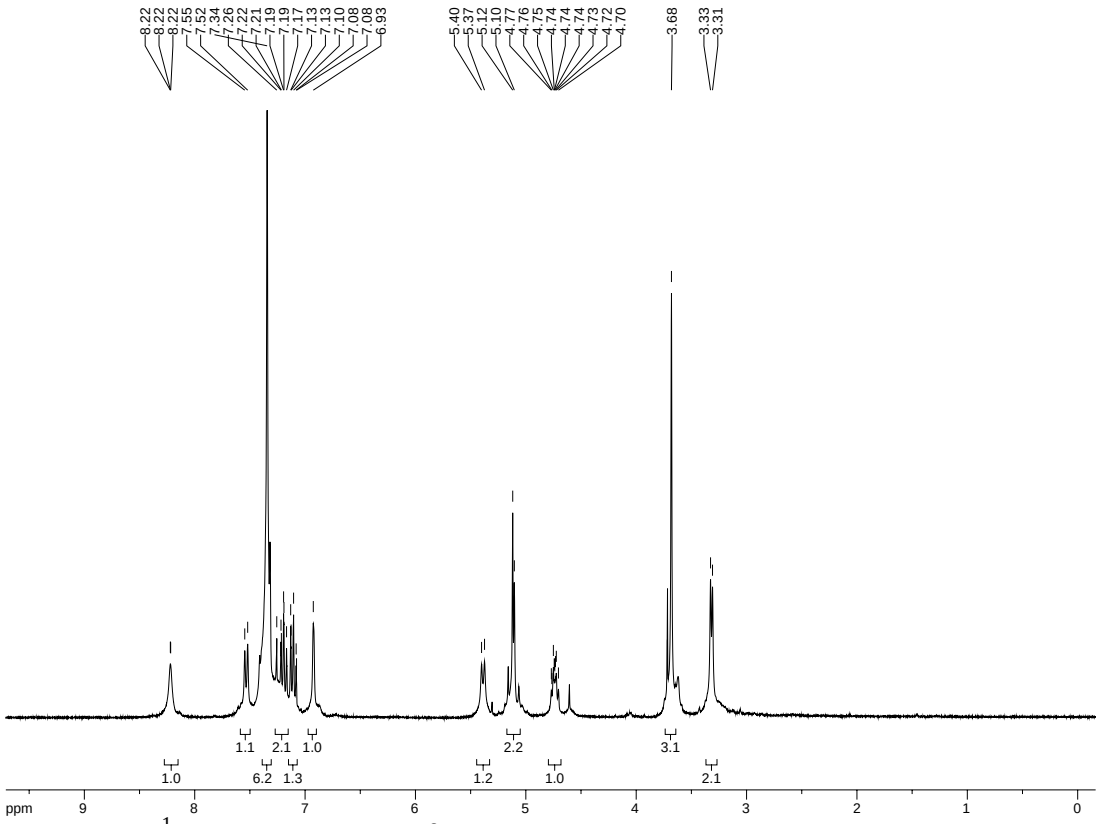

Figure 5.99a. ^{1}H NMR spectrum of compound **5.28**.

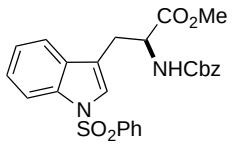

5.29

***N'*-SO_2Ph-*N*-Cbz-L-Trp-OMe (5.29)**. Phenylsulfonyl chloride (4.4 mL, 34.1 mmol) was added dropwise to a suspension of *N*-Cbz-L-Trp-OMe (10 g, 28.4 mmol), NaOH (3.4 g, 85.2 mmol), and Bu_4NHSO_4 (483 mg, 1.42 mmol) in CH_2Cl_2 (140 mL). The reaction was allowed to stir O/N at r.t., then to it added concentrated NH_4Cl and EtOAc. The organic layer was removed and the product further extracted into EtOAc (2x), then the combined organic extracts dried and concentrated to afford the title compound (13.31 g, 95% yield). ^{1}H-NMR (300 MHz; $CDCl_3$): δ 8.05 (d, *J* = 8.0 Hz, 1H), 7.97 (d, *J* = 8.3 Hz, 1H), 7.81 (d, *J* = 7.8 Hz, 2H), 7.64 (d, *J* = 8.0 Hz, 1H), 7.37 (sextet, *J* = 7.7 Hz, 9H), 7.20 (d, *J* = 7.4 Hz, 1H), 5.31 (d, *J* = 7.9 Hz, 1H), 5.16-5.06 (m, 2H), 4.70 (q, *J* = 6.6 Hz, 1H), 3.62 (s, 3H), 3.22 (t, *J* = 5.6 Hz, 2H).

REF: **TRW-II-452**.

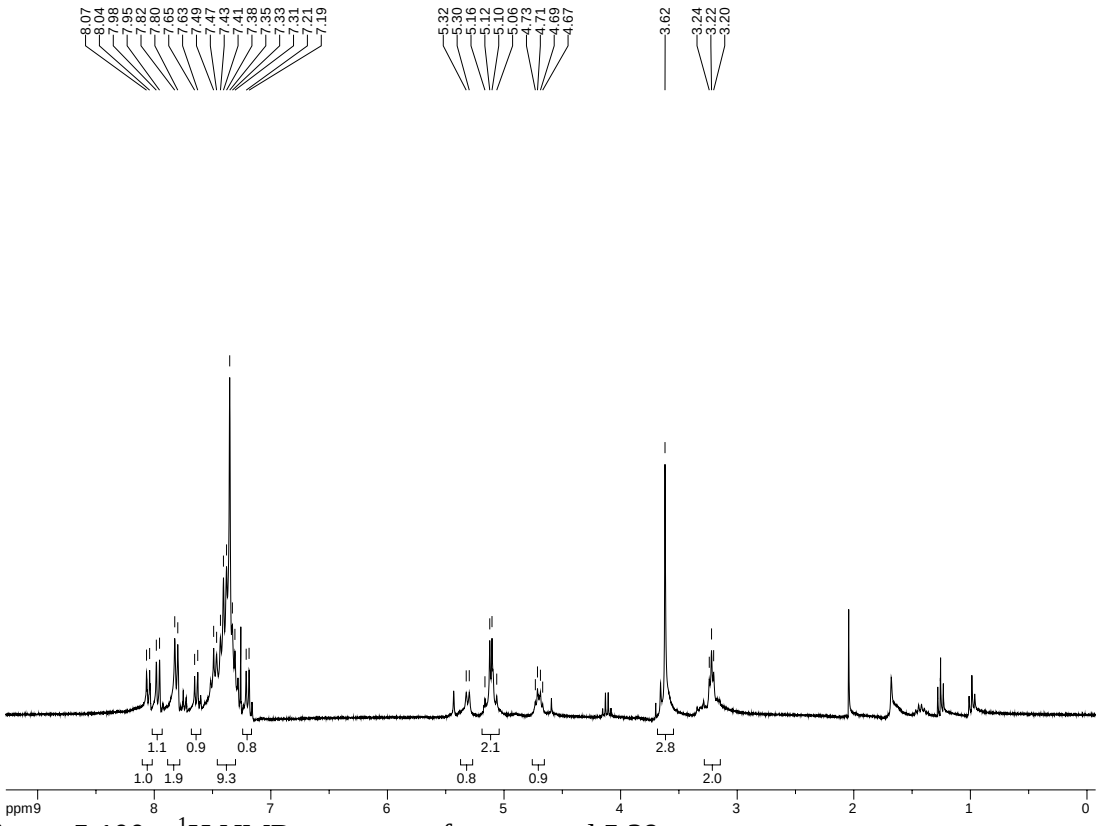

Figure 5.100a. ^{1}H NMR spectrum of compound **5.29**.

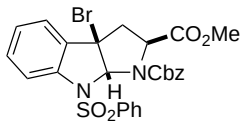

5.30

Bromopyrroloindoline (5.30). *N*'-SO_2Ph-*N*-Cbz-L-Trp-OMe (13.31 g, 27 mmol) was dissolved in CH_2Cl_2 (400 mL), and to the resulting solution added NBS (4.81 g, 27 mmol) and PPTS (6.78 g, 27 mmol). The reaction was allowed to stir O/N at r.t. $NaHCO_3$ (10% aq.) and $Na_2S_2O_4$ (10% aq.) were added in a 1:1 mixture, the organic layer removed, dried, and purified (SiO_2 chromatography, 1:1 H:E) to afford the title compound (11.46 g, 74% yield).

^{1}H-NMR (300 MHz; $CDCl_3$): δ 7.63 (d, *J* = 8.1 Hz, 1H), 7.50-7.45 (m, 3H), 7.36-7.34 (m, 8H), 7.26-7.25 (m, 2H), 7.19 (d, *J* = 7.4 Hz, 1H), 6.36-6.29 (bs, 1H), 5.42-5.22 (broad, 2H), 3.90-3.84 (m, 1H), 3.69-3.52 (broad, 3H), 3.09 (dd, *J* = 12.8, 6.0 Hz, 1H), 2.82-2.74 (m, 1H).

REF: **TRW-II-453**.

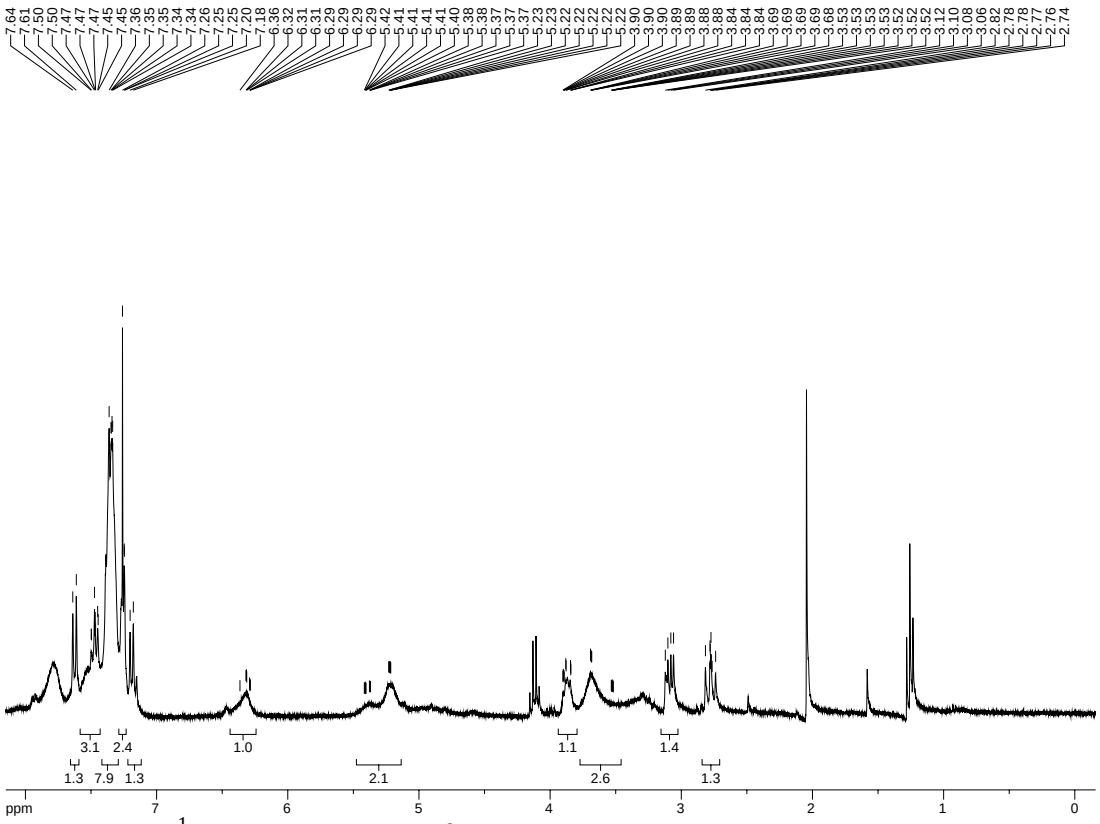

Figure 5.101a. ^{1}H NMR spectrum of compound **5.30**.

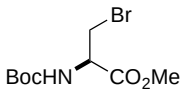

5.31

Methyl 3-bromo-2-(*tert*-butoxycarbonylamino)propanoate (5.31). To a solution of *N*-Boc-Ser-OMe (2.0 g, 9.1 mmol) in THF (50 mL) at 0 °C was added CBr_4 (4.54 g, 13.7 mmol) and PPh_3 (3.59 g, 13.7 mmol). The reaction was stirred at 0 °C for 10 minutes, then warmed to r.t. and stirred 4 h under Ar. The crude mixture was filtered through a bed of celite, diluted with ether, and washed with water and brine. The organic phase was dried over Na_2SO_4, filtered, and concentrated. The crude residue was purified by SiO_2 chromatography (3:1 hexanes:EtOAC) to afford bromide **5.31** (1.64 g, 64% yield).

^{1}H-NMR (300 MHz; $CDCl_3$): δ 5.42-5.39 (m, 1H), 4.78-4.73 (m, 1H), 3.81 (s, 3H), 3.71 (dd, *J* = 10.4, 3.4 Hz, 1H), 1.46 (s, 9H).

REF: **TRW-I-191**.

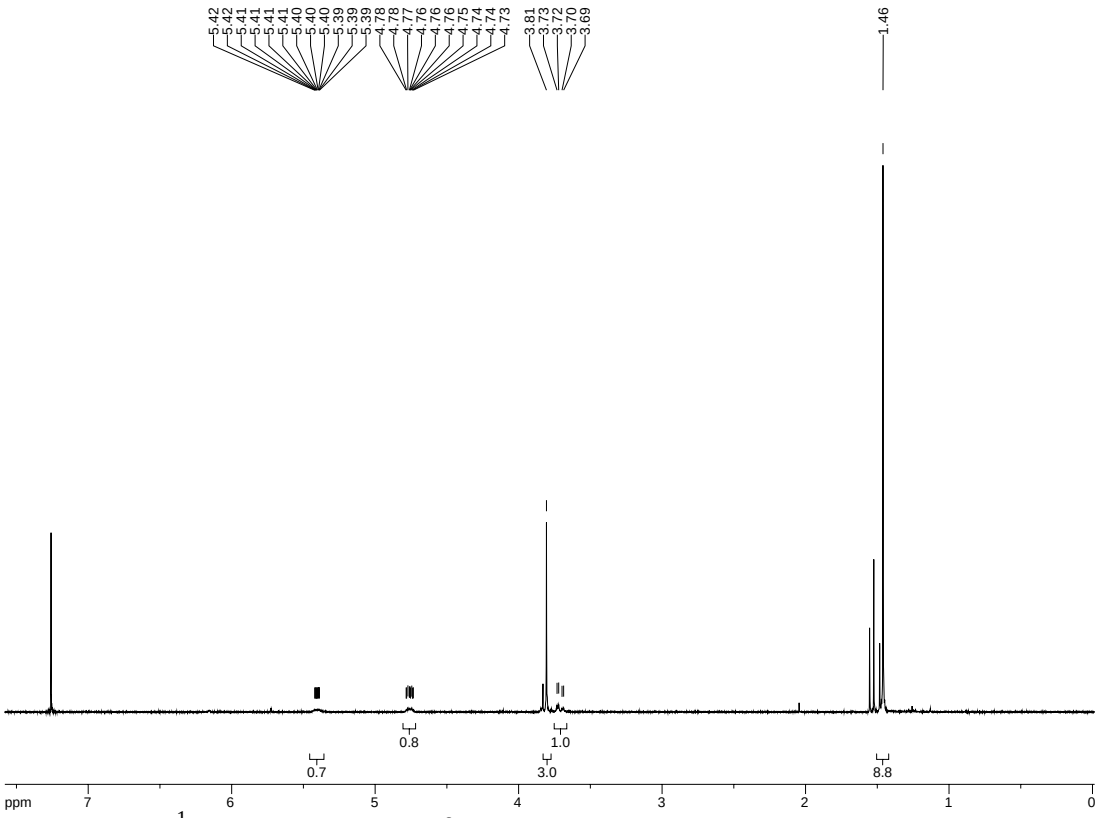

Figure 5.102a. ^{1}H NMR spectrum of compound **5.31**.

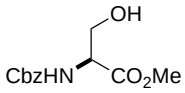

5.32

Methyl 2-(benzyloxycarbonylamino)-3-hydroxypropanoate (5.32). To a solution of Ser-OMe·HCl (5.0 g, 32.1 mmol) in MeOH:$NaHCO_3$ (1:1, 120 mL) was added CbzCl (5.75 g, 33.7 mmol). The reaction mixture was stirred at r.t. for 48 h, then 1 M HCl added. The crude mixture was concentrated and the resulting residue dissolved in EtOAc. The organic phase was washed with 1 M NaOH, dried over Na_2SO_4, filtered, and concentrated under reduced pressure to afford Cbz-amine **5.32** (8.12 g, 100% yield) as a clear oil, carried forward without additional purification.

^{1}H-NMR (300 MHz; $CDCl_3$): δ 7.37-7.34 (m, 5H), 5.72-5.67 (m, 1H), 5.13 (s, 2H), 4.47-4.43 (m, 1H), 4.01-3.93 (m, 2H), 3.79 (s, 3H).

REF: **TRW-I-256**.

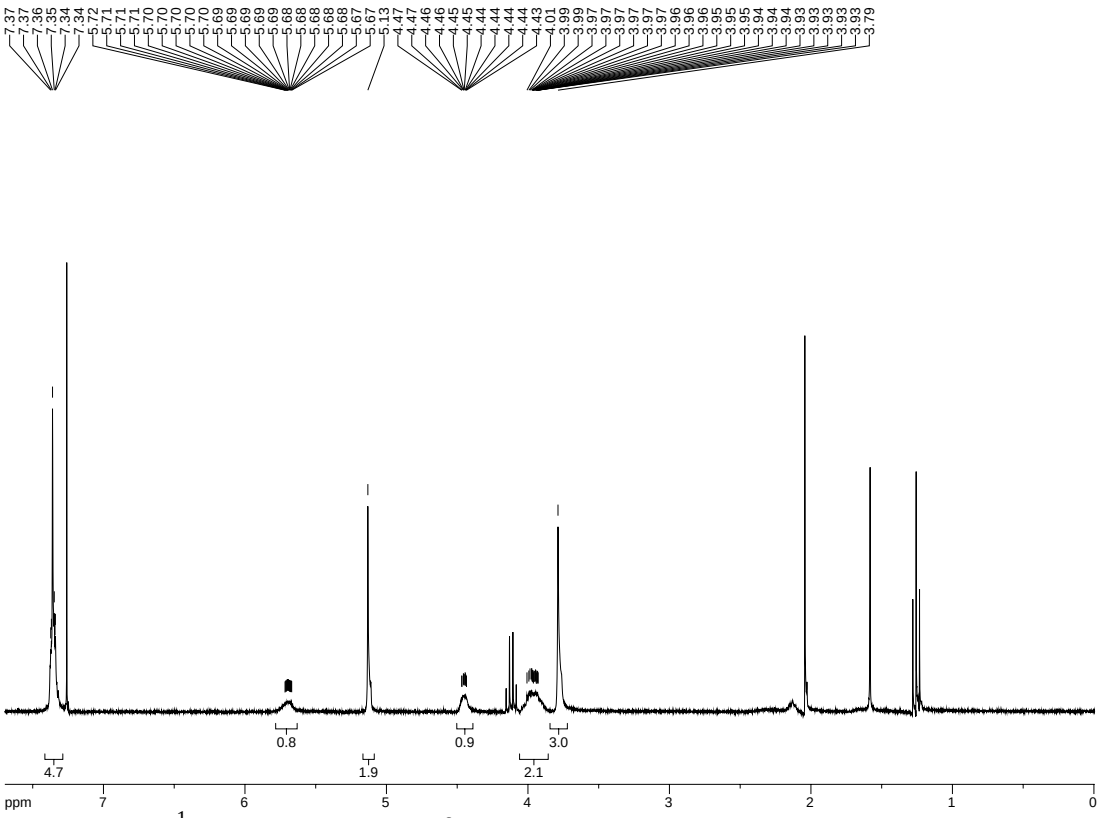

Figure 5.103a. ^{1}H NMR spectrum of compound **5.32**.

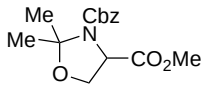

5.33

3-benzyl 4-methyl 2,2-dimethyloxazolidine-3,4-dicarboxylate (5.33). To a solution of Cbz-Ser-OMe (7.56 g, 30.0 mmol) in dry acetone (100 mL) was added 2,2-dimethoxypropane (40 mL), $BF_3 \cdot OEt_2$ (3.8 mL, 30.0 mmol), and Na_2SO_4 (10 g). The reaction mixture stirred overnight at r.t. under Ar, and then Et_3N (12 mL) was added. The resulting suspension was filtered and the filtrate concentrated under reduced pressure. The product was extracted with ether (3 x 75 mL), washed with $NaHCO_3$, washed with brine, dried over Na_2SO_4, and concentrated. The crude oil was purified by SiO_2 chromatography (5-50% EtOAc in hexanes) to afford **5.33** (7.20 g, 82% yield) as a mixture of rotamers. Crude oil was likely pure enough to carry forward without purification.

^{1}H-NMR (300 MHz; $CDCl_3$): δ 7.36-7.30 (m, 5H), 5.20-5.02 (m, 2H), 4.52 (ddd, *J* = 23.2, 6.6, 2.7 Hz, 1H), 4.19-4.07 (m, 2H), 3.69 (d, *J* = 40.4 Hz, 3H), 1.68 (d, *J* = 20.1 Hz, 3H), 1.58 (d, *J* = 9.5 Hz, 3H).

REF: **TRW-I-257**.

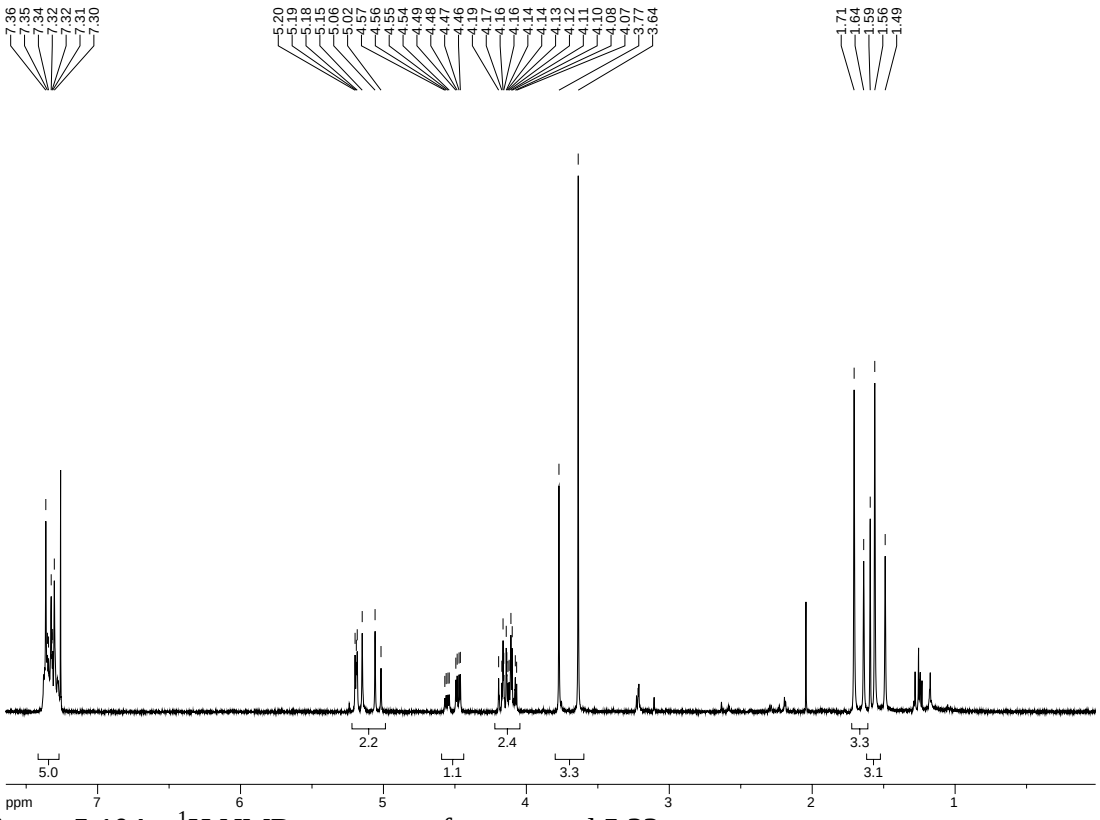

Figure 5.104a. ^{1}H NMR spectrum of compound **5.33**.

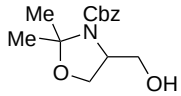

5.34

Benzyl 4-(hydroxymethyl)-2,2-dimethyloxazolidine-3-carboxylate (5.34). To a solution of ester **5.33** (1.0 g, 3.4 mmol) in THF (12 mL) at -10 °C was added $NaBH_4$ (517 mg, 13.6 mmol). The resulting mixture was stirred for 30 minutes at -10 °C, then MeOH (5 mL) added dropwise. The reaction was allowed to warm to r.t. while it stirred overnight under Ar. Water was added and the resulting suspension stirred for 30 minutes, concentrated under reduced pressure, diluted with brine, and the product extracted with EtOAc (3 x 15 mL). The combined organic layers were washed with brine, dried over Na_2SO_4, and concentrated to afford alcohol **5.34** (900 mg, 100% yield), deemed sufficiently pure to carry forward without additional purification.

^{1}H-NMR (300 MHz; $CDCl_3$): δ 7.36 (s, 5H), 5.17-5.12 (m, 2H), 4.15-4.13 (m, 1H), 4.04-3.98 (m, 2H), 3.83-3.59 (m, 3H), 3.39-3.36 (bs, 1H), 1.65-1.47 (m, 6H).

REF: **TRW-I-260**, TRW-I-263, TRW-I-267.

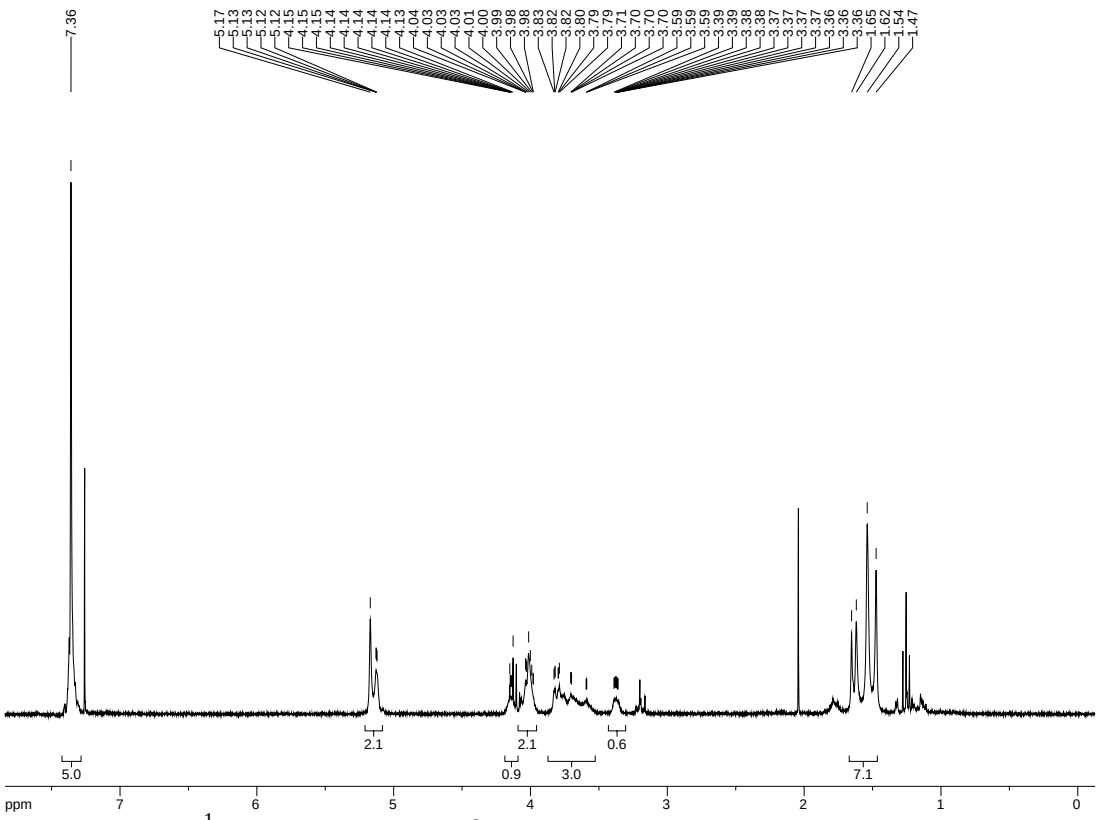

Figure 5.105a. ^{1}H NMR spectrum of compound **5.34**.

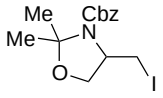

5.35

Benzyl 4-(iodomethyl)-2,2-dimethyloxazolidine-3-carboxylate (5.35). To a solution of Ph_3P (550 mg, 2.1 mmol) and imidazole (143 mg, 2.1 mmol) in CH_2Cl_2 (10 mL) at 0 °C was added I_2 (533 mg, 2.1 mmol) in 3 portions. The reaction mixture was warmed to r.t. for 10 minutes, then cooled to 0 °C before adding dropwise a solution of alcohol **5.34** (450 mg, 1.7 mmol) in 5 mL CH_2Cl_2. The resulting solution was stirred 1 h at 0 °C, then allowed to warm to r.t. as it stirred an additional 1.5 h. The crude reaction mixture was filtered through a plug of silica with 1:1 EtOAC/Hexanes. The filtrate was concentrated under reduced pressure and purified by SiO_2 chromatography (5-20% EtOAc in hexanes) to afford iodide **5.35** (30 mg, 8% yield).

^{1}H-NMR (300 MHz; $CDCl_3$): δ 7.36 (s, 5H), 5.15 (s, 2H), 4.25-4.19 (m, 1H), 4.08-4.02 (m, 2H), 3.54-3.35 (m, 1H), 3.21-3.10 (m, 1H), 1.62 (d, *J* = 20.1 Hz, 3H), 1.47 (d, *J* = 19.3 Hz, 3H); ^{13}C-NMR (75 MHz; $CDCl_3$): δ 128.9, 128.0, 67.69, 67.58, 67.0, 59.5, 58.9, 28.1, 27.2, 24.7, 23.2, 6.8, 6.5.

REF: **TRW-I-261**, TRW-I-266.

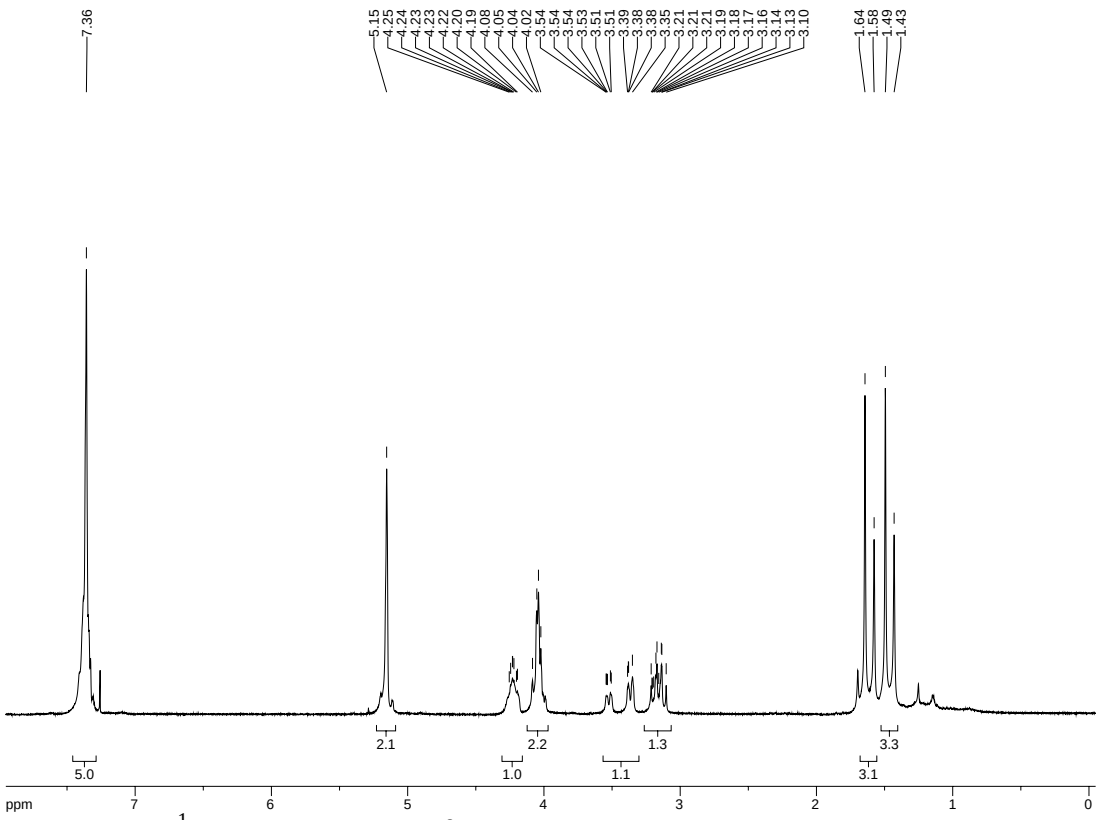

Figure 5.106a. ^{1}H NMR spectrum of compound **5.35**.

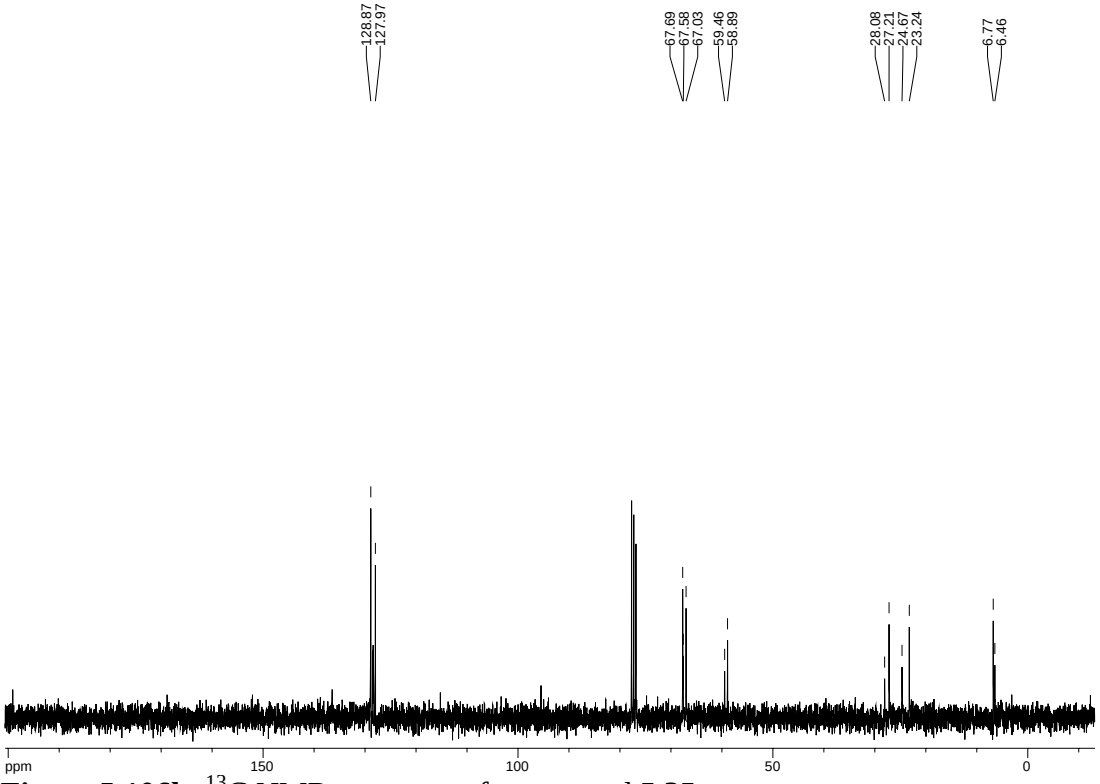

Figure 5.106b. ^{13}C NMR spectrum of compound **5.35**.

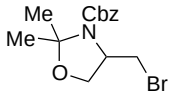

5.36

Benzyl 4-(bromomethyl)-2,2-dimethyloxazolidine-3-carboxylate (5.36). To a solution of alcohol **5.34** (450 mg, 1.7 mmol) in THF (9 mL) at 0 °C was added CBr_4 (862 mg, 2.6 mmol) and PPh_3 (681 mg, 2.6 mmol). The reaction was stirred at 0 °C for 10 minutes, then warmed to r.t. and stirred 4 h under Ar. The crude mixture was concentrated, diluted with ether, filtered through a bed of celite, and concentrated. The crude residue was purified by SiO_2 chromatography (5-20% EtOAc in hexanes) to afford bromide **5.36** (460 mg, 82% yield).

^{1}H-NMR (300 MHz; $CDCl_3$): δ 7.35 (s, 5H), 5.15 (s, 2H), 4.20-4.15 (m, 1H), 4.12-4.07 (m, 1H), 3.99 (ddd, *J* = 7.0, 5.1, 2.3 Hz, 1H), 3.68-3.49 (m, 1H), 3.30 (dt, *J* = 15.3, 10.0 Hz, 1H), 1.60 (d, *J* = 20.2 Hz, 3H), 1.48 (d, *J* = 19.8 Hz, 3H).

REF: **TRW-I-262**, TRW-I-269.

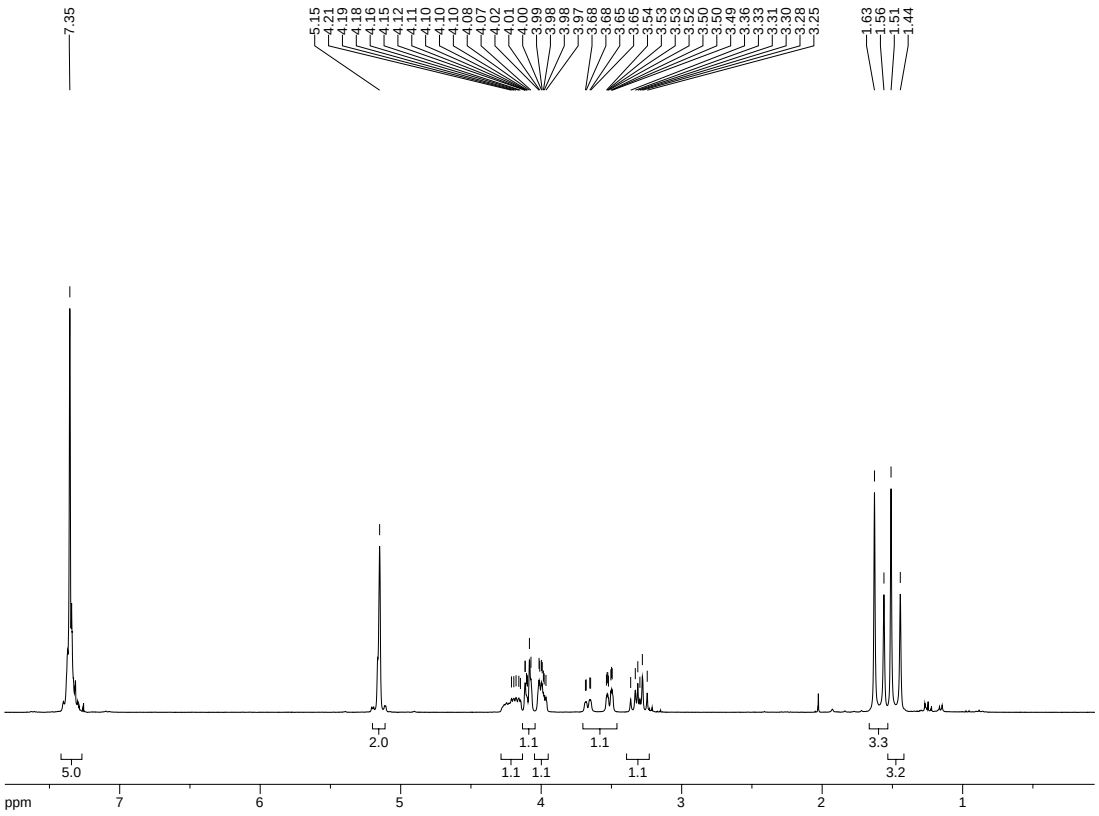

Figure 5.107a. ^{1}H NMR spectrum of compound **5.36**.

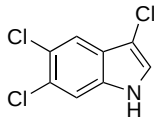

5.37

3,5,6-trichloroindole (5.37). NCS (1.75 g, 13.2 mmol) was added in one portion to a solution of 5,6-dichloroindole (2.45 g, 13.2 mmol) in DMF (65 mL) at rt. The reaction was stirred for 3 h at rt, and brine (50 mL) was added. The mixture was extracted with EtOAc (3 x 50 mL). The combined organic layers were washed with water (100 mL), brine (100 mL), dried (Na_2SO_4), and concentrated under reduced pressure. The residue was purified by flash chromatography eluting with hexanes/EtOAc (9:1) to give 1.95 g (67%) of **5.37** as a brown solid.

^{1}H NMR (300 MHz, $CDCl_3$) δ 8.11 (bs, 1 H), 7.71 (s, 1 H), 7.49 (s, 1 H), 7.20 (d, *J* = 2.6 Hz, 1 H); ^{13}C NMR (100 MHz, $CDCl_3$) δ 133.7, 127.5, 125.3, 125.1, 122.9, 119.7, 113.2, 106.5; IR (neat) 3442, 1448,1266, 1011 cm^{-1}; HRMS (ES/ApCl) calcd for $C_8H_3NCl_3$ (M-H) 217.9337, found 217.9347.

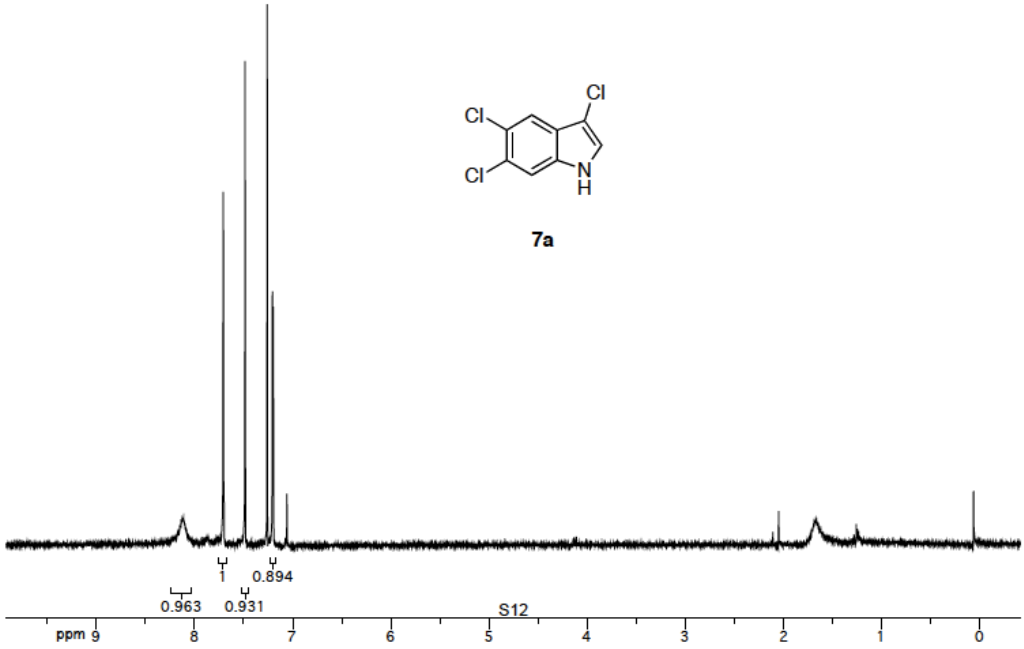

Figure 5.108a. ^{1}H NMR spectrum of compound **5.37**.

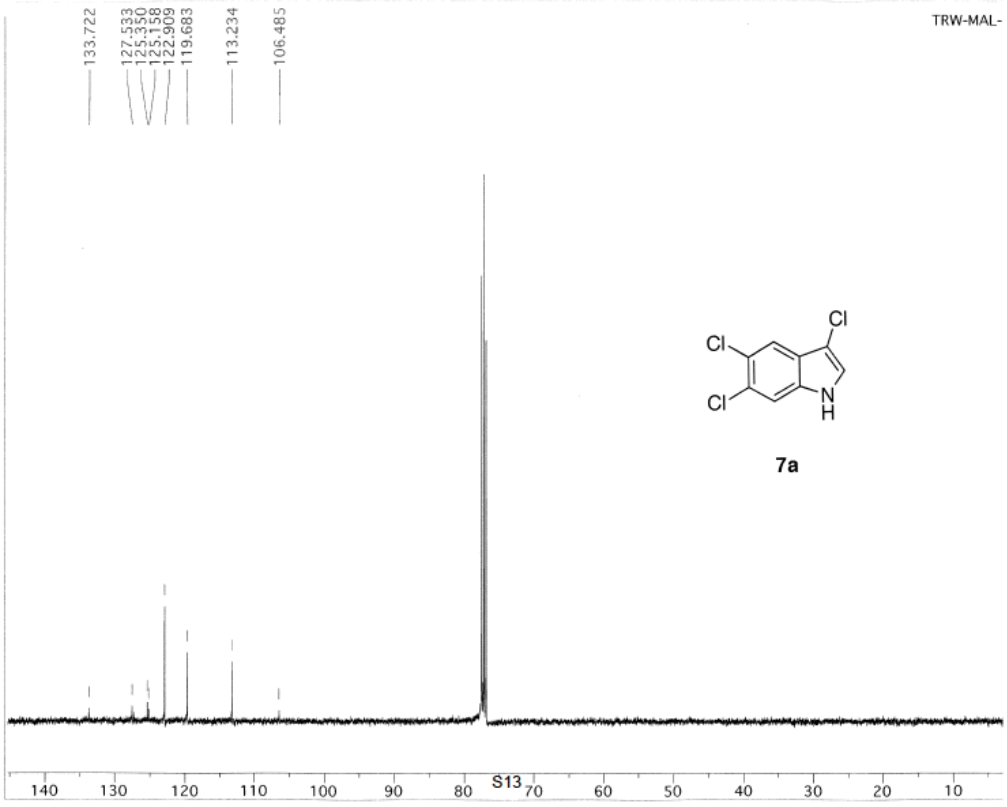

Figure 5.108b. ^{13}C NMR spectrum of compound **5.37**.

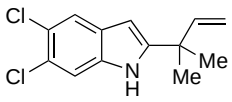

5.38

5,6-dichloro-2-(2-methylbut-3-en-2-yl)-1*H*-indole (5.38). Solid **5.37** (1.95 g, 8.84 mmol) was added in one portion to a solution of freshly prepared prenyl-9-BBN (26.52 mmol) and Et_3N (3.12 g, 30.94 mmol, 4.30 mL) in THF (53 mL) at rt. The reaction was stirred for 3 h, and then quenched with sat. $NaHCO_3$ (50 mL). The organic layer was separated and the aqueous layer was extracted with Et_2O (3 x 50 mL). The combined organic layers were washed with H_2O (100 mL), brine (100 mL), and dried (Na_2SO_4), and concentrated under reduced pressure. The residue was purified by flash chromatography eluting with hexanes/EtOAc (99:1) to give 1.80 g (80%) of **5.38** as a yellow oil.

^{1}H NMR (300 MHz, $CDCl_3$) δ 7.87 (bs, 1 H), 7.59 (s, 1 H), 7.38 (s, 1 H), 6.23 (m, 1 H), 6.01 (dd, *J* = 17.3, 10.6 Hz, 1 H), 5.15 (d, *J* = 10.6 Hz, 1 H), 5.09 (d, *J* = 17.3 Hz, 1 H), 1.46 (s, 6 H); ^{13}C NMR (75 MHz, $CDCl_3$) δ 148.2, 145.6, 134.9, 128.5, 125.0, 123.7, 121.1, 113.0, 112.0, 97.6, 38.5, 27.5; IR (neat) 3231, 2927, 1453, 1102 cm^{-1}; HRMS (FAB) calcd for $C_{13}H_{13}NCl_2$ (M+) 253.0425, found 253.0428.

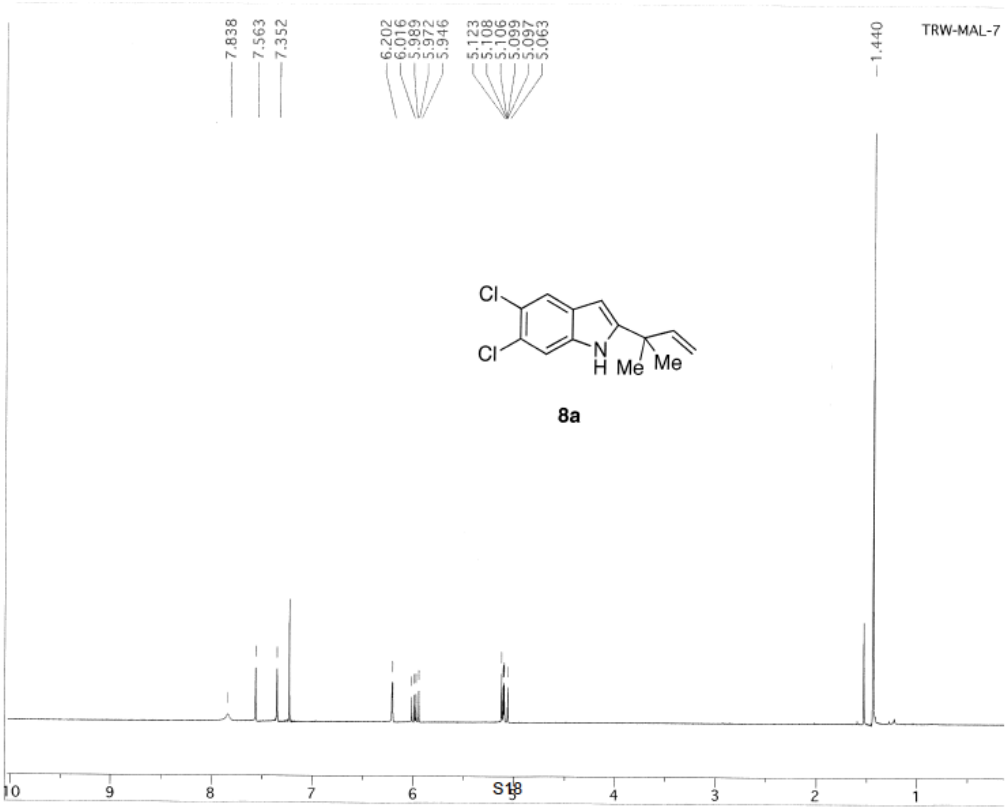

Figure 5.109a. ^{1}H NMR spectrum of compound **5.38**.

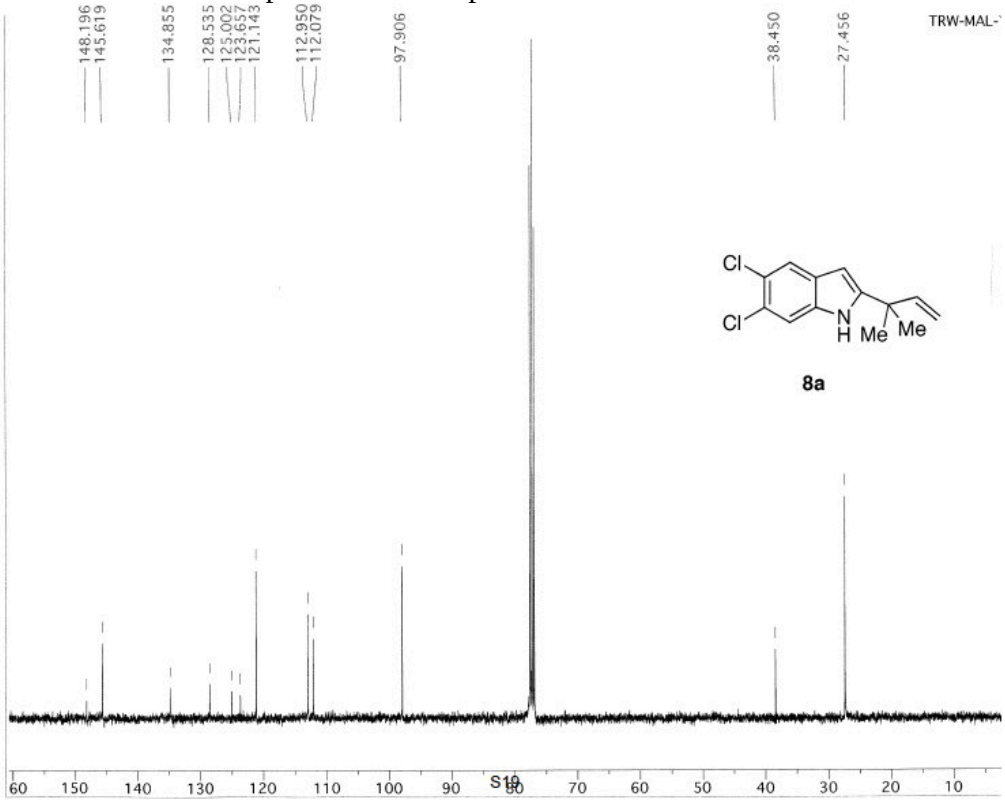

Figure 5.109b. ^{13}C NMR spectrum of compound **5.38**.

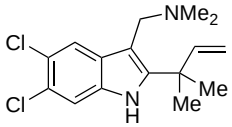

5.39

1-(5,6-dichloro-2-(2-methylbut-3-en-2-yl)-1*H*-indol-3-yl)-*N*,*N*dimethylmethanamine (5.39). A solution of Me_2NH (0.78 mL, 40% solution in H_2O, 6.00 mmol) and a solution of CH_2O (0.47 mL, 37% solution in H_2O, 6.00 mmol) were sequentially added to AcOH (2 mL) and the reaction stirred for 1 h. Neat **5.38** (1.45 g, 5.71 mmol) was added, and the reaction was stirred for 12 h at rt. 2N NaOH was added until pH ≈ 12. The reaction was extracted with Et_2O (3 x 20 mL). The combined organic layers were washed with H_2O (50 mL), brine (50 mL), and dried (Na_2SO_4), and concentrated under reduced pressure to give 1.66 g (90%) of **5.39** as a yellow oil which was used without further purification. ^1H NMR (400 MHz, $CDCl_3$) δ 7.86 (bs, 1 H), 7.76 (s, 1 H), 7.32 (s, 1 H), 6.08 (dd, *J* = 17.6, 10.0 Hz, 1 H), 5.14 (d, J = 10.0 Hz, 1 H), 5.12 (d, *J* = 17.6 Hz, 1 H), 3.49 (s, 2 H), 2.16 (s, 6 H), 1.52 (s, 6 H); ^{13}C NMR (100 MHz, $CDCl_3$) δ 145.7, 143.4, 132.9, 130.4, 124.9, 123.3, 120.6, 112.7, 111.8, 109.0, 54.1, 45.5, 39.5, 27.2; IR (neat) 3320, 2928, 1463, 1016 cm^{-1}; HRMS (+TOF) calcd for $C_{16}H_{21}N_2Cl_2$ (M+H) 311.1082, found 311.1020.

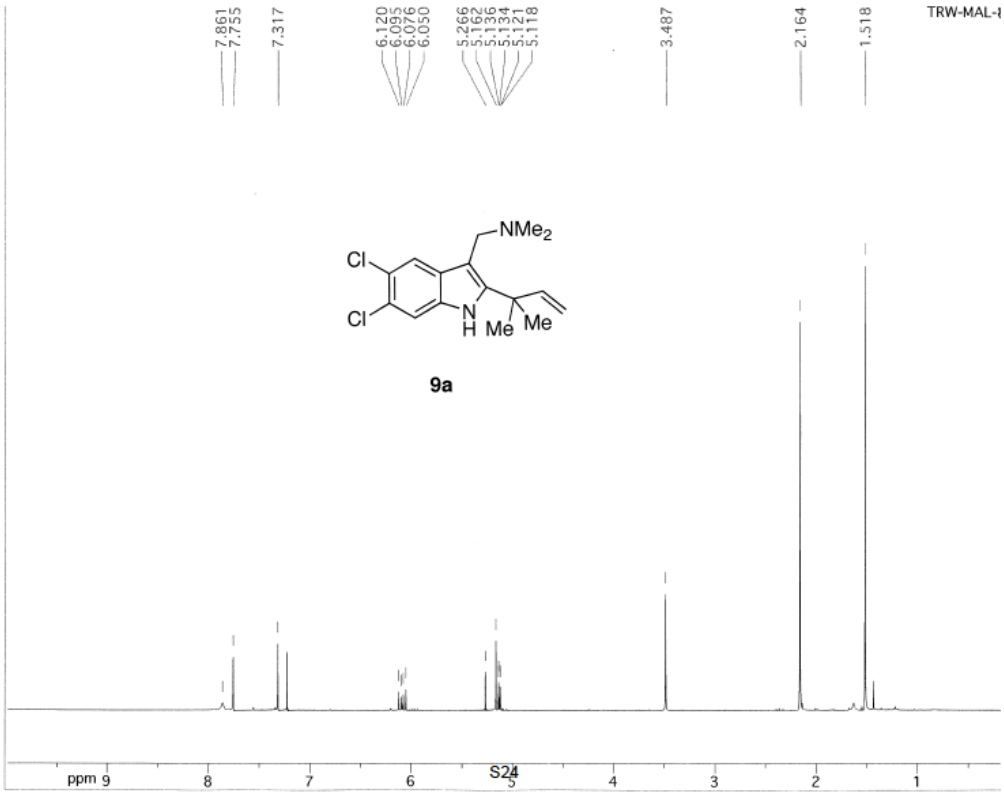

Figure 5.110a. ^{1}H NMR spectrum of compound **5.39**.

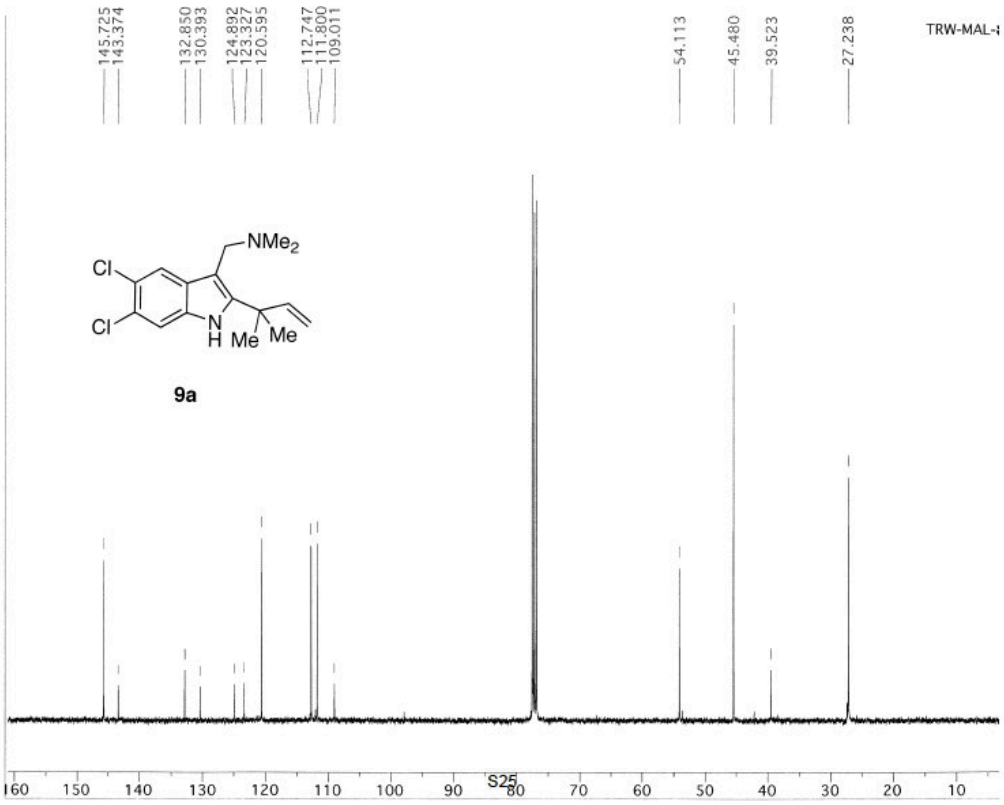

Figure 5.110b. ^{13}C NMR spectrum of compound **5.39**.

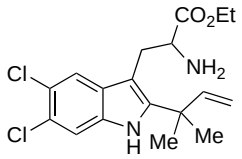

5.40

Ethyl 2-amino-3-(5,6-dichloro-2-(2-methylbut-3-en-2-yl)-1*H*-indol-3-yl)–propanoate (5.40). PBu_3 (346 mg, 1.72 mmol, 0.43 mL) was added to a solution of **5.39** (1.0 g, 3.43 mmol) and *N*-(Diphenylmethylene)glycine ethyl ester (832 mg, 3.12 mmol) in CH_3CN (30 mL) at rt. The reaction was heated to reflux and was stirred under Ar for 12 h. The reaction was cooled to rt and concentrated under reduced pressure. The residue was purified by flash chromatography eluting with hexanes/EtOAc (4:1) to give 1.19 g of a yellow oil which was dissolved in CH_2Cl_2 (25 mL). 1N HCl was added and the reaction was vigorously stirred for 12 h at rt. The organic layer was separated and the aqueous layer was extracted with CH_2Cl_2 (2 x 25 mL). The combined organic layers were concentrated under reduced pressure. The residue was purified by flash chromatography eluting with MeOH/CH_2Cl_2 (1:99-5:95) to give 848 mg (67%) of **5.40** as a yellow oil.

^{1}H NMR (400 MHz, $CDCl_3$) δ 7.89 (bs, 1 H), 7.59 (s, 1 H), 7.34 (s, 1 H), 6.08 (dd, *J* = 17.2, 10.8 Hz, 1 H), 5.16 (d, *J* = 10.8 Hz, 1 H), 5.15 (d, *J* = 17.2 Hz, 1 H), 4.09 (comp, 2 H), 3.73 (m, 1 H), 3.20 (dd, *J* = 14.8, 5.6 Hz, 1 H), 2.96 (dd, *J* = 14.8, 8.8 Hz, 1 H), 1.53 (s, 6 H), 1.16 (t, *J* = 7.2 Hz, 3 H); ^{13}C NMR (75 MHz, $CDCl_3$) δ 170.6, 145.6, 142.7, 133.1, 129.9, 125.3, 123.6, 119.9, 112.9, 112.0, 107.3, 61.2, 56.0, 39.5, 31.0, 27.8, 14.3; IR (neat) 3368, 2973, 2927, 1729, 1463, 1199 cm^{-1}; HRMS (TOF-) calcd for $C_{18}H_{21}N_2O_2Cl_2$ (M-H) 367.0986, found 367.0975.

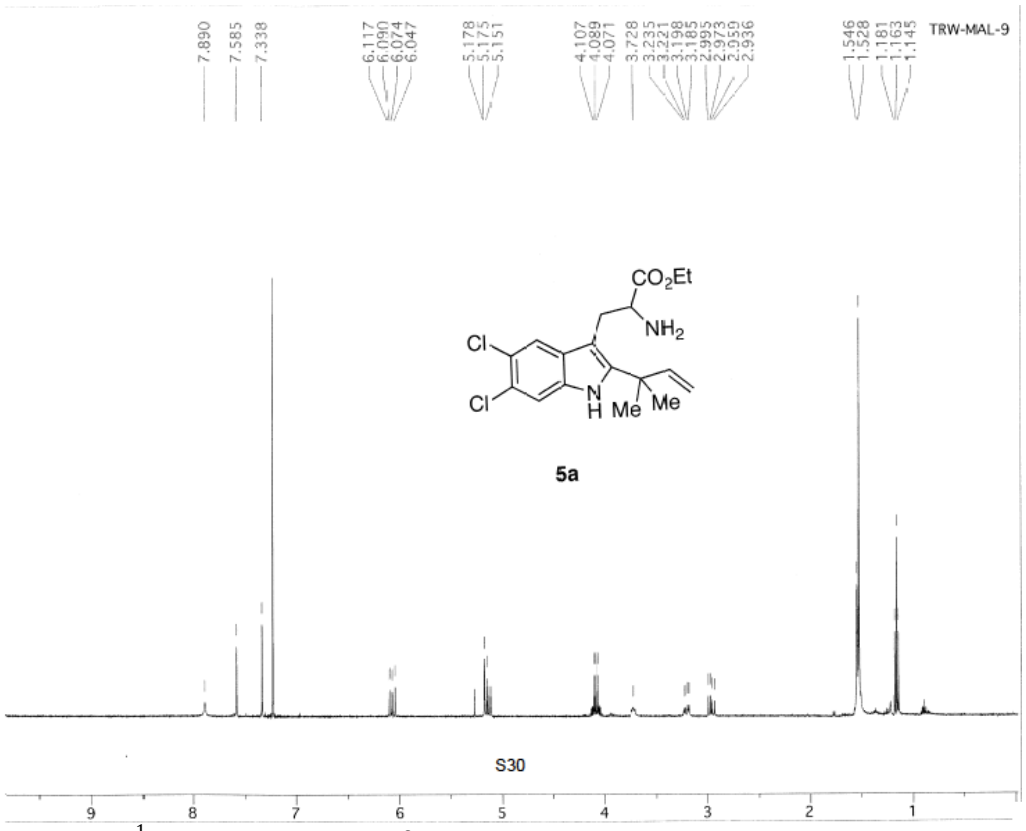

Figure 5.111a. ^{1}H NMR spectrum of compound **5.40**.

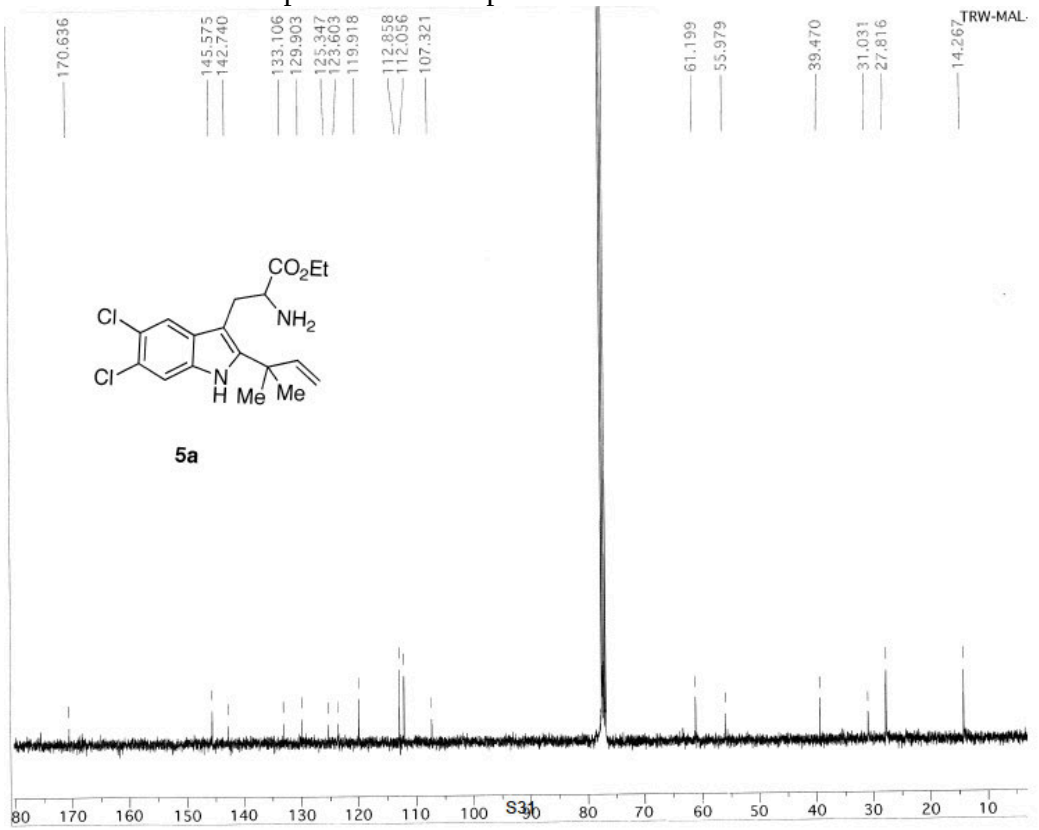

Figure 5.111b. ^{13}C NMR spectrum of compound **5.40**.

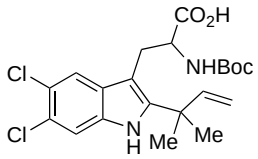

5.41

2-(*tert*-butoxycarbonylamino)-3-(5,6-dichloro-2-(2-methylbut-3-en-2-yl)-1*H*indol-3-yl)propanoic acid (5.41). 0.5M NaOH (4.5 mL, 2.25 mmol) and Boc_2O (586 mg, 2.69 mmol) were sequentially added to a solution of **5.40** (848 mg, 2.24 mmol) in dioxane (5 mL). The reaction was stirred at rt for 3 h, and then concentrated under reduced pressure to remove dioxane. 10% $KHSO_4$ was added until pH ≈ 2, and the solution was extracted with EtOAc (3 x 25 mL). The combined organic layers were dried (Na_2SO_4) and concentrated under reduced pressure. The residue was dissolved in 2:1 THF/H_2O (18 mL), and LiOH (280 mg, 11.25 mmol) was added in one portion. The reaction stirred at rt for 12 h. 10% $KHSO_4$ was added until pH ≈ 2, and the solution was extracted with EtOAc (3 x 25 mL). The combined organic layers were dried (Na_2SO_4) and concentrated under reduced pressure to afford 902 mg (91%) of a yellow solid which was used without further purification.

^{1}H NMR (300 MHz, $CDCl_3$) δ 11.0 (bs, 1 H), 8.19 (m, 1 H), 6.63 (m, 1 H), 7.31 (m, 1 H), 6.80 (bs, 1 H), 6.08 (m, 1 H), 5.18 (comp, 2 H), 4.56 (bs, 1 H), 3.37 (bs, 1 H), 3.14 (m, 1 H), 1.52 (s, 6 H), 1.28-1.02 (comp, 9 H); ^{13}C NMR (75 MHz, $CDCl_3$) δ 177.3, 176.3, 170.4, 156.6, 155.3, 145.4, 142.9, 133.0, 129.9, 129.7, 128.4, 125.0, 124.9, 123.5, 123.3, 119.7, 119.5, 112.9, 112.8, 106.6, 106.0, 81.4, 80.3, 55.4, 54.7, 39.2, 29.8, 28.6, 28.2, 27.8, 27.5; IR (neat) 3335, 2976, 2932, 1697, 1461 cm^{-1}; HRMS (TOF-) calcd for $C_{21}H_{25}N_2O_4Cl_2$ (M-H) 439.1197, found 439.1185.

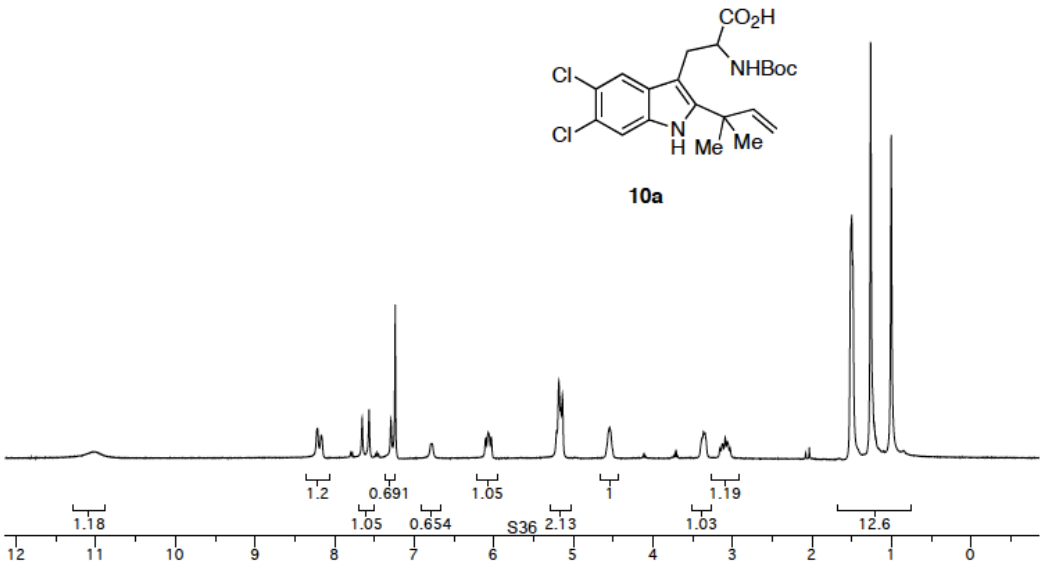

Figure 5.112a. ^{1}H NMR spectrum of compound **5.41**.

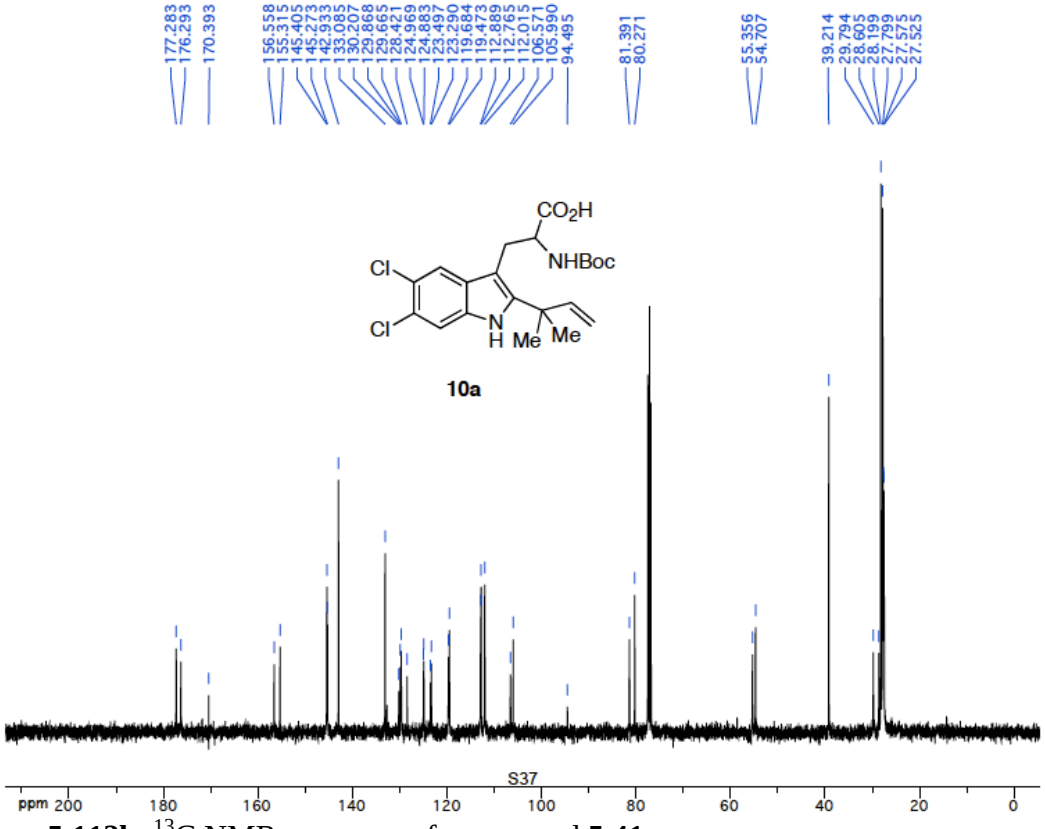

Figure 5.112b. ^{13}C NMR spectrum of compound **5.41**.

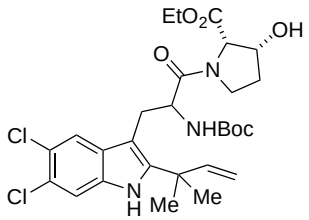

5.42

(2*S*,3*R*)-ethyl-1-(2-(*tert*-butoxycarbonylamino)-3-(5,6-dichloro-2-(2-methylbut-3-en-2-yl)-1*H*-indol-3-yl)propanoyl)-3-hydroxypyrrolidine-2-carboxylate (5.42). To a solution of **5.41** (280 mg, 0.63 mmol) in CH_3CN (6 mL) was sequentially added HATU (361 mg, 0.95 mmol), *i*Pr_2NEt (327 mg, 2.54 mmol), and *cis*-3-hydroxy-L-proline ethyl ester HCl (217 mg, 1.11 mmol). The reaction was stirred at rt for 3 h, and 2N HCl (10 mL) was added. The mixture was extracted with CH_2Cl_2 (3 x 25 mL), and the combined organic layers were dried (Na_2SO_4) and concentrated under reduced pressure. The residue was purified by flash chromatography eluting with hexanes/EtOAc (1:1) to give 252 mg (68%) of **5.42** as a colorless oil.

^{1}H NMR (300 MHz, $CDCl_3$) δ 8.73- 8.47 (m, 1 H), 7.58-7.32 (comp, 2 H), 6.11 (m, 1 H), 5.50 (m, 1 H), 5.17 (comp, 2 H), 4.63-3.04 (comp, 9 H), 1.57-1.14 (comp, 18 H); ^{13}C NMR (75 MHz, $CDCl_3$) δ 172.1, 169.3, 169.1, 169.0, 155.0, 154.8, 154.3, 145.7, 144.8, 144.7, 143.7, 143.3, 142.9, 133.1, 132.7, 129.9, 129.5, 129.2, 124.9, 124.7, 123.1, 119.6, 112.9, 112.6, 112.0, 105.9, 105.6, 79.6, 79.3, 71.7, 70.4, 70.1, 63.8, 63.3, 62.0, 61.4, 60.6, 53.0, 52.4, 45.2, 44.4, 44.3, 39.2, 33.5, 32.6, 30.8, 30.5, 30.2, 28.3, 28.0, 27.7, 21.1, 18.4, 14.2, 14.0; IR (neat) 3359, 2978, 2932, 1694, 1633, 1500, 1455 cm^{-1}; HRMS (TOF-) calcd for $C_{28}H_{36}N_3O_6Cl_2$ (M-H) 580.1987, found 580.1976.

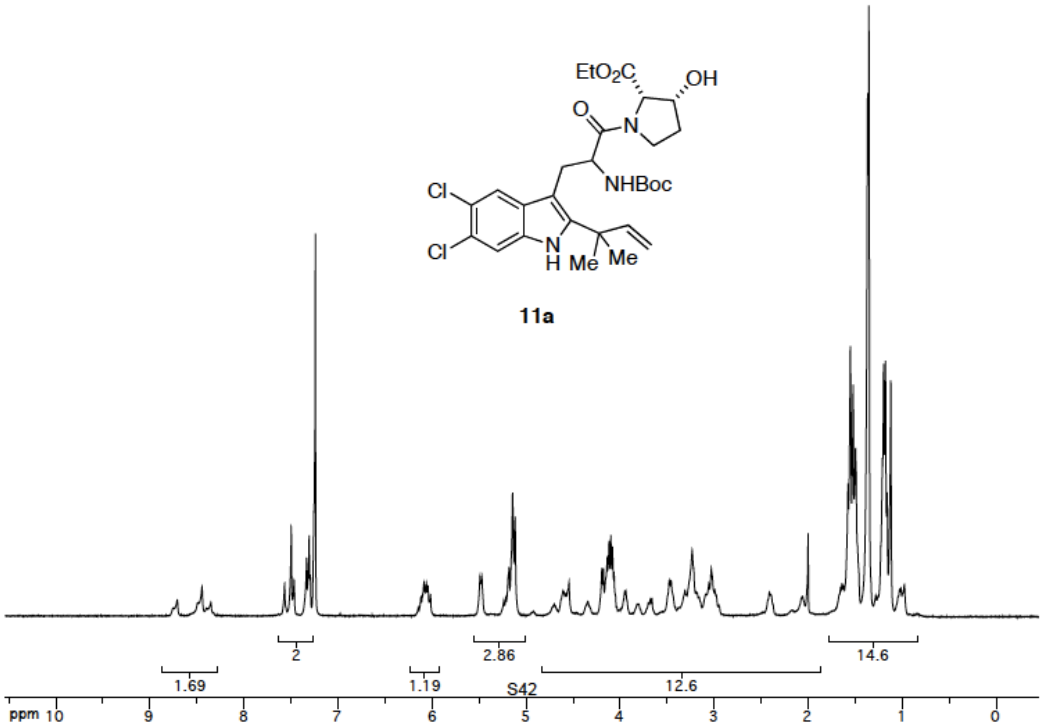

Figure 5.113a. ^{1}H NMR spectrum of compound **5.42**.

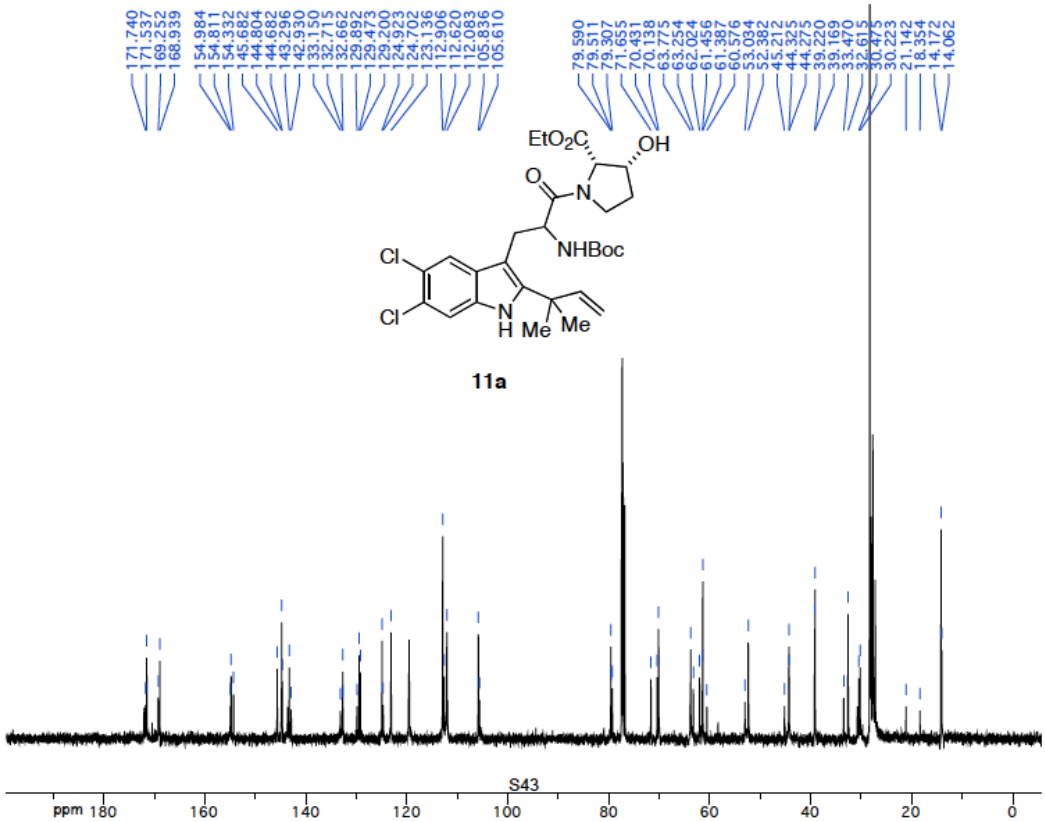

Figure 5.113b. ^{13}C NMR spectrum of compound **5.42**.

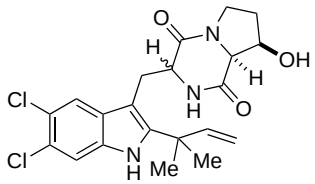

5.43

(8*R*,8a*S*)-3-((5,6-dichloro-2-(2-methylbut-3-en-2-yl)-1*H*-indol-3-yl)methyl)-8-hydroxyhexahydropyrrolo[1,2-*a*]pyrazine-1,4-dione (5.43). TFA (0.86 mL, 11.16 mmol) was added to a solution of **5.42** (252 mg, 0.43 mmol) in CH_2Cl_2 (9 mL). The reaction was stirred for 3 h, and sat. $NaHCO_3$ (30 mL) was added. The mixture was extracted with EtOAc (3 x 20 mL), and the combined organic layers were dried (Na_2SO_4) and concentrated under reduced pressure. The residue was dissolved in toluene (9 mL) and 2-hydroxypyridine (9 mg, 0.09 mmol) was added. The reaction was refluxed under Ar for 12 h, cooled to rt, and concentrated under reduced pressure. The residue was dissolved in CH_2Cl_2 (30 mL) and washed with 1N HCl (30 mL). The organic layer was dried (Na_2SO_4) and concentrated under reduced pressure to afford 156 mg (85%) of a beige solid which was used without further purification.

^{1}H NMR (300 MHz, $CDCl_3$) δ 8.14 (s, 1 H), 7.54 (s, 1 H), 7.43 (s, 1 H), 6.10 (dd, *J* = 17.4, 10.6 Hz, 1 H), 5.72 (bs, 1 H), 5.22 (d, *J* = 10.6 Hz, 1 H), 5.17 (d, *J* = 17.4 Hz, 1 H), 4.71-2.10 (comp, 9 H), 1.55 (s, 6 H); ^{13}C NMR (75 MHz, $CDCl_3$) δ 167.7, 165.5, 145.0, 144.1, 133.2, 128.8, 126.1, 124.3, 119.0, 113.6, 112.6, 104.5, 71.0, 64.7, 54.5, 44.2, 39.1, 30.3, 27.8, 26.3; IR (neat) 3352, 2973, 1647, 1459 cm^{-1}; HRMS (TOF+) calcd for $C_{21}H_{24}N_3O_3Cl_2$ (M+) 436.1189, found 436.1167.

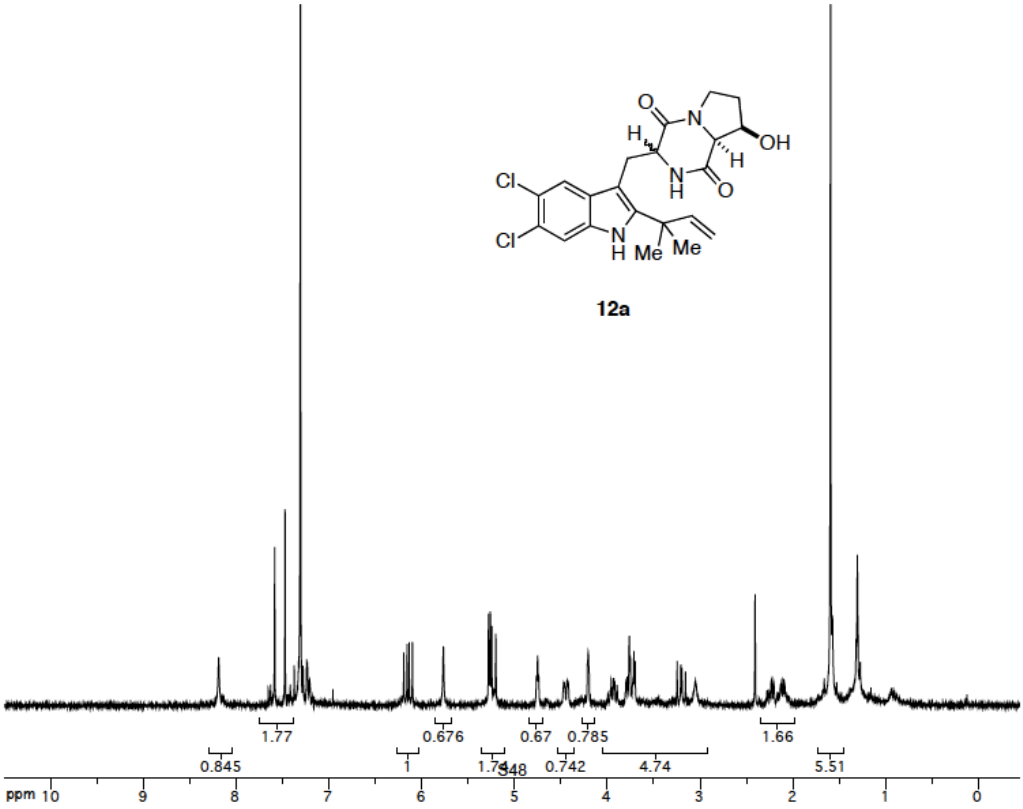

Figure 5.114a. ^{1}H NMR spectrum of compound **5.43**.

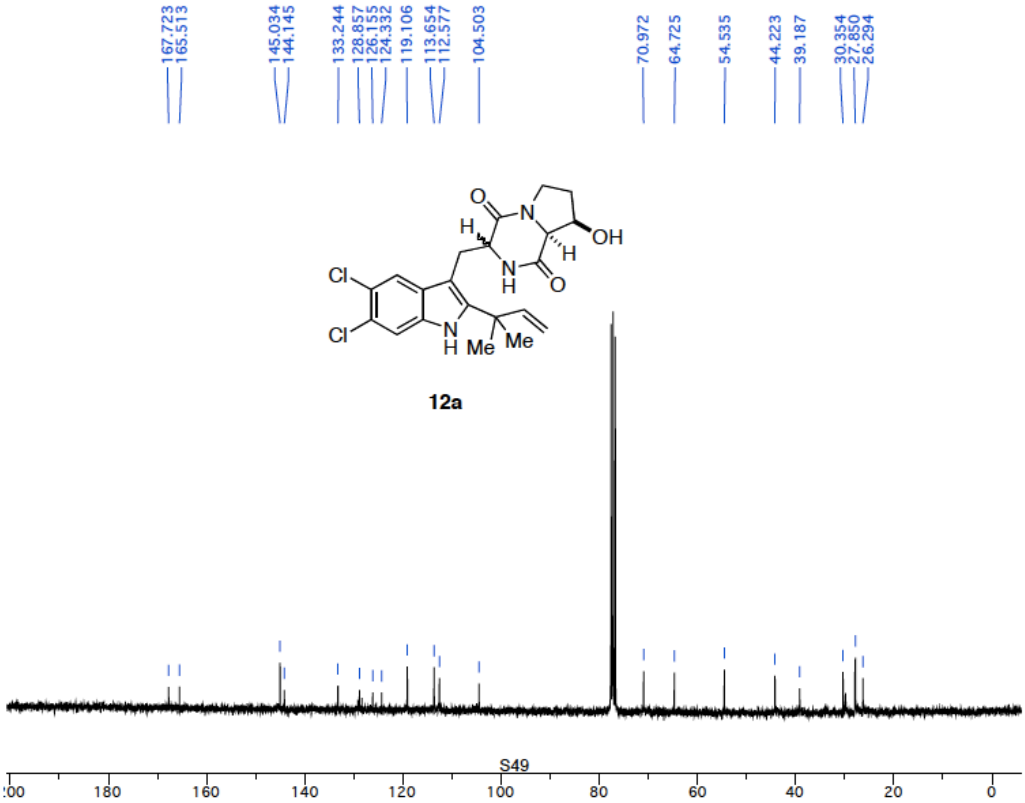

Figure 5.114b. ^{13}C NMR spectrum of compound **5.43**.

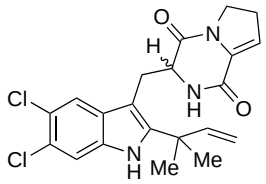

5.44

3-((5,6-dichloro-2-(2-methylbut-3-en-2-yl)-1*H*-indol-3-yl)methyl)-2,3,6,7-tetrahydropyrrolo[1,2-*a*]pyrazine-1,4-dione (5.44). DEAD (419 mg soln., 40% in toluene, 0.44 mL, 0.96 mmol) was added to a solution of **5.43** (140 mg, 0.32 mmol) in CH_2Cl_2 (10 mL). The reaction was stirred for 5 min, and PBu_3 (194 mg, 0.96 mmol) was added. The reaction was stirred for 3 h, and then concentrated under reduced pressure. The residue was purified by flash chromatography eluting with hexanes/EtOAc (1:1) to give 86 mg (64%) of **5.44** as a pale yellow oil.

^{1}H NMR (300 MHz, $CDCl_3$) δ 8.72 (s, 1 H), 7.52 (s, 1 H), 7.33 (s, 1 H), 6.05 (comp, 3 H), 5.09 (d, *J* = 17.3 Hz, 1 H), 5.09 (d, *J* = 10.6 Hz, 1 H), 4.42 (m, 1 H), 4.01 (comp, 2 H), 3.57 (dd, *J* = 14.6, 4.0 Hz, 1 H), 3.15 (dd, *J* = 14.6, 10.6 Hz, 1 H), 2.73 (comp, 2 H), 1.46 (s, 6 H); ^{13}C NMR (75 MHz, $CDCl_3$) δ 162.4, 156.8, 145.4, 144.3, 133.4, 132.8, 128.7, 125.5, 123.7, 119.4, 119.2, 112.6, 112.4, 104.3, 60.5, 57.2, 45.7, 39.2, 30.7, 27.8; IR (neat) 3323, 2971, 1681, 1644, 1446 cm^{-1}; HRMS (TOF+) calcd for $C_{21}H_{22}N_3O_2Cl_2$ (M+H) 418.1084, found 418.1089.

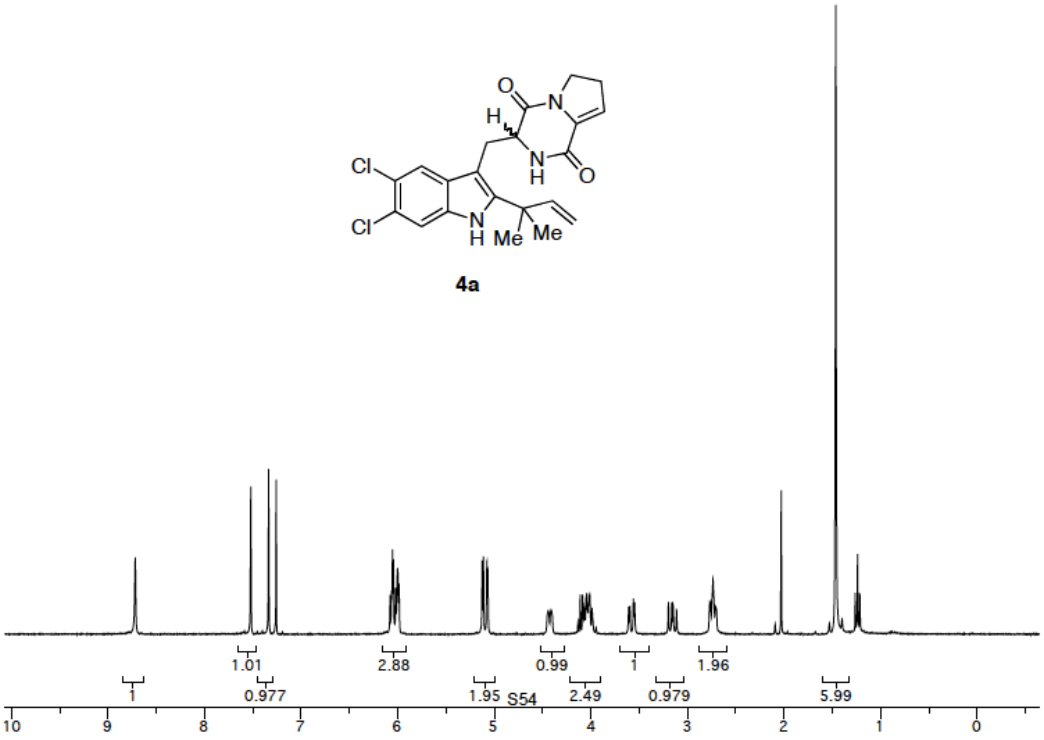

Figure 5.115a. ^{1}H NMR spectrum of compound **5.44**.

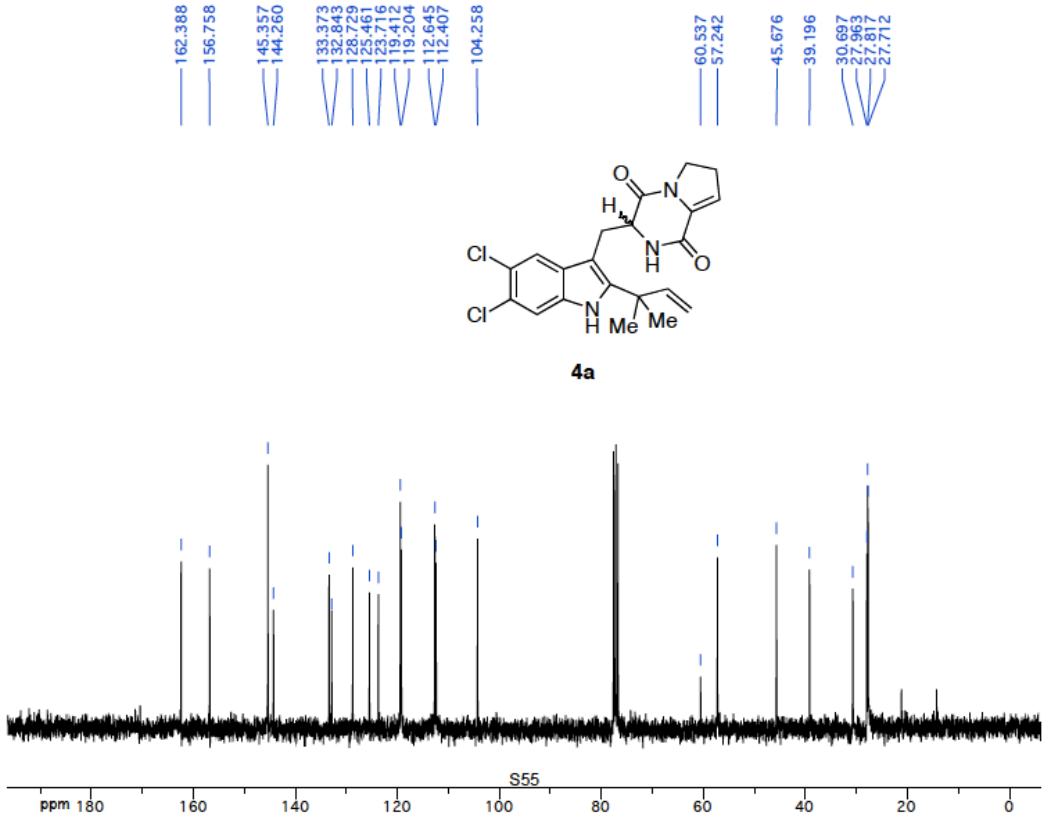

Figure 5.115b. ^{13}C NMR spectrum of compound **5.44**.

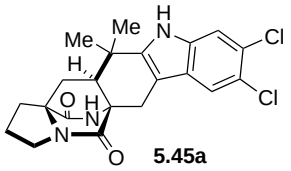

5.45a

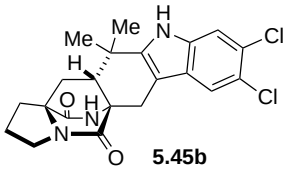

5.45b

Preparation of Cycloadducts 5.45a and 5.45b. To a solution of **5.44** (86 mg, 0.21 mmol) in MeOH (16 mL) at 0 °C was added 20% aqueous KOH (4 mL). The reaction was warmed to room temperature (rt) and was stirred for 12 h. The reaction was quenched with sat. NH_4Cl (30 mL) and extracted with CH_2Cl_2 (3x30 mL). The combined organic layers were dried (Na_2SO_4) and concentrated under reduced pressure. The residue was triturated with $CHCl_3$ (30 mL), and the suspension was filtered to provide 53 mg (60%) of **5.45a** as a white amorphous solid. Concentration of the filtrate gave 25 mg (29%) of **5.45b** as a white amorphous solid.

Data for major isomer **5.45a**: ^{1}H NMR (300 MHz, CD_3OD) δ 7.55 (s, 1 H), 7.40 (s, 1 H), 3.57 (d, *J*) 15.5 Hz, 1 H), 3.47 (m, 1 H), 2.74 (d, *J*) 15.5 Hz, 1 H), 2.60 (m, 1 H), 2.20-1.96 (comp, 6 H), 1.35 (s, 3 H), 1.11 (s, 3 H); ^{13}C NMR (75 MHz, CD_3OD) δ 175.7, 171.3, 144.3, 137.2, 128.1, 125.4, 123.3, 119.8, 113.1, 104.8, 68.3, 61.6, 50.8, 45.2, 36.2, 31.7, 30.1, 28.6, 25.4, 24.9, 22.3; IR (neat) 1663, 1428 cm^{-1}; HRMS (TOF+) calcd for $C_{21}H_{22}N_3O_2Cl_2$ (M + H) 418.1084, found 418.1084.

Data for minor isomer **5.45b**: ^{1}H NMR (300 MHz, $CDCl_3$) δ 9.78 (s, 1 H), 7.49 (s, 1 H), 7.33 (s, 1 H), 3.71 (d, *J*) 17.8 Hz, 1 H), 3.47 (comp, 2 H), 3.25 (s, 1 H), 2.78 (d, *J*) 17.8 Hz, 1 H), 2.67 (m, 1 H), 2.18- 1.78 (comp, 6 H), 1.24 (s, 3H), 1.16 (s, 3 H); ^{13}C NMR (75 MHz, CD_3OD /$CDCl_3$ (1:9)) δ 173.7, 169.6, 142.6, 135.7, 127.1, 125.0, 122.9, 119.1, 112.4, 102.9 67.2, 61.5, 45.8, 44.3, 34.8, 32.6, 29.8, 29.1, 28.4, 24.5, 23.2; IR (neat) 1676, 1453 cm^{-1}; HRMS (TOF+) calcd for $C_{21}H_{22}N_3O_2Cl_2$ (M + H) 418.1084, found 418.1079.

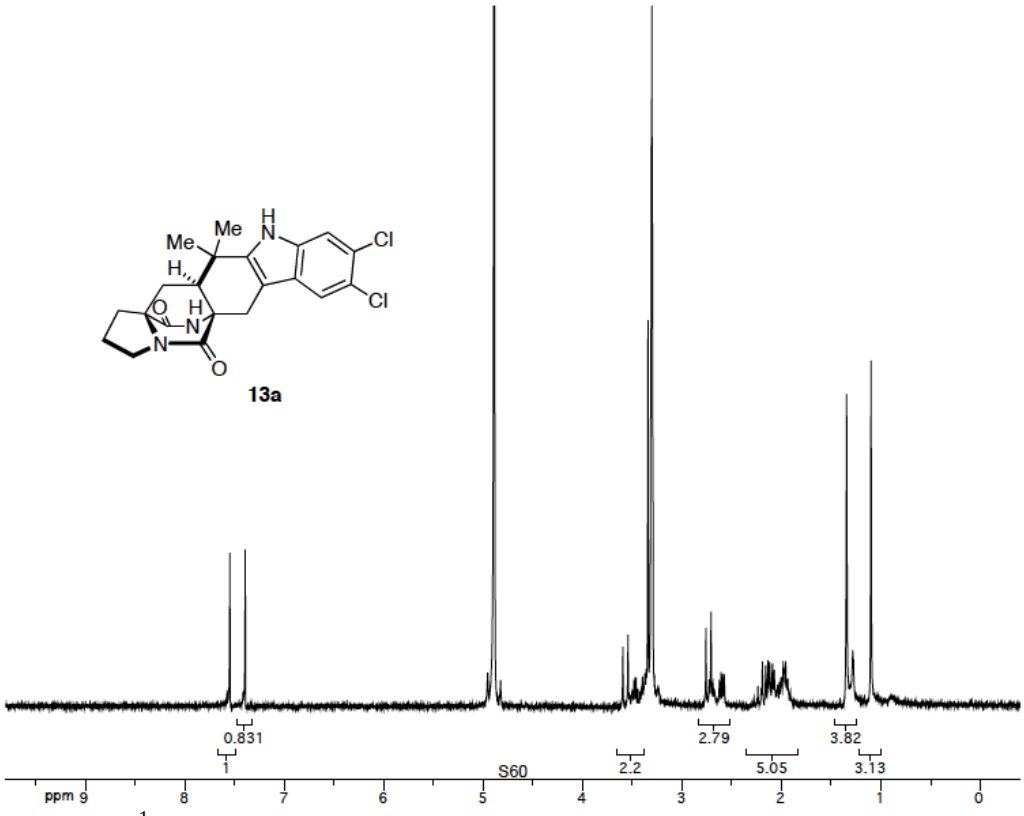

Figure 5.116a. ^{1}H NMR spectrum of compound **5.45a**.

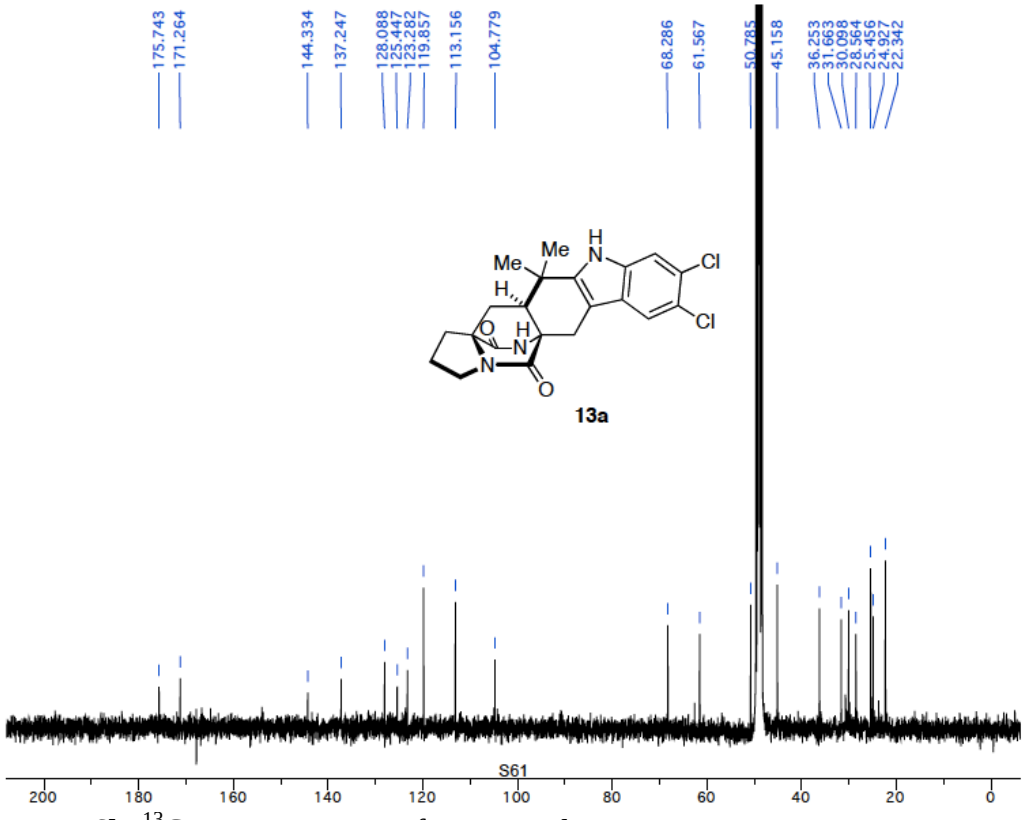

Figure 5.116b. ^{13}C NMR spectrum of compound **5.45a**.

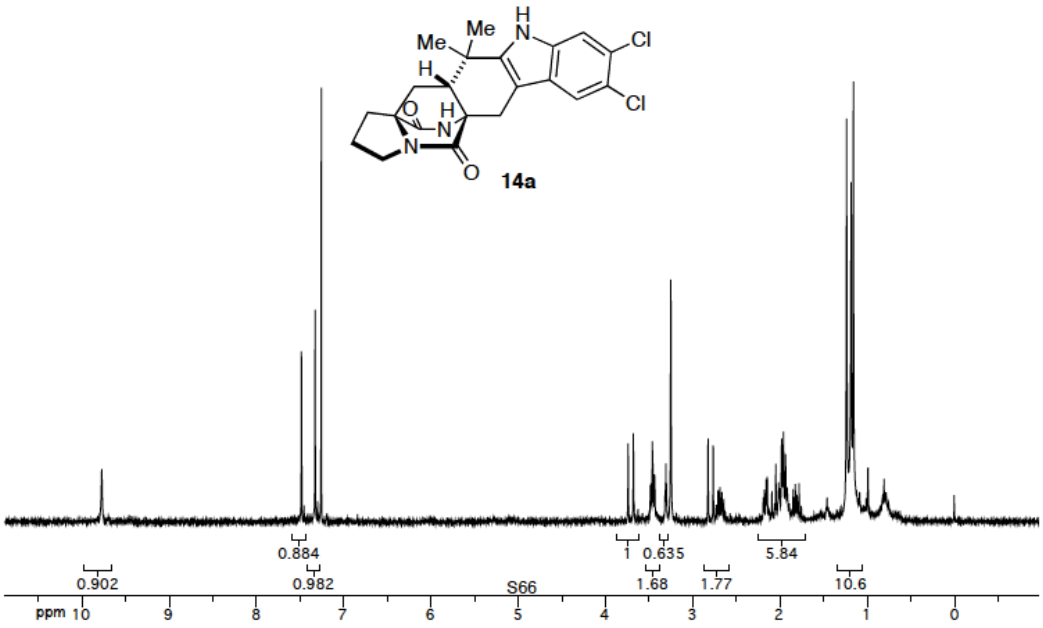

Figure 5.117a. ^{1}H NMR spectrum of compound **5.45b**.

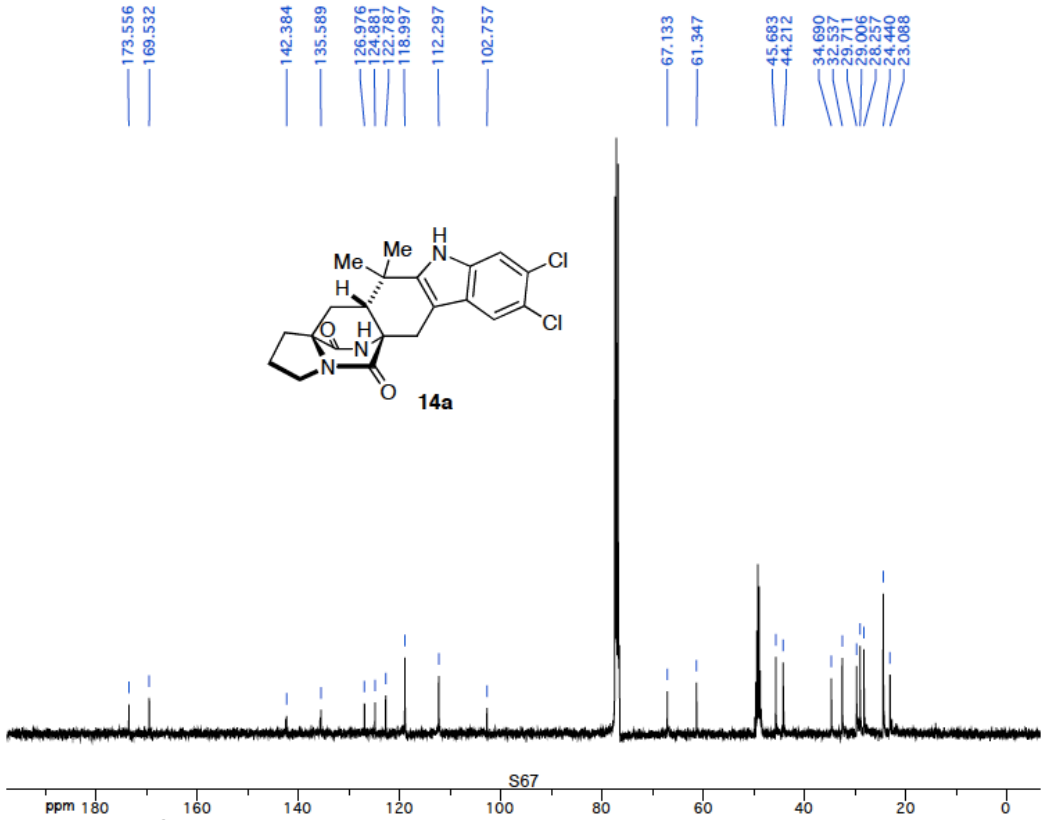

Figure 5.117b. ^{13}C NMR spectrum of compound **5.45b**.

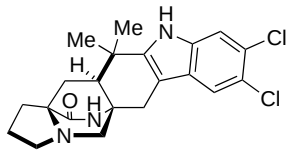

5.46

Synthesis of Malbrancheamide (5.46). DIBAL-H (0.70 mL, 1 M in toluene, 0.70 mmol) was added to a suspension of **5.45a** (15 mg, 0.036 mmol) in toluene (7 mL) at rt. The reaction was stirred at rt for 12 h, whereupon finely powdered Na_2SO_4-$10H_2O$ was added until bubbling ceased. The mixture was filtered with a medium porosity fritted funnel washing with EtOAc (50 mL) and MeOH (50 mL), and the filtrate was concentrated under reduced pressure. The residue was purified by flash chromatography eluting with MeOH/ CH_2Cl_2 (2:98) to give 12 mg (80%) of **5.46** as a white amorphous solid.

^{1}H NMR (400 MHz, CD_3OD) δ 7.48 (s, 1 H), 7.40 (s, 1 H), 3.43 (d, *J*) 10.3 Hz, 1 H), 3.06 (m, 1 H), 2.85 (comp, 2 H), 2.54 (m, 1 H), 2.27 (dd, *J*) 10.2, 1.5 Hz, 1 H), 2.20-1.18 (comp, 6 H), 1.43 (s, 3 H), 1.34 (s, 3 H); ^{13}C NMR (100 MHz, CD_3OD) δ 176.6, 145.1, 137.3, 128.2, 125.3, 123.2, 119.6, 113.1, 104.7, 66.1, 59.4, 57.4, 55.4, 48.5, 35.5, 32.4, 30.6, 30.0, 28.1, 24.2, 23.5; IR (neat) 3226, 1658, 1460 cm^{-1}; HRMS (TOF+) calcd for $C_{21}H_{24}N_3OCl_2$ (M + H) 404.1291, found 404.1290.

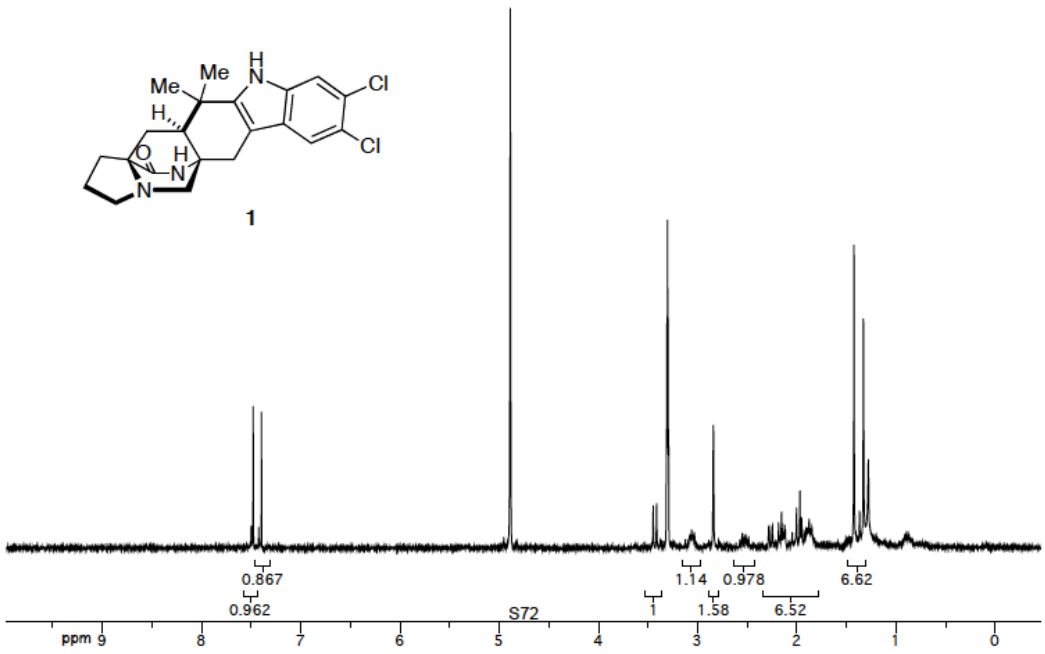

Figure 5.118a. ^{1}H NMR spectrum of compound **5.46**.

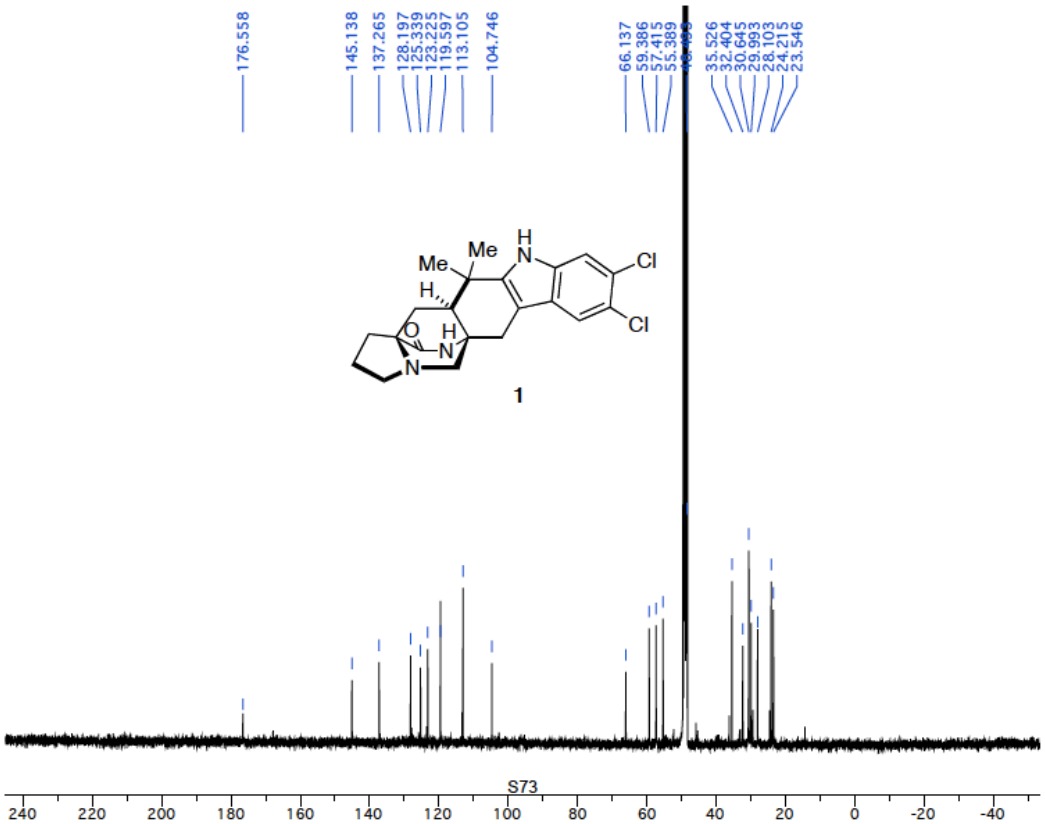

Figure 5.118b. ^{13}C NMR spectrum of compound **5.46**.

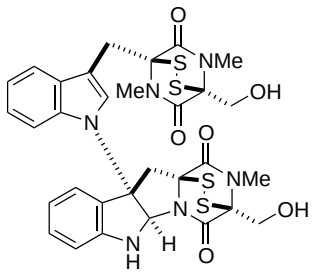

chetomin (**1.12**)

Chetomin (1.12). Authentic sample purchased from Santa Cruz Biotechnology.

^{1}H-NMR (400 MHz; $CDCl_3$): δ 7.66 (dd, *J* = 6.1, 3.0 Hz, 1H), 7.35-7.33 (m, 1H), 7.31-7.27 (m, 2H), 7.23-7.22 (m, 2H), 7.18 (s, 1H), 6.95 (t, *J* = 7.4 Hz, 1H), 6.80 (d, *J* = 8.0 Hz, 1H), 6.21 (s, 1H), 4.43 (s, 1H), 4.39 (d, *J* = 4.7 Hz, 1H), 4.35 (s, 1H), 4.31 (d, *J* = 3.5 Hz, 1H), 4.28 (s, 1H), 3.87 (d, *J* = 15.6 Hz, 1H), 3.71 (d, *J* = 15.4 Hz, 1H), 3.20 (s, 3H), 3.16 (s, 3H), 3.10 (s, 1H), 2.96 (s, 3H); ^{13}C-NMR (101 MHz; $CDCl_3$): δ 166.8, 165.51, 165.48, 163.2, 148.3, 134.0, 131.4, 130.4, 127.2, 126.5, 125.0, 122.8, 120.60, 120.40, 119.2, 111.4, 111.2, 107.7, 80.0, 76.5, 76.1, 74.7, 73.7, 73.5, 61.3, 60.7, 42.6, 28.2, 27.44, 27.34, 27.1.

FOR NMR FILES, SEE Tim/NMR/robot/trw-III-chetomin.

See also (for characterization data): Fujimoto, H.; Sumino, M.; Okuyama, E.; Ishibashi, M. Immunomodulatory Constituents from an Ascomycete, Chaetomium Seminudum. *J. Nat. Prod.* **2004**, *67*, 98-102.

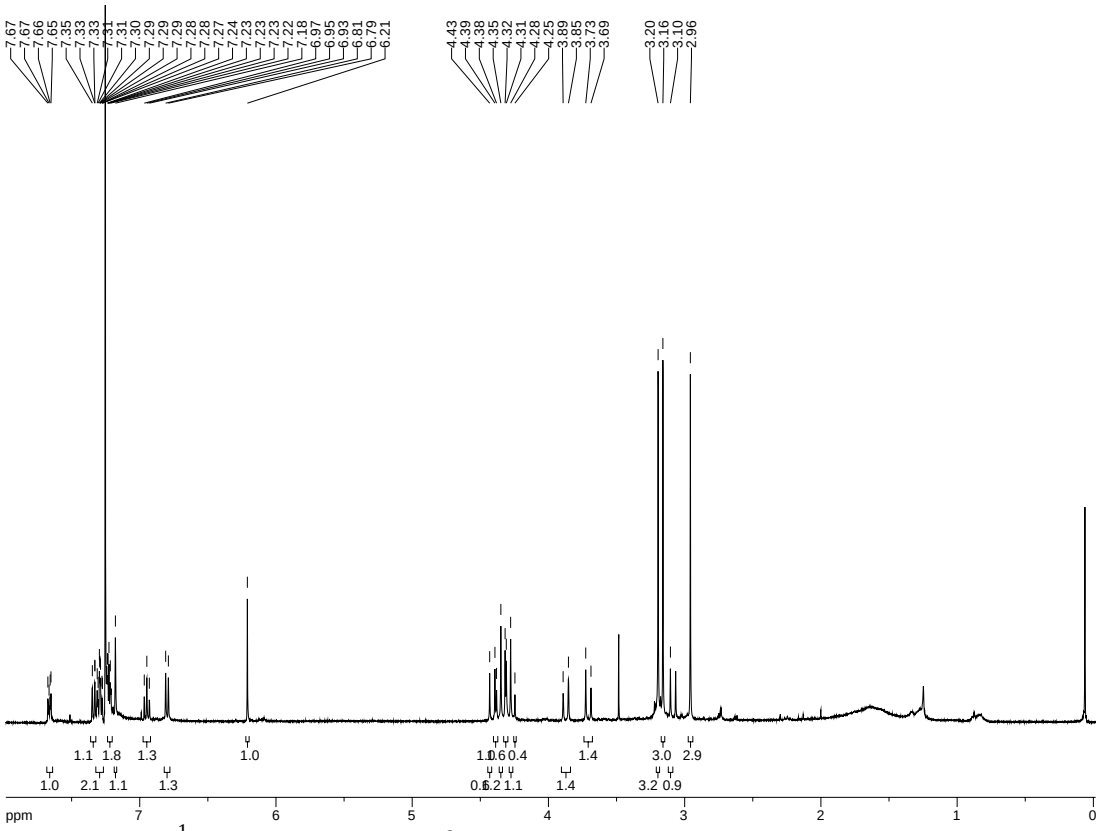

Figure 5.119a. ^{1}H NMR spectrum of compound **1.12**.

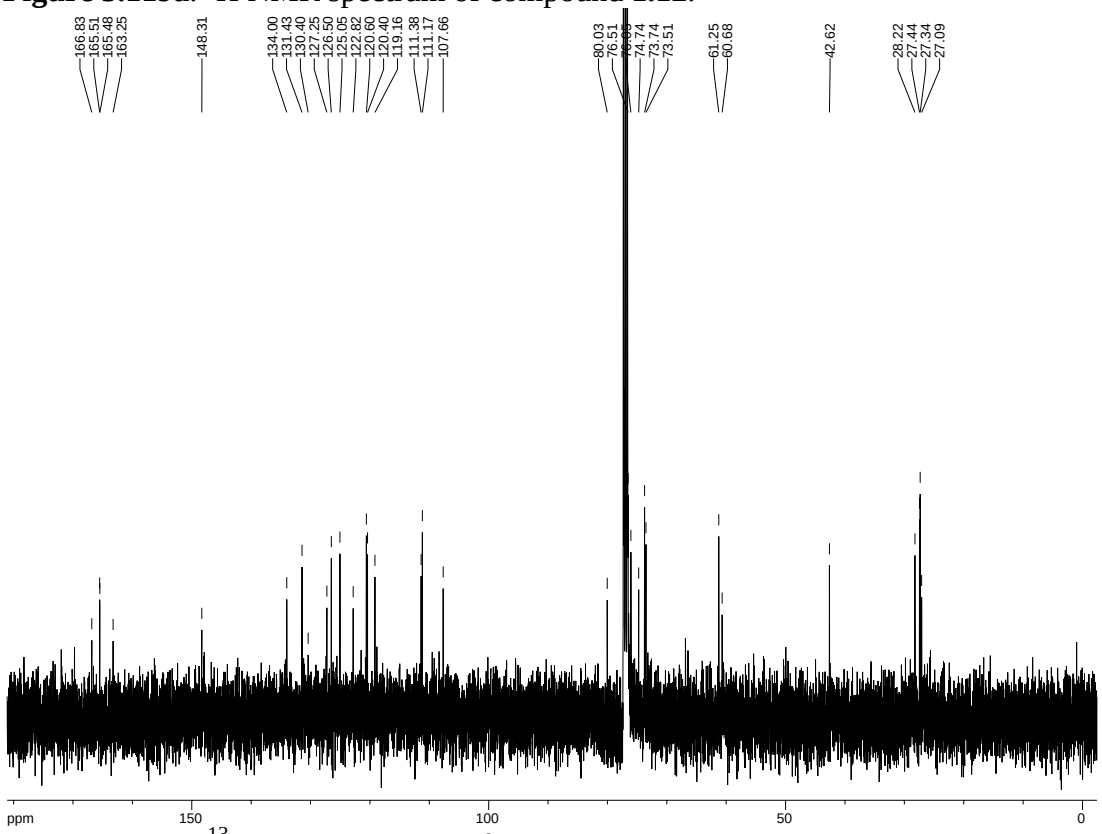

Figure 5.119b. ^{13}C NMR spectrum of compound **1.12**.

APPENDIX I

Publications

4
Biomimetic Synthesis of Alkaloids Derived from Tryptophan: Dioxopiperazine Alkaloids

Timothy R. Welch and Robert M. Williams

4.1
Introduction

Countless secondary metabolic indole alkaloids produced in both marine and terrestrial fungi are derived from tryptophan. Our crude attempts to synthesize some of the vast array of structurally diverse natural alkaloids only serves to showcase the efficiency and elegance with which Nature is able assemble the same molecules. Still, we strive to mimic and in turn better understand the mechanisms inside the cell that are able to produce molecular architecture of such synthetic complexity.

Moreover, it has often been found advantageous to exploit Nature's evolutionary creative design of alkaloids in search of new compounds of therapeutic potential. The rich subclass of biologically active, tryptophan-derived dioxopiperazines found in nature has inspired medicinal chemists to use the dioxopiperazine core in drug design efforts to mimic the interactions of natural peptides while reducing susceptibility to metabolic amide bond cleavage. Furthermore, a dioxopiperazine should pay a small entropic penalty upon binding to a target in comparison to an analogous peptide, as a direct consequence of the reduced conformational mobility inherent in the dioxopiperazine ring. In this chapter, we present a brief review of a select group of (partly) biomimetic syntheses of tryptophan-derived dioxopiperazine alkaloids (Figure 4.1). In most of these syntheses, a single step or key transformation has been deemed to constitute the ''biomimetic'' aspect of that particular work. As the actual biosynthetic pathways to most, if not all, of the alkaloid natural products covered here are either unknown or known only in part we have attempted, where appropriate, to point out the particular biomimetic step or transformation.

4.2
Prenylated Indole Alkaloids

Birch, Wright, and Russell first isolated brevianamide A from *Penicillium brevicompactum* in 1969 [1–3]. Several years later, Birch and coworkers determined that brevianamide A was biosynthetically derived from tryptophan, proline, and

Biomimetic Organic Synthesis, First Edition. Edited by Erwan Poupon and Bastien Nay.
© 2011 Wiley-VCH Verlag GmbH & Co. KGaA. Published 2011 by Wiley-VCH Verlag GmbH & Co. KGaA.

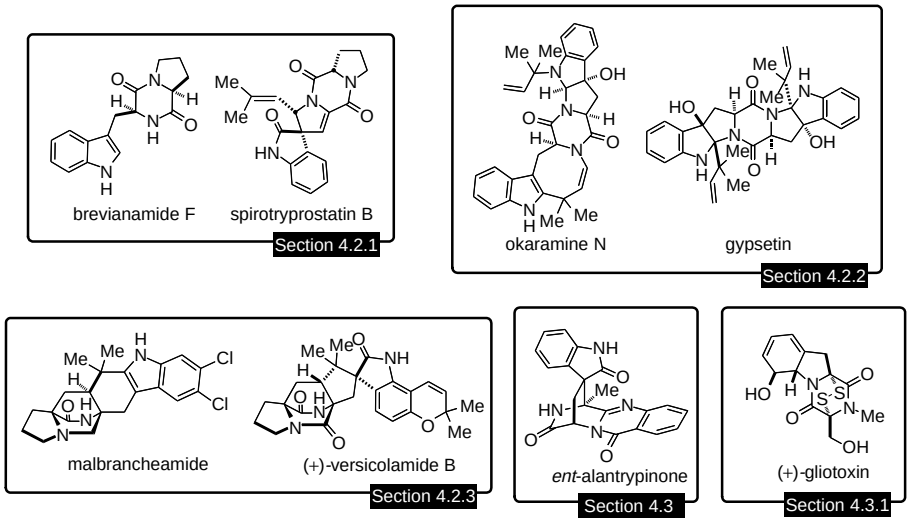

Figure 4.1 Representative molecules discussed in this chapter.

mevalonic acid through feeding experiments (Scheme 4.1) [4]. Furthermore, Birch showed that radiolabeled brevianamide F was incorporated into **5**. It was postulated at the time and later supported with experimental evidence by Williams and coworkers that deoxybrevianamide E was also a biosynthetic precursor [5].

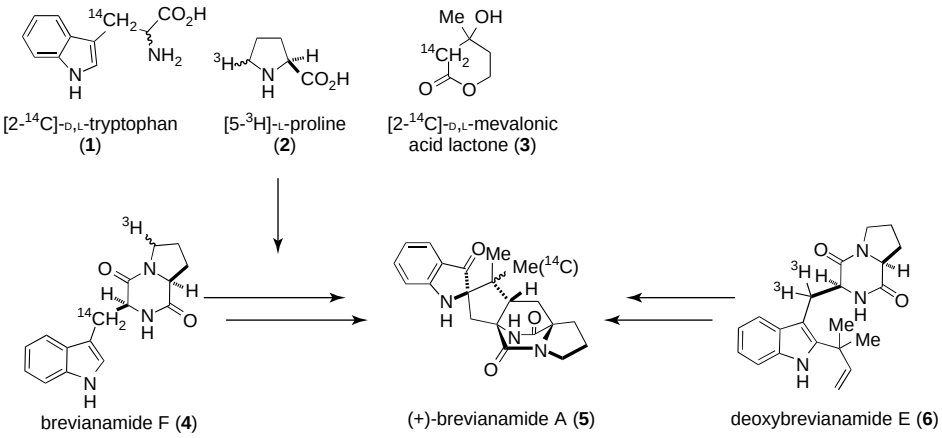

Scheme 4.1 Proposed biosynthesis of the brevianamides.

Since these early studies, Williams has developed a proposal for the biosynthesis of the brevianamides, with that of brevianamide E shown in Scheme 4.2. Derived from tryptophan and proline, **6** was proposed to undergo oxidation to hydroxyindolenine **7**. Irreversible nucleophilic ring closure was supposed to lead to brevianamide E (**8**), supported by incorporation of [8-$^3H_2$]**6** into **8** in significant radiochemical yield [5].

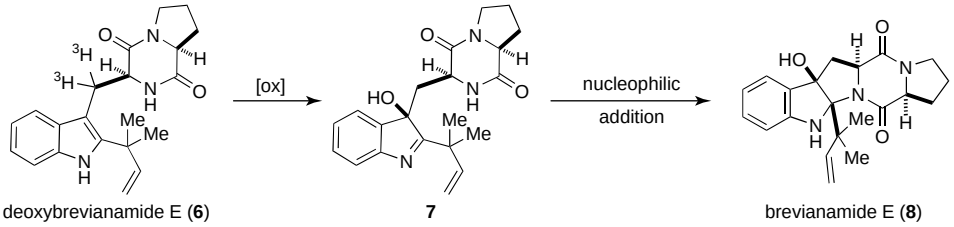

Scheme 4.2 Proposed biosynthesis of brevianamide E.

4.2.1
Dioxopiperazines Derived from Tryptophan and Proline

Brevianamide F (**12**) was first isolated in 1972 and is one of the simplest tryptophan-derived dioxopiperazine natural products. It is readily synthesized through amino acid coupling of *N*-Boc-tryptophan (**9**) to proline ethyl ester (**10**), Boc-deprotection, and ring closure, in modest overall yield (Scheme 4.3) (R.M. Williams, unpublished results).

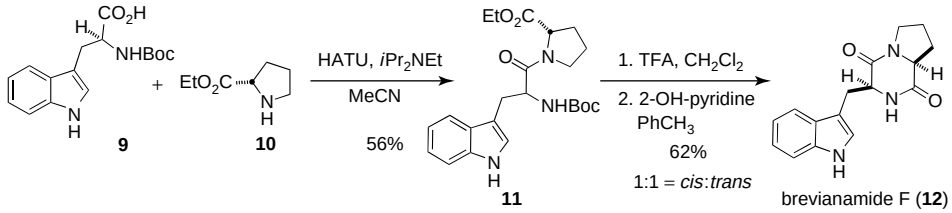

Scheme 4.3 Biomimetic synthesis of brevianamide F.

Brevianamide F lacks only the reverse prenyl group found in deoxybrevianamide E, which has been synthesized by Kametani and coworkers *en route* to brevianamide E (Scheme 4.4) [6]. *N*-Benzyloxycarbonyl-L-proline (**13**) was subjected to Schotten–Baumann conditions with dimethyl aminomalonate to give amide **14**. Debenzyloxycarbonylation of **14** followed by heating with catalytic 2-hydroxypyridine effected cyclization to dioxopiperazine **15** in 93% yield. Condensation with indole **16** gave a separable mixture of diastereomers, individually hydrolyzed to the corresponding free acids (**17**). Heating of the desired diastereomer in dioxane gave deoxybrevianamide E (**18**) and its epimer (**19**) in 29 and 55% yield, respectively. Irradiation of methanolic **18**, containing Rose Bengal in the presence of oxygen, followed by addition of dimethyl sulfide, resulted in the biomimetic hydroxylation of deoxybrevianamide E, furnishing brevianamide E (**8**) and **20** as a separable mixture of diastereomers.

Nineteen years later, a more efficient synthesis of brevianamide E was completed by Danishefsky and coworkers [7]. The synthesis commenced with C3 chlorination of the known phthaloylated tryptophan derivative **21**, followed by addition of fresh prenyl-9-borabicyclo[3.3.1]nonane (prenyl-9-BBN) to the resultant 3-chloroindolenine (Scheme 4.5). Hydrazinolysis in ethanol provided amino ester

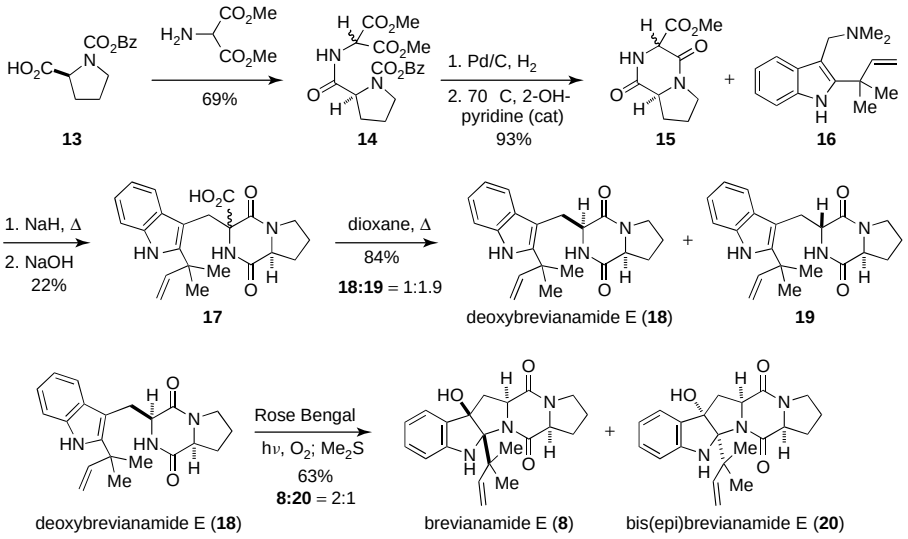

Scheme 4.4 Kametani's total synthesis of deoxybrevianamide E and brevianamide E.

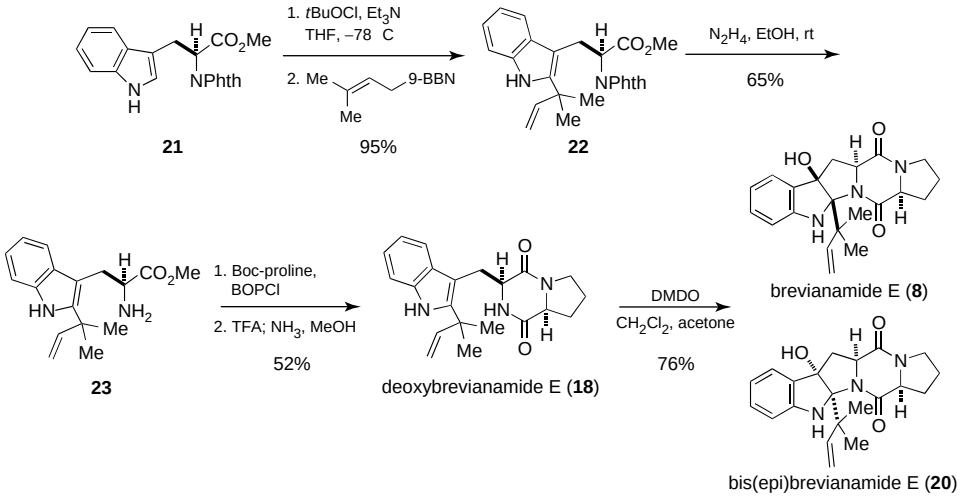

Scheme 4.5 Danishefsky's total synthesis of brevianamide E.

23 in 65% yield, which was coupled to *N*-Boc-L-proline, deprotected, and cyclized to afford deoxybrevianamide E (**18**) in 52% yield. Compound **18** was elaborated to brevianamide E (**8**) and bis(epi)brevianamide E (**20**) in a ratio of ~1 : 5 upon treatment with dimethyldioxirane (DMDO) in a biomimetic oxidative cyclization sequence reminiscent of the original Kametani work discussed above.

The structural similarities between deoxybrevianamide E and the then newly isolated natural products tryprostatin A and B did not escape notice of Danishefsky

and coworkers. While prenylation failed in attempts to use a reverse prenylborane nucleophile directly as in the method used to synthesize **22** above, a solution was found in treating chloroindolenine **24** with tri(*n*-butyl)prenylstannane and BCl_3 to afford the desired prenyl functionality at C_2 in excellent yield (Scheme 4.6). Phthalimide deprotection, peptide coupling, Boc-deprotection, and cyclization were achieved to afford tryprostatin B (**30**) in 43% overall yield [7].

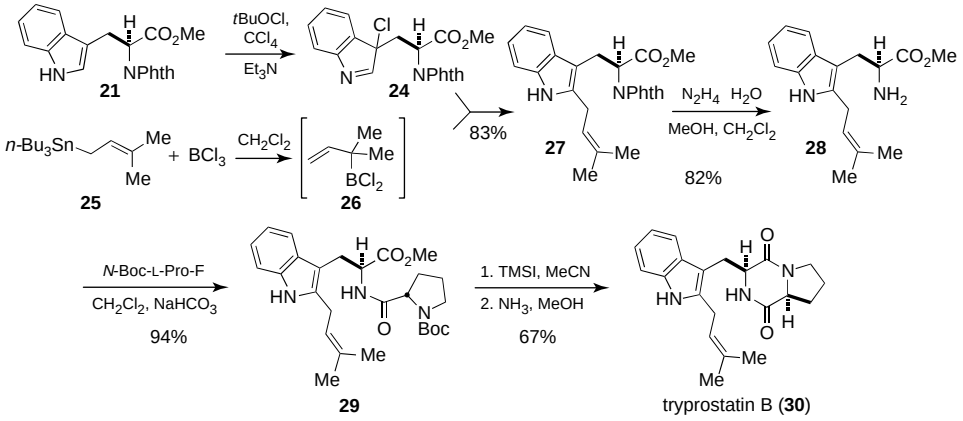

Scheme 4.6 Biomimetic total synthesis of tryprostatin B.

Danishefsky and coworkers also completed the total synthesis of the spirooxindole spirotryprostatin B [8]. L-Tryptophan methyl ester was converted into the oxindole derivative **32**, followed by addition of prenyl aldehyde under basic conditions to afford an inseparable four-component mixture of spirooxindoles (**33**–**36**, Scheme 4.7). Peptide coupling and subsequent treatment of the mixture with lithium bis(trimethylsilyl)amide (LHMDS) followed by selenylation presumably gave phenyl selenide mixture **38**. Oxidative elimination produced a mixture from which **39** was separated and elaborated to spirotryprostatin B (**40**) via Boc-deprotection and base-induced cyclization.

Danishefsky took a markedly different approach in the synthesis of spirotryprostatin A [9]. A potentially biomimetic Pictet–Spengler reaction of tryptophan derivative **42** with thioaldehyde **41** as a masked isoprene equivalent gave the desired *cis*-tetrahydrocarboline (**43**) with marginal selectivity (Scheme 4.8). *N*-Bromosuccinimide (NBS)-mediated oxidative rearrangement proceeded via intermediate **44** to the oxindole was followed by deprotection of the carbamate to give amine **45**. The modest yield of the sequence (57%) reflects the susceptibility of the oxindole to electrophilic aromatic bromination under the *spiro*-rearrangement conditions. Peptide coupling and Troc-deprotection resulted in cyclization to the dioxopiperazine, after which oxidation and sulfoxide elimination revealed the prenyl group to afford selectively spirotryprostatin A (**48**).

The synthesis of notoamide J was completed by Williams and coworkers, starting with the Boc-protection of 7-hydroxyindole (Scheme 4.9) [10]. Chlorination at C3 was followed by reverse prenylation of the resultant 3-chloroindolenine **51** to afford

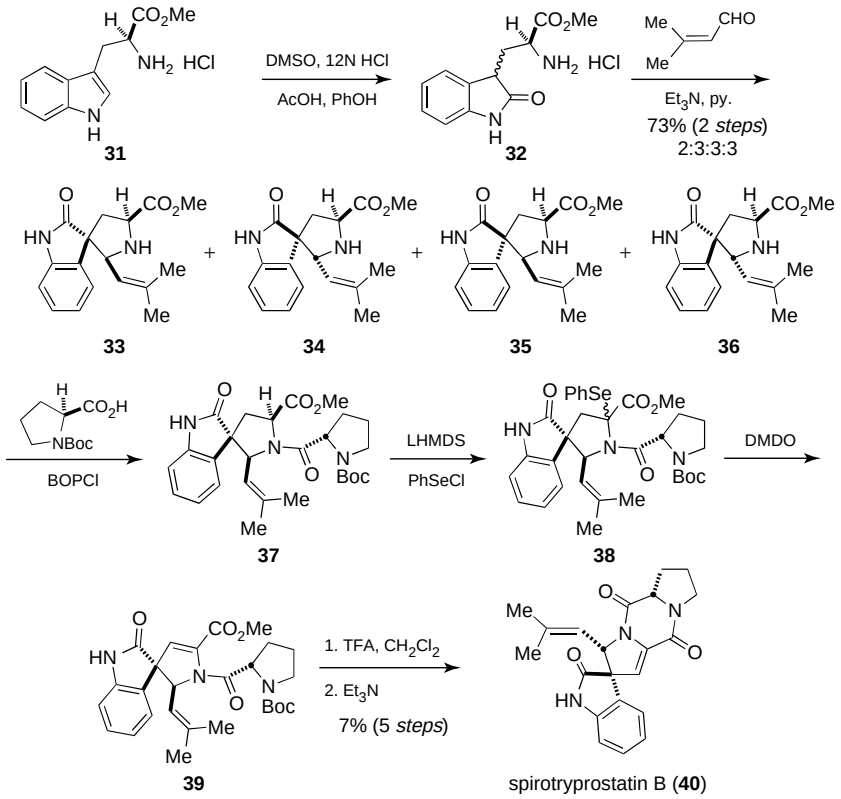

Scheme 4.7 Danishefsky's synthesis of spirotryprostatin B.

52. The corresponding gramine was prepared by treating **52** with formaldehyde and dimethylamine, and subsequent Somei–Kametani coupling and imine hydrolysis gave tryptophan derivative **54** in good yield. Protection of the free amine as the Boc-carbamate and ester hydrolysis gave **55**, which was coupled to proline ethyl ester in the presence of *O*-(7-azabenzotriazol-1-yl)-*N,N,N′,N′*-tetramethyluronium hexafluorophosphate (HATU) to afford amide **56**. Cyclization to dioxopiperazine **57** was followed by a biomimetic oxidation sequence accompanied by pinacol-type rearrangement to the oxindoles notoamide J (**58**) and 3-epi-notoamide J (**59**) in a 2 : 1 separable mixture.

4.2.2
Dioxopiperazine Derived from Tryptophan and Amino Acids other than Proline

Corey and coworkers designed a succinct synthesis of okaramine N, featuring a Pd-promoted dihydroindoloazocine formation [11]. Readily available tryptophan derivative **60** was reduced to indoline **61** and subsequently prenylated via copper(I)-catalyzed alkylation with butyne **62** (Scheme 4.10). Treatment with

Scheme 4.8 Danishefsky's synthesis of spirotryprostatin A.

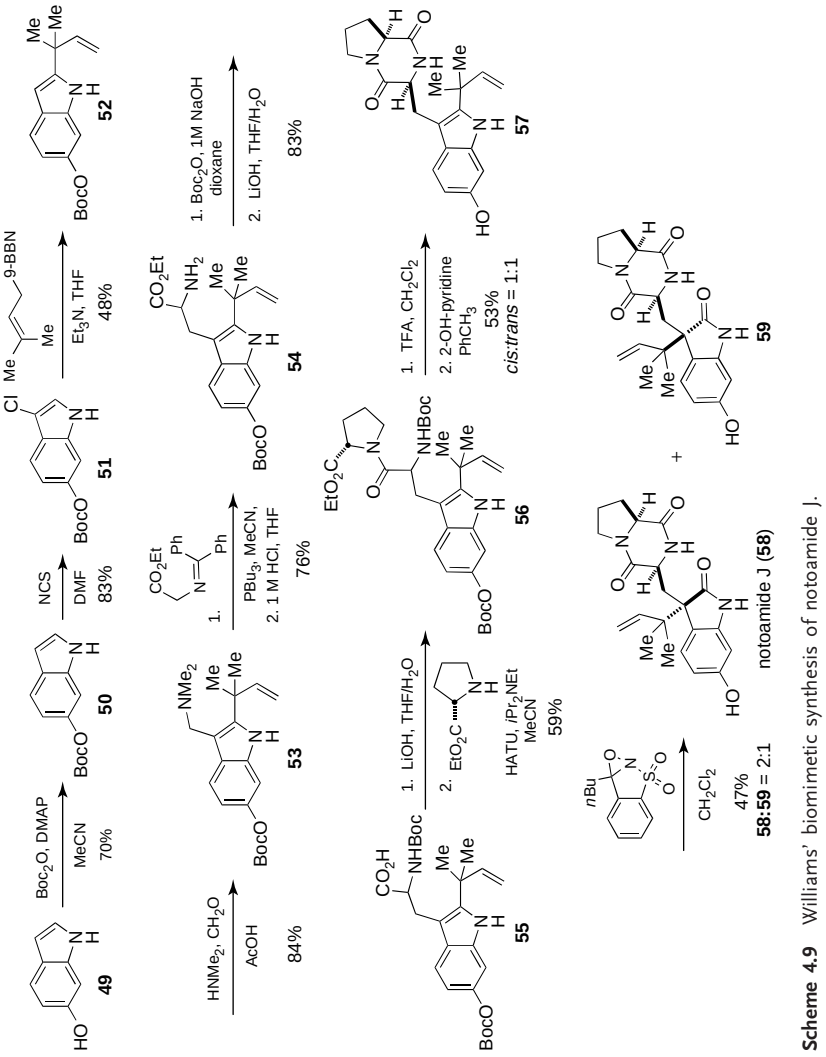

Scheme 4.9 Williams' biomimetic synthesis of notoamide J.

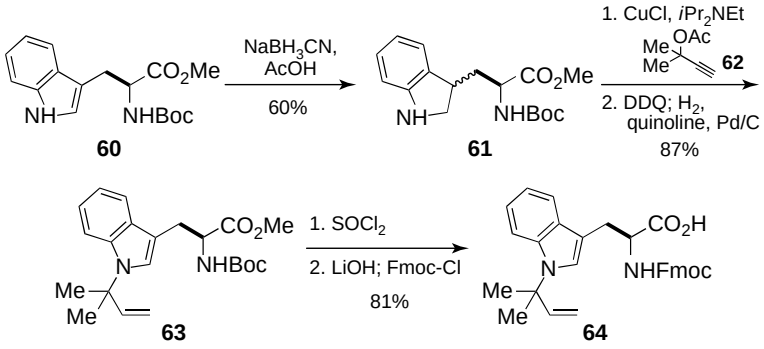

Scheme 4.10 Synthesis of the *N*-reverse-prenylated tryptophan derivative.

2,3-dichloro-5,6-dicyano-1,4-benzoquinone (DDQ) effected the dehydrogenation of the indoline, and the resulting tryptophan derivative **63** was deprotected, saponified, and reprotected as the N-Fmoc derivative (**64**).

The synthesis of okaramine N was completed through reductive amination of 3-methyl-buten-2-al onto L-tryptophan methyl ester, followed by coupling of the resultant product (**65**) with acid **64** to form the desired tetracycle (Scheme 4.11). Treatment of **66** with $Pd(OAc)_2$ provided the eight-membered ring (**67**) in modest yield (38%). The free amine obtained upon Fmoc cleavage underwent cyclization to form dioxopiperazine **68** in 95% yield. A potentially biomimetic oxidative cyclization was effected by treating **68** with *N*-methyltriazolinedione (MTAD), which reacted selectively with the N-unsubstituted indole subunit, and after photooxidation and

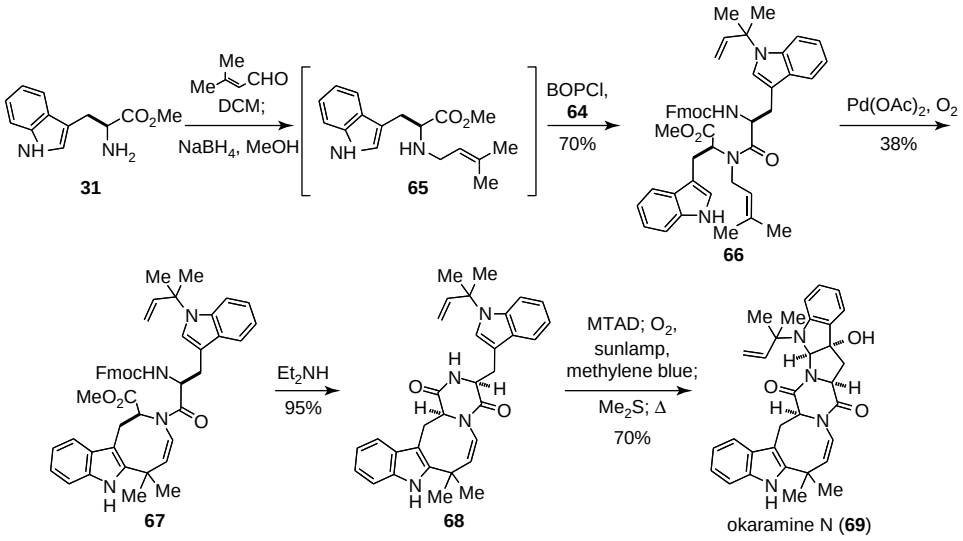

Scheme 4.11 Completion of the total synthesis of okaramine N.

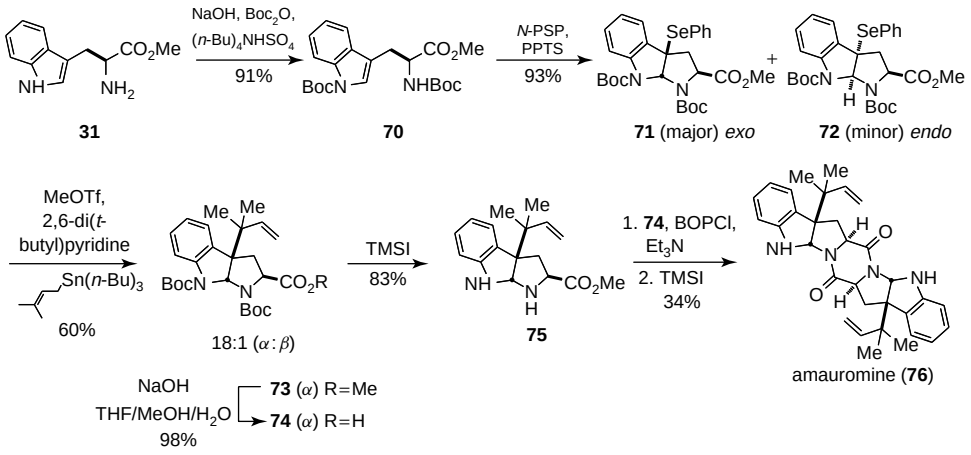

Scheme 4.12 Danishefsky's total synthesis of amauromine.

then reduction formed a hydroxylated octacycle that was directly converted into okaramine N (**69**) via thermolysis in 70% yield.

Amauromine was synthesized as shown in Scheme 4.12, starting with the bis(Boc) protection of L-tryptophan [12]. Conversion into the selenide by reaction with *N*-phenylselenophthalimide (*N*-PSP) in the presence of pyridinium *p*-toluenesulfonate (PPTS) afforded a mixture of **71** and **72** (9 : 1). Photolysis of the mixture in the presence of prenyltri(*n*-butyl)tin produced a mixture of reverse prenylated pyrrolodinoindolines, the desired major diastereomer of which was separated by crystallization from hexanes. The Boc groups were globally cleaved using iodotrimethylsilane (TMSI) to afford the ester (**75**). Coupling of **75** with acid **74** gave the amide, which readily cyclized to the desired dioxopiperazine (**76**, amauromine) upon treatment with TMSI.

Danishefsky and coworkers completed a total synthesis of gypsetin in the same fashion as their effort on brevianamide E [7]. The reverse prenylated amine, **23**, was synthesized as shown above (Scheme 4.5). Boc protection and cleavage of the methyl ester afforded acid **77**, which was coupled to amine **23**, deprotected, and cyclized to dioxopiperazine **78** (Scheme 4.13). Treatment with DMDO effected the biomimetic oxidative conversion into the natural product gypsetin (**79**).

4.2.3
Bicyclo[2.2.2]diazaoctanes

In 1970, Sammes proposed a hetero-Diels–Alder cycloaddition to be the biosynthetic origin of the bicyclo[2.2.2]diazaoctane core found in brevianamides A and B (Scheme 4.14) [13].

Support for this proposal was observed upon treating dihydroxypyrazine **82** with dimethyl acetylenedicarboxylate (**83**) or with norbornadiene (**84**) to give cycloadducts **85** or **86**, respectively (Scheme 4.15) [13].

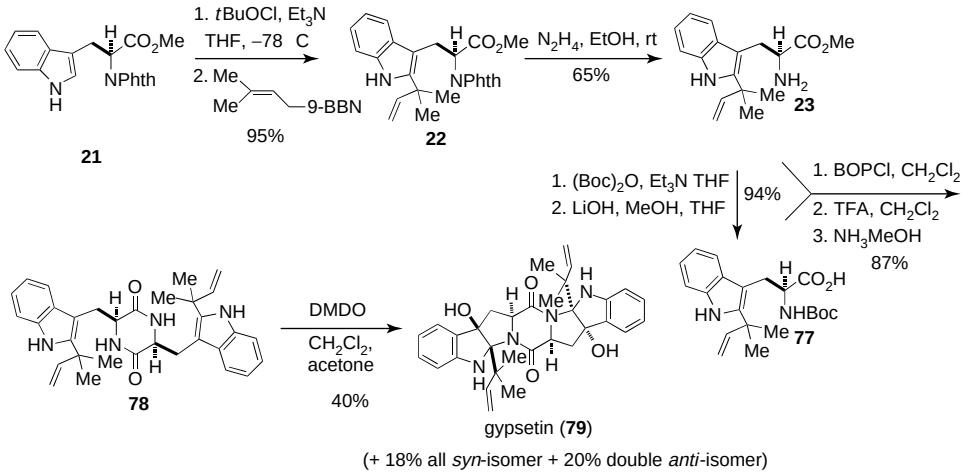

Scheme 4.13 Synthesis of gypsetin.

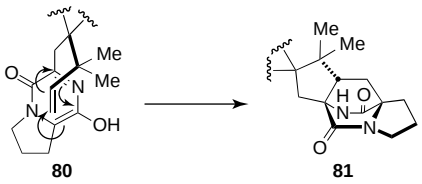

Scheme 4.14 Proposed hetero-Diels–Alder formation of bicyclo[2.2.2]diazaoctanes.

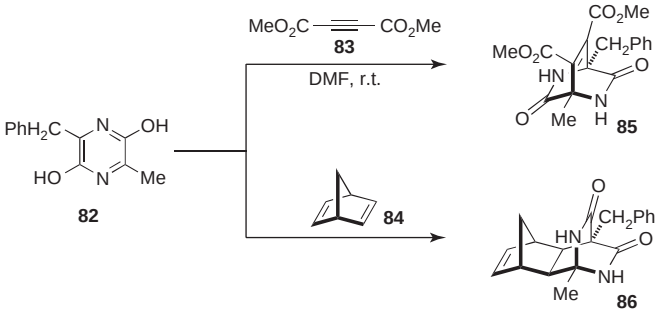

Scheme 4.15 Sammes' model study of proposed cycloaddition.

Williams and coworkers expanded on the pioneering work of Sammes with the following biosynthetic proposal for the brevianamides [5]. Deoxybrevianamide E (**18**) was thought to undergo oxidation to hydroxyindolenine **7**, which could undergo a pinacol-type rearrangement to indoxyl **87** (Scheme 4.16). Subsequent two-electron oxidation and enolization to azadiene **88**, followed by an intramolecular hetero-Diels–Alder reaction was, following from the original proposal of Sammes, envisioned to give the natural products (+)-brevianamide A and (+)-brevianamide

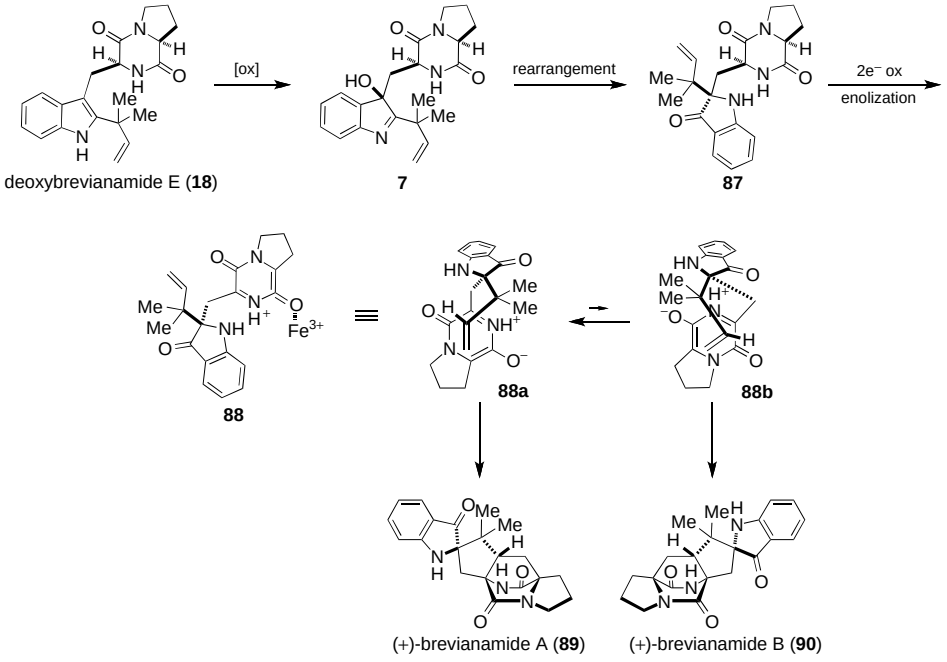

Scheme 4.16 Biosynthetic proposal for the brevianamides.

B. The pseudo-enantiomorphic relationship between the two natural products was envisaged to arise from the equilibrium between conformers **88a** and **88b**, which undergo cycloaddition to give **89** and **90**, respectively. *Ab initio* studies of the two transition states demonstrated that **88a** is the more stable of the two, which is consistent with the observed product ratios of **89** and **90**. The theoretical insights published by Domingo *et al.* lend support to the proposal of a biosynthetic intramolecular Diels–Alder reaction of intermediate **88** [14]. Unfortunately, experimental support for this pathway has been elusive to secure and thus it remains a speculative biogenetic construction.

The total synthesis of D,L-brevianamide B demonstrated the first congruent application of a biomimetic Diels–Alder reaction used to form the bicyclo[2.2.2]diazaoctane core common to the series of prenylated dioxopiperazines to be discussed in this section [15]. 9-Epi-deoxybrevianamide E (**19**) was converted into the lactim ether (**91**) and oxidized to give the Diels–Alder precursor **92** (Scheme 4.17). Treatment with aqueous methanolic KOH induced tautomerization to azadiene **93**, which underwent a potentially biomimetic intramolecular Diels–Alder cycloaddition to give a mixture of diastereomers (**94** and **95**, 2 : 1). Oxidation, pinacol-type rearrangement, and lactim ether deprotection of the minor diastereomer (**95**) afforded brevianamide B (**90**) in 65% overall yield from **96**. This study was one of the first to experimentally support the biogenetic origin of the core bicyclo[2.2.2] ring system as arising via a dioxopiperazine that undergoes a net two-electron oxidation to an azadiene moiety.

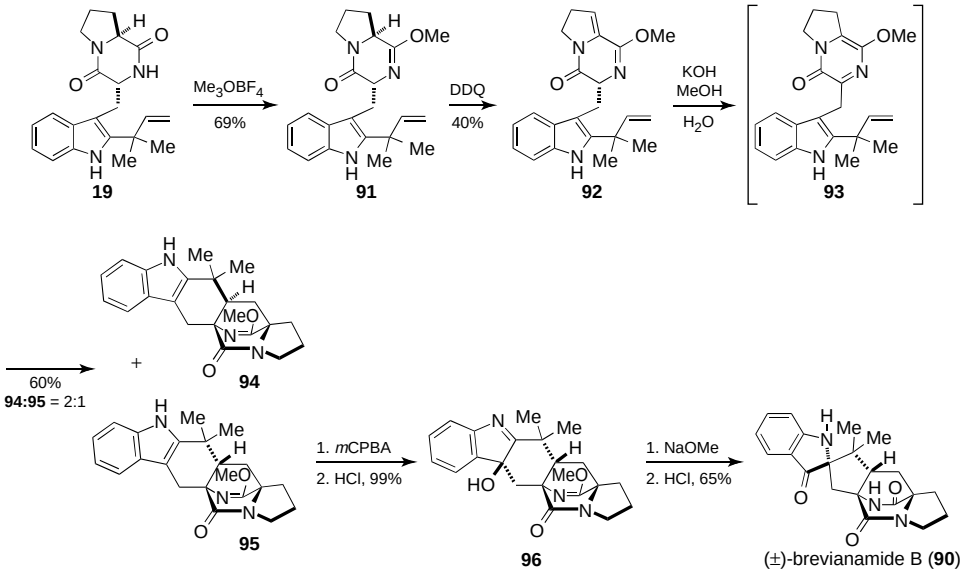

Scheme 4.17 Application of the proposed biomimetic Diels–Alder reaction.

Williams and coworkers also applied the intramolecular Diels–Alder reaction to the racemic synthesis of VM55599 [16]. The reverse-prenylated tryptophan derivative **97** was coupled to β-methyl-β-hydroxyproline ethyl ester **98** to afford dipeptide **99** (Scheme 4.18). *N*-Boc deprotection and cyclization afforded dioxopiperazine **100**, and elimination with thionyl chloride gave enamide **101**. Formation of the lactim ether (**102**) and treatment with aqueous KOH gave azadiene **103**, which spontaneously suffered intramolecular Diels–Alder reaction to give a separable mixture of all four possible racemic diastereomers (**104**–**107**, 2.6 : 3.7 : 1.0 : 1.6, respectively). Cleavage of the lactim ether and diisobutylaluminum hydride (DIBAL-H) reduction gave VM55599 in 73% yield from **105**.

The synthesis of VM55599 allowed for assignment of the absolute stereochemistry of the molecule, which places the methyl group at the β-position of the proline residue *syn*- to the bridging isoprene moiety [16]. In stark contrast, the analogous methyl group of paraherquamide A is *anti* to the bridging isoprene unit. Scheme 4.19 outlines a possible unified biosynthesis for VM55599 and paraherquamide A, arising from dimethylallyl pyrophosphate (DMAPP), L-isoleucine, and L-tryptophan. If a Diels–Alder cycloaddition is to be invoked, approach of the isoprene moiety must occur from the same face as the methyl group on the proline ring for synthesis of VM55599, and from the opposite face to the methyl group to give paraherquamide A. The diastereofacial selectivity of the Diels–Alder reaction gave a preponderance of the *syn*-relative stereochemistry *alpha* to the *gem*-dimethyl group in both molecules. As VM55599 is a very minor metabolite of *Penicillium* sp. IMI332995, it is plausible that cyclization of **112**→**114** is preferred and further metabolization gives paraherquamide A, whereas the minor cycloaddition via **113** produces VM55599 as a dead-end shunt metabolite. As shown in Scheme 4.18

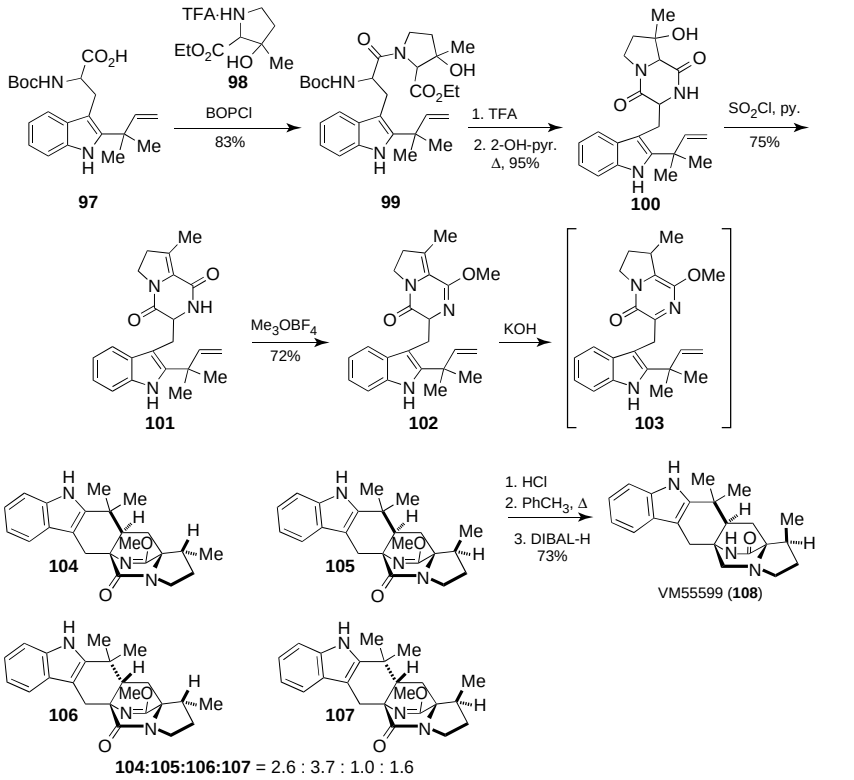

Scheme 4.18 Williams' biomimetic total synthesis of VM55599.

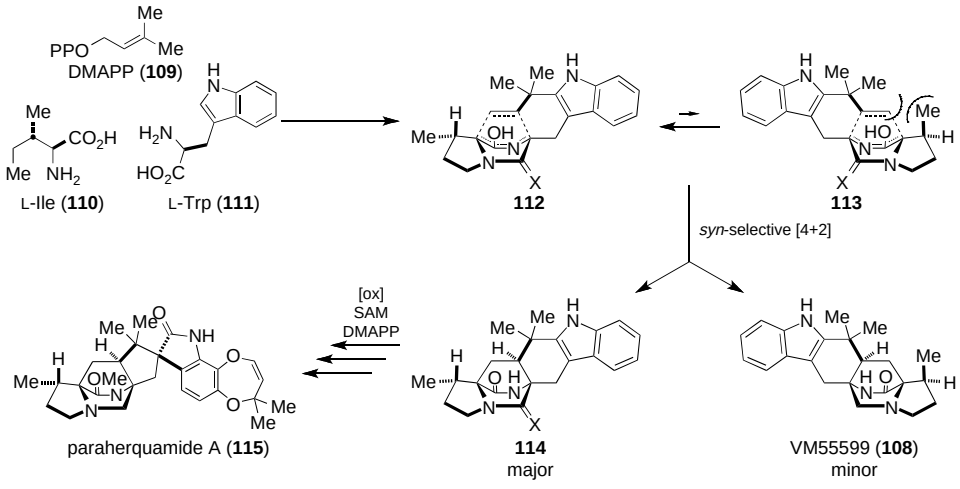

Scheme 4.19 Proposed biosynthesis of paraherquamide A and VM55599.

above, the intrinsic diastereofacial bias of the Diels–Alder reaction is modest at best, giving a slight excess (1.47 : 1) of cycloaddition from the same face as the methyl group, and favoring the *syn*-relative stereochemistry to the extent of 2.4 : 1. Such observations suggest that the biosynthesis may rely on protein organization of the precyclization conformers to stereoselectively produce the *syn*-isomers.

A report from Liebscher and coworkers showed promise in terms of improving the diastereoselectivity of the Diels–Alder cycloaddition, using neutral conditions to prepare the azadiene in contrast to the basic conditions employed by Williams [17]. Compound **118** was prepared by a Horner–Wadsworth–Emmons reaction of aldehyde **116** with phosphonate **117** (Scheme 4.20). Treatment of **118** with neat acetyl chloride for 20 days gave the Diels–Alder product **119** as a single diastereomer in 48% yield.

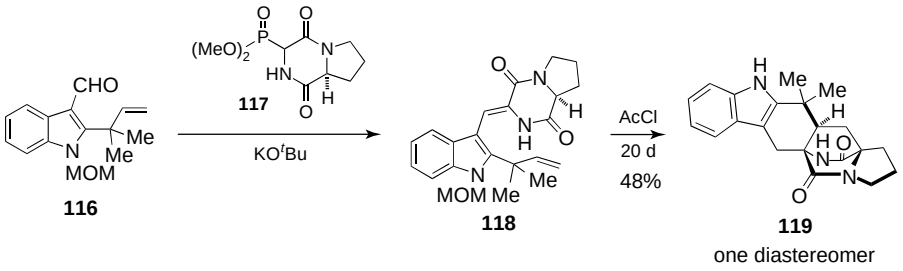

Scheme 4.20 Liebscher's Diels–Alder work.

The precedent set by Liebscher's work was applied to an asymmetric total synthesis of VM55599 [18]. The loss of stereochemistry observed at the proline methyl group in **101** above led Williams to employ a dehydrotryptophan derivative as the Diels–Alder azadiene precursor, allowing for the preparation of VM55599 in an enantioselective fashion. Williams has demonstrated that the β-methylproline residue of paraherquamide A and VM55599 are biosynthetically derived from L-Ile. In a biomimetic construct, L-Ile was converted into optically pure β-methylproline **120** using Hoffman–Löffler–Freytag conditions in 45% yield (Scheme 4.21).

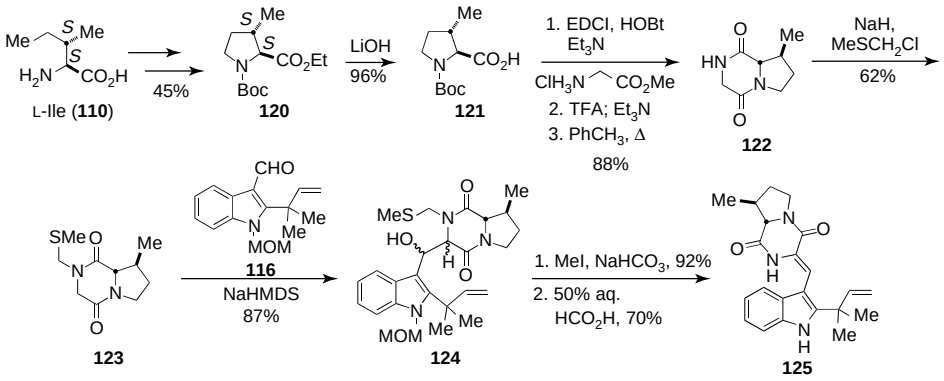

Scheme 4.21 Key dioxopiperazine synthesis.

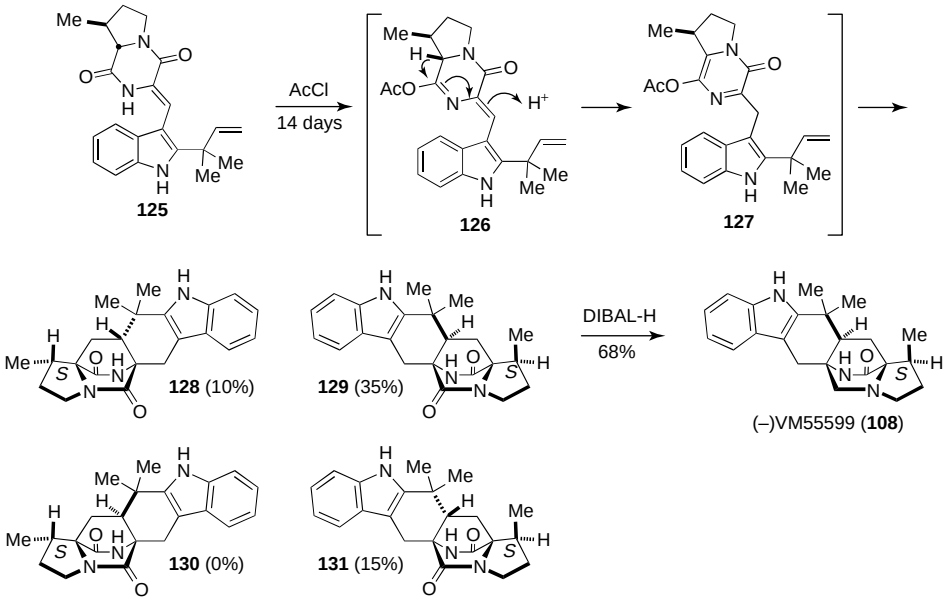

Scheme 4.22 Completion of the asymmetric total synthesis of (−)-VM55599.

Cleavage of the ethyl ester, peptide coupling to glycine methyl ester hydrochloride, Boc deprotection, and cyclization gave dioxopiperazine **122** in good overall yield. Protection of the secondary amide and subsequent condensation with aldehyde **116** gave an epimeric mixture of dioxopiperazines, which gave selectively *(Z)*-isomer **125** following deprotection and dehydration.

Following Liebscher's protocol, **125** was treated with acetyl chloride for 14 days, yielding a mixture of three diastereomers (Scheme 4.22). The reaction is thought to proceed by initial acylation to the *O*-acyl lactim **126**, tautomerization to azadiene **127**, which suffers intramolecular Diels–Alder reaction from three of the four possible diastereomeric transition states, followed by loss of acetate to give compounds **128–131**. The major diastereomer **129** was treated with excess DIBAL-H to effect reduction to (−)-VM55599 (**108**). Interestingly, cycloadduct **130** was not observed from the cycloaddition reaction. *Penicillium* sp. produces paraherquamide A in large excess over VM55599 (>600 : 1), so it is surprising that this provocative biogenetic precursor to paraherquamide A is not observed in laboratory cycloaddition reactions. Despite the structural differences between the laboratory and biological Diels–Alder precursors, the intrinsic facial selectivity of the cyclization does not appear to mimic the bias toward paraherquamide stereochemistry one would expect given the observed product ratios of the fungal metabolites.

As many of the bicyclo[2.2.2]diazaoctane natural products differ only at the substitution of the indole ring, a convergent approach utilizing a Fischer indole synthesis was undertaken in an alternative racemic synthesis of brevianamide B [19]. This work had the objective of validating other possible biosynthetic pathways

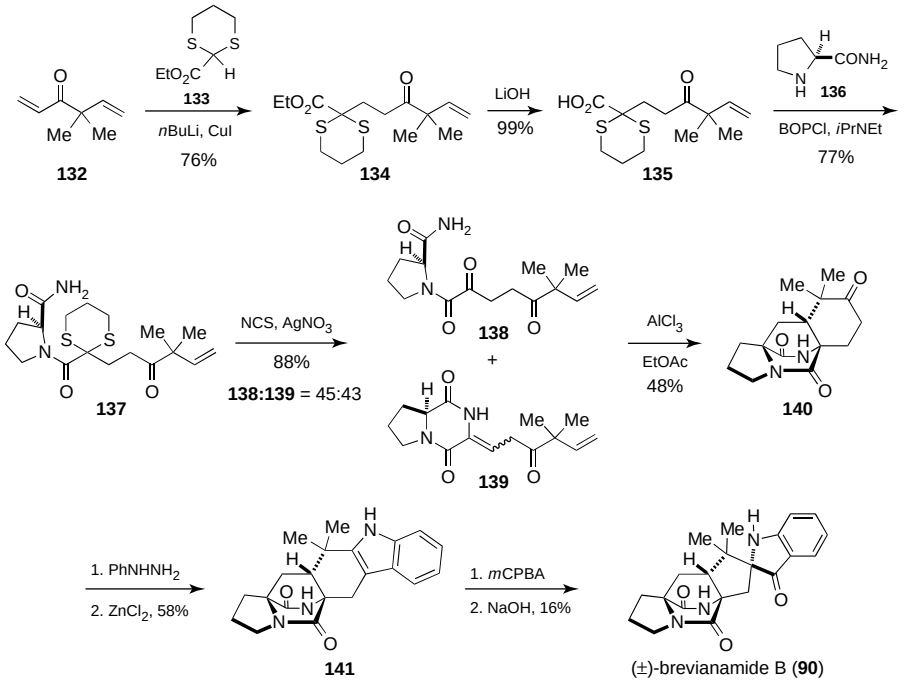

Scheme 4.23 Concise synthesis of brevianamide B.

to reach the oxidation state of the azadiene. In the present instance, the α-ketoamide species (**138**) was posed to serve as a surrogate for the possible biosynthetic oxidative deamination of the tryptophan moiety and coupling to a proline amide species (Scheme 4.23). Conjugate addition of carboxylate **133** to ketone **132** gave ester **134** in 76% yield. Saponification, peptide coupling with L-proline amide, and dithiane deprotection gave a mixture of the uncyclized amide **138** and dioxopiperazine **139**. Aluminum trichloride was added to the mixture to give the Diels–Alder cycloadduct (**140**) in exclusively the *anti*-configuration, whereas mixtures of both the *syn*- and *anti*-cycloadducts were observed in previous syntheses of VM55599 and brevianamide B discussed above. A Fischer indole synthesis was completed by treatment of **140** with phenyl hydrazine followed by $ZnCl_2$, affording **141** in good yield. Oxidation and pinacol-type rearrangement of this known intermediate gave brevianamide B. While an appealing convergent approach towards the synthesis of other related bicyclo[2.2.2]diazaoctanes, the utility of this strategy is limited to those natural products containing the *anti*-stereochemistry observed in formation of compound **140**, the remainder of which must be able to withstand the harsh conditions of the Fischer indole synthesis.

The same biomimetic Diels–Alder disconnection was exploited in the total synthesis of stephacidin A [20]. Starting with reverse prenylated tryptophan derivative **142** (prepared in eleven steps from 6-hydroxyproline), dipeptide **144** was prepared through bis(2-oxo-3-oxazolindinyl)phosphinic chloride (BOPCl) mediated coupling

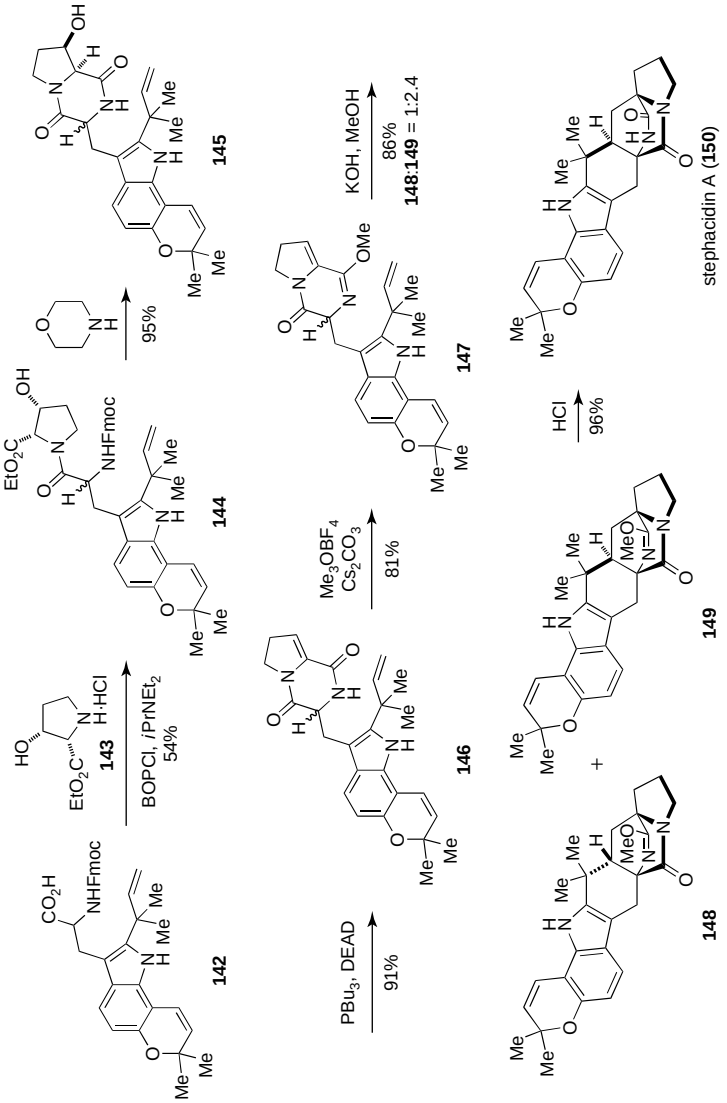

Scheme 4.24 Synthesis of stephacidin A.

with *cis*-3-hydroxyproline ethyl ester (**143**, Scheme 4.24). Fmoc deprotection resulted in the cyclization to dioxopiperazine **145**, which upon treatment with tributyl phosphine and diethyl azodicarboxylate (DEAD) underwent Mitsunobu dehydration to give enamide **146**. Formation of the lactim ether (**147**) was followed by intramolecular Diels–Alder reaction to give a mixture of epimers enriched with the *syn*-isomer (**149**, 2.4 : 1). Deprotection of **149** gave stephacidin A (**150**) in excellent yield.

Williams found that the bicyclo[2.2.2]diazaoctane core could be accessed directly from compound **145** by treating it with excess PBu_3 and DEAD, effecting the dehydration, tautomerization, and Diels–Alder reaction in one pot to afford stephacidin A and its epimer (Scheme 4.25) [21].

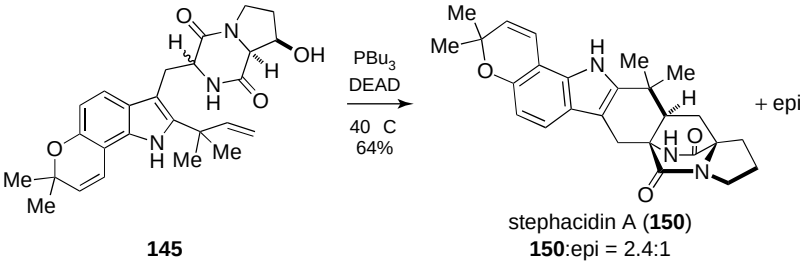

Scheme 4.25 Improved biomimetic synthesis of stephacidin A.

Myers and coworkers, in the course of their total synthesis of avrainvillamide, discovered that synthetic (−)-**152** spontaneously dimerized to stephacidin B under several mild conditions, including addition of triethylamine or exposure to silica gel [22, 23]. Baran and coworkers later determined that stephacidin A could be readily converted into avrainvillamide through reduction to indoline **151** followed by Somei oxidation (Scheme 4.26). In accord with Myers' observations, dimerization to stephacidin B occurred readily upon exposure to silica gel, triethylamine, or on evaporation from dimethyl sulfoxide (DMSO) [24–26]. Myers has further demonstrated that the observed biological activity of stephacidin B may be due to the formation of **152** from **153** *in vivo* [22].

Stephacidin A is of particular biogenetic interest, as both enantiomers have been isolated in nature: (+)-stephacidin A from *Aspergillus ochraceus* [27] and from a marine-derived *Aspergillus* sp. [28] and (−)-stephacidin A from terrestrial Aspergillus versicolor [29–31]. Operating under the assumption that the biosynthesis of stephacidin A proceeds through a common, *achiral* intermediate, Williams and coworkers have proposed notoamide S (**154**) as the point of divergence in the two biosyntheses [32]. Oxidation of **154** could give achiral azadiene **155**, which is postulated to undergo intramolecular Diels–Alder reaction to give either (+)- or (−)-stephacidin A depending on the enantiofacial selectivity of the reaction (Scheme 4.27).

Tryptophan derivative **142** used in the above synthesis of stephacidin A was also employed in the biomimetic total synthesis of marcfortine C (**164**) [33]. Pipecolic acid derivative **156** was coupled to acid **142** to form amide **157**, which underwent cyclization to the dioxopiperazine following Fmoc-deprotection to give **158** as

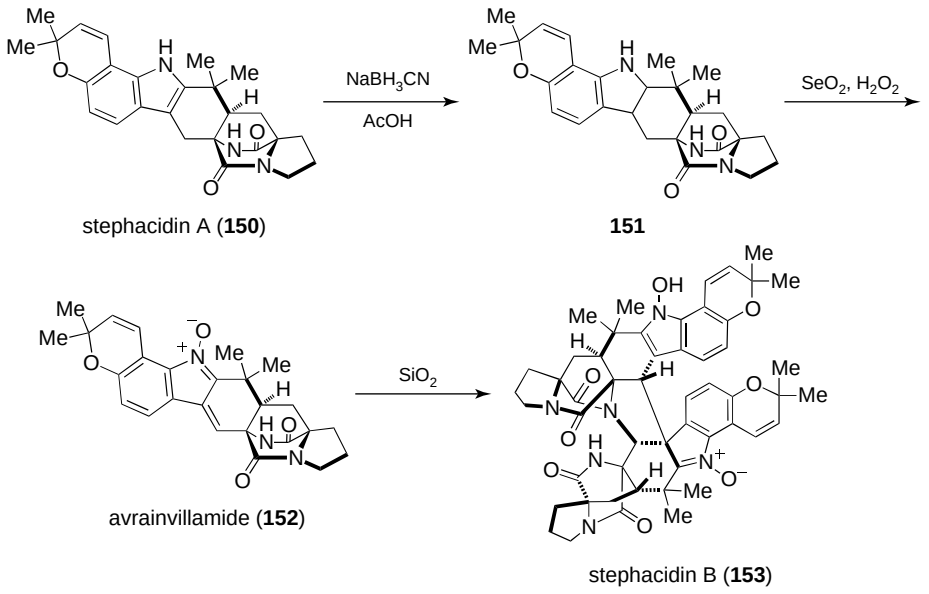

Scheme 4.26 Biomimetic conversion of stephacidin A into stephacidin B.

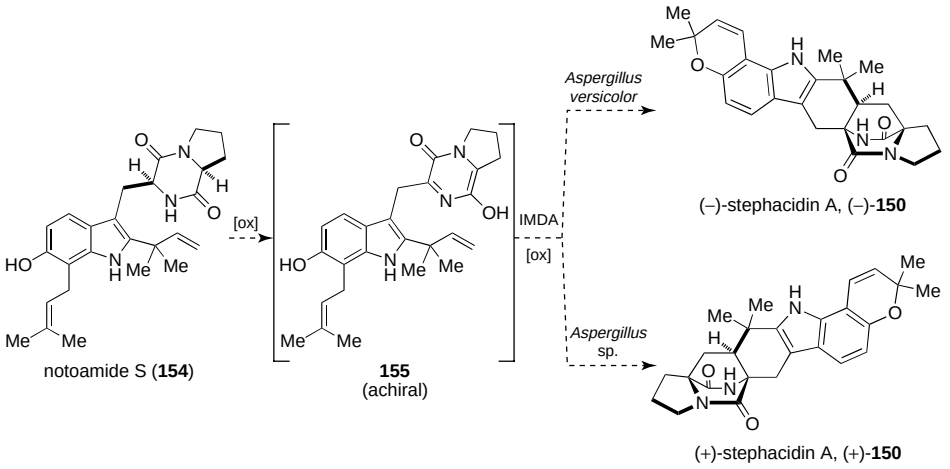

Scheme 4.27 Proposed biosynthesis of (+)- and (−)-stephacidin A through notoamide S.

an inconsequential mixture of diastereomers (Scheme 4.28). The biomimetic Diels–Alder reaction preferred the *syn*-diastereomer **160** in 2.4-fold excess, as expected. Excess DIBAL-H selectively reduced the tertiary amide of **160**, and amine salt formation followed by a biomimetic oxidative rearrangement gave marcfortine C **(164)**.

Malbrancheamide and malbrancheamide B were synthesized via the biomimetic Diels–Alder reaction of enamides **165** and **166** to afford both *syn*-cycloadducts **167**

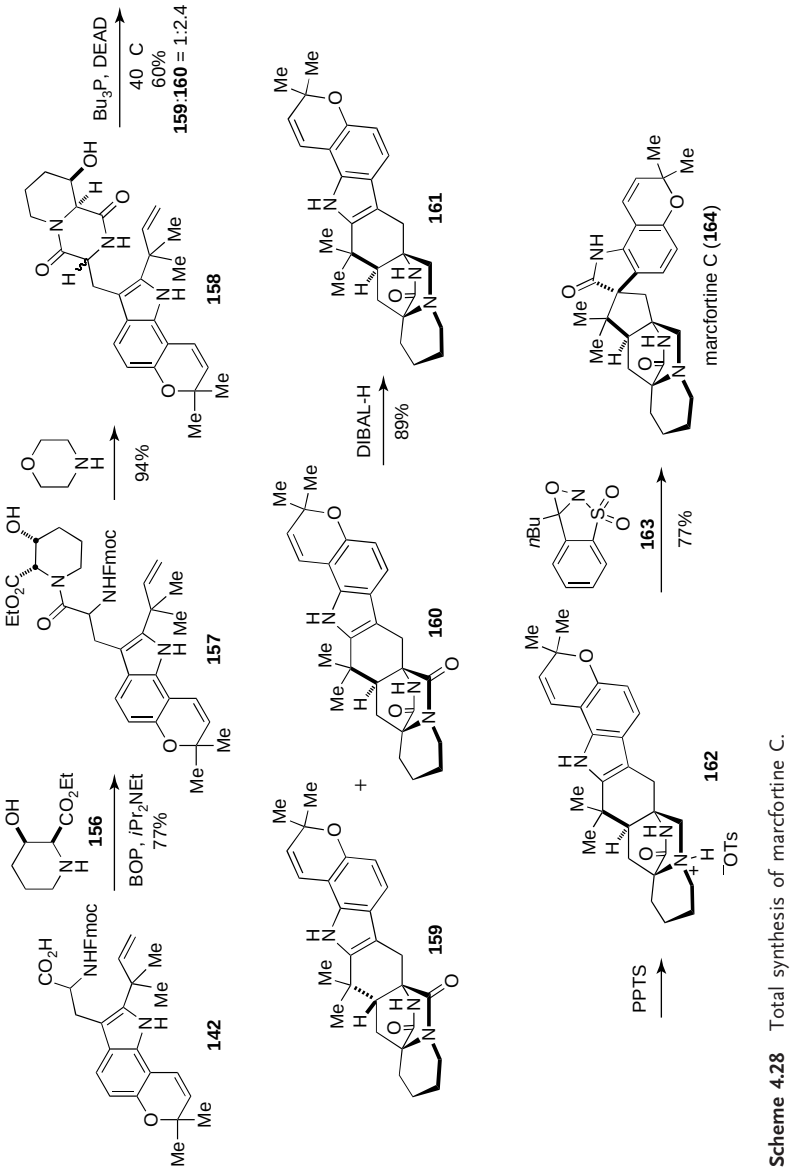

Scheme 4.28 Total synthesis of marcfortine C.

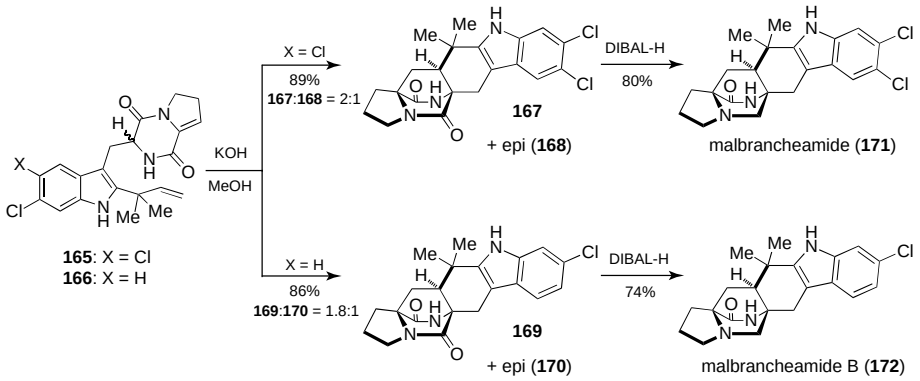

Scheme 4.29 Completion of the total syntheses of the malbrancheamides.

and **169**, as well as the *anti*-epimers **168** and **170** (Scheme 4.29) [34]. Treatment of the *syn*-cycloadducts with excess DIBAL-H gave either malbrancheamide or malbrancheamide B.

As the malbrancheamides were the first of this family of prenylated indole alkaloids to possess a halogenated indole ring, Williams and coworkers probed the biosynthesis to establish the timing of the chlorination event [35]. Malbrancheamide is proposed to arise from tryptophan, proline, and dimethylallyl diphosphate, leading to deoxybrevianamide E (**18**, Scheme 4.30). Oxidation of **18** could give intermediate **174**, which is expected to suffer intramolecular Diels–Alder reaction

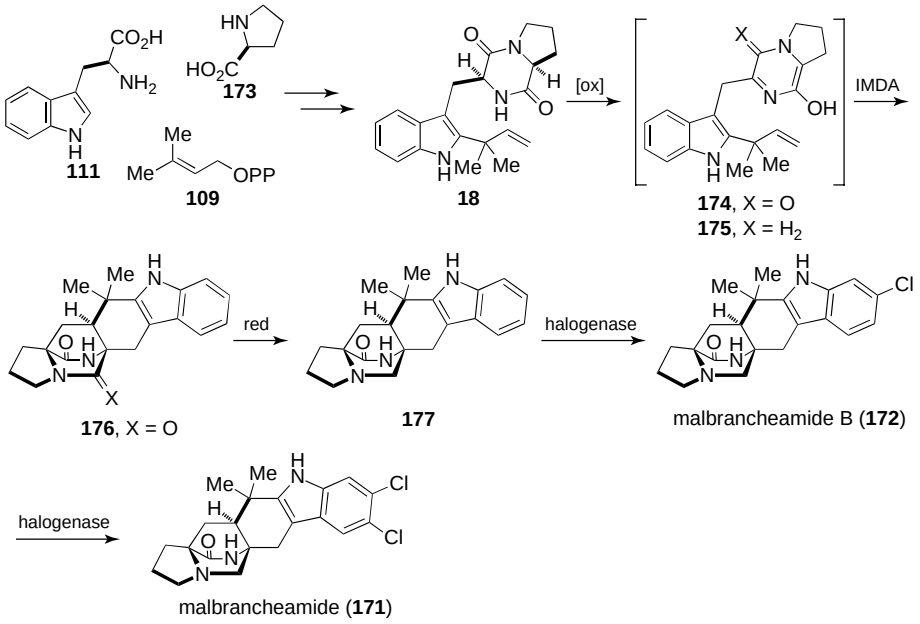

Scheme 4.30 Proposed biosynthesis of the malbrancheamides.

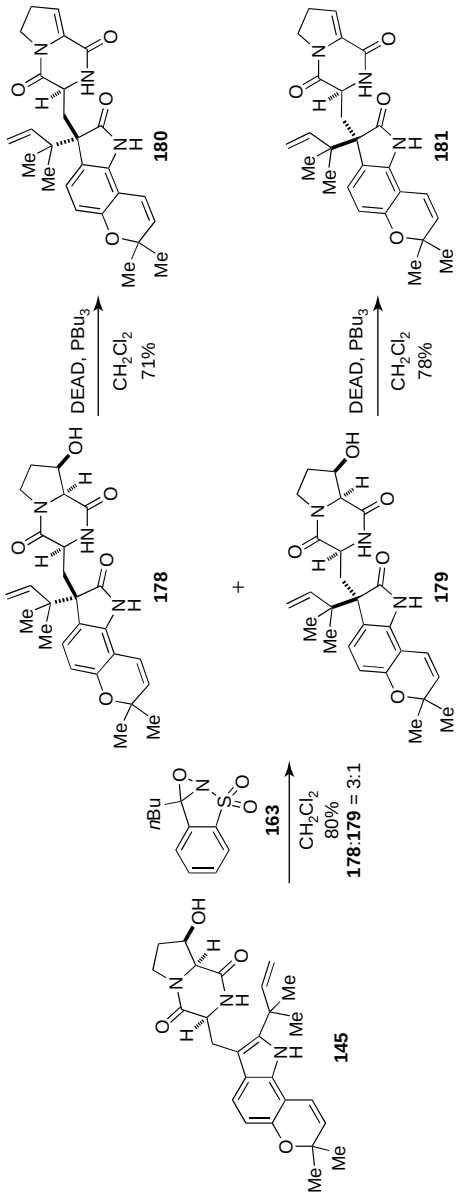

Scheme 4.31 Synthesis of key oxindoles.

(IMDA) to cycloadduct **176**. Reduction of the tertiary amide would provide premalbrancheamide (**177**). Alternatively, **18** could suffer reduction of the tertiary amide to **175**, providing **177** directly upon cycloaddition. Premalbrancheamide is proposed to undergo subsequent halogenation events to give both malbrancheamide B and malbrancheamide. In feeding studies, labeled dioxopiperazine **176** and premalbrancheamide (**177**) were added to separate cultures of *Malbranchea aurantiaca*, but interestingly only premalbrancheamide **177** was incorporated into malbrancheamide B. This suggests that reduction of the tertiary amide must precede Diels–Alder construction of the bicyclo[2.2.2]diazaoctane core through an intermediate analogous to monooxopiperazine **175**.

Williams has reported that–like stephacidin A and notoamide B, which are produced in Nature as distinct enantiomers–the minor metabolite versicolamide B is likewise produced as distinct enantiomers in different strains of *Aspergillus* sp. The asymmetric syntheses of both (+)- and (−)-versicolamide B (**182**) have recently been accomplished by deploying compound **145**, previously used in the synthesis of stephacidin A (Scheme 4.31). Oxaziridine oxidation of **145** and pinacol-type rearrangement consequent to oxidation of the indole gave a 3 : 1 separable mixture of **178** and **179** [36]. As previously reported, treatment with tributyl phosphine and DEAD induced Mitsunobu dehydration to give enamides **180** and **181**.

Treatment of **180** and **181** individually with potassium hydroxide in methanol induced the intramolecular Diels–Alder reaction to afford either (+)- or (−)-versicolamide B (**182**), along with the minor *anti*-diastereomers (+)-**183** or (−)-**183** (Scheme 4.32). As previous biomimetic Diels–Alder reactions containing indole-based azadienes display *syn*-selectivity (typically ∼2.5 : 1 *syn : anti*), the exclusive selectivity for the *anti*-products in the versicolamide B syntheses is of particular interest. The authors suggest that the *anti*-preference stems from a stable transition state leading to the *anti*-cycloadduct when an oxindolic azadiene is employed, whereas the *syn*- and *anti*-transition states arising from an indolic azadiene are of roughly equal stability [14, 37].

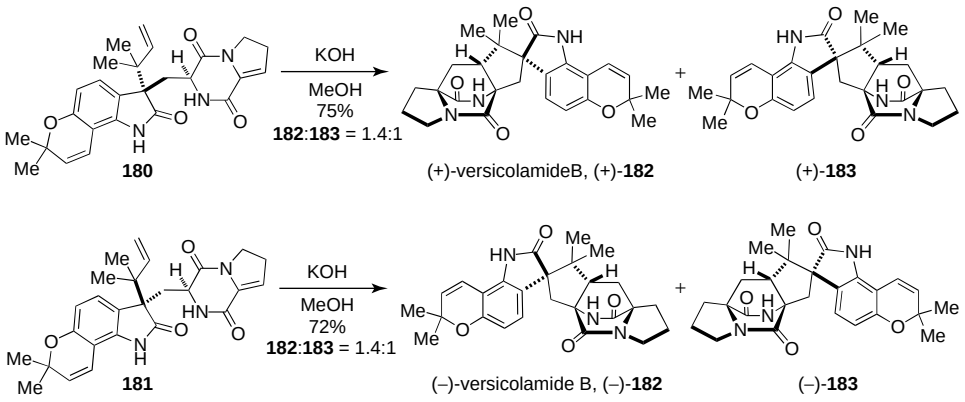

Scheme 4.32 Completion of the asymmetric syntheses of the versicolamides.

While the above syntheses have differed in the approach to the azadiene, all share a common biomimetic intramolecular Diels–Alder reaction to give the bicyclo[2.2.2]diazaoctane core featured in the molecules presented in this section.

4.3
Non-prenylated Indole Alkaloids

Hart and coworkers have expressed interest in the biosynthesis of the fumiquinazoline family of alkaloid natural products, and reported a biomimetic synthesis of *ent*-alantrypinone as the initial effort at a synthetic program to access more complex, related substances [38]. L-Tryptophan methyl ester was coupled to isatoic anhydride to afford amide **184** in good yield (Scheme 4.33). Acylation of **184** with acyl chloride **186** (prepared in two steps from *S*-methyl-L-cysteine, **185**) under Schotten–Baumann conditions furnished diamide **187**, which underwent cyclodehydration to iminobenzoxazine **188**. Treatment with excess $Li[Me_3AlSPh]$ effected the rearrangement to quinazolinone **189**, and Fmoc deprotection was accompanied by amide formation to give **190**. Oxidation of **190** provided the sulfoxide, which was converted into enamide **191** upon heating in benzene with triphenylphosphine. Trifluoroacetic acid induced the conversion into bicycle **192**, presumably through intramolecular electrophilic attack of an intermediate *N*-acyliminium ion onto indole. Conversion into the oxindole proceeded via oxidative rearrangement of **192** with NBS to give the polybrominated indolinone, which was hydrogenolyzed over platinum on carbon to give *ent*-alantrypinone (**193**), along with *ent*-17-epi-alantrypinone (**194**).

Three dimeric tryptophan-derived dioxopiperazines have succumbed to biomimetic total syntheses, all completed by Movassaghi and coworkers, namely, (+)-WIN 64821, (−)-ditryptophenaline, and (+)-11,11′-dideoxyverticillin A [39, 40]. Syntheses of the former two began with cleavage of the Boc carbamate to effect the cyclization to dioxopiperazine **196** (Scheme 4.34) [40]. Treatment with bromine then gave a separable mixture of two diastereomers, *endo*-(+)-**197** and *exo*-(−)-**198**. *endo*-Bromide (+)-**197** was carried on to (+)-WIN 64821 (**201**) by, first, treatment with tris(triphenylphosphine)cobalt chloride to afford the dimerized product **199**, which was globally deprotected upon exposure to samarium diiodide. (+)-WIN 64821 was thus obtained in 75% yield. Similarly, (−)-ditryptophenaline (**202**) was synthesized following methylation of *exo*-(−)-**198**, dimerization, and deprotection to give the product in 79% yield.

4.3.1
Epidithiodioxopiperazines

(+)-11,11′-Dideoxyverticillin A (**211**) differs from dimers **201** and **202** in that it is likely derived from L-tryptophan and L-alanine, rather than from L-phenylalanine. Additionally, the dioxopiperazines are bridged by a disulfide, adding a difficult challenge to the synthetic construction of the molecule. Similar to their previous

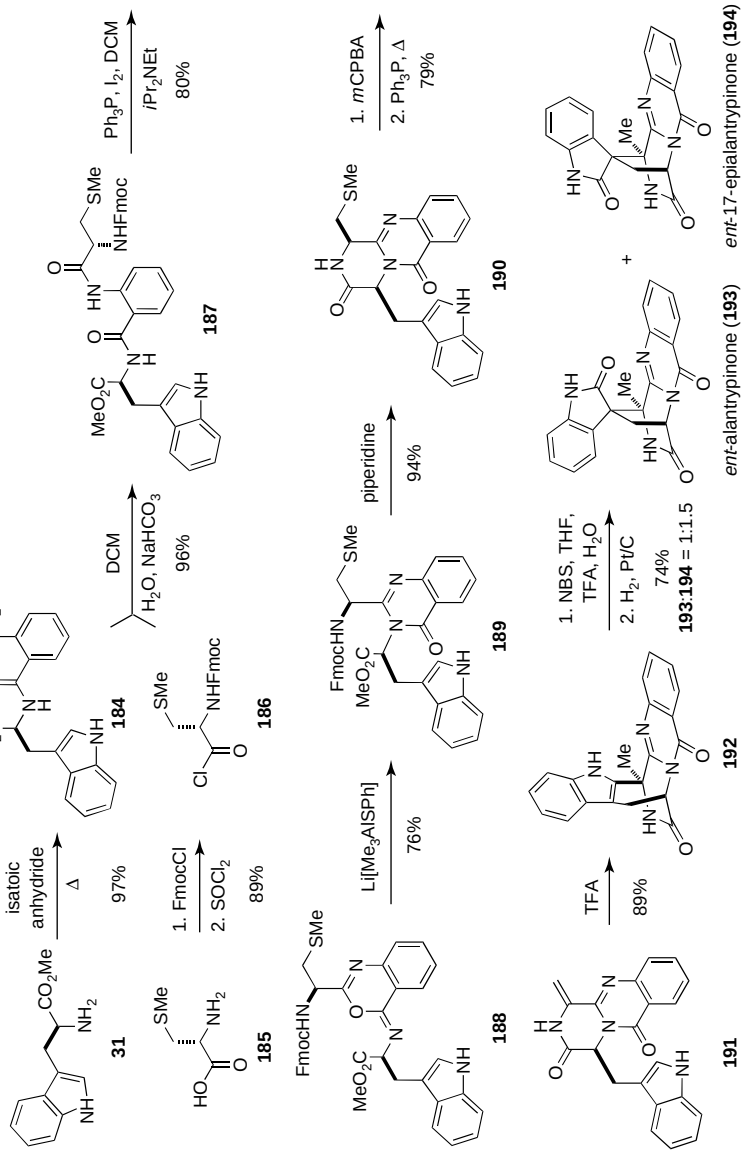

Scheme 4.33 Synthesis of *ent*-alantrypinone.

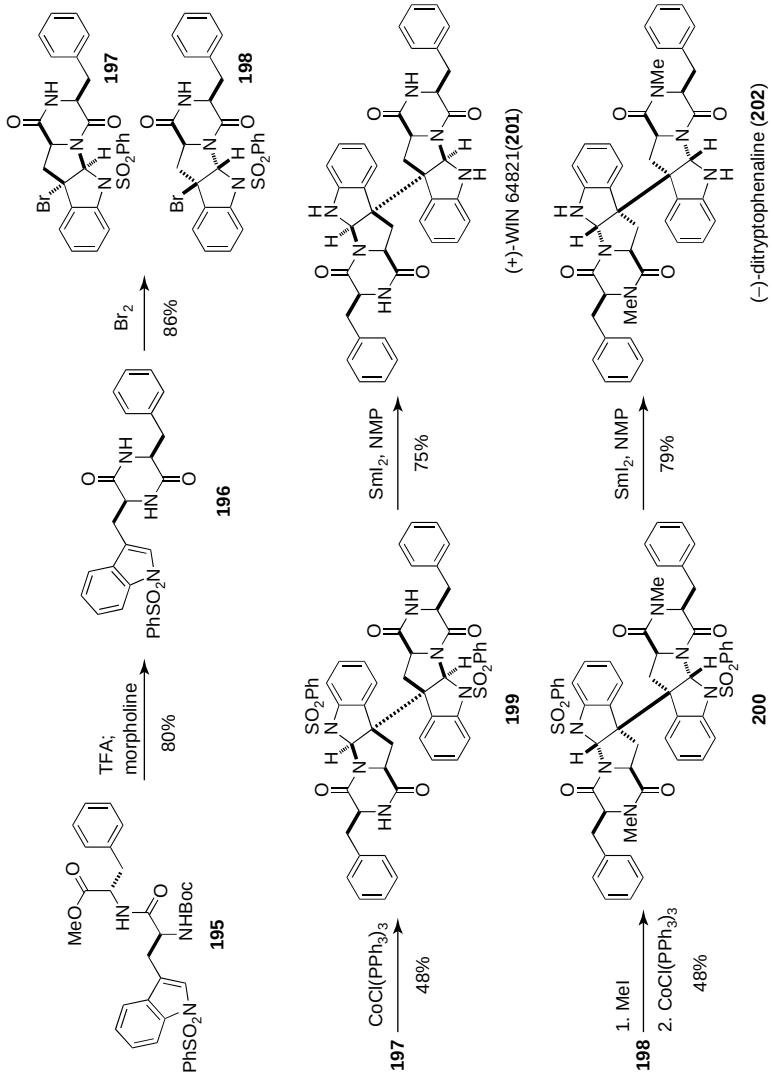

Scheme 4.34 Concise total syntheses of (+)-WIN 64821 and (−)-ditryptophenaline.

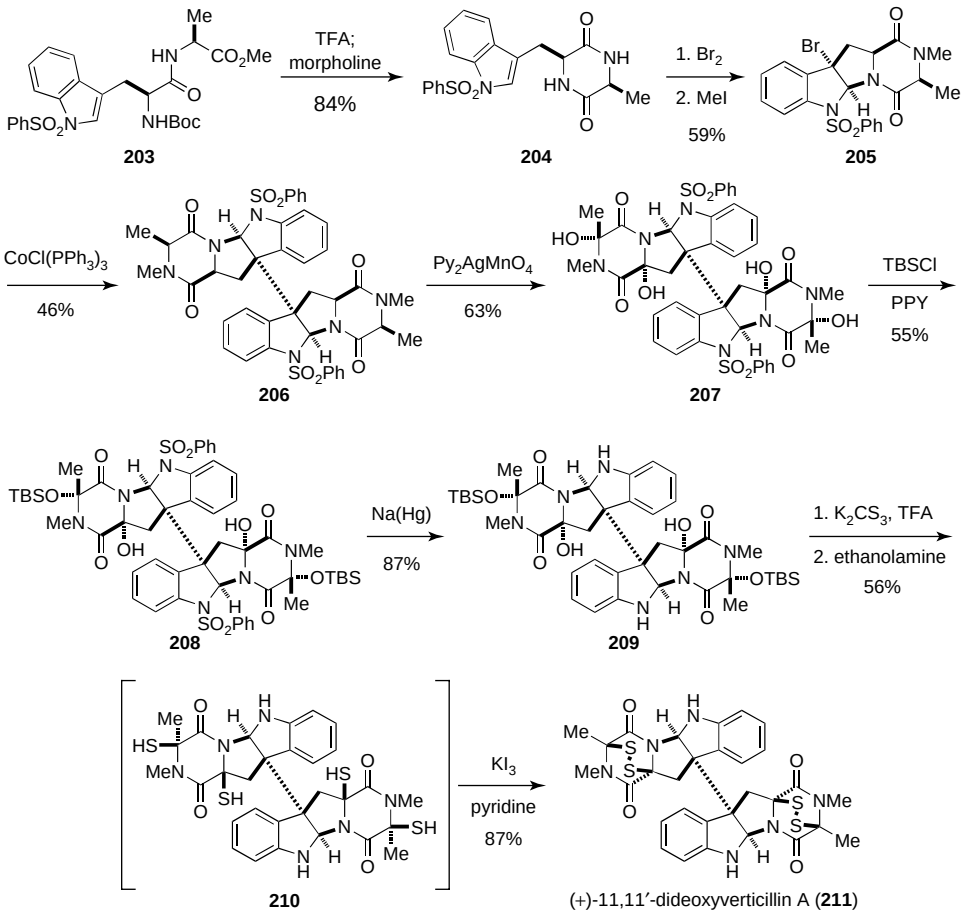

Scheme 4.35 Biomimetic total synthesis of (+)-11,11′-dideoxyverticillin A.

work, Movassaghi and coworkers showed that cleavage of the *N*-Boc carbamate was accompanied by cyclization to dioxopiperazine **204** (Scheme 4.35) [39]. Exposure of **204** to bromine produced the 3-bromopyrroloindoline, and the amides were subsequently methylated upon treatment with iodomethane. Reductive dimerization with the cobalt(I) complex as before gave the desired dimeric intermediate **206**. The dimer was oxidized with bis(pyridine)-silver(I) permanganate to octacycle **207**, and exposure to Fu's *(R)*-(+)-4-pyrrolidinopyridinyl(pentamethylcyclopentadienyl)iron (PPY) catalyst with t-butyldimethylsilyl chloride (TBSCl) gave selectively the alanine-derived protected hemiaminals of **208**. Removal of the benzenesulfonyl groups with sodium amalgam revealed diaminodiol **209**. Treatment of **209** with K_2CS_3 followed by ethanolamine gave diaminotetrathiol **210**, which readily oxidized to (+)-11,11′-dideoxyverticillin A (**211**) when partitioned between aqueous hydrochloric acid and dichloromethane and treated with potassium triiodide.

The total synthesis of sporidesmin A was completed by Kishi and coworkers in 1973. In a series of communications, Kishi described a novel strategy for the synthesis of epidithiodioxopiperazines using a dithioacetal moiety as a protecting group for the disulfide bridge [41–43]. Thus protected, the dithioacetal is stable to acidic, basic, and reducing conditions, allowing for the introduction of thiol groups at an early stage in a total synthesis. Synthesis of the sporidesmins began with the treatment of dioxopiperazine **212** with the dithiane derivative of *p*-anisaldehyde in the presence of acid to afford dithioacetal-protected dioxopiperazine **213** (Scheme 4.36) [43]. Condensation with acid chloride **214** and subsequent methoxymethyl deprotection gave compound **215**. Treatment of ketone **215** with DIBAL-H at −78 °C resulted in stereoselective reduction to the alcohol, which was then converted into acetate **216** in 80% yield. Cyclization to the diacetate (**217**) proceeded upon addition of iodosobenzene diacetate, and hydrolysis of the acetates gave the corresponding diol. Treatment of the diol with *m*-chloroperbenzoic acid (*m*CPBA) afforded an intermediate sulfoxide, which decomposed to the disulfide upon exposure to strong Lewis acid, revealing (±)-sporidesmin A (**218**).

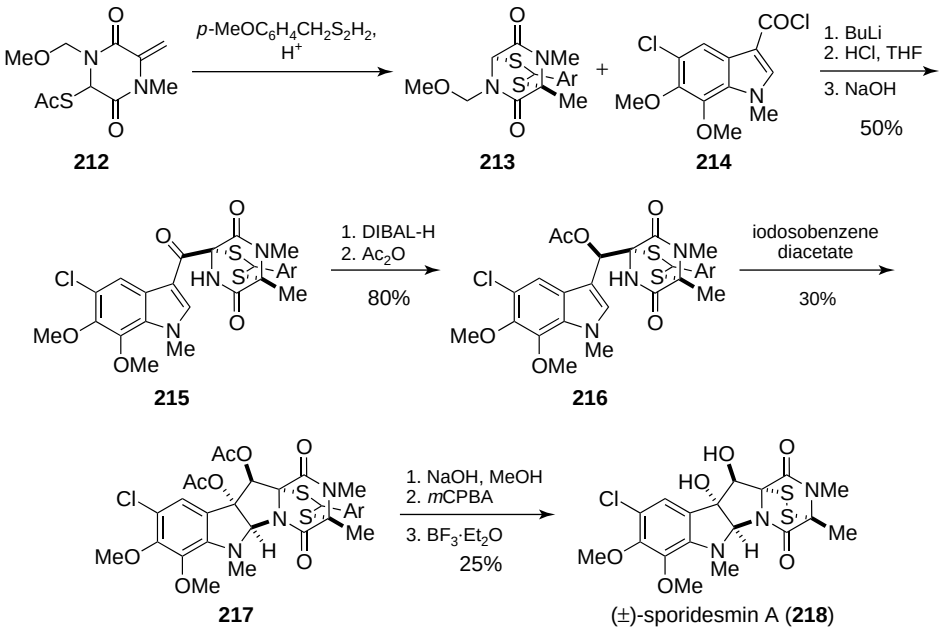

Scheme 4.36 Total synthesis of (±)-sporidesmin A.

The biosynthesis of gliotoxin is believed to proceed through the intramolecular nucleophilic ring-opening of a phenylalanine-derived arene oxide and has been the subject of considerable speculation and interest. Kishi and coworkers drew inspiration from these biogenetic hypotheses in devising a brilliant total synthesis of gliotoxin. The total synthesis of (±)-gliotoxin was completed in 1976 utilizing the same disulfide protecting strategy as deployed above for the sporidesmins, and was re-engineered in 1981 by the same route starting from optically pure

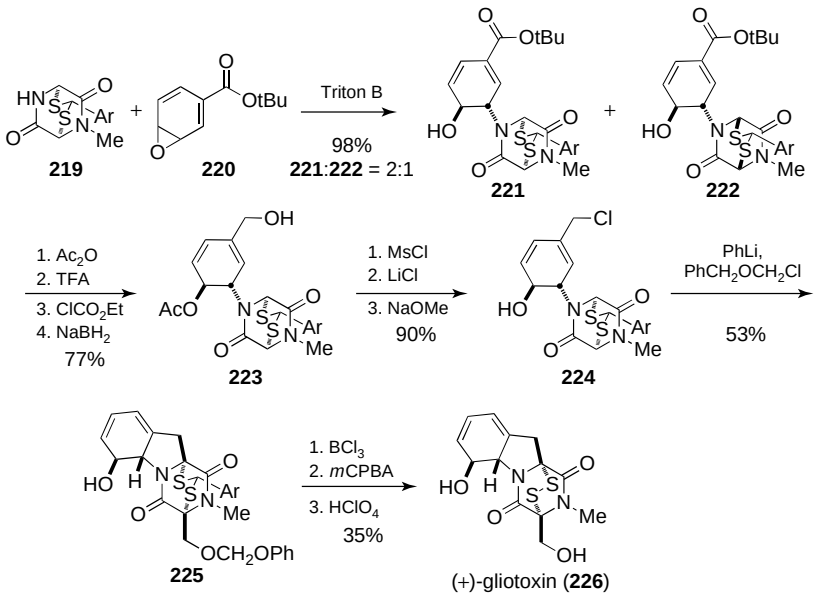

Scheme 4.37 Kishi's total synthesis of (±)- and (+)-gliotoxin.

dithioacetal **219** obtained from resolution (Scheme 4.37) [44, 45]. Coupling of **219** with *t*-butoxy arene oxide **220** in the presence of triton B afforded **221** and **222** in a 2 : 1 ratio. Acylation, deprotection, mixed anhydride formation, and reduction gave alcohol **223** in 77% yield. Alcohol **223** was converted into the chloride following mesylation, and then deprotected to reveal alcohol **224**. The key stereoselective cyclization–alkylation reaction was achieved upon addition of phenyllithium to **224** and phenoxymethyl chloride, affording cycloadduct **225** in modest yield (53%). The primary alcohol was revealed upon removal of the benzyl ether, and the thioacetal oxidatively removed to afford either (±)- or (+)-gliotoxin (**226**).

4.4 Conclusion

Dioxopiperazine alkaloids cover an astonishing array of molecular architecture and, with that, corresponding synthetic challenges to construct such substances. The biosynthesis of many of the natural substances touched on in this chapter has, in some instances, been studied going back several decades, and many workers have sought to exploit insights from Nature's strategic bond constructions in a synthetic laboratory context. Advances in whole genome sequencing have brought new and invigorated interest in elucidating the biosynthesis of structurally intriguing and biomedically relevant secondary metabolites. The insights to be gained from educated guess work on what specific compounds might lie along a possible biosynthetic pathway, traditionally accomplished by isolation and structural

elucidation to map metabolite co-occurrence in conjunction with isotopically labeled precursor incorporation experiments, is in the process of giving way to a much higher resolution picture of secondary metabolism in microorganisms and plants. With the advent of powerful new genomics and proteomics tools to study and manipulate secondary metabolite production, advances in our understanding of Nature's creative synthetic palette will surely explode in the coming years. The fruits of these insights will undoubtedly be extensively exploited by synthetic chemists working at the forefront of complex molecule synthesis. In addition, many new natural products–the biosynthetic intermediates themselves, often isolated in trace amounts if at all–will provide and constitute worthy new synthetic targets and substrates for various important applications.

Acknowledgment

R.M.W. is grateful to the National Institutes of Health (GM068011; CA70375; CA85419) for financial support.

References

1. Birch, A.J. and Russell, R.A. (1972) *Tetrahedron*, **28**, 2999–3008.
2. Birch, A.J. and Wright, J.J. (1969) *J. Chem. Soc., Chem. Commun.*, 644–645.
3. Birch, A.J. and Wright, J.J. (1970) *Tetrahedron*, **26**, 2329–2344.
4. Baldas, J., Birch, A.J., and Russell, R.A. (1974) *J. Chem. Soc., Perkin Trans. 1*, 50–52.
5. Sanz-Cervera, J.F., Glinka, T., and Williams, R.M. (1993) *Tetrahedron*, **49**, 8471–8482.
6. Kametani, T., Kanaya, N., and Ihara, M. (1980) *J. Am. Chem. Soc.*, **102**, 3972–3975.
7. Schkeryantz, J.M., Woo, J.C.G., Siliphaivanh, P., Depew, K.M., and Danishefsky, S.J. (1999) *J. Am. Chem. Soc.*, **121**, 11964–11975.
8. von Nussbaum, F. and Danishefsky, S.J. (2000) *Angew. Chem., Int. Ed.*, **39**, 2175–2178.
9. Edmondson, S., Danishefsky, S.J., Sepp-Lorenzino, L., and Rosen, N. (1999) *J. Am. Chem. Soc.*, **121**, 2147–2155.
10. Finefield, J.M. and Williams, R.M. (2010) *J. Org. Chem.*, **75**, 2785–2789.
11. Baran, P.S., Guerrero, C.A., and Corey, E.J. (2003) *J. Am. Chem. Soc.*, **125**, 5628–5629.
12. Depew, K.M., Marsden, S.P., Zatorska, D., Zatorski, A., Bornmann, W.G., and Danishefsky, S.J. (1999) *J. Am. Chem. Soc.*, **121**, 11953–11963.
13. Porter, A.E.A. and Sammes, P.G. (1970) *J. Chem. Soc., Chem. Commun.*, 1103.
14. Domingo, L.R., Sanz-Cervera, J.F., Williams, R.M., Picher, M.T., and Marco, J.A. (1997) *J. Org. Chem.*, **62**, 1662–1667.
15. Williams, R.M., Sanz-Cervera, J.F., Sancenon, F., Marco, J.A., and Halligan, K. (1998) *J. Am. Chem. Soc.*, **120**, 1090–1091.
16. Stocking, E.M., Sanz-Cervera, J.F., and Williams, R.M. (2000) *J. Am. Chem. Soc.*, **122**, 1675–1683.
17. Jin, S.D., Wessig, P., and Liebscher, J. (2001) *J. Org. Chem.*, **66**, 3984–3997.
18. Sanz-Cervera, J.F. and Williams, R.M. (2002) *J. Am. Chem. Soc.*, **124**, 2556–2559.
19. Adams, L.A., Valente, M.W.N., and Williams, R.M. (2006) *Tetrahedron*, **62**, 5195–5200.

20. Greshock, T.J., Grubbs, A.W., Tsukamoto, S., and Williams, R.M. (2007) *Angew. Chem. Int. Ed.*, **46**, 2262–2265.
21. Greshock, T.J. and Williams, R.M. (2007) *Org. Lett.*, **9**, 4255–4258.
22. Herzon, S.B. and Myers, A.G. (2005) *J. Am. Chem. Soc.*, **127**, 5342–5344.
23. Myers, A.G. and Herzon, S.B. (2003) *J. Am. Chem. Soc.*, **125**, 12080–12081.
24. Baran, P.S., Guerrero, C.A., Ambhaikar, N.B., and Hafensteiner, B.D. (2005) *Angew. Chem. Int. Ed.*, **44**, 606–609.
25. Baran, P.S., Guerrero, C.A., Hafensteiner, B.D., and Ambhaikar, N.B. (2005) *Angew. Chem. Int. Ed.*, **44**, 3892–3895.
26. Baran, P.S., Hafensteiner, B.D., Ambhaikar, N.B., Guerrero, C.A., and Gallagher, J.D. (2006) *J. Am. Chem. Soc.*, **128**, 8678–8693.
27. Qian-Cutrone, J., Huang, S., Shu, Y.Z., Vyas, D., Fairchild, C., Menendez, A., Krampitz, K., Dalterio, R., Klohr, S.E., and Gao, Q. (2002) *J. Am. Chem. Soc.*, **124**, 14556–14557.
28. Kato, H., Yoshida, T., Tokue, T., Nojiri, Y., Hirota, H., Ohta, T., Williams, R.M., and Tsukamoto, S. (2007) *Angew. Chem. Int. Ed.*, **46**, 2254–2256.
29. Deyrup, S.T., Swenson, D.C., Gloer, J.B., and Wicklow, D.T. (2006) *J. Nat. Prod.*, **69**, 608–611.
30. Mudur, S.V., Gloer, J.B., and Wicklow, D.T. (2006) *J. Antibiot.*, **59**, 500–506.
31. Shim, S.H., Swenson, D.C., Gloer, J.B., Dowd, P.F., and Wicklow, D.T. (2006) *Org. Lett.*, **8**, 1225–1228.
32. McAfoos, T.J., Li, S., Tsukamoto, S., Sherman, D.H., and Williams, R.M. (2010) *Heterocycles*, **82**, 461–472.
33. Greshock, T.J., Grubbs, A.W., and Williams, R.M. (2007) *Tetrahedron*, **63**, 6124–6130.
34. Miller, K.A., Welch, T.R., Greshock, T.J., Ding, Y.S., Sherman, D.H., and Williams, R.M. (2008) *J. Org. Chem.*, **73**, 3116–3119.
35. Ding, Y.S., Greshock, T.J., Miller, K.A., Sherman, D.H., and Williams, R.M. (2008) *Org. Lett.*, **10**, 4863–4866.
36. Miller, K.A., Tsukamoto, S., and Williams, R.M. (2009) *Nat. Chem.*, **1**, 63–68.
37. Domingo, L.R., Zaragoza, R.J., and Williams, R.M. (2003) *J. Org. Chem.*, **68**, 2895–2902.
38. Hart, D.J. and Magomedov, N.A. (2001) *J. Am. Chem. Soc.*, **123**, 5892–5899.
39. Kim, J., Ashenhurst, J.A., and Movassaghi, M. (2009) *Science*, **324**, 238–241.
40. Movassaghi, M., Schmidt, M.A., and Ashenhurst, J.A. (2008) *Angew. Chem. Int. Ed.*, **47**, 1485–1487.
41. Kishi, Y., Fukuyama, T., and Nakatsuk, S. (1973) *J. Am. Chem. Soc.*, **95**, 6492–6493.
42. Kishi, Y., Fukuyama, T., and Nakatsuk, S. (1973) *J. Am. Chem. Soc.*, **95**, 6490–6492.
43. Kishi, Y., Nakatsuk, S., Fukuyama, T., and Havel, M. (1973) *J. Am. Chem. Soc.*, **95**, 6493–6495.
44. Fukuyama, T. and Kishi, Y. (1976) *J. Am. Chem. Soc.*, **98**, 6723–6724.
45. Fukuyama, T., Nakatsuka, S., and Kishi, Y. (1981) *Tetrahedron*, **37**, 2045–2078.

JOC*Article*

Biomimetic Total Synthesis of Malbrancheamide and Malbrancheamide B

Kenneth A. Miller,[†] Timothy R. Welch,[†] Thomas J. Greshock,[†] Yousong Ding,[‡] David H. Sherman,[‡] and Robert M. Williams*[,†,§]

Department of Chemistry, Colorado State University, Fort Collins, Colorado 80523-1872, University of Colorado Cancer Center, Aurora, Colorado, 80045, and Life Sciences Institute, and Departments of Medicinal Chemistry, Chemistry, Microbiology & Immunology, The University of Michigan, 210 Washtenaw Avenue, Ann Arbor, Michigan 48109-2216

rmv@lamar.colostate.edu

Received January 17, 2008

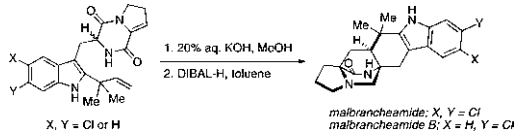

The biomimetic total syntheses of both malbrancheamide and malbrancheamide B are reported. The synthesis of the two monochloro species enabled the structure of malbrancheamide B to be unambiguously assigned. The syntheses each feature an intramolecular Diels−Alder reaction of a 5-hydroxypyrazin-2(1*H*)-one to construct the bicyclo[2.2.2]diazaoctane core, which has also been proposed as the biosynthetic route to these compounds.

Introduction

Our research group has exhibited a long-standing interest in the synthesis and biosynthetic study of a number of unique prenylated indole alkaloids containing a characteristic bicyclo-[2.2.2]diazaoctane core.[1] This class of natural products includes such highly biologically active fungal metabolites as the paraherquamides,[2] brevianamides,[3] notamides,[4] and stephacidins,[5] among others, which we have shown all arise biogenetically from tryptophan, mevalonate-derived isoprene units, and proline or derivatives of proline.[1] Sammes originally proposed that the bicyclo[2.2.2]diazaoctane core common to all of these natural products arises in *Nature* via an intramolecular hetero-Diels−Alder reaction of a 5-hydroxypyrazin-2(1*H*)-one,[6] and work from this laboratory has extensively supported such a proposal.[1] In fact, we have applied such a [4+2] hetero-Diels−Alder cycloaddition strategy to the total synthesis of several of these prenylated indole alkaloids, including stephacidin A,[7] brevianamide B,[8] marcfortine C,[9] notoamide B,[7b] and VM55599.[10]

Malbrancheamide (**1**)[11] and malbrancheamide B (**2**) were recently isolated from *Malbranchea aurantiaca* RRC1813, a

[†] Colorado State University.
[‡] The University of Michigan.
[§] University of Colorado Cancer Center.

(1) (a) Williams, R. M.; Cox, R. J. *Acc. Chem. Res.* **2003**, *36*, 127. (b) Williams, R. M. *Chem. Pharm. Bull.* **2002**, *50*, 711. (c) Williams, R. M.; Stocking, E. M.; Sanz-Cevera, J. F. *Top. Curr. Chem.* **2000**, *209*, 98.

(2) (a) Yamazaki, M.; Okuyama, E. *Tetrahedron Lett.* **1981**, *22*, 135. (b) Ondeyka, J. G.; Goegelman, R. T.; Schaeffer, J. M.; Kelemen, L.; Zitano, L. *J. Antibiot.* **1990**, *43*, 1375. (c) Liesch, J. M.; Wichmann, C. F. *J. Antibiot.* **1990**, *43*, 1380. (d) Banks, R. M.; Blanchflower, S. E.; Everett, J. R.; Manfer, B. R.; Reading, C. J. *J. Antibiot.* **1997**, *50*, 840.

(3) (a) Birch, A. J.; Wright, J. J. *J. Chem. Soc. Chem. Commun.* **1969**, 644. (b) Birch, A. J.; Wright, J. J. *Tetrahedron* **1970**, *26*, 2329. (c) Birch, A. J.; Russell, R. A. *Tetrahedron* **1972**, *28*, 2999.

(4) Kato, H.; Yoshida, T.; Tokue, T.; Nojiri, Y.; Hirota, H.; Ohta, T.; Williams, R. M.; Tsukamoto, S. *Angew. Chem., Int. Ed.* **2007**, *46*, 2254.

(5) (a) Qian-Cutrone, J.; Huang, S.; Shu, Y.-Z.; Vyas, D.; Fairchild, C.; Menendez, A.; Krampitz, K.; Dalterio, R.; Klohr, S. E.; Gao, Q. *J. Am. Chem. Soc.* **2002**, *124*, 14556. (b) Qian-Cutrone, J.; Krampitz, K.; Shu, Y.-Z.; Chang, L. P. U.S. Patent 6,291,461, 2001.

(6) (a) Porter, A. E. A.; Sammes, P. G. *J. Chem. Soc. Chem. Commun.* **1970**, 1103. (b) Baldas, J.; Birch, A. J.; Russell, R. A. *J. Chem. Soc., Perkin Trans I* **1974**, 50.

(7) (a) Greshock, T. J.; Williams, R. W. *Org. Lett.* **2007**, *9*, 4255. (b) Greshock, T. J.; Grubbs, A. W; Tsukamoto, S.; Williams, R. W. *Angew. Chem., Int. Ed.* **2007**, *46*, 2262.

(8) (a) Williams, R. M.; Sanz-Cervera, J. F.; Sancenón, F.; Marco, J. A.; Halligan, K. *J. Am. Chem. Soc.* **1998**, *120*, 1090. (b) Williams, R. M.; Sanz-Cervera, J. F.; Sancenón, F.; Marco, J. A.; Halligan, K. *Bioorg. Med. Chem.* **1998**, *6*, 1233. (c) Sanz-Cervera, J. F.; Williams, R. M.; Marco, J. A.; López-Sánchez, J. M.; González, F.; Martínez, M. E.; Sancenón, F. *Tetrahedron* **2000**, *56*, 6345. (d) Adams, L. A.; Valente, M. W. N.; Williams, R. M. *Tetrahedron* **2006**, *62*, 5195.

(9) Greshock, T. J.; Grubbs, A. W.; Williams, R. M. *Tetrahedron* **2007**, *63*, 6124.

(10) (a) Stocking, E. M.; Sanz-Cervera, J. F.; Williams, R. M. *J. Am. Chem. Soc.* **2000**, *122*, 1675. (b) Sanz-Cervera, J. F.; Williams, R. M. *J. Am. Chem. Soc.* **2002**, *124*, 2556.

10.1021/jo800116y CCC: $40.75 © 2008 American Chemical Society
Published on Web 03/18/2008

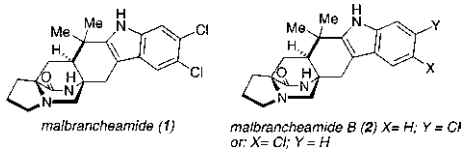

FIGURE 1. Malbrancheamide and malbrancheamide B.

fungus collected on bat detritus collected in a cave in Mexico by Mata and co-workers. These new substances are the first alkaloids in this class of prenylated indole alkaloids to contain a halogenated indole ring (Figure 1). The lack of a tertiary amide in the bicyclo[2.2.2]diazaoctane core also serves to characterize the malbrancheamides. In addition to these notable structural features, malbrancheamide has been shown to be a calmodulin (CaM) antagonist that inhibits the activity of CaM-dependent phosphodiesterase (PDE1) in a concentration dependent manner.[11] The chemotherapeutic potential of PDE1 inhibitors includes applications in the treatment of neurodegenerative diseases, cancers, and vascular diseases, due to the effect on intracellular cAMP and cGMP concentrations.[12] New pharmacological properties of malbrancheamide may be discovered through the study of malbrancheamide, malbrancheamide B, and other analogs, as specific PDE1 inhibitors are scarce and the exact function of the enzyme has not been fully characterized.

Although compelling spectroscopic evidence indicated that the structure of **1** was as shown,[11] the precise structure of malbrancheamide B (**2**) was less certain. Isolation and structural characterization of **2** indicated the presence of a single chlorine on the indole ring, and further, preliminary biosynthetic experiments indicated that malbrancheamide B (**2**) is a putative biosynthetic precursor to **1**,[13] which is thought to arise by sequential halogenation events. However, the question as to whether malbrancheamide B (**2**) was constituted as the 5-chloro or the 6-chloro derivative was unclear from the preliminary characterization data due to the scarce supply of the natural material. With these issues at the forefront, we undertook the synthesis of both natural substances to determine the exact identity of malbrancheamide B. To this end, we envisioned that malbrancheamide (**1**) and malbrancheamide B (**2**) would arise from the aforementioned hetero-IMDA of the 5-hydroxypyrazin-2(1*H*)-one **3**, which we could access by enolization and tautomerization of the enamide **4** (Scheme 1). Using chemistry previously established in our laboratory,[7a] we planned on assembling the enamide **4** from a reverse prenylated tryptophan **5**, which could be obtained in a few steps from the corresponding chlorinated indole **6**.

Results and Discussion

Installation of the reverse prenyl group at the indole 2-position was carried out using a two-step protocol developed by Danishefsky and co-workers.[14] Chlorination at the 3-position

SCHEME 1. Retrosynthetic Plan

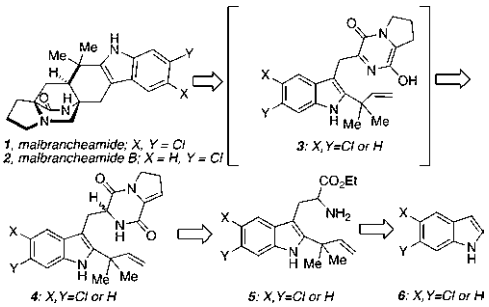

SCHEME 2. Reverse Prenylated Tryptophan Derivatives

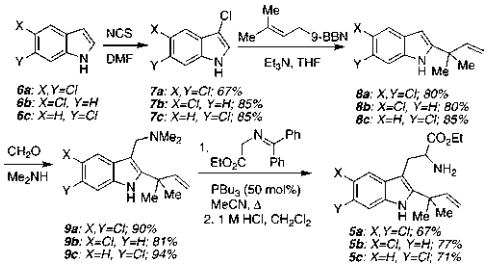

of indoles **6a**−**c**[15] using NCS in DMF gave **7a**−**c** (Scheme 2), which were treated with prenyl-9-BBN in the presence of Et_3N to afford the reverse prenylated indoles **8a**−**c**.[14] The corresponding gramines **9a**−**c** were prepared by treating **8a**−**c** with formaldehyde and dimethylamine, and subsequent Somei−Kametani coupling[16] and imine hydrolysis gave the tryptophan derivatives **5a**−**c** in good yields.

The free amine moieties in **5a**−**c** were protected as the corresponding BOC-carbamates followed by ester hydrolysis under standard conditions to yield acids **10a**−**c** (Scheme 3). Coupling of *cis*-3-hydroxyproline ethyl ester with the tryptophan derivatives **10a**−**c** in the presence of HATU delivered the amides **11a**−**c** as inseparable mixtures of diastereomers. Treatment of **11a**−**c** with TFA led to carbamate deprotection and the resulting amino esters were immediately cyclized to the corresponding diketopiperazines **12a**−**c** after refluxing with 2-hydroxypyridine. Dehydration of **12a**−**c** under Mitsunobu conditions gave the enamides **4a**−**c**, which would serve as the respective IMDA substrates.[17]

Treatment of the enamides **4a**−**c** with aqueous KOH in MeOH gave intermediate hydroxy-azadienes by enolization and tautomerizaion, and subsequent IMDA gave mixtures of **13a**−**c** and **14a**−**c** favoring the desired *syn*-isomers **13a**−**c** in ratios of (2−1.6):1 (Scheme 4). The observed preference for the IMDA to provide the *syn*-isomers **13a**−**c** as the major products mirrors

(11) (a) Martinez-Luis, S.; Rodriguez, R.; Acevedo, L.; Gonzalez, M. C.; Lira-Rocha, A.; Mata, R. *Tetrahedron* **2006**, *62*, 1817. (b) Figueroa, M.; del Carmen González, M.; Mata, R. Unpublished results.

(12) (a) Zhu, H. J.; Wang, J. S.; Guo, Q. L.; Jiang, Y.; Liu, G. Q. *Biol. Pharm. Bull.* **2005**, *28*, 1974. (b) Leisner, T. M.; Liu, M. J.; Jaffer, Z. M.; Chernoff, J.; Parise, L. V. *J. Cell Biol.* **2005**, *170*, 465.

(13) Ding, Y.; Sherman, D. H.; Williams, R. M. Unpublished results.

(14) Schkeryantz, J. M.; Woo, J. C. G.; Siliphaivanh, P.; Depew, K. M.; Danishefsky, S. J. *J. Am. Chem. Soc.* **1999**, *121*, 11964.

(15) For the preparation of 5,6-dichloroindole see: Bromidge, S. M.; et al. *J. Med. Chem.* **1998**, *41*, 1598.

(16) (a) Somei, M.; Karasawa, Y.; Kaneko, C. *Heterocycles* **1981**, *16*, 941. (b) Kametani, T.; Kanaya, N.; Ihara, M. *J. Chem. Soc., Perkin Trans. 1* **1981**, 959.

(17) Curiously, attempts to effect the one-step dehydration/IMDA reaction sequence from **12a**−**c** directly to **13a**−**c** + **14a**−**c** failed under the same conditions used successfully for stephacidin A (ref 7a) and marcfortine C (ref 9).

SCHEME 3. Enamide Diels−Alder Precursors

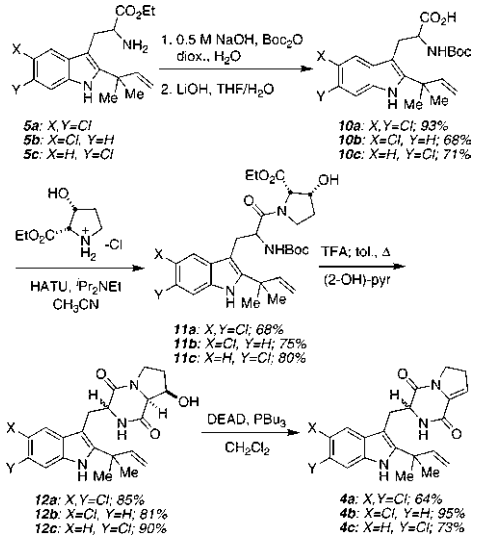

SCHEME 4. Hetero-IMDA Reactions

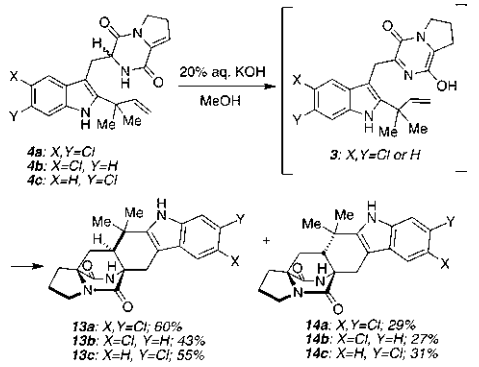

the preference we have noted for this cycloaddition in the past.[7−9] Considering that previous optimization efforts to improve the *syn*:*anti* ratio in related IMDAs were not productive when a variety of solvents and temperatures were studied, we elected to simply separate the major isomers **13a**−**c** and continue the total syntheses without further optimization.[7−9]

Completion of the syntheses required selective reduction of the tertiary amide in the presence of the secondary amide, and to that end, **13a**−**c** were treated with excess DIBAL-H,[18] which cleanly provided malbrancheamide (**1**) from **12a** (80%) and malbrancheamide B (**2**) from **12c** (74%) (Scheme 5). Synthetic **1** was identical in all respects (^{1}H, ^{13}C, HRMS) to the natural product.[11] Comparison of the ^{1}H NMR spectrum of **15**, the 5-chloro derivative, to that of natural malbrancheamide B revealed significant differences in the aromatic region revealing that the correct structure contained a 6-chloroindole ring.

(18) Fukuyama, T.; Liu, G. *J. Am. Chem. Soc.* **1996**, *118*, 7426−7427.

SCHEME 5. Amide Reductions

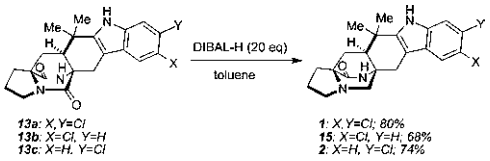

Gratifyingly, synthetic **2** was identical in all respects (^{1}H, HRMS) to natural malbrancheamide B.

It is striking that the initial halogenation of the indole ring during the biosynthesis of malbrancheamide B, occurs at the less-activated 6-position as opposed to the more electron-rich 5-position. Studies to clone and express the putative halogenase from *M. aurantiaca* are currently under investigation in these laboratories.

In summary, the first total synthesis of malbrancheamide (**1**) and malbrancheamide B (**2**) have been completed in twelve steps in 5.3% and 8.2% overall yield, respectively. In addition, the structure of malbrancheamide B (**2**) was confirmed though the synthesis of both the 5-chloro and the 6-chloro regioisomers. Experiments to establish the biosynthetic relationship between **1** and **2** and their putative progenitors are in progress and will be reported in due course.

Experimental Section

Representative Procedure for the Hetero-Diels−Alder Reaction of Enamides 4. Preparation of Cycloadducts 13a and 14a. To a solution of **4a** (86 mg, 0.21 mmol) in MeOH (16 mL) at 0 °C was added 20% aqueous KOH (4 mL). The reaction was warmed to room temperature (rt) and was stirred for 12 h. The reaction was quenched with sat. NH_4Cl (30 mL) and extracted with CH_2Cl_2 (3 × 30 mL). The combined organic layers were dried (Na_2SO_4) and concentrated under reduced pressure. The residue was triturated with $CHCl_3$ (30 mL), and the suspension was filtered to provide 53 mg (60%) of **13a** as a white amorphous solid. Concentration of the filtrate gave 25 mg (29%) of **14a** as a white amorphous solid. Data for major isomer **13a**: ^{1}H NMR (300 MHz, CD_3OD) δ 7.55 (s, 1 H), 7.40 (s, 1 H), 3.57 (d, J = 15.5 Hz, 1 H), 3.47 (m, 1 H), 2.74 (d, J = 15.5 Hz, 1 H), 2.60 (m, 1 H), 2.20−1.96 (comp, 6 H), 1.35 (s, 3 H), 1.11 (s, 3 H); ^{13}C NMR (75 MHz, CD_3OD) δ 175.7, 171.3, 144.3, 137.2, 128.1, 125.4, 123.3, 119.8, 113.1, 104.8, 68.3, 61.6, 50.8, 45.2, 36.2, 31.7, 30.1, 28.6, 25.4, 24.9, 22.3; IR (neat) 1663, 1428 cm^{-1}; HRMS (TOF+) calcd for $C_{21}H_{22}N_3O_2Cl_2$ (M + H) 418.1084, found 418.1084. Data for minor isomer **14a**: ^{1}H NMR (300 MHz, $CDCl_3$) δ 9.78 (s, 1 H), 7.49 (s, 1 H), 7.33 (s, 1 H), 3.71 (d, J = 17.8 Hz, 1 H), 3.47 (comp, 2 H), 3.25 (s, 1 H), 2.78 (d, J = 17.8 Hz, 1 H), 2.67 (m, 1 H), 2.18−1.78 (comp, 6 H), 1.24 (s, 3H), 1.16 (s, 3 H); ^{13}C NMR (75 MHz, CD_3OD /$CDCl_3$ (1:9)) δ 173.7, 169.6, 142.6, 135.7, 127.1, 125.0, 122.9, 119.1, 112.4, 102.9 67.2, 61.5, 45.8, 44.3, 34.8, 32.6, 29.8, 29.1, 28.4, 24.5, 23.2; IR (neat) 1676, 1453 cm^{-1}; HRMS (TOF+) calcd for $C_{21}H_{22}N_3O_2Cl_2$ (M + H) 418.1084, found 418.1079.

Cycloadducts 13b and 14b. Prepared from **4b** in to give 43% of **13b** as a white amorphous solid and 27% of **14b** as a white amorphous solid according to the representative procedure described above for **13a** and **14a**. Data for major isomer **13b**: ^{1}H NMR (300 MHz, CD_3OD) δ 7.54 (s, 1 H), 7.44 (s, 1 H), 7.22 (d, J = 8.6 Hz, 1 H), 7.04 (d, J = 8.6 Hz, 1 H), 3.68 (d, J = 15.4 Hz, 1 H), 3.55−3.40 (comp, 2 H), 2.77 (d, J = 15.4 Hz, 1 H), 2.76 (m, 1 H), 2.61 (m, 1 H), 2.25−1.92 (comp, 5 H), 1.37 (s, 3 H), 1.12 (s, 3 H); ^{13}C NMR (100 MHz, CD_3OD) δ 175.8, 171.4, 143.4, 136.8, 129.2, 125.2, 122.1, 118.2, 112.8, 104.5, 68.3, 61.6, 50.8, 45.2, 36.2, 31.7, 30.1, 28.7, 25.5, 25.0, 22.4; IR (neat) 1678, 1441 cm^{-1}; HRMS

(TOF+) calcd for $C_{21}H_{23}N_3O_2Cl$ (M + H) 384.1473, found 384.1460. Data for minor isomer **14b**: ^{1}H NMR (300 MHz, CD_3OD) δ 7.91 (s, 1 H), 7.41 (d, J = 2.0 Hz, 1 H), 7.23 (d, J = 8.6 Hz, 1 H), 7.01 (dd, J = 8.6, 2.0 Hz, 1H), 3.71 (d, J = 17.6 Hz, 1H), 3.53 (comp, 2 H), 2.90 (d, J = 17.6 Hz, 1 H), 2.70 (m, 1 H), 2.23−1.89 (comp, 6 H), 1.34 (s, 3 H), 1.27 (s, 3 H); ^{13}C NMR (100 MHz, CD_3OD) δ 175.4, 171.7, 143.4, 136.8, 129.7, 125.3, 122.1, 118.1, 112.8, 103.8, 68.6, 62.7, 47.3, 45.2, 35.9, 33.3, 30.8, 29.9, 28.7, 25.4, 24.8, 23.8; IR (neat) 1675, 1461 cm^{-1}; HRMS (TOF+) calcd for $C_{21}H_{23}N_3O_2Cl$ (M + H) 384.1473, found 384.1468.

Cycloadducts 13c and 14c. Prepared from **4c** in to give 55% of **13c** as a white amorphous solid and 31% of **14c** as a white amorphous solid according to the representative procedure described above for **13a** and **14a**; data for major isomer **13c**: ^{1}H NMR (400 MHz, DMSO-d_6) δ 8.75 (s, 1 H), 7.40−6.98 (comp, 3 H), 3.42 (d, J = 15.3 Hz, 1 H), 3.30 (comp, 2 H), 2.68 (d, J = 15.3 Hz, 1 H), 2.50 (comp, 1 H), 2.10−1.70 (comp, 6 H), 1.27 (s, 3 H), 0.99 (s, 3 H); ^{13}C NMR (100 MHz, DMSO-d_6) δ 173.0, 168.4, 142.0, 136.8, 125.3, 125.2, 118.9, 118.5, 110.4, 103.8, 66.0, 59.6, 48.9, 43.6, 34.6, 30.0, 28.7, 27.9, 24.0, 23.7, 21.6; IR (neat) 1671, 1409 cm^{-1}; HRMS (TOF+) calcd for $C_{21}H_{23}N_3O_2Cl$ (M+H) 384.1473, found 384.1470. Data for minor isomer **14c**: ^{1}H NMR (400 MHz, CD_3OD/$CDCl_3$ (1:9)) δ 9.58 (s, 1 H), 7.33 (d, J = 8.4 Hz, 1 H), 7.23 (d, J = 1.8 Hz, 1 H), 6.97 (dd, J = 8.4, 1.8 Hz, 1 H), 3.75 (d, J = 17.8 Hz, 1 H), 3.47 (comp, 2 H), 3.30 (bs, 1 H), 2.84 (d, J = 17.8 Hz, 1 H), 2.70 (m, 1 H), 2.23−1.77 (comp, 6 H), 1.25 (s, 3 H), 1.18 (s, 3 H); ^{13}C NMR (100 MHz, DMSO-d_6) δ 172.43, 169.0, 142.0, 136.8, 125.8, 125.3, 119.0, 118.5, 110.4, 103.1, 79.2, 66.4, 60.5, 45.4, 43.7, 34.2, 31.6, 28.6, 27.7, 24.0, 22.5; IR (neat) 1672, 1410 cm^{-1}; HRMS (TOF+) calcd for $C_{21}H_{23}N_3O_2Cl$ (M + H) 384.1473, found 384.1468.

Representative Procedure for the Selective Reduction of Tertiary Amides with Excess DIBAL-H. Synthesis of Malbrancheamide (1). DIBAL-H (0.70 mL, 1 M in toluene, 0.70 mmol) was added to a suspension of **13a** (15 mg, 0.036 mmol) in toluene (7 mL) at rt. The reaction was stirred at rt for 12 h, whereupon finely powdered Na_2SO_4•$10H_2O$ was added until bubbling ceased. The mixture was filtered with a medium porosity fritted funnel washing with EtOAc (50 mL) and MeOH (50 mL), and the filtrate was concentrated under reduced pressure. The residue was purified by flash chromatography eluting with MeOH/CH_2Cl_2 (2:98) to give 12 mg (80%) of **1** as a white amorphous solid: ^{1}H NMR (400 MHz, CD_3OD) δ 7.48 (s, 1 H), 7.40 (s, 1 H), 3.43 (d, J = 10.3 Hz, 1 H), 3.06 (m, 1 H), 2.85 (comp, 2 H), 2.54 (m, 1 H), 2.27 (dd, J = 10.2, 1.5 Hz, 1 H), 2.20−1.18 (comp, 6 H), 1.43 (s, 3 H), 1.34 (s, 3 H); ^{13}C NMR (100 MHz, CD_3OD) δ 176.6, 145.1, 137.3, 128.2, 125.3, 123.2, 119.6, 113.1, 104.7, 66.1, 59.4, 57.4, 55.4, 48.5, 35.5, 32.4, 30.6, 30.0, 28.1, 24.2, 23.5; IR (neat) 3226, 1658, 1460 cm^{-1}; HRMS (TOF+) calcd for $C_{21}H_{24}N_3OCl_2$ (M + H) 404.1291, found 404.1290.

Isomalbrancheamide B (15). Prepared from **13b** in 68% yield as a white amorphous solid according to the representative procedure described above for **1**: ^{1}H NMR (400 MHz, DMSO-d_6) δ 8.39 (s, 1 H), 7.33 (s, 1 H), 7.26 (d, J = 8.5 Hz, 1 H), 7.01 (d, J = 8.5 Hz, 1 H), 3.33 (d, J = 7.2 Hz, 1 H), 3.26 (d, J = 9.9 Hz, 1 H), 2.76 (s, 2 H), 2.42 (m, 1 H), 2.15−1.73 (comp, 7 H), 1.33 (s, 3 H), 1.27 (s, 3 H); ^{13}C NMR (100 MHz, DMSO-d_6) δ 173.1. 143.4, 134.9, 127.7, 122.8, 120.4, 116.7, 112.1, 103.4, 64.1, 58.6, 55.3, 53.9, 47.0, 34.0, 31.1, 30.0, 28.7, 26.6, 23.7, 22.5; IR (neat) 3311, 1637, 1458 cm^{-1}; HRMS (TOF+) calcd for $C_{21}H_{25}N_3OCl$ (M + H) 370.1680, found 370.1675.

Malbrancheamide B (2). Prepared from **13c** in 74% yield as a white amorphous solid according to the representative procedure described above for **1**: ^{1}H NMR (400 MHz, DMSO-d_6) δ 8.41 (s, 1 H), 7.32 (d, J = 8.4 Hz, 1 H), 7.27 (d, J = 1.7 Hz, 1 H), 6.95 (dd, J = 8.4, 1.7 Hz, 1 H), 3.36 (s, 1 H), 3.27 (d, J = 10.0 Hz, 1 H), 2.95 (m, 1 H), 2.76 (s, 2 H), 2.43 (m, 1 H), 2.13 (d, J = 9.9 Hz, 1 H), 2.10−1.70 (comp, 6 H), 1.32 (s, 3 H), 1.26 (s, 3 H); ^{13}C NMR (100 MHz, DMSO-d_6) δ 173.1, 142.6, 136.8, 125.3, 125.2, 118.7, 118.5, 110.3, 103.7, 64.1, 58.5, 55.3, 53.9, 47.0, 34.0, 31.1, 30.0, 28.7, 26.6, 23.7, 22.5; IR (neat) 3297, 1652, 1457 cm^{-1}; HRMS (TOF+) calcd for $C_{21}H_{25}N_3OCl$ (M + H) 370.1680, found 370.1670.

Acknowledgment. Financial support from the National Institutes of Health (CA70375 to R.M.W) and the Hans W. Vahlteich Professorship (to D.H.S.) is gratefully acknowledged. We are grateful to Prof. Rachel Mata and Dr. María del Carmen González of the Departamento de Farmacia, Facultad de Química, Universidad Nacional Autónoma de México for providing ^{1}H NMR spectra of natural malbrancheamide and malbrancheamide B as well as an authentic specimen of malbrancheamide. We also acknowledge Prof. Mata for sharing a pre-print of their manuscript describing the structural elucidation of malbrancheamide B (ref 11b). We thank Dr. Anthony E. Glenn of the USDA for providing M. aurantiaca RRC1813 strain (originally obtained from Dr. María del Carmen González). Mass spectra were obtained on instruments supported by the NIH Shared Instrumentation Grant GM49631.

Supporting Information Available: Spectroscopic data and experimental details for the preparation of all new compounds as well as copies of ^{1}H NMR and ^{13}C NMR spectra. This material is available free of charge via the Internet at http://pubs.acs.org.

JO800116Y

APPENDIX II

Research Proposal

Principal Investigator: Welch, Timothy R. 6.4

Plans for Work Under Fellowship

B. Research Plan: Targeting STAT5 in Prostate Cancer Cells with DNA Binding Polyamides

I. Specific Aims

Prostate cancer was responsible for approximately 33720 deaths in 2011.[1] While patients with metastatic prostate cancer typically respond to surgical or medicinal androgen deprivation initially, all will eventually progress to an androgen independent state termed castration-resistant prostate cancer (CRPC). The progression of prostate cancer cells to the androgen independent phenotype occurs concomitantly with an increase in the constitutive activation of the transcription factors androgen receptor (AR) and signal transducer and activator of transcription 5 (STAT5).[2] AR is established as a relevant target for the treatment of CRPC, and several therapies targeting the AR signaling pathway are available or in development.[3,4] While the exact role of STAT5 in CRPC is not as well defined, it appears to be equally important to prostate cancer cell growth and survival, as evidenced by the following: (1) STAT5 is overactive in 95% of CRPCs,[5] (2) STAT5 activity is associated with highly aggressive (high Gleason grade) prostate cancers,[6,7] and (3) inhibition of STAT5 by siRNA results in massive apoptotic cell death in human prostate cancer cell lines.[8] STAT5 represents a promising target for the treatment of CRPC, a disease for which no effective therapy currently exists. To date, no small molecule inhibitors of STAT5 transcriptional activity have been reported.

Our *long term goal* is to develop small molecule inhibitors of STAT5 function for the treatment of malignancies displaying aberrant STAT5 activity. The *overall objective* of this proposal is to determine the therapeutic potential of DNA binding pyrrole-imidazole polyamides that target STAT5 for the treatment of CRPC. *We hypothesize that polyamides can be designed to downregulate the expression of a subset of genes required for CRPC cell survival*. Polyamides containing *N*-methylpyrrole (Py) and *N*-methylimidazole (Im) comprise the **only** known class of programmable small molecules capable of binding specific DNA sequences.[9,10] Previous studies from the Dervan group have shown that polyamides are cell permeable,[11-13] access nuclear chromatin,[14-16] inhibit specific protein–DNA interfaces,[17] and modulate gene expression in cell culture.[18-23] Polyamides represent a promising approach toward the pursuit of small molecule inhibitors of STAT5 transcription for the treatment of CRPC. The specific aims proposed below will determine the suitability of this approach while contributing to the overall understanding of STAT5 signaling in prostate cancer.

AIM 1. **Synthesize a series of Py/Im polyamides designed to target the STAT5 response element and evaluate their DNA binding interactions in vitro.** Polyamides designed to target the consensus STAT5 binding sequence 5'-TTCNNNGAA-3'[†] will be synthesized by solid phase methodology. DNA binding interactions of the polyamides will be evaluated in vitro using melting temperature analysis and electrophoretic mobility shift assay (EMSA).

AIM 2. **Examine nuclear localization and characterize gene regulatory potency of polyamides.** Laser-scanning confocal microscopy will be used to examine cellular uptake and localization of high-affinity polyamides in several cancer cell lines. The expression of STAT5 regulated oncogenes *BCL-2*,[24-27] *BCL-X_L*,[28,29] and *CYCLIN-D1*[2,8,30] in prostate cancer cells will be examined following polyamide treatment using quantitative real-time RT-PCR (qRT-PCR). The global effects of polyamides that are shown to modify gene expression will then be studied

[†] Abbreviations for degenerate nucleotides: N = any base; W = A or T.

with chromatin immunoprecipitation coupled with sequencing (ChIP-seq) and mRNA sequencing (RNA-seq).

AIM 3. **Investigate polyamide induced apoptosis in prostate cancer cell lines and in mice bearing xenograft tumors.** General cell death will be analyzed following polyamide treatment in both normal and prostate cancer cell lines. Polyamide effects on C4-2 tumor growth will be studied in a murine model at the Caltech Animal Facility.

The aims in this proposal represent a new approach toward the development of inhibitors of STAT5 regulated gene expression. The proposed experiments will provide thorough and systematic understanding of the activity, mechanism, and specificity of polyamides in prostate cancer. If successful, the proposed research could produce the first known *specific* inhibitors of STAT5 regulated gene expression for the treatment of CRPC.

II. Background and Significance

A limited set of transcription factors has been implicated in a large number of diverse oncogenic signaling pathways.[31] Selective inhibition of a single transcription factor would thus influence the expression of numerous upstream oncogenes, many of which are currently individually targeted by discrete inhibitors. Signal transducer and activator of transcription (STAT) proteins are overactive in a variety of cancers, promote cancer cell survival and proliferation, and are susceptible to inhibition, making them ideal targets for cancer therapy.[32-34] STATs are latent cytoplasmic proteins that, once activated by tyrosine kinase phosphorylation, dimerize, traffic to the nucleus, and bind specific response elements of target gene promoters (***Figure 1***).[32,35-37] In normal cells, STAT activation has a role in cell survival, angiogenesis, immune function, and in controlling cell growth.[38,39] However, disregulation of this activity can contribute to tumor cell growth and proliferation.[32,40]

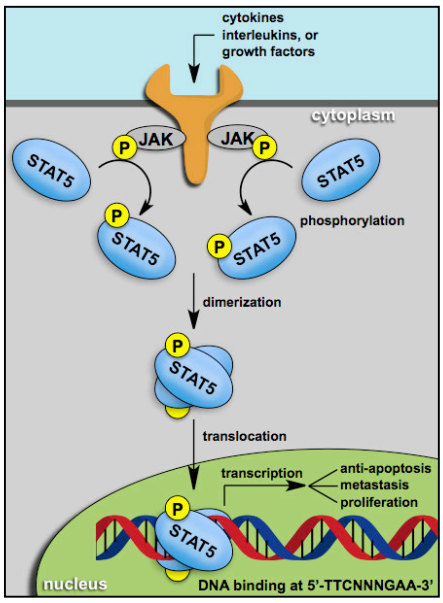

Figure 1. Canonical STAT5 signaling pathway.

Persistent activity of STAT5, a member of the STAT family of proteins, is associated with prostate cancer,[5,6,8,41,42] lung, head, and neck cancers,[43] and several types of leukemia[44-47] and lymphomas.[35,48] The link to prostate cancer is particularly strong, with 95% of castration-resistant prostate cancers (CRPC) displaying constitutive STAT5 activity.[5] Active STAT5 in prostate cancer predicts early disease recurrence and is associated with high Gleason grade prostate cancers characterized by an aggressive phenotype and poor patient outcome.[6,7] Furthermore, active STAT5 has been shown to increase the motility of prostate cancer cells, enhancing the intrinsic ability of the disease to metastasize.[49] STAT5 is a generic term for two highly homologous protein isoforms, 94-kDa STAT5a and 92-kDa STAT5b.[50] Both isoforms share a conserved DNA binding domain that permits binding of STAT5 to consensus motifs (5'-TTCNNNGAA-3') found in target gene promoters, including the oncogenes encoding anti-apoptotic (BCL-X_L, BCL-2) and pro-proliferative (Cyclin-D1) proteins.[2,8,24-30,51] STAT5 binding to this consensus motif

found at non-canonical recognition sites has additionally been shown to activate several novel and potentially oncogenic genes, including TNFRSF13b, MKP-1, and C3ar1.[52]

Numerous studies have shown that inhibition of STAT5 results in massive apoptotic cell death in human prostate cancer cell lines, regardless of the inhibitory method employed (adenoviral expression of dominant-negative mutants of STAT5, siRNA, or antisense oligonucleotides).[2,8,41,53] STAT5 inhibition by antisense oligonucleotides has specifically been shown to suppress the expression of Cyclin-D1 and BCL-X_L in LNCaP, C4-2, and DU145 prostate cancer cell lines at both the mRNA and protein levels, resulting in increased apoptotic death and decreased cell growth.[2,8] In mouse xenograft models, the progression of CRPC was delayed significantly by STAT5 inhibition with antisense oligonucleotides.[2] *These findings imply prostate cancers depend on persistent STAT5 activation for cell growth and survival*. Chemotherapeutic small molecules targeting STAT5 signaling could thus have a substantial impact on the treatment of CRPC, a disease for which no effective pharmacological therapy currently exists. STAT5 inhibitors published to date indiscriminately downregulate STAT5 regulated transcription and lack practical therapeutic potential. Herein, we describe a new, promising approach for the selective inhibition of STAT5 mediated gene expression in prostate cancer, using DNA binding polyamides to disrupt the STAT5–DNA interface.

Polyamides containing *N*-methylpyrrole (Py) and *N*-methylimidazole (Im) comprise a class of programmable small molecules that can be designed to bind specific DNA sequences with affinities

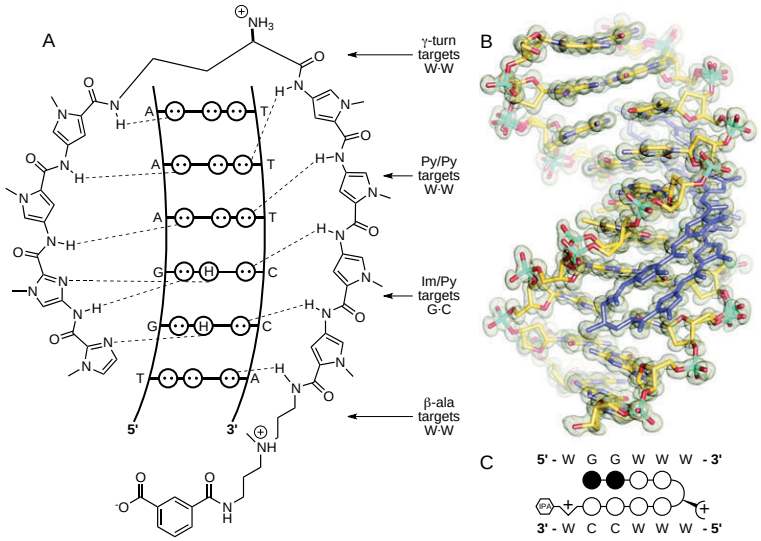

Figure 2. Molecular recognition of the minor groove of DNA by a hairpin polyamide. (**A**) Model of an eight ring hairpin polyamide (ImImPyPy-(R)^{H_2N}-γ-PyPyPyPy-β-IPA) bound to a 5'-TGGAAA-3' sequence. Putative hydrogen bonds are represented by dashed lines. (**B**) X-ray crystal structure of a cyclic polyamide (blue) in complex with dsDNA (0.95Å resolution). (**C**) Ball-and-stick model of the polyamide in **2A**. Closed and open circles represent *N*-methylimidazole and *N*-methylpyrrole monomers, respectively. Diamonds, β-alanine; triangle with positive charge, triamine linker; curved line substituted with positive charge, α-amino-substituted γ-turn. The isophthalic acid derived tail is represented by a hexagon.

comparable to native DNA binding proteins.[9] Sequence specificity of Py/Im polyamides is determined by side-by-side pairing of the heterocyclic amino acids to form distinct hydrogen bonds to nucleotides in the minor groove of DNA (***Figure 2***).[54] Im/Py pairs distinguish G•C from C•G, whereas Py/Py pairs degenerately bind A•T and T•A.[10] Hairpin polyamides designed as such have been shown to bind DNA with high affinities,[55] inhibit interactions with DNA binding proteins,[17] bind chromatin,[14-16] and traffic to the nucleus in a variety of cell types.[11-13] Recently, analyses have shown that 8-ring cyclic polyamides allosterically perturb the DNA helix through a 4Å widening of the minor groove and consequent major groove compression.[56] This significant change provides a mechanistic basis for disruption of protein–DNA interfaces by hairpin polyamides.

To evaluate the specific inhibition of STAT5 mediated gene expression by cell permeable, sequence specific DNA binding polyamides, we propose the synthesis, biochemical evaluation, and biological study of a small library of Py/Im polyamides designed to specifically disrupt the interactions of STAT5 with regulatory regions of pro-proliferative and anti-apoptotic genes.

III. Preliminary Studies

This proposal builds upon known chemical and biological techniques developed in the Dervan group. The study highlighted here shows precedence for the use of polyamides in the modulation of endogenous gene expression (***Figure 3***). In the study, hypoxia inducible factor (HIF-1α) binding to the sequence 5'-WWWCGW-3' found in the vascular endothelial growth factor (VEGF) hypoxia response element (HRE) was perturbed by a hairpin polyamide.[21,22] The polyamide reduced occupancy of HIF-1α at the VEGF HRE and suppressed VEGF mRNA expression. Only a subset of genes induced by deferoxamine (DFO)—a small molecule used to mimic hypoxia in cells—was inhibited by polyamide, whereas HIF-1α siRNA and the DNA-binding natural product echinomycin inhibited most of the DFO induced transcripts. This demonstrated the relative selectivity of Py/Im polyamides compared to other methods used to perturb HIF-1α activity.

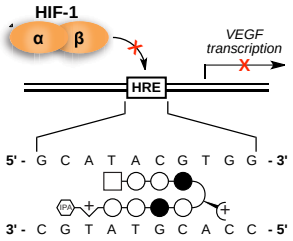

Figure 3. Polyamide mediated inhibition of HIF-1 DNA binding to the HRE suppresses *VEGF* expression. (The square symbol represents chlorothiophene.)

A second investigation key to the design of this proposal was detailed in a series of publications from the Dervan group in which the nuclear localization of a library of over 120 polyamide-fluorophore conjugates was described.[11-13] Cellular uptake profiles of the polyamides were assayed in 13 cell lines using confocal microscopy. The reported nuclear uptake trends suggest the following structural features to be conducive to uptake: an eight-ring hairpin or cyclic core, a positive charge on the amino substituent of the γ-aminobutyric acid (GABA) turn, and either a conjugated fluorescein fluorophore (FITC) or isophthalic acid (IPA) moiety on the hairpin tail. Polyamides targeting 5'-WGWWGW-3' and 5'-WGGWWW-3' similar to those proposed below were shown to have strong nuclear localization in PC-3 and LNCaP prostate cancer cell lines.[11,12]

The transition from cell culture work to murine models is an important next step in Py/Im polyamide research that is focused on biomedical applications of the technology. Recent studies undertaken in the Dervan laboratory have provided basic pharmacokinetic analyses of polyamides in C57/BL6 wild type mice.[57] Micromolar blood levels of Py/Im polyamides were achieved for multiple hours following a single injection of the compound subcutaneously or intraperitoneally. An example is shown in **Figure 4a** (a representative HPLC trace) and **4B** (a representative pharmacokinetic profile for a hairpin Py/Im polyamide). Decline in hairpin polyamide concentration was observed over the course of multiple hours,

with a peak concentration noted between 1-3h depending on route of administration. Compound plasma levels were below detection level 24h after the injection. The polyamide was well tolerated by the animals. Multiple administrations (i.p. or s.c. at 120 nmol per injection per animal) did not result in any significant reduction in body weight. Weight loss is a commonly used criterion for health deterioration in mice (**Figure 4C, D**).[57]

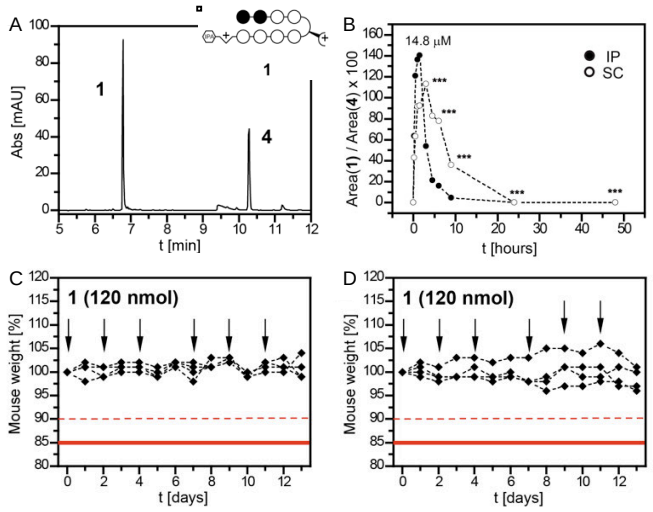

Figure 4. Pharmacokinetic data for hairpin polyamide **1** in C57/BL6 wild type mice. (**A**) HPLC analysis of a blood sample collected retro-orbitally 1.5 h post intraperitoneal (i.p.) injection of **1**. Plasma was isolated by centrifugation and pre-cleared from protein by methanol precipitation. (**4** = internal reference standard). (**B**) Plasma levels of **1** as a percent of reference standard **4** following i.p. or subcutaneous (s.c.) injection. (**C**, **D**) Weight of four individual mice in response to polyamide dosing regimen. 120 nmol doses were administered either i.p. (**C**) or s.c. (**D**) at intervals denoted by arrows in the plot. The solid red line indicates the 15% weight loss mark considered an endpoint criterion for the mice.

The Dervan group has recently gained broad experience with xenograft experimentation in immunocompromised mice, encompassing the engraftment of human cancer cell lines A549, LNCaP, U251, and T47D. FITC-labeled polyamides injected subcutaneously on the flank opposite the tumor were shown by confocal microscopy to access the tumor derived cell nuclei. *Moreover, gene expression changes have been observed in engrafted A549 tumors following polyamide treatment*.[58]

The studies outlined above demonstrate the validity of targeting the transcription factor–DNA interface as a means of modulating gene expression. Furthermore, evaluation of nuclear uptake trends allows for the rational design of new polyamides that are structurally optimized for nuclear localization. The Dervan group has also recently developed a gram-scale synthesis of hairpin polyamides and shown that polyamides are bioavailable in mice, eliminating two major obstacles in the evaluation of polyamides in animal models.[59,60] Tumor engraftment protocols, established tolerable dosing conditions, and general animal care and handling expertise found in the Dervan group will be invaluable during in vivo testing of the proposed STAT5-targeting polyamides. We are confident the methods established by these studies can be extended to the proposed research and will increase the probability of success.

IV. Research Design and Methods

An estimated timeline for completion of the specific aims is given in ***Figure 5***. The proficiency of the Dervan group with these techniques coupled with the outstanding equipment, facilities, and expertise found at Caltech will provide strong support for the success of this research project. We are confident that the proposed objectives will be thoroughly pursued during the planned three year period.

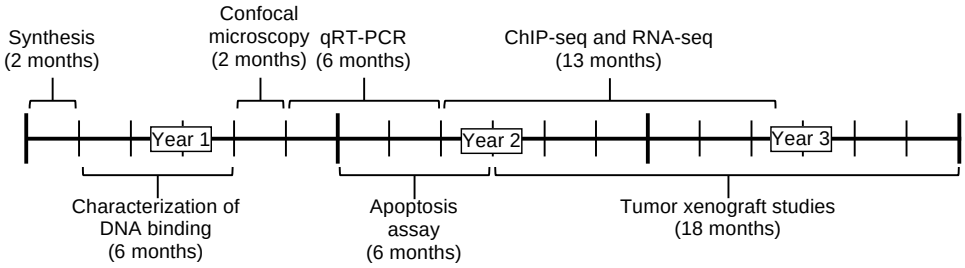

Figure 5. Predicted timetable for the proposed research.

AIM 1. Synthesize a series of Py/Im polyamides designed to target the STAT5 response element and evaluate their DNA binding interactions in vitro.

Three oncogenes shown in the literature to be functionally activated by STAT5 and to contain a STAT5 binding site characterized at the sequence level were selected as targets for polyamide inhibition (***Table 1***). The three degenerate base pairs found in the middle of the consensus STAT5 binding sequence (5'-TTC**NNN**GAA-3') represent the great degree of diversity of the binding sequences on target genes, allowing for the design of polyamides with greater DNA site sequence specificity than the native transcription factor. Three polyamides (***Figure 6***) are proposed to bind the sequences 5'-WGWWGW-3' (**1**, found in *BCL-X*$_L$), 5'-WWCGGW-3' (**2**, found in *BCL-X*$_L$), and 5'-WGGWWW-3' (**3**, found in *BCL-2* and *CYCLIN-D1*).[27,30] Polyamide **3** is also expected to bind non-canonical STAT5 binding sites found in *MKP-1*, *TNFRSF13b*, and *C3ar1*.[52] Mismatch controls will be prepared for each compound by substituting a Py for an Im (structures not shown). Polyamides **1**-**3** and the three mismatch controls will be synthesized using solid-phase methodology established in the Dervan laboratory.[18,61,62] Preparative reverse-phase high performance liquid chromatography (RP-HPLC) will be used to purify crude reaction products. Chemical purity of polyamides will be determined by analytical HPLC and the chemical composition of each confirmed by matrix-assisted laser desorption ionization time-of-flight mass spectrometry (MALDI-TOF).

Gene	*Function*	*STAT5 Binding Sequence*
BCL-X$_L$	anti-apoptotic	5'-GCAT**TTCGGAGAA**GACG-3'
BCL-2	anti-apoptotic	5'-CAAG**TTCCAGGAA**AGCG-3'
CYCLIN-D1	pro-proliferative	5'-GGCG**TTCTTGGAA**ATGC-3'

Table 1. Promoter sequences for selected genes demonstrated to be STAT5 dependent. The consensus sequence is specified in bold.

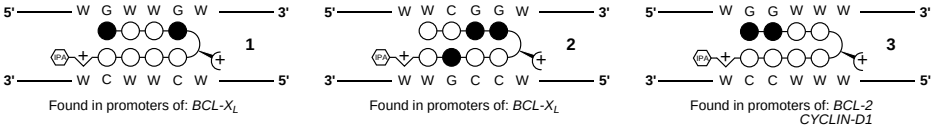

Figure 6. Proposed library of polyamide inhibitors of STAT5. Structural abbreviations are defined in Figure 2.

The ability of synthesized polyamides **1**-**3** to bind DNA will be determined using melting temperature (T_m) analysis. The degree to which both match and mismatch polyamides stabilize 14 base pair DNA duplexes containing the appropriate match sequence will be measured. Previous results have shown a correlation between the increase in T_m of DNA duplexes and DNA binding affinity.[63-65] Polyamides

identified to bind DNA with high affinity will be subjected to electrophoretic mobility shift assay (EMSA) to evaluate their ability to disrupt STAT5 binding to their cognate sequences. Published protocols from the Dervan laboratory will be followed using commercially available STAT5 and ^{32}P-labelled oligonucleotides purchased from Abcam and Integrated DNA Technologies, respectively.[19-21,63]

AIM 2. Examine nuclear localization and characterize gene regulatory potency of polyamides.

Fluorescent (FITC) derivatives of polyamides **1**-**3** will be evaluated in cell culture to examine their uptake and localization properties. Cells treated with varying concentrations of fluorescent polyamides will be examined using confocal microscopy as previously described.[11-13] Several prostate cancer cell lines will be studied to establish general cellular uptake trends, including LNCaP, C4-2, DU145, and PC-3 (***Table 2***). All have been previously used in the Dervan laboratory or are commercially available and will be cultured and propagated according to recommended American Type Culture Collection (ATCC) procedures.

Polyamides will then be screened for the ability to suppress gene expression in cells by quantitative real-time RT-PCR (qRT-PCR).[22] Specifically, we will examine the mRNA expression profiles of STAT5 regulated genes *BCL-X_L*, *BCL-2*, and *CYCLIN-D1* in the presence of polyamides following induction of STAT5 activity by interleukin 3 (IL-3) in four different prostate cancer cell lines. *A reduction in IL-3 induced expression is expected if a polyamide disrupts STAT5 activation of the gene under investigation*. Mismatch polyamides will serve as a negative control, while STAT5 siRNA known to inhibit expression of all three target genes will be used as a positive control for comparison.[8] Since constitutive STAT5 activation is most prevalent in cells expressing an androgen independent phenotype, cell lines for this experiment were selected based on androgen dependence (***Table 2***). Polyamide binding is expected to impart a greater change on gene expression in androgen independent cell lines C4-2 and DU145 than on androgen sensitive LNCaP cells. PC-3 cells do not express STAT5 and are included as a negative control for STAT5 regulated gene expression.

Cell Line	***Androgen Dependence***	***STAT5 (+/-)***	***Commercial source***
LNCaP	sensitive	+	ATCC
C4-2	independent	+	UroCor Labs
DU145	independent	+	ATCC
PC-3	independent	-	ATCC

Table 2. Proposed prostate cancer cell lines.

The *global effects of polyamide treatment* on prostate cancer cells will be investigated through chromatin-immunoprecipitation coupled with sequencing (ChIP-seq) and cellular mRNA sequencing (RNA-seq). To probe the mechanism of polyamide induced gene suppression in prostate cancer cells, ChIP-seq will be conducted to assess STAT5 occupancy in nuclear chromatin. In the absence of polyamide or in the presence of the mismatched control, amplification of DNA isolated from anti-STAT5 antibody (purchased from Santa Cruz) pull-down is expected, demonstrating normal STAT5–DNA binding. *A decrease in pull-down efficiency from polyamide treated cells would support an inhibitory mechanism in which displacement of STAT5 is attributable to polyamide binding to gene promoters*. Isolated DNA will be submitted to high throughput sequencing using the Illumina Genome Analyzer at Caltech. Sequencing results mapped to the human genome will be compared between the untreated, mismatch control, and match polyamide experiments to identify specific genomic sites susceptible to polyamide-mediated STAT5 displacement. A consensus polyamide binding site will also be characterized, providing valuable insight as to the *sequence specificity* of the polyamide. The *global effect* of polyamides on gene expression can be evaluated using RNA-seq. STAT5 activity will be induced in cells with IL-3, then either (1) left untreated, or treated with (2) mismatch polyamide, (3) polyamide, or (4) STAT5 siRNA. Total mRNA will be isolated from each experiment, sequenced, and scanned for a 2-fold or greater alteration in expression. Our hypothesis that polyamides can be designed to selectively inhibit

a subset of STAT5 regulated genes will be supported if fewer IL-3 induced transcripts are affected by polyamide than by siRNA. A sequence specific mechanism of polyamide mediated perturbation is also supported if the mismatch control suppresses fewer induced gene transcripts than the matched polyamide.

AIM 3. Investigate polyamide induced apoptosis in prostate cancer cell lines and in mice bearing xenograft tumors.

The effect on cell apoptosis of the proposed polyamides will be evaluated in each of the prostate cancer cell lines mentioned above. Cells will be incubated with varying concentrations of polyamide, then the effect on cell cycle population analyzed by flow cytometry, caspase-3 activity, and cleaved poly ADP ribose polymerase (PARP) expression.[2,53] Polyamide induced apoptosis would be characterized by dose-dependent increases in the fraction of cells in the sub-G_0/G_1 phases of the cell cycle, caspase-3 activity, and in the expression of cleaved PARP. STAT5-negative PC-3 cells will serve as a necessary negative control. *The selectivity of polyamide induction of apoptosis in cancerous versus normal cell lines will be determined by comparing these results to those found in an analogous experiment on HUVEC and NHDF cell lines*.

Polyamide effects on the C4-2 cell line will be further studied in an in vivo murine model. All experiments are to be conducted at the Caltech Animal Facility following the experimental procedures outlined in the IACUC protocol of the Dervan laboratory (#1638-11, date of approval: 9/21/11). Male immunocompromised mice will be injected subcutaneously (s.c.) with up to 10^7 C4-2 cells in PBS. Following a 1-2 week tumor engraftment period, Py/Im polyamides will be injected intraperitoneally (i.p.) at doses not exceeding 40 mg/kg over the course of up to 12 weeks. The animals will be injected with polyamide up to three times a week with a resting period of at least onea day between injections. A vehicle-treated reference control group will be maintained throughout the experiment. Recent investigations conducted in the Dervan laboratory showed that micromolar concentrations of polyamide in murine blood could be achieved following i.p. injection of polyamides with varying sequences.[57,58] Tumor volume will be monitored at least once a week using caliper measurements. Retro-orbital blood samples will be collected weekly and levels of tumor-specific secreted factor PSA measured by enzyme-linked immunosorbent assay (ELISA). After four weeks of polyamide treatment, the mice will be sacrificed by asphyxiation (CO_2 chamber, 60%). Tumors will be excised and sectioned for histological blood vessel quantification. RNA-seq experiments will further be conducted to determine global polyamide effects on the tumor transcriptome in comparison to the vehicle treated group.

Potential Problems with this Proposal

Three possible problems with this proposal are presented and addressed.

(i) *The proposed polyamides are not sufficiently specific to be considered therapeutic candidates for the selective inhibition of STAT5 in the context of the human genome.*

The human genome likely contains over a million potential binding sites for a compound that targets six base pair sequences. However, many of these sites are inaccessible in the context of nuclear chromatin. Boyle and coworkers have shown using DNase I hypersensitivity maps that only 2.1% of the genome is accessible in $CD4^+$ T-cells.[66] Moreover, polyamide binding at non-promoter sequences of accessible DNA does not affect transcription, as RNA polymerase dislodges polyamides from DNA during transcription.[67] Despite the prevalence of six base pair sequences targeted by 8-ring polyamides in the genome, the HIF-1 studied mentioned above shows that polyamides have a relatively small effect on *global* gene expression.

(ii) *The STAT family of proteins share a similar DNA binding domain, so polyamides designed to target a six base pair STAT5 sequence will invariably target other members of the family of transcription factors.*

STAT5 and STAT3 site sequences share the most homology (5'-TTCNNNGAA-3' and 5'-TTCCNGGAA-3', respectively) among the STAT family.[68] Polyamides **1** and **2** target STAT consensus sequences with at least two mismatched sites and are expected to be selective for STAT5 over STAT3. Polyamide **3** matches the STAT3 consensus when N=W and will likely inhibit some binding of both STAT3 and STAT5 to the cognate sequence. Comparison of the gene regulatory activity of polyamides **1**-**3** will allow us to analyze selectivity of the proposed polyamides. Binding specificity could be improved by expanding the Py/Im core to target seven or eight base pair sequences (***Figure 7***). However, disruption of STAT3 activated gene expression would not necessarily be an undesired consequence of polyamide binding, as constitutive STAT3 activity has also been implicated in the malignant phenotype of numerous cancers.[32] For this reason, polyamide **3** was deliberately included in this proposal.

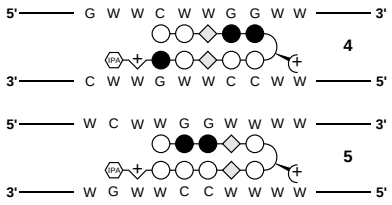

Figure 7. Polyamide modifications: extended hairpins targeting 7 bp sequences of *CYCLIN-D1* promoter.

(iii) *Inhibition of STAT5 target gene expression is not selective for cancer cells.*

CRPC tumors are dependent upon persistent STAT5 activity for malignant cell growth and survival. It has been suggested that even partial inhibition of STAT5 mediated transcription would be fatal to tumor cells as a consequence of this increased STAT5 dependence.[32] Normal cells could plausibly survive with low levels of active STAT5 or utilize other survival pathways. Indeed, even STAT5 null mice remain viable, despite impaired mammary gland development and abnormalities in hematopoiesis.[36,69] Conversely, disruption of STAT5 signaling in tumor cells causes massive apoptosis. ***Aim 3*** will provide a direct comparison of polyamide treatment on normal versus cancerous cells.

Closing Remarks

The primary aim of this proposal is the development of a small library of polyamides designed to inhibit the binding of STAT5 to its cognate promoter site sequences. We hypothesize that the disruption of STAT5 binding events should suppress gene expression necessary for tumor cell growth and survival, resulting in apoptosis of CRPC cells. Inhibition of STAT5 transcriptional activity at the protein–DNA interface represents a new approach toward the treatment of CRPC. Accordingly, extensive experimentation has been proposed to fully elucidate the binding affinities and specificities of polyamides **1**-**3** for the cognate DNA sequences, to determine if the polyamides are able to traffic to the nucleus, and to quantify the effect of polyamide treatment on gene expression in prostate cancer cells. The ability of polyamides to reduce the viability of cancer cells will then be examined in cell lines and in mice bearing xenograft tumors. Results of these studies will reveal the therapeutic potential of polyamides in the treatment of CRPC and contribute to the understanding of STAT5 signaling in prostate cancer cells.

Literature Cited

1. Siegel, R.; Ward, E.; Brawley, O.; Jemal, A. Cancer statistics, 2011: the impact of eliminating socioeconomic and racial disparities on premature cancer deaths. *CA Cancer J Clin* **2011**, *61*, 212-236.
2. Thomas, C.; Zoubeidi, A.; Kuruma, H.; Fazli, L.; Lamoureux, F.; Beraldi, E.; Monia, B. P.; MacLeod, A. R.; Thuroff, J. W.; Gleave, M. E. Transcription factor Stat5 knockdown enhances androgen receptor degradation and delays castration-resistant prostate cancer progression in vivo. *Mol Cancer Ther* **2011**, *10*, 347-359.
3. Antonarakis, E. S.; Carducci, M. A.; Eisenberger, M. A. Novel targeted therapeutics for metastatic castration-resistant prostate cancer. *Cancer Lett* **2010**, *291*, 1-13.
4. Ryan, C. J.; Tindall, D. J. Androgen receptor rediscovered: the new biology and targeting the androgen receptor therapeutically. *J Clin Oncol* **2011**, *29*, 3651-3658.
5. Tan, S. H.; Dagvadorj, A.; Shen, F.; Gu, L.; Liao, Z.; Abdulghani, J.; Zhang, Y.; Gelmann, E. P.; Zellweger, T.; Culig, Z.; Visakorpi, T.; Bubendorf, L.; Kirken, R. A.; Karras, J.; Nevalainen, M. T. Transcription factor Stat5 synergizes with androgen receptor in prostate cancer cells. *Cancer Res* **2008**, *68*, 236-248.
6. Li, H.; Ahonen, T. J.; Alanen, K.; Xie, J.; LeBaron, M. J.; Pretlow, T. G.; Ealley, E. L.; Zhang, Y.; Nurmi, M.; Singh, B.; Martikainen, P. M.; Nevalainen, M. T. Activation of signal transducer and activator of transcription 5 in human prostate cancer is associated with high histological grade. *Cancer Res* **2004**, *64*, 4774-4782.
7. Li, H.; Zhang, Y.; Glass, A.; Zellweger, T.; Gehan, E.; Bubendorf, L.; Gelmann, E. P.; Nevalainen, M. T. Activation of signal transducer and activator of transcription-5 in prostate cancer predicts early recurrence. *Clin Cancer Res* **2005**, *11*, 5863-5868.
8. Dagvadorj, A.; Kirken, R. A.; Leiby, B.; Karras, J.; Nevalainen, M. T. Transcription factor signal transducer and activator of transcription 5 promotes growth of human prostate cancer cells in vivo. *Clin Cancer Res* **2008**, *14*, 1317-1324.
9. Dervan, P. B.; Edelson, B. S. Recognition of the DNA minor groove by pyrrole-imidazole polyamides. *Curr Opin Struct Biol* **2003**, *13*, 284-299.
10. Trauger, J. W.; Baird, E. E.; Dervan, P. B. Recognition of DNA by designed ligands at subnanomolar concentrations. *Nature* **1996**, *382*, 559-561.
11. Best, T. P.; Edelson, B. S.; Nickols, N. G.; Dervan, P. B. Nuclear localization of pyrrole-imidazole polyamide-fluorescein conjugates in cell culture. *Proc Natl Acad Sci U S A* **2003**, *100*, 12063-12068.
12. Edelson, B. S.; Best, T. P.; Olenyuk, B.; Nickols, N. G.; Doss, R. M.; Foister, S.; Heckel, A.; Dervan, P. B. Influence of structural variation on nuclear localization of DNA-binding polyamide-fluorophore conjugates. *Nucleic Acids Res* **2004**, *32*, 2802-2818.
13. Nickols, N. G.; Jacobs, C. S.; Farkas, M. E.; Dervan, P. B. Improved nuclear localization of DNA-binding polyamides. *Nucleic Acids Res* **2007**, *35*, 363-370.
14. Dudouet, B.; Burnett, R.; Dickinson, L. A.; Wood, M. R.; Melander, C.; Belitsky, J. M.; Edelson, B.; Wurtz, N.; Briehn, C.; Dervan, P. B.; Gottesfeld, J. M. Accessibility of nuclear chromatin by DNA binding polyamides. *Chem Biol* **2003**, *10*, 859-867.
15. Suto, R. K.; Edayathumangalam, R. S.; White, C. L.; Melander, C.; Gottesfeld, J. M.; Dervan, P. B.; Luger, K. Crystal structures of nucleosome core particles in complex with minor groove DNA-binding ligands. *J Mol Biol* **2003**, *326*, 371-380.
16. Edayathumangalam, R. S.; Weyermann, P.; Gottesfeld, J. M.; Dervan, P. B.; Luger, K. Molecular recognition of the nucleosomal "supergroove". *Proc Natl Acad Sci U S A* **2004**, *101*, 6864-6869.
17. Gottesfeld, J. M.; Neely, L.; Trauger, J. W.; Baird, E. E.; Dervan, P. B. Regulation of gene expression by small molecules. *Nature* **1997**, *387*, 202-205.

18. Chenoweth, D. M.; Harki, D. A.; Phillips, J. W.; Dose, C.; Dervan, P. B. Cyclic pyrrole-imidazole polyamides targeted to the androgen response element. *J Am Chem Soc* **2009**, *131*, 7182-7188.
19. Muzikar, K. A.; Nickols, N. G.; Dervan, P. B. Repression of DNA-binding dependent glucocorticoid receptor-mediated gene expression. *Proc Natl Acad Sci U S A* **2009**, *106*, 16598-16603.
20. Nickols, N. G.; Dervan, P. B. Suppression of androgen receptor-mediated gene expression by a sequence-specific DNA-binding polyamide. *Proc Natl Acad Sci U S A* **2007**, *104*, 10418-10423.
21. Nickols, N. G.; Jacobs, C. S.; Farkas, M. E.; Dervan, P. B. Modulating hypoxia-inducible transcription by disrupting the HIF-1-DNA interface. *ACS Chem Biol* **2007**, *2*, 561-571.
22. Olenyuk, B. Z.; Zhang, G. J.; Klco, J. M.; Nickols, N. G.; Kaelin, W. G., Jr.; Dervan, P. B. Inhibition of vascular endothelial growth factor with a sequence-specific hypoxia response element antagonist. *Proc Natl Acad Sci U S A* **2004**, *101*, 16768-16773.
23. Dickinson, L. A.; Burnett, R.; Melander, C.; Edelson, B. S.; Arora, P. S.; Dervan, P. B.; Gottesfeld, J. M. Arresting cancer proliferation by small-molecule gene regulation. *Chem Biol* **2004**, *11*, 1583-1594.
24. Buitenhuis, M.; Baltus, B.; Lammers, J. W.; Coffer, P. J.; Koenderman, L. Signal transducer and activator of transcription 5a (STAT5a) is required for eosinophil differentiation of human cord blood-derived CD34+ cells. *Blood* **2003**, *101*, 134-142.
25. Wierenga, A. T.; Vellenga, E.; Schuringa, J. J. Maximal STAT5-induced proliferation and self-renewal at intermediate STAT5 activity levels. *Mol Cell Biol* **2008**, *28*, 6668-6680.
26. Weber-Nordt, R. M.; Egen, C.; Wehinger, J.; Ludwig, W.; Gouilleux-Gruart, V.; Mertelsmann, R.; Finke, J. Constitutive activation of STAT proteins in primary lymphoid and myeloid leukemia cells and in Epstein-Barr virus (EBV)-related lymphoma cell lines. *Blood* **1996**, *88*, 809-816.
27. Li, G.; Miskimen, K. L.; Wang, Z.; Xie, X. Y.; Brenzovich, J.; Ryan, J. J.; Tse, W.; Moriggl, R.; Bunting, K. D. STAT5 requires the N-domain for suppression of miR15/16, induction of bcl-2, and survival signaling in myeloproliferative disease. *Blood* **2010**, *115*, 1416-1424.
28. Gesbert, F.; Griffin, J. D. Bcr/Abl activates transcription of the Bcl-X gene through STAT5. *Blood* **2000**, *96*, 2269-2276.
29. Horita, M.; Andreu, E. J.; Benito, A.; Arbona, C.; Sanz, C.; Benet, I.; Prosper, F.; Fernandez-Luna, J. L. Blockade of the Bcr-Abl kinase activity induces apoptosis of chronic myelogenous leukemia cells by suppressing signal transducer and activator of transcription 5-dependent expression of Bcl-xL. *J Exp Med* **2000**, *191*, 977-984.
30. Ehret, G. B.; Reichenbach, P.; Schindler, U.; Horvath, C. M.; Fritz, S.; Nabholz, M.; Bucher, P. DNA binding specificity of different STAT proteins. Comparison of in vitro specificity with natural target sites. *J Biol Chem* **2001**, *276*, 6675-6688.
31. Darnell, J. E. Transcription factors as targets for cancer therapy. *Nature Reviews Cancer* **2002**, *2*, 740-749.
32. Yu, H.; Jove, R. The STATs of cancer--new molecular targets come of age. *Nat Rev Cancer* **2004**, *4*, 97-105.
33. Frank, D. A. STAT signaling in cancer: insights into pathogenesis and treatment strategies. *Cancer Treat Res* **2003**, *115*, 267-291.
34. Turkson, J.; Jove, R. STAT proteins: novel molecular targets for cancer drug discovery. *Oncogene* **2000**, *19*, 6613-6626.
35. Ferbeyre, G.; Moriggl, R. The role of Stat5 transcription factors as tumor suppressors or oncogenes. *Biochim Biophys Acta* **2011**, *1815*, 104-114.
36. Levy, D. E.; Darnell, J. E., Jr. Stats: transcriptional control and biological impact. *Nat Rev Mol Cell Biol* **2002**, *3*, 651-662.
37. Darnell, J. E., Jr. STATs and gene regulation. *Science* **1997**, *277*, 1630-1635.

38. Akira, S. Roles of STAT3 defined by tissue-specific gene targeting. *Oncogene* **2000**, *19*, 2607-2611.
39. Nevalainen, M. T.; Ahonen, T. J.; Yamashita, H.; Chandrashekar, V.; Bartke, A.; Grimley, P. M.; Robinson, G. W.; Hennighausen, L.; Rui, H. Epithelial defect in prostates of Stat5a-null mice. *Lab Invest* **2000**, *80*, 993-1006.
40. Libermann, T. A.; Zerbini, L. F. Targeting transcription factors for cancer gene therapy. *Curr Gene Ther* **2006**, *6*, 17-33.
41. Ahonen, T. J.; Xie, J.; LeBaron, M. J.; Zhu, J.; Nurmi, M.; Alanen, K.; Rui, H.; Nevalainen, M. T. Inhibition of transcription factor Stat5 induces cell death of human prostate cancer cells. *J Biol Chem* **2003**, *278*, 27287-27292.
42. Dagvadorj, A.; Collins, S.; Jomain, J. B.; Abdulghani, J.; Karras, J.; Zellweger, T.; Li, H.; Nurmi, M.; Alanen, K.; Mirtti, T.; Visakorpi, T.; Bubendorf, L.; Goffin, V.; Nevalainen, M. T. Autocrine prolactin promotes prostate cancer cell growth via Janus kinase-2-signal transducer and activator of transcription-5a/b signaling pathway. *Endocrinology* **2007**, *148*, 3089-3101.
43. Xi, S.; Zhang, Q.; Dyer, K. F.; Lerner, E. C.; Smithgall, T. E.; Gooding, W. E.; Kamens, J.; Grandis, J. R. Src kinases mediate STAT growth pathways in squamous cell carcinoma of the head and neck. *J Biol Chem* **2003**, *278*, 31574-31583.
44. Lin, T. S.; Mahajan, S.; Frank, D. A. STAT signaling in the pathogenesis and treatment of leukemias. *Oncogene* **2000**, *19*, 2496-2504.
45. Schwaller, J.; Parganas, E.; Wang, D.; Cain, D.; Aster, J. C.; Williams, I. R.; Lee, C. K.; Gerthner, R.; Kitamura, T.; Frantsve, J.; Anastasiadou, E.; Loh, M. L.; Levy, D. E.; Ihle, J. N.; Gilliland, D. G. Stat5 is essential for the myelo- and lymphoproliferative disease induced by TEL/JAK2. *Mol Cell* **2000**, *6*, 693-704.
46. Huang, M.; Dorsey, J. F.; Epling-Burnette, P. K.; Nimmanapalli, R.; Landowski, T. H.; Mora, L. B.; Niu, G.; Sinibaldi, D.; Bai, F.; Kraker, A.; Yu, H.; Moscinski, L.; Wei, S.; Djeu, J.; Dalton, W. S.; Bhalla, K.; Loughran, T. P.; Wu, J.; Jove, R. Inhibition of Bcr-Abl kinase activity by PD180970 blocks constitutive activation of Stat5 and growth of CML cells. *Oncogene* **2002**, *21*, 8804-8816.
47. Levis, M.; Allebach, J.; Tse, K. F.; Zheng, R.; Baldwin, B. R.; Smith, B. D.; Jones-Bolin, S.; Ruggeri, B.; Dionne, C.; Small, D. A FLT3-targeted tyrosine kinase inhibitor is cytotoxic to leukemia cells in vitro and in vivo. *Blood* **2002**, *99*, 3885-3891.
48. Kelly, J. A.; Spolski, R.; Kovanen, P. E.; Suzuki, T.; Bollenbacher, J.; Pise-Masison, C. A.; Radonovich, M. F.; Lee, S.; Jenkins, N. A.; Copeland, N. G.; Morse, H. C., 3rd; Leonard, W. J. Stat5 synergizes with T cell receptor/antigen stimulation in the development of lymphoblastic lymphoma. *J Exp Med* **2003**, *198*, 79-89.
49. Gu, L.; Vogiatzi, P.; Puhr, M.; Dagvadorj, A.; Lutz, J.; Ryder, A.; Addya, S.; Fortina, P.; Cooper, C.; Leiby, B.; Dasgupta, A.; Hyslop, T.; Bubendorf, L.; Alanen, K.; Mirtti, T.; Nevalainen, M. T. Stat5 promotes metastatic behavior of human prostate cancer cells in vitro and in vivo. *Endocr Relat Cancer* **2010**, *17*, 481-493.
50. Liu, X.; Robinson, G. W.; Gouilleux, F.; Groner, B.; Hennighausen, L. Cloning and expression of Stat5 and an additional homologue (Stat5b) involved in prolactin signal transduction in mouse mammary tissue. *Proc Natl Acad Sci U S A* **1995**, *92*, 8831-8835.
51. Horvath, C. M.; Wen, Z.; Darnell, J. E., Jr. A STAT protein domain that determines DNA sequence recognition suggests a novel DNA-binding domain. *Genes Dev* **1995**, *9*, 984-994.
52. Basham, B.; Sathe, M.; Grein, J.; McClanahan, T.; D'Andrea, A.; Lees, E.; Rascle, A. In vivo identification of novel STAT5 target genes. *Nucleic Acids Res* **2008**, *36*, 3802-3818.
53. Gu, L.; Dagvadorj, A.; Lutz, J.; Leiby, B.; Bonuccelli, G.; Lisanti, M. P.; Addya, S.; Fortina, P.; Dasgupta, A.; Hyslop, T.; Bubendorf, L.; Nevalainen, M. T. Transcription factor Stat3 stimulates metastatic behavior of human prostate cancer cells in vivo, whereas Stat5b has a preferential

role in the promotion of prostate cancer cell viability and tumor growth. *Am J Pathol* **2010**, *176*, 1959-1972.
54. Chenoweth, D. M.; Dervan, P. B. Structural basis for cyclic Py-Im polyamide allosteric inhibition of nuclear receptor binding. *J Am Chem Soc* **2010**, *132*, 14521-14529.
55. Hsu, C. F.; Phillips, J. W.; Trauger, J. W.; Farkas, M. E.; Belitsky, J. M.; Heckel, A.; Olenyuk, B. Z.; Puckett, J. W.; Wang, C. C.; Dervan, P. B. Completion of a Programmable DNA-Binding Small Molecule Library. *Tetrahedron* **2007**, *63*, 6146-6151.
56. Chenoweth, D. M.; Dervan, P. B. Allosteric modulation of DNA by small molecules. *Proc Natl Acad Sci U S A* **2009**, *106*, 13175-13179.
57. Raskatov, J. A.; Hargrove, A. E.; So, A. Y.; Dervan, P. B. Pharmacokinetics of Py-Im Polyamides Depend on Architecture: Cyclic versus Linear. *J Am Chem Soc* **2012**, Submitted.
58. Raskatov, J. A.; Nickols, N. G.; Dervan, P. B. *Unpublished results*, **2012**.
59. Chenoweth, D. M.; Harki, D. A.; Dervan, P. B. Solution-phase synthesis of pyrrole-imidazole polyamides. *J Am Chem Soc* **2009**, *131*, 7175-7181.
60. Harki, D. A.; Satyamurthy, N.; Stout, D. B.; Phelps, M. E.; Dervan, P. B. In vivo imaging of pyrrole-imidazole polyamides with positron emission tomography. *Proc Natl Acad Sci U S A* **2008**, *105*, 13039-13044.
61. Baird, E. E.; Dervan, P. B. Solid phase synthesis of polyamides containing imidazole and pyrrole amino acids. *J Am Chem Soc* **1996**, *118*, 6141-6146.
62. Belitsky, J. M.; Nguyen, D. H.; Wurtz, N. R.; Dervan, P. B. Solid-phase synthesis of DNA binding polyamides on oxime resin. *Bioorg Med Chem* **2002**, *10*, 2767-2774.
63. Dose, C.; Farkas, M. E.; Chenoweth, D. M.; Dervan, P. B. Next generation hairpin polyamides with (R)-3,4-diaminobutyric acid turn unit. *J Am Chem Soc* **2008**, *130*, 6859-6866.
64. Pilch, D. S.; Poklar, N.; Baird, E. E.; Dervan, P. B.; Breslauer, K. J. The thermodynamics of polyamide-DNA recognition: hairpin polyamide binding in the minor groove of duplex DNA. *Biochemistry* **1999**, *38*, 2143-2151.
65. Muzikar, K. A.; Meier, J. L.; Gubler, D. A.; Raskatov, J. A.; Dervan, P. B. Expanding the Repertoire of Natural Product-Inspired Ring Pairs for Molecular Recognition of DNA. *Org Lett* **2011**, *ASAP*.
66. Boyle, A. P.; Davis, S.; Shulha, H. P.; Meltzer, P.; Margulies, E. H.; Weng, Z.; Furey, T. S.; Crawford, G. E. High-resolution mapping and characterization of open chromatin across the genome. *Cell* **2008**, *132*, 311-322.
67. Gottesfeld, J. M.; Belitsky, J. M.; Melander, C.; Dervan, P. B.; Luger, K. Blocking transcription through a nucleosome with synthetic DNA ligands. *J Mol Biol* **2002**, *321*, 249-263.
68. Chen, X.; Xu, H.; Yuan, P.; Fang, F.; Huss, M.; Vega, V. B.; Wong, E.; Orlov, Y. L.; Zhang, W.; Jiang, J.; Loh, Y. H.; Yeo, H. C.; Yeo, Z. X.; Narang, V.; Govindarajan, K. R.; Leong, B.; Shahab, A.; Ruan, Y.; Bourque, G.; Sung, W. K.; Clarke, N. D.; Wei, C. L.; Ng, H. H. Integration of external signaling pathways with the core transcriptional network in embryonic stem cells. *Cell* **2008**, *133*, 1106-1117.
69. Teglund, S.; McKay, C.; Schuetz, E.; van Deursen, J. M.; Stravopodis, D.; Wang, D.; Brown, M.; Bodner, S.; Grosveld, G.; Ihle, J. N. Stat5a and Stat5b proteins have essential and nonessential, or redundant, roles in cytokine responses. *Cell* **1998**, *93*, 841-850.

LIST OF ABBREVIATIONS

Ac_2O	Acetic anhydride
AcCl	Acetyl Chloride
AcOH	Acetic acid
AIBN	Azobisisobutyronitrile
AQN	Anthraquinone
ATP	Adenosine-5’-triphosphate
9-BBN	9-Borabicyclo[3.3.1]nonane
Bn	Benzyl
BnBr	Benzyl bromide
Boc	*tert*-Butoxycarbonyl
Boc_2O	Di-*tert*-butyldicarbonate
BOMCl	Benzyloxymethyl chloride
BOP	(Benzotriazol-1-yloxy)tris(dimethylamino) phophonium hexafluorophosphate
CbzCl	Benzyl chloroformate
cod	1,5-Cyclooctadiene
CREB	cAMP response element-binding
d	Day
Davis’s oxaziridine	2-(Phenylsulfonyl)-3-phenyloxaziridine
DEAD	Diethyl azodicarboxylate
Dess-Martin or DMP	Triacetoxy *o*-iodoxybenzoic acid
DBU	1,8-Diazabicyclo[5.4.0]undec-7-ene
DHQD	Dihydroquinidine
DIBAL-H	Diisobutylaluminium hydride
DMAP	4-(Dimethylamino)-pyridine

DMDO	Dimethyldioxirane
DME	Dimethoxyethane
DMF	Dimethylformamide
DMS	Dimethylsulfide
DMSO	Dimethyl sulfoxide
dppf	1,1'-*Bis*(diphenylphosphino)ferrocene
DTBMP	2,6-*di*-*tert*-butyl-4-methylpyridine
EDCI	*N*-(3-dimethylaminopropyl)-*N*'-ethylcarbodiimide
ee	Enantiomeric excess
e.r.	Enantiomeric ratio
Et_3N	Triethylamine
EtOAc	Ethyl Acetate
Et_2O	Diethyl ether
EtOH	Ethanol
Fmoc	Fluorenylmethyloxycarbonyl
FmocOSu	9-Fluorenylmethyl *N*-succinimidyl carbonate, *N*-(9-fluorenylmethoxycarbonyloxy)succinimide
GSH	Glutathione
h	Hour
HATU	*O*-(7-Azabenzotriazol-1-yl)-*N*,*N*,*N*',*N*'-tetramethyluronium hexafluorophosphate
HIF-1	Hypoxia-inducible factor 1
h*v*	Irradiation with light
*i*Bu	Isobutyl
*i*Pr	Isopropyl
iPr_2NEt	*N*,*N*-Diisopropylethylamine
Imid	Imidazole
KO*t*Bu	Potassium *tert*-butoxide
LDA	Lithium *N*,*N*-diisopropylamide
LHMDS	Lithium bis(trimethylsilyl)amide
*m*CPBA	*m*-Chloroperbenzoic acid

Me	Methyl
MeCN	Acetonitrile
MeI	Methyl iodide
MeOH	Methanol
min	Minute
MOMCl	Methyl chloromethyl ether
MRSA	Methicillin-resistant *Staphylococcus aureus*
MsCl	Methanesulfonyl chloride
NADPH	Nicotinamide adenine dinucleotide phosphate
NaHMDS	Sodium bis(trimethylsilyl)amide
NBS	*N*-Bromosuccinimide
NCS	*N*-Chlorosuccinimide
NIS	*N*-Iodosuccinimide
*n*BuLi	*n*-Butyllithium
N-PSP	Diphenyl diselenide
O/N	Overnight
$Pd(OAc)_2$	Palladium(II) acetate
Pd/C	Palladium on carbon
Ph	Phenyl
$PhI(OAc)_2$	Iodobenzene diacetate
PhMe	Toluene
PPTS	Pyridinium *p*-toluenesulfonate
PPY	(*R*)-(+)-4-pyrrolidinopyridinyl(pentamethylcyclo-pentadienyl)iron
Py. or Pyr.	Pyridine
No Rxn	No reaction was observed
RT or r.t.	Room temperature
Sat'd	Saturated aqueous solution
T3P	Propane phosphonic acid anhydride
TBAF	Tetrabutyl ammonium fluoride
TBDMSCl or TBSCl	*tert*-Butyldimethylsilyl chloride

TBDPS	*tert*-Butyldiphenylsilyl
TBSOTf	*tert*-Butyldimethylsilyl trifluoromethanesulfonate
Teoc	2-(trimethylsilyl)ethoxycarbonyl
TES	Triethylsilyl
Tf	Trifluoromethanesulfonate
TFA	Trifluoroacetic acid
TFAA	Trifluoroacetic anhydride
Tf_2O	Trifluoromethanesulfonyl anhydride
THF	Tetrahydrofuran
TIPS	Triisopropylsilyl
TLC	Thin layer chromatography
TMS	Trimethylsilyl
TMSOTf	Trimethylsilyl trifluoromethylsulfonate
Tr	Trityl (triphenylmethyl)
Triton B	Benzyltrimethylammonium hydroxide
*p*TsOH or *p*TSA	*p*-Toluenesulfonic acid
µw	Microwave irradiation
V-70	2,2'-Azobis(4-methoxy-2,4-dimethyl valeronitrile)
VRE	Vancomycin-resistant *Enterococcus*